



U.S. DEPARTMENT OF COMMERCE
Environmental Science Services Administration

COLLECTED REPRINTS-1968



ATLANTIC-PACIFIC
OCEANOGRAPHIC LABORATORIES



U. S. DEPARTMENT OF COMMERCE

Maurice H. Stans, Secretary

ENVIRONMENTAL SCIENCE SERVICES ADMINISTRATION

Robert M. White, Administrator

RESEARCH LABORATORIES

Wilmot N. Hess, Director

Collected Reprints-1968

ATLANTIC-PACIFIC OCEANOGRAPHIC LABORATORIES

ISSUED SEPTEMBER 1969

Atlantic Oceanographic and Meteorological Laboratories
Miami, Florida 33130

Pacific Oceanographic Laboratories
Seattle, Washington 98105

For sale by the Superintendent of Documents, U.S. Government Printing Office, Washington, D.C. 20402
Price \$3.25

FOREWORD

Knowledge of the ocean and its processes develops slowly. It is the result of the work of many researchers in this country and throughout the world. To be useful, however, each new increment of knowledge must be disseminated so that the other workers will know of it and be able to build upon it.

Because the published results of the scientific and technical work of ESSA's Atlantic Oceanographic Laboratories and Pacific Oceanographic Laboratories are scattered through the literature, they are being brought together in a series of annual publications. These publications provide to researcher and to interested layman alike a convenient summary of the results of the work of these two oceanographic laboratories of the Environmental Science Services Administration of the U.S. Department of Commerce.

This volume, the third in the series, holds the published papers for the year 1968.

Harris B. Stewart, Jr.
Director
Atlantic Oceanographic and
Meteorological Laboratories

TABLE OF CONTENTS

PHYSICAL OCEANOGRAPHY

1. Hazelworth, John B., Water temperature variations resulting from hurricanes: *J. Geophys. Res.* 73, No. 16, 5105-5123.
2. Hansen, Donald V., A Review of: Riches of the sea; the new science of oceanology: Norman Carlisle, Sterling Publ. Co., New York, in *The Science Teacher* 35, No. 3, 67.
3. Larsen, J. C., Electric and magnetic fields induced by deep sea tides: *Geophys. J. R. astr. Soc.* 16, 47-70.
4. Reed, R. K., et al., New feature of the East Australian Current: *Nature* 218, No. 5141, 557-558.
5. Reed, R. K., Transport of the Alaskan Stream: *Nature* 220, No. 5168, 681-682.
6. Zetler, Bernard D., Tide talk: *Go Magazine*, Oct., Nov., Dec., 1968.

MARINE GEOLOGY AND GEOPHYSICS

7. Bassinger, B. G., Marine magnetic study in the northeast Chukchi Sea: *J. Geophys. Res.* 73, No. 2, 683-687.
8. Boon, John D. III, and William G. MacIntyre, The barosalinity relationship in estuarine sediments of the Rappahannock River, Virginia: *Chesapeake Sci.* 9, No. 1, 21-26.
9. Boon, John D. III, Trend surface analysis of sand tracer distributions on a carbonate beach, Bimini, BWI, *J. Geol.* 76, No. 1, 71-87.
10. Dietz, Robert S., Shatter cones and star wounds: *New Scientist* 40, No. 625, 501-503.
11. Dietz, Robert S., Shatter cones in cryptoexplosion structures: in *Shock Metamorphism of Natural Materials*, ed. Beven M. French and Nicholas M. Short, (Mono. Book Corp., Baltimore, Md.), 267-283.
12. Dietz, Robert S., A reply to A.A. Meyerhoff's "Arthur Holmes: Originator of Spreading Sea Floor Hypothesis": *J. Geophys. Res.* 73, No. 20, 6567.

13. Dietz, Robert S., The origin of continental slopes: Documenta Geigy, No. 4, Nautilus, Basle, Switz., 4-5.
14. Dietz, Robert S., Barringer meteor crater: in Intern. Dictionary Geophys. 1, 134-136 (Pergamon Press, New York, N.Y.), p.3.
15. Dietz, Robert S., and Rhodes W. Fairbridge, Wave base: Encycl. Geomorph., ed. R.W. Fairbridge, Reinhold, N.Y., 1224-1228.
16. Dietz, Robert S., Miogeoclines (Miogeosynclines) in space and time: A reply: J. Geol. 76, No. 1, 119-121.
17. Dietz, Robert S., and Harley J. Knebel, Survey of Ross's original deep sea sounding site: Nature 220, No. 5169, 751-753.
18. Dietz, Robert S., and Walter P. Sproll, Miogeoclines (Miogeosynclines in space and time): A reply: J. Geol. 76, No. 1, 113-116.
19. Dietz, Robert S., Harley J. Knebel, and Lee H. Sommers, Cayar Submarine Canyon: Bull. Geol. Soc. Am. 79, No. 12, 1821-1828.
20. Harbison, R. N., Geology of DeSoto Canyon: J. Geophys. Res. 73, No. 16, 5175-5183.
21. Harrison, W., et al., A time series from the beach environment: ESSA Tech. Memo. RLTM-AOL 1.
22. Harrison, W., Empirical equation for longshore current velocity: J. Geophys. Res. 73, No. 22, 6929-6936.
23. Keller, George H., Shear strength and other physical properties of sediments from some ocean basins: Proc. Conf. on Civil Engineering in the Oceans, Sept. 1968, Amer. Soc. Civil Engr., 391-417.
24. Keller, George H. and R. H. Bennett, Mass physical properties of submarine sediments in the Atlantic and Pacific Basins: Proc. XXIII Intern. Geol. Cong. Prague 8, 33-50.
25. Keller, G. H., and G. Peter, East-west profile from Kermadec Trench to Valparaiso, Chile: J. Geophys. Res. 73, No. 22, 7154-7157.

26. Malloy, Richard J. Depositional anticlines versus tectonic "reverse drag": Trans. Gulf Coast Assoc. of Geol. Soc. 18, 114-123.
27. Naugler, Frederick P., and Barrett H. Erickson, Murray Fracture Zone: Westward extension: Science 161, No. 3846, 1142-1145.
28. Peter, George, and R. E. Burns, Island arcs, general: Encycl. Geomorph., ed. R. W. Fairbridge, Reinhold, N.Y., 564-568.
29. Ryan, T. V., and P. J. Grim, A new technique for echo sounding corrections: Intern. Hydro. Rev. 45, No. 2, 41-58.
30. Smith, R. E., J. D. Gassaway, and H. N. Giles, Iron-manganese nodules from Nares Abyssal Plain: Geochemistry and Mineralogy: Science 161, No. 3843, 780-781.
- * Starr, Robert B., and B. G. Bassinger, Marine geophysical observations of eastern Puerto Rico-Virgin Islands region: Proc. Vol., Fifth Caribbean Geol. Conf.

* Reprint not available.

GENERAL

31. Harrison, W., Where the sea meets the land, ESSA World 3, No. 2, 14-16, U.S. Dept. of Commerce, Rockville, Md.
32. Sokolowski, T. J., and G. R. Miller, Deep sea release mechanism: ESSA Tech. Memo RLTM-POL 1.
33. Stewart, Harris B., Jr., Ocean-wide surveys, both meteorological and oceanographic: Calif. Mar. Res. Comm., CalCOFI Rept. No. 12, 43-49.
34. Stewart, Harris B., Jr., You'll love it--don't let it kill you: ESSA World 3, No. 3, 4-6, U.S. Dept. of Commerce, Rockville, Md.
35. Stewart, Harris B., Jr., Issues and programs--Environmental Science Services Administration, Dept. of Commerce: Gulf Univ. Res. Corp. Pub. No. 107, 31-34.

36. Stewart, Harris B., Jr., Florida's future, oceanographically speaking: Orlando (Fla.) Sentinel, Fla. Industries Expo., Sec. G., 5-6.
37. Stewart, Harris B., Jr., Scientists aid weekend sailors: The Miamian, Dec., 66-67.
38. Stewart, Harris B., Jr., Science, surveys, and the continental shelf: Transactions, Natl. Symposium on Ocean Sciences and Engineering of the Atlantic Shelf, Marine Technol. Soc., Philadelphia, Pa., Mar. 19, 1968, 1-7.
39. Stewart, Harris B., Jr., The Southside Fleet: The Miamian, Jan., 18-23.

MAPS

- Lattimore, Robert K., B. G. Bassinger, and Omar DeWald,
Transcontinental Geophysical Survey (35⁰- 39⁰N)
Magnetic Map from the Coast of California to 133⁰
Longitude, Miscellaneous Geologic Investigations,
Map I-531-A.
- Lattimore, Robert K., Sam A. Bush, and Patricia A. Bush,
Transcontinental Geophysical Survey (35⁰-39⁰N)
Gravity and Bathymetric Map from the coast of
California to 133⁰W Longitude, Miscellaneous
Geologic Investigations, Map I-531-B.

Water Temperature Variations Resulting from Hurricanes

JOHN B. HAZELWORTH

*Physical Oceanography Laboratory, Atlantic Oceanographic Laboratories
Environmental Science Services Administration, Miami, Florida 33130*

Daily variations in sea surface temperature at several coastal and lightship stations and the Nomad buoy during the passages of ten hurricanes are presented. The temperature variations are given for the coastal stations and Nomad buoy for a period from 10 days before to 36 days after the hurricane passed. Generally, marked cooling of the sea surface occurred during the passage of a hurricane. However, examples are noted where a rise in temperature occurred. A comparison was made of the daily temperature variation due to hurricanes as recorded at the coastal and deep water sites. The mean temperatures decrease for the eleven coastal examples and for the thirteen lightship examples was 3.1°F, and for the three Nomad examples was 6.4°F. The extent of cooling of the surface water appears to be related to storm intensity and orientation with respect to the recording station. The temperature decreases at the Nomad buoy during the passage of hurricanes were quite large compared with the changes at other times during the 47-day periods, but factors other than hurricanes appear to cause larger temperature variations at the coastal sites. The length of time for the water temperature to return to normal after passage of a hurricane was computed for all stations. For the coastal and lightship stations the temperature returned to normal in less than one month, with mean time of 13 and 10 days, respectively. At the Nomad buoy, near prehurricane surface temperature conditions were recorded within 10 days. These observations indicate the rapidity with which hurricane effects are modified by subsequent environmental events.

INTRODUCTION

Evidence of marked cooling of the sea surface following the passage of hurricanes and typhoons has been reported by several authors. These include *Leipper* [1965], *Uda* [1954], *Jordan* [1965], *Jordan and Frank* [1964], *Fisher* [1958], and *Stevenson and Armstrong* [1965]. Several theories explaining this phenomenon have been advanced. *McFadden* [1967] summarized the various proposed theories and also reported sea-surface temperatures taken by an infrared radiometer aboard a research aircraft following the passage of hurricane Betsy. In brief, the theories on the lowering of water temperature include the following processes: (1) loss of heat to the hurricane, (2) maximum upwelling in the center of the storm plus horizontal advection, (3) maximum upwelling in the region of maximum turbulent shearing stress, (4) vertical mixing induced by mechanical stirring.

Usually, the data analyzed by the various authors have been recorded by ship injection thermometers during individual traverses through the area, certainly not a very adequate sampling technique. Only *Leipper* [1965] and

Uda [1954] have systematically obtained sea-surface and subsurface temperature observations soon after the passage of a hurricane. None has presented day-by-day variations in water temperature at a point before, during, and following the passage of a hurricane. Inasmuch as such data are regularly recorded, an inspection was made to see if these data could possibly lead to a better understanding of the effects of a hurricane on the ocean thermal structure.

THE DATA

The U. S. Coast and Geodetic Survey continuously records sea-surface temperatures at Galveston, Miami, Atlantic City, New York, and Boston. The U. S. Navy obtains sea-surface temperature from the Nomad¹ buoy in the center of the Gulf of Mexico (25°N, 90°W) [*Marcus*, 1964]. Also, the U. S. Coast Guard records daily bathythermograms and sea-

¹The Nomad buoy has been in operation since 1958. However, as the equipment is still undergoing technical evaluation, the data should be regarded as of unknown quality.

surface salinity observations at a number of lightship stations located along the Atlantic coast. Since 1956 these data have been published annually by the U. S. Fish and Wildlife Service [Day, 1963; Chase, 1964, 1967].

A survey was made of hurricanes occurring between 1960 and 1965 that passed within 185 km of an observation point. Ten were found that passed in the vicinity of at least one of the Coast and Geodetic Surveys' recording stations. Three passed in the vicinity of lightships. In some cases the hurricane passed near two or more stations. Table 1 lists the hurricanes, the dates of occurrences, and nearest distance between the center of the hurricane and the

station. The letter (G) follows the hurricane's name if it was listed by Kraft [1966] as a great hurricane in the vicinity of the recording station. The letters (R) or (L) following the shortest distances indicate whether the station was to the right or to the left of the path of the hurricane. Figure 1 shows the paths the various hurricanes followed. Figure 2 shows the locations of the lightships, the Coast and Geodetic Survey recording stations, and the Nomad buoy. In general, no data were recorded aboard the lightships on the day that the hurricane passed the station. Usually, bathythermograms and surface salinity observations were made every day except the day the storm passed.

TABLE 1. List of Hurricanes

Hurricane	Station	Shortest Distance from Hurricane to Station, km	Date of Hurricane Passage
Donna (G)	Miami	Less than 110 (R)	Sept. 10, 1960
Donna	Atlantic City	Less than 93 (L)	Sept. 12, 1960
Donna	Boston	Less than 18 (R)	Sept. 12, 1960
Donna	Portland Lightship	37 (R)	Sept. 12, 1960
Donna	Boston Lightship	37 (R)	Sept. 12, 1960
Donna	Ambrose Lightship	85 (L)	Sept. 12, 1960
Donna	Winter Quarter Lightship	28 (L)	Sept. 12, 1960
Donna	Chesapeake Light- ship	65 (L)	Sept. 12, 1960
Donna	Barnegat Lightship	35 (L)	Sept. 12, 1960
Donna	Five Fathom Bank Lightship	56 (L)	Sept. 12, 1960
Donna (G)	Frying Pan Shoals Lightship	Passed over	Sept. 11, 1960
Donna	Diamond Shoals Lightship	28 (R)	Sept. 11, 1960
Donna (G)	Savannah Lightship	111 (L)	Sept. 11, 1960
Ethel	Nomad	Passed over	Sept. 14, 1960
Carla (G)	Nomad	About 111 (R)	Sept. 9, 1961
Carla (G)	Galveston	About 167 (R)	Sept. 11, 1961
Esther	Atlantic City	About 185 (L)	Sept. 20, 1961
Esther	Boston	About 74 (L)	Sept. 26, 1961
Esther	Boston Lightship	74 (L)	Sept. 26, 1961
Esther	Portland Lightship	9 (L)	Sept. 26, 1961
Alma	Miami	18 (L)	Aug. 26, 1962
Arlene	Bermuda	Passed over	Aug. 9, 1962
Cleo	Miami	Passed over	Aug. 26, 1964
Hilda	Nomad	About 74 (R)	Oct. 1, 1964
Isbell	Miami	Less than 93 (R)	Oct. 14, 1964
Isbell	Frying Pan Shoals Lightship	130 (L)	Oct. 16, 1964
Isbell	Diamond Shoals Lightship	74 (R)	Oct. 16, 1964
Betsy (G)	Miami	Less than 18 (R)	Sept. 8, 1965

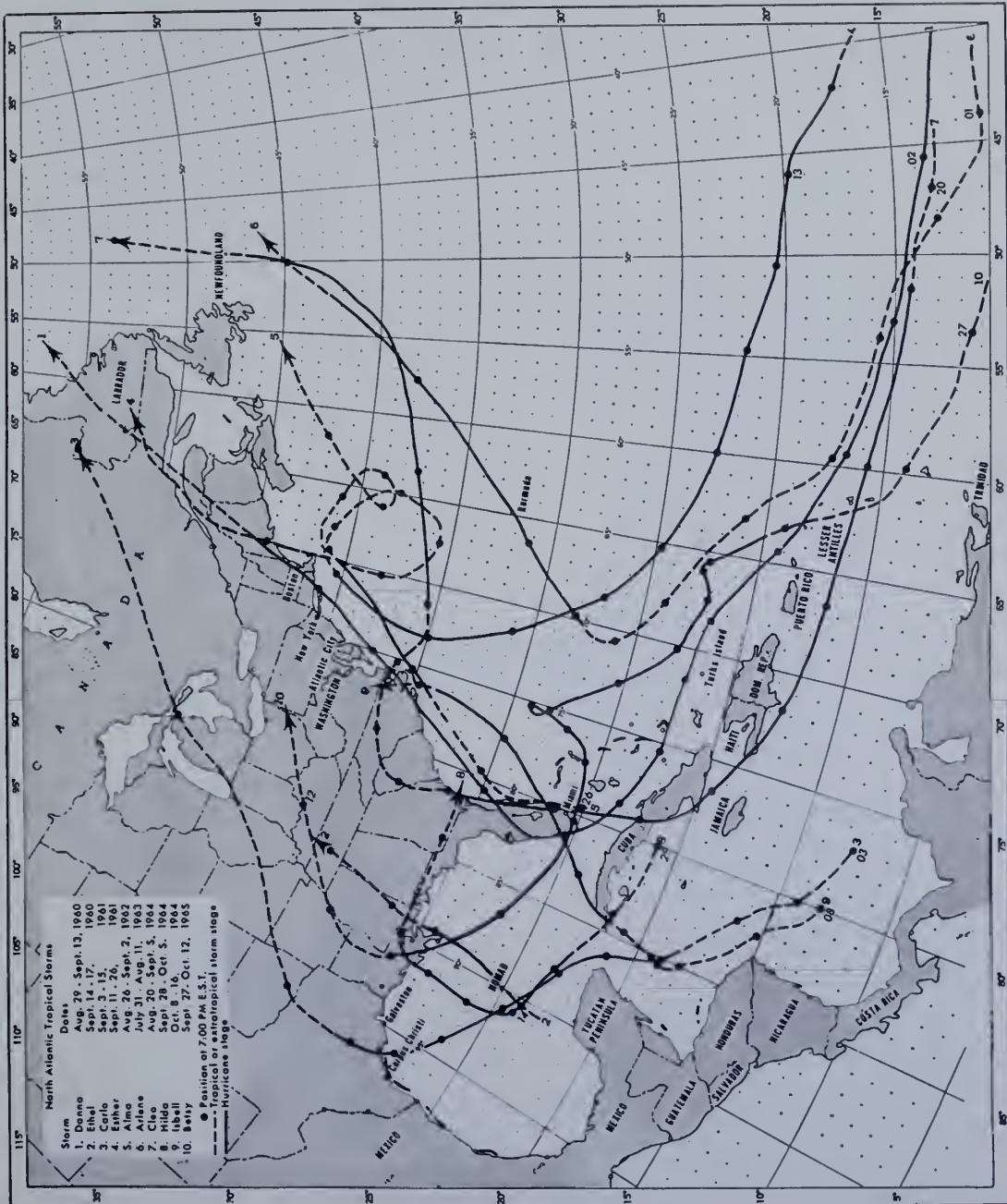


Fig. 1. The paths the various hurricanes followed.

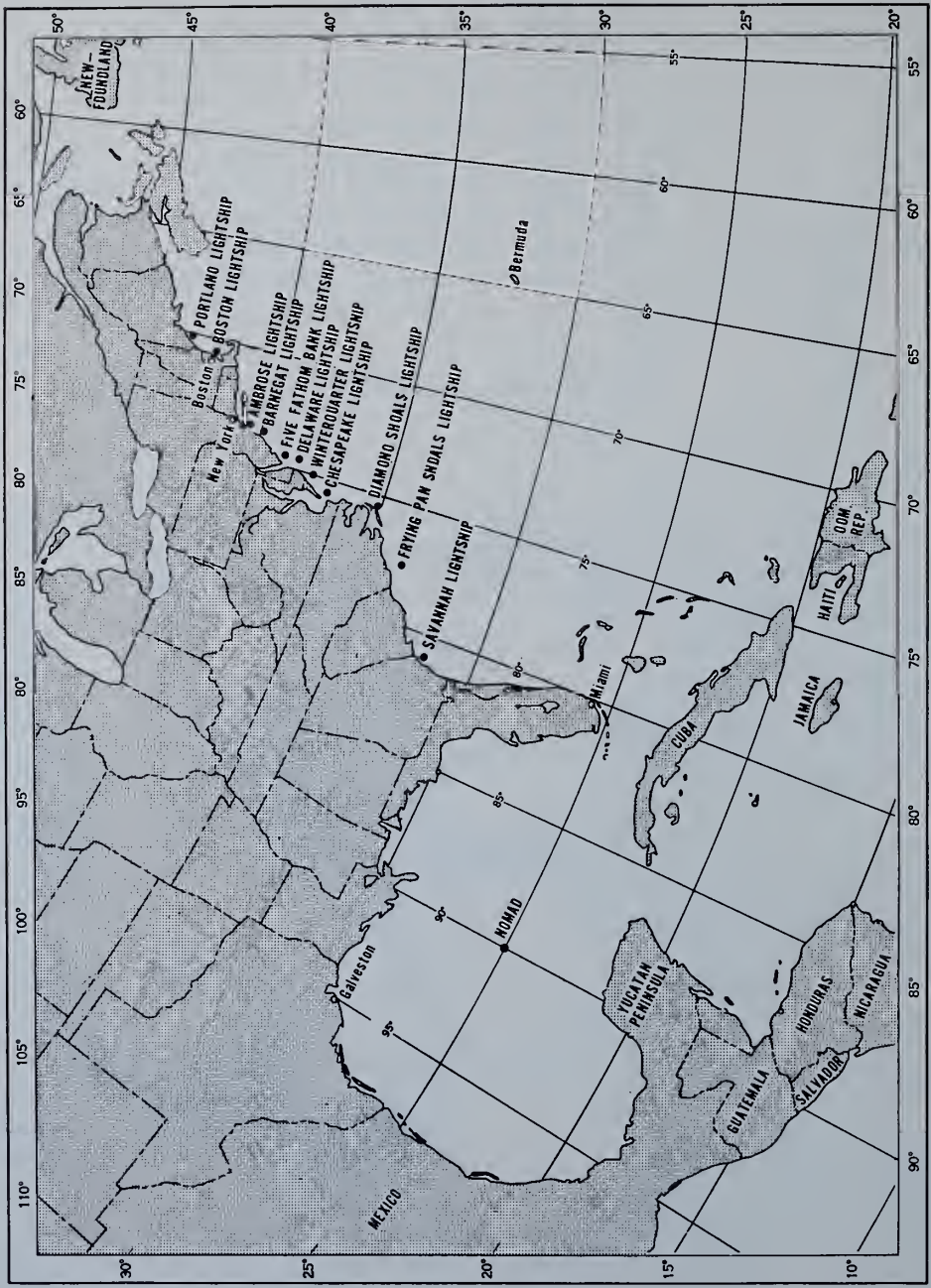


Fig. 2. Locations of the Coast Guard lightships, Coast and Geodetic Survey recording stations, and the Nomad buoy.

Temperatures from the bathythermograms were tabulated at several levels and are reproduced as Figure 3. The small '1' below the temperature trace indicates the pre-hurricane condition and the '2' the post-hurricane condition. The surface sigma- t observations were read from tables. These data are presented as Table 2. Figures 4 through 10 show the mean daily surface water temperature for each station for the period of 10 days before until 36 days after the passage of the respective storm.

Some variations in accuracy of the sea-surface temperature occur because of the recording methods. At Bermuda the sea-surface temperature was measured by a bucket thermometer. As only one observation is made each day, a tidal effect might be included in the data. The Nomad temperature sensor is mounted 18 inches below the sea surface. As the daily means were computed by using four to six observations, any tidal effect should be averaged out. The temperature sensors at the coastal stations are at a constant depth off the bottom, and so their depth below the sea surface varies with the tide. The means of the daily water temperature were computed from hourly observations, canceling out any tidal effect. The lightship temperature was recorded by a bathythermograph. A single observation was made each day.

Also shown on Figures 4 through 10 is the difference between the daily sea-surface temperature and the normal daily sea-surface temperature. The normal daily sea-surface temperatures were established for the coastal stations by computing sea-surface temperature means for each day, from at least 10 years of historical temperature data. Periods when the water was disturbed by the passage of a hurricane were omitted from these computations. Normal daily sea-surface temperature values were established for the Nomad buoy and the lightships in the same manner. The buoy was not operative until 1958, and, because of missing data, the normal daily mean temperatures were computed from two to six observations. The lightship oceanographic program was started in 1956; the normal daily mean temperatures were computed from three to eight observations.

DISCUSSION OF THE DATA

As expected, in nearly every case the water temperature dropped during the passage of the

hurricane. However, during the passage of Esther (1961), the Atlantic City and Boston stations, and the Portland lightship recorded a temperature increase.

The mean change for the 11 coastal examples for the 5-day period of 2 days before until 3 days after the passage of the hurricane was 3.1°F. For the 3 cases that passed the Nomad buoy, the mean drop was 6.4°F, and, for the 13 cases that passed the lightships, the mean drop was 3.1°F. These results are summarized in Table 3. The water temperature reached its minimum value within 3 days after the passage of the hurricane. In approximately 50% of the cases the minimum surface water temperature occurred the day after the hurricane passed.

The mean variation in sea-surface temperature was -4.0°F for the 11 cases when the stations were to the right of the hurricane track but only -3.0°F for the 12 cases when the stations were to the left. This difference supports the observations reported by Jordan [1965] and McFadden [1967]. Also, it is to be expected because on the right-hand side of the hurricane the wind blows in the direction that the storm is moving, and consequently the seas are highest and mixing should be greatest. The extent of cooling of the surface waters appears to be related to storm intensity. The mean temperature decrease during the 5-day hurricane period is 5.1°F when great hurricanes pass the shore stations but only 2.3°F for other hurricanes.

A plot was made between the decrease in surface temperature and the distance from the hurricane to the nearshore recording station. No correlation existed. Temperature decrease ranged from 0.2° to 4.8°F when a hurricane passed over a station. In all other cases the temperature decrease fell within this same range regardless of distance from the recording station. Obviously, this lack of correlation is limited to cases where the hurricane passes within 185 km of the station (the limit of this data sample). A comparison was made between the temperature change that occurred during the passage of a hurricane and the maximum change within any other 5 consecutive days during the rest of the tabulated 47-day periods. For the eleven examples at the coastal sites the mean of these maximum changes was 5.1°F, whereas it was only 3.1°F during the passage of hurricanes.

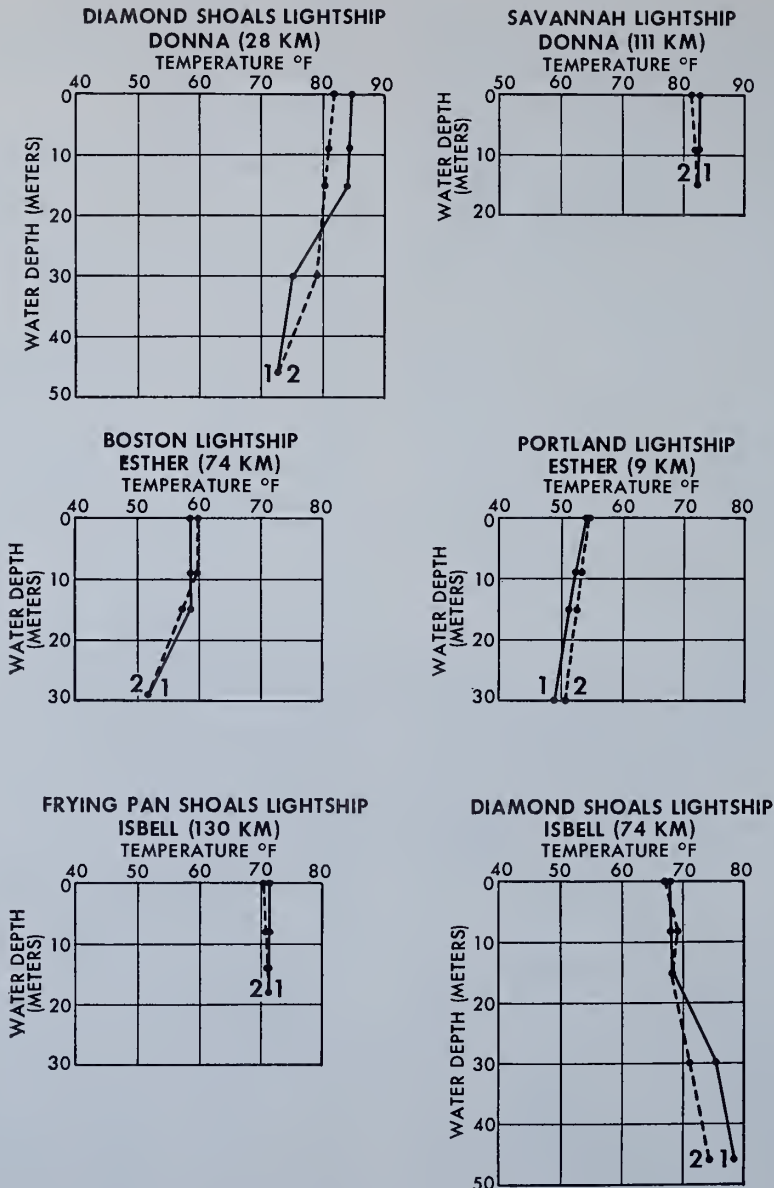


Fig. 3. Thermal structure before and after the passage of a hurricane at the lightships.

However, the temperature changes at the Nomad buoy during the passages of hurricanes were quite large compared with the maximum daily temperature changes during the rest of the periods. At the coastal stations and at the lightships, factors other than hurricanes appear to cause larger water temperature variations than do hurricanes. An outstanding example of this occurred at Galveston (Pleasure Pier). Dur-

ing the passage of hurricane Carla the largest water temperature drop was 1.5°F from the day before until the day the storm passed. On the other hand, 21 days later the water temperature dropped 8.8°F within a 1-day period. During this same day the prevailing wind shifted from south to north and the air temperature dropped from 3°F above normal to 8°F below normal, suggesting a relation between

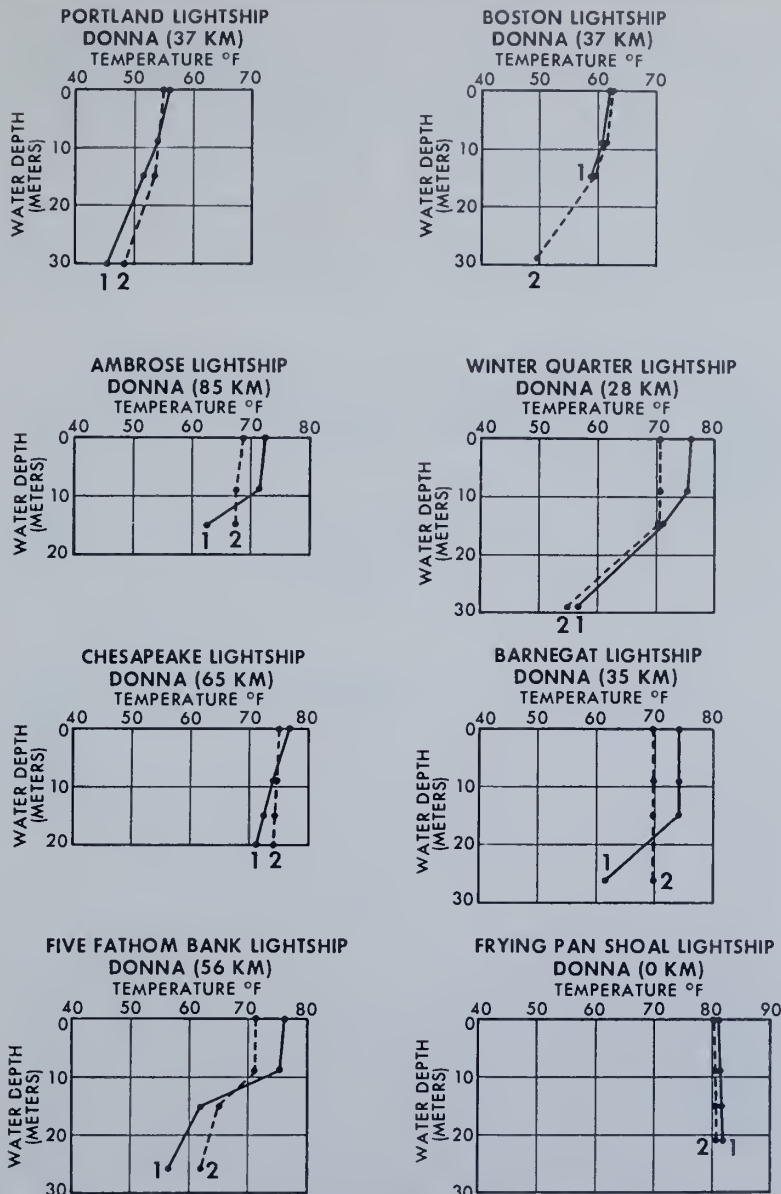


Fig. 3. Thermal structure before and after the passage of a hurricane at the lightships.

the air and sea-surface temperatures. By using the entire 45 days of data, a correlation coefficient between the departure from normal of the air and sea-surface temperature of $r = 0.72$ was computed. Horizontal advection may also have made a significant contribution to the sea-surface temperature drop. An inspection of the other examples revealed that in some cases the large water temperature changes did follow large air temperature changes, whereas in other cases

large water temperature changes appeared to be unrelated.

From Figures 4 through 10 it is possible to obtain some idea of the duration of the effect of the hurricane on the water temperature. This was accomplished by first determining the mean normal daily water temperature for each station. Then, a prehurricane water temperature variation from normal was determined. The temperature variation from normal resulting

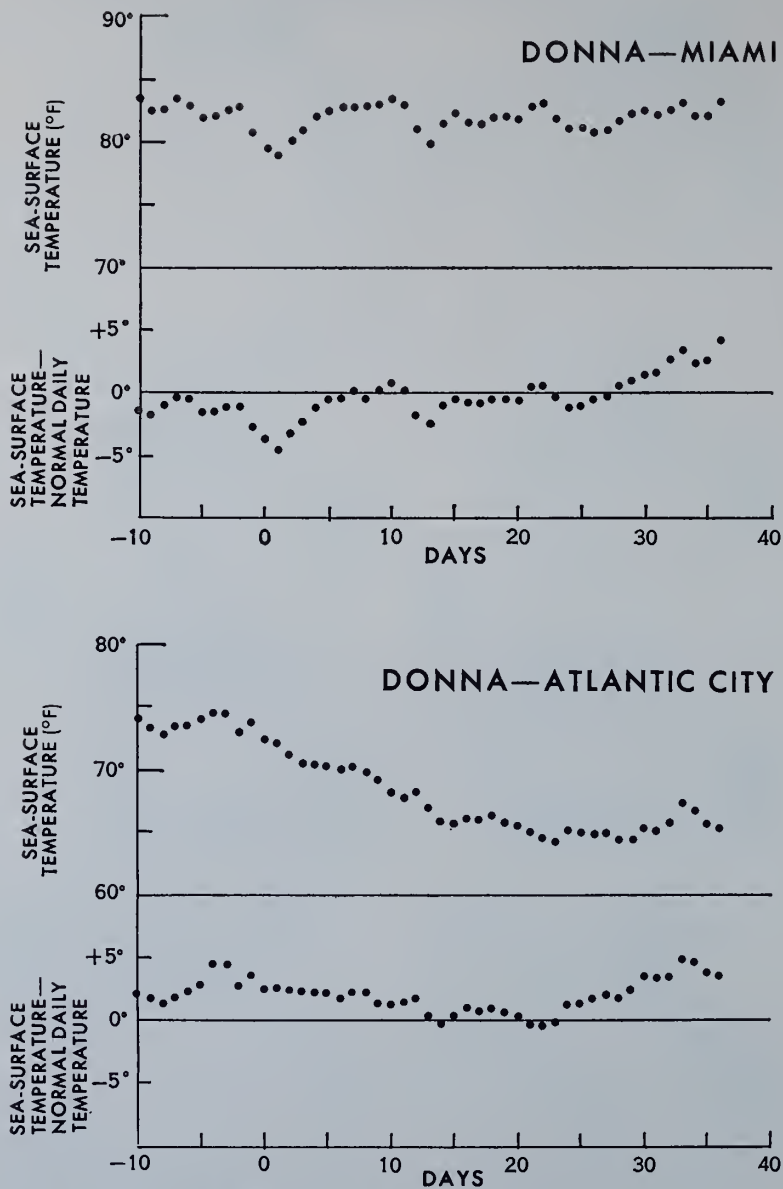


Fig. 4. Mean daily sea-surface temperature and difference between daily sea-surface temperature and normal sea-surface temperature, Donna-Miami and Donna-Atlantic City.

from the hurricane was then determined. Finally the number of days required for the water to return to the prehurricane variation from normal for the appropriate date was determined.

Having established the normal daily means for each station, it was a simple matter to compute the daily variation from the normal during each hurricane period. Prehurricane

temperature variations from normal were computed by averaging the daily variations for days $D - 10$ to $D - 3$ (10 to 3 days before the hurricane passed). Extreme variations from normal during the hurricane period ($D - 2$ to $D + 3$) were next computed. Finally, the number of days for the water to return to the prehurricane variation from normal conditions

was tabulated. The results are given in Table 4. There was considerable difference in time required for the water temperature to return to prehurricane conditions from one hurricane to another. However, at the coastal and light-ship stations, water temperatures returned to prehurricane conditions within one month. In fact, the mean times were only 13 and 10 days, respectively. The return to prehurricane con-

ditions was not determined at the Nomad buoy, as only three cases were recorded. In one case prehurricane conditions were regained within 7 days. In the other two cases, although total recovery did not occur within one month, the major part of the variation had dissipated within 10 days. An insignificant correlation was found between the temperature variation from normal and the number of days it took the

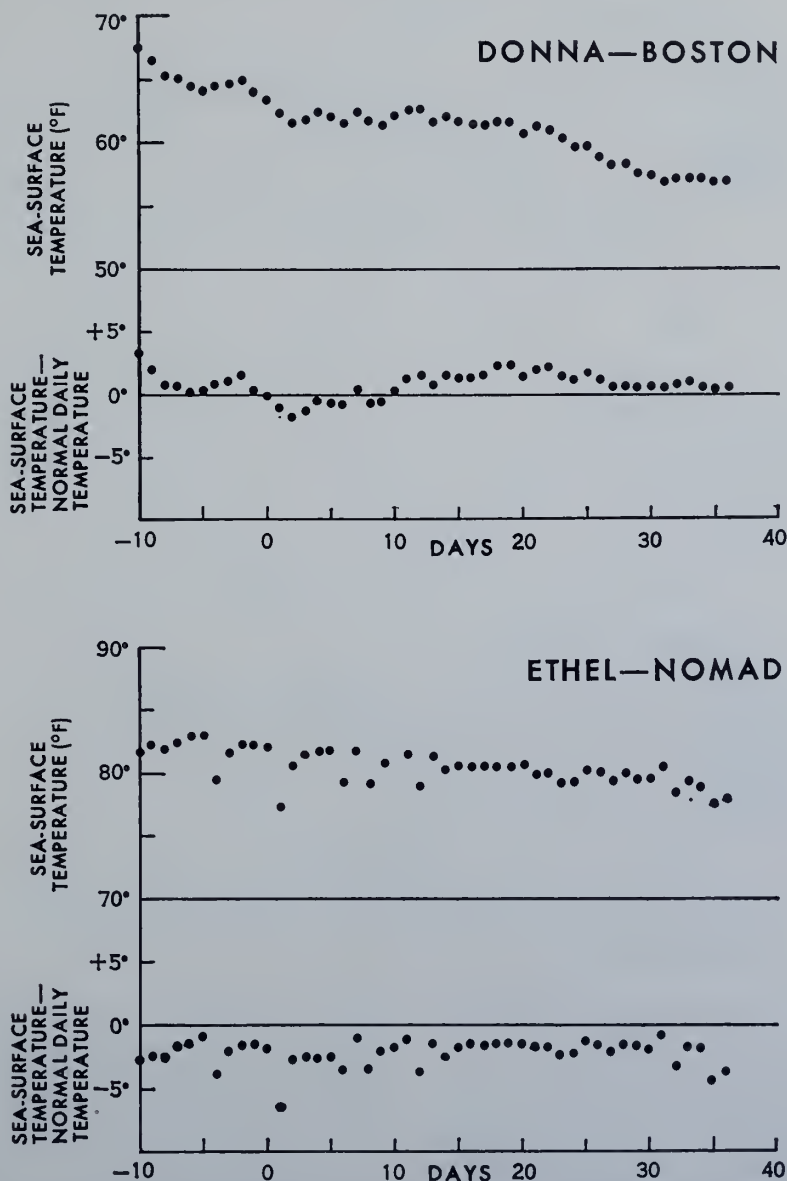


Fig. 5. Mean daily sea-surface temperature and difference between daily sea-surface temperature and normal sea-surface temperature, Donna-Boston and Ethel-Nomad.

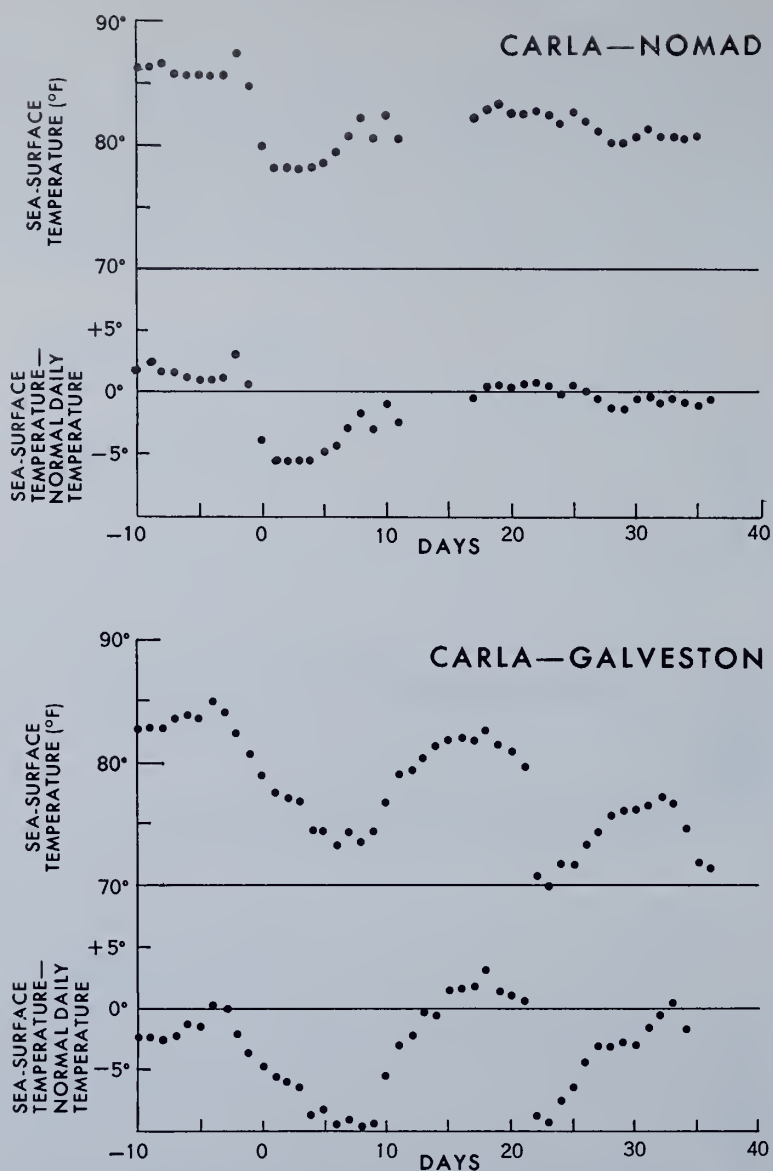


Fig. 6. Mean daily sea-surface temperature and difference between daily sea-surface temperature and normal sea-surface temperature, Carla-Nomad and Carla-Galveston.

temperature to return to normal (data from Table 4).

The lightship data given in Table 2 do not exhibit any consistent thermal structure variation pattern following the passage of hurricanes. As previously noted, in general, the sea-surface temperature is colder. If the colder water is the result of upwelling, then there should be a corresponding increase in salinity.

Also, the thermocline should be appreciably shallower. In only four cases did the salinity increase when the surface water became colder, and no examples were recorded where the thermocline became shallower. Therefore, it would appear that upwelling was not a principal process affecting lower surface temperatures.

Conversely, if the colder water resulted from turbulent mixing, the thermocline should be

found at greater depth (heat added at depth at the expense of the surface water). This phenomenon occurred at Barnegat, Ambrose, Five Fathom Bank, Diamond Shoals, Winter Quarter, and Chesapeake lightships following the passage of Donna.

Besides the redistribution of heat through the water column by vertical transport, heat

may be added to or removed from the water column. Rain may add cold water to the surface and thereby lower the average surface temperature. Also rain may tend to evaporate in the air above the sea and reduce the air temperature, thereby increasing conductive transfer of heat from the sea to the air. Reduced heat content was observed at Barnegat,

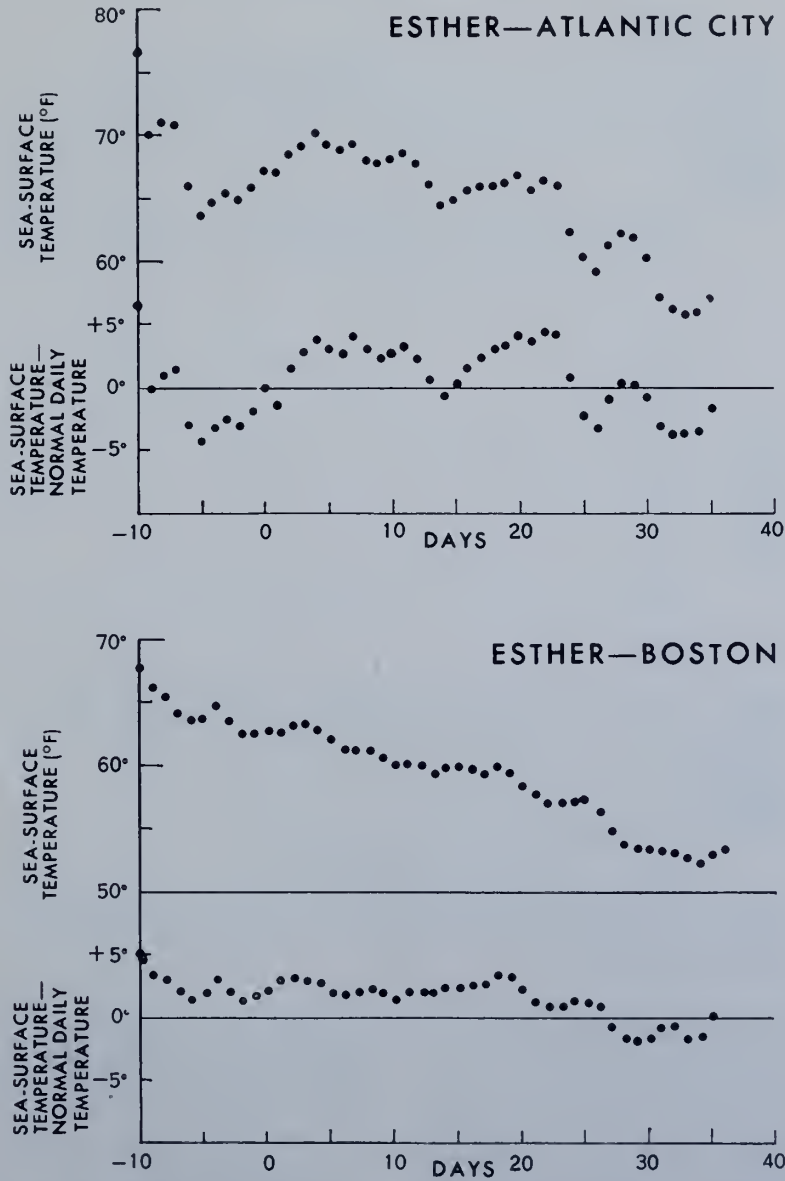


Fig. 7. Mean daily sea-surface temperature and difference between daily sea-surface temperature and normal sea-surface temperature, Esther-Atlantic City and Esther-Boston.

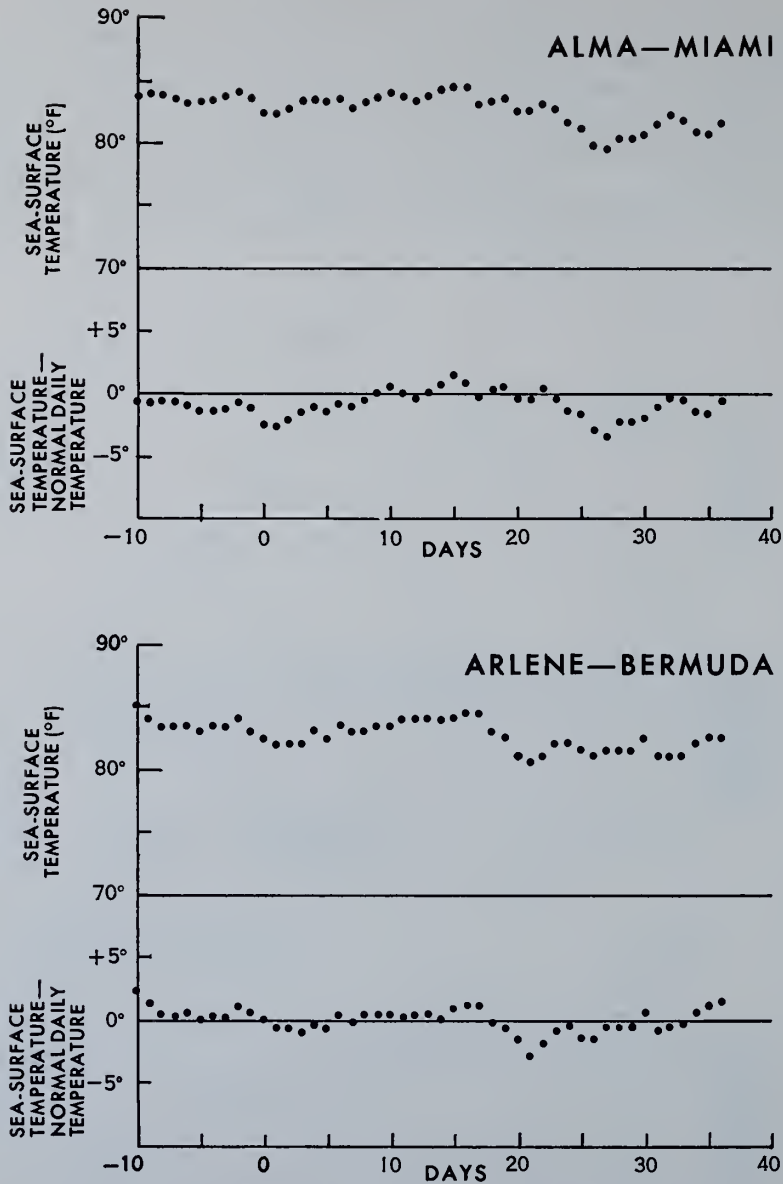


Fig. 8. Mean daily sea-surface temperature and difference between daily sea-surface temperature and normal sea-surface temperature, Alma-Miami and Arlene-Bermuda.

Ambrose, Diamond Shoals, Frying Pan Shoals, and Savannah lightships following the passage of Donna, and at Frying Pan Shoals and Diamond Shoals lightships following the passage of Isbell. The addition of heat to the water column is suggestive of horizontal advection. Higher heat content was observed at Portland, Boston, Chesapeake, and Five Fathom light-

ships following the passage of Donna and at Portland and Boston lightships following the passage of Esther.

CONCLUDING REMARKS

The observations given in the preceding sections raise some interesting points. Undoubtedly the passage of tropical storms over water

often does cause a sharp drop in water temperature. However, occasionally a temperature rise is recorded, apparently due to horizontal advection. The transfer of energy between the water and the air is a complex one.

The physical processes that cause surface cooling have been summarized by *Jordan and Frank* [1964]. They contend that surface

cooling during the passage of a hurricane due to horizontal advection, radiation losses, rain cooling, evaporative cooling, and sensible heat loss under typical open ocean conditions is limited to 1.3°F. Even though a somewhat higher value is given for extreme conditions, these processes apparently cannot account for the large recorded temperature variations at

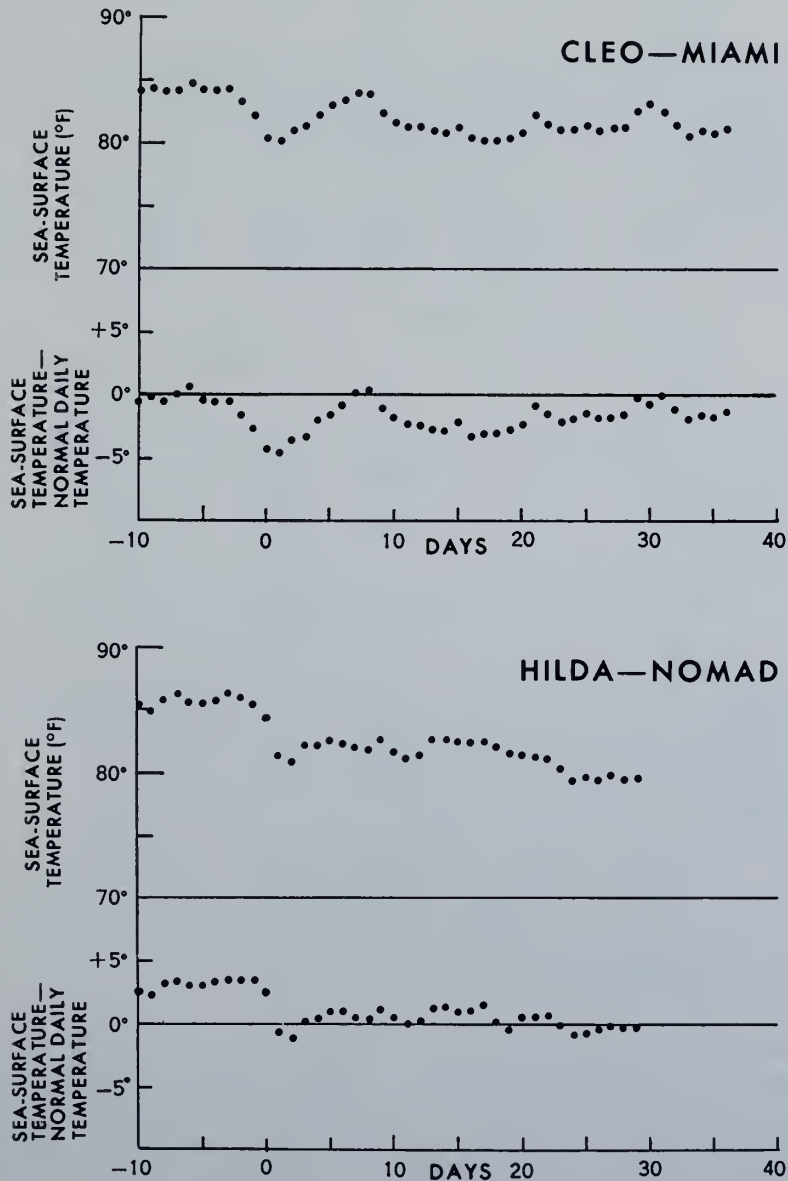


Fig. 9. Mean daily sea-surface temperature and difference between daily sea-surface temperature and normal sea-surface temperature, Cleo-Miami and Hilda-Nomad.

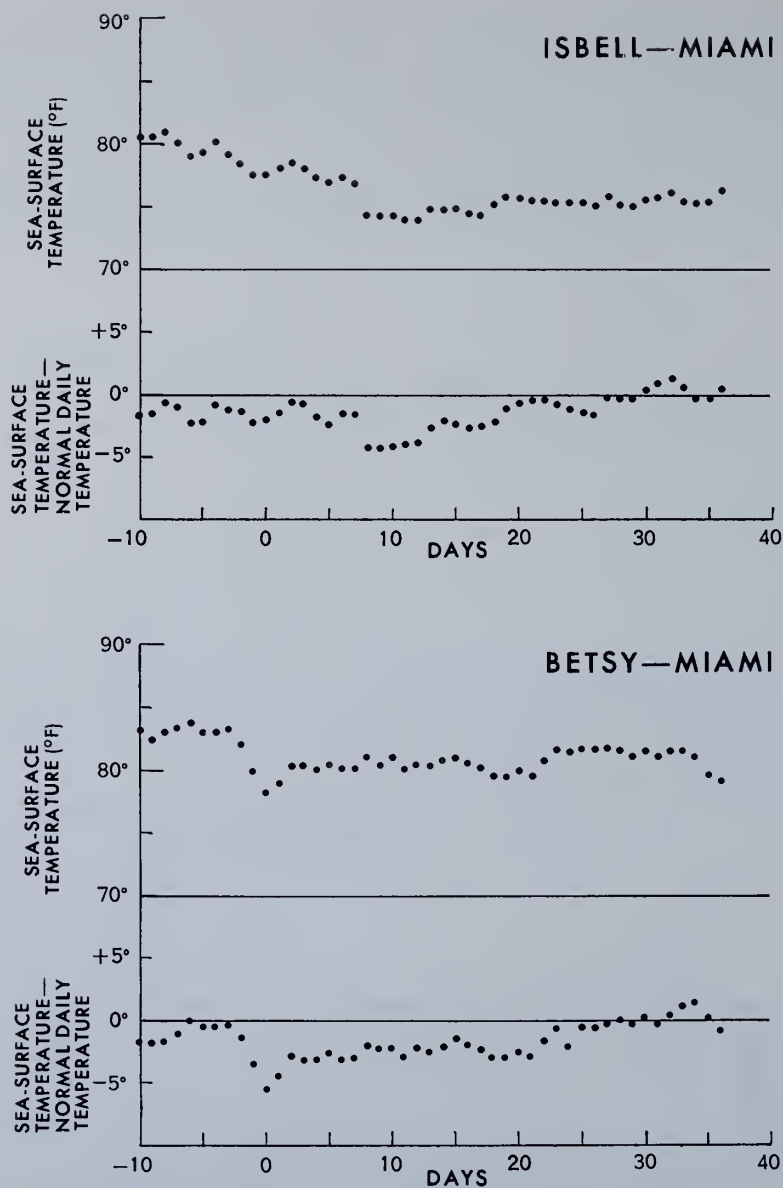


Fig. 10. Mean daily sea-surface temperature and difference between daily sea-surface temperature and normal sea-surface temperature, Isbell-Miami and Betsy-Miami.

the Nomad buoy, nor could they be expected to apply to nearshore areas. Nearshore at the coastal and lightship stations, where the surface temperature variation is somewhat less, these factors are limited by the water depth. Nearshore, turbulent mixing plus horizontal advection or evaporative and rain cooling plus mixing appear to be most important. Examples

of these processes occurred at the Barnegat and Ambrose lightships following the passage of Donna. The evidence is not conclusive, however, whether upwelling or turbulent mixing is more important in the open ocean.

Significant temperature increases were recorded at the Boston, Atlantic City, and Portland lightships following the passage of

TABLE 2. Water Temperature at Several Levels and Surface Salinity and Sigma-*t* Observations from the Lightship Stations

<i>Portland Lightship, Hurricane Donna, September 12, 1960</i>						
Date	Temperature				Salinity	Sigma- <i>t</i>
	0 m	9 m	15 m	30 m		
9/11/60	55.6	53.8	51.3	45.4	31.72	23.86
9/13/60	55.0	54.0	53.3	48.0	31.64	23.86
9/14/60	56.2	55.4	54.6	51.7	31.65	23.75
<i>Boston Lightship, Hurricane Donna, September 12, 1960</i>						
Date	Temperature				Salinity	Sigma- <i>t</i>
	0 m	9 m	15 m	29 m		
9/11/60	62.0	60.8	58.7	N.D.	31.31	22.77
9/13/60	62.2	61.4	59.3	49.2	31.59	22.97
9/14/60	60.1	60.0	59.8	N.D.	31.57	23.23
<i>Ambrose Lightship, Hurricane Donna, September 12, 1960</i>						
Date	Temperature			Salinity	Sigma- <i>t</i>	
	0 m	9 m	15 m			
9/11/60	72.1	71.8	62.9	30.71	20.91	
9/12/60	71.6	71.4	71.0	30.69	20.98	
9/13/60	68.3	67.6	67.2	29.41	20.48	
9/14/60	67.2	68.1	68.4	29.52	21.16	
<i>Winter Quarter Lightship, Hurricane Donna, September 12, 1960</i>						
Date	Temperature				Salinity	Sigma- <i>t</i>
	0 m	9 m	15 m	29 m		
9/9/60	76.0	75.4	71.0	56.5	29.82	20.38
9/14/60	70.2	70.4	70.1	55.0	30.04	21.24
<i>Chesapeake Lightship, Hurricane Donna, September 12, 1960</i>						
Date	Temperature				Salinity	Sigma- <i>t</i>
	0 m	9 m	15 m	20 m		
9/11/60	76.9	73.1	72.2	71.0	27.41	17.68
9/13/60	75.0	74.2	74.3	74.4	29.63	19.62
9/14/60	75.0	73.5	73.7	73.7	30.06	19.97
<i>Barnegat Lightship, Hurricane Donna, September 12, 1960</i>						
Date	Temperature				Salinity	Sigma- <i>t</i>
	0 m	9 m	15 m	26 m		
9/11/60	74.2	74.2	74.0	61.8	31.07	20.82
9/14/60	69.9	69.9	69.9	69.9	31.02	21.45

TABLE 2 (continued)

<i>Five Fathom Bank Lightship, Hurricane Donna, September 12, 1960</i>						
Date	Temperature				Salinity	Sigma-t
	0 m	9 m	15 m	26 m		
9/11/60	76.0	75.2	61.8	56.2	30.80	20.47
9/13/60	71.5	71.2	64.8	61.9	30.97	21.24
9/14/60	71.8	71.3	70.8	58.9	30.79	21.02

<i>Frying Pan Shoals Lightship, Hurricane Donna, September 11, 1960</i>						
Date	Temperature				Salinity	Sigma-t
	0 m	9 m	15 m	21 m		
9/10/60	81.0	81.7	81.9	81.9	36.11	23.50
9/13/60	80.8	80.7	80.8	80.6	35.56	23.13

<i>Diamond Shoals Lightship, Hurricane Donna, September 11, 1960</i>							
Date	Temperature					Salinity	Sigma-t
	0 m	9 m	15 m	30 m	46 m		
9/10/60	84.8	84.2	84.1	75.1	72.7	36.03	22.74
9/13/60	81.8	80.8	80.8	79.0	72.6	35.69	23.16
9/14/60	79.8	79.8	79.7	78.3	70.3	35.87	23.59

<i>Savannah Lightship, Hurricane Donna, September 11, 1960</i>						
Date	Temperature			Salinity	Sigma-t	
	0 m	9 m	15 m			
9/10/60	82.8	82.5	82.3	34.56	22.02	
9/12/60	81.5	82.0	82.0	32.60	20.78	
9/13/60	80.0	80.3	80.7	32.54	20.99	
9/14/60	82.0	82.0	82.0	33.98	21.72	

<i>Boston Lightship, Hurricane Esther, September 26, 1961</i>						
Date	Temperature				Salinity	Sigma-t
	0 m	9 m	15 m	29 m		
9/25/61	58.5	58.7	58.1	51.9	31.25	23.17
9/27/61	59.5	59.7	57.8	52.0	30.72	22.66
9/28/61	60.3	59.8	57.8	51.3	30.58	22.44

<i>Portland Lightship, Hurricane Esther, September 26, 1961</i>						
Date	Temperature				Salinity	Sigma-t
	0 m	9 m	15 m	30 m		
9/25/61	54.0	52.2	51.8	49.2	32.06	24.25
9/27/61	54.9	53.2	52.7	51.0	31.58	24.25
9/28/61	55.7	53.0	52.7	49.7	31.45	23.63

TABLE 2 (continued)

Date	<i>Frying Pan Shoals Lightship, Hurricane Isbell, October 16, 1964</i>					
	Temperature				Salinity	Sigma-t
	0 m	8 m	14 m	18 m	0 m	0 m
10/14/64	71.4	71.6	71.8	71.8	35.97	25.02
10/18/64	70.5	70.9	71.2	71.6	36.01	25.16

Date	<i>Diamond Shoals Lightship, Hurricane Isbell, October 16, 1964</i>						
	Temperature					Salinity	Sigma-t
	0 m	8 m	15 m	30 m	46 m	0 m	0 m
10/14/64	68.0	68.2	68.3	75.9	78.7	31.41	22.05
10/19/64	67.8	69.1	68.4	71.1	74.7	31.11	21.85

TABLE 3. Water Temperature Drop during 5-Day Hurricane Period* and Maximum Temperature Change within Five Days

Hurricane	Station	Temperature Decrease during Hurricane Period	Maximum Temperature Change within a 5-Day Period†
Donna (G)	Miami	3.8	3.6
Donna	Atlantic City	2.6	3.3
Donna	Boston	3.3	3.2
Donna	Portland Lightship	0.6	5.1
Donna	Boston Lightship	2.6	6.3
Donna	Ambrose Lightship	4.9	5.0
Donna	Barnegat Lightship	4.2	3.1
Donna	Five Fathom Lightship	4.5	3.8
Donna	Winter Quarter Lightship	No data	2.5
Donna	Chesapeake Lightship	2.6	3.3
Donna	Diamond Shoal Lightship	5.4	7.5
Donna (G)	Frying Pan Shoal Lightship	No data	2.0
Donna (G)	Savannah Lightship	3.0	2.6
Ethel	Nomad	4.8	3.2
Carla (G)	Nomad	9.3	4.0
Carla (G)	Galveston	7.7	12.7
Esther	Atlantic City	4.1	13.1
		(increase)	
Esther	Boston	0.8	4.1
		(increase)	
Esther	Portland Lightship	1.7	4.8
		(increase)	
Esther	Boston Lightship	1.6	7.9
Alma	Miami	1.8	3.6
Arlene	Bermuda	2.0	4.0
Cleo	Miami	3.2	2.6
Hilda	Nomad	5.0	2.1
Isbell	Miami	0.9	3.1
Isbell	Frying Pan Shoals Lightship	4.3	9.4
Isbell	Diamond Shoals Lightship	1.3	5.6
Betsy (G)	Miami	3.8	2.5
Mean	Coastal	3.1	5.1
Mean	Nomad	6.4	3.1
Mean	Lightships	3.1	4.9

* Period extends from 2 days before until 3 days after the hurricane passes.

† Within any 5-day period during rest of the tabulated days.

TABLE 4. Water Temperature Variation from Normal during Passage of Hurricane and Number of Days for Return to the Prehurricane Anomaly

Hurricane	Station	Prehurricane Temperature Anomaly, °F	Temperature Variation from Normal during Hurricane Period, °F	Number of Days to Prehurricane Temperature Anomaly
Donna	Miami	-1.1	-3.3	5
Donna	Atlantic City	+2.7	-0.3	30
Donna	Boston	+1.3	-2.9	11
Donna	Portland Lightship	-0.7	-1.3	2
Donna	Boston Lightship	+1.7	+1.1	11
Donna	Ambrose Lightship	+3.5	-0.8	5
Donna	Barnegat Lightship	+0.9	-0.9	4
Donna	Five Fathom Bank Lightship		Data incomplete	
Donna	Winter Quarter Lightship		Data incomplete	
Donna	Chesapeake Lightship	+1.0	0.0	8
Donna	Diamond Shoals Lightship	+4.0	+1.6	24
Donna	Frying Pan Shoals Lightship	+0.5	+0.1	19
Donna	Savannah Lightship	+0.6	-0.4	3
Ethel	Nomad	-2.1	-4.1	7
Carla	Nomad	+1.6	-7.3	>36
Carla	Galveston	-1.6	-7.9	13
Esther	Atlantic City	-2.8	+6.9	26
Esther	Boston	+2.3	-1.2	5
Esther	Portland Lightship	-1.1	-1.3	2
Esther	Boston Lightship	+1.1	+1.7	4
Alma	Miami	-1.0	-1.7	6
Arlene	Bermuda	+0.8	-1.7	15
Cleo	Miami	-0.3	-4.3	7
Hilda	Nomad	+3.2	-4.2	>30
Isbell	Miami	-1.4	-0.6	1
Isbell	Frying Pan Shoals Lightship	-3.1	-8.3	31
Isbell	Diamond Shoals Lightship	-3.3	-3.8	7
Betsy	Miami	-1.0	-4.6	23
Mean	(Coastal)			13
Mean	(Nomad)			>20
Mean	(Lightship)			10

hurricane Esther. At Atlantic City the water temperature dropped about 11°F within a 5-day period from 10 to 6 days before the hurricane passed. During this period the wind blew almost continuously from the south and southwest. Thus, it appears the warm water was driven offshore and replaced with colder water. Then for a period of 3 days before the hurricane until after the storm had passed the wind blew almost continuously from the northeast, possibly blowing back to Atlantic City the warmer water, somewhat cooled by the hurricane, that had been blown out several days earlier. It would appear that, at least on this occasion, horizontal advection and to a lesser extent other mechanisms for surface

cooling played significant roles in causing the observed water temperature variation.

A study of Table 2 and Figures 4 through 10 indicates that water temperature variations due to hurricanes are rapidly modified by subsequent environmental events. In most cases water temperature anomalies due to a hurricane are either completely destroyed or greatly modified within a week or two.

Synoptic data on the surface and subsurface thermal structure near a hurricane both before the storm passes and soon afterward are necessary to answer the questions concerning upwelling, mixing, and surface cooling. As pointed out by *McFadden* [1967], the only apparent way of obtaining these data appears

to be by using a research aircraft equipped with an airborne radiation thermometer and an expendable bathythermograph system. For example, such data could be used to check out the theory on upwelling and mixing developed and discussed by O'Brien and Reid [1967] and O'Brien [1967].

Acknowledgments. I greatly appreciate the assistance given in the compilation of the tables and figures by Ruth Payne, Lewis Pierce, and Sidney Marcus. I also wish to thank Robert Starr, Dale Leipper, Donald Hansen, James McFadden, and D. Lee Harris for their helpful suggestions during the preparation of this paper.

REFERENCES

- Chase, J., Oceanographic observations, 1961 east coast of the United States, *U.S. Fish and Wildlife Service, Data Rept. 1*, 176 pp., Washington, D. C., 1964.
- Chase, J., Oceanographic observations, 1964 east coast of the United States, *U.S. Fish and Wildlife Service, Data Rept. 18*, 181 pp., Washington, D. C., 1967.
- Day, C. G., Oceanographic observations, 1960 east coast of the United States, *U.S. Fish and Wildlife Service, Spec. Sci. Rept., Fisheries 406*, p. 59, Washington, D. C., 1963.
- Fisher, E. L., Hurricanes and the sea-surface temperature field, *J. Meteorol.*, *15*, 328-333, 1958.
- Jordan, C. L., Evidence of surface cooling due to typhoons, *Proc. Sea-Air Interaction Conf. Tallahassee, Florida, Feb. 23-25, 1965*, edited by J. Sparkman, pp. 185-190, *U.S. Dept. of Commerce Tech. Note 9-SAIL-1*, 1965.
- Jordan, C. L., and N. L. Frank, On the influence of tropical cyclones on the sea-surface temperature field, pp. 1-31, Florida State University, Tallahassee, Florida, 1964.
- Kraft, R. H., Great hurricanes, 1955-1965, *Mariners Weather Log*, *19*(6), 200-202, 1966.
- Leipper, D. F., The Gulf of Mexico after Hilda (Preliminary Results), *Proc. Sea-Air Interaction Conf. Tallahassee, Florida, Feb. 23-25, 1965*, edited by J. Sparkman, 163-183, *U.S. Dept. of Commerce Tech. Note 9-SAIL-1*, 1965.
- Marcus, S. O., Jr., Evaluation of Nomad 1 data for oceanographic and meteorological applications, Marine Technology Society, *Trans. Buoy Tech. Symp. 24-25 March 1964*, 311-333, 1964.
- McFadden, J. O., Sea-surface temperatures in the wake of hurricane Betsy (1965), *Monthly Weather Rev.*, *95*(5), 299-302, 1967.
- O'Brien, J. J., The nonlinear response of a two-layer, baroclinic ocean to a stationary, axially-symmetric hurricane, 2, Upwelling and mixing induced by momentum transfer, *J. Atmospheric Sci.*, *24*, 208-215, 1967.
- O'Brien, J. J., and R. O. Reid, The nonlinear response of a two-layer, baroclinic ocean to a stationary, axially-symmetric hurricane, 1, Upwelling induced by momentum transfer, *J. Atmospheric Sci.*, *24*, 197-207, 1967.
- Stevenson, R. E., and R. S. Armstrong, The modification of water temperature by hurricane Carla, *Proc. Sea-Air Interaction Conf., Tallahassee, Florida, Feb. 24-25, 1965*, edited by J. Sparkman, 191-208, *U.S. Dept. of Commerce Tech. Note 9-SAIL-1*, 1965.
- Uda, M., On the variation of water temperature due to the passage of typhoon, *Misc. Papers No. 6, Tokyo University of Fisheries*, 297-298, 1954.

(Received January 8, 1968;
revised April 10, 1968.)



RESOURCES / REVIEWS

Prepared by

The NSTA Science Teaching Materials Review Committee
 Chairman, Marjorie H. Gardner
 Associate Chairman, Charles J. La Rue
 The University of Maryland, College Park

* Book Reviews

Riches of the Sea; The New Science of Oceanology. Norman Carlisle. 128pp. \$3.95. Sterling Publishing Co., Inc., 419 Park Ave. South, New York 10016. 1967.

A brief "motherhood" statement on the vast economic potential of the ocean has been a common denominator among recent publications in oceanography. Carlisle has met the need for an introductory work summarizing the prospects and current activities directed to their realization without belaboring the complexity of, and impediments to operation in, the marine environment. The book also departs from others by including considerably more of what private industry and governmental oceanographers have been thinking about in recent years than has been the rule.

Ten chapters are devoted to developments in the tools and technology required to enable man to live and work effectively in and under the sea and aspirations and accomplishments relating to obtaining more food from the sea, undersea mining and oil drilling, obtaining fresh water and minerals from seawater, tidal and ocean thermal generation of electric power, environmental prediction and control, and exploration. The book is so well illustrated—averaging nearly three pictures per double page including a color section—as to interest many elementary pupils, yet so broad and up to date that few professional oceanographers will find nothing new. Such information is, however, highly perishable in this rapidly developing field. Some coverage, like the discussion of the Mohole project, is already out of date—a fair price for the relevance delivered. During its limited lifetime, this book is highly recommended for the science shelf, particularly for schools having a course in earth science.

Donald V. Hansen
 Research Oceanographer
 Institute for Oceanography, ESSA

Reprinted from THE GEOPHYSICAL JOURNAL OF THE ROYAL ASTRONOMICAL SOCIETY

Electric and Magnetic Fields Induced by Deep Sea Tides

J. C. Larsen

(Received 1967 November 29)

Summary

A lunar semidiurnal variation (12·4206 h period) induced by tides in the deep ocean is demonstrated in (i) a month's observations of the horizontal electric field and magnetic declination at a sea floor site located 600 km off the California coast in 4·4 km of water, in (ii) a month's observations of the vertical magnetic field at a coastal site near Cambria, California, and in (iii) two years' observations of the vertical magnetic field at the island magnetic observatory on San Miguel, Azores. Comparison of the sea floor, coastal, and island observations with simultaneous continental magnetic observations permits an estimation of that part of the variation due to a lunar ionospheric oscillation.

The observed oceanic induced variation at the sea floor and coastal sites are found to agree well with tidal induced fields computed for a model of the Earth's electrical conductivity and lunar semidiurnal tide. The model assumes (i) a flat semi-infinite ocean of uniform depth and conductivity, rotating at a uniform rate appropriate to the latitude of interest, (ii) non-conducting atmosphere, continent and upper mantle, and (iii) superconducting mantle at a uniform depth beneath the ocean.

The observed oceanic induced vertical magnetic field at San Miguel is found to agree qualitatively with tidal induced fields computed for an island model. This model assumes (i) a uniformly conducting small circular island, (ii) a flat infinite ocean of uniform depth and conductivity, rotating at a uniform rate appropriate to the latitude of interest, (iii) a non-conducting atmosphere and upper mantle, and (iv) a superconducting mantle at a depth much greater than the size of the island.

Introduction

Electromagnetic variations induced by oceanic tides depend on the distribution of tidal currents and on the distribution of electrical conductivity beneath the ocean. If either were known perfectly, the measurements would serve to give some precise information of the other. The actual situation is that very little is known of either deep sea tides or conductivity beneath the ocean and the approach here must be to check the consistency of the observed variations with *reasonable* models.

The first part of this study contains a discussion of tidal induced electromagnetic fields in the ocean off California. Observations of electromagnetic field variations at a sea floor and coastal site are shown to contain a lunar semidiurnal periodicity due predominantly to an oceanic source. Tidal induced fields, computed for a model of the Earth's electrical conductivity and lunar tide along

California, agree well with the observed fields. The second part contains a discussion of tidal induced magnetic fields at island stations. Magnetic hourly data from the island stations, Honolulu, Hawaii and San Miguel, Azores are analysed to determine whether a lunar semidiurnal tidal induced field is present. Computed oceanic tidal induced fields based on an island model are shown to be qualitatively consistent with the observations.

Previous investigations. Lunar magnetic variations have been observed and discussed since the 1850's. A review of contributions is included in Chapman (1919), Chapman & Bartels (1940) and Matsushita & Maeda (1965). Most investigators have concentrated their efforts on explaining magnetic lunar variations which are caused entirely by an external source such as tidal motion in the ionosphere. An exception was van Bemmelen (1912, 1913) who separated the lunar magnetic variations into an internal and external part and thought that some of the internal part might be due to tidal motion in the ocean. Chapman (1919), however, disagreed and believed that he had demonstrated that the internal part was due merely to an external source. Evidence that oceanic tidal induced magnetic variations are detectable is suggested by a lunar frequency analysis of the coastal magnetic variations at Amberley, New Zealand (Bullen & Cummack 1953). Their computations showed a relatively large lunar semidiurnal vertical component with slight seasonal dependency whereas the horizontal components in contrast showed a much stronger seasonal dependency. It seems likely that oceanic tidal motion caused the lunar semidiurnal variations in the vertical component for otherwise its seasonal change should follow closely the seasonal change of the horizontal components of the lunar semidiurnal variations. This conclusion is consistent with the fact that oceanic tidal induced magnetic variations should show practically no seasonal dependency. From a comparison with the solar daily variation, Egedal (1956) has suggested that the Amberley lunar vertical component ' . . . may be due to sea electric currents produced by local oceanic currents, the speed of which contains a lunar-diurnal term '.

The electric field in the ocean, on the other hand, has been suspected since the days of Faraday of having a part clearly induced by oceanic tidal motion. Observations that first showed evidence of oceanic tidal induced electric fields were made in the 1850's using submarine telegraph cables. Longuet-Higgins (1949) treated theoretically the case appropriate for the English Channel where effects of time variations of the induced magnetic field can be ignored. These effects, however, become important for tidal induced fields in the open ocean and are included in the present study. Stommel (1954) has investigated the potential differences between widely separated stations in the Atlantic using submarine telegraph cable. He found rather poor agreement between the theoretical tidal currents and the lunar semidiurnal electric fields which he attributed to the poor knowledge of tidal motion in the open ocean. He took for the electric field $\mathbf{E} = -\mathbf{u} \wedge \mathbf{F}$ where \mathbf{u} is the horizontal water motion and \mathbf{F} is the geomagnetic field. Thus the poor fit may be due to his neglect of electric currents which are associated with time variations of the magnetic field. Finally, observations of potential differences between widely separated stations in the Pacific have been made by Runcorn (1964) using submarine telegraph cables. He showed that the times of high and low water of a nearby tide station agreed with the times of high and low values of the potential differences.

1. Tidal induced fields at sea floor and coastal sites

1.1 Sea floor and coastal electromagnetic observations

Observations. Measurements of the horizontal electric field and east component of the magnetic field on the deep sea floor at a site 600 km off the California coast (32° 46' N, 127° 07' W, at 4.4 km depth) and the three components of the magnetic

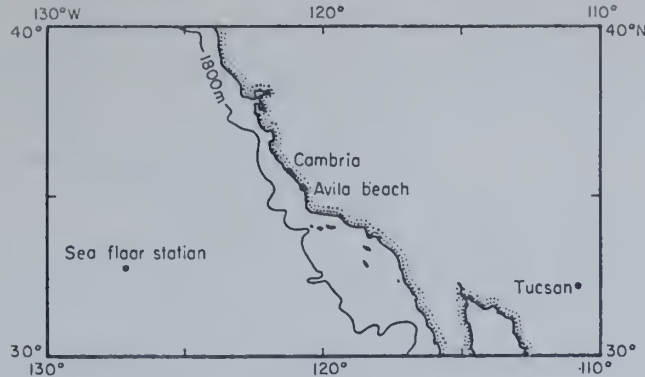


FIG. 1. Location of stations.

field at Cambria on the California coast ($35^{\circ} 36' N$, $121^{\circ} 06' W$), see Fig. 1, were analysed to determine whether tidal induced fields could be detected. A comparison with simultaneous observed magnetic fields at Tucson, Arizona ($32^{\circ} 15' N$, $110^{\circ} 50' W$, about 500 km from the coast) permits an estimate of that part of the field due to an ionospheric source. A comparison was also made with the tidal observations at Avila Beach, California. Table 1 lists the observed components, azimuths and times.

The magnetic variations at Cambria were recorded by a portable Askania variograph with about one gamma resolution. Magnetic variations on the sea floor were recorded by a newly developed magnetometer (Filloux 1967) that registered ΔD (azimuth $106^{\circ} T$ for this location) with one gamma resolution. T indicates true azimuth measured clockwise with respect to geographic north and $10^9 \gamma = 1 \text{ Wb/m}^2$, $\gamma = \text{gamma}$. Readings were made every 2.5 min. The components of the magnetic variation are: ΔD (horizontal, positive magnetic east variation), ΔH (horizontal, positive magnetic north variation), and ΔZ (vertical, positive down variation).

Horizontal electric field observations on the sea floor, designated ΔE_A and ΔE_B , were made by two separate instruments which recorded the potential difference between pairs of Ag-AgCl electrodes spaced one kilometre apart in a known direction. Azimuth for ΔE_A was $199^{\circ} T$, and for ΔE_B , $159^{\circ} T$. Readings were made every

Table 1

Horizontal electric field			
Station	Component	Azimuth*	Time (1965)
Sea floor	ΔE_A	$199 \pm 2^{\circ} T$	3/18-4/10
Sea floor	ΔE_B	$159 \pm 5^{\circ} T$	3/17-4/02
Magnetic field			
Station	Component	Azimuth*	Time (1965)
Sea floor	ΔD	$106^{\circ} T \dagger$	4/28-5/23
Tucson	ΔD	$103^{\circ} T \dagger$	4/28-5/23
Tucson	ΔH	$13^{\circ} T \dagger$	4/28-5/23
Cambria	ΔD	$105^{\circ} T \dagger$	3/18-4/10
Cambria	ΔH	$15^{\circ} T \dagger$	3/18-4/10
Cambria	ΔZ	Down	3/17-4/09
Tucson	ΔD	$103^{\circ} T \dagger$	3/18-4/10
Tucson	ΔH	$13^{\circ} T \dagger$	3/18-4/10
Tucson	ΔZ	Down	3/17-4/09

* T indicates true azimuth measured clockwise with respect to geographic north.

† Azimuths of Earth's steady magnetic field.



FIG. 2. Fortnightly examples of observations (U.T. 1965) from stations at sea floor, Cambria and Tucson.

2.5 min with approximately 0.05 mV/km resolution. The method of electric field measurements is described by Filloux & Cox (1967).

The records were digitized at 10 min intervals except for sea floor ΔD which was digitized at 12 min intervals. Two slight adjustments of the observations were made. Cambria ΔZ was corrected for a small linear drift due to an instrumental drift and sea floor ΔE_B was corrected for a monotonically increasing drift due to a gradually worsening leak in the insulation of the electrode wire. Fortnightly examples of the observations are plotted in Fig. 2.

Harmonic analysis. The spectral lines corresponding to harmonics of the solar daily variation of 24, 12, 8 and 6 h periods (designated S_1 , S_2 , S_3 and S_4) and the principal lunar semidiurnal variation of 12.4206 hour period (designated M_2) were determined by a least squares fit (Larsen 1966). After removing the above periodicities from each record, the harmonic coefficients of the background were determined. Figs 3 and 4 present the harmonic amplitudes of the spectral lines and the background for the components and stations listed in Table 1. The M_2 amplitudes and phases and \mathcal{R} (the estimate of the rms amplitude of the background) are listed in Table 2. \mathcal{R} is determined from the nearest ten harmonic amplitudes of the background about the spectral line. According to Fisher (1929), there is a 1 in 20 chance that a single frequency estimate of a Gaussian noise will exceed 2.1 times the estimate \mathcal{R} . It is evident from Table 2 that the M_2 amplitudes for sea floor ΔD , ΔE_A and ΔE_B and Cambria ΔZ , are well above the 5 per cent level. This establishes the presence of the M_2 periodicity. The M_2 periodicity, if present in the other observed components, is lost in the background.

For a Gaussian background, there is a 63 per cent chance that a frequency estimate plotted on a harmonic dial will lie within a circle of error having a radius equal to the r.m.s. amplitude. Then \mathcal{R} is an estimate of the uncertainty (with the above probability) associated with the estimates of the amplitude and phase of the periodic signal. The M_2 amplitude for sea floor ΔD is thus 2.4 ± 0.8 gammas and for Cambria ΔZ , 1.6 ± 0.4 gammas. The electric field measured along two horizontal

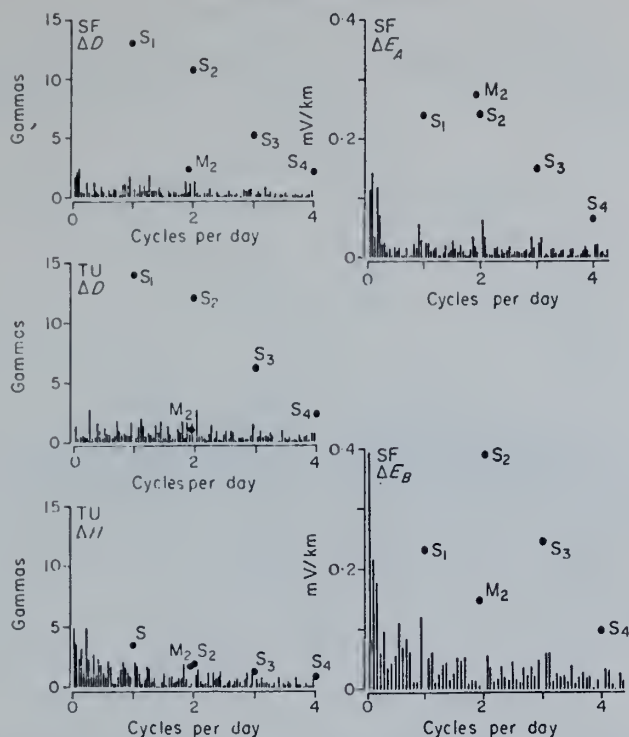


FIG. 3. Harmonic amplitudes for various components at sea floor site and Tucson. The dots are the amplitudes of the signal at the exact periods 24, 12, 8, 6 and 12·4206 h which are labelled respectively S_1 , S_2 , S_3 , S_4 and M_2 . The vertical bars are harmonic amplitudes of the background after the above periodicities have been removed from the record. These analyses are for the first five entries in Table 1.

Table 2

Lunar M_2 variation $A \cos(\omega t + \theta)$ and r.m.s. amplitude \mathcal{R} . Phases refer to zero hour, 1965 January 1 U.T.

Station	Horizontal electric field			\mathcal{R} (mV/km)
	Component	A (mV/km)	θ^* (°)	
Sea floor 3/18-4/10	ΔE_A	0·27	85	0·03
Sea floor 3/17-4/02	ΔE_B	0·15	270	0·03
Station	Magnetic field			\mathcal{R} (γ)
	Component	A (γ)	θ^* (°)	
Sea floor 4/28-5/23	ΔD	2·4	226	0·8
Tucson 4/28-5/23	ΔD	1·1†	346	1·3
Tucson 4/28-5/23	ΔH	1·7†	56	1·0
Cambria 3/18-4/10	ΔD	0·8†	256	0·9
Cambria 3/18-4/10	ΔH	2·1†	36	1·2
Cambria 3/17-4/09	ΔZ	1·6	210	0·4
Tucson 3/18-4/10	ΔD	0·9†	296	0·9
Tucson 3/18-4/10	ΔH	1·7†	35	1·1
Tucson 3/17-4/09	ΔZ	0·5†	194	0·5

* Add 2 times west longitude of station $-45\cdot2^\circ$ to convert to local mean lunar time (Bartels & Fanslau 1937).

† Not significant.

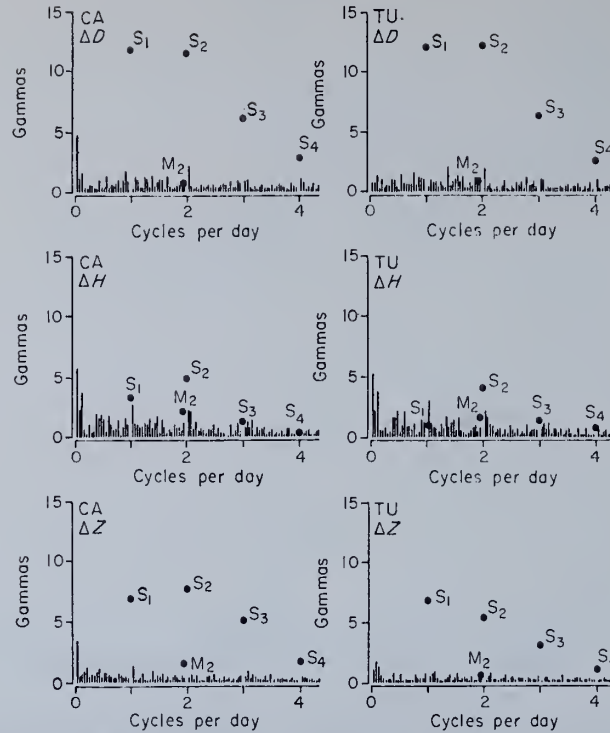


FIG. 4. Harmonic amplitudes of various components at Cambria and Tucson. See legend for Fig. 3. These analyses are for the last six entries in Table 1.

directions allows a computation of the hodograph of the M_2 oscillations. The ratio of major to minor axis is found to be $70:1$. The horizontal M_2 electric field is therefore essentially linearly polarized in the direction $83 \pm 6^\circ T$, a direction skew to the trend ($148^\circ T$) of the 1800 metre isobath off the California coast. The amplitude is 0.62 ± 0.10 mV/km.

Discussion of results. The sea floor observations have been previously discussed (Larsen & Cox 1966). The main conclusion was that the M_2 periodicity in the sea floor electromagnetic fields was due predominantly to an oceanic source and not to an ionospheric source. If the converse were true, the ratios of M_2 to both the r.m.s. background amplitude and amplitudes of the solar daily variation, which are due predominantly to an ionospheric source, would be nearly the same as Tucson and the sea floor site. The same type of reasoning also implies a predominantly oceanic source for the M_2 periodicity in ΔZ at the coastal station, Cambria.

1.2 Model of barotropic ocean tide

Tidal motions in the open ocean are essentially unknown. Therefore, in order to compare the observed tidal induced fields with coastal tide observations, we adopt a free wave model of the tide, consistent with the hydrodynamic equations. The model assumes a flat ocean of uniform depth h , rotating at a uniform rate appropriate to the latitude of interest. Solutions of the hydrodynamic equations can then be found that make it possible to solve the electromagnetic problem. Here the Kelvin wave solution is described and compared with the observed lunar M_2 tide along western North America. We choose throughout a right-handed coordinate system (x, y, z) with unit vectors \hat{i} northerly and parallel to the coast, \hat{j} westerly and \hat{k} up and with the ocean confined to the space

$$(-\infty \leq x \leq \infty, 0 \leq y \leq \infty, -\frac{1}{2}h \leq z \leq \frac{1}{2}h).$$

Hydrodynamic equations. The linearized equations of motion for free barotropic water waves (Lamb 1945) are

$$\frac{\partial u_x}{\partial t} - fu_y = -g \frac{\partial \zeta}{\partial x}$$

and

$$\frac{\partial u_y}{\partial t} + fu_x = -g \frac{\partial \zeta}{\partial y}$$

and the continuity equation is

$$\frac{\partial \zeta}{\partial t} = -\frac{\partial}{\partial x} (hu_x) - \frac{\partial}{\partial y} (hu_y),$$

where u_x and u_y are the horizontal particle velocities in the directions x and y respectively, ζ is the wave height and f is the Coriolis parameter assumed constant.

Kelvin wave solution. The Kelvin wave solution (Lamb 1945) is

$$\zeta = Ae^{-(f/\omega)ky} e^{i(kx - \omega t)},$$

$$u_x = \left(\frac{\omega A}{kh}\right) e^{-(f/\omega)ky} e^{i(kx - \omega t)},$$

and

$$u_y = 0,$$

where $i = (-1)^{\frac{1}{2}}$, k is the longshore wave number, ω the frequency, and $\omega/k = (gh)^{\frac{1}{2}} > 0$. For the northern hemisphere these waves propagate only in the positive x direction. One sees that the particle motion is always parallel to the coastline and dies away exponentially from the coast. Also, the vertical motion at the surface compared with the horizontal motion is $-ikh$ so that the vertical motion, for low frequencies, can be ignored.

Comparison of Kelvin wave with lunar tidal observations along western North America. The M_2 tidal amplitudes and phases for exposed coastal tide stations along western North America are given in Fig. 5. The values are plotted as a function of distance south from Vancouver, B. C. From the 6th point (San Francisco) to the 14th point (central Baja California) the M_2 amplitude is nearly constant at 0.50 m and the phase changes almost uniformly as the tide sweeps northward along the coast. The magnitude and direction of the longshore phase velocity is consistent

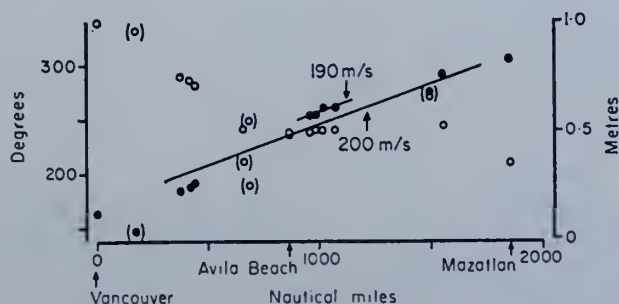


FIG. 5. Lunar M_2 tide along western North America as a function of distance south from Vancouver, along the rumb line, $148^\circ T$, parallel to the central California coast. Open circles are amplitudes and solid circles are phase leads relative to zero hour, 1965 January 1 U.T. Stations near entrances of bays are in parenthesis. Longshore phase velocity noted in metres per second.

with that predicted (200 m/s) by the Kelvin wave solution for an ocean depth of approximately 4 km. The overall fit seems reasonably good and suggests that the Kelvin wave solution may be used as a model of the M_2 tide along the California coast. Of course there is no guarantee that the actual M_2 tide decreases exponentially from the coast as a Kelvin wave would. Comparison of the observed with the computed oceanic tidal induced electromagnetic fields in a later section suggest, however, that the M_2 tide does decrease offshore.

Effects of bottom topography. It may be conjectured that bottom topography offshore might radically change the nature of the Kelvin wave solutions. Theoretical studies of the effect of a single step topography (Larsen 1966) show, however, that the shelf region off central California could change the Kelvin wave solution (amplitude, phase and particle velocity) by only a few per cent.

The effects of the borderland region off the southern California coast on the Kelvin wave solutions were also computed. One effect is to slow the Kelvin wave down by 5 per cent (190 m/s). Another effect is to cause the water particles at the outer edge of the borderland region to move counter-clockwise about ellipses with 1:6 axis ratio and major axis parallel to the coast. These results are consistent with bottom current measurements just beyond the borderland region (Isaacs *et al.* 1966). Their measurements at most sites gave semidiurnal tidal currents of several cm/s magnitude for which the water particles moved counterclockwise about ellipses with major axes parallel to the trend of the coast. The axis ratios ranged from 1:2 to 1:6. There is a possibility, however, that the current measurements also contained internal wave motion of tidal frequency which confuse the interpretation.

1.3 Model of Earth's electrical conductivity

Previous investigations indicate that the principal conducting elements of the Earth are: (i) an ionosphere about one hundred kilometres above the Earth's surface, (ii) an ocean with a layer of conducting bottom sediments, and (iii) a conducting mantle at a depth of a few hundreds of kilometres. Table 3 summarizes the information about the Earth's electrical conductivity. The model adopted here, appropriate for tidal induced fields, has the following features: (i) an ocean represented by a flat sheet of uniform conductivity σ and thickness h which can be treated as a thin conducting sheet because the skin depth, $d = (\frac{1}{2}\mu\omega\sigma)^{-\frac{1}{2}} \sim 60$ km, and tidal wave number, $k \sim 10^{-3}$ km $^{-1}$, are such that $h \ll d$ and $kh \ll 1$, (ii) a negligible ionospheric and bottom sediment conductivity since their integrated conductivity is much less than that of the ocean, (iii) a non-conducting atmosphere, crust and upper mantle and (iv) a superconducting mantle at a depth H_a . Thus, given the tidal motion, it is now possible to determine the solutions for the tidal induced electromagnetic fields.

Solutions for the induced fields in an infinite sheet spaced H_a above a superconducting mantle are found to be nearly equivalent to solutions for a sheet above a

Table 3

Material	Height or depth (km)	Electrical conductivity		References
		σ (Ω^{-1}/m)	$\int \sigma dz$ (Ω^{-1})	
Ionosphere	90-140	$< 10^{-3}$	10-50	Data: Chapman (1956) Formula: Ratcliffe & Weekes (1960) Gish (1951)
Atmosphere	0-20	$10^{-14}-10^{-12}$		
Ocean	0-4.4	4.6-3.0	1.43×10^4	Data: SIO-CCOFI 6304 Table: Horne & Frysinger (1963)
Bottom sediments	4.4-5.4	~ 1.4	$\sim 1.4 \times 10^3$	Cox, personal communication
Crustal rocks	1	$< 10^{-3}$		Watt <i>et al.</i> (1963)
Continental mantle	80	0.03		Cantwell & Madden (1960)
Oceanic mantle	30	0.4		Filloux (1967)

finite conducting σ_m mantle at a depth H_m with $H_a = H_m + (\mu\omega\sigma_m)^{-1/2}$ provided $\mu\omega\sigma_m \gg k^2$ (Larsen 1966). For M_2 frequencies, the Cantwell-Madden estimates of continental mantle conductivity and depth give a value $H_a = 514$ km and the Filloux estimates of oceanic mantle conductivity and depth give a value $H_a = 149$ km. The advantage of a model having a superconducting mantle is that the boundary condition along the superconducting boundary can be easily satisfied by negative image currents at a depth $2H_a$.

The agreement of the model with the real world probably is limited most by the assumption that the conductivity within the Earth is uniformly stratified and the assumption of an abrupt ocean-continental conductivity transition. Neglect of sphericity will also introduce errors but it can be shown that sphericity effects will be less than 10 per cent for electric and magnetic fields if $H_a/R < 0.1$ and $kR < 5$ where R is the Earth's radius and k the horizontal wave number. For the semidiurnal tide we estimate $kR \sim 4.5$. Finally, electromagnetic induction of distant ocean tides should be negligible at the region of interest because of the shielding effect of the highly conducting mantle.

1.4 Tidal induced electric and magnetic fields

The observed M_2 electromagnetic fields of oceanic origin will be shown here to be reasonably consistent with the computed tidal induced fields based on the models. Included is a discussion of the governing electromagnetic equations appropriate for the models, a discussion of the solutions, and a comparison of the computed and observed fields.

Governing equations. The phase velocity ω/k of barotropic tidal motion in the ocean is negligibly small compared with c , the speed of light. Therefore displacement currents can be ignored for tidal-induced fields and Maxwell's equations (Feynman, Leighton & Sands 1964) are

$$-\frac{\partial \mathbf{B}}{\partial t} = \nabla \wedge \mathbf{E},$$

$$\nabla \wedge \mathbf{B} = \mu \mathbf{J},$$

$$\nabla \cdot \mathbf{B} = 0,$$

and

$$\nabla \cdot \mathbf{E} = \frac{q}{\epsilon},$$

where \mathbf{B} is the magnetic field, \mathbf{E} the electric field, \mathbf{J} the electric current density, q the electric charge density, and $\mu = 4\pi \times 10^{-7}$ Ω s/m the magnetic permeability which is assumed to be the same everywhere as *in vacuo*. The dielectric constant is $\epsilon = 1/(\mu c^2)$. Since the particle velocity \mathbf{u} is small, the induced magnetic fields will be negligible compared with the steady geomagnetic field \mathbf{F} . Then by Ohm's law, the electric current within the moving ocean of uniform conductivity σ is

$$\mathbf{J} = \sigma(\mathbf{E} + \mathbf{u} \wedge \mathbf{F})$$

and in the non-conductors above and below the ocean it is zero. These equations imply that $\nabla \cdot \mathbf{J} = 0$ which means that if one can ignore displacement currents, one can ignore the term $\partial q/\partial t$ in the electric current continuity equation (Backus 1958). The electric current normal to the ocean at the top and bottom vanish to the same order of approximation.

The thin sheet approximations of Maxwell's equations, which govern the electromagnetic field in the ocean, have been generalized (Larsen 1966) from Price (1949) to include the case of barotropic motion. The horizontal and vertical components

are subscripted respectively s and z . Following Price, the electric current, since it is essentially horizontal, can be represented by a stream function ψ as

$$\mathbf{I}_s = -\hat{\mathbf{k}} \wedge \nabla_s \psi,$$

where

$$\mathbf{I}_s = \int_{-\frac{1}{2}h}^{\frac{1}{2}h} \mathbf{J}_s dz$$

is the vertically integrated electric current and $\nabla_s = \hat{\mathbf{i}}\partial/\partial x + \hat{\mathbf{j}}\partial/\partial y$ is the horizontal gradient operator. The thin sheet approximations combine to form the single equation at the ocean,

$$\nabla_s \cdot \left(\frac{\nabla_s \psi}{\sigma h} \right) - \frac{\partial B_z}{\partial t} = \nabla_s \cdot (\mathbf{u} F_z),$$

with B_z continuous. The terms from the left are resistance, induction and source.

The horizontal electric field, which is nearly uniform from top to bottom is

$$\mathbf{E}_s = -\hat{\mathbf{k}} \wedge \left(\frac{\nabla_s \psi}{\sigma h} - \mathbf{u} F_z \right).$$

Schmucker (1966) has pointed out that \mathbf{E}_s is strictly uniform from top to bottom only if $h \ll H_a$ for $kH_a < 0.2$. These conditions are satisfied for tidal motion.

The magnetic field by the Biot-Savart law is

$$\mathbf{B} = \frac{\mu}{4\pi} \iiint \frac{\mathbf{J} \wedge \mathbf{r}}{r^3} dx' dy' dz',$$

where \mathbf{r} is directed toward the point (x, y, z) from a small current element $\mathbf{J} dx' dy' dz'$ at the point (x', y', z') . Replacing the electric current by the stream function and integrating over the thickness of the thin sheet, the magnetic field is

$$\mathbf{B} = \frac{\mu}{4\pi} \hat{\mathbf{k}} \int_0^\infty \int_0^\infty \mathbf{K} \cdot \nabla_s' \psi dx' dy' - \frac{\mu}{4\pi} \int_0^\infty \int_0^\infty \mathbf{K} \cdot \hat{\mathbf{k}} \nabla_s' \psi dx' dy',$$

where

$$\nabla_s' = \hat{\mathbf{i}}\partial/\partial x' + \hat{\mathbf{j}}\partial/\partial y'.$$

For $\boldsymbol{\rho} = \hat{\mathbf{i}}(x-x') + \hat{\mathbf{j}}(y-y')$, $\mathbf{r} = \boldsymbol{\rho} + \hat{\mathbf{k}}(z-z')$, and $\zeta = z-z'$, the kernel \mathbf{K} is

$$\mathbf{K} = \frac{\boldsymbol{\rho}}{h} \int_{z-\frac{1}{2}h}^{z+\frac{1}{2}h} (\zeta^2 + \rho^2)^{-\frac{3}{2}} d\zeta + \frac{\hat{\mathbf{k}}}{h} \int_{z-\frac{1}{2}h}^{z+\frac{1}{2}h} \zeta (\zeta^2 + \rho^2)^{-\frac{3}{2}} d\zeta,$$

where

$$\rho^2 = (x-x')^2 + (y-y')^2.$$

Since B_z must vanish at the interface of the superconducting mantle which is at depth H_a , we imagine, at a depth $2H_a$, a thin layer of electric currents which are the negative image of the ocean electric currents. Then, because of symmetry, B_z vanishes at the interface and \mathbf{B} can be expressed as a function of the electric currents in the ocean and the negative image currents in the mantle. Also, since the continent is assumed non-conducting, the stream function will be constant at the coast line and this constant can be arbitrarily set to zero along this particular boundary. Then performing an integration by parts and using the boundary condition, $\psi = 0$ for $y = 0$, our 'thin sheet' equation, after substitution of B_z , becomes

$$\nabla_s \cdot \left(\frac{\nabla_s \psi}{\sigma h} \right) + \frac{\mu}{4\mu} \frac{\partial}{\partial t} \int_0^\infty \int_{-\infty}^\infty \psi G dx' dy' - \frac{\mu}{h} \frac{\partial \psi}{\partial t} = \nabla_s \cdot (\mathbf{u} F_z),$$

where $G = (\rho^2 + \frac{1}{4}h^2)^{-\frac{1}{2}} - (\rho^2 + 4H_a^2)^{-\frac{1}{2}} + 12H_a^2(\rho^2 + 4H_a^2)^{-\frac{3}{2}}$.

This integro-differential equation, applying to $-\infty \leq x \leq \infty$, $0 \leq y \leq \infty$, and $-\frac{1}{2}h \leq z \leq \frac{1}{2}h$, is independent of z because of the thin sheet ocean approximation. Therefore, given $\mathbf{u}F_z$ in terms of x and y , the equation can be solved for the stream function and the solutions for the electric and magnetic field can then be determined. Two alternate forms of this equation have been found but the above form is the most useful for numerical purposes because the kernel is non-singular for $\rho = 0$ and differentials of ψ do not appear in the integrand. If self-induction were negligibly small, the second and third terms on the left-hand side would vanish and the equation would reduce to a d.c. resistance type problem. For tidal induced fields in the open ocean, however, self-induction effects must be included.

Fields induced by Kelvin wave. The source term $\nabla_s \cdot (\mathbf{u}F_z)$, by the continuity equation for uniform water depth h , becomes $-(F_z/h)\partial\zeta/\partial t + \mathbf{u} \cdot \nabla_s F_z$. For the Kelvin solution we have

$$\nabla_s \cdot (\mathbf{u}F_z) = \frac{i\omega}{h} F_z(1 - i\beta)\zeta$$

where $\beta = (\partial F_z/\partial x)(kF_z)^{-1}$ is the fractional change of F_z in distance k^{-1} along the coast. To a first approximation β and F_z are assumed constant with values appropriate to the latitude of interest.

Since the source term is proportional to $\exp(i(kx - \omega t))$, the stream function and fields will also be proportional to the same factor and the stream function and fields may be non-dimensionalized to $\Phi = \psi(\sigma h U F_z/k)^{-1}$, $\hat{\mathbf{E}} = \mathbf{E}(U F_z)^{-1}$, and $\hat{\mathbf{B}} = \mathbf{B}(k U F_z/\omega)^{-1}$, where $U = \omega A(kh)^{-1} \exp(i(kx - \omega t))$ is the water motion at the coast. Suitable non-dimensional parameters are $Q = \frac{1}{2}\mu\omega\sigma h/k$, $\gamma = 2kH_a$, and $\delta = \frac{1}{2}kh$. The non-dimensional stream function then satisfies the integro-differential equation

$$\frac{d^2\Phi}{dY^2} - \Phi - iQ \left[\int_{-Y}^{\infty} \Phi(\eta + Y) G_1(\eta, \delta, \gamma) d\eta - \frac{\Phi(Y)}{\delta} \right] = i(1 - i\beta) e^{-(f/\omega)Y}$$

and the boundary condition $\Phi = 0$ for $Y = 0$, where $Y = ky$. The kernel G_1 is

$$G_1 = \frac{1}{\pi} \left\{ \frac{K_1[(\eta^2 + \delta^2)^{\frac{1}{2}}]}{(\eta^2 + \delta^2)^{\frac{1}{2}}} + \frac{\gamma^2 K_0[(\eta^2 + \gamma^2)^{\frac{1}{2}}]}{(\eta^2 + \gamma^2)} - (\eta^2 - \gamma^2) \frac{K_1[(\eta^2 + \gamma^2)^{\frac{1}{2}}]}{(\eta^2 + \gamma^2)^{\frac{3}{2}}} \right\}.$$

where K_0 and K_1 are modified Bessel functions of the second kind.

The horizontal components of the electric field within the ocean, from Ohm's law for a moving conductor, are

$$\hat{E}_x(Y) = \frac{d\Phi}{dY},$$

and

$$\hat{E}_y(Y) = -i\Phi + (1 - i\beta) e^{-(f/\omega)Y}.$$

The components of the magnetic field at the Earth's surface, by the Biot-Savart law after integrating out the x dependency, are

$$\hat{B}_x^{(\pm)}(Y) = iQ \int_{-Y}^{\infty} \Phi(\eta + Y) G_2^{(\pm)}(\eta, \delta, \gamma) d\eta,$$

$$\hat{B}_y^{(\pm)}(Y) = Q \int_{-Y}^{\infty} \frac{d\Phi(\eta + Y)}{dY} G_2^{(\pm)}(\eta, \delta, \gamma) d\eta,$$

and

$$\hat{B}_z(Y) = -Q \int_{-Y}^{\infty} \Phi(\eta + Y) G_1(\eta, \delta, \gamma) d\eta + \frac{Q}{\delta} (Y),$$

where, for the superscript (\pm), plus is taken for the top and minus for the bottom of the ocean. The kernel $G_2^{(\pm)}$ is

$$G_2^{(\pm)} = \frac{(\pm 1)}{2\delta\pi} \{K_0[(\eta^2 + 4\delta^2)^{\pm}] - K_0[|\eta|]\} + \frac{\gamma}{\pi} \frac{K_1[(\eta^2 + \gamma^2)^{\pm}]}{(\eta^2 + \gamma^2)^{\pm}}.$$

Solutions. Solutions for the stream function and the fields at M_2 frequency were determined by a finite difference approximation of the equations. Because the kernels G_1 and $G_2^{(\pm)}$ have singularities in the complex plane, special care must be used in the finite difference approximation of the integrals. These difficulties were avoided in the present study by finding asymptotic expressions for G_1 and $G_2^{(\pm)}$ near the singularities which could be integrated analytically. Further away from the singularities, the kernels were computed using a polynomial approximation of the Bessel functions (Lee 1963). A solution for the stream function was then found by a matrix inversion of the finite difference approximation of the integro-differential equation using 70 grid points. The electromagnetic fields were then computed from the stream function.

Solutions were found for the following three cases: (1) $f/\omega = 0.519$, $H_a = 149$ km, (2) $f/\omega = 0.519$, $H_a = 514$ km, and (3) $f/\omega = 0$, $H_a = 149$ km. Oceanic and continental mantle conductivity give, respectively, the values $H_a = 149$ and 519 km. For 30° N latitude we have $f/\omega = 0.519$. Cases 1 and 2 were computed to compare the differences due to a change in H_a . Case 3 was computed to show the effects of a wave whose amplitude does not decrease off shore. The solution far from the coast for this case was found to be within one per cent of the plane wave solution for an ocean without boundaries. The amplitudes and phase leads (relative to the water motion) for the stream function Φ , the emf source $S = i(1 - i\beta) \exp(-Yf/\omega)$, the electric field \hat{E} , and the magnetic field \hat{B} for the three cases are plotted in Figs 6-8 as functions of $Y = ky$ (distance off shore). Values used in computation, appropriate for the ocean off California, were $\omega/k = 207$ m/s, $h = 4.4$ km, $\sigma = 3.26\Omega^{-1}/\text{m}$ and $\beta = 0.28$.

Discussion of solutions. Some common features are: The stream function is a smoothly varying function of Y . The horizontal electric field, the magnetic field normal to the coast and the vertical magnetic fields are enhanced at the ocean's boundary due in part to the assumed abrupt ocean-continental conductivity transition that concentrate electric currents along it and in part to the edge effect of the water motion. The horizontal magnetic field is enhanced beneath the ocean, a consequence of the induced electric currents in the conducting mantle.

Some differences of the solutions between the cases are the following: cases 1 and 2 show that, for smaller depths to the conducting mantle, the horizontal magnetic field beneath the ocean and the horizontal electric and vertical magnetic field at the coast are more enhanced. Cases 1 and 3 show that the horizontal magnetic field beneath the ocean is much larger for a wave which remains constant offshore than for a Kelvin wave.

Comparison of computed and observed fields. The observed M_2 variations are compared in Table 4 with the computed values for cases 1-3. Case 3 can be immediately ruled out but the other cases seem to fit the observed values reasonably well. Cases 1 and 2 probably give similar results because the observation sites are close to the edge of the ocean so that the coastal enhancement masks the mantle enhance-

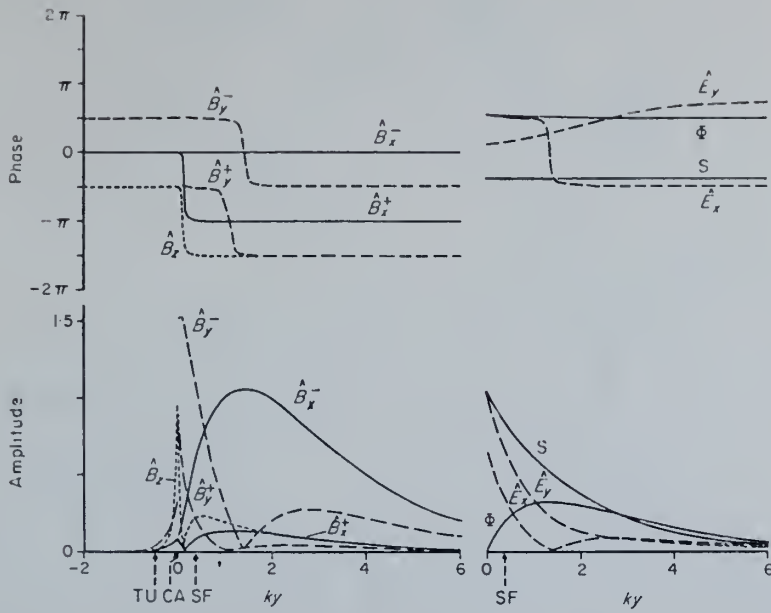


FIG. 6. Case 1. Semidiurnal tidal induced fields for $H_a = 149$ km, $f/\omega = 0.519$. Upper curves phase lead relative to water motion and lower curves non-dimensional amplitudes plotted as function of ky , positive for offshore distances. Outer edge of continental shelf at $y = 0$ and stations Tucson, Cambria and Sea Floor are noted. Superscripts (+) and (-) refer respectively to values above and below ocean. Solid line \hat{B}_x ; dashed \hat{B}_y ; dotted \hat{B}_z . See text for further description.

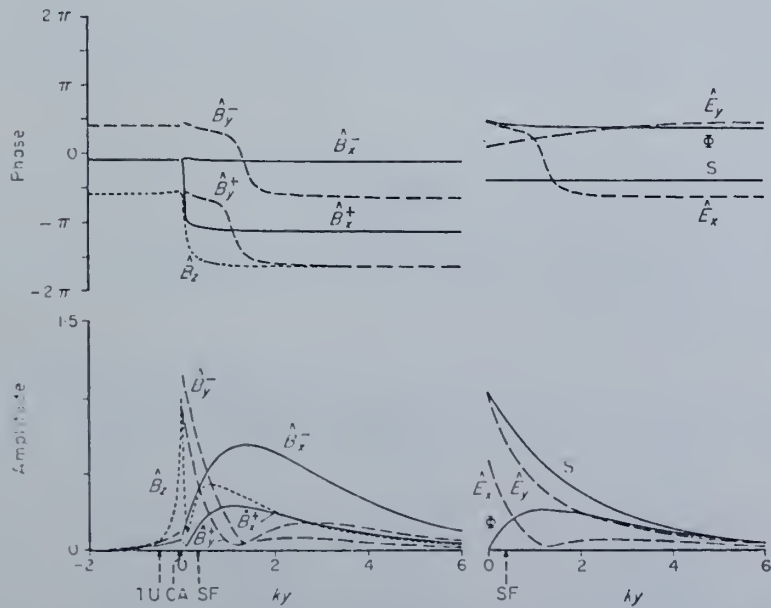


FIG. 7. Case 2. Semidiurnal tidal induced fields for $H_a = 514$ km, $f/\omega = 0.519$. See legend for Fig. 6.

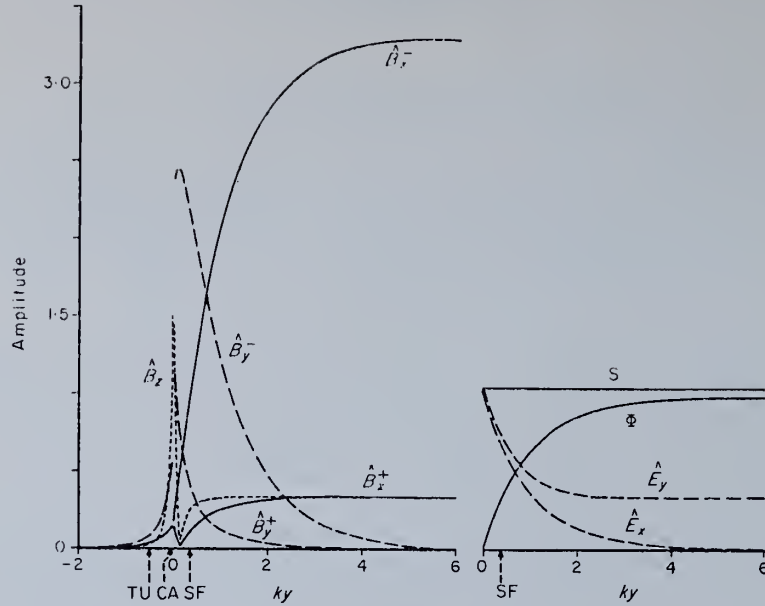


FIG. 8. Case 3. Semidiurnal tidal induced fields for $H_a = 149$ km, $f/\omega = 0$. See legend for Fig. 6.

ment. Therefore the observations are inadequate to determine the mantle conductivity. The computed fields suggest, however, that the observed M_2 fields at the station sites are induced by barotropic tidal motion similar in some respects to a Kelvin wave. The fit, however, is not perfect as the model is only an approximation of the tides and conductivity. The possibility that part of the variation might be induced by baroclinic tidal motion has been investigated (Larsen 1966). It was shown there that baroclinic tidal induced fields will be negligible compared with barotropic tidal induced fields.

Table 4

Observed and computed M_2 tidal induced fields for various cases using observed tide height at Avila Beach $\zeta = 0.5 \cos(\omega t + 235^\circ)$ m. Fields tabulated as cosine wave $A \cos(\omega t + \theta)$ where phase is relative to zero hour, 1965 January 1 U.T.

$$F_z = -0.38 \text{ gauss}$$

Station		Observations	Case 1	Case 2	Case 3
			$H_a = 149$ km $f/\omega = 0.519$	$H_a = 514$ km $f/\omega = 0.519$	$H_a = 149$ km $f/\omega = 0$
Sea floor ΔE	Amplitude (mV/km)*	0.62 ± 0.10	0.62	0.68	0.77
	Phase (deg)	267 ± 15	261	262	284
	Azimuth ($^\circ T$)*	83 ± 6	72	76	97
	Axis ratio	0.01 ± 0.04	0.45	0.25	0.63
	Rotation	ccw†	ccw†	ccw†	ccw†
Sea floor ΔD	Amplitude (γ)	2.4 ± 0.8	3.2	2.7	5.6
	Phase (deg)	226 ± 19	259	250	256
Cambria ΔZ	Amplitude (γ)	1.6 ± 0.4	1.9	2.4	3.1
	Phase (deg)	210 ± 16	146	131	146

* Values for semi-major axis of ellipse.

† ccw—counterclockwise.

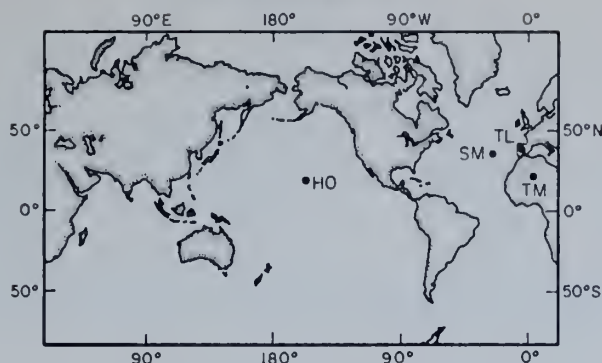


FIG. 9. Location of stations.

2. Tidal induced fields at island stations

2.1 Island magnetic observations

Magnetic data from two pairs of island–continental magnetic observatories (see Fig. 9) were analysed to determine the lunar semidiurnal magnetic variation. The observatories were (Honolulu, Hawaii; Tamanrasset, Algeria), (San Miguel, Azores; Toledo, Spain). For each pair, the stations were selected for their similar geographic and geomagnetic latitude, see Table 5, with the expectation that the ionospheric lunar magnetic variations would be nearly the same except for an obvious phase difference due to longitude differences. A comparison of the lunar variations between the continental and island station then permits an estimation of that part due to an oceanic source.

Observations. Hourly values of the magnetic components from the sun spot minimum years 1951–56 were obtained from the various stations. The components were ΔD (horizontal, positive magnetic east variation), ΔD (horizontal, positive magnetic north variation), and ΔZ (vertical, positive down variation). Table 6 lists the record lengths which were analysed for the various components at the various stations.

Missing hourly values were replaced by the mean of the daily variation of the two days directly preceding and following the gaps. The individual gaps were never longer than three days and the number of gaps for any one component amounted to less than 1.2 per cent of the record length. The hourly values were then smoothed by a low pass filter with sharp cutoff at 3.72 c/d to give eight readings per day (tri-hourly values). No correction for the filter response was needed at the lunar semidiurnal frequency.

Results of harmonic analysis. The data for each component from the various stations were divided into seasonal groups centred on the equinoxes and solstices from 1951–56. The seasons being spring, Sp; summer, S; fall, F; winter, W. Each

Table 5

Position of magnetic observatories

Station	Geomagnetic		Geographic	
	Latitude	Longitude	Latitude	Longitude
Honolulu	21.1° N	266.5° E	21° 19' N	158° 06' W
Tamanrasset	25.4° N	79.6° E	22° 48' N	5° 32' E
San Miguel	45.6° N	50.9° E	37° 47' N	25° 39' W
Toledo	43.9° N	74.7° E	39° 53' N	4° 03' W

Table 6

Hourly values

Station	Component	Azimuth	Time
Honolulu	$\Delta D, \Delta H, \Delta Z$	$101.5^\circ T, 11.5^\circ T$, down	1951-56
Tamanrasset	ΔD	$84.5^\circ T$	1953-56
Tamanrasset	$\Delta H, \Delta Z$	$-5.5^\circ T$, down	1951-56
San Miguel	$\Delta D, \Delta H$	$74^\circ T, -16^\circ T$	1951-56
San Miguel	ΔZ^*	Down	11/VII/1951-56
Toledo	$\Delta D, \Delta H, \Delta Z$	$81.5^\circ T, -8.5^\circ T$, down	1951-56

* San Miguel ΔZ variations appear to be in error from VI/52 to VI/56 and the data for this period were ignored.

group consisted of 107 lunar days of data which was faded by a $\sin x/x$ type fading function. Then, harmonic coefficients a_n and b_n , for twenty frequencies, $(200+n)/T$, $n = 1, \dots, 20$, $T = 107$ lunar days, were computed for each component, station and seasonal group.

Power spectral estimates for each component at the various stations were determined by an ensemble average over all available seasonal groups of the squares of the harmonic coefficients, $\frac{1}{2}T \langle a_n^2 + b_n^2 \rangle$ gamma²/cycles per lunar day. The results are presented in Fig. 10. Most of the spectra show a peak at the M_2 frequency (2 cycles per lunar day). The peaks are broadened somewhat due to fading of the time series. In addition to the peak at the M_2 frequency, the spectrum for San Miguel ΔZ shows a peak close to the N_2 tidal frequency (1.962 cycles per lunar day). There appear to be no other prominent peaks present in this frequency interval. The increase of the spectra to the right is due to the continuum about the solar semi-diurnal variation.

Seasonal and yearly means of the harmonic coefficients $\langle a_n \rangle$ and $\langle b_n \rangle$ for each component at the various stations were determined from the individual seasonal groups. Table 7 lists the seasonal and yearly mean amplitudes and phases of the

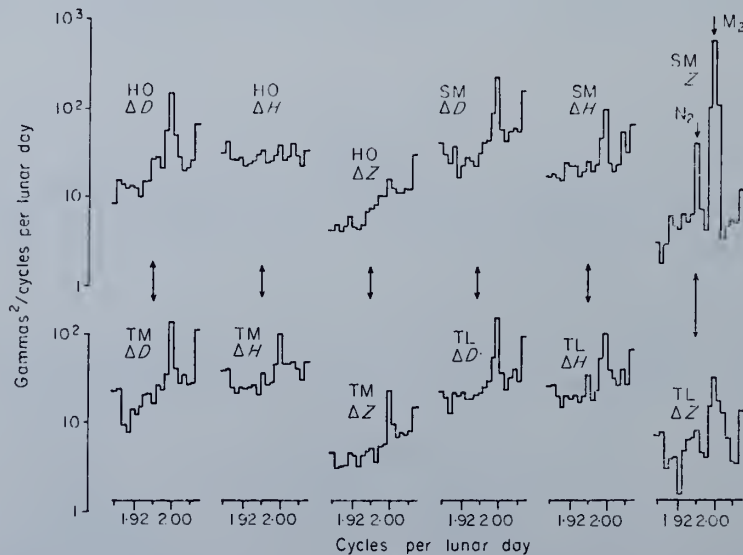


FIG. 10. Power spectral estimates of magnetic variations of the various components at Honolulu, San Miguel, Tamanrasset and Toledo. Frequencies range from $201/T$ to $220/T$ where $T = 107$ lunar days. The double arrow is the 95 per cent confidence limits for spectra directly above and below it, both of which are based on simultaneous data available from 1951-56, see Table 6.

Table 7

Seasonal and yearly mean M_2 variation $A \cos(\omega t + \theta)$. Phases refer to zero hour, 1951 January 1 U.T. r.m.s. amplitude \mathcal{R} of background based on 15 harmonic terms nearest M_2 frequency

Station	Component	Season	A (γ)	θ † (deg)	\mathcal{R} (γ)	Station	Component	Season	A (γ)	θ † (deg)	\mathcal{R} (γ)
San Miguel 1951-56	ΔD	Spring	0.7*	226	0.4	Honolulu 1953-56	ΔD	Spring	0.5*	296	0.3
		Summer	2.6	268	0.3			Summer	2.1	24	0.3
		Fall	2.2	311	0.4			Fall	1.7	27	0.4
		Winter	0.6*	187	0.3			Winter	0.8	84	0.3
		Year	1.2	273	0.2			Year	1.1	28	0.2
San Miguel 1951-56	ΔH	Spring	0.2*	68	0.3	Honolulu 1951-56	ΔH	Spring	0.3*	156	0.4
		Summer	1.5	62	0.3			Summer	0.3*	140	0.2
		Fall	1.5	87	0.3			Fall	0.4*	93	0.3
		Winter	0.4*	162	0.3			Winter	0.6*	150	0.3
		Year	0.8	81	0.2			Year	0.4*	136	0.2
San Miguel 1951-52 1956	ΔZ	Spring	3.8	144	0.3	Honolulu 1951-56	ΔZ	Spring	0.2*	281	0.1
		Summer	3.1	148	0.2			Summer	0.3*	44	0.2
		Fall	3.4	142	0.2			Fall	0.4*	350	0.2
		Winter	3.4	146	0.2			Winter	0.6	245	0.1
		Year	3.4	145	0.1			Year	0.2	306	0.1
Toledo 1951-56	ΔD	Spring	0.6*	278	0.4	Tamanrasset 1953-56	ΔD	Spring	0.9	231	0.4
		Summer	2.1	322	0.3			Summer	1.8	353	0.2
		Fall	1.8	359	0.3			Fall	1.6	29	0.3
		Winter	0.5*	245	0.2			Winter	1.4	177	0.3
		Year	1.0	324	0.1			Year	0.3*	359	0.2
Toledo 1951-56	ΔH	Spring	0.2*	214	0.3	Tamanrasset 1951-56	ΔH	Spring	0.4*	230	0.3
		Summer	1.6	120	0.3			Summer	0.6	206	0.2
		Fall	1.1	135	0.2			Fall	1.0	232	0.3
		Winter	0.8	232	0.3			Winter	1.3	282	0.4
		Year	0.7	147	0.1			Year	0.7	247	0.1
Toledo 1951-52 1956	ΔZ	Spring	0.6*	58	0.3	Tamanrasset 1951-56	ΔZ	Spring	0.2*	56	0.2
		Summer	0.7	28	0.2			Summer	0.6	93	0.1
		Fall	1.0	77	0.2			Fall	0.9	98	0.1
		Winter	0.4*	49	0.2			Winter	0.2*	171	0.1
		Year	0.7	57	0.1			Year	0.4	100	0.1

* Not significant

† Add 2 times west longitude of station—172.1° to convert to local mean lunar time (Bartels & Fanslau 1937).

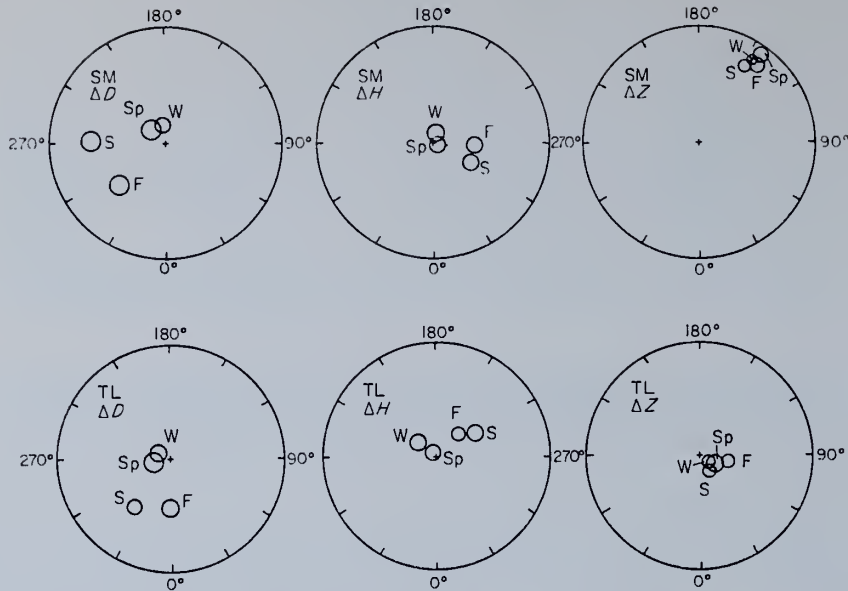


FIG. 11. Harmonic dials of seasonal mean lunar M_2 magnetic variation $A \cos(\omega t + \theta)$ of the various components for San Miguel and Toledo. Seasonal means (Sp, spring; S, summer; F, fall; W, winter) based on data available from 1951–56. Phases refer to zero hour, 1951 January 1 U.T. Large outer circles correspond to four gammas amplitude. Small circles have radii equal to rms amplitude of background and are centred on mean amplitudes and phases.

lunar M_2 magnetic variations and Table 8, the N_2 variation. The rms amplitudes \mathcal{R} of the background were determined from the mean coefficients excluding $n = 10, 13, 14, 15$ and 20 .

Seasonal and yearly mean amplitudes and phases from Table 7 are presented pictorially as harmonic dials in Figs 11 and 12 for the various components and stations. Circles having radii equal to the r.m.s. amplitude \mathcal{R} of the background are centred on the mean M_2 amplitude and phase. If the background is Gaussian noise there is a 63 per cent chance that the circle contains the true value of the periodic part of the signal.

Discussion of results. The seasonal mean of the M_2 magnetic variation for San Miguel ΔD changes, season by season, quite similarly as Toledo ΔD , see Fig. 11. For example, the phase of Toledo ΔD differs, season by season, from the phase of San Miguel ΔD by an amount which is nearly twice the difference in longitude between the two stations while the amplitudes, season by season, are nearly the same. The same applies for the seasonal changes of San Miguel ΔH and Toledo ΔH . The seasonal changes for San Miguel ΔZ and Toledo ΔZ , however, are not similar. After correcting the phases for the difference in longitude, one finds that the amplitude of ΔZ for San Miguel is about four gammas larger with slight seasonal dependency. The interpretation of these results is the following:

The horizontal M_2 variations at San Miguel are probably due entirely to an ionospheric source because the seasonal changes compare so well with those at Toledo. This conclusion is consistent with the relative phase shift (50° as determined from Fig. 11) being nearly that expected ($43^\circ =$ twice the difference in longitude of stations) for an ionospheric semidiurnal progressive wave travelling westwards. The small consistent differences in amplitudes and phases are probably due to ionospheric induced currents in the ocean. The vertical M_2 variation at San Miguel, however,

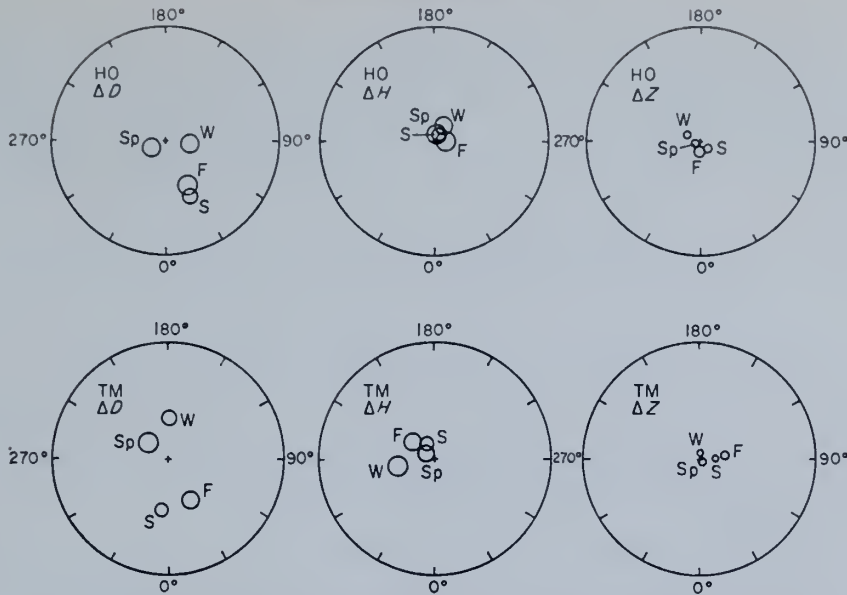


FIG. 12. Harmonic dials of seasonal mean lunar M_2 magnetic variation $A \cos(\omega t + \theta)$ of the various components for Honolulu and Tamanrasset. See legend for Fig. 11.

is due mostly to an oceanic source because of its large amplitude relative to Toledo ΔZ . The oceanic part is estimated to have an amplitude 3.8 gammas and a phase 153° relative to zero hour, 1951 January 1 U.T. The small seasonal changes of the vertical M_2 variation at San Miguel are probably due to an ionospheric source. These conclusions are consistent with the facts, (i) that oceanic tidal induced variations should show negligible seasonal dependency, and (ii) that if there were only an ionospheric source present, the vertical M_2 magnetic variation at San Miguel should follow closely the seasonal change of the horizontal variations at San Miguel. The N_2 vertical magnetic variation, detected at San Miguel, see Table 8, lends supporting evidence that the vertical lunar semidiurnal variations at San Miguel are due mostly to an oceanic source. For example, the yearly mean for San Miguel ΔZ gives an amplitude ratio $N_2/M_2 = 0.25$ and phase difference $\theta_{N_2} - \theta_{M_2} = 58^\circ$, similarly the tides at San Miguel yield $N_2/M_2 = 0.23$ and $\theta_{N_2} - \theta_{M_2} = 42^\circ$.

Interpretation of the harmonic dials (Fig. 12) for Honolulu and Tamanrasset is not quite as clear. This is probably a result of the large differences in longitude between the two stations. Comparison of the harmonic dials suggest a possibility that part of the M_2 variation in Honolulu ΔD has an oceanic source. This variation is estimated to have an amplitude 0.5 gammas and phase 22° . The evidence for this variation of oceanic origin, however, is highly tenuous.

Table 8

Seasonal and yearly mean lunar N_2 magnetic variation $A \cos(\omega t + \theta)$ and r.m.s. amplitude \mathcal{R} . Phases refer to zero hour 1965 January 1 U.T. and r.m.s. amplitude based on 15 harmonic terms nearest M_2 frequency

Station	Component	Season	A (γ)	θ (deg)	\mathcal{R} (γ)
San Miguel 1951-1952, 1956	ΔZ	Spring	0.9	204	0.3
		Summer	0.9	186	0.2
		Fall	0.8	220	0.2
		Winter	0.9	203	0.2
		Year	0.9	203	0.1

2.2 Tidal induced electric and magnetic fields

The observed oceanic tidal induced magnetic field, which was large at San Miguel and small at Honolulu, is shown in the present section to be qualitatively consistent with the computed field based on a model study of the island effect on oceanic tidal induced fields. Observations of the island effect of fields induced by ionospheric sources have been studied by Mason (1963), Parkinson (1962), Voppel (1964), Swift & Wescott (1964), Rikitake (1964) and Ashour & Chapman (1965).

Model. Choose a right-handed coordinate system where the z coordinate with unit vector \hat{k} , is up and the rectangular coordinates (x, y) or polar (r, θ) are in the plane of the ocean (θ measured counter clockwise from x axis). The model consists of a circular island of radius $r = b$ having a uniform conductivity ν times that of sea water and having vertical walls for a coastline. The island is imagined to be in an infinite ocean, of uniform depth h and conductivity σ , rotating at a uniform rate appropriate to the latitude of interest, and spaced above a superconducting mantle at depth H_a . The crust and mantle above H_a and the atmosphere are assumed non-conducting. The tide, distant from the island, is represented by a free plane wave with wave height

$$\zeta = A e^{ikx} e^{-i\omega t},$$

where $k = (\omega^2 - f^2)^{\frac{1}{2}} / (gh)^{\frac{1}{2}}$ is the horizontal wave number and ω the frequency. The solution for the wave height near the island (Proudman 1914), where $kr \ll 1$ and $kb(1 - f^2/\omega^2)^{-1} \ll 1$, is approximately $A \exp(-i\omega t)$, i.e. the scattered wave is negligible. Then the horizontal components of the water motion near the island in the direction of increasing r and θ are approximately

$$u_r = \frac{\omega A}{kh} \left(1 - \frac{b^2}{r^2}\right) \left(\cos \theta - i \frac{f}{\omega} \sin \theta\right) e^{-i\omega t},$$

and

$$u_\theta = -\frac{\omega A}{kh} \left(1 + \frac{b^2}{r^2}\right) \left(\sin \theta + i \frac{f}{\omega} \cos \theta\right) e^{-i\omega t}.$$

Electric and magnetic fields. In the absence of an island the electric current, for vanishing wave number but $\omega/k = (gh)^{\frac{1}{2}}$ finite and uniform vertical geomagnetic field F_z (Larsen 1966), is

$$I_f = \frac{\omega \sigma A F_z}{k(1 - iQ_f)} e^{-i\omega t}$$

and flows in the y direction. The self-induction factor, for $2kH_a \ll 1$ (Larsen 1966), is

$$Q_f = \mu \omega \sigma h H_a.$$

With an island we separate the electric current stream function into a local part Ψ_l and a far part Ψ_f such that Ψ_l vanishes far from the island and $\Psi_f = -I_f r \cos \theta$. The contribution to the electric current by the scattered wave can be shown to be negligible for $kb \ll 1$. Furthermore, the self-induction associated with Ψ_l , the local electric currents, will be negligible provided $\mu \omega \sigma h b \ll 1$. Then the integro-differential equation governing the stream function (see Section 1.4) simplifies to

$$\nabla^2 \Psi_l = 0.$$

Solutions (Ashour & Chapman 1965) are then

$$\psi_l = I_f \kappa \frac{b^2}{r} \cos \theta, \quad \text{for } r \geq b,$$

and

$$\psi_i = I_f \kappa r \cos \theta, \quad \text{for } 0 \leq r \leq b,$$

where $\kappa = (1-\nu)/(1+\nu)$ is a factor depending on the island-ocean conductivity contrast. One sees that the island behaves as a dipole current source which modifies the uniform electric currents flowing in the ocean. To the above approximation, we can then compute the electric and magnetic field from ψ_i and ψ_f by the thin sheet approximations (Section 1.4) of the electromagnetic equations. We first non-dimensionalize the fields to $\hat{\mathbf{E}} = \mathbf{E}(\sigma h/I_f)$ and $\hat{\mathbf{B}} = \mathbf{B}(\mu I_f)^{-1}$.

The horizontal components of the electric field at the point (r, θ) within the ocean ($r \geq b$) are found to be

$$\hat{E}_r = \left(1 - \kappa \frac{b^2}{r^2}\right) \sin \theta - (1 - iQ_f) \left(1 + \frac{b^2}{r^2}\right) \left(\sin \theta + i \frac{f}{\omega} \cos \theta\right),$$

and

$$\hat{E}_\theta = \left(1 + \kappa \frac{b^2}{r^2}\right) \cos \theta - (1 - iQ_f) \left(1 - \frac{b^2}{r^2}\right) \left(\cos \theta - i \frac{f}{\omega} \sin \theta\right).$$

The first term on the right is the field due to the electric currents within the ocean and the second term is $\mathbf{u} \wedge \mathbf{F}$. On the island ($r \leq b$) the horizontal components are found to be

$$\hat{E}_r = (1 + \kappa) \sin \theta,$$

and

$$\hat{E}_\theta = (1 + \kappa) \cos \theta.$$

This field is linearly polarized in the direction of the wave crest.

The magnetic field due to the image of the local electric current at depth $2H_a$ will be negligible (to within a few per cent) provided $2H_a/b > 5$. Then the components of the magnetic field at the point (r, θ) and height z above mid-ocean depth, for vanishing h , are found to be

$$\hat{B}_r = -\frac{\kappa}{2} \cos \theta \left[1 - \frac{z}{\pi} \int_0^\pi \int_b^\infty \left(1 + \left(\frac{b}{r'}\right)^2 \cos 2\theta'\right) Pr' dr' d\theta'\right],$$

$$\hat{B}_\theta = \frac{\kappa}{2} \sin \theta \left[1 - \frac{z}{\pi} \int_0^\pi \int_b^\infty \left(1 - \left(\frac{b}{r'}\right)^2 \cos 2\theta'\right) Pr' dr' d\theta'\right],$$

and

$$\hat{B}_z = \frac{\kappa}{2\pi} \cos \theta \int_0^\pi \int_b^\infty \left[r' \cos \theta' - r + \left(\frac{b}{r'}\right)^2 (r' \cos \theta' - r \cos 2\theta')\right] Pr' dr' d\theta',$$

where

$$P = (r^2 + r'^2 - 2rr' \cos \theta' + z^2)^{-\frac{1}{2}}.$$

If the island were as conducting as sea water, $\kappa = 0$, and the magnetic field would vanish. For $\theta = 0^\circ$, one sees that $\hat{B}_\theta = 0$ and for $\theta = \pm 90^\circ$, $\hat{B}_r = \hat{B}_\theta = 0$. For $r = 0$, we find $\hat{B}_r = -\frac{1}{2}\kappa \cos \theta [1 - z/(z^2 + b^2)^{\frac{1}{2}}]$, $\hat{B}_\theta = \frac{1}{2}\kappa \sin \theta [1 - z/(z^2 + b^2)^{\frac{1}{2}}]$, and $\hat{B}_z = 0$, and for $z = 0$ and $r \leq b$, we have $\hat{B}_z = \frac{1}{2}\kappa \cos \theta (r/b)$.

The components of the fields are plotted in Fig. 13 as a function of distance r/b from the centre of a non-conducting island ($\kappa = 1$) for directions $\theta = 0^\circ$ and -90° . The electric field was computed using the values $h = 4$ km, $\sigma = 3\Omega^{-1}/\text{m}$, $H_a = 150$ km, and $k = 10^{-3} \text{ km}^{-1}$, appropriate for the ocean about San Miguel and for M_2 tidal frequency. The magnetic field, for height $z/b = 0.1$, was computed by numerical integration and the values agree with the solution for an equivalent electromagnetic problem (Ashour & Chapman 1965).

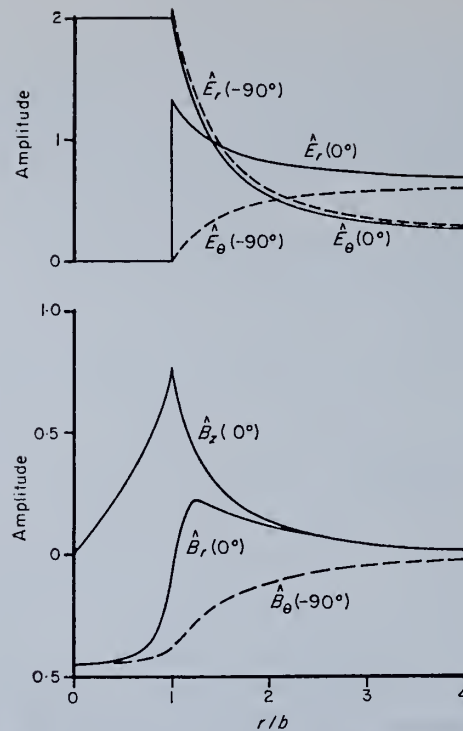


FIG. 13. Island effect on tidal induced electric and magnetic fields for a small circular, non-conducting island of radius b spaced above a superconducting mantle at a depth much greater than the size of the island. Non-dimensional amplitudes plotted as functions of distance r/b from centre of island for the directions $\theta = 0^\circ$ (solid line) and -90° (dashed line) relative to the propagation direction of tide.

Discussion of solutions. The principal features of the solution are the following: (i) the vertical magnetic field and horizontal electric field are enhanced at the edge of a non-conducting island (the magnetic field is enhanced because of the concentration of electric currents at the edge of the island while the electric field in the ocean is enhanced by the concentration of both the electric and tidal currents near the edge), (ii) the horizontal magnetic field near the centre of the island is linearly polarized normal to the wave crest, (iii) the horizontal electric field within the island is linearly polarized parallel to the wave crest, (iv) the phases of the magnetic field or the electric field on the island do not depend on r . Hence, observed phases of the fields might be used to determine the phase and direction of tidal induced currents in the deep ocean.

Comparison of solutions with observations. We approximate the islands for the stations San Miguel and Honolulu by circular islands of radius $b = 50$ km. Then for semidiurnal frequency we find that $kb(1-f^2/\omega^2)^{-1} = 0.07$, $\mu\omega\sigma hb = 0.11$, $2kH_a = 0.3$, and $2H_a/b = 6$ so that the approximations assumed appear to be reasonably valid for the region $r/b < 4$.

Quantitative interpretation of the observed tidal induced magnetic fields at the island stations with the computed fields for the island model, however, is impossible as, (i) there is only one magnetic station per island, (ii) the electric field was not measured, and (iii) the island's conductivity and its distribution is relatively unknown. The observations, however, are qualitatively consistent with the features of the computed fields. For example, the San Miguel station, because it has a large vertical magnetic field of oceanic tidal origin, is probably located near the edge of a relatively

non-conducting island. This conclusion is consistent with the fact that an oceanic tidal induced horizontal field was not observed and hence must be much smaller. The lack of an oceanic tidal induced vertical field at the Honolulu station has the following possible explanations: (i) the station is near the centre of the island, (ii) the island has a conductivity near that of sea water, or (iii) there are no oceanic tidal induced electric currents near Hawaii. The third possibility probably can be ruled out.

Although the phases are relatively unaffected by the island, it was not possible to infer, from the observations, either the tidal motion in the open ocean or the mantle conductivity because more information is needed about tidal motion in the deep ocean.

3. Conclusions

The principal conclusions for part 1 are the following: (i) the lunar semidiurnal periodicity (12.4206 h period) in the electromagnetic field at the sea floor site and in the magnetic field at the coastal site has a predominant oceanic origin, (ii) the observed periodicities are consistent with the fields computed using a model of the Earth's electrical conductivity and a Kelvin wave model of the barotropic lunar semidiurnal tide along the California coast, (iii) baroclinic induced fields of tidal frequency are unlikely to be detected because the fields are many times smaller than those for the barotropic tides, (iv) the tidal variations were inadequate to determine the distribution of mantle conductivity. Because of the above, it is concluded that the observed lunar semidiurnal periodicity is caused by a barotropic tide in the ocean and that the Kelvin wave solution may be a reasonable model of the lunar semidiurnal tide along the California coast.

The principal conclusions for part 2 are the following: (i) the lunar semidiurnal periodicity (12.4206 h period) in the vertical component of the magnetic field at San Miguel has a definite oceanic tidal origin, (ii) this variation appears to be qualitatively consistent with computed fields for an island model, (iii) it is not possible to conclude definitely that there is an oceanic tidal induced field at Honolulu, (iv) the lack of deep ocean tidal measurements or electric field observations makes it impossible to determine the distribution of mantle conductivity.

These conclusions suggest the possibility that other types of barotropic water motion such as tsunamis or planetary waves may induce observable electromagnetic fields at coastal, island, or oceanic stations. Also, the possibility that other coastal or island magnetic observatories may contain a significant oceanic tidal induced variation cannot be arbitrarily ruled out.

4. Acknowledgments

This investigation formed part of a thesis submitted to the Scripps Institution of Oceanography, La Jolla, California. The author wishes to express his gratitude to Dr Charles S. Cox for the inspiration to undertake this study and for his help and guidance in carrying it through, and to the other committee members, Drs Carl H. Eckart, Walter H. Munk, George E. Backus, and Douglas L. Inman for their assistance. The author is very much indebted to Dr Ulrich Schmucher for making available the Cambria magnetic data and for many helpful discussions, and to Dr Jean H. Filloux and Dr Charles S. Cox whose instrumentation and support made it possible to obtain the sea floor electric and magnetic data.

This research was supported by the Office of Naval Research, National Science Foundation, and Bendix Corporation while the author was at the Scripps Institution of Oceanography.

*Joint Tsunami Research Effort,
Environmental Science Services Administration,
University of Hawaii.
1967 November.*

References

- Ashour, A. & Chapman, S., 1965. *Geophys. J. R. astr. Soc.*, **10**, 31.
 Backus, G., 1958. *Ann. Physics*, **4**, 372.
 Bartels, J. & Fanslau, G., 1937. *Z. Geophysik*, **13**, 311.
 Bullen, J. & Cummack, C., 1953. *J. geophys. Res.*, **58**, 554.
 Cantwell, T. & Madden, T., 1960. *J. geophys. Res.*, **65**, 4202.
 Chapman, S., 1919. *Phil. Trans. R. Soc.*, **A218**, 1.
 Chapman, S., 1956. *Nuovo Cimento, Suppl.*, **4**, 1385.
 Chapman, S. & Bartels, J., 1940. *Geomagnetism*, Vols 1 & 2, Clarendon Press, Oxford.
 Egedal, J., 1956. *J. geophys. Res.*, **61**, 784.
 Feynman, R., Leighton, R. & Sands, M., 1964. *The Feynman Lectures on Physics*, Vol. 2. Addison-Wesley, New York.
 Filloux, J., 1967. Ph.D. Thesis, University of California, San Diego.
 Filloux, J., 1967. *Geophysics*, **32**, 978.
 Filloux, J. & Cox, C., 1967. A self-contained sea floor recorder of the electric field, *Contribution from the Scripps Institution of Oceanography*, New Series.
 Fisher, R., 1929. *Proc. R. Soc.*, **A125**, 54.
 Gish, O., 1951. *Compendium of Meteorology*, 101.
 Horne, R. & Frysinger, G., 1963. *J. geophys. Res.*, **68**, 1967.
 Isaac, J., Reid, J., Schick, G. & Schwartzlose, R., 1966. *J. geophys. Res.*, **71**, 4297.
 Lamb, H., 1945. *Hydrodynamics*, 6th edn Cambridge Univ. Press.
 Larsen, J. & Cox, C., 1966. *J. geophys. Res.*, **71**, 4441.
 Larsen, J., 1966. Ph.D. Thesis, University of California, San Diego.
 Lee, W. H. K., 1963. *Inter. Comput. Centre Bull.*, **2**, 1.
 Longuet-Higgins, M., 1949. *Mon. Not. R. astr. Soc., Geophys. Suppl.*, **5**, 295.
 Mason, R., 1963. Spatial dependence of time-variations of the geomagnetic field in the range 24 h–3 min on Christmas Island, Imperial College of Science and Technology, Vol. 3.
 Matsushita, S. & Maeda, H., 1965. *J. geophys. Res.*, **70**, 2559.
 Parkinson, W., 1962. *Geomagnetica*, publicação comemorativa do 50.º aniversário do Observatório Magnético de S. Miguel, Azores, 97.
 Price, A., 1949. *Q. J. mech. appl. Math.*, **2**, 283.
 Proudman, J., 1914. *Proc. Lond. Math.*, **14**, 89.
 Ratcliffe, J. & Weekes, K., 1960. *Physics of the Upper Atmosphere*, ed. by Ratcliffe, J., p. 378, New York.
 Rikitake, T., 1964. *J. Geomagn. Geoelec.*, **16**, 31.
 Runcorn, S., 1964. *Nature, Lond.*, **202**, 10.
 Schmucker, U., 1966. *Marine Physical Laboratory Report*, University of California, San Diego.
 Stommel, H., 1954. *Arch. Met. Geophys. Bioklim.*, Ser. A, **7**, 292.
 Swift, D. & Wescott, E., 1964. *J. geophys. Res.*, **69**, 4149.
 van Bemmelen, W., 1912. *Meteorol. Z.*, **29**, 218; 1913. *Meteorol. Z.*, **30**, 589.
 Voppel, D., 1964. *Deutsche Hydrogr. Z.*, **17**, 179.
 Watt, A., Mathews, F. & Maxwell, E., 1963. *Proc. Inst. elect. electron. Engrs*, **51**, 897.

(Reprinted from *Nature*, Vol. 218, No. 5141, pp. 557-558,
May 11, 1968)

New Feature of the East Australian Current

As part of the global cruise of the Coast and Geodetic Survey ship *Oceanographer*, a brief investigation of the East Australian Current was conducted in September 1967 by personnel from the Pacific Oceanographic Research Laboratory and the Division of Fisheries and Oceanography. The results reported here are from oceanographic casts along 31° S. extending eastward 170 km from the Australian continental shelf. Closely spaced observations, made feasible by the satellite navigation system on board the ship, revealed some previously unknown details of the current.

Most of the previous observations of this current were presented and discussed by Hamon^{1,2}. The current is typically present as a narrow stream near the shore. South of 33° S., detached, fast-moving eddies are common, and the current location and pattern is quite variable with time. The current system eventually trends to the east and in part returns to the north far offshore. It is typical of western boundary currents in some but not all respects.

Density structure is frequently used to compute geostrophic flow relative to a selected reference level. Hopefully, this level has no horizontal motion; otherwise, all computed velocities are in error by its motion. For this study, the method of Defant³ was used to select zones of minimum shear which, he argued, represent zones of least horizontal motion.

The geostrophic flow across 31° S. is shown in Fig. 1. The south going East Australian Current, with peak speeds above 140 cm s⁻¹, is highly structured with speeds in excess of 50 cm s⁻¹ over a horizontal extent of about 40 km. From these data, volume transport of the East Australian Current was computed to be 29×10^6 m³ s⁻¹. A previously unreported counter-current is found shoreward of station 4. A maximum speed above 40 cm s⁻¹ is indicated at 200 m; volume transport above 1,000 m was computed to be 4×10^6 m³ s⁻¹.

Other data obtained on this cruise show that the East Australian Current diverged from the edge of the shelf in this area. It is possible that the observed counter-current was part of a local entrainment process, rather than a permanent feature of the current itself.

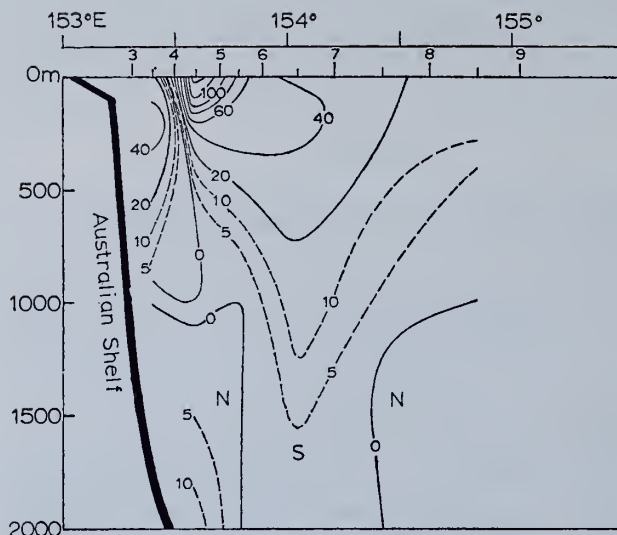


Fig. 1. Vertical section of geostrophic flow (cm s^{-1}), based on a reference level of variable depth, along 31°S , September 21–22, 1967. N and S indicate north and south flow, respectively.

Between stations 4 and 5, a deep northerly flow is indicated beneath the East Australian Current. This brings to mind similar flows reported under the Gulf Stream⁴⁻⁶. Volkmann⁵ found a counter-current from surface to bottom inshore of the Gulf Stream, but his near-surface speeds were much less than those reported here. Our data density, however, is inadequate to show if continuity exists between the upper and lower counter-currents.

R. K. REED
T. V. RYAN

Pacific Oceanographic Research Laboratory,
Environmental Science Services Administration,
Seattle, Washington.

B. V. HAMON
F. M. BOLAND

CSIRO Division of Fisheries and Oceanography,
Cronulla, New South Wales.

Received March 22, 1968.

¹ Hamon, B. V., *CSIRO Austral. Div. Fish. Oceanogr. Tech. Pap.*, No. 11 (1961).

² Hamon, B. V., *Deep-Sea Res.*, 12, 899 (1965).

³ Defant, A., *Physical Oceanography* (Macmillan, New York, 1961).

⁴ Swallow, J. C., and Worthington, L. V., *Deep-Sea Res.*, 8, 1 (1961).

⁵ Volkmann, G., *Deep-Sea Res.*, 9, 493 (1962).

⁶ Barrett, J. R., *Deep-Sea Res.*, 12, 173 (1965).

(Reprinted from *Nature*, Vol. 220, No. 5168, pp. 681-682,
November 16, 1968)

Transport of the Alaskan Stream

THE Alaskan Stream, a westward flow along the south side of the Alaska Peninsula and Aleutian Islands, has been known to exist for decades, but its westward extent, true speeds and other details were not generally recognized until much later. Based on observations made in the summer of 1959, Favorite¹ described the system and concluded that the Alaskan Stream is a narrow, western boundary current with peak surface speeds exceeding 50 cm/s. An analysis of data obtained by the Scripps Institution of Oceanography in January 1966 and by the Pacific Oceanographic Research Laboratory in September 1966 and 1967 shows that appreciable changes occur in volume transport and width of the Stream.

I wish to discuss here the volume transport in the upper 1,000 m only, because the more sparse deeper data indicate that variations in relative transport (assuming zero speed at 1,000 m) imply real changes in the system.

At 165° W the relative volume transport of the Stream in January 1966 was computed to be $8 \times 10^6 \text{ m}^3 \text{ s}^{-1}$. Results from a section very near 165° W in September 1966 indicate that the relative volume transport was $5 \times 10^6 \text{ m}^3 \text{ s}^{-1}$. The transports computed for September 1966 and September 1967 for an adjacent section differed by only $0.4 \times 10^6 \text{ m}^3 \text{ s}^{-1}$. These data also indicate that near 165° W the Stream was approximately twice as wide in winter as in summer. Farther west, Bureau of Commercial Fisheries data for 1965 and 1966 show winter and summer differences in transport and width very similar to these.

Uda^{2,3} concluded that northward transport into the Gulf of Alaska varies directly with the difference in atmospheric pressure in the Aleutian Low and North American Arctic High. This difference is large in winter and much smaller in summer⁴. The winter and summer differences in volume transport reported here are consistent with Uda's hypothesis, and the results imply that flow of the Alaskan Stream west of the Gulf of Alaska is correlated with the seasonal pressure systems.

I thank Dr Donald V. Hansen and Mr T. V. Ryan of the Environmental Science Services Administration for helpful suggestions.

R. K. REED

Pacific Oceanographic Research Laboratory,
Environmental Science Services Administration,
Seattle, Washington.

Received September 23, 1968.

¹ Favorite, F., *Intern. North Pac. Fish. Comm. Bull.*, 21 (1967).

² Uda, M., *Abst. Symp. Pap. Tenth Pacific Science Congress*, 345 (1961).

³ Uda, M., *J. Fish. Res. Bd. Canada*, 20, 119 (1963).

⁴ Dodimead, A. J., Favorite, F., and Hirano, T., *Intern. North Pac. Fish. Comm. Bull.*, 13 (1963).



TIDE TALK

By Bernard D. Zetler
Atlantic Oceanographic
Laboratories, Miami.

GO OCTOBER 1968

The Editor has invited me to write a column, hopefully monthly, combining a training of many years in tides with an abysmal lack of knowledge of local waters, of boating in general and of fishing. He has also informed me that I will not be permitted to hide behind horrendous mathematical formulas. I'm willing to try!

Although the ESSA Atlantic Oceanographic Laboratories arrived only recently in Miami, we receive a remarkably large number of phone inquiries requesting tide information for nearby waters. Although I try to oblige to the best of my ability, I am haunted by the thought that most of the callers don't want tide information and that what they really want is tidal current information. For example, in navigating small craft, the problem of current-induced drift is frequently more significant than the available depth of water at a given time. The question then is whether the caller knows enough of the local relationship between tide and tidal current to properly use the tide information. The relationship is not constant but varies from place to place. The time of slack water does not generally coincide with the time of high or low water nor does the time of maximum current usually coincide with the time of most rapid change in the vertical height of the tide. At stations located on a tidal river or bay, the time of slack water may differ from one to three hours from the time of high or low water. It is for this reason that the U.S. Coast and Geodetic Survey publishes tidal current tables as well as tide tables.

GO NOVEMBER 1968

A number of years ago, we were informed that on occasion the pilots were having a hard time bringing large aircraft carriers into the Brooklyn Navy Yard. We were somewhat horrified to find that, although tidal current predictions were available, the pilots were using a rule of thumb correction to tide predictions to obtain times of slack water. We ran tests and found that the rule of thumb conversion was ordinarily but not always dependable. The moral is— use tidal current predictions if they are available. (Tidal Current Tables, Atlantic Coast of North America, is an annual publication of the Coast and Geodetic Survey. Cost \$2. Information parallels copy of annual tide tables.)

The reason why tides and tidal currents do not have a set time relationship is that there are two types of tide waves, progressive and stationary (standing). A progressive wave is essentially what you will see if you throw a pebble into a still pond. A train of waves will move away from the starting point. If you could examine the water particle motion in the wave train, you would find that the maximum current forward is found at the crest (high water), the maximum current in the opposite direction is found at the trough (low water) and halfway between (mean water level) there is no horizontal motion.

A standing wave is easily imagined in a rectangular tank partially full of water when one end is suddenly tilted. The water will slosh back and forth with high water at one end occurring simultaneously with low water at the other and a nodal (no tide) line in the middle. At this moment there is no current anywhere in the tank. Then the water flows in the opposite direction with maximum speed when the level at the ends is at mid-water.

The observed tide at any point is some undetermined combination of progressive and standing waves and therefore the associated current is not readily inferred.

GO DECEMBER 1968

I have previously recommended that, if you need tidal current predictions, use the tidal current tables rather than the tide tables with some rule of thumb correction. You will find however that there are many places in the tide tables that are not covered in the tidal current tables. The reason is that, unlike tide observations, tidal current observations are quite difficult and expensive to obtain.

One could, if need be, install a marked ruler vertically in the water and read the height at fixed intervals of time to obtain reasonable good tide records. What is more, the data would be fairly representative of the tide at a number of nearby places. Tide gauges are inexpensive and require little attention. With current measurements, however, you need calibrated meters to measure both the direction and speed of the flow. You need to note the depth of the meter because at the same position but a different depth the current may be flowing in the opposite direction. Nearby you may have an eddy with different speeds and directions. All of this takes ships, buoys and expensive equipment. Consequently, we have current data for fewer places than we have tide observations, the observed series are usually shorter and the reliability of the observations is frequently poorer.

Marine Magnetic Study in the Northeast Chukchi Sea

B. G. BASSINGER

Institute for Oceanography, ESSA, Silver Spring, Maryland 20910

During the 1961 and 1962 field seasons, the U. S. Coast and Geodetic Survey conducted sea magnetometer operations off the northwest coast of Alaska. Tracklines, primarily oriented in a north-south direction and spaced at intervals of 10 km or less, provided adequate coverage for the delineation of prominent magnetic anomalies. A distinct change in character of the residual magnetic intensity contours occurs at about 165°30'W. Very little magnetic relief exists east of this longitude, but, to the west, a north-south trending magnetic feature with anomalies of up to 450 gammas was mapped. The feature appears to be more closely related to north-south structures associated with the Tigara uplift than to the east-west trends of the Colville geosyncline. The increase in magnetic intensity is interpreted as a shallowing of the basement surface that indicates a northern continuation of the Tigara uplift.

Introduction. As part of a systematic survey off the northwest coast of Alaska, the U. S. Coast and Geodetic Survey ship *Surveyor* collected total magnetic field intensity data during July, August, and September of 1961 and 1962. Survey operations were conducted over an area of approximately 47,300 km² (Figure 1), in a region where bottom topography is of very low relief and water depths seldom exceed 55 meters. The ship's position, primarily along north-south oriented tracklines spaced at intervals of 10 km or less, was determined by Raydist navigation control. Although the study area is located at latitudes where magnetic disturbances occur frequently, the density of data provides adequate coverage for the delineation of prominent magnetic anomalies.

Geology. As a result of seismic studies in Naval Petroleum Reserve 4, the arctic slope of northern Alaska was found to be a large sedimentary basin with the deepest part of the basin in the foothills north of the Brooks Range. Principal rocks of the basin are Cretaceous in age and range in thickness from about 0.5 km in the Point Barrow area to 4.5 to 6.0 km near the Brooks Range [Woolson *et al.*, 1962]. To the west of this area, Miller *et al.* [1959] have described the Chukchi basin as having a thick sequence of Cretaceous sedimentary rocks. In the Cape Lisburne area of northwestern Alaska, Payne [1955] indicates that the Tigara uplift contains Paleozoic and Triassic rocks upfaulted and lying adjacent to great thicknesses of Mesozoic rocks.

Off the northwest coast of Alaska, the shelf varies in width from 75 km north of Point Barrow to 750 km in the Chukchi Sea. The shelf is of low relief with average depths of 45 to 55 meters and gradients of 1 m/km to local maximum gradients of 40 m/km [Creager and McManus, 1965]. In the Chukchi Sea area, the investigations of Dietz *et al.* [1964] suggest that the shelves are ancient peneplains that have been modified by many transgressions and regressions of the sea. This suggestion has been supported for part of the northeast Chukchi Sea, as a result of seismic reflection studies conducted by Moore [1964].

Magnetic data. A Varian nuclear resonance magnetometer was used to measure the earth's total magnetic field intensity. The sensing unit was towed behind the ship at a minimum distance of 135 meters, resulting in the effect of the ship's field on the measured values to be less than 10 gammas for north-south oriented tracklines.

Magnetic data collected aboard ship were evaluated by correlation between adjacent tracklines and by comparison with magnetograms from Barrow Magnetic Observatory. When disturbances at the observatory were greater than 100 gammas in vertical intensity and/or no correlation of adjacent lines was possible, the total magnetic intensity values were not used in the contouring process. Although approximately 25% of the data was judged to be questionable, the survey provided

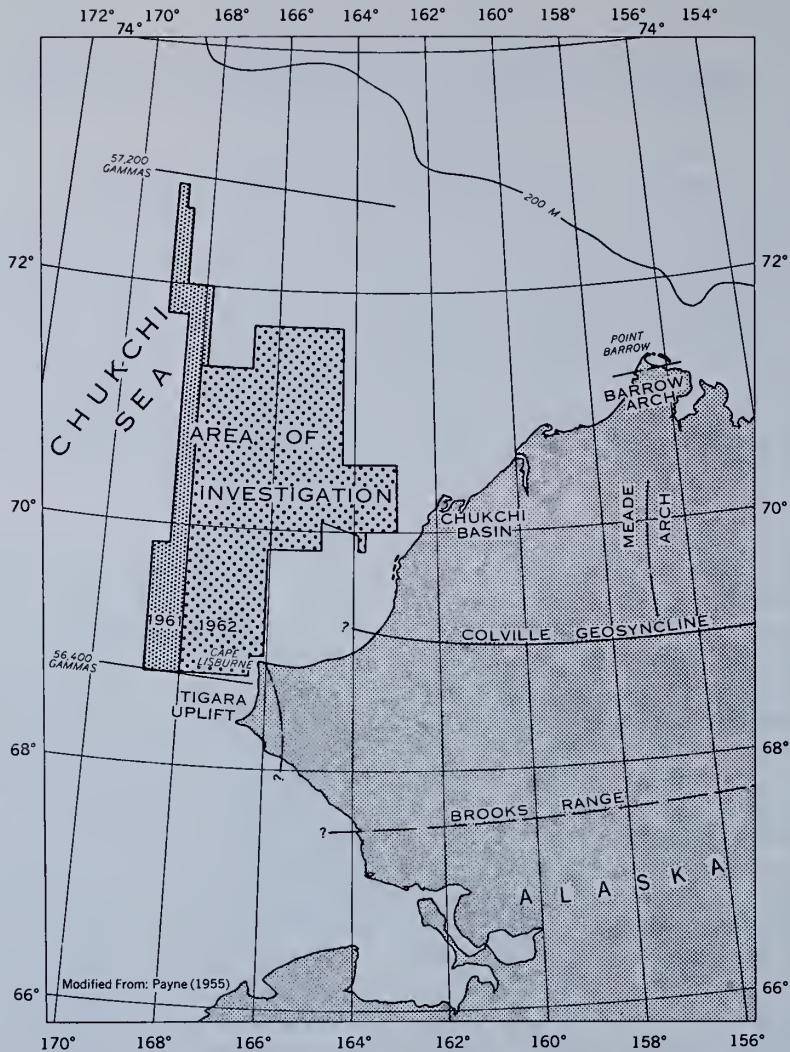


Fig. 1. Index map showing geologic trends and regional magnetic field.

a line spacing of acceptable values of 10 km or less.

Magnetic data obtained on the project were not corrected for temporal variations. A comparison of adjacent tracklines revealed that neither daily nor secular variations of the magnetic field effected the observed values enough to justify a correction. Nevertheless, all discrepancies between observed magnetic values were smoothed in the contouring process.

Anomaly map. A regional gradient of the total magnetic field intensity was determined from Hydrographic Office Chart 1703 (1955). The chart was corrected to 1962 and adjusted

to the observed magnetic values for conformity. No adjustment was required at 68°N, but, at 71°N, these data indicate that the residual field is 400 gammas lower than the field shown by the world chart. This discrepancy probably reflects a lack of control in the compilation of the 1955 world chart.

Two iso-gamma lines that represent the magnitude and direction of the earth's magnetic field are shown in Figure 1. A linear interpolation between the lines defines the plane used to determine residual values. Shaded areas of the residual map (Figure 2) represent zones where observed values exceeded the regional field,

and, conversely, areas that are not shaded indicate zones where observed values were lower than the regional field.

The residual magnetic field contour map indicates two prominent features: a central magnetic high and a northern magnetic high. In the study area west of 165°30'W, the central magnetic high and its corresponding western low form a dominant trend over a major portion of the anomaly map. The magnetic high indicates a prominent north-south lineation with anomalies of up to 450 gammas. This feature compares favorably with observations made during a regional seaborne magnetic survey

[*Ostenseo and Parks, 1964*]. The northern magnetic high centered at about 71°15'N and 168°15'W is the sharpest magnetic feature observed in the study area. It reveals an anomaly of up to 650 gammas with about a north 45° east strike. The anomaly's position and orientation agree with an anomaly previously reported by *Ostenseo* [1962]. Also, several other magnetic traverses in the Chukchi Sea appear to indicate that the high is part of a continuous feature that crosses the shelf.

East of the central magnetic high, the magnetic field is of very low relief. This widely spaced contour interval agrees favorably with

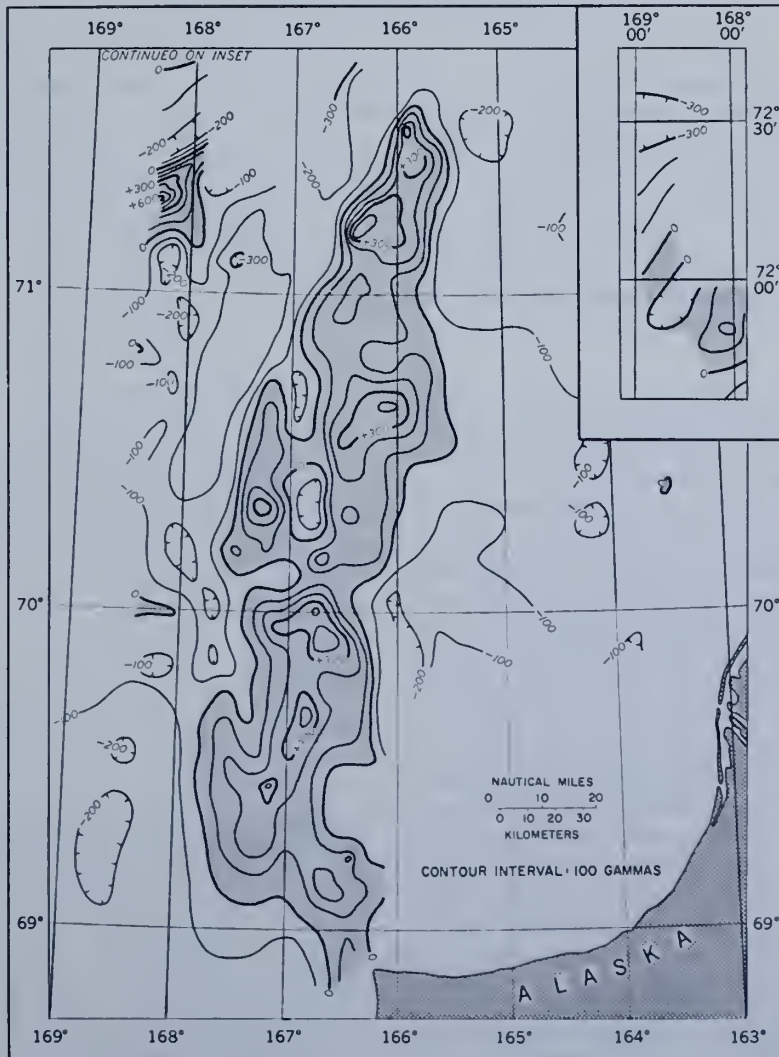


Fig. 2. Residual magnetic field intensity contour map.

an adjacent airborne magnetic survey by the Naval Petroleum Reserve [Woolson *et al.*, 1962].

Discussion. Bathymetric data reveal no significant features that could account for the magnetic anomalies found in the study area. Therefore, these anomalies are the result of either an intrabasement contrast or a relief on the basement surface. Gravity and seismic reflection data give supporting evidence for the latter interpretation.

The central magnetic high is the most significant magnetic feature. A seismic reflection profile crosses the magnetic feature along approximately $70^{\circ}25'N$ and indicates a fault with upthrown side to the west at the eastern margin of the central magnetic high [Moore, 1964]. To the west of the fault, a zone of east dip is indicated from about $167^{\circ}W$ to the indicated fault, a traverse of approximately 45 km, whereas, to the east of the fault, tighter folding with some faulting is present. This change in the nature of subbottom structures at the fault and the corresponding difference in the character of magnetic contours suggest that the origin of the fault may be related to a displacement in the basement rock complex. The eastern margin of the uplifted section apparently can be traced over a major portion of the study area and appears to be related to the Tigara uplift.

A free-air anomaly map by Ostenso and Parks [1964] correlates well with the magnetic anomaly map. Although their map is based on a limited number of gravity observations, it does show a north-south contour development with an increase in gravity coincident with the magnetic anomaly. Not enough is known about the subsurface structure and lithology to make a reliable correlation, but, considered together, the magnetic and gravity data suggest that the Tigara uplift, identified in the Cape Lisburne area west of about $165^{\circ}30'W$, is part of a much larger geologic feature to the north.

Low magnetic relief shown on the eastern part of the anomaly map could be the result of either a thick sedimentary cover or crystalline rocks of low magnetic susceptibility at shallow depths. However, with a thick sedimentary cover known to exist in the Chukchi basin, it would appear that this cover extends westward into the study area to approximately $165^{\circ}30'W$.

Depth estimates based on gravity and magnetic data support the conclusion that the central magnetic high is a result of a basement ridge. Assuming lateral density stability and a density differential of 0.2 g/cm^3 between sediments and basement rocks, the 30-mgal increase in gravity from east to west over the study

area, indicated by Ostenso and Parks [1964], could represent a decrease in sedimentary cover of 3.6 km. Peters' method [Dobrin, 1952] was used to estimate depths on some of the individual magnetic anomalies associated with the central magnetic high. They indicate an average depth of 2.7 km to the upper surface of the magnetic source. This depth is considerably shallower than the 4.5-km minimum depth of Cretaceous sediments indicated in the basin. Therefore, the central magnetic high is interpreted as a shallowing of the basement surface that indicates a northern continuation of the Tigara uplift.

The northern magnetic high is the most prominent magnetic anomaly. Its sharpness is indicative of a near surface source. An increase in gravity associated with this feature suggests that the anomaly is caused by a geologic body of high density and high magnetic susceptibility. It could be a result of basaltic intrusions, as suggested by Ostenso [1962].

Acknowledgments. I am grateful to the officers and men of the U. S. Coast and Geodetic Survey ship *Surveyor* and to geophysicists who participated in this project. I am particularly indebted to G. Peter, R. K. Lattimore, and R. J. Malloy of the Institute for Oceanography for their helpful suggestions.

REFERENCES

- Creager, J. S., and D. A. McManus, Pleistocene drainage patterns on the floor of the Chukchi Sea, *Marine Geol.*, **3**, 279, 1965.
- Dietz, R. S., A. J. Carsola E. C. Buffington, and C. J. Shipek, Sediments and topography of the Alaskan shelves, in *Papers in Marine Geology*, edited by R. L. Miller, pp. 241-256, Macmillan, New York, 1964.
- Dobrin, M. B., *Introduction to Geophysical Prospecting*, McGraw-Hill, New York, 1952.
- Miller, D. J., T. G. Payne, and G. Gryc, Geology of possible petroleum provinces in Alaska, *U. S. Geol. Surv. Bull.*, **1094**, 1959.
- Moore, D. G., Acoustic-reflection reconnaissance of continental shelves: Eastern Bering and Chukchi seas, in *Papers in Marine Geology*, edited by R. L. Miller, pp. 319-362, Macmillan, New York, 1964.
- Ostenso, N. A., Geophysical investigations of the Arctic Ocean Basin, *Univ. Wisconsin, Geophys. Polar Res. Ctr., Res. Rept.* **62-4**, 1962.
- Ostenso, N. A., and P. E. Parks, Jr., Seaborne magnetic measurements in the Chukchi Sea, *Univ. Wisconsin, Geophys. Polar Res. Ctr., Res. Rept.* **64-5**, 1964.
- Payne, T. G., Mesozoic and Cenozoic tectonic elements of Alaska, *U. S. Geol. Surv. Misc. Geol. Invest. Map I-84*, 1955.
- Woolson, J. R., et al., Seismic and gravity surveys of Naval Petroleum Reserve No. 4 and adjoining areas, *U. S. Geol. Surv. Prof. Paper 304-A*, 1962.

(Received August 7, 1967.)

The Boron-salinity Relationship in Estuarine Sediments of the Rappahannock River, Virginia¹

JOHN D. BOON III

*Land and Sea Interaction Laboratory
Institute for Oceanography, ESSA
Norfolk, Virginia 23510*

WILLIAM G. MACINTYRE

*Virginia Institute of Marine Science
Gloucester Point, Virginia 23062*

ABSTRACT: Twelve sediment cores from the lower Rappahannock estuary in Virginia were analyzed for boron concentration, clay-silt ratio, and percent organic carbon. Clay-silt ratios and percent organic carbon, along with distance upstream in nautical miles and average water salinity, were used as independent variables in linear regression plots with boron concentration as the dependent variable. The results show a lack of correlation between boron concentration and either the clay-silt ratio or the percent organic carbon; however, both a negative correlation with distance upstream and positive correlation with salinity appear to be real. This is taken as evidence supporting the theory of boron incorporation in fine-grained sediments in amounts proportional to the salinity of the depositional environment.

Introduction

Minor amounts of boron in argillaceous sediments are thought to have been derived from overlying saline waters. Research efforts to date strongly suggest that boron concentration in marine sediments is a function of the depositional environment, a relationship which the present study seeks to explore through analysis of contemporaneous sediments and environmental conditions.

Relatively high concentrations of boron (in the ppm range) were first noticed in marine shales by Goldschmidt and Peters (1932). Landergren (1945, 1958) later demonstrated a direct linear relationship between boron in ancient clays and the paleosalinity of the depositional environ-

ment. Other workers (Degens *et al.*, 1957, 1958; Ernst *et al.*, 1958; Walker and Price, 1963; Ernst, 1963; Potter *et al.*, 1963) conducted investigations hoping to confirm Landergren's relationship over wider areas and conditions. Landergren (1964) suggested a two-step mechanism for boron incorporation in marine sediments, assuming an adsorption process, followed by a more permanent incorporation of the element in the lattice structure of clay minerals.

Recently, various aspects of the boron-paleosalinity relationship have been criticized. Hirst (1962) pointed out that differing rates of deposition will affect boron concentrations in sediments laid down under similar salinity conditions. Other authors (e.g. Spears, 1965) have shown that terrigenous source material contains varying amounts of boron and such deposits may reflect local weathering conditions. Hirst (1962) concluded that the

¹Contribution 13, Land and Sea Interaction Laboratory (LASIL) 439 West York Street, Norfolk, Virginia 23510.

Contribution 265, Virginia Institute of Marine Science, Gloucester Point, Virginia 23062.

greater part of the boron located in clay minerals in modern sediments from the Gulf of Paria arrived in the basin of deposition fixed this way. Unusually high boron concentrations in some Japanese rivers have been related to vulcanism (Livingstone, 1963), while argillaceous rocks of evaporitic or desert-type environments evidence a possible climatic factor as the cause of their high boron contents (Ernst, 1963). The consequences of extensive reworking of marine illitic clays have been examined by Harder (1961) and others.

Goldberg and Arrhenius (1958) studied the bonding of boron in pelagic clays and concluded that the element exists in authigenic ferromagnesian minerals or substitutes for silicon in the tetrahedral layer of certain clay minerals. Levinson and Ludwick (1966), on the other hand, proposed that river water is the source of most of the boron in marine clays, and that boron in sea water somehow behaves differently than boron in river water. The boron in freshwater is adsorbed in part or completely by fine sediment particles in suspension when a salinity gradient is met in an estuary. The authors, who referred mainly to a deltaic environment, concluded that boron-enriched fine sediment from rivers does not settle out until it has traveled some distance from land. Hence, according to them, the observed boron-salinity relationship is coincidental, the real relationship being between boron concentration and particle size gradation with distance from shore.

A further complication has been treated by Eager (1962) and Curtis (1964), who advocated a negative correlation between boron and organic carbon content such as they had observed in certain British coal measure sediments. Moreover, Bader (1962) demonstrated that clay minerals could quickly adsorb up to 350% of their own mass of soluble organic matter from solution. He supposed that strong bonding of organic material to individual clay particles provided an effective barrier against further inclusion of ionic boron.

In spite of the controversial aspects of boron and its relation to marine deposits, a substantial amount of empirical data has

been gathered in support of its use as a paleosalinity indicator. The foremost study of this type is that of Potter *et al.*, (1963), who examined groups of ancient and modern, marine and non-marine sediments taken from many different depositional basins. Their analyses for several trace elements, including boron, were used as variables in multivariate discriminant tests attempting separation of the marine and freshwater environments. The most efficient discriminant function was based on boron and vanadium alone for 33 modern sediments. Using this combination to test 33 ancient sediments whose depositional environments were known, 85% of the samples were correctly identified as marine or non-marine. Similar results have been obtained with boron and gallium (Degens *et al.*, 1957) and boron and lithium (Keith and Bystrom, 1959).

Area of Investigation

The lower Rappahannock estuary (Fig. 1) was selected for an investigation of the boron-salinity relationship in modern sediments because of its known salinity gradient, over the range of 3 to 18‰, and its predominantly silt and clay bottom sediments, which were likely to produce significant amounts of boron in whole-sample analyses. Also the presence of industrial contaminants was less evident here than in other Chesapeake Bay estuaries.

The lower portion of the Rappahannock varies from 1 to 2 miles wide and has mid-channel depths of between 15 and 70 feet. The geometry of this estuary is largely the product of subaerial erosion during the Pleistocene epoch, the present bathymetry resulting from the drowning of the ancient river valley. Relatively sluggish bottom currents near the center of the channel make this area an effective settling basin for fine-grained sediments.

Twelve short cores, each 2 inches in diameter, were obtained near the center of the river channel at intervals of approximately 3 nautical miles, beginning due east of Urbanna, Virginia, near Towles Point (Fig. 1) and proceeding upstream. Two adjacent cores were taken at the same location near the mid-range point (Fig. 1, Sta-

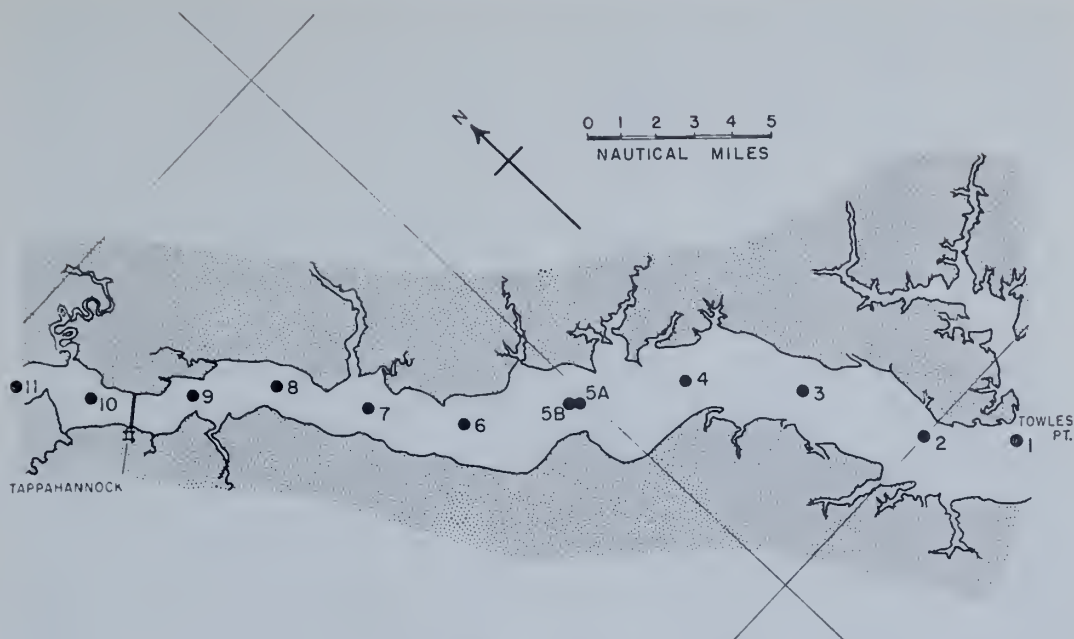


Fig. 1. Coring stations in the Rappahannock River.

tion 5) as a check on local variation. The sealed cores were frozen shortly after collection to prevent biochemical action.

Analytical Method

The sediment cores were thawed and extruded; the top centimeter of sediment was removed, washed, and a portion of it dried. Dried portions were ground powder-fine in an agate mortar and stored in plastic vials.

The carminic acid spectrophotometric method of Hatcher and Wilcox (1950), in combination with the standard means of dissolving rock samples by sodium carbonate fusion in a platinum crucible, was used for analysis of sample boron content. Although the carminic acid is not as sensitive as other color forming complexors such as 1-1' dianthrimide (Werner, 1959), it has the advantages of rapid color development and a reproducible standard curve that permit efficient analysis.

Duplicate analyses were made on each sediment sample, except for Station 1 where a part of the sample was lost. Mixtures of 0.50 g of sample and 2.50 g of sodium carbonate were fused, then dissolved in sufficient hydrochloric acid to attain a

pH of 5.7–5.8. The resultant precipitate, mostly silica, trivalent iron oxide, and alumina, was removed by centrifugation and the remaining solution evaporated to dryness at 95 C. The dried residue was taken up with 5.00 ml of dilute hydrochloric acid and centrifuged so that a 2.0 ml aliquot of the clear liquid could be drawn off. Each aliquot was combined with two drops of concentrated hydrochloric acid and 10 ml of concentrated sulphuric acid in a small flask and allowed to cool. After cooling, 10.0 ml of 0.05% carmine (alum lake) in concentrated sulphuric acid was added to the solution, which was then mixed and allowed to stand 50 minutes for color development.

The absorbance of each sample was determined at 585 $m\mu$ in 1 cm quartz cells using a Coleman Model 30 Autoset spectrophotometer. All concentrations were derived from a standard curve based on 2.0 ml aliquots of sodium borate solution covering the range 0 to 10 ppm. Due to the small quantity of sample (0.5 g) ingested during fusion and the minute quantities of boron involved, actual boron concentration for each sample could be obtained from the standard curve by multiplying each read-

TABLE 1. Boron concentrations (ppm) in Rappahannock River sediment.

Core no.	Run 1	Run 2	*Distance (N. Mi.)
1	36.0	—	0.0
2	42.5	47.0	3.0
3	62.0	63.0	6.4
4	33.0	30.0	9.3
5A	21.5	19.5	12.7
5B	51.5	43.5	12.7
6	21.0	27.5	15.9
7	22.0	28.5	18.4
8	51.0	48.5	20.9
9	25.0	13.5	23.4
10	34.5	42.5	26.1
11	25.5	18.5	28.9

* Linear distance upstream from first core at buoy R"6" off Towles Point.

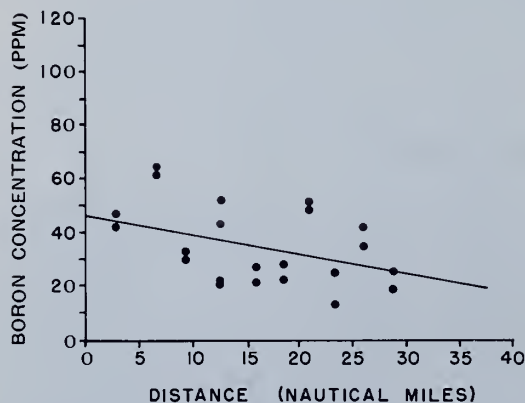


Fig. 2. Boron concentration vs distance upstream.

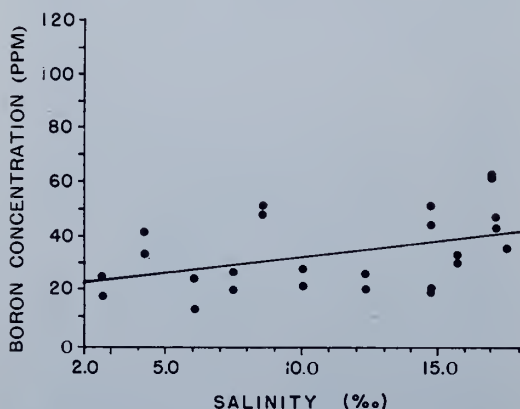


Fig. 3. Boron concentration vs average salinity.

ing in ppm by a factor of ten. The standard rock sample W-1 of the U.S. Geological Survey was analyzed as a check for the absolute accuracy of the technique. Values

of 3 to 14 ppm were obtained by the author, as compared to the reported value of 17 ppm. These low readings are believed to result from incomplete separation of boron from the ferromagnesian matrix material of W-1, a diabase, so that a loss of boron and inclusion of interfering elements may have occurred during its analysis. Standard clays are not now available and acidic rock standards contain no appreciable boron.

To avoid contamination, Nalgene labware was used exclusively, the only exceptions being some Pyrex centrifuge bottles coated inside with Gulf Microwax, and the necessary platinum hardware.

In addition to the boron analyses, pipette analyses (Krumbein and Pettijohn, 1938) were run on the undried portions of the initial samples and sand-silt-clay percentages were determined. Also, organic carbon analyses were made on the remaining portions of the samples using a Leco carbon analyzer (after washing the samples with dilute acid to remove carbonate).

Results

Results of the boron analyses are presented in Table 1. Boron concentrations were plotted against distances upstream in nautical miles (Fig. 2) and average salinity (Fig. 3) as determined from cruise data of the Virginia Institute of Marine Science, Gloucester Point, Virginia. Linear regressions of distance upstream and salinity on boron concentration yielded correlation coefficients of -0.43 and 0.41 , respectively. Thus, the direct relationship between boron and salinity appears to hold but amid considerable sample variation. In an attempt to account for this variation, boron values were plotted against clay-silt ratios (Fig. 4); a positive correlation coefficient of 0.16 was obtained, offering no support for the common theory that finer-sized material and particularly clay minerals should contain more boron than the coarser fractions. Furthermore, a plot of boron concentrations against percent organic carbon (Fig. 5) produced a similarly low correlation coefficient of 0.15 although a significant organic carbon content was evident in most samples (mean = 2.0%).

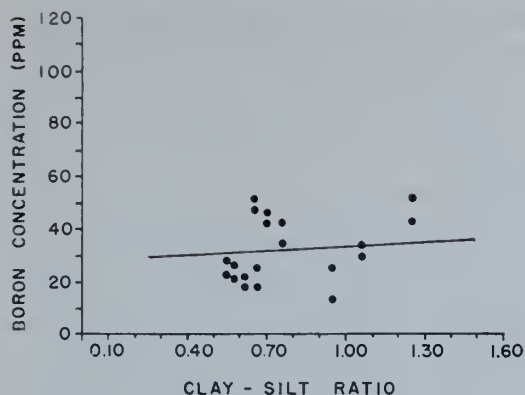


Fig. 4. Boron concentration vs clay-silt ratio.

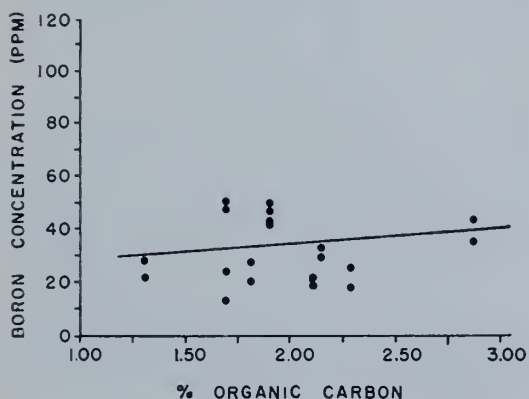


Fig. 5. Boron concentration vs % organic carbon.

For the boron data alone, a mean difference of 5.5 ppm between duplicates of each sample compares to an overall sample standard deviation of ± 14.1 ppm. This suggests that the apparent local variation of boron concentration is real and not the result of the analytical method. Cores 5A and 5B, taken within a few feet of one another, show a boron difference of almost 30 ppm, far more than could be accounted for by the experimental procedure. The mean boron concentration of all samples was 35.1 ppm. This appears low compared to some estuarine muds unless high carbon content is considered. (Eager, 1962, quotes an average value of 48 ppm for some highly organic sediments in England.)

Discussion

Although the data of this study indicate a direct relationship between boron concentration and salinity, considerable de-

viation from the predicted boron values of the regression analysis was seen within the area of concern. The factors suspected of contributing to this deviation, namely the clay-silt ratio and the percent organic carbon, proved to be of little significance and other factors as yet unknown must be important. For example, other elements in the sediment may interfere in the analyses, or perhaps industrial wastes containing boron are nonrandomly distributed in the estuary.

In view of the results of the present study, little can be offered in the way of support for the theory of Levinson and Ludwick (1966), which stipulates that the boron contained in river water is adsorbed in increasingly greater amounts by the finer-grained estuarine and marine sediments. If this were a major process, one should expect some correlation between boron concentration and the clay-silt ratio of the Rappahannock sediments (Fig. 4). Distance upstream and salinity appear to be only variables evidencing any correlation with boron concentration.

Evidence of chemical difference between freshwater and sea water boron, as proposed by Levinson and Ludwick (1966) is not conclusive. These authors referred to Noakes and Hood (1961) as stating that boron occurs in both organic and inorganic form in sea water. However, Noakes and Hood report that the amount of boron occurring as organic complexes is only 0.0 to 0.8% of the total dissolved boron. This is in agreement with the theoretical calculations of Williams and Strack (1966). Lerman (1966), meanwhile, performed laboratory experiments showing that the uptake of boron by clays in bottles of artificial sea water was proportional to the amount of dissolved inorganic boron in the bottles. Because the boron content of natural sea water is directly proportional to the salinity, Lerman's results constitute prima facie evidence that the boron-salinity relationship is real and that organic complexing of boron is not essential to boron uptake by sediments.

The question of selective acquisition of boron by certain types of clay minerals, such as illite, must remain unanswered in

the present study. Nelson (1960) qualitatively discussed the clay mineralogy of the lower Rappahannock, but little is known in a quantitative way of the distribution of the various clay mineral species.

Conclusion

The accumulated evidence in the literature and the results of this study tend to confirm the boron-salinity (paleosalinity) relationship. Nevertheless, certain complicating factors such as varying rates of deposition, addition of terrigenous or reworked marine material of varying boron content, and other local effects must be taken into account before attempting to use boron concentrations in sediments to predict salinity conditions. Probably the most convincing paleosalinity data results when argillaceous rock and sediment analyses for a pair of chemical indicators are used in statistical procedures such as the multivariate discriminant test.

REFERENCES CITED

- BADER, R. G. 1962. Some experimental studies with organic compounds and minerals. *University of Rhode Island Occasional Pub. No. 1*.
- CURTIS, C. D. 1964. Studies on the use of boron as a paleoenvironment indicator. *Geochim. Cosmochim. Acta*, 28:1125-1137.
- DEGENS, E. T., WILLIAMS, E. G., AND KEITH, M. L. 1957. Environmental studies of carboniferous sediments: Part I. Geochemical criteria for differentiating marine and fresh water shales. *Bull. Amer. Ass. Petrol. Geol.* 41: 2427-2455.
- , ———, AND ———. 1958. Environmental studies of carboniferous sediments: Part II. Application of geochemical criteria. *Bull. Amer. Ass. Petrol. Geol.* 42:981-997.
- EAGER, R. M. C. 1962. Boron content in relation to organic carbon in certain sediments of the British Coal Measures. *Nature Long.* 196:428-431.
- ERNST, W. 1963. Diagnose der Salinitätsfazies mit Hilfe des Bors. *Fortschr. Geol. Rheinland Westfalen*, 10:253-266.
- , KREJCL-GRAF, K., AND WERNER, H. 1958. Parallelisierung von Leithorizonten im Ruhrkarbon mit Hilfe des Bor-Gehaltes, *Geochim. Cosmochim. Acta*, 14:211-222.
- GOLDBERG, E. S., AND ARRHENIUS, G. O. S. 1958. Chemistry of Pacific pelagic sediments. *Geochim. Cosmochim. Acta*, 13:153-212.
- GOLDSCHMIDT, V. M., AND PETERS, C. 1932. Zur geochemie des Bors II. *Nachr. Ges. Wiss. Göttingen* 4:528p.
- HARDER, H. 1961. Einbau von Bor in detritische Tonminerale. *Geochim. Cosmochim. Acta*, 21: 669-694.
- HATCHER, J. T., AND WILCOX, L. V. 1950. Colorimetric determination of boron using carmine. *Anal. Chem.* 22(4):567-569.
- HIRST, D. M. 1962. The geochemistry of modern sediments from the Gulf of Paria II: The location and distribution of the trace-elements. *Geochim. Cosmochim. Acta*, 26:1147-1187.
- KEITH, M. L., AND BYSTROM, A. M. 1959. Comparative analyses of marine and fresh-water shales. *Penn. State Univ., Mineral Inds. Expt. Sta. Bull.*
- KRUMBEIN, W. C., AND PETTIJOHN, F. J. Manual of sedimentary petrography. New York: Appleton-Century-Crofts, Inc., (1938). 549p.
- LANDERGRÉN, S. 1945. Distribution of boron in some Swedish sediments, rocks and iron-ores. *Ark. Kemi. Min. Geol.* 19A:1-31.
- . 1958. On the distribution of boron on different size classes in marine clay sediments. *Geol. Foren. Stockholm Forh.*, 80:104-107.
- . 1964. On the geochemistry of deep-sea sediments. *Rep. Swedish Deep-Sea Expedition 1947-1948, Vol. X, Special Investigations No. 5*.
- LERMAN, A. 1966. Boron in clays and estimation of paleosalinities. *Sedimentology*, 6:267-286.
- LEVINSON, A. A., AND LUDWICK, J. C. 1966. Speculation on the incorporation of boron into argillaceous sediments. *Geochim. Cosmochim. Acta*, 30:855-861.
- LIVINGSTONE, D. A. 1963. Chemical composition of rivers and lakes. *U. S. Geol. Surv. Profess. Paper 440-G*.
- NELSON, B. W. 1960. Clay mineralogy of the bottom sediments. Rappahannock River, Virginia. *Seventh Natl. Conf. Clays Clay Minerals*: 135-147.
- NOAKES, J. E., AND HOOD, D. W. 1961. Boron-boric acid complexes in sea-water. *Deep-Sea Res.* 8:121-129.
- POTTER, P. E., SHIMP, N. F., AND WITTERS, J. 1963. Trace elements in marine and fresh-water argillaceous sediments. *Geochim. Cosmochim. Acta*, 21:669-694.
- SPEARS, D. A. 1965. Boron in some British carboniferous rocks. *Geochim. Cosmochim. Acta*, 29:315-328.
- WALKER, C. T., AND PRICE, N. B. 1963. Departure curves for computing paleosalinity from boron in illites and shales. *Bull. Am. Assoc. Petrol. Geologists*, 47:833-843.
- WERNER, H. 1959. Serienbestimmung von Bor in Sedimentgesteinen. *Anal. Chem.* 168:266-268.
- WILLIAMS, P. M., AND STRACK, P. M. 1966. Complexes of boric acid with organic cis-diols in seawater. *Limn. and Ocean.* 11(3):401-404.

Reprinted from Journal of Geology Vol.76, No.1

TREND SURFACE ANALYSIS OF SAND TRACER DISTRIBUTIONS ON A CARBONATE BEACH, BIMINI, B.W.I.¹

JOHN D. BOON III²

Land and Sea Interaction Laboratory, Institute for Oceanography, ESSA

ABSTRACT

Two-dimensional trend surface analyses were performed on areally distributed tracer-concentration data for three different fluorescent sand tracers recovered from four depth intervals of the foreshore. The tracers had been affected by the swash, breakers, and longshore currents of one tidal cycle. Analysis of the statistical significance of trend surfaces for each depth interval showed that only the upper 2.5 cm. of the sand column evidenced definite trend components. Differential sorting of tracers of different shapes and mean grain sizes was probably negligible, as deduced from the similarity in direction of orthogonals to the trend surface contours for the various tracer data.

The advantage of the trend surface method of describing sand movement patterns on beaches lies in its ability to represent, in an objective manner, the average movement of sand grains by means of a single representative equation. Furthermore, for time scales of the order of minutes to several hours, the motion of sand is seldom parallel to the shore line. Studies attempting to define over-all particle drift at such time scales will be more meaningful where areal concentration data are objectively analyzed, as opposed to the subjective analysis of linear concentration data from samples collected parallel to the shore line.

INTRODUCTION

The following is a technique study, combining two comparatively new innovations—that of tracing the movement of beach sand with particles coated with fluorescent dye, and two-dimensional trend surface analysis of tracer-concentration data.

Investigators of the drift of beach sand have difficulty in predicting long-term trends because of the irregularities in rate and direction of movement resulting from the inherent variability in the hydrodynamic conditions of the littoral zone. Many attempts have been made with varying degrees of success to equate beach changes with environmental conditions (e.g., Caldwell, 1956; Miller and Zeigler, 1958; Zeigler and Tuttle, 1961; Harrison, Pore, and Tuck, 1965). In order further to refine future investigations of this nature, it is desirable to describe observed patterns of sand movement in a more objective way. The present exploratory study is concerned with the description of the movement of sand during one tidal cycle in the foreshore zone of a carbonate beach on the island of North Bimini, B.W.I. (fig. 1).

¹ Manuscript received January 26, 1967.

² Contribution 10, Land and Sea Interaction Laboratory (LASIL), 439 West York Street, Norfolk, Virginia 23510.

The Bimini Islands are located at the extreme northwestern corner of the Great Bahama Bank, approximately 50 nautical miles east of Miami, Florida (fig. 1, *inset*). A short distance from the western shore of these islands lie the Florida Straits and the Florida Current. During most of the year, the islands are subject to light easterly trade winds; however, storms with northwesterly winds commonly occur during winter months.

The area chosen for study was an uninterrupted strip of beach northeast of Paradise Point (fig. 1) on North Bimini. This beach is exposed to deep-water waves generated to the west and north and is unprotected from northwest winds. At the time of the present experiment, the beach slope just seaward of the berm was 11 degrees; the slope angle diminished gradually to 5 degrees at the low-tide position. The foreshore was smooth, with little debris. A slight cusp development was present near the berm crest. The width of the foreshore from the low-water line to the berm crest was approximately 15 m.

DESIGN OF EXPERIMENT

PREVIOUS INVESTIGATIONS

Wright (1962) assumed that tracer sand of a given size would move within a narrow band parallel to the beach contours in

following the general direction of particle drift on the foreshore. At Sandy Hook, New Jersey, Wright observed tracer-particle frequency decreasing with increasing distance from the injection point parallel to the beach contours. He also observed the

pattern of tracer concentration along a number of azimuths extending outward from a point of tracer injection and stated: "The results of Trial D in which movement was generally up the beach slope as well as parallel to the contours, despite the falling

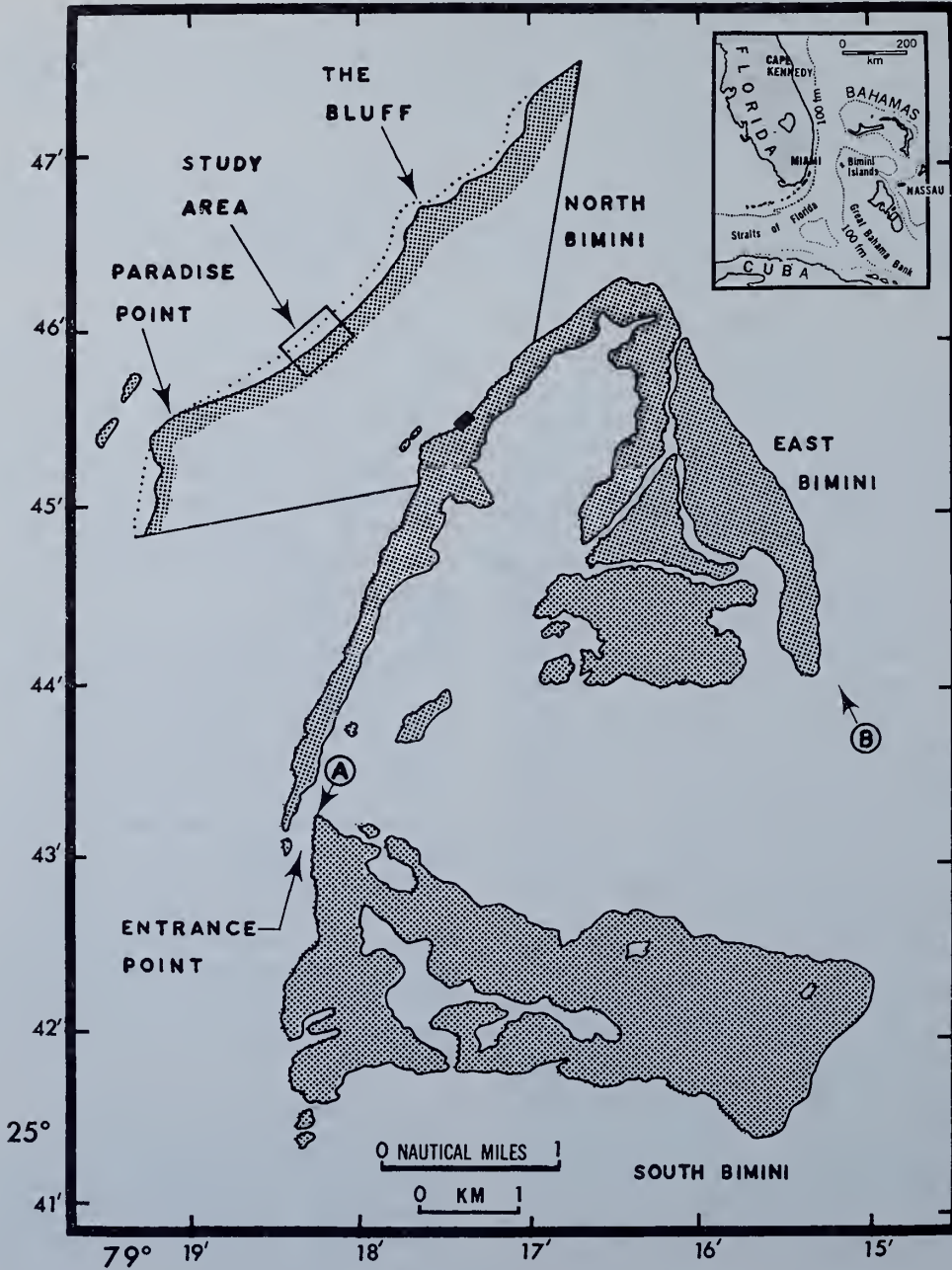


FIG. 1.—Location map showing Bimini Islands and area of study

tide during the study period, are also of interest and deserve more study" (p. 19).

Russell (1960) investigated the use of pebble tracers to obtain quantitative estimates of littoral drift. This he achieved by continual point injection of tracer material at 1-week intervals, noting the variation of tracer concentration with distance and applying a special dilution theory to the observed distribution patterns. He assumed that particles of a given size would seek specific beach contours and would confine their movement to these zones, a closed two-way system of transport, in effect. Russell counted only surface particles, leaving open the question of variation of particle concentration with depth.

A comprehensive report on beach sand movement has been presented by Ingle (1966). A portion of his work was devoted to quantitative results in which he correlated average grain velocity at the surface with relative alongshore wave energy. Average grain velocity was estimated by first measuring the area between grain-concentration contours at different times to determine the depletion rate or percentage of the original number of grains leaving the study area during specific time intervals. The average grain velocity was then obtained by dividing the average distance of tracer travel (injection point to main exit from the study area) by the time required for one-half of the initial tracer quantity to become depleted. Again, certain problems in interpretation of rates of grain drift may result from the decision to ignore tracer distribution below the beach surface.

Another approach to estimating sand particle velocity has been that of the time-integration method. Using this method, the arrival of "modes" or maximums of particle concentration is noted along with elapsed times at a collection point a known distance downdrift from the injection point (Bruun, 1965; Yasso, 1965). Average velocity is obtained by dividing distance by elapsed time.

All of the above techniques of tracing the movement of foreshore sand have employed subjective analysis of tracer-particle distribution patterns with the exception of the

time-integration method. It is thus important that an objective and reproducible method for description of tracer grain distribution be employed where quantitative statements about the sand motion are to be made. Also, there is a need for examining statistically the validity of any underlying trend in the variable tracer-concentration data upon which average or interpolative values of the direction and rate of particle movement depend.

PRESENT STUDY

As tracer methods are likely to receive more attention in the future, with increasing emphasis on practical application, ambiguities must be resolved concerning basic assumptions made about them. With this in mind, the present study seeks to investigate the nature of particle dispersion on a beach, particularly that dispersion which shows a definite trend, as opposed to mere randomness of movement. In addition to determining movement in two dimensions on the surface, some idea of the areal distribution of particles at discrete levels *below* the surface is desirable. Also, the variable dispersion of differing particle sizes and shapes is to be investigated, especially the extent to which a given size "seeks" a specific zone on the foreshore.

To accomplish these objectives, the present experiment employed a radial sampling grid (fig. 2), laid out on the foreshore at low tide. Three sand tracers coated with different fluorescent dyes were released at the intersection of the radii. Short cores (≈ 15 cm. long) were obtained at the sampling points during the following low tide. Sections of these cores were examined for dyed grains, using a long-wave ultraviolet light source.

A single tidal cycle was selected for study of the patterns of grain motion because it is a basic unit of time associated with swash zone drift and a logical beginning point for exploratory research. Strahler (1964) has demonstrated that three distinct phases of alteration of a natural foreshore occur as the result of hydrodynamic forces acting during a single tidal cycle: *initial deposition*

during the beginning of the flood stage, *scour* during the high-water stage, and a *final deposition* at the conclusion of the cycle. These forces are superimposed on the long-term conditions affecting the beach and produce no net erosion or deposition in themselves. One must consider, however, that individual particle motion may be misleading in studies using a travel time representing only a portion of the full tidal cycle. In this respect, sand transport on

more objectively, a statistical method known as trend surface analysis was employed. Essentially, this method provides a means of separating the main types of variability and evaluating the significance of major trends present. These trends may be represented by simple mathematical formulas.

Miller (1956) first utilized trend surfaces in relating sediment size parameters to current and wave systems. Since Miller's work,

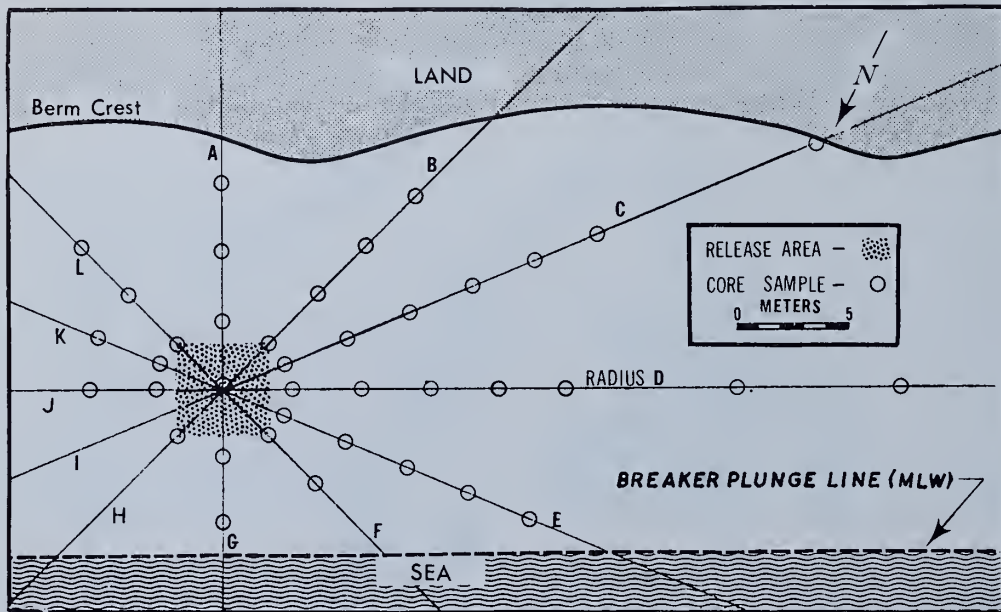


FIG. 2.—Study area showing foreshore limits and sample locations

beaches influenced by the tide is not analogous to sand transport by streams whose rate of flow is more or less steady.

TREND SURFACE ANALYSIS

According to the present approach, hand-contoured maps of observed tracer distributions are not considered adequate information in themselves. In constructing contour maps, subjective interpretations are unavoidable; correct visual interpretation of trends over the range of values spread out horizontally may well be impossible due to the masking effect of local variability. To treat the concentration data of this study

others (e.g., Grant, 1957; Krumbein, 1959) have explained the utility of trend surfaces in the areal analysis of geophysical data. Whitten (1963) presents a computer program for surface-fitting procedures for geological models involving areally distributed data. A brief résumé of the pertinent points of trend surface analysis follows.

In beach studies, it is clear that any set of observations of some measurable property over a given area will exhibit variation. This variation may be divided into two components: (1) a mathematically defined trend component and (2) a residual component, the deviation. The form of the

trend component is a surface defined by the general polynomial function

$$X_n = a_0 + a_1U + a_2V + a_3U^2 + a_4UV + a_5V^2 + a_6U^3 + a_7U^2V + \dots, \quad (1)$$

in which U and V are coordinate values locating the n th observation point on a rectangular grid, X_n is the value of a given property at that point measured along an ordinate perpendicular to the grid, and a_0, a_1, a_2, \dots are coefficients. Given the first three coefficients, the surface is linear; increasing the number of coefficients to six yields the quadratic, and to ten, the cubic surface. In two dimensions, the projection of any of these surfaces onto the horizontal plane yields equal value contours, or isopleths. To achieve the best fit of these contours to the observed data points, coefficients a_0, a_1, a_2, \dots are evaluated for n equations (n observations) so that the sum of squares of the deviation as expressed by

$$\Sigma (X_{\text{obs}} - X_{\text{comp}})^2 \quad (2)$$

is a minimum, where X_{obs} is the observed value of the property and X_{comp} is the computed value at the same point. Substituting a_0, a_1, a_2, \dots in equation (1) yields computed values for all observation points and permits trend surface maps to be constructed.

EXECUTION OF EXPERIMENT

SELECTION OF TRACER SAND

Three separate quantities of sand were collected, each sand having a different mean grain size and shape characteristics. These were coded by coating them with different fluorescent colors. The first quantity of sand to be dyed was taken at the injection point (fig. 2) in the study area during low tide and designated "in situ sand." Microscopic examination of the sand revealed that the in situ tracer consisted of shell and coral fragments. A second quantity of sand, obtained from the northwestern shore of South Bimini near Entrance Point (fig. 1,A), contained shell fragments primarily and was designated "shell hash sand." The third quantity of sand, from a shallow bank near East

Bimini (fig. 1,B), was a pure oölite sand that exhibited a high degree of sphericity. Subsequent size analyses of the three tracers were made. Mean grain size (M_z) was calculated from cumulative size-frequency curves using the formula

$$M_z = \frac{\phi_{16} + \phi_{50} + \phi_{84}}{3},$$

where $\phi = -\log_2$ diameter in millimeters. Also computed were values of the "inclusive graphic standard deviation" (sorting index), as defined by Folk and Ward (1957).

$$S_I = \frac{\phi_{84} - \phi_{16}}{4} + \frac{\phi_{95} - \phi_5}{6.6}.$$

The results, presented in table 1, are intended to show the differences in mean grain size and sorting index between tracers. A size analysis was also conducted using the top 2.5 cm. of a sample taken at the injection point as part of the main sampling scheme. The latter gives an indication of the variability of beach sand size over the period of time between collection of the sand for dye coating and the termination of the experiment.

DYE COATING TRACER SANDS

Various methods of marking sand grains have been summarized by Wright (1962). On the whole, the techniques vary mainly in the type of dye selected. For the present study, the method of Yasso (1965) was adopted; it utilizes a commercial grade of fluorescent acrylic lacquer whose application is simple, economical, and effective. The only departure from Yasso's technique was the method of dye application. About 0.25 liter of dye solution was added to 11.2 kg. of sand and the mixture shaken by hand in a large plastic bag. Colors used to identify the three tracers were Day-Glo No. 202-15 (blaze orange) for in situ, Day-Glo No. 202-46 (lightning yellow) for shell hash, and Day-Glo No. 202-11 (aurora pink) for oölite.

TRACER INJECTION AND SAMPLING

Approximately 22.5 kg. of each tracer were combined and the mixture raked into

the beach at low tide the morning of October 26, 1965. The marked sand was raked in to a depth of about 3 cm. within an area 4.6 m. on a side. Sampling was conducted during the subsequent low tide, following the sampling pattern of figure 2. Samples were taken at 3.05-m. intervals along the radii; the actual pattern of sampling was designed to favor the prevailing direction of longshore drift at the beginning of the study. In all, thirty-nine samples were obtained with a view toward examining the distribution in three dimensions. Each sample was collected using a 30-cm. length of 3.8-cm. I.D. plastic core liner inserted into the beach by hand to

ate" one. No attempt was made to correlate environmental factors and tracer distributions.

LABORATORY WORK

The sand cores were opened in the laboratory, impregnated with liquid gelatin, and cooled to 4° C. Once the gelatin hardened, the plastic core liner could be cut away and the core sliced into 2.5-cm. lengths using a wire "cheese slicer." Each length thus cut was further sampled with a thin-walled 2.5-cm. diameter tube so as to remove peripheral sediment which might contain grains that could have been forced downward along the

TABLE 1
STATISTICAL MEASURES OF SAND TRACERS AND NORMAL BEACH
SAND AT THE TIME AND PLACE OF INJECTION

Designation	Mean Size M_z (mm.)	Inclusive Graphic Stand- ard Deviation (Sorting Index)	Verbal Scale (Sorting Index)
Oolite	0.31	0.29	Very well sorted
Shell hash69	.18	Very well sorted
In situ35	.64	Moderately sorted
Sample*	0.52	0.88	Moderately sorted

* Normal sand sample taken at injection point 0.0-2.5-cm. depth interval.

an average depth of 15 cm. A rubber stopper was applied to the upper end of each core liner after its insertion to act as a closed valve so that disturbance or loss of material was prevented upon withdrawal of the core.

ENVIRONMENTAL CONDITIONS

At the time the foreshore was completely submerged by the swash zone, the following environmental conditions were observed: wind direction, 050°; wind speed, 0-5 knots; breaker height, 0.5-0.8 m.; breaking wave period, 9.1 sec.; angle made by breaking wave and shore line, about 6° (opening to west); swash drift, 0.27 m/sec; longshore current, breaker zone, 0.26 m/sec toward west; water temperature, 24.0° C.

These conditions give an idea of the relative energy level in the foreshore region. This energy level may be termed a "moder-

margin of the core liner. Four to six subsamples were obtained from each core, depending on the length of the original core. Each subsample contained 12.3 cm³. These samples were washed in hot water (to remove the gelatin), dried, and examined under long-wave ultraviolet light. Fluorescent grains were removed with a fine brush, identified, and counted under a low-power stereomicroscope. Where large numbers of dyed grains were encountered, the sample was split from one to three times, depending on the total concentration, using a CARPCO micro-sample splitter. The total grain count was then derived by multiplying the number counted by (2)ⁿ, where *n* = the number of times the sample was split. In general, for each color type, the sample was not split until the count exceeded fifty grains.

DATA ANALYSIS

OBSERVED DISTRIBUTION OF TRACER

A number of maps of observed tracer distribution were constructed from the grain count data, each one integrating a vertical interval of 2.5 cm., beginning with 0.0 cm. at the beach surface. Several of these maps are shown in figures 3-14. It is obvious from the observed concentration contours for the three tracers at the 0.0-2.5-cm. level that the dispersal of grains followed no simple pattern, and, as both Wright (1962) and Ingle (1966) found, much of the total movement was up the beach slope as well as in the downdrift direction. Furthermore, no striking differences between the patterns of the three tracers were noted. Considering the successively lower levels, all tracers appeared to be restricted to two or three small areas within which the grains were highly concentrated; maximum counts on the order of 2,000 grains were found near the origin in the 2.5-5.0-cm. interval. (Shell hash counts were everywhere lower relative to the finer tracers, due to larger size and fewer individual grains per unit weight. This does not detract from the main objective of the study, to analyze the relative distribution of each tracer irrespective of size.)

Some subjectivity was employed in constructing the tracer-distribution maps, especially in the downdrift or southwest portion of the study area where the radial sampling grid reached its maximum divergence. Trend surface analysis of the data reduced the subjectivity involved here.

TREND SURFACE ANALYSIS

Coefficients for equation (1) were determined using a computer program and the data from the thirty-nine cores; computed trend surface values, as well as the deviation of these from the observed values, were obtained for each sample location for surfaces of degrees one through three. Sufficient grain counts were found to compute surfaces down to the fourth 2.5-cm. depth interval. Below this level, only a few cores contained tracer grains. In fact, it became

obvious that a bothersome number of "zero" counts were present at almost all levels, and as the computer regarded a zero count the same as no observation at all (minimum number of observations was mandatory), an arbitrary value of 1 count was added to all observations.

The trend component given by a linear surface will account for a certain portion of the total variability of the data, and surfaces of successively higher degree account

TABLE 2

Sand	Linear	Quadratic	Cubic
Oölite.....	19.45	23.03	45.86
In situ.....	10.23	13.65	33.29
Shell hash.....	13.00	33.40	38.54

for still more, so that the deviation is constantly reduced. The portion of the total variability accounted for by any combination of surfaces, expressed as a percentage, is:

$$\frac{\sum X^2_{\text{comp}} - (\sum X_{\text{comp}})^2/n}{\sum X^2_{\text{obs}} - (\sum X_{\text{obs}})^2/n} \times 100. \quad (3)$$

Typically, a combination including degree-three coefficients accounts for the major portion of the total variability. The unaccounted deviation then consists almost entirely of local variation (of possible geologic significance) and random variation or "noise." The trend component of systematic variation holds primary interest in this study. However, the deviation will be examined for its significance as well.

The computer output included the per cent sum of squares for each surface, as given by equation (3). A comparison of these values revealed that the interval 0.0-2.5 cm. contained the greatest amount of systematic variation. The per cent sum of squares values for this interval is shown in table 2.

Considering that the per cent sum of squares values for lower depth intervals and for all intervals combined were generally minimal (as little as 2.3 per cent for the linear, 5.4 per cent for the quadratic, and

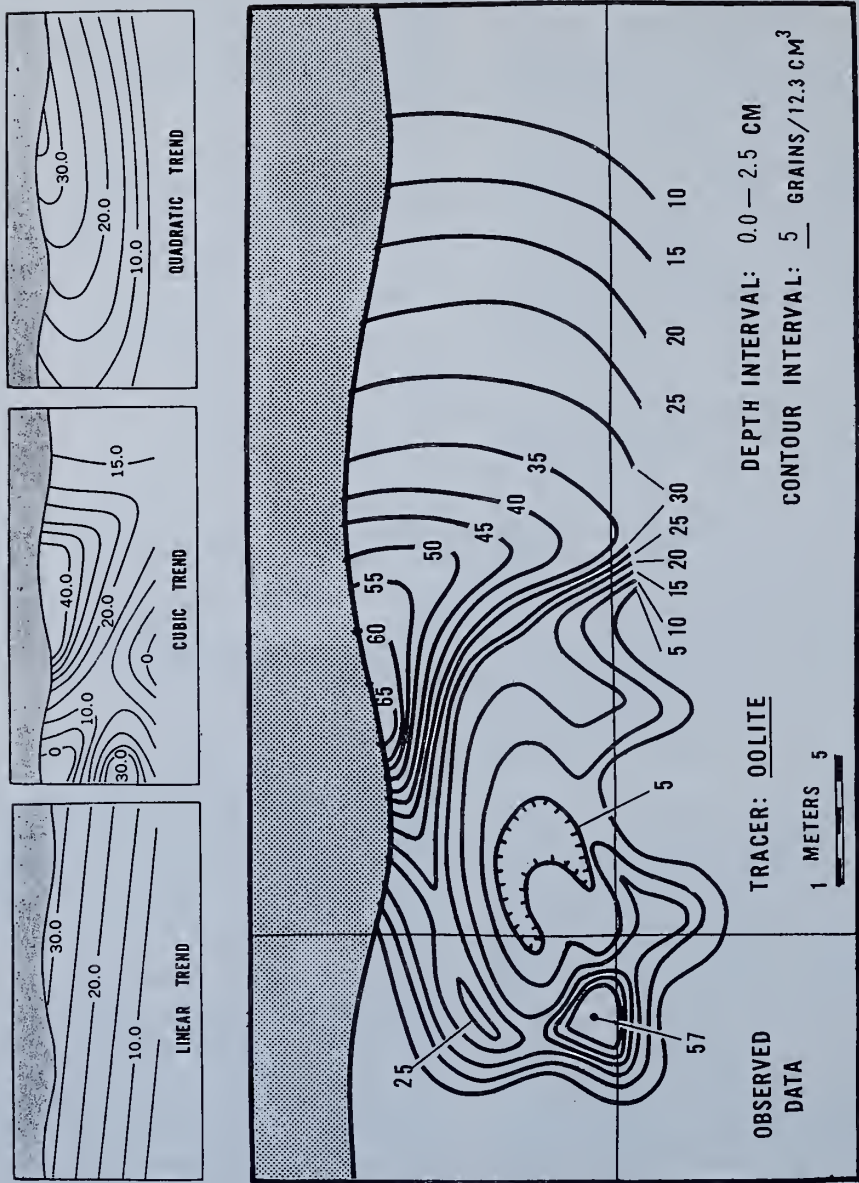


FIG. 3.—Map of observed oölite distribution and trend surfaces, 0.0-2.5-cm. depth interval

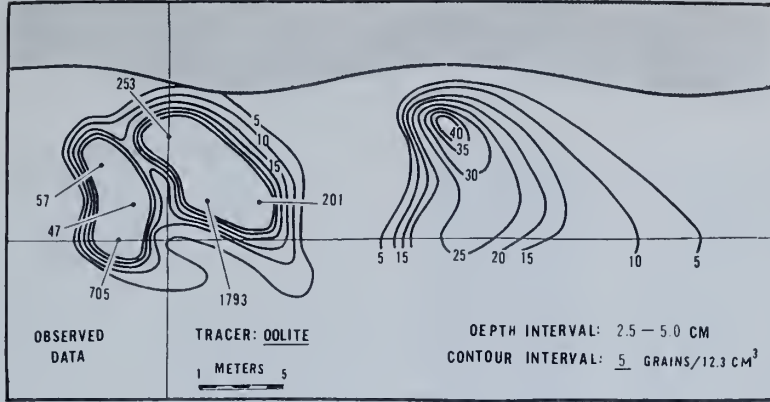


FIG. 4.—Map of observed oölite distribution, 2.5-5.0-cm. depth interval

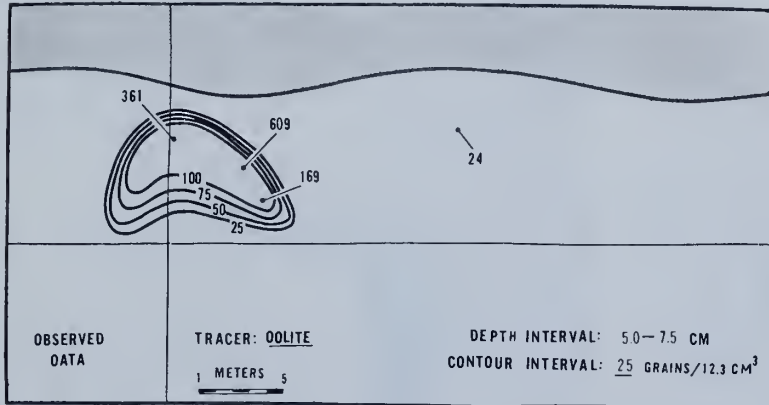


FIG. 5.—Map of observed oölite distribution, 5.0-7.5-cm. depth interval

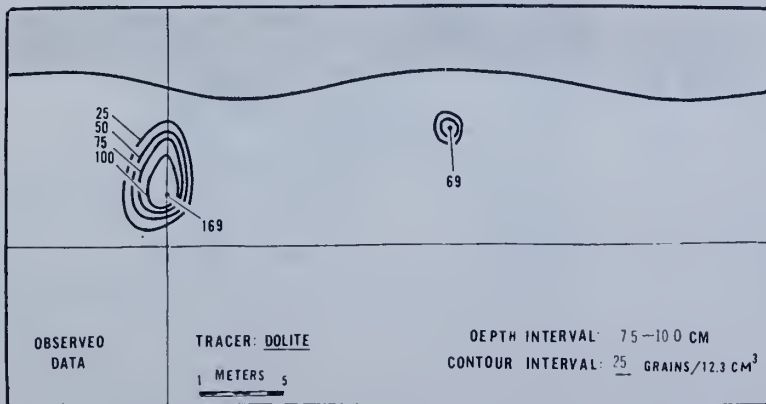


FIG. 6.—Map of observed oölite distribution, 7.5-10.0-cm. depth interval

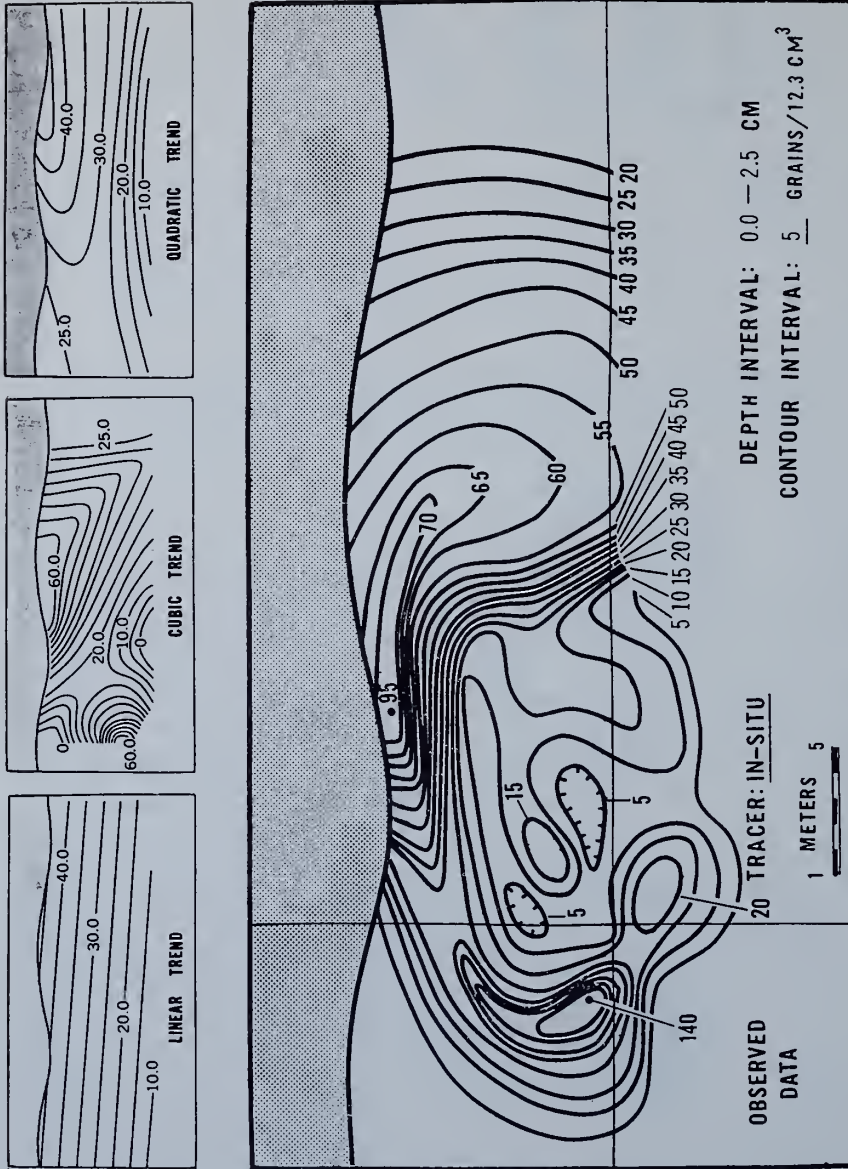


FIG. 7.—Map of observed in situ distribution and trend surfaces, 0.0-2.5-cm. depth interval

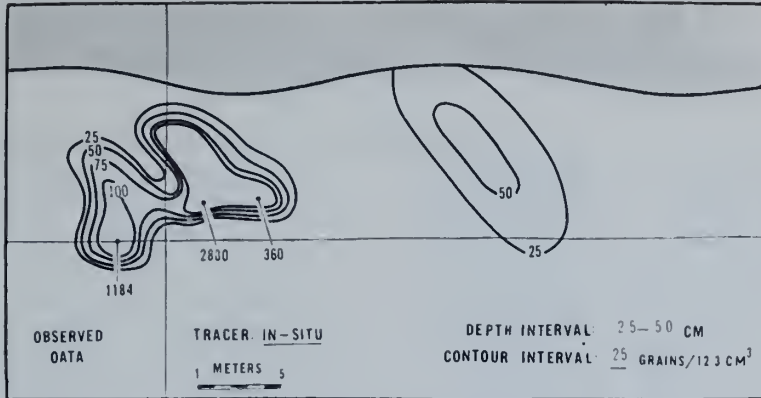


FIG. 8.—Map of observed in situ distribution, 2.5-5.0-cm. depth interval

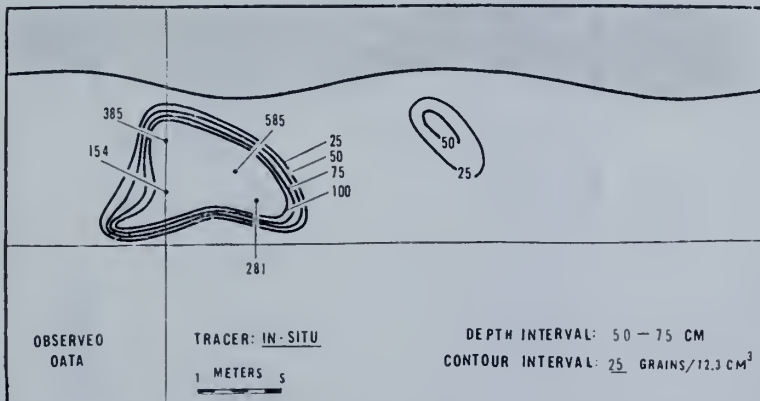


FIG. 9.—Map of observed in situ distribution, 5.0-7.5-cm. depth interval

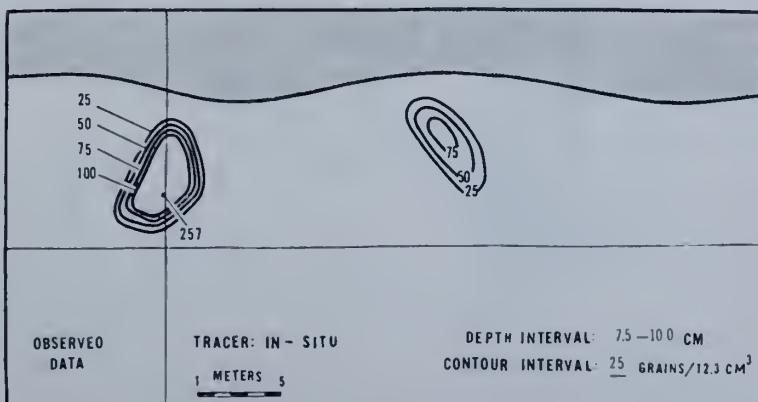


FIG. 10.—Map of observed in situ distribution, 7.5-10.0-cm. depth interval

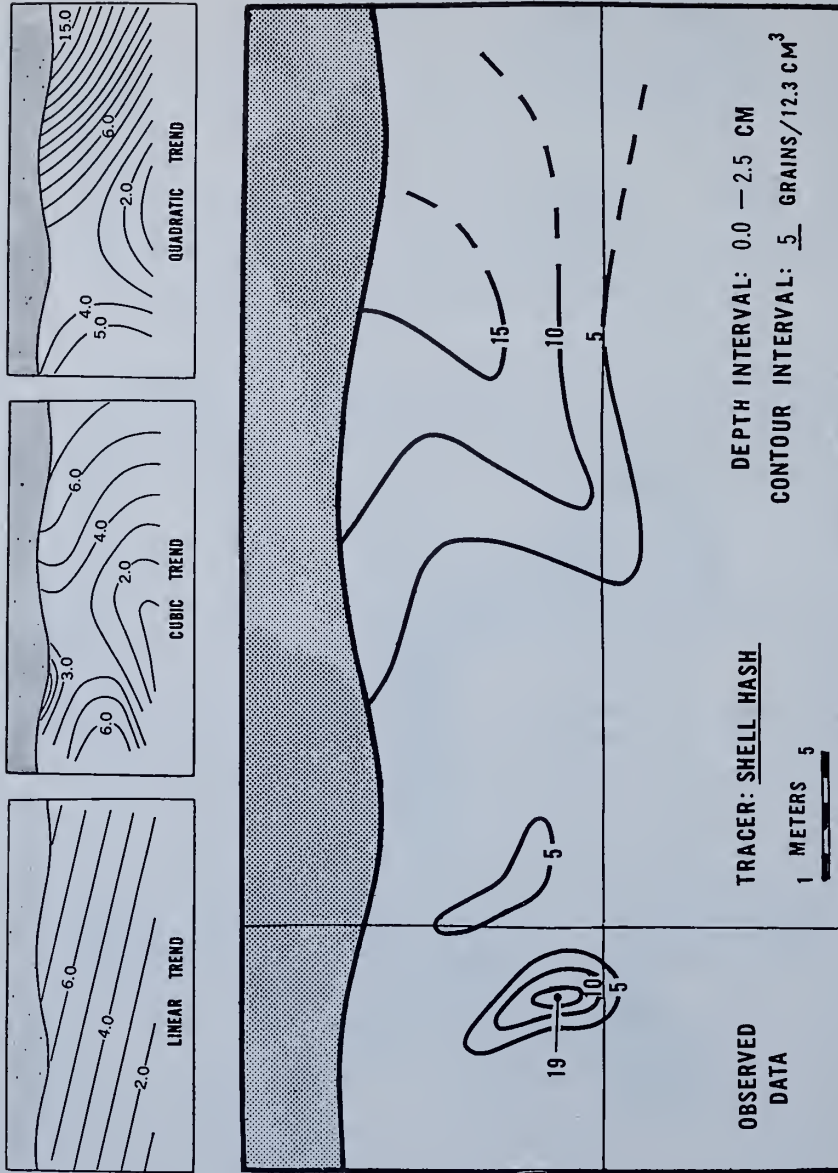


Fig. 11.—Map of observed shell hash distribution and trend surfaces, 0.0-2.5-cm. depth interval

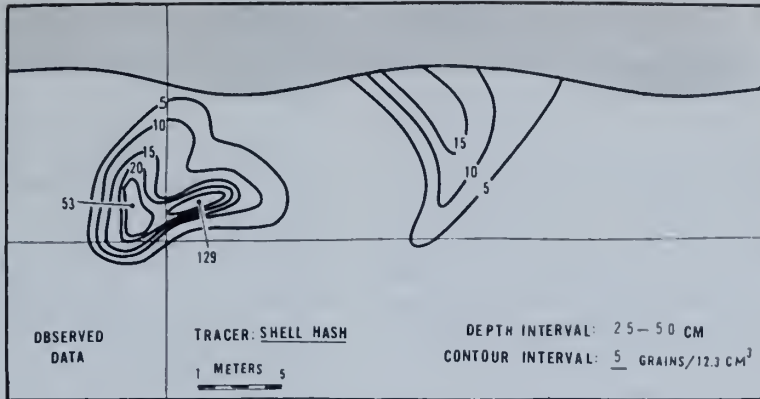


FIG. 12.—Map of observed shell hash distribution, 2.5-5.0-cm. depth interval

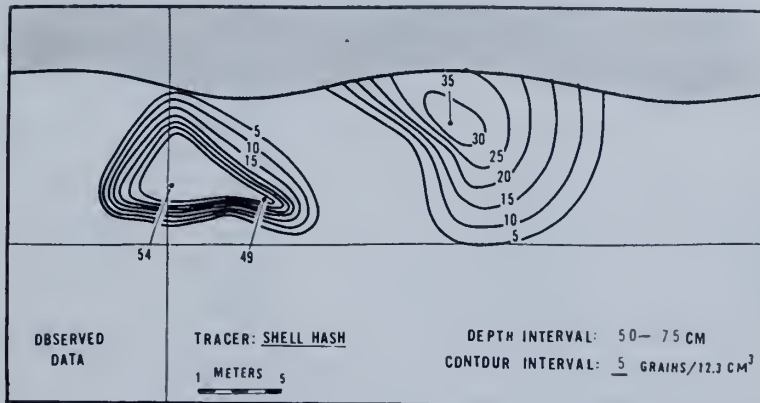


FIG. 13.—Map of observed shell hash distribution, 5.0-7.5-cm. depth interval

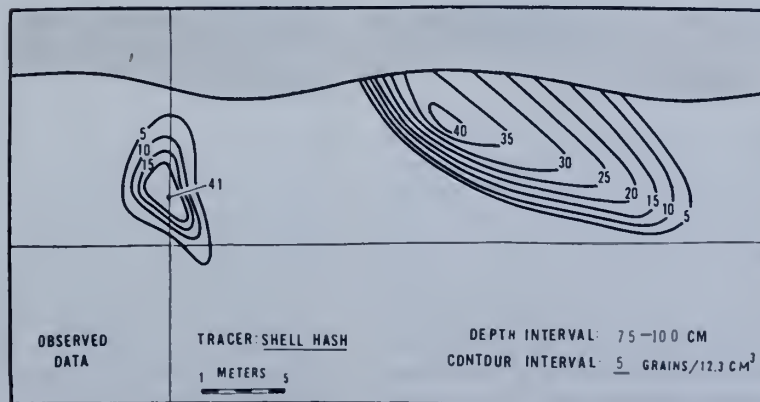


FIG. 14.—Map of observed shell hash distribution, 7.5-10.0-cm. depth interval

10.2 per cent for the cubic surface), trend surfaces for these intervals were not drawn. These low values merely confirmed the local distributions evidenced by the observed data; that is, high tracer concentrations locally with but slight distribution of tracer grains at the lower depth intervals. A further piece of evidence was obtained by an analysis of variance of trend surface data (after Allen and Krumbein, 1962) for the oölite tracer as shown in table 3.

four depth intervals combined were non-significant.

Based on the above considerations, trend surface maps were constructed for all three tracers at the surface only. They are presented as part of figures 3, 7, and 11. It will be noted that linear surfaces for the three grain types do not differ significantly in the orientation of their isopleths, only in their gradients. Orthogonals to these isopleths may be regarded as indicators of the direc-

TABLE 3
ANALYSIS OF VARIANCE OF TREND SURFACE DATA, OÖLITE TRACER

Variation Source	Sums of Squares	Degrees of Freedom	Mean Square	F Value	Confidence Level (Percentage)
0.0-2.5-cm. Interval					
Total.....	10,907.590	38
Linear.....	2,121.234	2	1,060.617	4.35	97
Deviation.....	8,786.356	36	244.065
Quadratic.....	2,512.152	3	837.384	4.40	99
Deviation.....	6,274.204	33	190.127
Cubic.....	5,002.303	4	1,250.576	28.51	>99
Deviation.....	1,271.901	29	43.859
Combined 0.0-10.0-cm. Interval					
Total.....	4,450,562.875	38
Linear.....	238,668.797	2	119,334.398	1.02	<75
Deviation.....	4,211,893.500	36	116,997.042
Quadratic.....	443,085.656	3	147,695.219	1.29	<75
Deviation.....	3,768,807.844	33	114,206.298
Cubic.....	961,150.289	4	240,287.572	2.48	92
Deviation.....	2,807,657.555	29	96,815.778

According to normal statistical usage, a confidence level below 95 per cent indicates that any separation of a given trend effect from the over-all deviation after a single experiment may have been the result of chance; that is, a replication of the same number of samples might yield a decidedly different trend surface, all other factors being the same. Conversely, confidence levels greater than 95 per cent indicate significant or "real" trends. The data of table 3 show that all of the trend surfaces for the 0.0-2.5-cm. interval were significant, whereas all of the trend surfaces for the

tion of mean particle movement for each of the three tracers (see Ingle, 1966, p. 58-59). This similarity in orientation also exists for the quadratic and cubic surfaces. The trend surface patterns, then, offer evidence of a lack of significant segregation (or sorting) of the different grain types represented over the interval of time involved. Assuming the synchronous areal distribution of tracers, any tendency of the grains to accumulate within and travel along discrete "bands" parallel to the shore line should be reflected in the trend surfaces as distinctly different patterns of isopleths. The major differences

in the patterns of figures 3, 7, and 11, however, are in the gradients of the isopleths, not their orientation.

For trend surfaces having low per cent sum of squares values, as for the combined interval data above, the deviation may deserve closer examination. Allen and Krumbain (1962) suggest that the deviation may often contain small-scale or secondary trends that have been superimposed on the large-scale major trend. A map of the deviation from the oölite cubic trend surface for the combined 0.0-10.0-cm. interval data is presented in figure 15. This map indicates

therefore derive greater benefits from an analysis that utilizes an areal spread of observations.

Figure 16 compares several cross sections along radius D (fig. 2) for the 0.0-2.5-cm. interval. This graph shows that the observed data vary so much with distance that simple curves fitted to them are meaningless. The curves for the three trend surfaces for oölite, however, take their form from a consideration of the entire areal distribution. Again, if the synchronous areal distribution of tracer grains may be assumed, the curves for the oölite trend surfaces (fig.

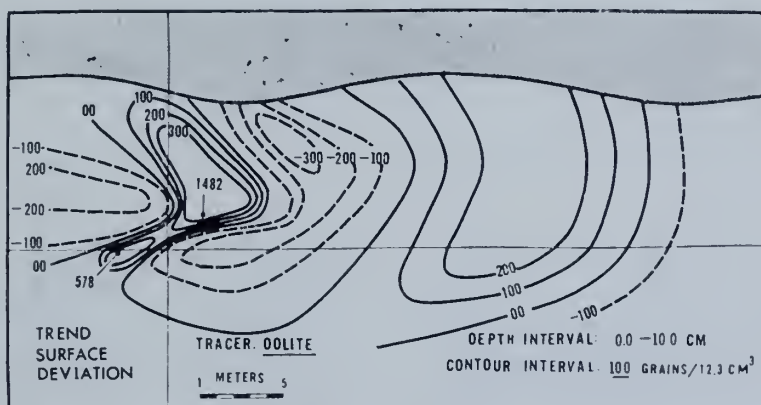


FIG. 15.—Map of deviation from cubic trend surface, combined 0.0-10.0-cm. depth interval

two areas of positive deviation, or superabundance of grains, one near the injection point and the other centered about a point 20 m. downdrift that could possibly be interpreted as a particle "mode" and be used as such in a time-integration method for calculation of average particle velocity (see Yasso, 1965).

It should be noted that tracer-concentration data taken from any vertical section of a given trend surface may be used to produce a regression line corresponding to those produced from tracer-concentration data obtained from a simple linear sampling of a foreshore (e.g., Wright, 1962). The difference is that a cross section of a trend surface is based on the tracer distribution over the entire study area, rather than the distribution along a single line. A study attempting to define total particle drift on a beach will

16) will be more meaningful representations of tracer distribution along the D radius than will curves fitted to the data actually observed along this radius.

DISCUSSION

It has been shown that reliable trend components are restricted to the upper 2.5 cm. of the foreshore under investigation. Below this level, large concentrations of tracer grains occur at two or three points. It is probable that these major concentrations are the result of burial during an early stage of the tidal cycle. When buried, these grains are effectively removed from the dynamic environment acting on the grains remaining near the surface. Figure 15 shows a large "tongue" of negative deviation values which could well define a sediment mass moving in from the upper-left corner

of the study area and overriding the tracer grains locally. Such interaction of moving sand masses may be typical of "zigzag" swash-backwash patterns, accentuated here by the slight cusp development (fig. 2) near the berm crest.

Assuming that portions of the total tracer input were randomly removed from the active drift zone by burial, it is not surprising to find a lack of trend components for the combined tracer-particle distribution. The alternative use of strictly surface trends in

points, such as the immediate sediment-water interface and breaker plunge line; as a result, the limits of a given dynamic zone through time are hard to define.

CONCLUSIONS

The statistical evidence of this experiment disclosed that sediment movement in the foreshore zone of the beach under study exhibited a significant trend within 2.5 cm. of the surface only, and over a single tidal cycle, no clear-cut differences developed be-

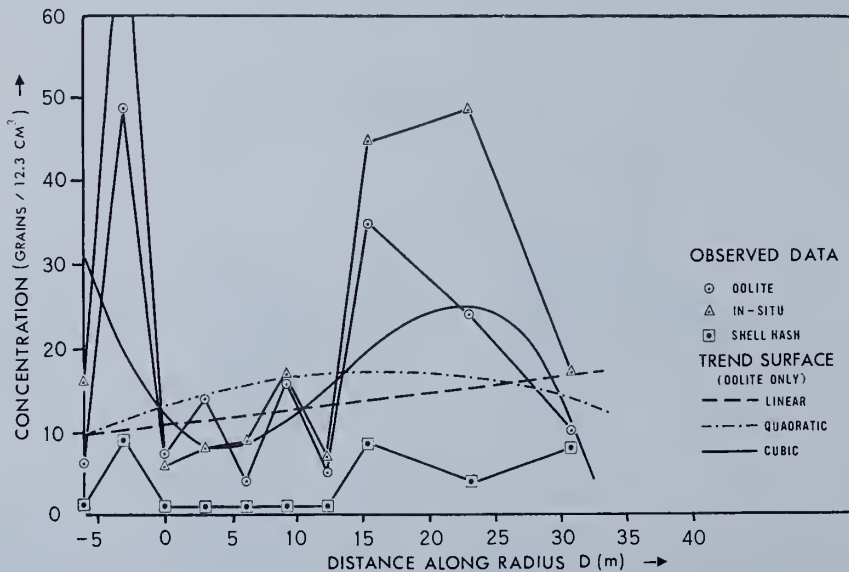


FIG. 16.—Tracer concentration versus distance along radius D from injection point

defining tracer movement requires a certain amount of caution, as a portion of the total tracer quantity is necessarily ignored.

A complicating factor in the study of core sections of a beach lies in the assumption of synchronous areal distribution and the correlation of time with depth. Unless deposition (or erosion) occurs simultaneously and at the same rate at all points, tracers recovered at a given depth may have moved at widely different times and come under the influence of wholly different dynamic forces before being recovered. Practically, this problem will not be overcome without some difficulty inasmuch as field measurements are restricted to certain physical reference

tween the patterns of tracer-particle distribution representing different grain sizes and shapes. Furthermore, trend surfaces for successively lower levels were all non-significant. Thus, a device sampling too deep will obtain data containing little or nothing in the way of significant trends, as was the case for the 0.0–10.0-cm. depth interval.

The results of this study may be regarded as expectable, perhaps, but they are not necessarily typical of all beach conditions. Any quantitative tracer study of beach drift in the swash-backwash zone must take into account the possible effect of random removal (or dilution) of tracer grains from the more active surface layers through buri-

al (or admixing) by adjacent sand. If the synchronous areal distribution of tracer grains can be assumed, contour maps of the combined interval (total depth) trend deviations may provide the most comprehensive means of defining modes of high particle concentration for use in determining an average particle velocity. If the basic assumption of synchronism *cannot* be adopted, however, provision must be made in the design of a tracer experiment for sampling over time intervals that represent uniform depositional dynamics.

The value of trend surface analysis in describing the drift of beach sand lies in its ability to combine a large number of observations in a single representative equation. It is conceivable that a set of equations could be found which would predict the sediment distribution pattern, in the form of a trend surface of n th degree, for any

combination of relevant dynamic variables that might occur at a given locality. With the increasing use of automatic data acquisition systems, the time is approaching in which continuous analysis of such environmental variables will permit prediction of the pattern of net sand movement on beach foreshores. At present, such a practical application seems contingent upon the development of rapid methods for estimating sediment transport rates through use of tracers.

ACKNOWLEDGMENTS.—I am indebted to Dr. Wyman Harrison for much helpful guidance and advice during the course of this study. I am also grateful to Dr. Stephen Murray, J. J. Norcross, Dr. Robert L. Miller, and Dr. James C. Ingle, Jr., for critically reading the manuscript. Field support for this study was provided by the Lerner Marine Laboratory, Bimini, B.W.I.

REFERENCES CITED

- ALLEN, P., and KRUMBEIN, W. C., 1962, Secondary trend components in the top ashdown pebble bed: a case history: *Jour. Geology*, v. 70, no. 5, p. 507-538.
- BRUNN, P., 1965, Quantitative tracing of littoral drift: U.S. Dept. Agri. Misc. Pub. 970, p. 756-768.
- CALDWELL, J. M., 1956, Wave action and sand movement near Anaheim Bay, California: U.S. Army Beach Erosion Board Tech. Mem. 68, 21 p.
- FOLK, R. L., and WARD, W. C., 1957, Brazos River bar: a study in the significance of grain size parameters: *Jour. Sed. Petrology*, v. 27, no. 1, p. 3-26.
- GRANT, R., 1957, A problem in the analysis of geophysical data: *Geophysics*, v. 22, p. 309-344.
- HARRISON, W., PORE, N. A., and TUCK, D. R., JR., 1965, Predictor equations for beach processes and responses: *Jour. Geophys. Research*, v. 70, no. 24, p. 6103-6109.
- INGLE, J. C., JR., 1966, The movement of beach sand: New York, Elsevier Publishing Co., 221 p.
- KRUMBEIN, W. C., 1959, Trend surface analysis of contour-type maps with irregular control-point spacing: *Jour. Geophys. Research*, v. 64, p. 823-834.
- MILLER, R. L., 1956, Trend surfaces. I. The relation of sediment size parameters to current-wave systems and physiography: *Jour. Geology*, v. 64, p. 425-446.
- and ZEIGLER, J. M., 1958, A model relating dynamics and sediment pattern in equilibrium in the region of shoaling waves, breaker zone, and foreshore: *Jour. Geology*, v. 66, p. 417-441.
- RUSSELL, R. C. H., 1960, The use of fluorescent tracers for the measurement of littoral drift: *Coastal Eng. Conf.*, 7th, The Hague, Proc., v. 1, p. 418-444.
- STRAHLER, A. N., 1964, Tidal cycle of changes in an equilibrium beach, Sandy Hook, New Jersey: Office Naval Research, Geog. Br., Tech. Rept. 4, 51 p.
- WHITTEN, E. H. T., 1963, A surface-fitting program suitable for testing geological models which involve areally-distributed data: Office Naval Research, Geog. Br., Tech. Rept. 2, 56 p.
- WRIGHT, F. F., 1962, The development and application of a fluorescent marking technique for tracing sand movements on beaches: Office Naval Research, Geog. Br., Tech. Rept. 2, 19 p.
- YASSO, W. E., 1965, Fluorescent tracer particle determination of the size-velocity relation for foreshore sediment transport, Sandy Hook, New Jersey: *Jour. Sed. Petrology*, v. 35, p. 989-993.
- ZEIGLER, J. M., and TUTTLE, S. D., 1961, Beach changes based on daily measurements of four Cape Cod beaches: *Jour. Geology*, v. 69, p. 583-599.

Shatter cones and star wounds

Shatter cones are a distinctive form of fracture structure produced in rocks by intense shock forces. Volcanic explosions seem inadequate to account for them; instead, they are probably the best criterion we have for identifying the scars of ancient meteorite impacts

With the Moon and Mars covered with numerous meteorite craters, one wonders why the Earth does not bear obvious evidence of similar bombardment. Of course, erosion quickly erases the surficial expression of terrestrial craters, but the discerning eye of the geologist should still be able to detect the remnant root structures.

Actually, in the past two decades we have been able to sort out perhaps threescore probable ancient cosmic impact scars on the Earth which we term *astrolemes* (from a Greek word meaning "star wounds"). The difficulty has been trying to find impact scars among the welter of other crypto-explosive geologic structures, most of which are volcanic. The breakthrough has been achieved by the identification of mineralogic criteria for intense shock far greater than can be expected from endogenic or internal Earth processes such as a volcanic steam explosion. The subject of this shock metamorphism is too extensive to cover here, but a good example is the shock transformation of common quartz to the more dense polymorph of silica, the mineral named *coesite*, which apparently is formed by a shock overpressure of about 20 kilobars. As a more tightly packed atomic phase, coesite bears the same relationship to quartz that diamond does to graphite. My further remarks here will be confined to the fracturing of rock by shock waves.

Let us briefly envision the effect of hypervelocity impact of a giant meteorite or comet head striking the Earth. The kinetic energy of this cosmic "cannon ball" is such that a great explosion ensues creating a circular geologic scar of crushed, jumbled, and deranged rock. It is mainly a shock event since the velocity of impact may range from 12 to

72 km per second, which is many times the speed of an elastic wave in rock. From ground zero an intense shock wave moves out through the rock along a hemispherical front which is rapidly damped mainly by crushing and fracturing rock. If this fracturing has some distinctive appearance, it would be a most useful criterion for identifying ancient impact scars. One type of shock fracturing *does* seem to produce distinctive striated cones which we term shatter cones.

It is a matter of common knowledge that when a missile strikes a plate-glass window a conical percussion fragment often pops out. Shatter coning bears a vague relationship to this phenomenon, but shock waves (and especially an elastic precursor shock wave) are involved at shock overpressures probably in the range from 10 to 70 kb depending upon the Hugoniot—the pressure/density relationship—of the substance. Unlike percussion coning, which forms only a single cone, myriads of cones are formed along the advancing spherical front of the shock wave spreading out from a giant meteorite impact. Actually, a really definitive theory of shatter coning is still lacking, but it is quite certain that steam explosions related to volcanism cannot create them.

It takes a photograph to describe shatter coning, so some examples are presented in Figures 1 and 2. The most distinctive aspect is formed by the horse-tail-like packets of flaring striations on the master cone. In fine detail these striations are convex ridges, so that the "mould" or negative face of a shatter cone is quite unlike the positive face—an aspect which serves to distinguish them from the slickensides formed by rock slippings in fault zones.

Dr Robert Dietz

is a research oceanographer at the Atlantic Oceanographic Laboratories of the Environmental Science Services Administration in Miami, Florida



Figure 1 A group of large shatter cones in the upturned southern margin of the Sudbury astrobleme in Ontario, Canada. These conical fractures were created 1.7 billion years ago as a shock wave raced out from ground zero—the impact point of a giant meteorite more than two miles in diameter. A plastic pulse immediately following the shock wave then threw up the strata to their present vertical position so that the cones now point skyward

Figure 2 Shatter-coned dolomite from the Sierra Madera Structure, Texas. Note the formation of parasitic cones, a feature of this type of fracturing which distinguishes it from all other forms of conical failure. (Actual size)



A certain amount of discrimination is needed to identify shatter cones, as there are many other natural conical structures and striated or fluted rocks. The most common mis-identification arises from cone-in-cone structures often termed "shales with beef" by British miners. These cones, which have nothing to do with shock fracturing, occur in thin beds of rock and are marked with horizontal rings rather than vertical striations. They are common in the Carboniferous Coal Measures. When well developed, shatter cones are easily identified and admit of no confusion. We now know of 19 shatter-coned explosion scars from various parts of the world (Figure 3). They are mostly concentrated in North America, largely because the most intensive search has been carried on there.

Most shatter-coned astroblemes are of moderate size, a few miles across, but two of Precambrian age attain diameters of a few tens of miles across—the Sudbury structure in Canada and the Vredefort Ring of South Africa. In addition to shatter coning, both of these structures bear evidence of what might be termed "geologic overkill"—that is, deformation which seems to exceed by far the principle of least work. At Vredefort scattered pods of black vitreous rock called pseudotachylite occur which appear to have been shock-melted rock. Through the application of shock waves, and only in this manner, it is possible to melt the interior of a rock mass while the exterior remains comparatively cool.

As well as indicating the passage of an intense shock wave, shatter cones also permit a reconstruction of the applied force field since the cone apices point in the direction of the oncoming shock wave. At several shatter-coned sites it is possible to tell that the force was applied from above and centrally—that is, with the bull's-eye of the structure as ground zero for the explosion. This is, of course, good evidence for their impact origin. At Gosses Bluff astrobleme in central Australia, shatter-coned exposures are sufficiently good to permit a reconstruction of the hemispherical shock front and, in turn, demonstrate that the impacting missile (presumably a comet head in this case) was about one mile across.

A curious aspect of many presumed astroblemes is their so-called "damped-wave" form—a central domal uplift surrounded by an annular depression or syncline, and sometimes other ring elevations and depressions of rapidly diminishing amplitude. Thus they resemble the *rebound* form of the disturbance created on a water surface after a stone has been dropped in it. It would seem as though rocks under the impulsive load of a hypervelocity impact react like a liquid rather than a solid. Indeed, the strength of rocks is minute compared to the tremendous megabar pressures (a megabar equals a million atmospheres) generated at the point of impact. The mechanics of impact, however, remain poorly understood, as they cannot begin to be duplicated in the laboratory either in scale or intensity.

Perhaps a reasonable explanation of the damped-wave form is that under a low-velocity impact, such as by a bullet, the target material is plastically

pushed aside to accommodate the impinging object. But with the hypervelocity impact of a meteorite, and with the generation of shock waves instead of elastic waves, the target material is not "forewarned" of the impinging bolide. So it does not move aside, but is compressed into a core immediately beneath the oncoming bolide. When its energy is spent, the core rebounds and becomes damped or frozen as a dome by the formation of tension fractures.

The validity of the shatter-cone criterion is greatly strengthened if it proves useful in prediction. The 1967 discovery of the Malbaie astrobleme near Quebec is a case in point. Striated cones in limestone and gneiss were first discovered by a local geologist who did not realize their special significance and termed them "cats' paws." They were then shown to another geologist who recognized them as shatter cones and who, in turn, alerted the Dominion Observatory where a group

of scientists are actively working on Canadian astroblemes. P. B. Robertson, of that group, was soon able to demonstrate the existence of a 37-km-diameter, deeply eroded meteorite impact scar of early Palaeozoic age. This was the first time that shatter cones were noticed prior to the discovery of an associated crypto-explosion structure.

In summary, shatter coning appears to be a most useful criterion for geologic structures created by intense shock, and by inference these must be astroblemes. While normal volcanic explosions appear to be eliminated as a cause of shatter coning, there remains an outside possibility that an unknown geologic mechanism could generate sufficient shock intensities—as, for example, an explosive phase change in the material deep within the Earth. And to be quite sure that we are dealing with impact structures, we need still to find remnants of the cosmic missile. Like traces of TNT in a bomb crater, these still elude our search.



KNOWN SHATTER-CONED STRUCTURES

No	Structure	Location	Date and first published reference	Notes
1	Steinheim Basin	Germany	1905 Branca & Frass	Elegant shatter-coning. Coesite spherules and meteoritic spherules in "Sister" Reis Basin structure
2	Kentland	Indiana	1933 Shrock & Malott	Coesite. Formerly excellent shatter cones
3	Bosumtwi Crater	Ghana	1934 Rohleder	Needs reconfirmation
4	Wells Creek Basin	Tennessee	1936 Bucher	Excellent shatter cones
5	Crooked Creek	Missouri	1954 Hendriks	Fair shatter cones
6	Serpent Mound	Ohio	1960 Dietz	Fair shatter cones. Coesite reported but needs confirmation
7	Flynn Creek	Tennessee	1960 Dietz	Shatter-coning poorly developed
8	Sierra Madera	Texas	1960 Dietz	Excellent shatter-coning
9	Vredefort Ring	South Africa	1961 Hargraves	Grand scale shatter-coning
10	Decaturville	Missouri	1963 Dietz	Fair shatter-coning
11	Carswell Lake	Canada	1964 Innes	Poorly known
12	Clearwater Lake West	Canada	1964 Dence	Shatter-cone development poorly known
13	Sudbury	Canada	1964 Dietz	Excellent cones
14	Middlesboro	Kentucky	In press Dietz	Poor cones
15	Manicouagan	Canada	Unpublished Dence & Manton	Poorly known
16	Nicolson Lake	Canada	Unpublished Dence	(?)
17	Gosse's Bluff	Australia	1967 Crook & Cook	"Abundant shatter cones"
18	Malbaie	Quebec, Canada	1967 Robertson	Shatter cones found prior to identification of the impact structure
19	Kaalijarv Crater	Estonia, USSR	1964 Krinov	Modern meteorite crater

Reprinted from SHOCK METAMORPHISM OF NATURAL MATERIALS
B.M. French and N.M. Short, Eds. Mono Book Corp. Balt.

SHATTER CONES IN CRYPTOEXPLOSION STRUCTURES

ROBERT S. DIETZ¹

Institute for Oceanography, ESSA, Silver Spring, Maryland 20910

Shatter cones are now known from 18 sites around the world, including 16 cryptoexplosion structures and two meteorite craters (Bosumtwi in Ghana and Kaalijarv in Estonia). The cryptoexplosion structures with known shatter-coning are Steinheim Basin in Germany; Kentland, Wells Creek, Crooked Creek, Serpent Mound, Flynn Creek, Sierra Madera, Decaturville and Middlesboro in the United States; Sudbury, Clearwater Lake West, Carswell Lake, Manicouagan, and Nicholson Lake in Canada; Vredefort Ring in South Africa; and Gosses Bluff in Australia. A review of their characteristics reinforces the belief that shatter cones are useful field criteria for shock-wave fracturing and so constitute presumptive evidence for astroblemes—ancient meteorite impact scars. The recent Kaalijarv discovery by Krinov provides a new example of shatter-coning at a modern meteorite crater. The question of shatter cone orientation is discussed as are other types of natural coning which have been mistaken for shatter cones. New work at Sudbury and Vredefort has added some support for an impact origin.

INTRODUCTION

For more than two decades, I have attempted to relate shatter-coning to astroblemes (ancient meteorite impact scars). No full review of this subject will be made here as my findings and opinions have already been covered in earlier papers and so are in the public domain (Dietz: 1947, 1959, 1960, 1961a, 1961b, 1963, 1964, and 1966c, and Dietz and Butler, 1964). It suffices here to add new information so as to update this fascinating problem.

Shatter cones are a peculiar type of rock fracturing apparently caused by the passage of intense shock waves. Their orientations, where measured, are such that these shock waves apparently arrived from a source above their present locations. Bona fide examples, now known from 18 localities, are invariably from cryptoexplosion structures—sites proposed to result from natural explosions, as based on evidence quite apart from the presence of shatter cones. The possibility of an intraterrestrial origin, even as an additional cause of shatter-coning, seems unlikely to me but cannot be definitely ruled out. The usual max-

imum pressure associated with volcanism (steam explosions of low *brisanse*) are generally cited as being about 0.6 kilobar. Gorshkov (1959) quotes 3 kb for the eruption of Bezymianny in Kamchatka; but it remains unknown if even such an explosion produces other than elastic waves. We are still faced with the problem of identifying a definitive astrobleme—e.g., by the discovery of associated meteorite debris or similar compelling evidence. In recent years the case for many so-called cryptovolcanic structures actually being astroblemes has become ever stronger, critics notwithstanding (e.g., Bucher, 1963).

The term *fossil meteorite crater* is sometimes used to refer to many of the presumed impact sites in Canada. While the term is quite descriptive for certain sites like Holleford and Brent, it is not an apt description of Manicouagan, which is dominated by a central uplift. And certainly, it fails to describe essentially all of the presumed astroblemes in the United States, like Wells Creek or Sierra Madera. Also the use of the adjective *fossil* is not correct, as this term specifically applies to some impression or trace of *life* preserved in rock. Furthermore, the object which produced an impact scar may not have been a meteorite. Many, perhaps most, such structures may have been formed by comet heads or by other, as yet

¹ New address: Institute for Oceanography, ESSA, 901 S. Miami Ave., Miami, Florida 33130.

undescribed, packets of cosmic energy that may conceivably exist. The term *astrobleme*, from Greek roots meaning *star-wound*, would seem preferable. The structures are of sufficient importance to justify the coining of this new term (Dietz, 1963).

In the last decade there has been a gradual acceptance by most geologists of the existence of at least some meteoritic impact structures on the earth. It would seem that those who still deny that *any* cryptoexplosion structures are astroblemes would apply their best efforts to find other structures which permissively might qualify as impact sites. Unfortunately, some critics seem indisposed to help out in this respect. An extreme (and I hope, not typical) opinion is, for example, expressed by Amstutz (1964) who flatly rejects "exogenous creationistic theories" and "epi-exo-myths." He writes: "This process of thought from epi-exo-patterns to syn-endo-patterns is one which takes place all the time in fields of human culture, including the sciences. It suffers relapses, of course, as recently seen when the myth of flying saucers and of meteor impact structures swept around the world and even affected the scientists."

THE SHATTER-CONING PHENOMENON

Shatter cones are striated cup-and-cone structures, most common in carbonate rocks, but also known from shale, sandstone, quartzite, granite, and other lithologies. The striated surfaces radiate from small parasitic horsetail-like half-cones on the face of the master cone—a pattern which serves to differentiate these striations from the parallel grooving of slickensides. Unlike slickensides, shatter cones also have positive faces on the cone and negative faces on the cup. The apical angle varies but is usually close to 90 degrees. Cones vary greatly in size from less than 1 cm to as much as 12 m in length. With shatter cones, "a picture is worth a thousand words" as seen in some examples shown in Plates I and II.

An illuminating theoretical study of shatter-coning has recently been made by Johnson and Talbot (1964). They conclude that shatter cones are shock-fractures formed along a traveling boundary between plastic and elastic shock re-

sponse of the medium, defined by the dynamic elastic limit. The horsetail-like striations may be caused by the plastic domain moving relative to an elastic domain. They also note that no other known type of fracture displays this remarkable pattern of radiating ridges and grooves, which adds credence to the judgment that shatter cones result from some unusual type of fracture mechanism. They conclude that: (1) shatter cones are produced as a result of the interaction of an elastic precursor in a shock front with an inclusion or inhomogeneity; (2) the susceptibility to shatter-coning is a function of the shape of the Hugoniot for the rock in which the shock wave is propagating; (3) shatter cone formation requires shock-wave intensities of magnitudes rarely produced (if ever—author's note) in a volcanic explosion; (4) the distribution of shatter cones should be symmetrical, about the point of origin of the shock wave; (5) if the transmitting medium is stratified rock, certain strata may contain shatter cones, while others may not, depending on the susceptibility of individual strata to shatter-coning; (6) shatter cones will be oriented with their axes directed toward the point of impact or explosion; (7) it is impossible to predict the size of shatter cones in terms of present theory; (8) the majority of shatter cones will have apical angles very close to 90 degrees; (9) the intensity of shatter-coning will depend upon the number of inclusions in the rock; and (10) fine-grained, more homogeneous rock will favor shatter cone formation.

The Johnson and Talbot analysis is in accord with many field observations: (1) Shatter cones generally seem to be oriented toward ground zero, implying that the shatter-coning event preceded upheaval of the rocks that contain them. (2) In small shatter-coned structures, the shatter cones are developed in the central "bull's-eye," but in large structures such as Vredefort and Sudbury they occur far out in the upturned ring. This is consistent with shatter-coning not being developed in the domain of the plastic shock wave near ground zero, but only farther away where the impulse has degenerated to the level where an elastic precursor shock wave is formed. (3) High-pressure phases (coesite, stishovite,



Plate I—Shatter Coning from Wells Creek Basin

Shatter-coned block of Knox dolomite collected from the center of the Wells Creek Basin cryptoexplosion structure in Tennessee. Note the common orientation of all cones, blunted apices of cones, and the stacking (but not mutual intersection) of cones. Characteristic also are the striations or horsetails on each cone. Photo by C. W. Wilson.

maskelynite, etc.) have not been found associated with shatter cones. These observations suggest that shatter cones are formed outside of the region of most intense shock overpressures, and may develop at pressure ranges from 20 to 100 kilobars, depending on the Hugoniot of the rock. However, x-ray diffraction studies (Simons and Dacheille, 1965; Dacheille, Gigl, and Simons, *this vol.*, p. 555) have yielded evidence of shock damage in single crystals of quartz and calcite from several shatter cones provided by the author. Carter (1965) has also found basal quartz deformation lamellae in a shatter cone from Vredefort Ring. He has noted the same features at Meteor Crater, and he suggests that impact shock

overpressures between 35 and 60 kilobars are indicated; these values are consistent with dynamic elastic limits for these rocks. Basal quartz deformation lamellae have also been recently noted in shatter cones from Sudbury (Wm. Scott, unpublished information).

Johnson's and Talbot's analysis is the first attempt to provide a sound theoretical basis for the shatter-coning phenomenon. Undoubtedly, their conclusions will be revised as further study is made, but it is certainly a good beginning. To date, experimental work and theoretical analysis on shatter-coning have been quite limited so that empiricism still rules—a gap which should be eliminated. However, the work done thus far



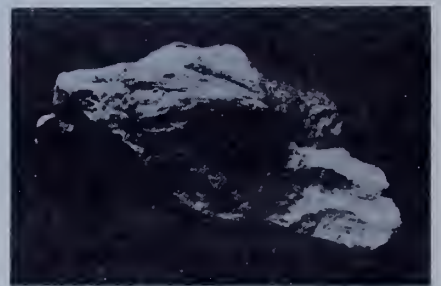
(A)



(B)



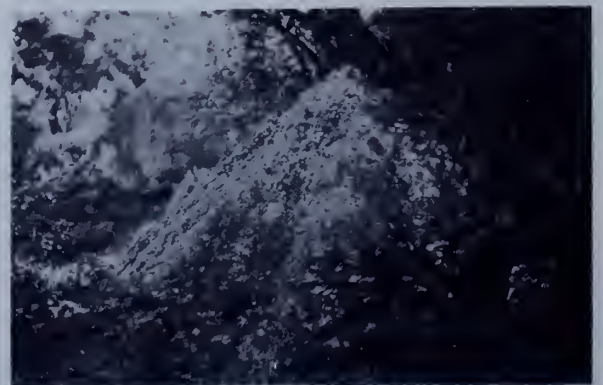
(C)



(D)



(E)



(F)

generally has added support to the belief that shatter cones may well be a criterion for astroblemes.

DISTRIBUTION OF SHATTER-CONED SITES

My preference for the astrobleme interpretation of shatter cone sites is based upon an assessment of all known localities where such fracturing is found. At the time of my summary paper (Dietz, 1959), only four such sites were known, but this number has increased in recent years, and currently 18 sites are known; these are listed in Table I, chronologically by time of discovery. Although little can be learned from any single shatter-coned site, the observations from this group of similar structures provide support for the impact origin. For example, the proponent of "cryptovolcanism" might reasonably explain away absence of hydrothermal effects or volcanic products at any particular site, but not collectively at all shatter-coned structures. Similarly, one might reasonably explain the upward orientation of shatter cones in a single structure as the result of the explosion of a steam pocket trapped above the presently preserved structure, but this reasoning is not convincing when it can be shown that an upward or inward orientation is general. Of course, this reasoning depends upon there being only one cause for shatter-coning.

As already noted, the identification of shatter-coning can be problematical. I have always tended to consider the shatter cones at Flynn Creek to be of rather marginal quality, and not as fully confirmed as those which I have collected elsewhere. However, Roddy (1963 and personal communication), who is mapping the structure in great detail, assures me that Flynn Creek is

definitely shatter-coned in its center although there is a very limited outcrop area of shatter-coned rock.

The Canadian "fossil meteorite craters" of Beals and his associates were studied for many years without any shatter cones being observed. Recently, however, they have been reported from Carswell Lake (Innes, 1964), from Clearwater Lake West (Dence, 1964), and from Manicouagan, where they have been discovered by Dence and Manton, marginal to the large central uplift (personal communication). I can personally agree that those from Carswell Lake and Clearwater Lake West are rather poor but nevertheless probably genuine examples of shatter cones, so far as one can judge from seeing only a hand specimen. They are developed in gneiss, and such coarsely crystalline rocks tend not to display the phenomenon in fine detail. Both of these identifications were made by observers well acquainted with shatter-coning phenomena elsewhere. Another new Canadian locality for shatter cones apparently is Nicholson Lake, N.W.T. (Dence *et al.*, *this vol.*, p. 339), an irregularly-shaped lake approximately 7 miles in diameter which forms part of the Dubawnt River drainage system. The deformation affects Precambrian granitic rocks, and reconnaissance geological and geophysical work during June 1965 is said to strongly support a meteoritic origin.

An interesting cryptoexplosion structure within the United States at which no shatter cones have been found is Jephtha Knob, Kentucky. I have personally searched the area twice without success. Seeger (1966) has recently made a detailed restudy of Jephtha Knob in which he confirms that it is similar to the other structures originally described by Bucher as cryptovolcanic. Seeger

Plate II—Shatter Cones from Various Localities

A. A group of shatter cones (about 8 cm long) from the Steinheim Basin, Germany, the locality where these shock-generated cones were first discovered.

B. A large (2 m.) shatter cone from the Kentland astrobleme in Indiana, showing rich development of parasitic cones on the master cone. The beds are upended with their tops being to the left; hence the cone would point skyward when the beds are turned to their pre-event position. This relation indicates that the shock wave came from above.

C. A typical shatter cone (10 cm. high) from Kentland. Right side shows characteristic horsetailing of the striations; left side is weathered.

D. Small shatter cone (3 cm. long) from the main Kaalijarv meteorite crater in Estonia. Photo by E. Kriinov.

E. Hand specimen of a 10 cm. long shatter cone from the Vredefort Ring of South Africa.

F. Large (1 m. high) weathered shatter cone in the alkali granite in the upthrown rim of the Vredefort Ring.

TABLE
List of Known Shatter-

No.	Structure	Location	First published reference	Location of shatter cones
1	Steinheim Basin	Germany	Branca and Fraas, 1905	Central uplift
2	Kentland	Indiana	Shrock and Malott, 1933	Center
3	Lake Bosumtwi	Ghana	Rohleder, 1934	
4	Wells Creek Basin	Tennessee	Bucher, 1936	Central uplift
5	Crooked Creek	Missouri	Hendriks, 1954	Central uplift
6	Serpent Mound	Ohio	Dietz, 1960	Central uplift
7	Flynn Creek	Tennessee	Dietz, 1960	
8	Sierra Madera	Texas	Dietz, 1960	Central uplift Periphery
9	Vredefort Ring	South Africa	Hargraves, 1961 Dietz, 1961a	Central uplift Periphery
10	Decaturville	Missouri	Dietz, 1963	Center
11	Carswell Lake	Saskatchewan, Canada	Innes, 1964	Periphery
12	Clearwater Lake West	Quebec, Canada	Dence, 1964	Central uplift
13	Sudbury	Ontario, Canada	Dietz, 1964	Periphery
14	Middlesboro	Kentucky	Dietz, 1966a	
15	Manicouagan-Mushalagan	Quebec, Canada	Dence and Manton, unpubl.	Central uplift
16	Nicholson Lake	N.W. Territories, Canada	Innes and Dence, 1965	
17	Gosses Bluff	Australia	Cook, 1966 Crook and Cook, 1966	Central uplift Periphery
18	Kaalijarv	Estonian SSR	Aaloe and Krinov, unpub.	

rules out an endogenic origin for Jeptha Knob and regards it as most likely the scar of the hypervelocity impact of a meteorite or comet head; he, too, has been unable to find shatter coning. This is really not too surprising since the entire central area of the structure is capped with post-event Paleozoic rocks.

GOSSES BLUFF, AUSTRALIA

A recently discovered shatter-coned structure of exceptional interest is the Gosses Bluff astrobleme in the Amadeus Basin of central Australia (latitude 23°48'S, longitude 132°18'E), 150 miles west

of Alice Springs (Cook, 1966; Crook and Cook, 1966; Dietz, 1967). Gosses Bluff also appears on a Gemini IV space photo (V-2-22). The structure was originally described (Prichard and Quinlan, 1962) as a diapir caused by subsurface flow of the incompetent Bitter Springs limestone; however, the hypothesized plug of this limestone was not encountered in a test drilling to more than 4,000 feet. A drill-core cutting which shows a portion of a shatter cone in limestone was kindly sent to me in early 1966 by the Australian Bureau of Mineral Resources in Canberra. Although only a section of a cone is present, the details of the fracture pattern are sufficiently good to identify it as an

1

Coned Structures

Rock types which show shatter-coning	Remarks
Limestones	Coesite, stishovite, and nickel-iron spherules found in "sister" Ries Basin astrobleme.
Limestone, shale, sandstone	Excellent shatter-coning now mostly quarried away. Coesite reported (Cohen, Bunch, and Reid, 1961). Rohleder (1934) reported a possibly shatter-coned fragment in explosion debris of north wall of crater; needs reconfirmation.
Dolomite	Excellent shatter cones.
Limestone	Cones are small, only fair quality. Found along creek beds only in central uplift.
Limestone	Cones are of only fair quality, limited to limestones in center of central uplift.
Limestone	Definite but poorly developed.
Limestone	Majority of cones found in central uplift, but recently discovered in peripheral rocks as well.
Sandstone	
Granite	Shatter-coning developed on a grand scale at more than 60 localities, mostly in rocks of uplifted annular collar, but also in central granite core.
Quartzite, granite, amygdaloid <i>et al.</i>	
Limestone	Cones are of fair quality.
Crystalline gneiss	Convincing but crude examples recovered from outer ring of structure.
Crystalline granitic gneiss	Crude but convincing examples found in various crystalline rocks. Widespread shock metamorphism present.
Quartzite, shale, granite, <i>et al.</i>	Excellent shatter cones at more than 100 localities, from uplifted annular ring surrounding irruptive. Developed in many lithologies, most spectacularly in Mississagi quartzite.
Shaly sandstone	Exhibits probable examples of poor shatter-coning. Shock-metamorphic features in quartz (N. M. Short, personal communication).
Crystalline gneisses (anorthosite, gabbro)	Crude but definite shatter cones found in various lithologies. Many other shock-metamorphic effects also present.
Crystalline gneisses	Good shatter cones present.
Limestone, sandstone, siltstone, mudstone	Abundant shatter cones in various lithologies, both on surface and in drill core to 3,000 ft. Most common in central uplift, but found as far as 5 mi. from center of structure. Glassy breccia, planar lamellae in quartz, are also present.
Dolomite	Segments of small shatter cones in dolomite found in explosion debris in wall of main crater. Only known example of shatter cones associated with meteorite fragments in an accepted meteorite crater.

unquestionable shatter cone. Shatter cones have also been found at the surface in the center of the structure (Plate III). Hence Gosses Bluff must be added to the list of shatter-coned structures.

Gosses Bluff is circular and has the typical damped-wave form of many other shatter-coned structures. A central domal uplift 3 miles across is surrounded by a ring syncline followed by a ring anticline so that the entire area of deformation is about 12 miles across. Ordovician and Silurian (?) beds include a wide variety of lithologic types which eventually should provide much information on shock effects for some rock types about which we now know little.

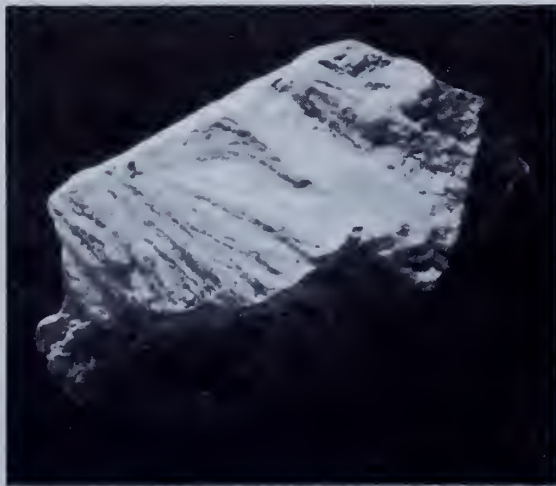
Cook (1966) writes that, from a recent restudy of Gosses Bluff, shatter cones are remarkably well developed and that the structure probably offers one of the best localities in the world for their study. The shatter cones are widespread; they are present in the center, in the rim of the central uplift, and out to at least 5 miles from the center. They occur in all types of rock—sandstone, limestone, siltstone, and mudstone, as either individual or multiple cones which range in length from less than 1 inch up to several feet. In the east rim they show a strong preferred orientation with the apices pointing upwards and parallel to bedding in vertically



(A)



(B)



(C)



(D)

Plate III—Gosses Bluff Cryptoexplosion Structure, Australia

A. Gemini IV space photo (no. V-2-22) giving a view of Gosses Bluff from near space. Central uplift (dark ring) about 3 miles across is surrounded by an outer ring syncline (ghost ring). NASA photo, taken August 27, 1965 from an altitude of 165 miles.

B. Aerial oblique view of Gosses Bluff in central Australia showing the central uplift of the cryptoexplosion structure which is presumably an astrobleme. Photo from P. Cook.

C & D. Shatter cones from Gosses Bluff structure are an indication that shock forces were involved in its creation. Photos from P. Cook and K. Crook. The specimen in C is about 3 cm. high and is from a drill core obtained at about 3,000 feet below the surface in the center of the structure.

upthrown beds. (This, of course, means that if the beds are returned to their pre-event position, the apices would point inward toward ground zero, the direction from which the shock wave arrived.) Elsewhere other shatter cones commonly have their apices normal to bedding planes.

In some areas, however, the apices show a random orientation with, for instance, three or four different orientations of shatter cones on a single hand specimen. A thorough quantitative study of the shatter cones will be necessary to establish or refute the existence of a preferred orientation of shatter cones at Gosses Bluff. The reality of cone apices pointing in random directions seems questionable. Cone segments alone may show orientations that are as much as 90 degrees apart owing to the master cone's apical angle of about 90 degrees (Manton, 1965). Fully inverted cones are sometimes found, but not random orientations. The astrobleme concept predicts that the cones should show a strongly preferred orientation toward ground zero, and I predict that a detailed study at Gosses Bluff eventually will confirm this orientation.

Cook states that subsurface shatter cones are fairly common. They occur down to 3,000 feet in the Gosses Bluff oil test well drilled in the center of the structure, and also in four other shallow wells drilled in the periphery for stratigraphic purposes.

Although Australian geologists remain skeptical about the astrobleme interpretation of Gosses Bluff, it seems to me to be an excellent and undoubted example of such a structure. The wide distribution of shatter cones away from the central eye suggests that Gosses Bluff may bridge the gap between small astroblemes where shatter cones occur only in the "bull's eye," and larger ones where they are found only far out in the periphery.

SHATTER CONES AT MODERN METEORITE CRATERS

Shatter cones have been almost entirely found in presumed astroblemes—ancient impact sites. It would obviously be useful to find them in modern meteorite craters as well. The early description of shatter cones from the Lake

Bosumtwi crater by Rohleder (1934) provides a possible connection with a highly probable young meteorite crater in which coesite-bearing impactite and meteoritic spherules have been found (Littler *et al.*, 1962; El Goresy, 1966). Although Rohleder's description is brief and is supported only by a poor sketch, his identification is probably valid, inasmuch as he was immediately struck by the similarity of these features with those from the Steinheim Basin in Germany. However, on recent visits to Lake Bosumtwi, both Monod and Chao (personal communications) were unable to locate definite shatter cones, and further study of this locality is sorely needed. A possibly shatter-coned piece of Coconino sandstone from Meteor Crater, Arizona, found by Chao and noted by Dietz (1963) is also questionable and cannot really be admitted as evidence for shatter-coning in a modern meteorite crater.

As noted above, the identification of shatter cones at Bosumtwi needs reconfirmation and thus does not provide a fully satisfactory tie-in between shatter cones and accepted modern meteorite craters. However, the finding by E. I. Krinov (unpublished) of shatter cones at the largest crater (110-m diameter) of the Kaalijärvi group in Estonia (Krinov, 1961) now bridges this gap. Two small shatter cones (2 cm high) recently discovered in dolomite were shown to me by Krinov (of the USSR Academy of Sciences' Committee on Meteorites) at Moscow in June 1966. Although they are not fully complete cones, they do display the usual conical shape and horsetail-packet striations in fine detail. There is no doubt that they are bona fide examples of this mode of shock fracturing. These shatter cones are being placed on display at the Mineralogical Museum along with impactites and meteorites previously collected from the Kaalijärvi craters. The shatter cones come from the main crater, the only one considered to be an explosion crater as evidenced, for example, by the quaquaversally uplifted dolomite strata. The cones were discovered in an exploratory pit in ejecta detritus inside the south wall of the main crater.

ORIENTATION OF SHATTER CONES

Both the reality and the significance of orientation of shatter cones have been questioned. How-

ever, the axes of shatter cones do show a remarkable preferred orientation within any particular rock unit although individual megabreccia blocks may be variously oriented. Exceptions to the common orientation do occur; the most frequent exceptions (although quite rare) are completely inverted cones. I have seen examples at Kentland, Decaturville, and the Steinheim Basin. The appearance of divergent axes commonly arises from seeing only cone segments rather than full cones which can occur 90 degrees or a little more apart. However, the plotting of numerous cone segments at Vredefort (Manton, 1965), Crooked Creek (Hendriks, 1954) and Wells Creek (Stearns *et al.*, *this vol.*, p. 323) has demonstrated a common orientation. Hendriks' plotting of several hundred cone segments at Crooked Creek (personal communication) showed that the cone axes have an upward orientation at a steep angle to bedding.

Even more detailed plotting at Wells Creek reveals orientation at a steep angle to bedding and directed either inward toward ground zero or, alternately, outward and away from ground zero (Stearns *et al.*, *this vol.*, p. 323). The uncertainty in this case arises from the fact that it is impossible to determine tops and bottoms of beds (which units are inverted and which are not). Stearns prefers to consider the upward orientation as being real, for it is difficult to envision a shock wave propagation toward a point of common convergence.

Shatter cone orientation similar to that at Vredefort Ring (inward-pointing cones when the upturned rocks are returned to their pre-event position) is found at Sudbury, although the observations are confined to a limited section along the south side of the structure (Dietz and Butler, 1964) (Plate IV). More recently, International Nickel Company geologists (Bray *et al.*, 1966) have confirmed this orientation in other portions of Sudbury Basin.

THE VREDEFORT RING AND THE SUDBURY STRUCTURE

Many geologists, and especially astrogeologists, are now inclined to accept the small shatter-coned structures like Wells Creek and Sierra Madera as

probable astroblemes (Plate V). However, some balk at the suggestion that large shatter-coned structures like the Vredefort Ring and Sudbury may also be astroblemes, and so doubt the significance of the shatter cone criterion. They may argue that shatter-coning can have many origins, or may suggest that the term is being applied to fracture patterns unlike those at the standard localities—i.e., Steinheim Basin and Wells Creek. In my opinion, both Vredefort and Sudbury are unquestionably shatter-coned and spectacularly so. It is pertinent to note that my interpretation of both Vredefort and Sudbury as astroblemes (Dietz, 1961a; Dietz, 1964) was not based upon the discovery of shatter cones. Instead, I considered that there was enough geologic evidence of shock effects at these structures to make the search for shatter cones worthwhile. Shatter cones were subsequently found at both structures, so that the astrobleme concept thus has the added support of successful predictions.

The origin of the Vredefort Ring is an intriguing and complex problem; for, if it is meteoritic, the impact event was comparable to that which created Copernicus on the Moon. My impression, upon visiting South Africa in 1964, was that most South African geologists were not favorably inclined toward the impact hypothesis. Since then, evidence supporting the impact origin of the Vredefort Ring has been supplied by the dating of the shatter-coned alkali granite which is intruded into the upturned ring of sedimentary rock surrounding this structure. At the time of my paper on Vredefort (Dietz, 1961a) it was thought that this alkali granite, on geologic grounds, was of the same age as the Pilansburg intrusive and its associated system of dikes in the Bushveld Complex or about 1400 million years old. If verified, this would have ruled out the impact hypothesis, for the Vredefort event has been radiometrically dated as 1970 m.y. (Nicolaysen, 1963), thus necessitating two shatter-coning events widely spaced in time, which is most unlikely. Dating of the alkali granite (Nicolaysen, 1963), however, revealed an age of 2030 m.y.—the granite is older as is required by the astrobleme hypothesis. These two dates are sufficiently close so as to overlap one another within the

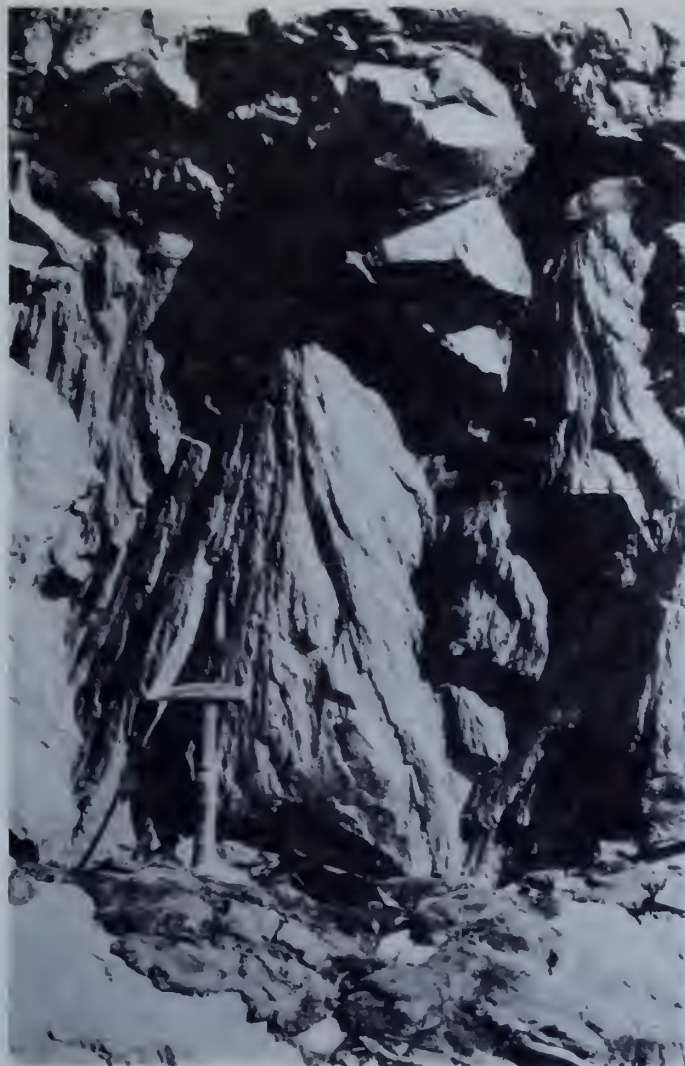


Plate IV—Sudbury Shatter Cones

A group of shatter cones nearly 2 m. high in the Mississagi quartzite from the south rim of the Sudbury Basin. The strata dip almost vertically at this point so that if the rocks are returned to their pre-event position, the cones would point toward the center of the Sudbury Basin. This is the direction of ground zero according to the astrobleme hypothesis. Photo by the author.

margin of error; hence the interpretation that the intrusion of the alkali granite pre-dated the Vredefort event is both permissible and likely, but not fully established.

Another finding supporting the meteorite impact origin of Vredefort has been made by Carter (1965; *this vol.*, p. 453), who has found basal quartz deformation lamellae in a shatter cone from the Vredefort Ring. He considers this a

definitive criterion of shock deformation resulting from meteorite impact. As noted above, shatter cones seem to form outside of the limits of intense impact metamorphism and crushing, and hence rarely show these effects.

On my first reconnaissance of Sudbury, disappointingly few shatter cones were found. Their presence was not emphasized in my first paper on the structure (Dietz, 1964), inasmuch



(A)



(B)

Plate V—Shatter Cones from Steinheim Basin and Sierra Madera

A. Shatter cone in dolomite from the Sierra Madera cryptoblastite structure in Texas. The horsetailing, or packets of striations on the surface, are a hallmark of shatter coning.

B. Shatter-coned limestone from the Steinheim Basin cryptoblastite structure in Germany where this shock fracturing has been known since about 1900. Specimen at

lower right shows a positive face while the upper specimen shows a negative face (or cone mold). The development of such negative faces offer a criterion whereby shatter cones may be differentiated from slickensides (fault slippage striations). The length of the upper specimen is about 8 cm.

as these rocks are ancient and have had a complex history wherein fractures resembling shatter cones might have been produced. During a subsequent visit, however, excellent and extensive shatter-coning was discovered once the search was extended several miles out in the wall rocks

to the south of the Sudbury lopolith (Dietz and Butler, 1964). It also became apparent that the shatter cones at these sites were oriented in such a way that if the rocks were returned to the horizontal (their presumed pre-event position) they would point inward toward Sudbury Basin;

i.e., to ground zero according to the impact concept.

Bray *et al.* (1966) have greatly extended the study of shatter-coning around Sudbury, with results in harmony with the astrobleme concept. Although my discovery of shatter cones was confined to the readily accessible southern margin of the Sudbury Basin, they have recorded shatter cones at nearly 100 sites in a belt 11 miles wide in the wall rocks completely around the Sudbury irruptive. The preferred orientation of the shatter cones is generally parallel to the bedding (as at Vredefort) and the orientation is directed toward the Sudbury Basin—this orientation is strongly enhanced when highly dipping beds are returned to the horizontal (their presumed pre-event position). Shatter-coning was not found outside of this belt although traverses were made out to 60 miles and in the same formations; e.g., the Mississagi quartzite at Blind River. Furthermore, shatter cones do not occur in the younger rocks across the Grenville Front south of Sudbury although they do occur in older Huronian rocks within a few hundred yards of this front. Those rocks which are intruded with the Sudbury breccia are also shatter-coned. Thus excluded from shatter-coning are younger diabase dikes which traverse the region, the Sudbury irruptive itself, and the overlying Whitewater sediments. These last named beds, according to my "extrusive lopolith" (Dietz, 1964) concept (and in contrast to the classical intrusive lopolith concept), are post-impact-event fillings of the Sudbury crater.

Bray *et al.* (1966, p. 245) conclude that "the form, distribution, and orientation of shatter cones at Sudbury . . . (are) not inconsistent with the predictions of Dietz's astrobleme theory. However, the precise origin and genetic significance of shatter cones in general are still open matters, and although Sudbury structure also possesses other features thought to be characteristic of cryptoexplosion structures, much additional information must be forthcoming . . ."

New evidence for the impact origin of Sudbury has recently been described by French (1967; *this vol.*, p. 383). He reports the occurrence of unusual deformation structures, similar to those

observed in rocks from known and suspected meteorite craters, in inclusions of "basement" rock in the Onaping formation at Sudbury, and concludes that "these features, which include planar sets in quartz parallel to the {0001} and {10 $\bar{1}$ 3} planes, suggest that the Onaping formation consists of shocked and melted material deposited immediately after a meteorite impact which formed the Sudbury basin." Fairbairn *et al.* (1967) have radiometrically dated the overlying sediments of the Whitewater series which cover the Sudbury irruptive. The sediments are found to be of essentially the same age as the Sudbury irruptive, a result which is consistent with the impact hypothesis (although not unique proof of this concept), under which the irruptive is an "extrusive lopolith" which welled up into an impact explosion basin.

GEOLOGIC STRUCTURES RESEMBLING SHATTER CONES

The shatter-coning phenomenon can be beautifully developed, as in the carbonates at Steinheim Basin or at Wells Creek Basin, or it can degenerate, particularly in coarser-grained rocks, to the point where it is difficult to differentiate shatter cones from more common types of rock fractures. The so-called slickensides found in some meteorites of the brecciated chondrite class probably are shock fractures closely related to shatter-coning (Dietz, 1966b).

On the other hand, many other structures of conical form have been confused with shatter cones. Among these we may list: cone-in-cone; coal cones; the "striated cones" of Cerro Colorado in New Mexico; and the fibrous crystalline conical habit such as found, for example, in the zeolite mineral pectolite. Of course, all natural cones are not necessarily shatter cones, just as all spherical rocks are not necessarily concretions. Some discretion must be used in identifying shatter cones, but, where well developed, shatter-coning invites no confusion. Non-conical striated surfaces such as slickensides, plumose fracturing, and stylolites, have also been confused with shatter cones but apparently never by those well acquainted with true shatter cones.

Bucher (1963) has described alleged "double shatter cones" in bituminous coal from West Virginia. Such coal cones are not shatter cones, although they bear a fairly close superficial resemblance. They were first described in the 19th century from England (Garwood, 1892; Gresley, 1892), and are now known from New Zealand and Poland. Tarr (1932) considers these coal cones to be a diagenetic structure related to cone-in-cone, but presumably of somewhat different origin. Price and Shaub (1963) describe these cone-in-cone features from West Virginia coal in some detail, and consider them to be pressure cones caused by loading or by tectonic stress. They compare them to the cones which can be generated by shearing in a cylinder of any brittle material (such as a cement pillar) during axial compression. Unfortunately the specimens studied were picked out of a coal bin and were not seen in place, a factor which seriously hampers understanding them. Tectonism appears to have played a role in the development of such cones in Poland (Gorzyca and Kwiecinska, 1963; Kwiecinska, 1963). Recently I have had an opportunity to examine several such specimens at the Newcastle-on-Tyne museum. These cones are not shatter cones, although a selected hand specimen may bear certain superficial resemblances to them.

In a treatment which is difficult for me to follow, Amstutz (1965) contends that the shatter cones present at both the Decaturville and Crooked Creek structures in Missouri are, in fact, not shatter cones at all. This is in marked contrast with the general consensus of opinion, which I share, that both of these cryptoexplosion structures contain, without question, bona fide shatter cones. In Amstutz' view, the cones at Crooked Creek are of a diagenetic type related to cone-in-cone, while those at Decaturville were somehow created by the regional tectonic stress field. In November 1965, I participated with about 75 other geologists in a Geological Society of America field trip through Missouri, which visited these two cryptoexplosion structures. In the discussions which ensued, no one questioned that the conical structures found in the central eye of both of these cryptoexplosion structures

were other than bona fide shatter cones. Of course, there was by no means universal agreement with my contention that both of these structures are astroblemes.

Monod (1963) quoted Karpoff as having found shatter cones in North Africa, confined to a thin horizon and extending for at least 15 km, an occurrence which has led Monod to dismiss the validity of shatter-coning as a shock criterion. It seemed evident that Karpoff was in fact describing a cone-in-cone layer, because this distribution is typical of cone-in-cone, whereas shatter cones massively and locally invade a rock mass. In the central United States carboniferous sediments, cone-in-cone horizons have been traced for as much as 500 miles from Indiana to Missouri (R. K. Wanless, personal communication). Shatter cones and cone-in-cone are strikingly different structures which should not be confused even in the hand specimen. They certainly cannot be confused in the field as cone-in-cone occurs along a thin stratum while shatter cones invade an entire rock mass. More distinctively, shatter cones occur in rocks of diverse lithologies and grain sizes, while cone-in-cone is generally restricted to impure calcareous rocks; also, cone-in-cone develops perpendicular to bedding planes while shatter cones may be variously oriented. The specimens in question were recently sent to me by Karpoff. They clearly are typical cone-in-cone, including even the common circular banding. To eliminate any subjectivity, the specimens were submitted to Drs. Carozzi and Wanless, of the University of Illinois, who agree that these specimens are indeed cone-in-cone.

Elston and Lambert (1965) have described what they consider to be possible shatter cones in an ancient volcanic funnel, Cerro Colorado near Albuquerque, New Mexico. Recognizing that these features are somewhat different from normal shatter cones, they have termed these "striated cones." They claimed that there are no objective criteria by which shatter cones can be distinguished from their striated cones. They do note the greater coarseness of the largest size of striated cones from Cerro Colorado, and the greater ease with which the Wells Creek shatter cones break out of the rock. In my opinion, these

striated cones and shatter cones bear virtually no resemblance to each other; it requires great imagination to see any similarity at all. Some points of difference may be listed as follows: (1) Some striated cone specimens show degrees of conical curvature but complete cones are not found. (2) The conical surfaces are weathering surfaces and not fracture planes, and it is impossible to obtain these striae on any freshly broken surface. (3) The striae on true shatter cones are rapidly lost when exposed to weathering but those on the Cerro Colorado striated cones are enhanced by weathering; in fact, they seem to be the result of differential weathering. (4) The so-called striae are not really striae at all but rugose markings. R. Hargraves, W. Manton, and N. Short (personal communications), all of whom have worked extensively with shatter cones, concur in my opinion that these definitely are not shatter cones. At this conference, Elston (*this vol.*, p. 287) read a paper pertaining to these cones entitled "Striated Cones: Wind Abrasion Features, not Shatter Cones" which indicates that he, too, now concurs in their not being shatter cones.

W. A. Cassidy (*this vol.*, p. 117) described and showed photographs at this conference of cone-shaped pieces of compressed clay from beneath a meteorite found in one of the Campo del Cielo craters of Argentina. He suggested these might be shatter cones. Although they are rudely conical, they lack the striations, and so I doubt that they are. More likely they are simply percussion or loading cones which would fit the fact that these craters are penetration funnels and not explosion craters.

ARTIFICIAL EXPLOSION AND IMPACT CONES

Explosion cones are produced in rocks by high explosives; an example of such a cone from a limestone quarry is shown in Plate VI. A rude cone results where the fracture appears to follow original lines of weakness in the rock. Similar conical explosion fractures may be commonly seen in road cuts, but cones with the geometric perfection and surface striations of shatter cones are never found. Quarrymen are primarily inter-

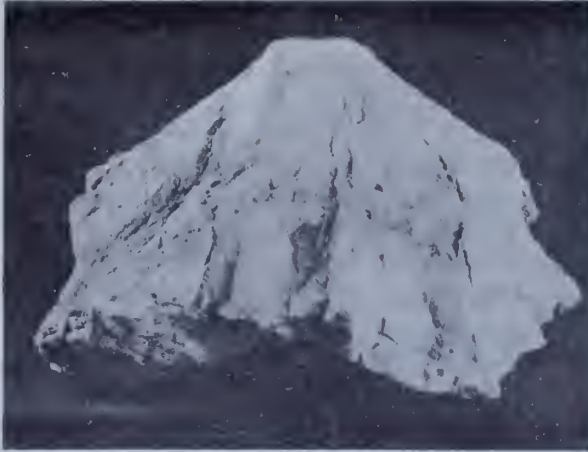
ested in heaving and moving rock rather than shattering it and so avoid high brisance explosives. By using a high-brisance military explosive (C-4, detonation wave velocity 25,000 ft./sec.), I have been able to create cones more perfect than TNT generated cones and with faint surface striations suggestive of shatter cones. By extrapolation, it would seem (perhaps naively) that if more intense explosives were available, shatter-coning might result. On the other hand, Shoemaker et al. (1961) have produced rather good, although minute, shatter cones in rock by using a hypervelocity bullet fired from a light gas gun. The apices of these cones produced in the impact-explosion crater point toward the point of impact.

CONCLUSIONS

The accumulated evidence that shatter-coned cryptoexplosion structures are astroblemes has become quite impressive, although the evidence at any particular site may be scant. Shatter-coning, together with coesite, impact metamorphic effects etc., still remains only an indication of shock; and hence of impact only by inference. There remains the possibility (although in my opinion an unlikely one) that the shock might have been generated by some intraterrestrial explosion triggered by a geologic process of an as yet unspecified nature. Without doubt we will continue to find new cryptoexplosion structures; the presence of shatter cones will sometimes provide the initial clue. With the continuing study of shatter cones the fascinating problems of the role of meteorite impacts in geology will be further illuminated.

NOTE ADDED IN PROOF

Since the preparation of this manuscript, I have been able to visit the Gosses Bluff cryptoexplosion structure in central Australia, which appears to be one of the most intensively shatter-coned structures in the world (Cook, 1968). In this structure, shatter-coning is developed on a remarkable scale, particularly in the northern sectors. Fragments of shatter-coned rocks are found in breccia zones, indicating that the formation of



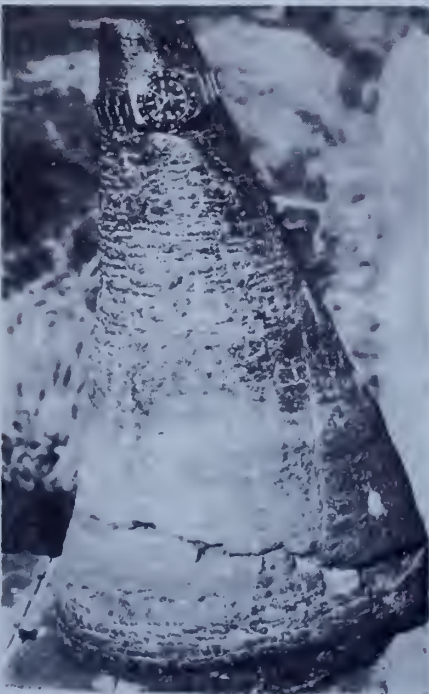
(A-1)



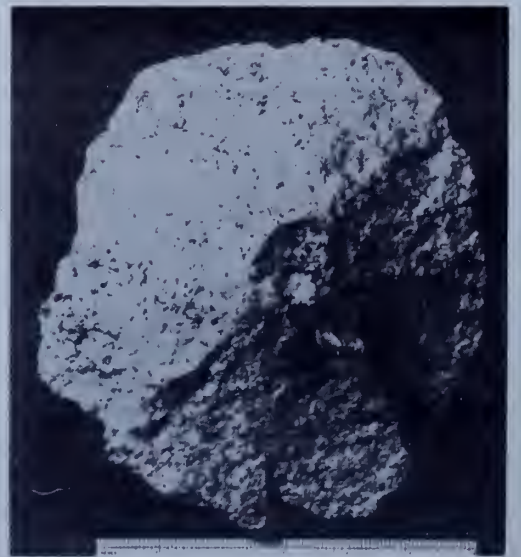
(A-2)



(B)



(C)



(D)

the shatter cones preceded formation of the breccias. The theory of impact origin for Gosses Bluff would require, however, that the two events were practically simultaneous.

Strong preferred orientation of the shatter cones at Gosses Bluff is also remarkably well exhibited. When the uplifted sedimentary rocks are graphically returned to the horizontal, the apices of shatter cones in the central part of the Gosses Bluff structure point upward, and the cone axes intersect in an area about 1.5 mi. in diameter. Somewhat further out from the center of the structure, the apices of shatter cones point both inward and upward; farther out, the cone apices point inward toward the center. These relations, which are identical to those observed at other cryptoexplosion structures (Manton, 1965; Stearns *et al.*, *this vol.*, p. 323), are interpreted to mean that the shock wave was impressed centrally and from above, and that the shock-producing body (presumably a comet head) had an effective diameter of about a mile (Dietz, 1967).

A detailed study of the Sierra Madera, Texas cryptoexplosion structure has recently been completed; the principal investigator now favors the astrobleme interpretation (H. Wilshire, personal communication). Shatter cones at Sierra Madera have been found to pre-date the folding and formation of the central uplift, and the impact origin would require that the shatter cones formed immediately previous to the uplift. Graphical restoration of the shatter-coned beds to the horizontal demonstrates that the shatter cone apices point upward and inward toward the center of the structure. The diapir-like uplift at Sierra Madera may be analogous to the central peaks of some lunar craters.

The information obtained from study of the Gosses Bluff structure emphasizes the growing

use of shatter cones as a field criterion for shock and for possible meteorite impacts; the impact origin of Gosses Bluff was not proposed until the extensive shatter-coning was discovered. More recently, a new shatter-coned locality, tentatively designated La Malbaie, has been discovered along the St. Lawrence River northeast of Quebec (Robertson, 1967). Significantly, the existence of this structure was not recognized until shatter cones were unexpectedly discovered by a French geologist who termed them "cat's paws"; John Murtaugh (personal communication) subsequently recognized them as excellent shatter cones. Subsequent study of the site (Robertson, 1967) has revealed petrographic shock features, and the structure is currently considered to be a 37-km-diameter, deeply eroded meteorite impact crater or astrobleme.

REFERENCES

- Anders, E., Diamonds in meteorites, *Sci. Am.*, 213, 26-36, 1965.
- Amstutz, G., Introduction, in *Developments in Sedimentology*, (G. Amstutz, Ed.), 2, New York, Elsevier Pub. Co., 1964.
- Amstutz, G., A morphological comparison of diagenetic cone-in-cone structures and shatter cones, *Ann. N.Y. Acad. Sci.*, 123, 1050-1056, 1965.
- Branco, W., and E. Fraas, Das kryptovulkanische Becken von Steinheim, *Akad. Wiss. Berlin, Phys.-math. kl., Abh.*, 1, 1-64, 1905.
- Bray, J. G., and geological staff, Shatter cones at Sudbury, *J. Geol.*, 74, 243-245, 1966.
- Bucher, W. H., Cryptovolcanic structures in the United States: *Intern. Geol. Congr. Rpt. 16th, USA, Wash., D.C.*, 2, 1055-1084, 1936.
- Bucher, W. H., Cryptoexplosion structures caused from without or from within the earth? (Astroblemes or Geoblems?), *Am. J. Sci.*, 261, 597-649, 1963.
- Carter, N., Basal quartz deformation lamellae—a criterion for recognition of impactites, *Am. J. Sci.*, 263, 786-806, 1965.

Plate VI—Natural and Artificial Cones Which Are *Not* Shatter Cones

The cones shown are examples of a few of the types of cones found in nature which are *not* shatter cones.

A. TNT cone. Top and side views of a TNT-explosion cone in limestone recovered from a quarry near Nashville. Circular apex marks the base of the drill hole where the TNT charge was emplaced. The rudimentary coning shows a tendency of the fracture surface to follow pre-existing lines of weakness.

B. Cone-in-cone. These cones, whose precise origin remains unknown, are common in impure limestones of the Carboniferous. The horizontal rugosities are typical. The two examples, about 12 cm. high, are from the Cambridge University collections.

C. Serpentine cone. An example of a large serpentine cone (50 cm. high) from an asbestos mine in Southern Rhodesia.

D. Granite cone. A natural cone in the Airy granite of Georgia presumably produced by weathering and spallation.

- Carter, N. L., Dynamic deformation of quartz, *this vol.*, p. 453.
- Cassidy, W. A., Meteorite impact structures at Campo del Cielo, Argentina, *this vol.*, p. 117.
- Cohen, A. J., T. E. Bunch, and A. M. Reid, Coesite discoveries establish cryptovolcanics as fossil meteorite craters, *Science*, *134*, 1624-1625, 1961.
- Cook, P. J., Gosses Bluff cryptoexplosion structures, *Aust. Bur. Miner. Resources, Geol. and Mining, Records*, *132*, 1966.
- Cook, P. J., The Gosses Bluff cryptoexplosion structure, *J. Geol.*, *76*, 123-139, 1968.
- Crook, K., and P. Cook, Gosses Bluff: diapir, cryptovolcanic structure or astrobleme? *J. Geol. Soc. Aust.*, *13*, 495-516, 1966.
- Dachille, F., P. Gigl, and P. Y. Simons, Experimental and analytical studies useful for the recognition of large impact structures, *this vol.*, p. 555.
- Dence, M. R., A comparative structural and petrographic study of probable Canadian meteorite craters, *Meteoritics*, *2*, 249-270, 1964.
- Dence, M. R., M. J. S. Innes, and P. B. Robertson, Recent geological and geophysical studies of Canadian craters, *this vol.*, p. 339.
- Dietz, R. S., Meteorite impact suggested by orientation of shatter cones at the Kentland, Indiana disturbance, *Science*, *105*, 42-43, 1947.
- Dietz, R. S., Shatter cones in cryptoexplosion structures (meteorite impact?), *J. Geol.*, *67*, 496-505, 1959.
- Dietz, R. S., Meteorite impact suggested by shatter cones in rock, *Science*, *131*, 1781-1784, 1960.
- Dietz, R. S., Vredefort Ring structure: meteorite impact scar? *J. Geol.*, *69*, 499-516, 1961a.
- Dietz, R. S., Astroblemes, *Sci. Amer.*, *205*, 2-10, 1961b.
- Dietz, R. S., Astroblemes: ancient meteorite impact structures on the earth, in *The Moon, Meteorites and Comets* (B. M. Middlehurst and G. P. Kuiper, eds.), Chicago, Univ. of Chicago Press, pp. 285-300, 1963.
- Dietz, R. S., Sudbury structure as an astrobleme, *J. Geol.*, *72*, 412-434, 1964.
- Dietz, R. S., Shatter cones at the Middlesboro Structure, Kentucky, *Meteoritics*, *3*, 27-29, 1966c.
- Dietz, R. S., Striated surfaces on meteorites; shock fractures, not slickensides, *Meteoritics*, *3*, 31-330, 1966b.
- Dietz, R. S., Shatter cones and astroblemes, Proc. Oregon Lunar Geological Field Conference, Bend, Oregon, 1966c.
- Dietz, R. S., Shatter cone orientation at Gosses Bluff astrobleme, *Nature (Lond.)*, *216*, 1082-1084, 1967.
- Dietz, R. S., and L. Butler, Shatter-cone orientation at Sudbury, Canada, *Nature*, *204*, 4955, 1964.
- El Goresy, A., Metallic spherules in Bosumtwi crater glasses, *Earth and Planetary Science Letters*, *1*, 23-24, 1966.
- Elston, W., and P. Lambert, Possible shatter cones in a volcanic vent near Albuquerque, New Mexico, *Ann. N.Y. Acad. Sci.*, *123*, 1003-1016, 1965.
- Elston, W. E., P. W. Lambert, and E. I. Smith, Striated cones: wind-abrasion features, not shatter cones, *this vol.*, p. 287.
- Fairbairn, H., G. Faure, W. Pinson, and P. Hurley, Rb-Sr whole-rock age of the Sudbury lopolith and basin sediments (Abs.), *Trans. Am. Geophys. Un.*, *48*, 241, 1967.
- French, B. M., Sudbury structure, Ontario: some petrographic evidence for origin by meteorite impact, *Science*, *156*, 1094-1098, 1967.
- French, B. M., Sudbury structure, Ontario: some petrographic evidence for an origin by meteorite impact, *this vol.*, p. 383.
- Garwood, E. J., *Geol. Mag.*, *29*, 334-335, 1892.
- Gorczyca, S., and B. Kwiecinska, Microstructure of cone-in-cone coals from the Lower Silesian coal basin, *Bull. Acad. Polon. Sci., Ser. Sci. Geol. Geogr.*, *11*, 207-210, 1963.
- Gorshkov, G., Gigantic eruption of the volcano Bezymianny, *Bull. Volcanologique*, ser. 2, *20*, 77-113, 1959.
- Gresley, W. S., *Geol. Magazine*, *29*, 432, 1892.
- Hargraves, R. B., Shatter cones in the rocks of the Vredefort Ring, *Trans. Geol. Soc. S. Africa*, *64*, 147-161, 1961.
- Hendriks, H., The geology of the Steelville Quadrangle, Missouri, Missouri Div. Geol. Surv., and Water Resources (Rept.), ser. 2, *36*, 82 p., 1954.
- Innes, M. J. S., Recent advances in meteorite crater research at the Dominion Observatory, Ottawa, Canada, *Meteoritics*, *2*, 219-241, 1964.
- Innes, M. J. S., and M. R. Dence, Nicholson Lake and Pilot Lake Craters, N.W.T. Canada (Abs.), Meteoritical Soc. meeting, Odessa, Texas, October, 1965.
- Johnson, G. P., and R. J. Talbot, A theoretical study of the shock wave origin of shatter cones, M.S. Thesis, Air Force Institute of Technology, Wright-Patterson AFB, Ohio, 1964.
- Krinov, E. L., Kaalijarv meteorite craters on Saaremaa Island, Estonian SSR, *Am. J. Sci.*, *259*, 430-440, 1961.
- Kwiecinska, B., Cone-in-cone coals in the Lower Silesian coal basin, *Bull. Acad. Polon. Sci., Ser. Sci. Geol. Geogr.*, *11*, 201-206, 1963.
- Littler, J., J. Fahey, R. S. Dietz, and E. C. T. Chao, Coesite from the Lake Bosumtwi Crater, Ashanti, Ghana, *Geol. Soc. America Sp. Paper*, *68*, 218, 1962.
- Manton, W. I., The orientation and origin of shatter cones in the Vredefort Ring, *Ann. N.Y. Acad. Sci.*, *123*, 1017-1049, 1965.
- Monod, Th., Contribution to setting up a list of circular disturbed areas of known, possible or supposed meteoritic origin (in French), Inst. Franc. Afrique Noire, Dakar, Senegal, 1963.
- Nicolaysen, L., A. Burger, and C. van Niekerk, Origin of the Vredefort Ring structure in the light of new isotopic data (Abs.), Internat. Un. Geodesy and Geophysics meeting, Berkeley, California, 1963.
- Price, P. H., and B. S. Shaub, Cone-in-cone in coal, *West Virginia Geol. and Econ. Surv., Rept. Invest.* *22*, 1963.
- Pritchard, C. E., and T. Quinlan, The geology of the southern half of Hermannsburg 1:250,000 sheet, *Austral. Bur. Min. Res., Geology and Geophys.*, *Rept. 61*, 39 p., 1962.
- Robertson, P. B., The Malbaie structure, Quebec—an

- ancient meteorite impact site (abs.), paper presented at the 30th Ann. meeting, Meteoritical Society, Moffett Field, California, Oct. 25-27, 1967.
- Roddy, D. J., Geologic section across the Flynn Creek structure, *U.S. Geol. Survey, Astrogeologic studies, ann. rept., Aug. 1962 to July 1963, Pt. B*, 53-73, 1963.
- Rohleder, H., On the finding of fracture phenomena and striated surfaces on the basin rim of the cryptovolcanic Lake Bosumtwi, Ashanti (in German), *Zentralbl. Mineralogie., Geologie, u. Paläontologie, Abl. A, no. 10*, 316-318, 1934.
- Seeger, C. R., Origin of the Jephtha Knob structure, Ph.D. Thesis, Univ. of Pittsburgh, 1966.
- Shoemaker, E. M., D. E. Gault, and R. V. Lugin, Shatter cones formed by high speed impact in dolomite, *U.S. Geol. Survey Prof. Paper 424-D*, 365-368, 1961.
- Shrock, R., and C. Malott, The Kentland area of disturbed Ordovician rocks in northwestern Indiana, *J. Geol.*, 41, 337-370, 1933.
- Simons, P., and F. Daehille, Shock damage of minerals in shatter cones (Abs.), *Geol. Soc., Am., Kansas City meeting, Program*, p. 153-154, 1965.
- Stearns, R. G., C. W. Wilson, Jr., H. A. Tiedemann, J. T. Wilcox, and P. S. Marsh, The Wells Creek structure, Tennessee, *this vol.*, p. 323.
- Tarr, W. A., Cone in cone, in *Treatise on Sedimentation*, 2nd ed. (ed. by W. H. Twenhofel), pp. 719-721, Baltimore, Williams & Wilkins Co., 1932.

Reply

ROBERT S. DIETZ

Atlantic Oceanographic Laboratories, ESSA, Florida 33130

As Meyerhoff correctly points out, modern hypotheses have often been anticipated or somewhat developed in earlier writings. We see this, for example, in the continental drift concept in which Wegener was, in some respects, anticipated by earlier writers, although these are, at most, rather oblique references or partial expositions. British writers like to quote Sir Francis Bacon as originating continental drift, but it takes some tortured reasoning to extract this from his writing [see *Blackett*, 1965]. It seems to me entirely correct to regard Wegener as the originator of continental drift as a respectable scientific concept, with *Du Toit* [1937] fleshing it out with proper geologic evidence. Certainly Wegener formalized the concept of continental drift, although minor thoughts about drift exist in earlier literature.

As regards sea-floor spreading, Hess deserves full credit for the concept, as correctly noted by Meyerhoff, by reason of priority and for fully and elegantly laying down the basic premises. I have done little more than introduce the term *sea-floor spreading*, which now seems to have acquired a wide usage and a rather definite meaning, and apply it to such things as geosynclinal theory and the tectonic passiveness of the continental plates [*Dietz*, 1963, 1966].

I cannot see that Holmes 'fathered' sea-floor spreading, although perhaps he in some ways anticipated it. Perhaps his chief contribution was the employment of mantle convection as the primum mobile of tectonogenesis. In any event, Holmes' concept (as shown in Figure 1 of Meyerhoff's preceding discussion) is not really sea-floor spreading. He resorts to thinning the crust rather than creating new oceanic rind at the mid-ocean swell and destroying it in

trenches in the conveyor-belt fashion of sea-floor spreading. Also his mid-ocean swell is sialic (which we now know it is not and which would spoil the continental drift jigsaw fit). Holmes thus follows Wegener. Whereas Wegener considered the continents as active elements, Holmes' figure shows them as being passive and entrained by mantle convection, as with sea-floor spreading.

If scientific concepts survive at all, they evolve from speculations to hypothesis and finally to theories. The status of any concept at any point in time is largely a matter of subjective judgment (and, I suppose, semantics). Meyerhoff regards sea-floor spreading as an hypothesis, whereas I am inclined to regard it now as a theory. It seems to me that especially the paleomagnetic results have made it so, subsequent to the suggestion of Vine and Matthews that the sea-floor conveyor belt has a remnant magnetic imprint accounting for the striped anomalies. To these many scientists, too numerous to list here, belongs the real credit. They have advanced a body of speculative subject matter into a theory of sea-floor spreading which seems to be providing a workable framework for geotectonics.

REFERENCES

- Blackett, P. M. S., Introduction, *A Symposium on Continental Drift*, *Phil. Trans. Roy. Soc. London*, 1088, 323 pp., 1965.
 Dietz, R. S., Collapsing continental rises: An actualistic concept of geosynclines and mountain building, *J. Geol.*, 71(3), 314-333, 1963.
 Dietz, R. S., Passive continents, spreading sea floors, and collapsing continental rises. *Am. J. Sci.*, 264, 177-193, 1966.
 Du Toit, A. L., *Our Wandering Continent*, 366 pp., Oliver and Boyd, Edinburgh, 1937.

(Received May 22, 1968.)

Documenta
Geigy **nautilus**⁴

Augusto Gansser	Introduction
Hugh Bradner	Microseism measurements on the deep ocean bottom
Hans M. Bolli	Recent marine sediments on the Great Bahama Bank
Robert S. Dietz	The origin of continental slopes
Augusto Gansser	The geology of the oceans
John B. Saunders	The relationship between land and sea round the islands of Trinidad and Tobago, West Indies

Editors: Dr. Heinz Ambühl, Zurich
Dr. Günther Böhnecke, Hamburg
Prof. Augusto Gansser, Küsnacht
Dr. Hermann Heberlein, Lugano
Rear-Admiral Stanley Miles, Plymouth
Dr. Jacques Piccard, Lausanne
Prof. Adolf Portmann, Basle

The origin of continental slopes

The most striking geological anomaly is probably the continental slope separating the continents and continental shelves from the deep oceans. The continents consist of a crust on the average 35 kilometres thick, but under the oceans this measures only a few kilometres. Various theories have been advanced to account for this striking difference in thickness. The most likely possibilities are discussed in the article below.

Nature of continental slopes

Since water seeks its own level, one might suppose that the oceans have simply ponded in the low places on a world which has a crust that is structurally uniform but is characterized by domes and swales spoiling its exact roundness. With this notion in mind, it came as a surprise to science to find that the earth is characterized by two preferred surface levels—the continental

platforms and the 5-km-deep ocean floors. And these two levels are separated, not by a region of gentle transition, but everywhere by a steep escarpment about 3500 metres high. Abrupt *continental slopes* surround all of the continents, attaining a total extent of 110000 km. So the continents rise as table-like pedestals above the ocean bed, not as dome-like protuberances. These escarpments would comprise the world's grandest

scenery if they could be seen; in the sub-aerial world only the Himalayan rampart ringing northern India offers comparable relief. Why are the earth's surface features of the first order of magnitude, the continents and the ocean basins, so abruptly discontinuous? Surely an understanding of why continental slopes exist, and their composition and origin, is critical to the history of the earth.

In a general way we already know why the continents stand high. They are composed of light granitic rock about 35 km thick which literally floats in the earth's dense mantle much as an antarctic iceberg floats in the Southern Ocean. The density contrast between an iceberg and the ocean is such that the berg floats five-sixths submerged; the density contrast between the mantle and the continents gives the latter a roughly similar "freeboard" with respect to the ocean floor. But this does not really explain the continental slopes for, if the continents were lenticular bodies instead of tabular ones, they would still float in the mantle but without displaying any abrupt continental slope.

Catastrophic explanations for the continental slopes

It would be nice to explain the continental slopes as the rim scars left after some immense catastrophic event early in the earth's history. Many have proposed such schemes and indeed this idea pervades the lay literature about ocean basins. Already Sir George Darwin suggested that the moon is the daughter of our planet, having been torn from Mother Earth by solar tidal attraction, leaving the Pacific Ocean and its ringing continental slope as the birth scar. According to Darwin the earth, when still liquid, once rotated with a four-hour-day period. This being also the natural resonance period of the earth, the tides grew larger daily until a blob of molten rock completely separated, forming the moon. Actually this story has little intrinsic scientific merit and the long persistence of this theory in the lay literature must be ascribed to its poetic beauty. Another catastrophic proposal which is the inverse of Darwin's idea is that the primitive earth was blasted by cosmic bodies which fell into the earth, blasting gaping holes in the earth's crust which have persisted until today as the ocean basins; the continental slopes would be rim scars. The maria on the moon may be cited in

favour of such an interpretation for they indeed do seem to be giant explosion basins. And it seems clear that, if an asteroid as big as the 800-km diameter Ceres were to strike the earth, a scar as large as an ocean basin would be formed. However, it seems equally clear to geologists that such an event has never happened in earth history.

Perhaps the strongest objection to any catastrophic explanation for continental slopes is that they are geomorphically young. They are steep and rugged, which are attributes of geologic youth, rather than worn down and subdued. They must have been formed in the last 100 million years or so; any so recent a catastrophe would leave an indelible and evident geological record. For example, such a great catastrophe would seriously affect the delicate skein of organic evolution, causing the abrupt extinction of many organisms and perhaps even all the higher forms of life. Evidently we must seek an evolutionary explanation for continental slopes by which they have developed in some slow, continuous and orderly manner.

Continental slopes as wave-built terraces

This concept looks upon continental slopes as the advancing edges of a wave-built terrace, a talus of detritus shed from the continental block and laid down like a huge delta. It was presumed that waves dug away at the shore and carried detritus out to the shelf edge where it was suddenly dropped like an embankment of mine tailings (Fig. 2). This view has been generally discredited by marine geological evidence collected over the past few decades. While delta terraces do build out the continental slopes locally, the general concept of the ocean waves creating a sedimentary embankment at the shelf edge is unsound. The sedimentary covering on continental slopes usually is only a thin mantle covering underlying bed rock. Most continental slopes seem to be erosional domains as is shown by the submarine canyons cut into them. The slopes tend to erode back like a mountain front rather than prograde seaward. In short, deposition of sediments can only be a modifying influence and we still must search for some fundamental mode of structural origin for continental slopes.

A variant of the wave-built terrace idea is that continental slopes may be built up by carbonate sedimentation. Indeed atoll-like carbonate build

up may account for at least the upper part of some continental slopes such as around Florida and for the Yucatan region of Mexico. Reef limestones forming at the shelf edge would tend to impound detritus shed from the continent. Such reef build-up is capable of producing very steep slopes, as is known from the atolls of the Pacific Ocean. However, a pre-existing continental slope of structural origin is obviously required before this carbonate modification can begin. Hence, a carbonate slope can only be the special proximate cause of a particular continental slope but does not help in explaining continental slopes generally (Fig. 3).

Continental slopes as fault scarps

Still another interpretation is that the continental slopes are fault scarps created along the juncture between the light continental block and the heavy oceanic segment of the earth's crust. Earthquakes along some continental slopes, the tendency of the slopes to be straight, and their abrupt transsection of the mountain belts are cited as favourable evidence of this interpretation. But since the continental blocks of the ocean basins are in equilibrium, there appears to be little reason for adjustments other than by minor faulting along the continental slopes. Faulting should thus be of secondary importance rather than the primary cause of the continental slopes. The fault-origin supposition cannot be entirely discredited for it does have some appealing aspects, but for reasons developed below the writer does not think it provides the best solution (Fig. 4).

Continental slopes as rift scarps

In recent years much evidence has accumulated favouring the old but dormant theory of continental drift. I am among those scientists inclined to accept its reality for many reasons, not the least of which is that it offers a reasonable explanation for continental slopes. Quite likely the northern hemisphere continents were joined together across the Atlantic about 150 million years ago, forming the supercontinent of *Laurasia*. Similarly the southern hemisphere continents, plus India, were also together then forming *Gondwana*. Subsequently these large supercontinents rifted and drifted apart to their present position.

Accordingly many of the continental slopes around the Atlantic and Indian Oceans may be explained as modified rift scars, remnants of this continental fragmentation. The opposing continental slopes of Africa and South America provide an excellent example, for it is now known that they fit together with fine precision beyond any previous expectation—especially when this translation is done with careful scientific controls and considerations. Today the Gulf of California and the Red Sea probably provide examples of new rifts, not more than 15 million years old, where new continental slopes are being created as opposing land-masses move apart (Fig. 5).

Continental slopes as accretionary mountain belts

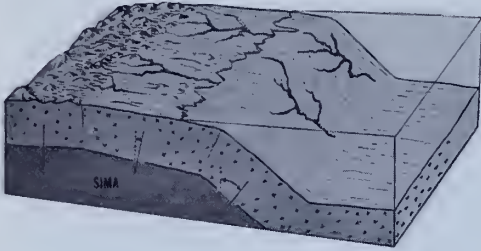
It is immediately evident that continental rifting and drifting apart cannot account for *all* continental slopes. In any such fragmentation new continental edges are created but the old ones remain as well! In other words, the original margins of Laurasia and Gondwana, now mostly facing the Pacific Ocean, cannot be rift scarps. What is their origin?

It seems quite likely that continents have grown through geological time by a process of accretion whereby new mountain belts are added to the periphery. Great prisms of sediment are laid down like aprons at the bases of the continental slopes around the world. From time to time the ocean floor underthrusts the continental blocks,

as seems to be taking place around the Pacific today. By this action belts of folded mountains are accreted to the continental margin, and a new continental slope is created as the seaward flank of this mountain belt. This process then seems to be the basic cause for the creation of continental slopes. Since it occurs at intervals over geological history, the slopes are from time to time renewed so that their geomorphic youth (ruggedness and steepness) is renewed. This process also meets the criterion of being a slow, evolutionary mode and so is in accord with geological history.

Robert S. Dietz
Institute of Oceanography (ESSA)
Washington, D.C.

1
Marginal downflexing has been proposed as a cause of continental slopes. It has been argued that this flexing would account for the submarine canyons incising the slopes as ancient river valleys. However, it is now known that canyons are cut by submarine processes.

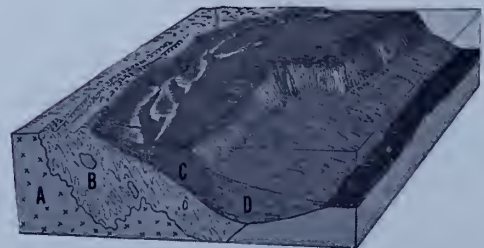
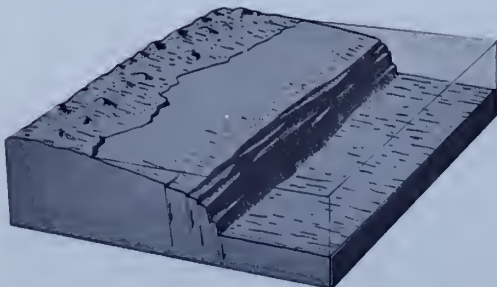
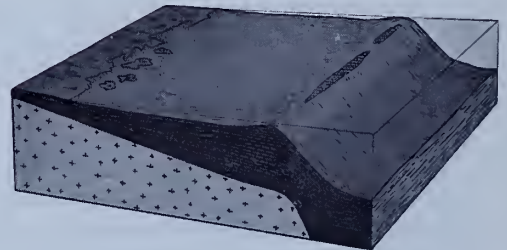
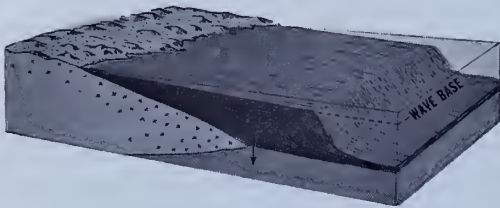


2
Another interpretation of continental slopes is that they are enormous sedimentary embankments of detritus carried out to the shelf edge.

3
A further explanation for sedimentary slopes is by a build-up of carbonate sediments deposited by reef corals along the margin of the continent.

4
Down-faulting along the continental margin offers still another interpretation for the origin of continental slopes.

5
The fundamental cause of continental slopes is presumably continental accretion whereby new margins are added to continents by the collapse of sedimentary prisms at the base of the continental slope. Underthrusting by the sea floor causes this accretion and generates a new continental slope.



Reprinted from "International Dictionary of Geophysics"

PERGAMON PRESS

OXFORD · LONDON · EDINBURGH · NEW YORK
TORONTO · SYDNEY · PARIS · BRAUNSCHWEIG

BARRINGER METEOR CRATER. The Barringer Crater, or Meteor Crater in Coconino County, Arizona, commands special scientific interest as it is the prototype, meteor impact crater on the face of the Earth, having been fully established as an impact site since 1930. Of all the world's meteorite craters, this one is the most elegant, most accessible and the best exposed. It is visited by a hundred and fifty thousand tourists each year.

The crater is nearly 4000 feet across and 570 feet deep, the rim is marked by upturned strata and debris piles rising 150 feet above the surrounding plain and containing some 300 million tons of fragmented rock. The rock units in the crater wall display a quaquaversal depth and locally are overturned. Regional jointing has exerted a control upon the shape of the crater which is somewhat squarish in outline rather than truly circular. The floor of the crater is underlain by debris, breccia, and covering lake beds attaining a thickness of about 100 feet. The ejected



An aerial view of Barringer Meteor Crater, Arizona, USA. North is to the right (Photo by Robert S. Dietz).

debris consists of unsorted angular fragments ranging from rock flour up to great blocks more than 100 feet across. The bedrock stratigraphy is preserved inverted, in the debris units. Permian to Triassic beds — the Moenocopic shale, the Kaibab limestone and the Coconino sandstone were all affected by the impact. Cores have shown that Supai siltstone and sandstone occurring at depths greater than 700 feet below the crater floor are undisturbed so that the disruption does not extend to depth.

Indians were familiar with Barringer Crater; the Hopi tribe gathered finely powdered white silica at the crater rim and used this rock flour in their ceremonies. Although discovered by white men in 1871, it first came to public attention in 1891 through the collection, in the environs, of a ton of meteorites by the mineralogist A. E. Foote. These meteorites achieved international interest when they were found to be diamondiferous, containing small nodules of minute black diamonds or carbonados of

great scientific interest but no commercial value. Unlike the diamonds found in certain other meteorites these are thought not to be cosmic, but created at the instant of impact by the shock transformation of the iron carbide mineral cohenite.

Foote did not directly associate the meteorites, which he called Canyon Diablo meteorites, and the nearby crater. So for almost 10 years after Foote's visit, the view persisted that "Crater Butte" was the last vestige of a once active volcano. This belief flourished despite the absence of any associated volcanic ash, lava or hydrothermal effects. First to recognize the impact origin of this crater was D. M. Barringer, a prominent mining engineer from Philadelphia. He acquired the property in 1903 and laid claim to the mineral rights and then spent the years from 1903 to 1929 attempting to exploit the mineral possibilities of the great mass of nickel iron he presumed to be present. Extensive drilling and other exploration was undertaken during this period in the hope of developing a nickel mine. This drilling showed the absence of any buried giant meteoritic 'cannon ball', but indicated considerable scattered cosmic debris.

It was not until 1930 that a consensus of opinion developed in the scientific community that this was indeed a meteoritic crater, an interpretation now beyond any dispute. Slowness of acceptance was mainly due to the crypto-volcanic interpretation of the prominent geologist G. K. Gilbert, who visited the site in 1891. Gilbert's interpretation is rather curious since he described the lunar craters as meteoritic in 1895 much along the lines still given to them today. Gilbert reasoned by analogy so he was unable to accept an exotic or unique interpretation for Barringer Crater. By the same token, once this crater was definitely shown to be meteoritic, many others were quickly located around the world based on criteria developed at this prototype. Even today much of the evidence for meteorite impact features both on the Earth and on the Moon is derived from this feature.

It is estimated that about 50 tons of Canyon Diablos have been recovered, the largest weighing nearly one ton. One half of this tonnage consists of fresh meteorites and the remainder of oxidized meteorites, known as "shale-ball" or oxidite. While the meteorites lying at the surface have been largely picked up, it is still a fairly simple matter to recover subsurface ones with a metal detector. Apparently the early Indians did not collect any significant amount of this iron for their arrow points or other purposes. Only one meteorite has been found in an Indian burial in the southwestern United States, apparently an amulet or fetish; it was not a Canyon Diablo.

Canyon Diablo meteorites reside in museums throughout the world. Without doubt it is the most widely distributed meteorite. Specimens command much public interest owing to their contorted form, pits and cavities. They conform to the laymans opinion as to what a meteorite should look like. Those parts of the meteorite which were highly shock-heated upon impact are devoid of the usual Widmanstätten figures. The Canyon Diablo meteorite is a siderite classed as a medium octahedrite and contains about 92% iron, 7% nickel, and traces of

many other elements. Meteorites from the small Odessa Meteorite Crater in Ector County, Texas, are virtually indistinguishable both chemically and mineralogically from Canyon Diablos. This has led to the suggestion that they may both be part of one fall many thousands of years ago.

Thoughts regarding the probable total mass of the bolide have undergone considerable revision over the years. Early estimates, which suggested an object of several millions of tons, appear to have been much too large. Estimates in the decades of the thirties and forties suggesting an object of a few tens of thousands of tons were underestimates. Recent studies suggest an object 100,000-300,000 tons depending largely on the actual impact velocities. In terms of energy, the impact is estimated to have been from 3 to 10 megatons-TNT-equivalent.

A number of geophysical surveys have been made searching for evidence of meteoritic material buried in the subsurface. These surveys disagree about the amount of buried meteorite debris but they concur in indicating a considerable amount of it. Very likely abundant fragments lie beneath the lake beds in the southwest quadrant of the crater as broken and shocked fragments.

Undoubtedly the meteorite was subjected to a considerable stripping, ablation and disintegration during its atmospheric flight. The amount of meteoritic substance existing today as fine particles around the crater far exceeds the ponderable meteorites recovered. Based upon 700 soil samplings, it has been calculated that about 12,000 tons of finely divided meteoritic debris is present in the immediate environs of the crater with the greatest concentration lying to the northeast, the explosion cloud having been moved in that direction by the prevailing winds.

The direction of approach of the bolide has been the subject of considerable discussion — all directions of the compass have been proposed except to the north. Based upon variations of the dip of the strata around the crater D.M. Barringer suggested the meteorite struck at a moderate angle of inclination toward the south. A general southerly direction appears to remain as the best interpretation. The velocity probably was also low. An impact velocity of about 15 km/sec is consonant with the observed geologic effect at Barringer Crater as inferred from the experimental equations of state of iron and inferred compressibility of the target rocks.

A form of impactite (shock metamorphosed rock) occurs at the crater consisting of altered Coconino sandstone. This curious rock consists of pulverized sand grains, silica glass or lechatelierite, and the dense polymorphs of silica coesite and stishovite. These polymorphs bear the relationship to normal forms of silica, like quartz, that diamond does to common carbon.

More than a hundred papers of scientific interest have been published concerning Barringer Crater but many aspects remain at best poorly known. For example the age of the crater has been only poorly determined. Perhaps the best recent estimate would place the impact event about 22,000 years ago. In spite of the early churn

drilling, the crater remains virtually unknown at depth. Diamond drilling, permitting core recovery, would greatly enhance our knowledge and add a new dimension to the understanding of meteorite craters generally.

Meteor craters, like lakes, are ephemeral features on the Earth's surface but their root scars persist into geologic antiquity. These older scars, no longer recognizable as craters, are called "fossil" craters or, better, *astroblemes* (i.e. star-wounds). Some probable examples include the Vredefort Ring in South Africa, the Rieskessel in Germany and the Wells Creek Basin Structure in Tennessee, U.S.A. There has been great interest in astroblemes in recent years. An organized and extensive search for them has been underway in Canada for a decade by the Dominion Observatory.

Barringer Crater is not the largest meteor crater on Earth; it probably ranks fifth among those now known. However, it is the largest definitely identified, based upon the presence of associated meteoritic debris (see table).

A list of the larger meteorite craters

	Diameter (ft)	Depth (ft)
1. Ashanti Crater (occupied by Lake Bosumtwi), Ghana	33,000	1,150*
2. New Quebec (Chubb) Crater, Ungava Peninsula, Canada	11,300	1,300*
3. Lonar Crater, India	6,000	570**
4. Talemzane, Algeria	5,600	—
5. Barringer Meteor Crater, Arizona	3,900	570
6. Pretoria Salt Pan, South Africa	3,400	500**
7. Wolf Creek Crater, Australia	2,700	200

* From top of rim to lake bottom.

** Top of crater rim to bottom of silt fill.

- Ashanti Crater is almost certainly a meteorite crater on the basis of morphology, structure, and indications of shock, (presence of shatter cones and coesite). No meteorites have been found.
- New Quebec Crater is almost certainly a meteorite crater on the basis of its morphology, but no meteorites have been found.
- Lonar Crater is probably a meteorite crater on the basis of morphology and structure but the degree of certainty is less than either Ashanti Crater or the New Quebec Crater.
- Very old, and deeply eroded, probably Pliocene.
- Barringer Meteor Crater is unequivocally a bona fide meteorite crater and is the world's prototype. The presence of meteorite fragments plus its morphology, structure and indications of shock including coesite demonstrate this.
- Probably a meteorite crater.

7. Wolf Creek Crater is unequivocally a meteorite crater. Oxidized meteorite fragments are associated. A fresh siderite has recently been reported.

In the absence of meteorite debris the following criteria are useful in establishing the identity of a possible meteorite crater:

1. A high degree of circularity,
2. A depth to diameter ratio, like that of Barringer Crater,
3. Crushed rock breccia lens beneath the bottom,
4. Quaquaversal dip of the rim rock,
5. Mounds of debris which lie around the rim,
6. Regional uniqueness of the depression (unlikely for a volcanic explosive feature, a subsidence caldera or a limestone collapse feature).
7. Presence of shock metamorphosed rock (*impactite*) with coesite or stishovite,
8. Shock fracturing effects such as shatter-coning,

These criteria have been developed mostly from studies at the Barringer Meteor Crater. It is evident, therefore, that this remarkable feature will continue to play a key role in the understanding of meteorite impact phenomena on both the Earth and the Moon.

Bibliography

- BALDWIN R. B. (1963) *The Measure of the Moon*, Chicago: The University Press.
- BARRINGER D. M. (1905) Coon Mountain and its crater: *Acad. Natl. Sci. Phil. Proc.*, **57**, 861.
- NINNINGER H. H. (1956) *Arizona's Meteorite Crater*. Denver: World Press.
- SHOEMAKER E. M. (1963) *Impact mechanics at Meteor Crater, Arizona*, in (Kuiper, G. P. Ed.) *The Solar System*, Vol. 4, *The Moon Meteorites and Comets*, Chicago: The University Press.
- SPENCER L. J. (1933) *Meteorite craters as topographical features on the Earth's surface*, *Geog. J.*, **81**, 227.
- R. S. DIETZ

WAVE BASE

In principle, wave base is the downward limit to which waves can move bottom particles. As defined by Gulliver (1899, pp. 76-77), wave base determines the ultimate depth of a platform of marine abrasion. No particular depth was specified, but in recent years several workers have placed its *effective* depth at about 10 meters, perhaps ultimately about twice this (Dietz and Menard, 1951; Fairbridge, 1952; Bradley, 1958). It is observed that unconsolidated clay-size particles may be stirred up by heavy swell down to nearly 200 meters, and this is *ultimate* wave base, but in no sense is this vigorous abrasion.

Marine abrasion of consolidated rock is largely conditioned by the pre-rotting or loosening of the coastal rocks by the subaerial chemical weathering action of ground water (Bartrum, 1926). The role of waves is thus primarily a mechanical one, to remove the debris (Fig. 1). Additional marine erosional forces are (a) mechanical abrasion, sand and boulders being propelled by wave action at the cliff foot, (b) hydraulic action (air compression in joints, etc.), and (c) biologic agencies (borers, algal buoyancy, etc.).

The principal locus of attack by all the above agencies is the intertidal belt. In exposed areas offshore, strong abrasion extends to the depth where waves begin to peak and, under storm conditions, break. More than 95% of wave energy is dissipated in this zone between about 10 meters and

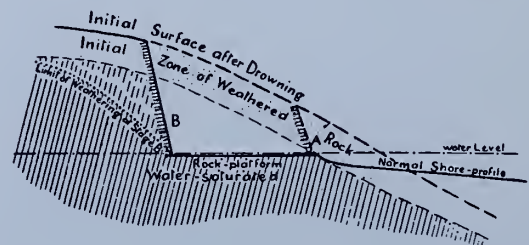


FIG. 1. The site of marine abrasion, involving the removal of subaerially rotted rock waste as visualized by Bartrum (1926). Wave action easily removes the "initial zone of weathered rock" to the point A, producing a cliff and "normal" offshore profile. Backwasting from point A favors further chemical weathering down to, but not below, the level of sea-water saturation. Marine abrasion thus tends to develop a horizontal platform, terminating at cliff B.

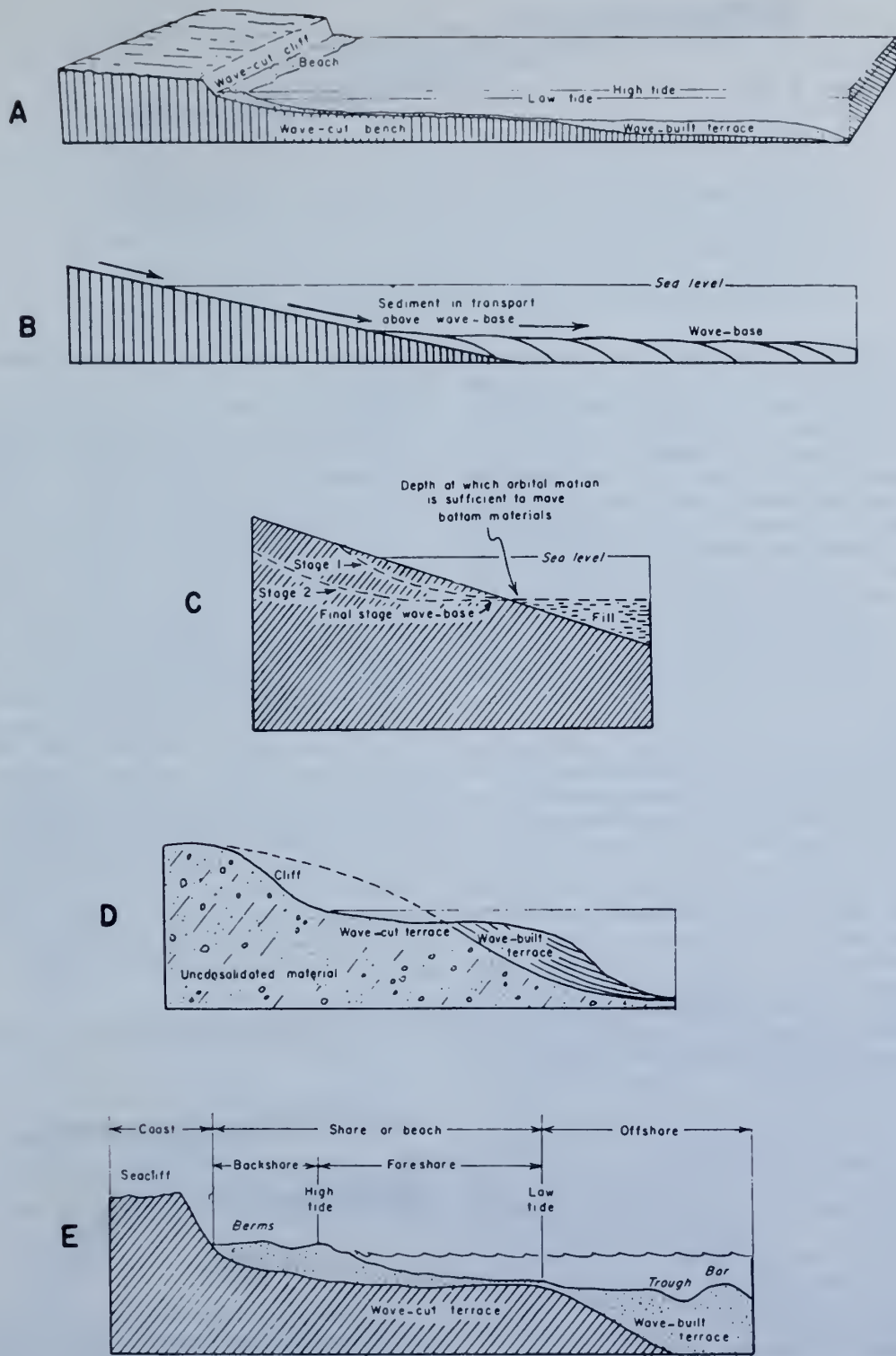


FIG. 2. Various views concerning the origin of the wave-cut and wave-built terraces, all of which imply a controlling effect of wave base. (A) After Longwell, Knopf, and Flint (1948); (B) after Clark and Stearn (1960); (C) after Garrels (1951); (D) after Von Engeln (1942); and (E) after Leet and Judson (1958).



FIG. 3. The delta terrace redrawn from Dunbar and Rodgers (1957, p. 47). Topset, foreset, and bottomset beds are shown to develop when a sediment-laden river enters a quiet body of water. Such delta terraces are common geomorphic forms; they should not be confused with the entirely hypothetical wave-built terrace. Note especially that the nick-point is at water level and not below; wave action would tend to modify or destroy the delta terrace. A rising water level would drown it, producing a feature which might erroneously be interpreted as a wave-built terrace.

the shore. Under extreme storm conditions, the outer limit may sometimes reach 20 meters. Strictly speaking, this should be called "surf base" or "surge base" as it is related to surf action rather than the depth of stirring by open-sea waves (Dietz, 1963). As Moore and Curray (1964) have pointed out, there is really a *zone* of wave base, effective for various sedimentary grades, shallow for boulders and gravel, deeper for silt and clay, that is activated in cycles up to a century or so.

Historically, there has been much confusion about the lower limit of wave base and marine abrasion. The traditional tendency was to relate the depth of the shelf edge, which is normally situated at about 100–200 meters, to the bottom friction of open-sea waves (see Fig. 1). One may certainly speak of a "feeling the bottom" by open sea waves, but this is unimportant as compared to the surf action, especially over long periods when it is combined with the large Quaternary oscillations of sea level. Several authors have remarked on the widespread evidence of late Pleistocene shore lines and undisturbed relic sediments on the outer shelf. Evidently this means that since the time that sea level has been at its approximate (modern) level (a matter of about 6000 years), there has been no large-scale abrasion on the outer shelf. In regions of little accumulation, clear, rock-cut terraces may be followed in steps right across the shelf (Carrigy and Fairbridge, 1954). In certain other areas, a considerable thickness of post glacial fine-grained sediments has accumulated here, strictly speaking an unconformable Holocene stratigraphic formation (see Fig. 1 of Moore and Curray, 1964). In neither of these regional types could there be any serious erosion below 10 meters.

"Wave base" when used in stratigraphic discussions essentially refers to the upper limits of medium- or fine-grained sediments that lack evidence of littoral action, beach facies, sand bars, boulder conglomerates, etc.

Wave-built Terrace

Related to wave base are two other concepts,

"wave-built terrace" and "marine profile of equilibrium."

The term "wave-built terrace" was first used for a prograding littoral deposit (on Lake Bonneville) by Gilbert (1890), but this was not in the sense later adopted by Johnson and others. Johnson (1919), and most text-book writers in recent decades, consider the entire continental shelf to be a wave-cut terrace in its inner part and a wave-built terrace in its outer part (see Fig. 2). Accordingly, the continental slope would always be the prograding face of a dipping series of clastic beds composed of detritus swept out from the shore and deposited as a talus. Modern survey work at sea rarely offers support for this model and, in fact, a simple hypothetical wave-built terrace of this sort seems to be fictitious. Shepard (1948, 1963) especially has shown that *continental shelves* (q.v. Vol. 1) are of great diversity and complexity, but none of them seem to correspond to Johnson's concept. It is important that this fallacy should be corrected, for it appears in almost every basic textbook.

The nearest equivalent to a wave-built terrace seems to be the *delta terrace* (see Fig. 3). When drowned by a rise of sea level, these are quite liable to false interpretation as wave-built terraces.

Wave-cut Terrace

From the evidence for the lower limit of effective

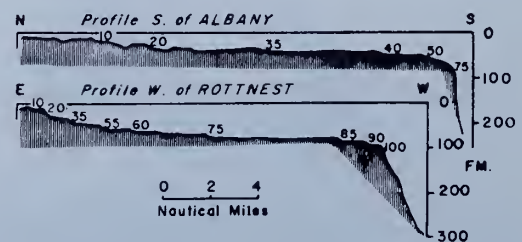


FIG. 4. Profile across the continental shelf off semi-arid Western Australia, showing abrasional notches corresponding to former eustatic sea levels (Carrigy and Fairbridge, 1954). Contemporary "wave-base" erosion, if effective down to -100 meters, would destroy such features.

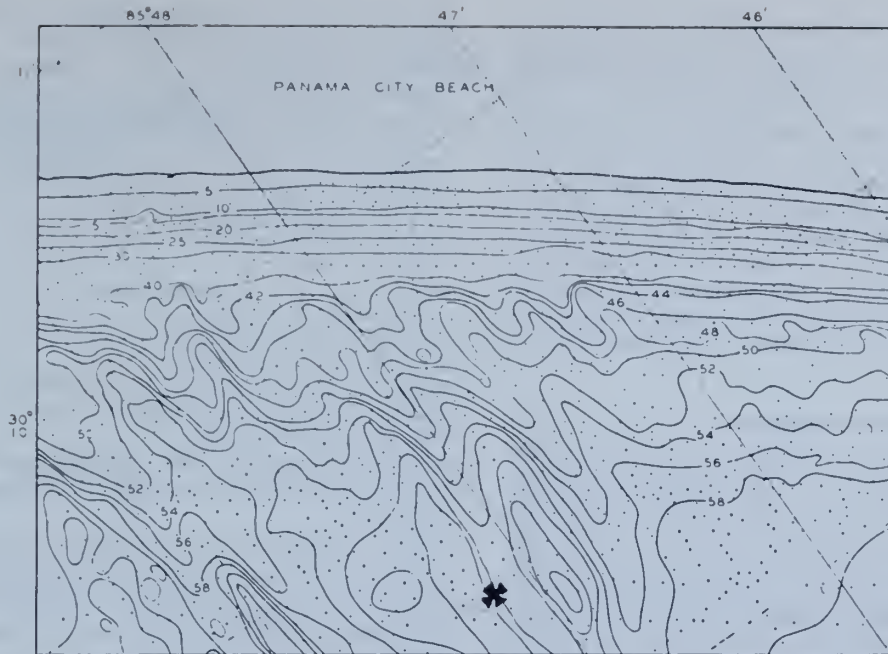


FIG. 5. Detailed topographic form of the inner shelf off Panama City, Florida, a region of elastic deposition (depths given in feet). A smooth-sloping gradient extends to a depth of 40 feet; presumably this is a near-shore marine profile of equilibrium. But greater depths are marked by a rough relict topography. A submerged forest is located at the point marked X having a radiocarbon date indicating an age in excess of 40,000 B.P. (after Dietz, 1963).

marine abrasion, noted above, it is clear that the continental shelf sediments cannot be underlain by a wave-cut terrace that was formed under the present sea-level regime.

However, sub-bottom acoustic profiling (Moore, 1960) has demonstrated many wave-cut terraces partly hidden beneath a thin veneer of late Holocene sediments. These terraces are separated from

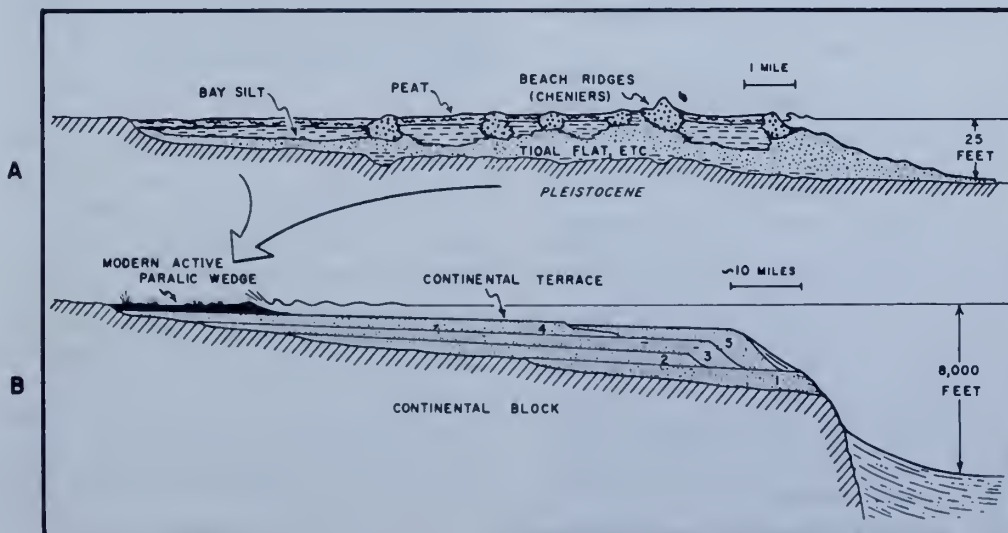


FIG. 6. Paralic wedge building up the continental terrace today off Louisiana (Dietz, 1963). (A) Detail of complex Holocene segment. No appreciable Holocene sediments are recorded beyond 25 feet (8 meters). (B) Progressive effect under eustatic control with steady subsidence.

one another by short escarpments and dip uniformly seaward. Along tectonically active coasts, such as that off southern California, these wave-cut terraces have evidently been warped and tilted seaward. On more stable coasts, e.g., off Western Australia (Carrigy and Fairbridge, 1954), such terraces are almost horizontal and seem to represent marine stillstands during the late and post-glacial eustatic changes of sea level (Fairbridge, 1961) (see Fig. 4). In areas of low sedimentary supply, especially on island shelves, the veneer of Holocene cover may be very slight, or longshore currents may keep them swept clear ("hard-grounds").

Marine Profile of Equilibrium

The concept of a profile of equilibrium applies well to rivers, where MSL (mean sea level) is the base level. However, the slope of continental shelves is in no sense analogous. Wave motion falls off asymptotically with depth, and a marine profile of equilibrium in loose sediments develops only to a depth of about 20 meters (Fig. 5). This paralic (i.e., nearshore) profile of equilibrium is created by the tendency of waves to push the tractive sand load onshore. A concave sand lens results which is balanced against the leveling effect of gravity.

The surface of the outer shelf is not a profile of equilibrium but rather a relict surface reflecting especially the effect of recently lower sea levels. A deep-water profile of equilibrium, as supposed by Johnson, simply does not exist.

A constructional continental terrace builds up from an active *paralic wedge* (Fig. 6) the locus of which shifts successively inward and outward across the continental margin as sea level rises and falls eustatically. Slow tectonic subsidence aids the progressive accumulation of such sediments.

ROBERT S. DIETZ
RHODES W. FAIRBRIDGE

References

- Bartrum, J. A., 1926, "'Abnormal' shore platforms," *J. Geol.*, **34**, 793-806.
- Bradley, W., 1958, "Submarine abrasion and wave-cut platforms," *Bull. Geol. Soc. Am.*, **69**, 967-974.
- Carrigy, M. A., and Fairbridge, R. W., 1954, "Recent sedimentation, physiography, and structure of the continental shelves of Western Australia," *J. Roy. Soc. W. Australia*, **38**, 65-95.
- Clark, T. and Stearn, C., 1960, "Geological Evolution of North America," New York, Ronald Press, 434pp.
- Dietz, R. S., 1963, "Wave-base, marine profile of equilibrium, and wave-built terraces: a critical appraisal," *Bull. Geol. Soc. Am.*, **74**, 971-990.
- Dietz, R. S., 1964, "Wave-base, marine profile of equilibrium, and wave-built terraces: reply," *Bull. Geol. Soc. Am.*, **75**, 1275-1282.
- Dietz, R., and Menard, H., 1951, "Origin of abrupt changes in slope at continental shelf margins," *Bull. Am. Assoc. Petrol. Geologists*, **35**, 1994-2016.
- Dunbar, C., and Rodgers, J., 1957, "Principles of Stratigraphy," New York, John Wiley & Sons, 356pp.
- Fairbridge, R., 1952, "Marine erosion," *Proc. Pacific Sci. Congr. Pacific Sci. Assoc.* **7th**, **3**, 347-358.
- Fairbridge, R. W., 1961, "Eustatic Changes of Sea Level," in "Physics and Chemistry," Vol. 4, pp. 99-185. Pergamon Press.
- Garrels, R., 1951, "Textbook of Geology," New York, Harper, 511pp.
- Gilbert, G. K., 1890, "Lake Bonneville," *U.S. Geol. Surv. Monograph*, **1**, 438pp.
- Gulliver, F., 1899, "Shoreline topography," *Proc. Am. Acad. Arts Sci.*, **34**, 151-258.
- Johnson, D., 1919 (1938, Second ed.), "Shore Processes and Shoreline Development," New York, John Wiley & Sons, 584pp.
- Leet, L. D., and Judson, S., 1958, "Physical Geology," Second edition, Englewood Cliffs, N.J., Prentice Hall, 502pp.
- Longwell, C., Knopf, A. K., and Flint, R., 1948, "Physical Geology," New York, John Wiley & Sons, 543pp.
- Moore, D., 1960, "Acoustic-reflection studies of the continental shelf and slope off Southern California," *Bull. Geol. Soc. Am.*, **71**, 1121-1136.
- Moore, D. G., and Curray, J. R., 1964, "Wave-base . . . discussion" (of Dietz, 1963), *Bull. Geol. Soc. Am.*, **75**, 1267-1273 (Reply, pp. 1275-1281).
- Shepard, F. P., 1948, "Submarine Geology," New York, Harper & Bros., 348pp.
- Shepard, F. P., 1963, "Thirty-five Thousand Years of Sea Level," in (Stevenson, R. E., editor), "Essays in Marine Geology in Honor of K. O. Emery," pp. 1-10, Los Angeles, Univ. South California Press.
- Von Engel, O., 1942, "Geomorphology," New York, MacMillan Co., 665pp.

Cross-references: *Abrasion; Base Level; Delta; Eustasy; Holocene; Littoral Processes; Nickpoint; Organisms as Geomorphic Agents; Platforms—Wave-cut; Profile of Equilibrium; Quaternary. Vol. 1: Continental Shelf; Mean Sea Level Changes; Ocean Waves.*

Reprinted from JOURNAL OF GEOLOGY Vol. 76 No.1

Reprinted from The Journal of Geology
Vol. 76, No. 1, January 1968
Copyright 1968 by The University of Chicago
Printed in U.S.A.

MIOGEOCLINES (MIOGEOSYNCLINES) IN SPACE AND TIME: A REPLY¹

ROBERT S. DIETZ²

I welcome this opportunity to reply to the discussion by Grant M. Young (this issue) of the paper "Miogeoclines (Miogeosynclines) in Space and Time" (Dietz and Holden, 1966). Hopefully, this exchange of views will bring into sharper focus some of the issues at stake.

Some points which suggest that the Grenville still may be an accretionary belt, in spite of the objection raised by Young, are presented elsewhere (Dietz and Sproll, 1968) and need not be repeated here. Regarding the non-eugeosynclinal lithofacies of many of the Grenville rocks, it is well to re-emphasize the concept of a continental embankment whereby, after a continental rise completely uplaps a continental slope, major prograding and extension of the continent occur, accompanied by the laying down of a surficial shallow-water bed. The Gulf Coast geosyncline is my type-example of such a dove-tailed sedimentary prism (Dietz, 1963*a*, 1963*b*, 1964). Along with many others (e.g., Muhlberger, 1965), I regard this modern, living geosyncline as being laid down on oceanic crust or sima. By analogy, the Grenville belt may simi-

larly be ensimatic, even though large areas of the sedimentary prism are covered by shallow-water deposits.

It should also be emphasized that in my actualistic concept of geosynclines, mountains, and continent-building, sedimentation of the eugeosynclinal prism in no way triggers orogeny, as is usually supposed. I regard this as an advantage, for it is not at all clear and is never convincingly specified why a geosyncline should slowly subside at a rate of a few hundred meters per million years for a few tens of millions of years (e.g., Kay, 1955) and then suddenly collapse like a beam being compressed within a vise. Instead, I suppose that sedimentation can continue indefinitely until, for some extraneous reason (sea-floor spreading?), decoupling of the continental plate and the ocean floor occurs (Dietz, 1961). Using the topographic contrast of $2\frac{1}{2}$ miles between the ocean floor and the continental plateau, plus isostatic sinking, a sedimentary prism may be laid down as a continental rise about 40,000–50,000 feet thick. Initially, this is synclinal in form, but with the prograding of a continental embankment, this syncline becomes flat-bottomed. The subsidence of the miogeosyncline is only active during the initial phase but then becomes isostatically dead. Thus, a long interval of time may ensue between the

¹ Manuscript received June 25, 1967.

² Institute for Oceanography, Environmental Science Services Administration, 901 South Miami Avenue, Miami, Florida 33130.

laying down of the miogeosyncline and the crumpling of the adjacent eugeosyncline. Perhaps we can explain the Huronian-to-Grenville orogenic event in this manner. It may also be that the initial collapse of the presumed continental-rise prism in the Sudbury region was related to the Penokean orogeny 1,600 m.y. ago (Card, 1964) rather than to the Grenville. Doubtless, the history of the Grenville belt is exceedingly complex; our figure was intended only as a simplified diagram to express a possibly permissible sequence of events.

Young's remark about the North American craton not being able to supply the sediments needed for the Cambrian to mid-Ordovician Appalachian miogeosyncline is most doubtful, as only a very limited amount of clastics is included in this wedge. The strata are mostly carbonates which were deposited chemically or biochemically directly from seawater. As noted by Pettijohn (1962, fig. 12), paleocurrent indicators reveal that the Weverton, the only true miogeosynclinal formation for which paleocurrent information is available, was derived from the craton. In contrast, the post-mid-Ordovician mollasse deposits came from Appalachia—presumably a peripheral mountain belt and not an offshore land of the Schuchert type. The paleocurrent data, as presently known, seem wholly in accord with my concept.

Detritus accumulated on a continental rise need not be derived from the immediately adjacent craton. We do not necessarily need to appeal to submarine canyons tapping the paralic zone or some other process for carrying detritus orthogonally across a carbonate miogeosynclinal belt. Heezen, Hollister, and Ruddiman (1966) show that much of this accumulation is laid down as redeposited turbidites, which they term "contourites," and is carried long distances more or less parallel to the continental margin. For example, distinctive rose-colored quartz silts, probably derived from Nova Scotia, have been found 1,000 miles south on the eastern flank of the Blake-Bahama outer ridge. These silts apparently

were transported in a direction parallel to the contours by the western-boundary undercurrent.

Any statement that no eugeosynclines were laid down ensimatically prior to the Mesozoic strikes me as unwarranted. For example, the crystalline Appalachian eugeosyncline was probably laid down mostly ensimatically off a continental margin (King, 1959, p. 62). Although I do not follow it, many accept the Kay (1951) model for eugeosynclines whereby this sedimentary prism was bounded oceanward by an island arc. Although not very specific, Kay apparently regarded eugeosynclines as ensialic, but, if we examine modern island arcs, they are separated from the mainland by deep basins which are now known to be underlain by oceanic crust. This is true for the Sea of Japan, the Philippine Sea, the Sea of Okhotsk, and the Bering Sea Basin (Menard 1964). Thus, modeled actualistically, the Appalachian eugeosyncline by the Kay model would have been laid down ensimatically. Statements in the literature regarding the ensialic emplacement of eugeosynclines are commonly "ex cathedra," with the details omitted. Generally, the nature of the basement is unexposed and unknown, as is to be expected if the tectonized prism is as thick as the continental plate and the basement is high-density simatic rock.

Greenschist and blueschist facies are common in eugeosynclines which seem to indicate upward tectonic transport after excessively deep burial—as deep as continents are thick. This, in turn, suggests that eugeosynclines encompass the entire continental plate down to the Moho or, in other words, are ensimatic and not ensialic. Continents would seem generally to be composed of accordion-pleated fold belts rather than having a "layer-cake" structure.

It is widely recognized that ancient eugeosynclinal graywackes have sialic provenance; but so do the sediments comprising modern continental rises, for they are derived from the continental block by being flushed down submarine canyons by tur-

bidity currents. This does not mean that continental-rise sediments are ensialic; obviously, the reverse is true: they are ensimatic. The composition of eugeosynclinal graywackes gives no clue as to the underlying basement.

An argument against the presence of an island arc off eastern North America prior to the collapse of the continental rise (by my concept) to form the *accretionary* fold belt of the crystalline Appalachians is the absence of any volcanic-ash beds (metabentonites) on the North American craton prior to the Middle Ordovician. At least twenty-

seven metabentonite beds are known from the Middle Ordovician, including one with a minimum volume of 24 cubic miles, suggesting that the collapse of the continental-rise prism was accompanied by subaerial volcanism and ash deposition on the old craton (Bowen, 1967). Prior to this initiation of the Appalachian orogeny (*sensu lato*), no cratonic ash beds appear in the geologic record. This is difficult to understand if an island arc indeed existed off eastern North America, as the associated subaerial volcanoes would have spewed much tephra.

REFERENCES CITED

- BOWEN, R. L., 1967, Volcanic events of the Middle Ordovician in eastern North America: *Am. Geophys. Union Trans.*, v. 48, no. 1, p. 226.
- CARD, K. H., 1964, Metamorphism in the Agnew Lake area, Sudbury district, Canada: *Geol. Soc. Amer. Bull.*, v. 75, p. 1011-1030.
- DIETZ, R. S., 1961, Continent and ocean basin evolution by spreading of the sea floor: *Nature*, v. 190, no. 4779, p. 854-857.
- 1963a, Collapsing continental rises: an actualistic concept of geosynclines and mountain building: *Jour. Geology*, v. 71, p. 314-333.
- 1963b, Wave base, marine profile of equilibrium and wave built terraces: a critical appraisal: *Geol. Soc. America Bull.*, v. 74, p. 971-990.
- 1964, Origin of continental slopes: *Am. Scientist*, v. 52, no. 1, p. 50-69.
- and HOLDEN, J. 1966, Miogeoclines (miogeosynclines) in space and time: *Jour. Geology*, v. 74, p. 566-583.
- and SPROLL, W., 1968, Miogeoclines (miogeosynclines) in space and time: a reply: *Jour. Geology*, v. 76, no. 1, p. 113-116.
- HEEZEN, B. S., HOLLISTER, C., and RUDDIMAN, W., 1966, Shaping of the continental rise by deep geostrophic contour currents: *Science*, v. 152, no. 3721, p. 502-508.
- KAY, M., 1951, North America geosynclines: *Geol. Soc. America Mem.* 48, 143 p.
- 1955, Sediments and subsidence through time: *Geol. Soc. America Spec. Paper* 62, p. 665-684.
- KING, P. B., 1959, *The evolution of North America*: Princeton, N.J., Princeton Univ. Press, 189 p.
- MENARD, N. W., 1964, *Marine geology of the Pacific*: New York, McGraw-Hill Book Co., 271 p.
- MUHLBERGER, W., 1965, Late Paleozoic movement along the Texas lineament: *New York Acad. Sci. Trans.*, ser. 2, v. 27, no. 3, p. 385-392.
- PETTIJOHN, F. J., 1962, Paleocurrents and paleogeography: *Am. Assoc. Petroleum Geologists Bull.*, v. 46, no. 8, p. 1468-1493.

(Reprinted from *Nature*, Vol. 220, No. 5169, pp. 751-753, November 23, 1968)

Reprinted from NATURE Vol. 220, No. 5169

Survey of Ross's Original Deep Sea Sounding Site

by

ROBERT S. DIETZ
HARLEY J. KNEBEL

Environmental Science Services Administration,
Atlantic Oceanographic Laboratories,
Miami, Florida

The first successful sounding of the ocean depths was carried out by Sir John Ross in 1840. As a commemorative gesture, in January of 1968 a survey was made over an area of 47 square miles in the vicinity of the Ross site, and soundings were recorded. In this article, the depth recorded during the survey is compared with Ross's original figures.

"On the 3rd of January [1840], in latitude 27° 26' S, longitude 17° 29' W, the weather and all other circumstances being propitious, we succeeded in obtaining soundings with two thousand four hundred and twenty-five fathoms of line, a depression of the bed of the ocean beneath its surface very little short of the elevation of Mount Blanc above it." This laconic statement was made by Captain Sir James C. Ross of HMS Erebus during the British Antarctic Expedition of 1839-1843 (ref. 1).

Although attempts to obtain deep soundings were made in the early 1500s², apparently none was successful before Ross made this sounding*. Before this time, the oceans

were either regarded as bottomless, or their depths were intuitively estimated. Many scientists argued, for example, that the oceans are as deep as the mountains are high. A more quantitative estimate was made by the astronomer Laplace. Based on a deduced relationship between oceanic depth and tide wave velocity, he placed the abyssal depth at 12 miles.

For the sounding, Ross prepared a line (stranded hemp?) "three thousand six hundred fathoms, or rather more than four miles in length fitted with swivels to prevent it unlaying in descent, and strong enough to support a weight of seventy-six pounds". The line was wound on a free-spooling reel and a plummet was attached to the outboard end. The apparatus was placed on one of the ship's small boats which was lowered over the side, and the plummet was dropped. While the weight was

* In 1818 Sir John Ross recovered bottom mud from depths of 1,000 and 1,050 fathoms (ref. 3). Although this also was a remarkable accomplishment, it cannot be considered an abyssal sounding because the hypsometric curve gives a mean depth of 2,555 fathoms for the oceanic basin province in the Atlantic Ocean⁴.

descending, oarsmen manoeuvred the small boat to compensate for currents and windage. Thus the sounding line was kept vertical so that line angle errors were minimized^{1,2}.

Ross identified the bottom by a decrease in the rate of pay out of line from the free-spooling reel. The velocity of descent was ascertained by noting the time between successive increments (100 fathoms) which had previously been marked on the 3,600 fathom line. An abrupt decrease in the rate of pay-out was indicative of bottom contact. This method was necessary because it is not feasible to "feel" bottom at abyssal depths. Maury³, who later formalized the rate-of-pay-out technique in his law of plummets descent, was aware that deep undercurrents could induce "swigging forces upon the bight" which could cause a line to run out for ever or, because sounding lines are of finite length, until the end spooled off and disappeared beneath the surface. Thus one could merely have measured the length of a piece of line rather than have determined the depth of the ocean.

We suppose that this is a calligraphic error in transcription, for a poorly handwritten "5" may appear to be a "6". There is certainly no justification for unravelling Ross's sounding because of the many inaccuracies involved in obtaining it. Similarly, the error in sounding location must have resulted from a creeping error in drafting without reference to the original source.

Because literally millions of soundings are now taken each year, it seemed appropriate to us to ask the USC and GSS Discoverer, while *en route* to Tristan da Cunha, to survey Ross's site as a commemorative gesture. The site is located about 600 miles NNW of Tristan and approximately half-way between the lower halves of South America and Africa.

On January 23, 1968, a brief survey was made over an area of 47 square miles in the vicinity of the Ross site. The survey was laid out in a butterfly pattern (Fig. 1) and was made during the early morning hours between reliable five-point morning and evening star fixes; positions were maintained by dead reckoning. We estimate

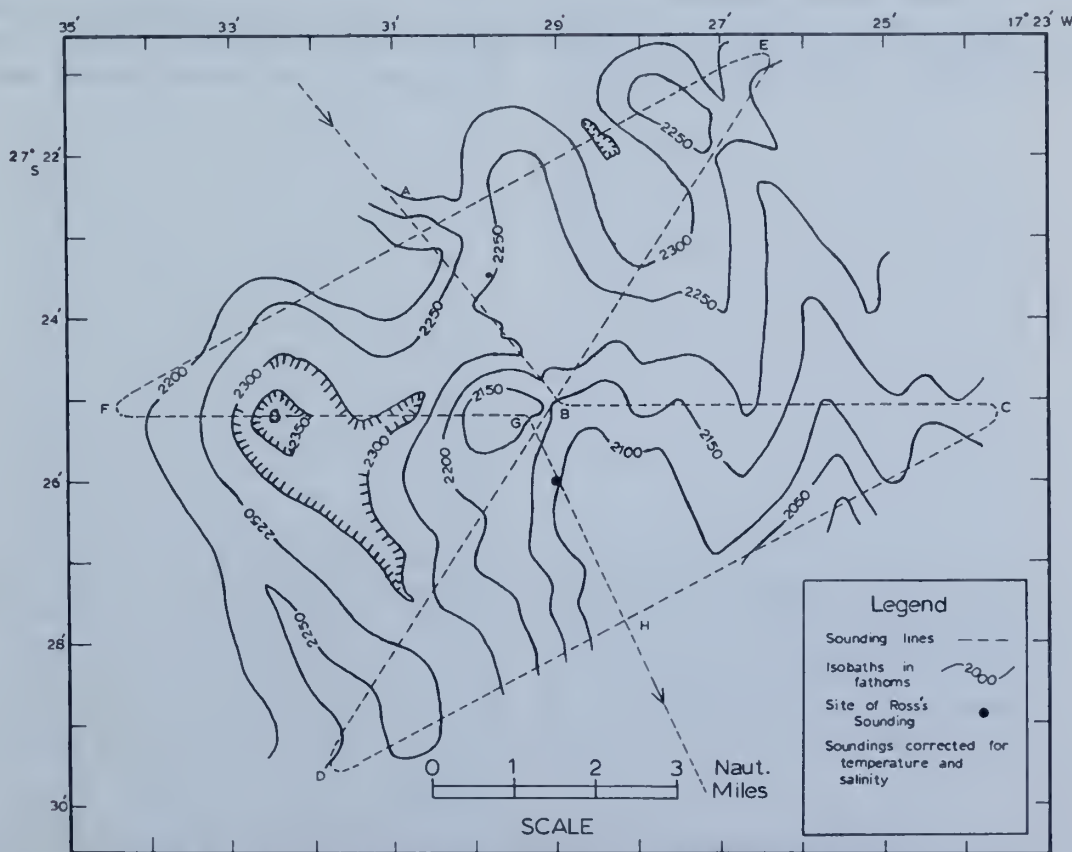


Fig. 1. Sonic sounding survey of the area around Sir James Ross's original abyssal sounding.

Ross's sounding is still retained on modern charts (for example, the US Navy Hydrographic Office Chart 5761), but its position has been slightly misplaced and it is given as 2,426 fathoms instead of 2,425 fathoms. Admiral G. S. Ritchie, the British hydrographer, has informed us that the sounding first appeared on Admiralty Chart No. 2203 in 1853 as 2,426 fathoms and has been recorded as such ever since. He stated that no evidence could be found in the records of the Hydrographic Department as to why one fathom had been added to Ross's measurement.

that the survey line positions are accurate to within about one nautical mile. The soundings were recorded on a precision depth recorder timed at 800 fathoms/s and were later corrected for salinity and temperature variations in seawater by using appropriate Coast and Geodetic Survey tables.

The relief of the area is bold and rugged; steep, isolated peaks separated by deep, V-shaped depressions are common. The north-western half of the region has a mean depth greater than 2,200 fathoms (4,023 m); the south-eastern half is shallower. The absolute relief observed

along the sounding lines was 404 fathoms. The depth at Ross's sounding site is 2,100 fathoms (3,843 m) (rounded to the nearest 5 fathoms), or it is 325 fathoms less than Ross's value. The maximum depth (2,400 fathoms; 4,392 m) was found in a hole in a broad depression in the north-western sector. This is about 3.5 miles away from the Ross site.

The Ross sounding was taken in the western flank province of the Mid-Atlantic Ridge. In this rugged region of abyssal hills substantial variations in depth occur in small horizontal distances. It would therefore be meaningless to speculate about the true error of the first abyssal sounding, for Ross's position can only have been approximate. None the less, it is interesting to compare the depth that Ross obtained with that which we obtained at his documented position. Ross's measurement of the depth is about 325 fathoms greater than ours. This amounts to an error of about 15 per cent. If, however, we select the maximum depth within the area, then Ross's sounding is only 25 fathoms more than ours and is in error by only 1 per cent.

We cannot determine with any certainty the reason for Ross's sounding being too deep, but two possibilities stand out: either the moment of bottom contact was not immediately recognized, or Ross's position was in error by 5 miles or more.

In the early days of sounding it was customary to use a cannonball as a plummet. Hence, to commemorate Ross's historic accomplishment, a cannonball about three centuries old, which was recovered by divers in the Florida Keys, was put over the side in a token lowering. In re-visiting this site, a hydrographic milestone was recognized and a part of oceanographic history was relived.

We thank Captain T. Treadwell, of the US Navy Oceanographic Office, and Admiral G. S. Ritchie for supplying information from their archives. We thank Captain Lorne Taylor and the officers and crew of the USC and GSS Discoverer, for carrying out the mission, especially Lieutenant Commander G. A. Maul, Lieutenant M. N. Walter, Lieutenant O. Staffin, Ensign P. Hitch and Chief C. Ellis.

Received May 24; revised July 22, 1968.

¹ Ross, Sir James C., *A Voyage of Discovery and Research in the Southern and Antarctic Regions During the Years 1839-43*, 1, 2 (John Murray, London, 1847).

² Carrington, E., *A Biography of the Sea*, 286 (Basic Books, Inc., New York, 1960).

³ Thomson, W., *The Depths of the Sea*, 527 (Macmillan Co., London, 1874).

⁴ Menard, H., and Smith, S., *J. Geophys. Res.*, 71, 4305 (1967).

⁵ Murray, J., and Hjort, J., *Depths of the Ocean*, 325 (Macmillan Co., London, 1912).

⁶ Maury, M. F., *Physical Geography of the Sea*, 493 (sixth ed.) (T. Nelson and Sons, London, 1859).

Reprinted from The Journal of Geology
Vol. 76, No. 1, January 1968
Copyright 1968 by The University of Chicago
Printed in U.S.A.

MIOGEOCLINES (MIOGEOSYNCLINES IN SPACE AND TIME): A REPLY¹

ROBERT S. DIETZ AND WALTER P. SPROLL
Institute for Oceanography, ESSA, Miami, Florida 33130

The purpose of a speculative paper such as "Miogeoclines (Miogeosynclines) in Space and Time" (Dietz and Holden, 1966) is to provoke critical appraisal, so we welcome the discussion and comments by P. M. Clifford and J. R. Henderson. A reply to their questions is attempted here.

HURONIAN MIOGEOCLINE

Clifford and Henderson reject the Huronian miogeocline concept mainly because an aeon separates the deposition of these rocks from the principal Grenville orogeny. However, if the Grenville Front was the cratonic (continental) edge upon which the Huronian wedge was deposited, we would expect a geologic development as follows: The continent edge would downflex as the ocean floor is loaded by a continental-rise prism. For reasons of isostasy, the continental-rise prism would grow to about 50,000 feet and the continental wedge to about 20,000 feet, judging from modern examples and assuming the continent/ocean relief was then the same as now, or 2.5 miles. This sedimentation would occur rather quickly so that, possibly after something like 200 m.y., the continental slope would become fully overlapped with the formation of a *continental embankment* (Dietz, 1964) in place of a continental slope. Additional sedimentation would then simply extend this embankment seaward (as in the Gulf Coast of the United States today). The terrace wedge, our future miogeocline, would become dead without further tendency to subside and accumulate sediment, regardless of the length of the interval between its original deposition and the next accretionary paroxysm which would collapse the continental-rise prism into a eugeosyncline.

¹ Manuscript received April 21, 1967.

Contrary to the common view, we do not consider that sedimentation per se triggers orogeny. Hence we do not regard the criticism by Clifford and Henderson as especially damaging to the concept of the Huronian sedimentary prism being a miogeocline. It is, of course, possible that we have overstepped in choosing the Huronian sedimentary wedge as a Precambrian example of a miogeocline, but the choice is tempting by its sudden "disappearance," as classically described by Quirke and Collins (1930). Our preferred explanation is, of course, that the "missing half" of the Huronian prism never existed. Instead, the prism was an ensialic continental margin wedge which thickened out—with the Grenville Front being the outcropping trace of an ancient continental slope, a moderately dipping plane. This, in turn, would nicely account for the front being the locus of some thrusting toward the craton and for the abrupt contrast in intensity of metamorphism and style of tectonism across it. It would be reminiscent of the contrast between the crystalline Appalachians and the folded Appalachians across the Blue Ridge line. The front is a most remarkable geologic boundary, as we would expect an ancient continent edge to be, even to the extent of localizing orogeny. In view of such considerations, it seems that the possibility of the Grenville Front marking the ancient continental edge should be kept open.

CRYSTALLINE APPALACHIANS AND CONTINENTAL ACCRETION

The case for continental accretion, as opposed to the alternate explanation of continental growth by reprocessing in some manner previously existing sial, probably will stand or fall upon the still unresolved question of whether the crystalline Appalachians constitute an accretionary belt. If it

proves to be so, it seems likely (although, of course, not necessarily so) that the Grenville belt may be similarly explained. Clifford and Henderson apparently reject the crystalline Appalachians as being an accretionary fold belt and quote the 1,100-m.y. age of the Baltimore gneiss as disproof.

This seems unreasonable to us, as explained elsewhere (Dietz, 1965). One of several possibilities of accommodating Grenville-aged rocks (*sensu lato*) into the Appalachian belt would be by interpreting the Baltimore gneiss as an uplifted portion of the pre-Appalachian continental slope of eastern North America. Modern, and presumably ancient, continental slopes have a declivity of only 3–5 degrees so that the inner portion of a continental-rise prism (a future eugeosynclinal orogen) is necessarily underlain by sialic rock. However, the Baltimore gneiss domes do seem a little too far distant (60 miles) from the Blue Ridge line to be readily accommodated by this interpretation, unless we take into account the great structural complexity of this reentrant in the Appalachian trend, where nothing is known for sure to be in place. Also, continental-slope regions sometimes extend far to sea in the modern world, for example the Blake Plateau.

The crux of the matter seems to be, should we try to accommodate a few anomalies to the concept of continental accretion by lateral growth, or should we discard it and embrace a concept of *virtually complete* reprocessing of an old continental plate into a new one. We prefer the former approach, until such time as there is more telling data.

GRENVILLE PROVINCE AND ACCRETION

Clifford and Henderson conclude that the Grenville province cannot be accretionary, based on the discovery by Grant (1964) of rocks of probable Kenoran age immediately across the Grenville Front in one area. This seems to be hardly a critical piece of evidence. For example, if the Grenville Front is not a nearly vertical plane but one gently

inclined to the east as was the former continental slope (as noted earlier), it would not be surprising to find uplifted older rocks along the inner margin of the front.

The critique, however, cites some evidence of metamorphosed Superior province rocks much further within the Grenville province; and apparently this is a common view among Canadian geologists. If such occurrences are found to be common, they would do strong damage to the accretionary concept, but we would prefer delaying any final judgment. Grant (p. 1050) noted that, although commonly claimed, it has not been demonstrated unequivocally that rocks of the Superior province have been metamorphosed during the Grenville orogeny.

If the Grenville province rocks are composed of a collapsed and plutonized eugeosynclinal suite originally laid down as a continental rise of flysch-type rocks or a continental embankment of mixed flysch and terrace wedge rocks, then they were largely derived from the Superior province. They would be sialic and contain much detritus of Kenoran age. With plutonization, some juvenile material would be added. Considering this and numerous other factors, what is the real geologic meaning of age dates as applied to continental accretion?

It has been claimed that the Grenville Front is a major fault with thrusting toward the west or cratonward, or that it is a major metamorphic transition. Most likely it is a combination of the two, but perhaps still more fundamentally it marks the former position of the continental margin. This would nicely account for the abrupt transition in metamorphism and for the localization of thrusting controlled by the plane of the continental slope. If the Grenville sediments are ensimatic, we could understand why they were mobilized and plutonized—by their basement eventually becoming a conveyor belt under sea-floor spreading. These features of the proposed geologic evolution are attractive enough to ask that the concept not be dismissed without serious consideration.

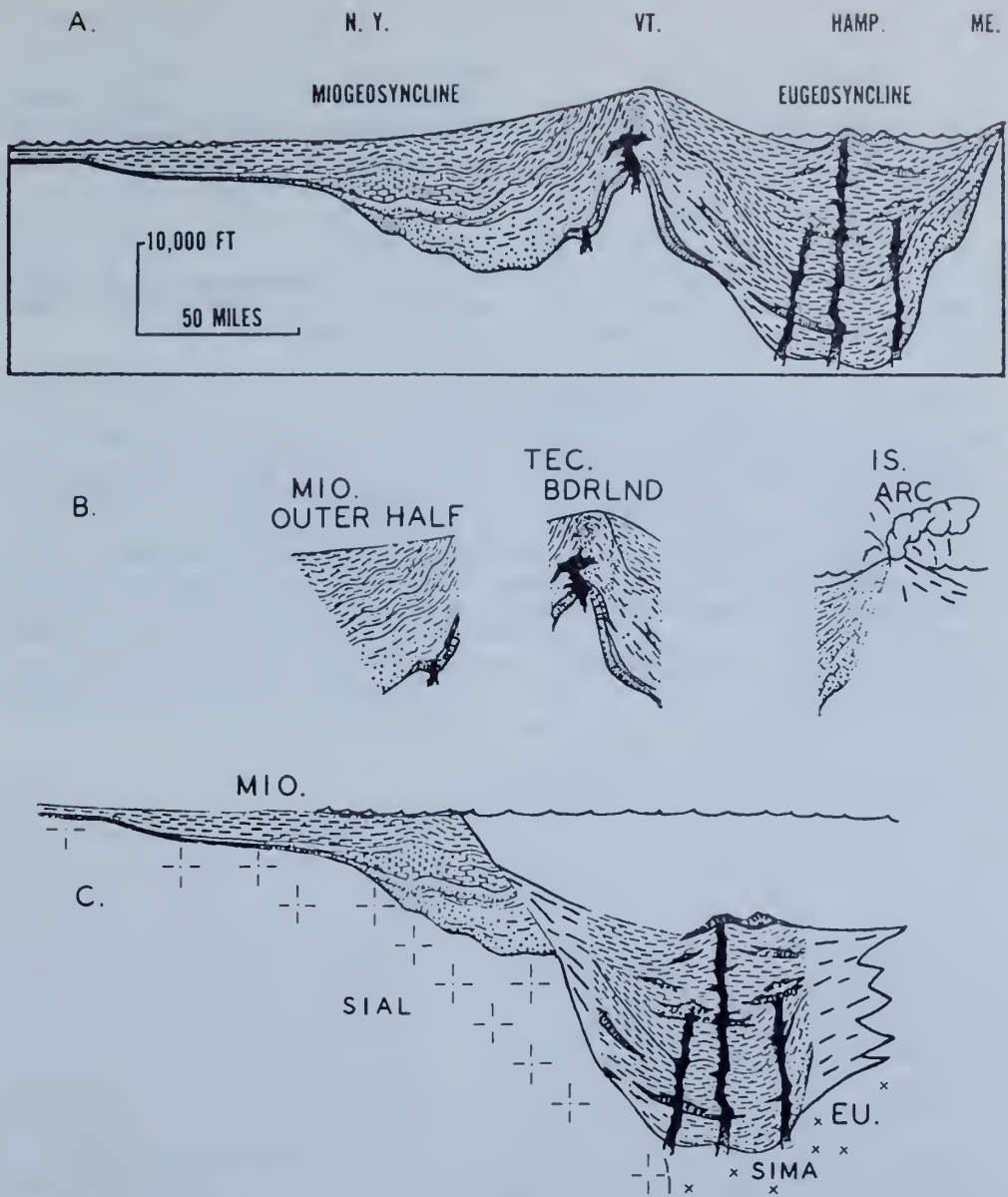


FIG. 1.—A diagram to show the elements which are deleted from the classical type of ensialic mio-eugeosynclinal couplet to transform it into an ensialic-ensimatic actualistic geosynclinal couplet. The outer half of the mioeugeosyncline, the tectonic borderland, and the island arc are eliminated; a continental slope is inserted. With the collapse of the continental-rise prism against the wall of the continental slope, continental accretion is effected. *A*, mio-eugeosynclinal couplet along eastern North America reconstructed as of the mid-Ordovician (after Kay, 1951). *B*, deleted elements. *C*, mio-eugeosynclinal couplet according to the actualistic concept of geosynclines (Dietz, 1963) by which the sedimentary prisms shown may be equated with sedimentary prisms along the modern continental edge of eastern North America.

CONCLUDING REMARKS

The post-mid-Mesozoic continental-rise prisms are by far the greatest sedimentary deposits on earth today. Where are their ancient equivalents? The present evidence of marine geology strongly suggests that there are no Precambrian deposits in modern deep ocean basins. So where have they gone? Their re-incorporation into the con-

tinental plates offers a reasonable solution to this impasse. This may be accomplished by sea-floor spreading which collapses continental-rise sedimentary prisms into accretionary eugeosynclinal fold belts. But to accomplish this, neither tectogenes nor ensialic marginal geosynclines of the classic description are adequate for the task. The actualistic concept of geosynclines is shown in figure 1 (Dietz, 1963, 1966).

REFERENCES CITED

- DIETZ, R. S., 1963, Collapsing continental rises: an actualistic concept of geosynclines and mountain building: *J. Geology*, v. 71, p. 314-333.
- 1964, Origin of continental slopes: *Am. Scientist*, v. 52, no. 1, p. 50-69.
- 1965, Collapsing continental rises: an actualistic concept of geosynclines and mountain building: a reply: *J. Geology*, v. 73, no. 6, p. 901-906.
- 1966, Passive continents, spreading sea floors and collapsing continental rises: *Am. Jour. Sci.*, v. 264, p. 177-193.
- 1967, Passive continents, spreading sea floors and collapsing continental rises: a reply: *Am. Jour. Sci.*, v. 265, p. 231-237.
- DIETZ, R. S., and HOLDEN, J. C., 1966, Miogeoclines (miogeosynclines) in space and time: *J. Geology*, v. 74, no. 5, p. 566-583.
- GRANT, J., 1964, Rubidium-strontium isochron study of the Grenville Front near Lake Timagami, Ontario: *Science*, v. 146, p. 1049-1053.
- KAY, M., 1951, North American geosynclines: *Geol. Soc. America Mem.* 48, 143 p.
- QUIRKE, T., and COLLINS, W., 1930, Disappearance of the Huronian: *Canada Geol. Survey Mem.* 160, 129 p.

Notes and Discussions

ROBERT S. DIETZ }
 HARLEY J. KNEBEL } *ESSA, Atlantic Oceanographic Laboratories, Miami, Florida*
 LEE H. SOMERS } *Department of Meteorology and Oceanography, University of Michigan, Ann Arbor, Michigan*

Cayar Submarine Canyon

Abstract: The characteristics of the Cayar Submarine Canyon off the coast of Senegal suggest that its evolution was controlled by submarine processes. This well-delineated, hitherto-unsurveyed canyon originates near the shoreline (10 to 20 m deep) on the upcurrent side of the Cape Verde peninsula and extends downslope to the oceanic basin. Its channel remains a prominent feature at 1800 fm (3294 m); its maximum width is 5 nautical miles (9 km).

The Cayar Canyon confirms the conditions which attend the development of canyons upcurrent from headlands: a supply of sediment available at the canyon head, a steep nearshore gradient, and a decrease in longshore current transport. The conspicuous absence of fluvial influence and the apparent lack of direct tectonic involvement in recent geologic time suggest that the canyon was developed by the movement of sediment downslope in response to a localized over-accumulation of continental detritus. This canyon is probably second only to the Congo Canyon in geologic importance around Africa.

INTRODUCTION

Early in 1968 one of the world's most prominent and well-delineated submarine canyons was surveyed just offshore from the fishing village of Cayar, Senegal, along the northwestern coast of Africa. Prior to this time only its extreme nearshore part had been sounded. This paper discusses the environment, bathymetry, and development of this canyon. The Cayar Canyon is of major importance for the entrapment of nearshore sediments and for funnelling them to the oceanic basin. It taps the paralic zone at the southern end of a coastal bight which extends 400 nautical miles (740 km) northward to Cape Blanc.

ACKNOWLEDGMENTS

We thank Captain Lorne G. Taylor and the officers and crew of the USC&GSS *Discoverer* for their cooperation and assistance during this survey. Thanks are also extended to J. P. Pinot and J. R. Vanney of the Institut de Géographie, University of Paris, P. Bouysse of B.R.G.M., Orleans, France, and C. M. Urien of the Argentine Hydrographic Office, Buenos Aires, for

their assistance and suggestions during this investigation.

GEOLOGY AND ENVIRONMENT

Regional Setting

In the area of the Cayar Canyon, the continental shelf is about 10 nautical miles (18 km) wide and the shelf break occurs at 50 to 60 fm (90 to 110 m). Toward the north the shelf widens (Fig. 1) and the depth at the shelf break increases to 70 to 80 fm. At the northern end of the bight the shelf extends offshore for more than 60 nautical miles (111 km).

Changes in the continental slope along this section of the coast are not pronounced; its width remains constant and a gradient of 2°00' is maintained. At least two smaller submarine canyons incise the slope between 17° and 18° N. latitude. These canyons have not been surveyed, and their shoreward limits are unknown.

The Senegal River is the only major waterway which contributes sediments to this part of the coast. This river, which is 913 nautical miles (1690 km) long, intersects the shoreline

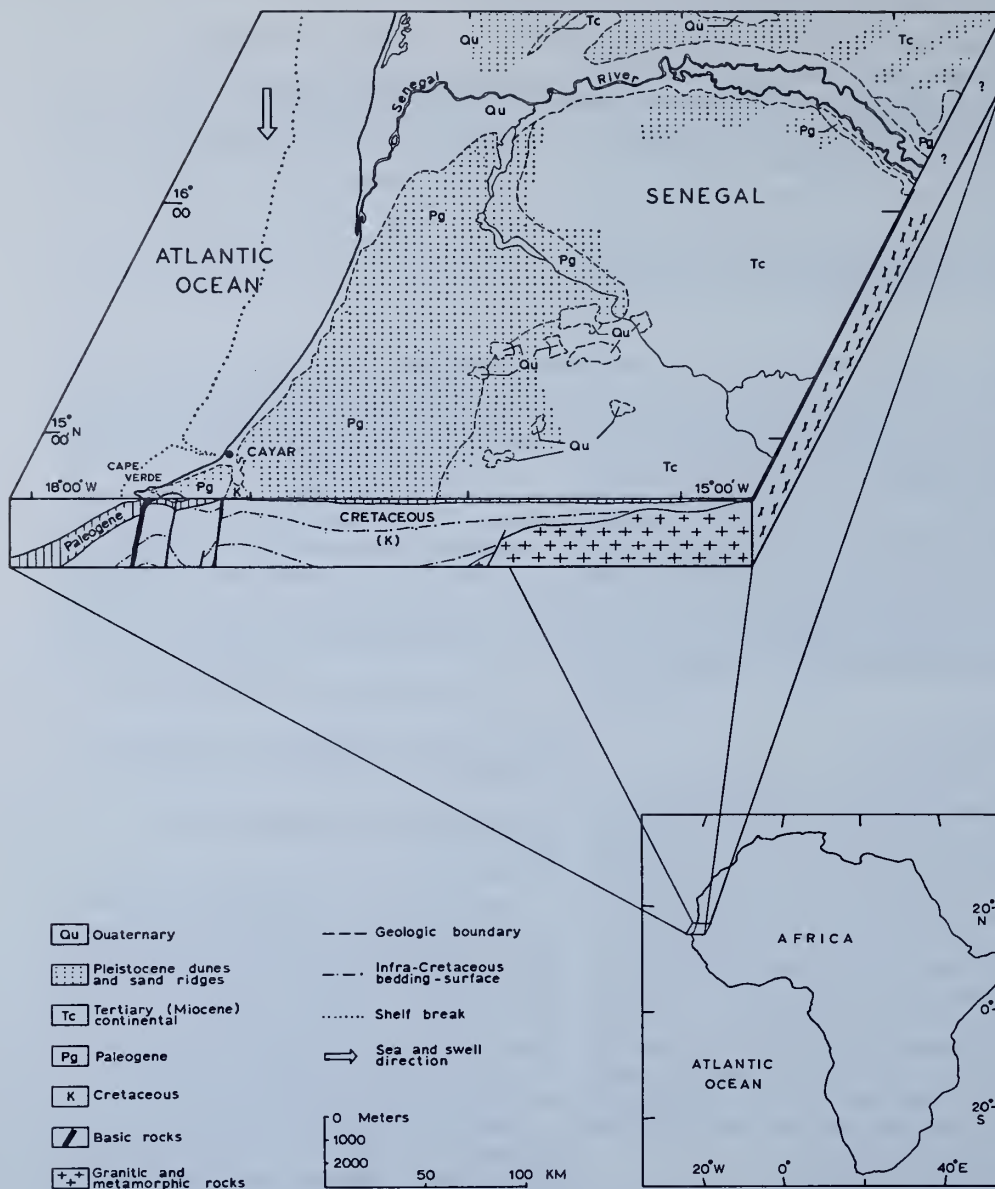


Figure 1. Geology and environmental conditions along the coast of Senegal north of the canyon area. Areal and subsurface geology obtained from Bureau de Recherches Géologiques et Minières (1960) and Spengler and others (1966), respectively. Offshore data from the U.S. Naval Oceanographic Office (1963) and the U.S. Navy Hydrographic Office (1943).

68 nautical miles (126 km) north of the canyon area. There its mouth is obscured by a narrow, southward-projecting spit (Fig. 1).

The sea and swell in this region are predominantly from the north. Only slight

changes in wave type and direction are observed throughout the year (U.S. Naval Oceanographic Office, 1963). The winds, however, are more capricious. Along the coast, the wind direction varies from northeast to north-

west. Inland, local variations and a moderate summer reversal preclude the establishment of a prevailing wind direction (Services Météorologiques De La France d'Outre-Mer, 1964).

Geologic Setting

The present shape of the Cape Verde peninsula is that of a tombolo, but its origin is more complex than this form suggests. From Late Cretaceous to middle Tertiary time, vertically acting forces produced the peninsula by undulating and fracturing a part of the seaward edge of the Mesozoic sedimentary basin that underlies most of western Senegal. This area was subsequently intruded, and volcanic rocks were extruded at several locations. As a result of this tectonic activity, Tertiary sedimentary and volcanic rocks underlie the surficial sands over much of the peninsula and Cretaceous sediments are exposed farther inland (Spengler and others, 1966) (Fig. 1).

Along the coast the bedrock is obscured by a cover of semiconsolidated detritus. This zone, which is about 57 miles (92 km) wide, is characterized by enormous Pleistocene sand ridges with smaller, present-day, longitudinal dunes in the interridge areas. Both the ridges and dunes are oriented in a northeast-southwest direction (Elouard, 1966). This belt parallels the shoreline in Senegal and extends northward into western Mauritania where it becomes a part of the Sahara Desert (Fig. 1).

There is no indication that there has been any direct fluvial influence in the Cayar region during recent geologic time. The uninterrupted cover of continental sediments which encompass the lower Senegal valley suggests that the course of the river has not changed significantly since Miocene time (Fig. 1). In addition, local fluvial involvement was probably limited by the coastal relief that was produced during the formation of the Cape Verde peninsula.

Finally, there is a marked difference in the size of the beach on either side of the canyon. Immediately south of its head (for approximately 1 km) the beach is practically non-existent. Farther down coast, the beach zone widens but remains conspicuously irregular (Fig. 2).

SURVEY RESULTS

Methods

Fathograms from 650 nautical miles (1203 km) of trackline were obtained from aboard the

USC&GSS *Discoverer* during February and March 1968. A Precision Depth Recorder coupled with an EDO transducer was used throughout the survey. The sound velocity was assumed to be 800 fm/sec (1463 m/sec), and the soundings were not corrected for velocity variations in the water column.

Two types of navigational control were used to position the sounding lines. Near shore, the fixes were established by visual sightings and radar bearings. Farther offshore, positions were maintained by dead reckoning with respect to land ties and celestial fixes, and a constant drift set was assumed. Positional accuracy for the nearshore area is probably within 1 nautical mile; offshore, the accuracy is slightly less.

Bathymetry

The Cayar Canyon originates just offshore (10 to 20 m deep) from a distinct coastal inflection approximately 26 nautical miles (48 km) northeast of the terminus of the Cape Verde peninsula and then proceeds toward the northwest across the continental shelf (Fig. 1). In this segment, the canyon is precipitous and symmetrical and has a gradient of $2^{\circ}09'$. At the shelf break its width and relief are 3 nautical miles (6 km) and 380 fm (695 m). One small tributary valley enters the canyon from the north about halfway across the shelf (Figs. 3, 4).

Below the shelf, the canyon turns toward the north and cuts orthogonally down the continental slope to about 1100 fm (2013 m). There the thalweg again turns westward. The average gradient in this section is less than $1^{\circ}00'$, despite the steep inclination of the canyon in the upper reaches of the continental slope. There is also a decrease in relief. In the lower slope, the depth to the valley floor is less than 150 fm (275 m). Along this stretch of the canyon the maximum width occurs at the confluence of several tributary valleys which enter from the north at $15^{\circ}17' N.$, $17^{\circ}54' W.$ Several other secondary valleys dissect the northern wall as well. The southern wall, on the other hand, is conspicuously uninterrupted (Figs. 3, 4).

Beyond the continental slope, the canyon maintains its westward trend and the gradient and relief continue to decrease. At the seaward edge of the survey area the axis is evident, but the walls are poorly defined due to the development of distributary channels. The re-

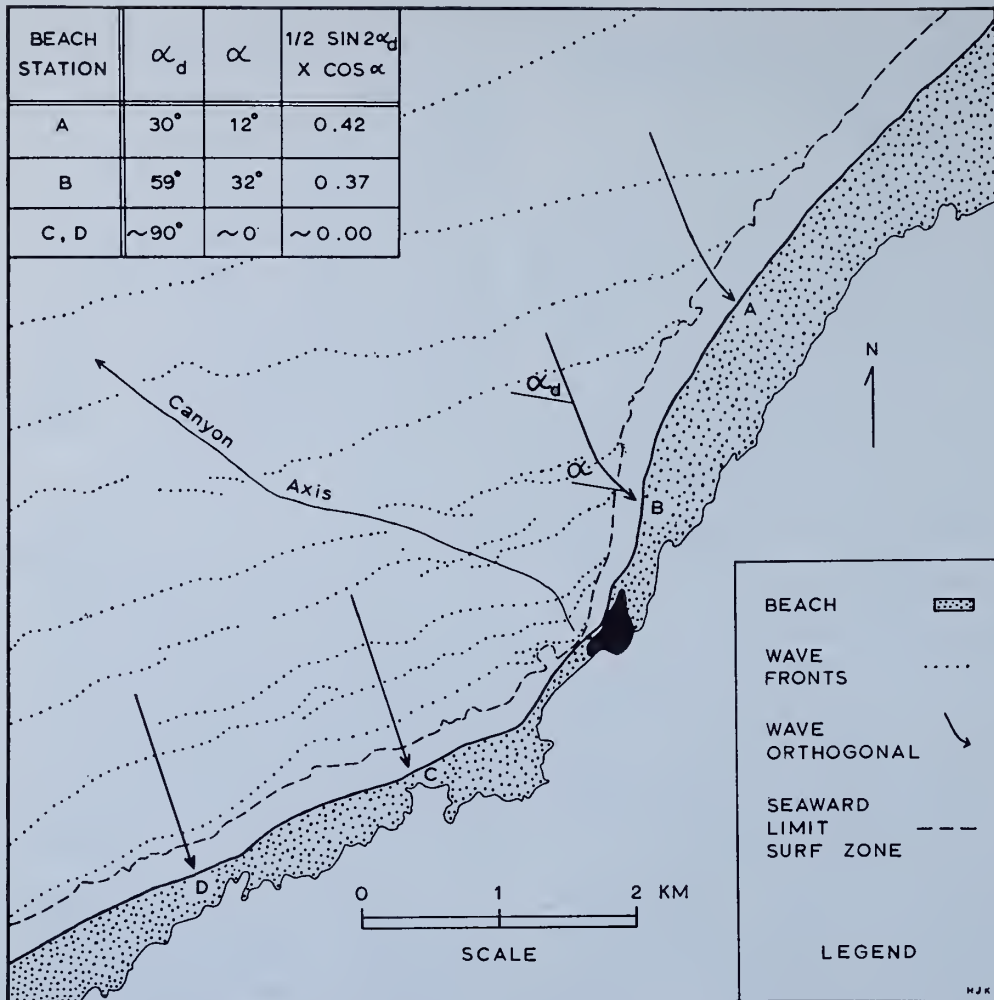


Figure 2. Environmental conditions and change in longshore-current transport near the head of the canyon. Diagrammatic reproduction of an aerial photograph taken over Cayar, Senegal, showing wave and beach conditions and the decrease in longshore transport rate. See text for explanation of symbols.

sulting trough is more than 7 nautical miles (13 km) wide. Well-developed, leveed banks border the canyon in this area (Figs. 3, 4).

DISCUSSION

The development of a submarine canyon is generally attributed to one or more of the following processes: subaerial erosion, faulting, mass movement of sediments, or turbidity currents. For the Cayar Canyon, the absence of fluvial involvement during recent geologic time eliminates subaerial erosion as an originative or developmental process. Furthermore, the apparent restriction of diastrophic activity

to the Cape Verde peninsula and the lack of proximal tectonic lineaments suggest that crustal deformation *per se* did not create the canyon. It is not improbable, however, that the course of the canyon was initiated or modified by tectonism. But, as a developmental process, faulting appears to have played a secondary role.

The most conspicuous geographic feature of the Cayar Canyon is that it occurs on the up-current side of a point of land. This position is not unique, for at least ten other submarine canyons are known to have this same relation with points (Shepard and Dill, 1966, p. 344-

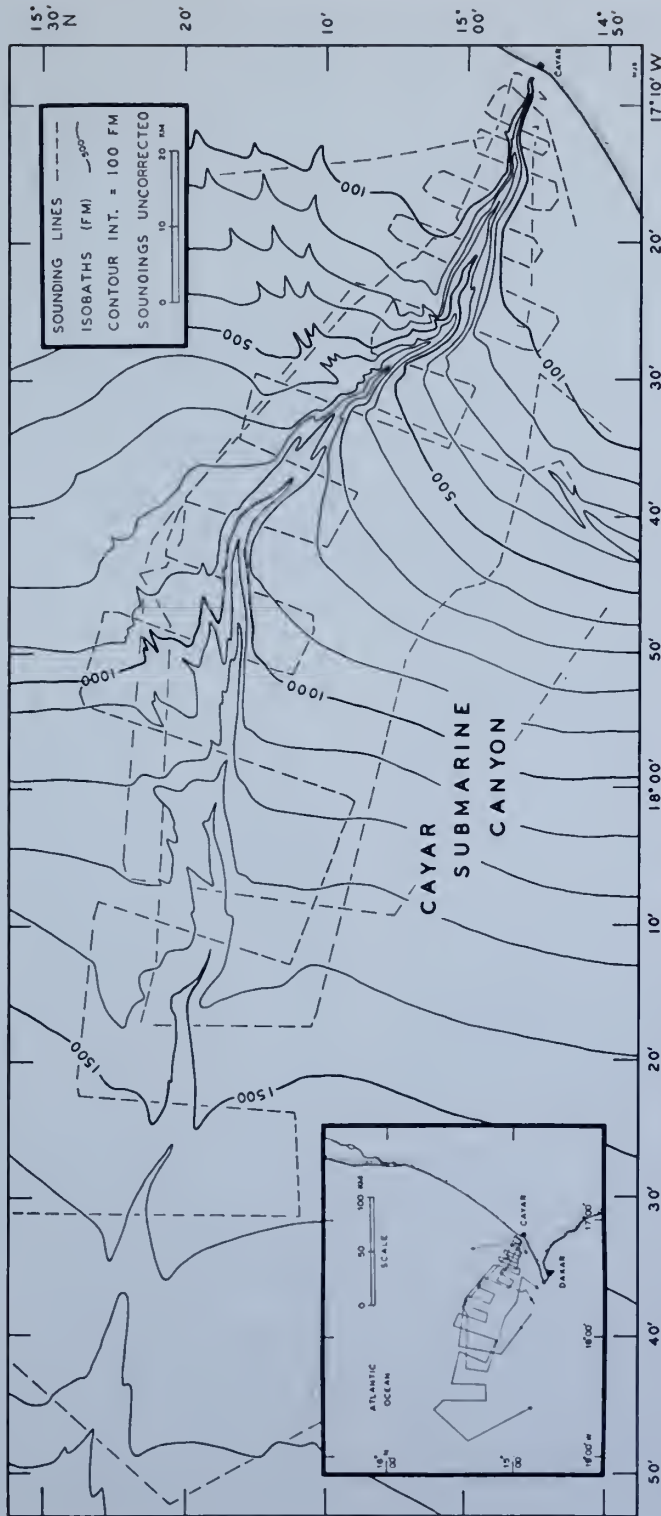


Figure 3. Bathymetric chart of Cayar Submarine Canyon. Soundings in fathoms at 800 fm/sec (1463 m/sec) and uncorrected for differential sound velocities. Isobaths are based on original data supplemented with soundings of various origins.

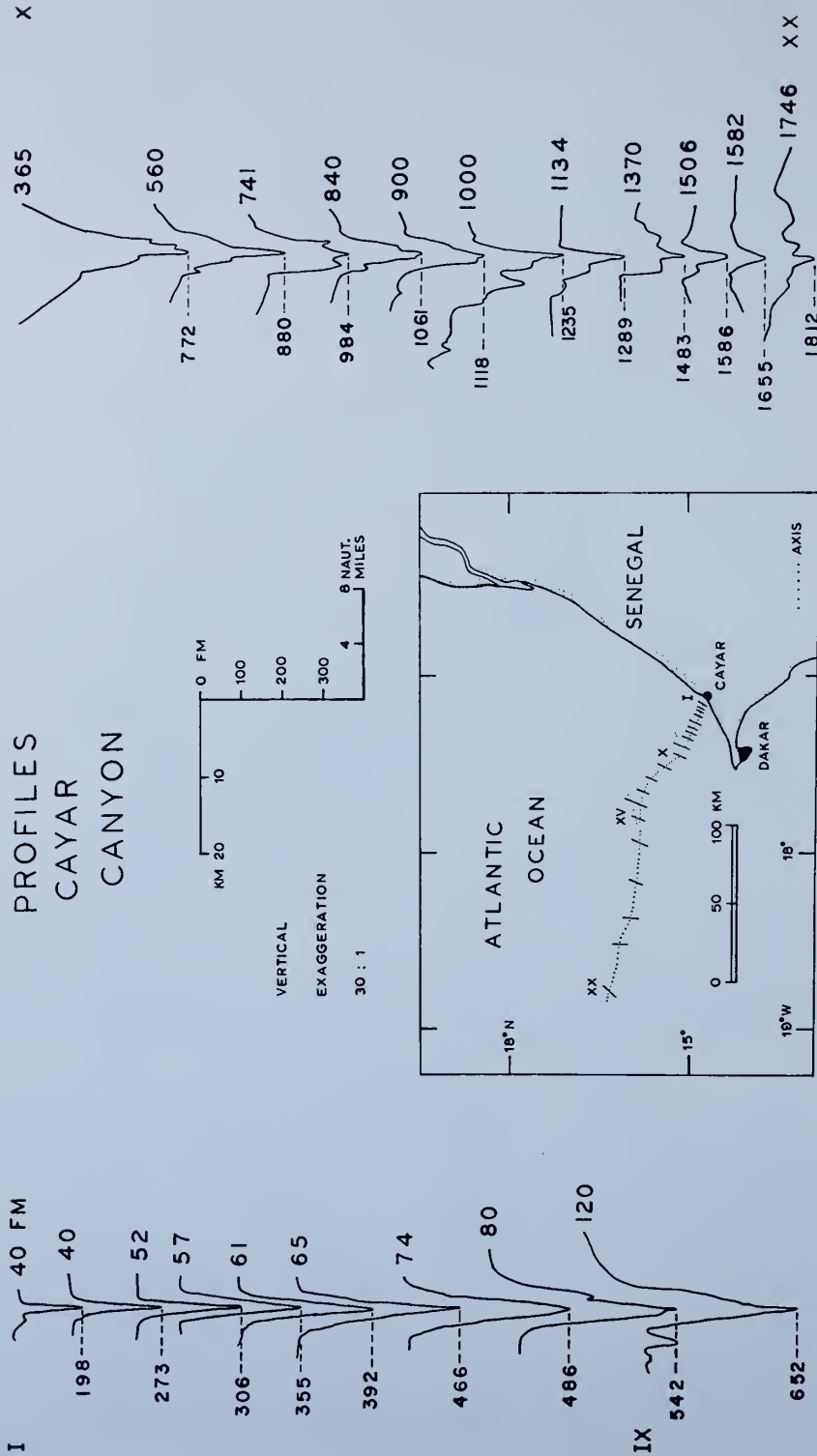


Figure 4. Vertical profiles of Cayar Submarine Canyon. Taken from Precision Depth Recorder. Roman numerals indicate profile number. Index map shows profile locations.

351). Several of these were included in a study by Crowell (1952) of the submarine canyons bordering central and southern California. For this section of the California coast, he found empirically that a source of sediment and a steep nearshore gradient were fundamental to canyon development. He stated that if these primary conditions have been present, canyons are found where sediment accumulates due to a decrease in the transportability of longshore currents.

These three conditions seem to be satisfied for the Cayar Canyon. The elongate zone of mobile detritus (Fig. 1) and the extensive beach area north of Cayar (Fig. 2) show that an ample supply of sediment is available along the coast. Furthermore, the northeast-southwest orientation of the longitudinal dune ridges and the northwest to northeast winds along the coast indicate that there is a net southwesterly movement of this sediment toward the head of the canyon. Petrographic evidence for this direction of sediment movement has been presented by Tourenq (1964). In addition to eolian transport, the Senegal River undoubtedly contributes some sediment as well. Its effect is restricted, however, by estuarine and climatic restraints.

Near the head of the canyon the submarine gradient is, indeed, steep. Here the declivity of the continental shelf is three times greater and its width is four times less than the world-wide average. In the Cayar region, the continental margin is constricted more than at any other place along the coastal bight.

Finally, it can be shown that there is a decrease in the transport rate of longshore currents in the vicinity of the Cayar Canyon. This decrease is due primarily to the coastal configuration, since there is very little change in either wave type or direction throughout the year and the nearshore submarine topography appears to be uniform. The differential wave refraction in this area is shown in Figure 2. North of Cayar the waves are greatly refracted and a strong southerly current is indicated. To the south, the wave orthogonals are almost normal to the coast and the longshore component is evidently very weak.

The decrease in transport rate can be shown quantitatively as well. For a given deep-water wave condition, the dynamic transport rate should be proportional to $\frac{1}{2} \sin \alpha_d \cos \alpha$, where α_d is the angle that deep-water waves make with the beach and α is the corresponding shallow-water angle (Inman and Bagnold, 1963,

p. 547-549). Four points were selected along the coast near the head of the canyon, and this variable was computed (Fig. 2). The values obtained indicate that the transport rate north of the canyon is several times greater than that to the south of it.

In addition to these fundamental conditions, the following points seem pertinent:

(1) The noticeable change in the size of the beach down coast shows that there is an appreciable loss of sediment from the paralic zone near the head of the canyon.

(2) The preferential development of tributaries along the northern wall indicates that their occurrence is not fortuitous and that they are probably due to the influx of clastics from the north.

(3) The nearshore divergence of waves over the canyon (Fig. 2) provides a quiescent depositional environment and an effective route for the offshore transport of sediment.

(4) The leveed banks in the lower reaches suggest that currents within the canyon are occasionally large enough to overflow the channel and to deposit detritus on the rim.

(5) The presence of the head of the canyon near sea level is indicative that the canyon is being cut by contemporary submarine processes that have kept pace with the postglacial rise in sea level.

(6) Evidence of turbidity currents causing cable breaks has been found in this area (Heezen, 1956).

SUMMARY AND CONCLUSIONS

The absence of direct fluvial and tectonic involvement during recent geologic time indicates that the evolution of the Cayar Canyon was controlled by submarine processes. Faulting may have determined the course of the canyon, but, as a genetic process, it appears to have been unimportant. The environmental conditions in this area are similar to those that have attended the development of canyons upcurrent from headlands off the coast of California: a supply of sediment available at the head of the canyon, a steep, nearshore gradient, and a decrease in the transport rate of longshore currents. These conditions favor both the mass movement of sediment and turbidity currents.

The influx of sediment into the canyon is evident from the decrease in the size of the beach near its head and from the dissection of the northern wall by numerous tributaries. The nearshore divergence of waves facilitates

deposition within the canyon. Apparently, sediments accumulate in the headward region until they become unstable; then they move seaward. Movement of detritus down the canyon is indicated by leveed banks and historical turbidity currents.

The head of the canyon has been maintained near sea level by erosion, and it now taps the paralic zone. The dimensions and environment

of the canyon suggest that the rate of sedimentary entrapment is considerably more than the estimate of 400,000 m³/yr made by Varlet (1958) for the Trou Sans Fond Submarine Canyon which occurs just offshore from Abidjan, Ivory Coast. The Cayar Canyon, therefore, is probably second only to the Congo Canyon (Heezen and others, 1964) in geologic importance around Africa.

REFERENCES CITED

- Bureau De Recherches Géologiques et Minières, 1960, Afrique occidentale carte géologique feuille no. 4 (Sénégal) (1:2,000,000), Paris.
- Crowell, J. C., 1952, Submarine canyons bordering central and southern California: *Jour. Geology*, v. 60, p. 58-83.
- Elouard, P., 1966, Le bassin quaternaire du Sénégal, in Reyre, D., *Editor*, Sedimentary basins of the African Coasts: Paris, Assoc. African Geol. Survey, p. 95-98.
- Heezen, B. C., 1956, The origin of submarine canyons: *Sci. American*, v. 159, p. 36-41.
- Heezen, B. C., Menzies, R. J., Schneider, E. D., Ewing, W. M., and Granelli, N. C. L., 1964, Congo submarine canyon: *Am. Assoc. Petroleum Geologists Bull.*, v. 48, p. 1126-1149.
- Inman, D. L., and Bagnold, R. A., 1963, Littoral processes, in Hill, M. N., *Editor*, The sea, v. 3: New York, John Wiley and Sons, p. 529-553.
- Services Météorologiques De La France d'Outre-Mer, 1964, Territoires français de l'Afrique noire: Paris, Annales, v. 1, p. 139-149.
- Shepard, F. P., and Dill, R. F., 1966, Submarine canyons and other sea valleys: Chicago, Rand-McNally and Co., 381 p.
- Spengler, A. de, Castelain, J., Cauvin, J., and Leroy, M., 1966, Le bassin secondaire tertiaire du Sénégal, in Reyre, D., *Editor*, Sedimentary basins of the African Coasts: Assoc. African Geol. Survey, Paris, p. 80-94.
- Tourenq, J., 1964, Contribution à l'étude de quelques sables de la presqu'île du Cap-Vert (Sénégal): *Soc. Geol. France Bull.*, v. 6, p. 666-673.
- U.S. Naval Oceanographic Office, 1963, Oceanographic atlas of the North Atlantic Ocean: Washington, D.C., U.S. Naval Oceanographic Office Pub. 700, sec. IV, 227 p.
- U.S. Navy Hydrographic Office, 1943, Chart 2197, 5th edition, Washington, D.C.
- Varlet, F., 1958, Le régime de l'Atlantique près Abidjan: *Inst. Fr. Afrique Noire, Études Éburnéennes*, no. 7, p. 97-222.

Geology of De Soto Canyon

R. N. HARBISON

Atlantic Oceanographic Laboratories, ESSA, Miami, Florida 33130

De Soto canyon is a curious S-shaped submarine canyon approximately 100 km south-southwest of Pensacola, Florida. Seismic reflection profiling shows that an east-west partially buried shoreline, the influence of at least five salt domes, and erosional and depositional structures are responsible for the peculiar shape of the canyon. The northern bank of the east-west part of De Soto canyon is underlain by what is interpreted as an old shoreline. The north-south-trending part of the canyon is formed by an erosional slope on the east and a depositional slope on the west. Erosion of the east bank and the transgression of the west bank has shifted the canyon bottom to the east. The southern part of the canyon trends south-west because of a subsurface structure, possibly a salt ridge. There is a sediment dam across the southern end of De Soto canyon causing a small basin (43 meters deep) to the north.

INTRODUCTION

De Soto canyon is located approximately 100 km south-southeast of Pensacola, Florida (Figure 1). A bathymetric map of the area shows the unusual S shape (Figure 2).

A reconnaissance seismic-reflection-profile study was initiated in 1963 to determine whether De Soto canyon was structural or erosional in origin. This 1000-joule-arcsec study conducted aboard the U.S. Coast and Geodetic Survey ship *Hydrographer* showed shallow faulting, an apparent domal closure, and erosional and depositional features.

In 1965 a more detailed seismic reflection study (Figure 1) was made in the area from the *Hydrographer* using the earlier reconnaissance results as a guide for track line locations. A 3000-joule arcsec supplied a broad-band energy spectrum whose characteristic output was concentrated between 150 and 300 hertz. The hydrophone array was 3.7 meters long and consisted of ten variable inductance phones. Reflected returns were not filtered. Loran A was used for navigation control. The profiles from the 1965 survey will be illustrated in this paper because they are better and because the track lines were more strategically oriented than during the 1963 reconnaissance study.

GENERAL MORPHOLOGY OF DE SOTO CANYON

De Soto canyon (Figure 1) is situated in the northeast 'corner' of the Gulf of Mexico, where the regional trend of peninsular Florida joins the regional east-west trend of the Gulf Coast.

Unlike most submarine canyons, De Soto canyon has a comparatively gentle gradient, is S-shaped, and has a closed bathymetric low in the southern part (Figure 2).

Northern De Soto canyon trends in an east-west direction for 11 km and has approximately 250 meters of relief. The slope of the north and south wall of this portion is about 9° .

The north-south-trending part of De Soto canyon is 17 km long and has a gradient of only $0^\circ 15'$. The eastern slope is $2\frac{1}{2}^\circ$, and the western slope is only 1° .

Southern De Soto canyon trends southwest-erly and contains a basin 13 km long and 43 meters in relief. The east and west slopes of this basin are approximately 8° .

Strata are labeled groups A, B, C, D, and E on the seismic reflection profiles for identification. Strata of groups A, B, and C are separated by unconformities visible on the profiles in several locations within the study area.

DOMES

Five domes were determined from at least two intersecting cross lines. Six other possible domes were observed by single crossings in the De Soto canyon area. Two domal features were also profiled by a reconnaissance line west of the canyon (Figure 1). Anomalous dip, apparent closure, shallow faulting, and collapse structures, which are commonly associated with salt domes in the Gulf Coast, are also associated with the domes and possible domes in the De Soto canyon area.

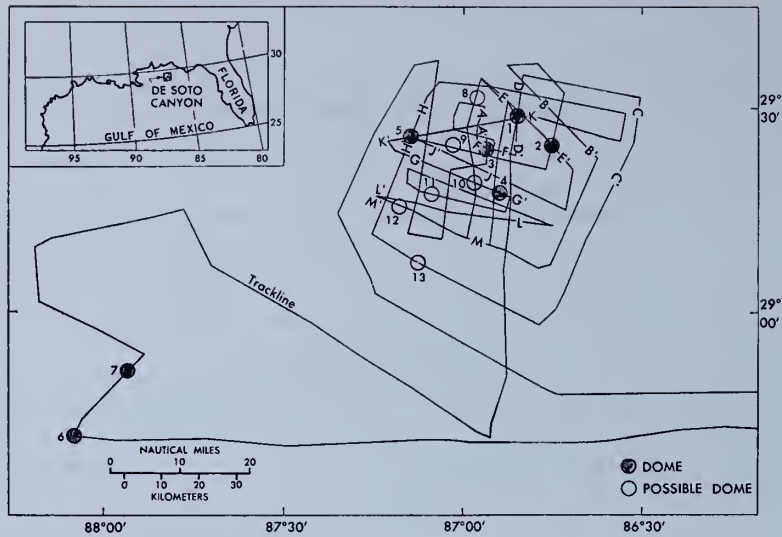


Fig. 1. Track line map showing location of domes, possible domes, and profiles AA' through MM'.

An unusual sea-floor high is present above dome 1 (profile DD', Figures 3 and 4). Although this high resembles a side echo on two seismic reflection profiles, fathograms taken simultaneously with the seismic profiles show that 75% of the sea-floor return is blocked out beneath this high, indicating that it is a true topographic

feature. A 'cartwheel' of four seismic reflection profiles shows that the feature is at least 400 meters wide and 60 meters high.

Group E strata may outcrop as a gentle knoll over dome 1 (Figure 4). A fathogram taken simultaneously with this seismic profile shows a side echo at 0.05 second below the sea floor

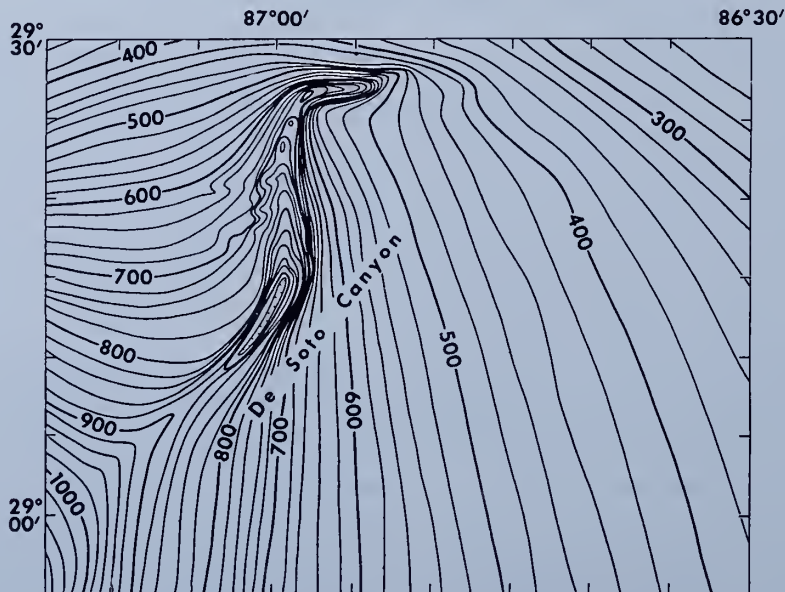


Fig. 2. Bathymetric map of De Soto canyon contoured in meters (made from original chart by Jordan [1951]).

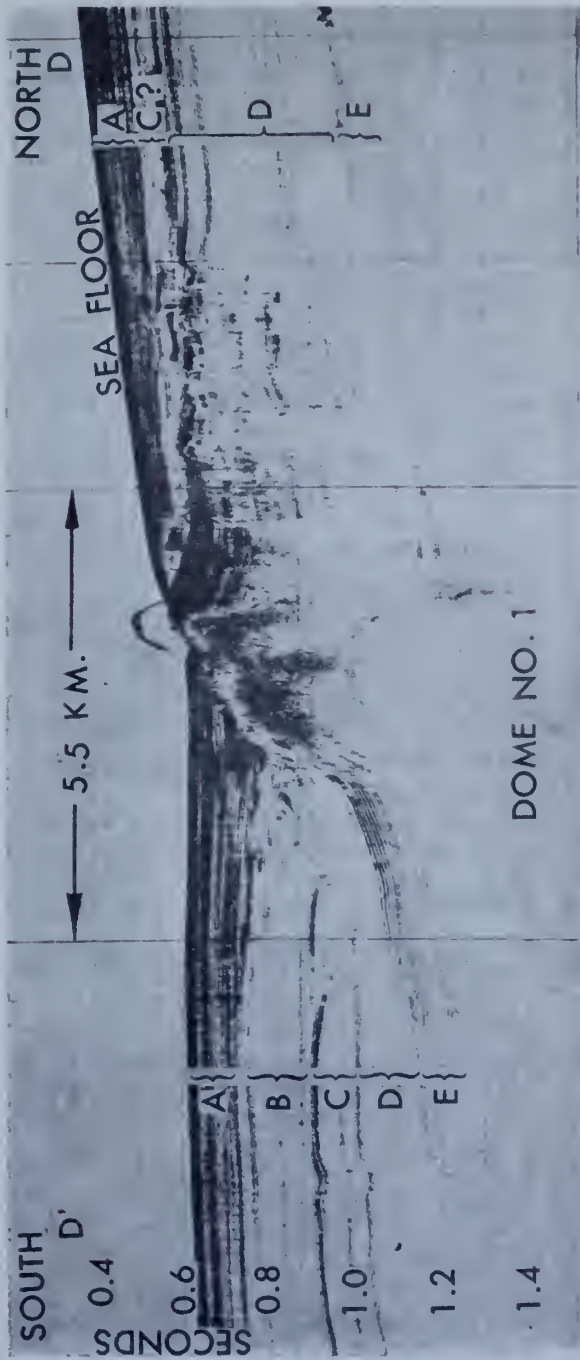


Fig. 3.

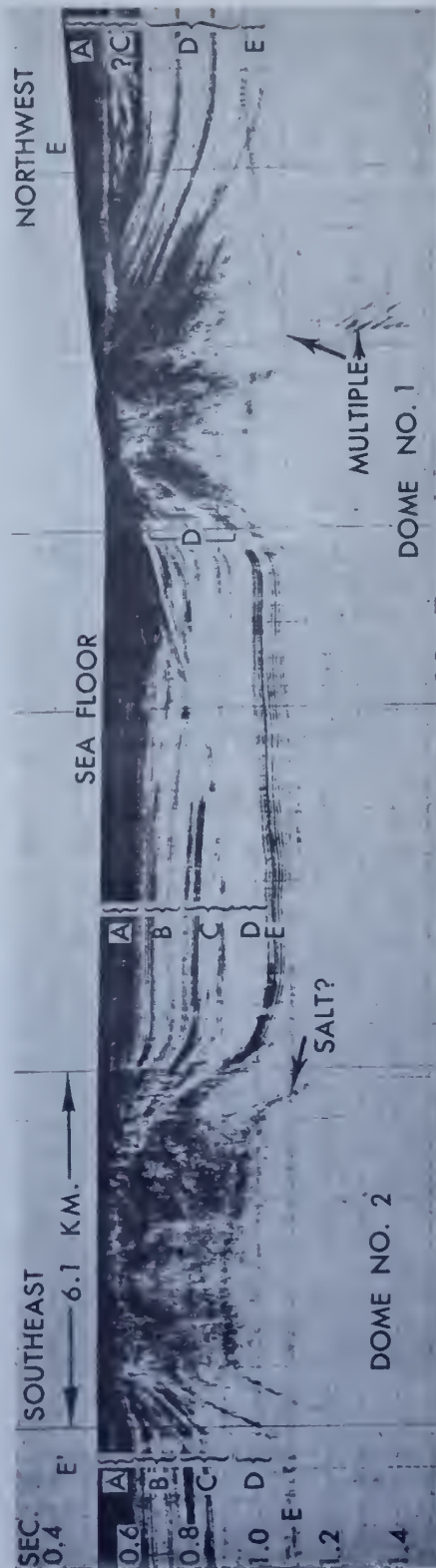


Fig. 4.

Fig. 3. North-south profile DD' illustrates local faulting within the plane of the profile north of dome 1. The topographic high above dome 1 is possibly an outcrop of strata of group D or E.

Fig. 4. Profile EE', a northwest-southeast profile through domes 1 and 2 showing the buried east-west erosional slope between the domes.

just northwest of the knoll. Computations show that this side echo probably comes from a topographic high about 250 meters away, at right angles to profile EE'. The author believes this topographic high may be a cuesta of group E or possibly group D strata which outcrops on the northwest quarter of dome 1 and is probably part of the topographic high previously discussed. Group D strata were possibly truncated by the erosion cycle that occurred after group B strata were deposited.

Domes 2 (Figure 4), 3 (Figure 5), 4 (Figure 6), and 7 (Figure 10) have collapse structures over their centers with associated faulting that extends up to the sea floor. The faults through strata of groups E, D, C, B, and A suggest that growth and collapse of the domes are continuing phenomena.

Domal features in the De Soto canyon area are interpreted as salt domes because of their size, shape, fault characteristics, and the collapse structures over their centers. Their frequency of occurrence and their geographical proximity to known salt domes and salt trends to the west and northwest further support this deduction. *Antoine* [1965] and *Antoine et al.* [1967] reported a salt dome in the De Soto canyon area. *Marsh* [1967] presented geophysical and geological evidence for the presence of deep-lying salt deposits extending from the Mississippi interior salt dome basin through southern Alabama, the Florida panhandle, and into De Soto canyon.

Magnetic studies by *Heirtzler et al.* [1966] combined with refraction studies by *Antoine and Harding* [1965] further suggest that a northeast-southwest-trending sediment trough extends from Apalachicola through the general area of De Soto canyon. This trough extending into the Gulf of Mexico would favor the accumulation of salt.

Collapse features over the domes and possible domes in the De Soto canyon area are common over known salt structures in the Gulf Coast and may be due to removal of salt by solution or localized isostatic adjustment.

EAST-WEST EROSIONAL SLOPE

One of the most interesting features in the De Soto canyon area is a partially buried east-west-trending erosional slope, which is best illustrated in northern De Soto canyon. This

unconformable surface has a southerly dip varying from 9° to less than 2°. The erosional slope is interpreted to extend 74 km along 29°27'N and 29°28'N across the area of the track line coverage (Figure 1) and possibly further.

A north-south profile (profile AA', Figure 8) shows a 9° erosional slope in group D strata that is unconformably covered by group A strata. Group E strata appear to die out south of the slope, possibly because of erosion or local faulting associated with dome 3. This crossing is on the northern slope of the canyon but shows part of the slumped sediments within the canyon as well.

More than half of group D strata have been removed on the east-west slope between domes 1 and 2 (profile EE', Figure 4). Groups A, B, and C have been unconformably deposited with a slight north dip against the erosional slope in group D strata. No faulting is associated with the slope, as indicated by continuous group E strata.

Profile BB' (Figure 9) and profile CC' (Figure 10) show group C strata built out on what may be the east-west slope eroded into group D strata. Group D reflectors show no changes of dip or thickness as they disappear beneath sloping group C strata. The author believes that the erosional slope in group D strata is present in profiles BB' and CC' because of its presence on all the other profiles to the west, and group D strata show no signs of pinching out. Older group C strata are built out as foreset beds over the slope, suggesting a shallow-water environment. Younger group C strata thicken to the south, where they provide two to three strong reflectors on the east side of the canyon.

Fig. 5. (*Opposite*) Profile FF' is an approximately east-west profile through dome 3 showing collapse of strata above the dome.

Fig. 6. (*Opposite*) East-west profile GG' crosses the north-south-trending part of De Soto canyon. Weak reflectors are inked in on possible dome 10 and the western slope of dome 4. The eastern canyon slope is formed by erosion, and the western slope is made up of eastward prograding strata.

Fig. 7. (*Opposite*) Profile HH' is an approximately north-south profile through dome 5. A graben extends above the dome into the vicinity of the sea floor. The east-west slope eroded into group D strata is present just north of dome 5.

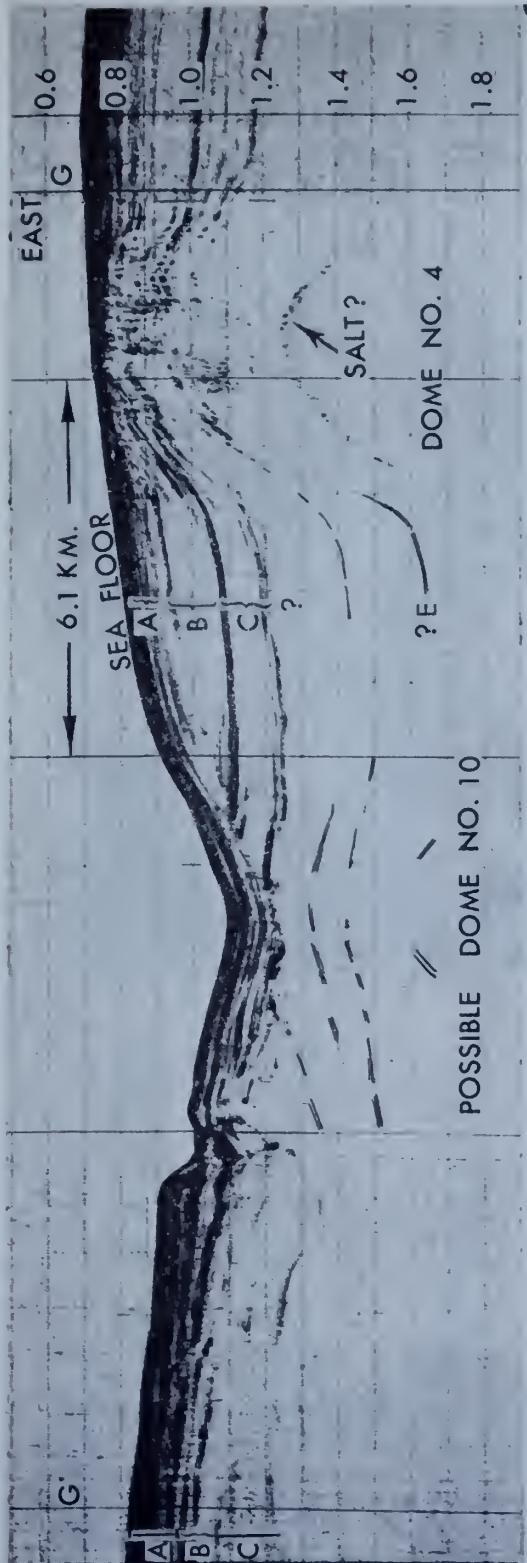


Fig. 6.

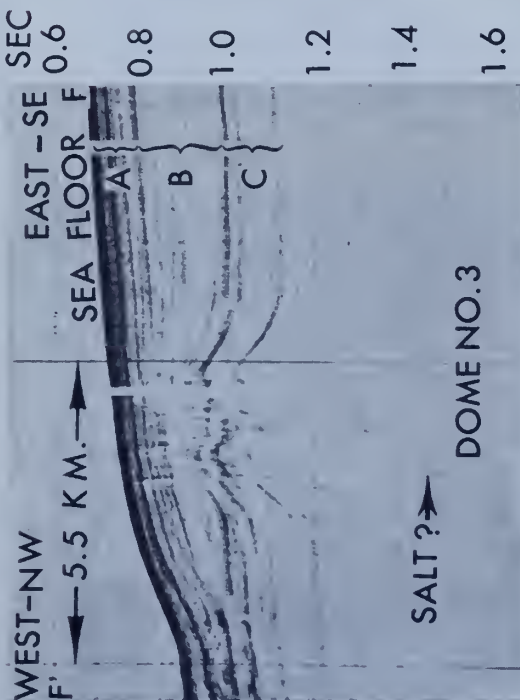


Fig. 5.

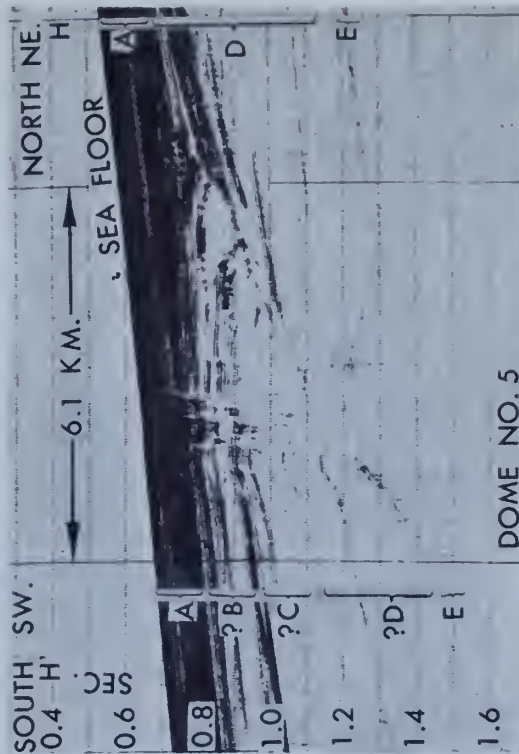


Fig. 7.

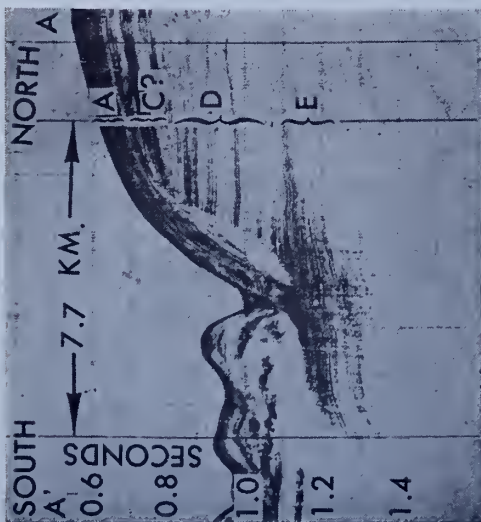


Fig. 8.

Fig. 8. Profile AA', a north-south profile through the east-west-trending area of northern De Soto canyon showing truncated group D strata.

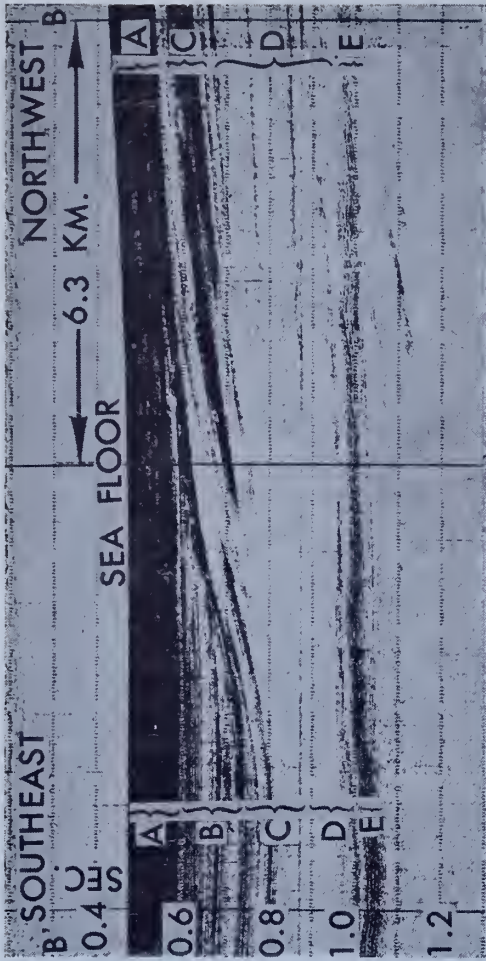


Fig. 9.

Fig. 9. Profile BB' is a northwest-southeast profile across a feature interpreted as an east-west shoreline.

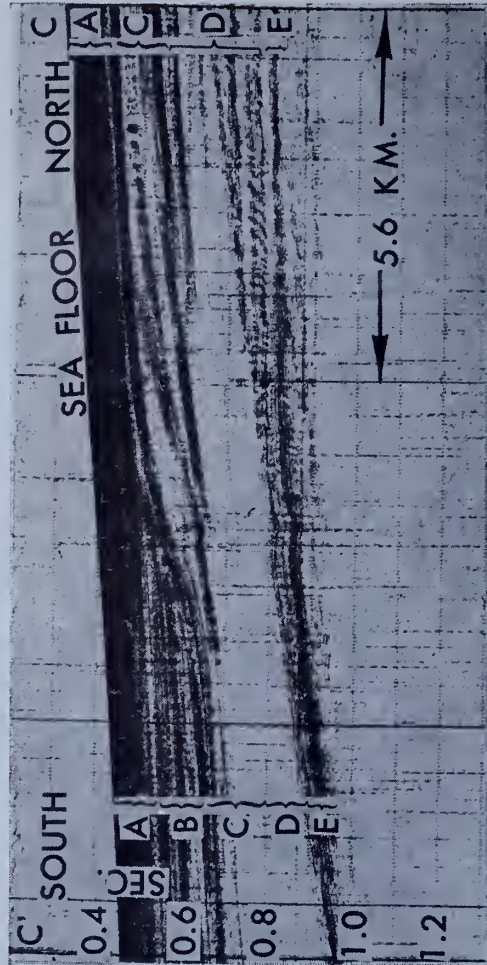


Fig. 10.

Fig. 10. Profile CC' is a north-south profile across the east-west shoreline on the eastern limits of track line coverage. Younger group C strata appear to have been built out as foreset beds, suggesting a near-shore environment.

In profiles BB' and CC', group B strata dip more gently and are thinner and more evenly stratified than the sloping group C strata against which they terminate unconformably. The distribution of group B strata suggests a slow deposition in deeper water. Group B thickens to the south and becomes acoustically transparent strata with no strong individual reflectors. Erosion apparently occurred after deposition of group B strata, removing all group B strata and much of the group C strata north of the slope. The erosion and reworking of group C strata north of dome 1 prevent positive correlation of these strata along the east-west profile north of 29°30'N. Group E strata are continuous beneath the eroded slope, indicating that the slope is not a fault scarp.

Profile HH' (Figure 7) shows the slope eroded into group D strata extending from the 0.8-second time mark in the north southward down to 1.0 second in the south near the center of dome 5. Strata interpreted as groups B and C reverse their dip and terminate dipping northward against eroded slope. Some slumping of these north-dipping strata may have occurred along their contact with the erosional slope, perhaps owing to sediment collapse over dome 5.

The cycle of erosion that occurred after deposition of group B strata formed an east-west-trending channel from 2000 to 3000 meters wide and from 180 to 300 meters deep. The channel extended 24 km west of the south flank of dome 1. Re-exposed group D strata along the old erosional slope formed the channel's north slope, and newly eroded strata of groups B and C formed the south slope. The general south-trending De Soto canyon joined the channel approximately between dome 3 and possible dome 9. Deposition of group A sediments buried all topographic expression of the channel except the portion that forms the present-day east-west-trending northern De Soto Canyon.

NORTH-SOUTH DE SOTO CANYON

Major faulting is not apparent parallel with the north-south axis of De Soto canyon. Profile KK' (Figure 12) trends approximately east-west between the southern flank of dome 1 and the southern flank of dome 5. Group E strata are unbroken, which indicates that there are no

north-south-trending faults through northern De Soto canyon.

Profile GG' (Figure 6) and profile JJ' (Figure 12) are two approximately east-west profiles. The erosion cycle that removed groups B and C strata from the east-west-trending erosional slope also removed these same strata from the north-south part of the canyon. Erosion continued to wear away the eastern slope of the canyon but ceased on the western slope as sediments from the north and west were built out in an eastwardly direction and buried the old western slope. This combination of erosion and deposition shifted the canyon eastward more rapidly in the south than in the north, therefore changing its channel from its northeast-southwest trend to its present north-south trend. A thin layer of group A sediments was deposited on the eroded eastern slope of the canyon, which indicates that the eastward erosion has ceased in this part of the canyon. Apparent slumping of group A sediments on the western slope near the center of the canyon is continuous in the north-south canyon and causes irregularities and small closures that appear on the bathymetric chart (Figure 2).

Correlation of groups B and C across the canyon in this general north-south portion is tenuous. Strata of groups B and C were eroded and covered by younger strata near present canyon slopes. Correlation was made mainly by projecting the identifiable group C strata from the east side to the west side of the canyon. The younger sediments on the west slope, possibly from the Mississippi River, cause the loss of character of the reflectors below. South of 29°27'N only the upper limits of group A and group E can be traced continuously from the east to the west side of the canyon (Figure 11, Profile KK').

NORTHEAST-SOUTHWEST DE SOTO CANYON

The northeast-southwest part of De Soto canyon is approximately 13 km long and contains a bathymetric low with 43 meters of closure. Profile LL' (Figure 13) crosses the deepest part of the basin and illustrates that the northeast-southwest-trending canyon has been shifted about eastward of its original position. This eastward movement has been the result of erosion of the east slope and the prograding of sediments eastward along the western slope.

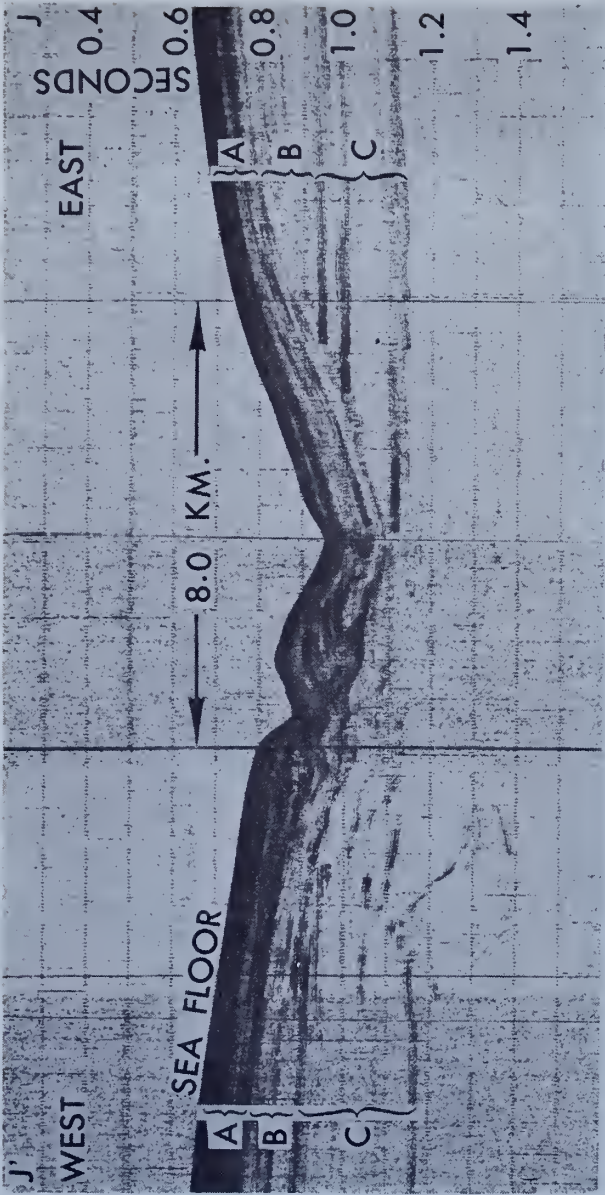


Fig. 12. Profile JJ' is an east-west profile through north-south De Soto canyon. Apparent slumping occurs just west of the center of the canyon and is a continuous feature throughout the north-south part of the canyon.

Fig. 11. Continuous group E strata indicate that there is no north-south fault through northern De Soto canyon along approximately east-west-trending profile KK'.



Fig. 11.

Fig. 12.

The prograding sediments partially covered the original eastern slope. Although the geological history is similar to the north-south portion of De Soto canyon, group A strata do not cover the bottom half of the present erosional eastern slope of the canyon. This lack of group A sediments is recorded along a section at least 7.5 km long, suggesting that the eastern slope of the canyon is presently being eroded.

Prograding sediments from the north and west have built the western slope of De Soto canyon completely out over the eroded east slope and have formed a sediment dam 96 meters high across the southwest end of the canyon (profile MM', Figure 14). Possible dome 12 is a gentle, closed subsurface high on the western side of the canyon, which may have contributed to the building of the 'dam' by structurally raising the strata during their deposition.

The northeast-southwest orientation of the closed low that forms southern De Soto canyon is apparently due to a gentle subsurface high or ridge extending southwestward from dome 4 to possible dome 13 (Figure 1). This gentle high may be caused by a salt ridge that has pushed up sediments above it. The subsurface high can be seen under the buried east slope of the canyon in Figure 14.

Water circulation studies at various depths have been made in the De Soto canyon area [Gaul, 1966]. One station, located at 29°10'N and 86°52.5'W, approximately 17 km southeast of the closed low, appeared to be the center of a current eddy. This eddy had an apparent radius of 100 km, and its direction varied from cyclonic to anticyclonic. At other times it did not exist. The flow measured from less than 0.01 to 0.3 m/sec, the latter value being in an easterly direction. Indications from these surveys are that quasi-steady currents, surface and subsurface, tend to align themselves with the bathymetric contours. The northeast-southwest-trending part of De Soto canyon is located where projections of regional bathymetric contours are perpendicular, possibly creating anomalous currents capable of erosion. The tectonic activity of domes in the area has influenced the morphology of the sea floor and, therefore, have probably influenced the direction of the currents.

SUMMARY

De Soto canyon is a topographic feature shaped by erosion, deposition, and structural highs associated with at least five domes. These domes are interpreted as salt domes which were probably tectonically active during several cycles of erosion and deposition. Seismic reflection data indicate that the canyon has not been formed as the direct result of major faulting.

An east-west slope is interpreted as having been eroded into group D strata by a northward transgressing sea along 29°27'N and 29°28'N within the limits of track line coverage. The transgressing sea apparently removed at least one-half of group D strata south of the slope. As sea level rose, group C strata were draped over the eroded slope first as foreset type beds and later as continuous beds that thickened to the south. Following this, a possibly higher sea deposited relatively flat, evenly bedded strata (group B) over the draped group C strata and completely buried the topographic expression of the erosional slope.

A period of erosion followed the deposition of group B strata, possibly caused by a drop in sea level or the presence of water currents capable of erosion. Most of group C strata and all of group B strata were removed north of the erosional slope in group D strata. An east-west channel was formed from south of dome 1 westward to within 14 km of dome 5 by the removal of strata of groups B and C along the east-west erosional slope in group D strata. The group D strata were re-exposed and formed the north slope of the east-west channel, while groups B and C strata formed the south slope. Another channel was cut through strata of groups B and C from the re-exposed east-west slope between dome 3 and possible dome 9 southwestwardly to the southern limit of the study area. De Soto canyon had an approximate T shape instead of its present S shape. Erosion of strata of groups B and C continued on the east slope of the general northeast-southwest-trending canyon during the same time period that the west slope was formed by eastward-prograding sediments. This process of eastward erosion of the east bank and the eastward prograding of sediments from the west bank shifted the channel eastward. The eastward migration of the channel proceeded faster in

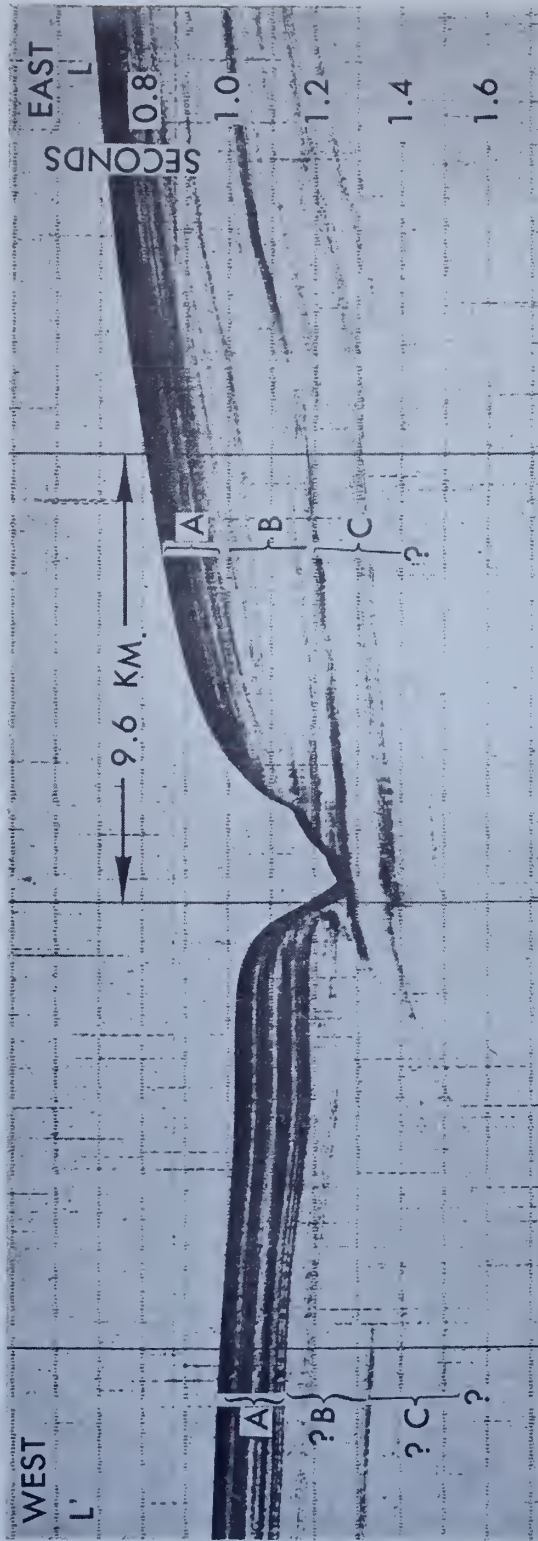


Fig. 13. East-west profile LL' crosses the closed bathymetric low in southern De Soto canyon. The lower half of the eastern slope is not covered by group A sediments, suggesting that this closed bathymetric low may be the only area in the canyon now being eroded.

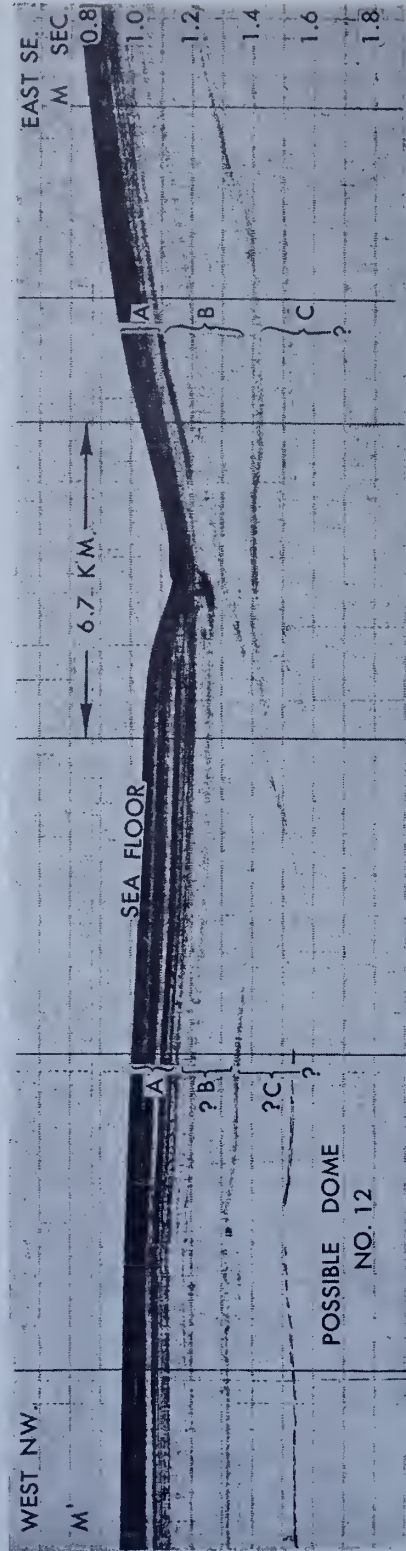


Fig. 14. Approximately east-west-trending profile MM' crosses the area just south of the closed low in southern De Soto canyon. Eastward prograding sediments have completely buried the eroded eastern slope, causing the bathymetric closure to the north. Weak reflector over possible dome 12 is inked in.

the south than in the north, causing the channel to change from its previous northeast-southwest trend to its present general north-south orientation, except in southern De Soto canyon.

Southern De Soto canyon trends northeast-southwest because of the influence of a gentle subsurface structural high extending from dome 4 southwestward to possible dome 13. This part of De Soto canyon contains a closed low with 43 meters of relief. The northern limits of the closed low were formed by possible dome 10 and the southern end by a wedge of sediments. These sediments were possibly transported from the west and north and built out eastwardly, completely covering the erosional eastern slope of the canyon. The eastern slope within the closed low is the only area in De Soto canyon that is presently being eroded. Group A strata have been deposited on all the other eroded surfaces of groups A and B. The old east-west erosional channel was buried by group A strata, except for the portion that forms the present east-west De Soto canyon.

Acknowledgments. The cooperation of Captain Reed and the officers and men of the USC&GSS *Hydrographer* is gratefully acknowledged. Helpful

suggestions by R. J. Malloy and George Peter of ESSA and Dr. E. Uchupi of Woods Hole Oceanographic Institution are appreciated.

REFERENCES

- Antoine, J. W., Structural features under continental shelf of Florida panhandle revealed by seismic reflection measurements (abstract), *Geophys. J.*, 30(6), 1228, 1965.
- Antoine, J. W., W. Bryant, and B. Jones, Structural features of continental shelf, slope, and scarp, northeastern Gulf of Mexico, *Bull. Am. Assoc. Petrol. Geologists*, 51(2), 257-262, 1967.
- Antoine, J. W., and J. L. Harding, Structure beneath continental shelf, northeastern Gulf of Mexico, *Bull. Am. Assoc. Petrol. Geologists*, 49, 157-171, 1965.
- Gaul, R. D., Circulation over the continental margin of the northeast Gulf of Mexico, *Texas A&M Res. Foundation, A&M Project 286-D*, 66-18T, 1966.
- Heirtzler, J. R., L. H. Burckle, and G. Peter, Magnetic anomalies in the Gulf of Mexico, *J. Geophys. Res.*, 71(2), 519-525, 1966.
- Jordan, G. F., Continental slope off Apalachicola, Florida, *Bull. Am. Assoc. Petrol. Geologists*, 35(9), 1978-1993, 1951.
- Marsh, O. T., Evidence for deep salt deposits in western Florida panhandle, *Bull. Am. Assoc. Petrol. Geologists*, 51(2), 212-222, 1967.

(Received July 31, 1967;
revised April 8, 1968.)

ESSA RESEARCH LABORATORIES
Atlantic Oceanographic Laboratories
Miami, Florida
January 1968

A Time Series From the Beach Environment



Technical Memorandum ERLTM-AOL 1

U.S. DEPARTMENT OF COMMERCE / ENVIRONMENTAL SCIENCE SERVICES ADMINISTRATION

U.S. DEPARTMENT OF COMMERCE
ENVIRONMENTAL SCIENCE SERVICES ADMINISTRATION
RESEARCH LABORATORIES

ESSA Research Laboratories Technical Memorandum -AOL 1

A TIME SERIES FROM THE BEACH ENVIRONMENT

W. Harrison
with
E. W. Rayfield, J. D. Boon III,
G. Reynolds, J. B. Grant, and D. Tyler
Land and Sea Interaction Laboratory
(LASIL)
Norfolk, Virginia

LASIL Contribution No. 12

ATLANTIC OCEANOGRAPHIC LABORATORIES
TECHNICAL MEMORANDUM NO. 1

MIAMI, FLORIDA
JANUARY 1968



FOREWORD

The time series of observations contained in this report was obtained as part of the Land and Sea Interaction Laboratory's continuing program of documenting interaction in the beach-ocean-atmosphere system. The Laboratory seeks on the one hand to develop valid predictor equations for use in beach forecast systems and on the other to understand the mechanisms underlying various "process-response" relationships in the beach environment. Comprehensive time series from various natural beaches offer means to these ends. Those published here also will allow other researchers to test hypotheses or to experiment with analytical procedures without going through the expensive and somewhat arduous task of obtaining the data.

This report is the first of a continuing series of publications concerning LASIL's documentation of interactions in various nearshore environments.

ABSTRACT

A continuous, 26-day series of measurements of the following variables was made at Virginia Beach, Virginia, during August and September, 1966: depth of the water table in the foreshore, altitude of the foreshore surface (at 16 stations), tidal elevation, angle between breaker crest and shoreline, height of breaking waves, period of breaking waves, rainfall, radiant energy balance over water, water temperature, air temperature, wind speed, wind direction, velocity of longshore current, position of the top of the uprush, position of the inshore margin of the breaker zone, and the height and period of significant waves 240 m offshore. Water and sand samples were also collected. Additional measurements derived from the samples or field data consisted of: significant breaker height, foreshore slope, quantity of foreshore sand eroded or deposited in one tidal cycle, mean time for sand samples to fall 1.0 m in fresh water, nominal grain diameter and sorting coefficient of foreshore samples, length of unsaturated foreshore surface from outcrop of water table to swash reach, length of saturated foreshore surface from water table outcrop to trough in front of breaking wave, elevation of water table outcrop above trough level at breaking, rate of rise or fall of the tidal plane, density of the sea water, and relative density of midforeshore sand grains.

Most of the variables were measured every 4 hr; a few were measured every 6.25 hr, at times of high or low water, and three variables were measured continuously. Plots of the variables were prepared, smooth curves drawn, and the curves digitized using 1-hr interval. A listing of the basic time series is presented, together with details of measurement techniques, analytical procedures, and operational definitions for each variable.

A second listing of the data is included, consisting of dimensionless variables derived from the basic time series and used for the study of changes in the quantity of sand on the foreshore over a single tidal cycle, where the change in foreshore volume is expressed as a function of nine independent variables distributed over nine possible lag periods. Nine precision charts of the nearshore bottom topography, indicating the character of the bottom beyond the breakers during the study period are also presented.

TABLE OF CONTENTS

	<u>Page</u>
1. INTRODUCTION	1
2. ENVIRONMENTAL CHARACTERISTICS	2
3. MEASUREMENT SCHEDULE	4
4. VARIABLES MEASURED	5
4.1 Continuous Measurements	5
4.1.1 Elevation of Tidal Plane (E_t)	5
4.1.2 Rainfall (r)	5
4.1.3 Net Radiation (R_n)	5
4.2 Measurements Made Every Four Hours	5
4.2.1 Position of Inshore Margin of Breaker Zone (B)	5
4.2.2 Position of Top of Swash (S)	5
4.2.3 Mean Height of Breaking Waves (\bar{H}_b)	5
4.2.4 Significant Breaker Height (H_{bs})	9
4.2.5 Mean Period of Breaking Waves (\bar{T}_b)	9
4.2.6 Mean Acute Angle Between the Shoreline and the Crests of Breaking Waves ($\bar{\alpha}_b$)	9
4.2.7 Mean Crest Length of Breaking Waves (\bar{l}_b)	9
4.2.8 Mean Trough to Bottom Distance in Front of a Breaking Wave (z)	9
4.2.9 Mean Longshore-Current Velocity (\bar{V})	12
4.2.10 Significant Wave Height (H_s)	12
4.2.11 Significant Wave Period (T_s)	12
4.2.12 Elevation of Beach Surface at Reference Station (E_b)	12
4.2.13 Elevation of Groundwater Table (E_w)	12
4.2.14 Density of Liquid (Sea Water) (ρ_g)	15
4.2.15 Temperature of the Air (t_a)	15
4.2.16 Temperature of the Water (t_w)	15
4.2.17 Mean Wind Direction (\bar{W}_d)	15
4.2.18 Mean Wind Speed (\bar{W}_s)	16

TABLE OF CONTENTS - (continued)

	<u>Page</u>
4.3 Measurements Made at Time of Low and High Water	16
4.3.1 Mean Nominal Grain Diameter of Sand Samples of the Mid-Foreshore (\bar{D})	16
4.3.2 Density of Solids (Sand Grains) on the Mid-Foreshore (ρ_s)	16
4.3.3 Standard Fall Velocity (\bar{v})	16
4.4 Measurements Derived From the Field Data	17
4.4.1 Mean Foreshore Slope (\bar{m})	17
4.4.2 Distance Between Outcrop of Water Table on Foreshore and Inshore Margin of Breakers (d)	17
4.4.3 Hydraulic Head (h)	17
4.4.4 Length of Unsaturated Beach Surface Between Outcrop of Water Table on Foreshore and Top of Swash (u)	17
4.4.5 Quantity of Sand Eroded From or Deposited Upon the Foreshore in One Tidal Cycle (Q_f)	20
4.4.6 Rate of Rise or Fall of the Still-Water Level ($\pm\eta$)	20
5. DATA PROCESSING	20
6. ACKNOWLEDGMENTS	21
7. REFERENCES	22
APPENDIX A	A-1
APPENDIX B	B-1
APPENDIX C	C-1

A TIME SERIES FROM THE BEACH ENVIRONMENT

by

W. Harrison

with

E.W. Rayfield, J.D. Boon, III, G. Reynolds,
J.B. Grant, and D. Tyler

1. INTRODUCTION

A time series is a set of observations taken at specified times, usually at equal intervals. The purpose of this study was to obtain a comprehensive time series from an ocean beach for use in the investigation of a number of "process-response" relationships in the beach-ocean-atmosphere system. Among the specific relationships to be investigated were the following:

- 1) the response of the foreshore to waves, tides, currents, and the movement of groundwater through the foreshore face,
- 2) the response of the groundwater table to waves and tides,
- 3) the dependency of the velocity of the longshore current on changes in foreshore slope and on wave characteristics, and
- 4) the response of nearshore water temperature to the local balance of radiant energy and to local winds.

The set of observations actually obtained permits analysis of many more relationships than those mentioned above. All the measurements are published here. Their ready availability will provide raw material for those involved with time-series and multivariate analysis of natural phenomena, as well as supply new data to those concerned with specific mechanisms in the beach-ocean-atmosphere system.

A 26-day time series from an oceanic beach is, of course, in itself but a sample of a nearly infinite series into which all possible combinations of all the variables measured could enter. So also is the environment of Virginia Beach but a sample of a very large population of possible beach environments. Analyses of the measurements presented in this report will be limited in their application to beaches similar, in composition and geometry, to the one investigated, and to beaches which undergo forces of similar frequency, duration, and magnitude.

2. ENVIRONMENTAL CHARACTERISTICS

The data of this time series were collected at Virginia Beach, Virginia, from two locations south of Cape Henry (fig. 1A). Variables were measured at a fishing pier at 15th Street (fig. 1C), and at a beach (fig. 1C) about 2800 m south of the pier. Between the pier and the beach is a relatively small controlled inlet. Its influence on the adjacent beaches is confined to a zone only 150 to 300 m to either side of its mouth, however, as shown by Harrison, Krumbein, and Wilson (1964).

Surveys (U.S. Congress, 1953, p. 13) by the U.S. Army Corps of Engineers show that beach slopes in the foreshore area range from about 1:17 to 1:28, while slopes between roughly the 3- and 6-m contours range between 1:50 and 1:60. An earlier study of profile modifications at the beach has been presented by Harrison and Wagner (1964), along with several maps of the nearshore bottom that show bar-trough rhythms.

The nature of the nearshore bottom topography was documented during the present study by use of the Sears Sea Sled (Kolessar and Reynolds, 1966, p. 47) and precision leveling techniques. Nine bathymetric maps (plates A - I, following the "References") were constructed from the sled data. The contours are accurate to about ±0.1 ft (0.03 m).

Physical and dynamic properties of 219 sand samples from the area were studied by Harrison and Morales-Alamo (1964), and the averages of several properties for various dynamic zones of the beach are summarized in table 1.

Table 1. - Physical and Dynamic Properties of Foreshore Sands

Zone	Mean grain size in mm		Sorting Coefficient $S_o = \frac{P80-P20}{P50}$	Reynolds Number†
	Nominal dia.	dia.*		
Shoaling-wave	0.25	0.22	0.70	4.8
Breaking-wave	0.30	0.27	0.70	8.1
Swash	0.28	0.25	0.55	6.2
Swash-berm	0.37	0.33	0.54	12.0

*Converted from nominal diameter (Inter-Agency Comm. Water Res., 1957, fig. 5).

†Based on fall velocity under average sea-water conditions and nominal diameter.

Sand samples with values for mean grain size approximating the above average values exhibit about 10 percent (by number) of heavy minerals and 2 percent or less of rock or shell fragments. Thus, the beach is composed largely of medium to fine quartz sand. Small samples of the average sized sand of the beach exhibit relatively low Reynolds numbers under average temperature and salinity conditions of the sea water.

Tides at Virginia Beach are of the semidiurnal (equal) type and have a mean range of 0.9 m with a spring range of 1.1 m. Tidal currents in the study area are dominated by the ebb and flood currents through the entrance to Chesapeake Bay. They are generally reversing in nature and parallel to the shore. According to Harrison, Brehmer, and Stone (1964, fig. 4), peak tidal-current velocities 915 m from shore and about 1 m above the bottom do exceed 0.25 m/s. Peak velocities, measured 1 m above the bottom at the end of the 15th Street pier, approximate 0.21 m/s.

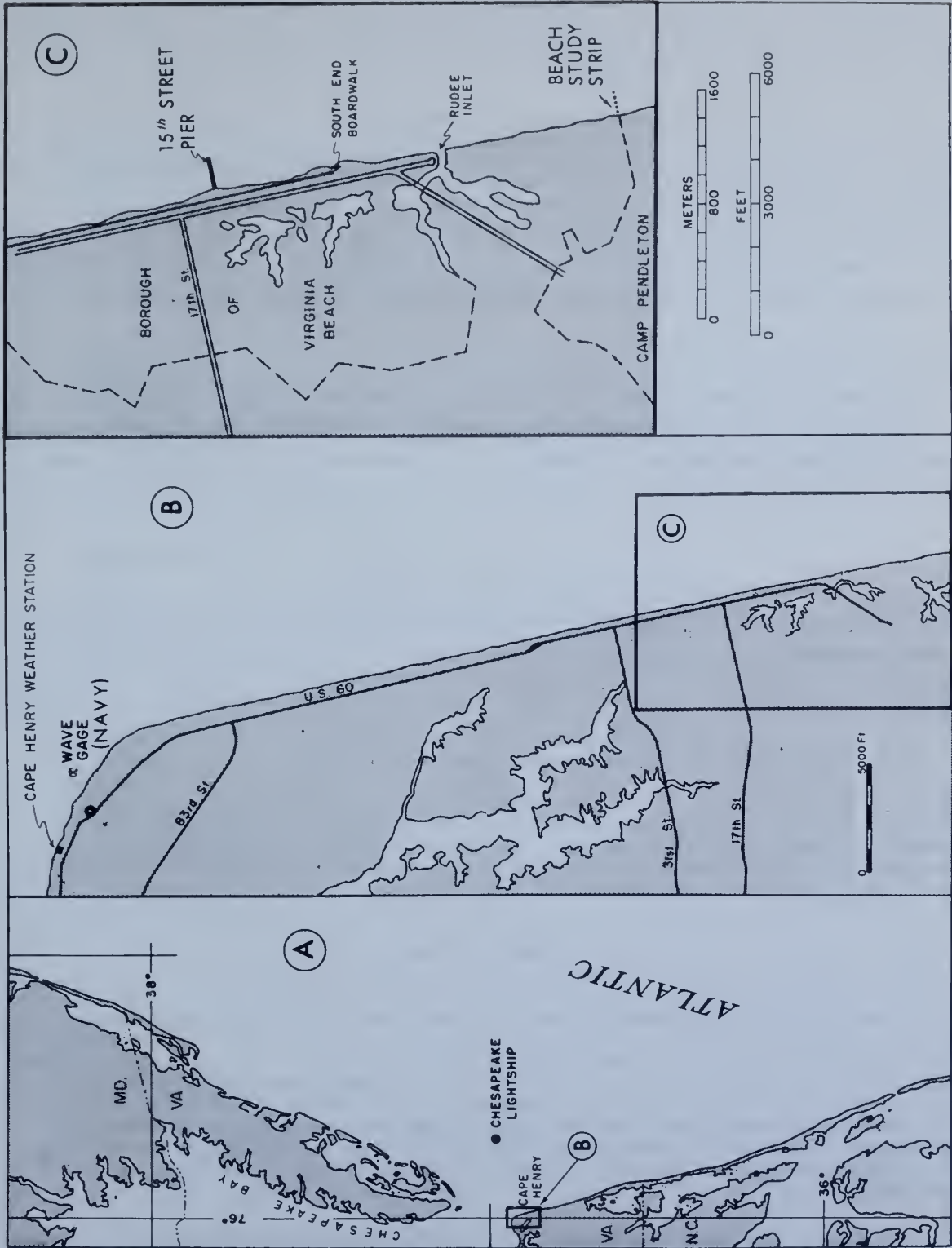


Fig. 1. Maps showing general area of investigation, pier station, and beach study strip.

Wind data (U.S. Congress, 1953, plate 5) from the Weather Bureau's Cape Henry station (fig. 1B) for a 16-yr period show that, whereas prevailing winds are from the southern quadrants, velocities and total wind movements are greater from the northern quadrants. Northeast winds tend to be most common in September.

The wave climate for the study area may be estimated from an analysis (Harrison and Wilson, 1964, app. G) of 4 yr of wave records from a stepped-resistance wave gage (fig. 1B) maintained by the U.S. Navy in 6.2 m of water off Cape Henry, and from 5 yr of wave observations at Chesapeake Lightship (fig. 1A), in 8.2 m of water. The summary data of table 2 give an indication of the approximate directions from which the waves that strike Virginia Beach come. The mean heights and periods of these waves are relatively low.

Table 2. - Summary of Offshore Wave Data for Virginia Beach

Significant wave analysis				Visual swell observation	
Wave period		Wave height		Direction from which swells come	
Mean (s)	1st Mode (s)	Mean (m)	1st Mode (m)	Direction	Percent of total swells
5.3	4.0	0.5	0.6	NE	30.0
				E	20.0
				SE	18.0

A breakdown of the 15 most frequent associations of wave period, height, and angle of approach at the Chesapeake Lightship is given in Harrison and Wilson (1964), together with details of the refraction of these wave fronts as they move into the study area.

Surf statistics at the Virginia Beach Life Boat Station, 2.4 km north of Rudee Inlet (fig. 1C), have been compiled by Helle (1958). Three years' records, for observations every 4 hr, reveal that the surf is 1.2 m or higher 10 percent of the year, 0.9 m or higher 50 percent of the year, and 0.6 m or higher 95 percent of the year. It tends to be highest in early fall when the angle-of-wave approach tends to be from the east (or ENE). The surf is also high in January, when it is largely out of the northeast. The average period of the surf tends to be greatest from April through July (around 6.0 s).

3. MEASUREMENT SCHEDULE

In documenting environmental processes and responses, it is desirable to obtain continuous measurements wherever possible and then digitize the continuous records at an interval determined by the type of analytical procedure to be used. From a practical standpoint, continuous measurements are usually impossible and measurements are made instead according to a schedule that will allow a sampling frequency that will sufficiently portray the significant variations in the phenomena under study. Most of the measurements of this study were made every 4 hr, at 0000, 0400, 0800, 1200, 1600, and 2000 EDT. A few were made every 6.25 hr, being keyed to times of high and low water. Only three variables were measured continuously.

A description of each variable measured follows, the variables being grouped according to whether they were measured continuously, every 4 hr, or at the time of high and low water. Six additional variables, derived from the measured ones, are also described.

4. VARIABLES MEASURED

Table 3 is a resumé of the variables described below.

4.1 Continuous Measurements

4.1.1 Elevation of tidal plane (E_t)

The position of the tidal plane was monitored because of its importance in modulating the expenditure of wave energy as the tidal plane translates up and down the foreshore. Hourly values of height of the tide were determined by the Coast and Geodetic Survey from continuous records obtained at a C&GS tide house (fig. 2) on the 15th Street pier. All values appearing in appendix A are relative to an arbitrary height datum of 1.0 m below MLW.

4.1.2 Rainfall (r)

This variable was monitored because of its expected effect on the elevation of the water table in the foreshore. A continuously recording, weighing rain gage was used to measure rainfall at the 15th Street pier (fig. 2). No measurable rainfall was recorded during the entire period of study. A trace of rainfall was recorded at the study strip (fig. 1C) on August 23 and 25, and September 7, 13, and 14. The September 13 precipitation was from the fringe of a thunderstorm and penetrated only a few centimeters into the dry beach sands.

4.1.3 Net radiation (R_n)

Variations in the radiant energy balance over water were studied because they are of first-order importance in determining variations in surface water temperature. A Thorntwaite net radiometer (Model 605) was mounted approximately 250 m offshore, perpendicular to one side of the fishing pier (fig. 2), and 5.0 m (± 1.2 m depending upon tides and waves) above the water surface. The radiometer protruded 3.1 m from the side of the pier and was free from effects of all structures. Continuous records of net radiation were obtained on a Rustrak recorder. The values of net radiation in appendix A are accurate to about ± 0.10 g cal/cm²/s.

4.2 Measurements Made Every Four Hours

4.2.1 Position of inshore margin of breaker zone (B)

The measurements for B and S (below) document the instantaneous boundaries of the swash zone as it translates up and down the sloping foreshore. The relative positioning of these boundaries on the foreshore and their relation to the outcrop of the water table are of considerable importance to erosion and deposition on the foreshore. The letter designation for the station (fig. 3) most often nearest to the inshore margin of the breakers ("B", fig. 4) at a given measuring time was noted on the field sheets. The error in this measurement ranged from about 0.6 to 2.2 m when the breaker zone was well defined. Some 10 percent of the time, breakers of various height were spread over so many stations that the position of the inshore margin was probably valid to only ± 1.8 m. Values for B are given in appendix A.

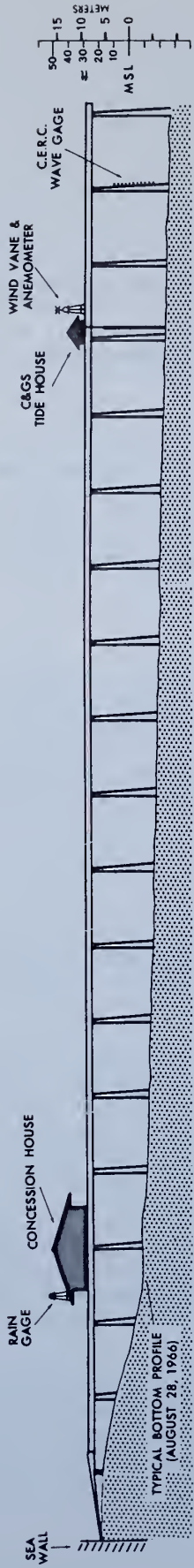
4.2.2 Position of top of swash (S)

The letter designation for the station (fig. 3) most often nearest to the top of the swash at a given measuring time was noted on the field sheets. The error in this measurement ("S", fig. 4) ranged from about 0.3 to 1.8 m, depending mainly upon the proximity of the top of the swash to the nearest reference station.

4.2.3 Mean height of breaking waves (\bar{H}_b)

The characteristics of the breaking waves were monitored, as described below, for studies of longshore current generation and erosion and deposition on the foreshore. Two methods were used for measuring the heights of breaking waves. The first, which was employed only a few days, utilized a battery-operated, stepped-resistance wave staff. The readout

PROFILE



PLAN

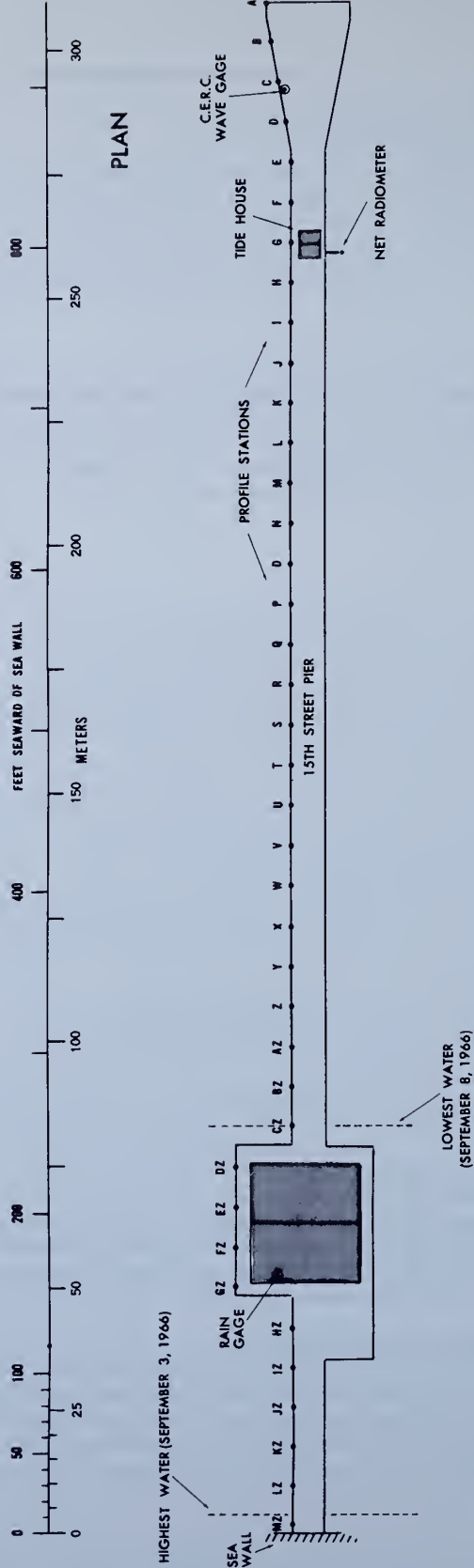


Fig. 2. Locations of instruments and profile stations at 15th Street fishing pier.

TABLE 3. - Variables Measured or Derived in Development of Time Series, their Dimensions, Schedule of Measurement, and Ranges in Value

Symbol	Dimensions	Description (refer to fig. 2, 3, or 4)	Measurement Schedule	Range in Values	Probable Error
B	0	Position of inshore margin of breaker zone (in terms of nearest reference station)	Every 4 hr and at times of high and low water	A to M	0.6 to 2.2 m (± 1.8 m, 10% of time)
d	L	Distance between outcrop of water table on foreshore and inshore margin of breakers	Derived (every 4 hr)	6.0 to 57.0 m	± 1.5 m
\bar{D}	L	Mean nominal grain diameter of sand samples taken at mid-foreshore	Every 6.25 hr (high and low water)	0.187 to 0.411 mm	± 0.02 mm
E_b	L	Elevation of beach surface at a reference station	Every 4 hr and at high and low water	0.47(K) to 2.76(M) m	± 2.0 mm, above water; ± 10 mm below
E_t	L	Elevation of tidal plane at tide gage	Continuous	1.036 to 2.560 m	± 0.15 m
E_w	L	Elevation of ground water table at a well point	Every 4 hr and at high and low water	1.01(X) to 1.14(Y) m	± 0.002 m
h	L	Vertical distance between horizontal plane passing through water table outcrop and horizontal plane through bottom of trough in front of breaking wave (fig. 4)	Derived (every 4 hr)	-0.20 to +1.60 m	± 0.04 m
\bar{H}_b	L	Mean height of breaking waves (fig. 4)	Every 4 hr	0.15 to 0.89 m	± 6.0 cm, low waves; ± 12.0 cm, high
H_{bs}	L	Height of significant breaking waves	Derived from H_b (every 4 hr)	0.20 to 1.20 m	± 6.0 cm, low waves; ± 12.0 cm, high
H_s	L	Significant wave height, 900 ft offshore	Every 4 hr	0.18 to 1.89 m	± 0.1 m
\bar{L}_b	L	Mean crest length of breaking wave	Every 4 hr	10.0 to 235.0 m	within 10%
\bar{m}	0	Mean slope of foreshore (tan)	Derived from E_b	0.0210 to 0.1263	$\pm 0.2^0$
Q_f	L ³	Quantity of sand eroded from or deposited on foreshore in one tidal cycle (fig. 3)	Derived every 6.25 hr (high and low water) from E_b	-5.73 m ³ to +3.00 m ³	± 0.05 m ³
r	L	Rainfall	Continuous	trace	
R_n		Net radiation, as measured at a point 800 ft offshore	Continuous	-0.12 to +0.60 g cal/cm ² /s	± 0.10 g cal/cm ² /s
S	0	Position of top of the swash (in terms of closest reference stake)	Every 4 hr and at high and low water	A + 40 ft to J	0.3 to 1.8 m

TABLE 3. - (continued)

Symbol	Dimensions	Description (refer to fig. 2, 3, or 4)	Measurement Schedule	Range in Values	Probable Error
t_a	0	Temperature of air, 800 ft offshore	Every 4 hr	14.5 to 32.7°C	$\pm 0.2^\circ$ to $\pm 0.7^\circ\text{C}$
t_w	0	Temperature of sea water	Every 4 hr	21.1 to 26.4°C	$\pm 0.2^\circ\text{C}$
\bar{T}_b	T	Mean period of breaking waves	Every 4 hr	4.0 to 12.4 s	± 0.2 s
T_s	T	Period of significant waves, 900 ft offshore	Every 4 hr	3.0 to 13.8 s	± 0.25 s to ± 0.5 s
u	L	Unsaturated beach surface between outcrop of water table on foreshore and swash reach	Derived (every 4 hr)	0.0 to 11.8 m	± 0.3 to ± 1.0 m for low & high values, respectively
\bar{v}	LT ⁻¹	Mean rate for sand sample to settle 1.0 m in pure water at 24°C	Every 6.25 hr (high and low water)	1.6(I) to 8.3(H) cm/s	± 0.02 cm/s
\bar{V}	LT ⁻¹	Mean longshore current velocity	Every 4 hr	0.00 to 1.40 m/s	± 0.06 m/s
W_d	0	Mean wind direction, 800 ft offshore	Every 2-4 hr	-----	$\pm 3.0^\circ$
W_s	LT ⁻¹	Mean wind speed, 800 ft offshore	Every 2-4 hr	1.0 to 12.0 m/s	± 0.5 to 1.0 m/s
\bar{z}	L	Mean trough to bottom distance in front of breaking wave (fig. 4)	Every 4 hr	0.07 to 0.98 m	± 0.005 m
α_b	0	Acute angle between shoreline and crest of breaking wave. (Tangent of angle is used)	Every 4 hr	0.0000 to 0.3172 or 0.0° to 17.6°	± 1.0 to 2.0° , per wave
$\pm\eta$	0	Rate of rise (+) or fall (-) of still water level at tide gage	Derived from E_t	-0.42 to +0.39 m/hr	± 0.015 m/hr
ρ_l	ML ⁻³	Density of liquid (sea water)	Every 4 hr	1.0169 to 1.0202 g/cm ³	± 0.00005 g/cm ³
ρ_s	ML ⁻³	Relative density of solids (sand grains) on foreshore surface	Every 6.25 hr (high and low water)	2.6172 to 2.6740 g/cm ³	± 0.0005 g/cm ³

module recorded wave heights to the nearest 15 cm. The second method involved exchanging the staff for a surveyor's rod graduated to tenths of a foot, with large labels for easy reading. In either case, the staff or the rod was held firmly in the zone of breaking waves by one man while values for wave heights were recorded by another man standing well inshore of the breakers. The breaker height, H_b (fig. 4), and the breaker type (plunging, spilling, or bore) of 50 successive waves was recorded, as well as the starting and ending time, to the nearest second, of the interval during which heights were measured. The probable error in water level measurements was ± 5.0 cm for the surveyor's rod (for high breakers) and ± 3.0 cm (for low breakers). Because the rod or staff could not be positioned beneath the exact crest of every single wave, the values obtained have an additional error. This error is difficult to estimate, but it is probably always less than ± 12.0 cm for high waves and ± 6.2 cm for low waves. Values for H_b (app. A) were calculated for 50 consecutive waves.

4.2.4 Significant breaker height (H_{bS})

This value (app. A) was obtained by calculating the mean height of the one-third highest breakers in a given set of 50 consecutive waves.

4.2.5 Mean period of breaking waves (\bar{T}_b)

The starting and ending times of the interval over which 50 successive wave heights were measured were recorded to the nearest second and \bar{T}_b was calculated using this elapsed time. The representativeness of \bar{T}_b is largely a function of the regularity of breaker heights and shapes. Where large and small breakers are intermixed, some of the small ones may be missed in counting or, alternatively, when they are counted they may in fact introduce unwanted variability in the calculation of a meaningful \bar{T}_b that would reflect only the higher waves. It is desirable to be able to calculate the period of the higher breakers, but instrumentation for this purpose was unavailable at the time this study began. Under the best conditions, the error in determining \bar{T}_b (app. A) is probably about ± 0.2 s.

4.2.6 Mean acute angle between the shoreline and the crests of breaking waves ($\bar{\alpha}_b$)

Three to eight determinations of $\bar{\alpha}_b$ were made, just before or just after determination of \bar{V} , using a tripod-mounted azimuthal circle equipped with sights. The tripod was set up as close to the inshore margin of the breaker zone as possible and values for α_b were measured to the nearest degree. For the first half of the study period, a base line parallel to the shoreline was estimated by eye. For the other half, the center of the tripod was lined up with two steel rods previously positioned on a base line determined to be "parallel to the shoreline". Such positioning of the tripod reduced observer variability as far as determination of the bearing of one side of angle α_b was concerned. The bearing of the other side of α_b was determined by sighting down the crests of breaking waves at some distance (50-500 m) from the tripod. Because of the straightness of the shoreline in the study area and the lack of significant beach rhythms during the study period (cf. plates A-I), the mean value obtained for the α_b 's is believed valid for the immediate area in which \bar{V} was determined.

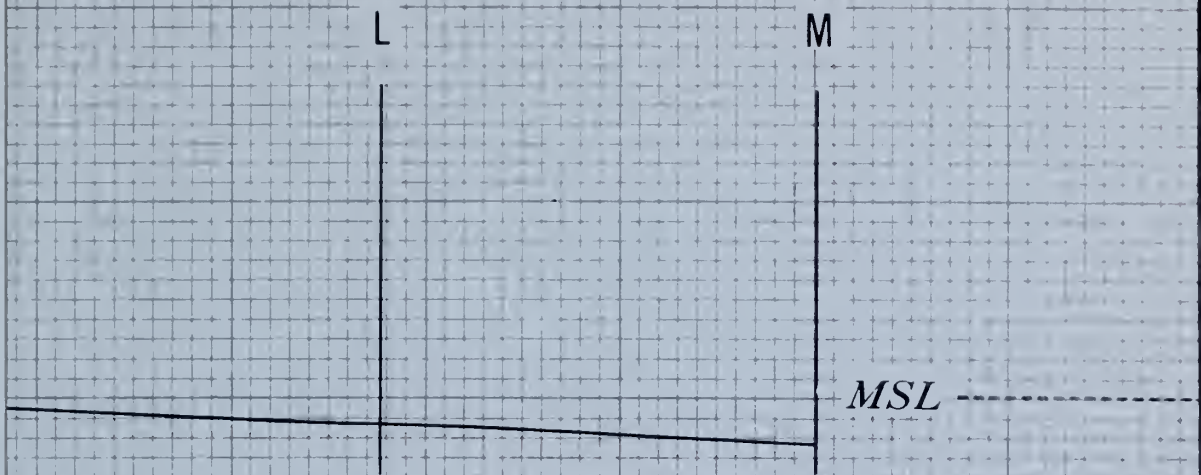
4.2.7 Mean crest length of breaking waves ($\bar{\ell}_b$)

The minimum and maximum crest length of breaking waves was estimated visually by comparison with a measured course on shore. At times, considerable variability was noted in crest length, and the "mean crest-length" values were only crude estimates. The significance of ℓ under such circumstances is open to question. For a number of longshore current measurement times, during a period of high \bar{V} , high H_b , and high ℓ (≈ 400 m), the mean crest-length values in appendix A are probably valid to within 10 percent.

4.2.8 Mean trough to bottom distance in front of a breaking wave (\bar{z})

This distance (\bar{z} , fig. 4) was measured directly with a meter stick. About 5 to 10 z values were read and an average value noted on the field sheets. The error in an individual measurement is about ± 0.5 cm. The representativeness of a given \bar{z} value (app. A) is variable, however, depending upon such things as the variability in size and type of breakers and their distribution throughout the breaker zone.

PROFILE



50

PLAN

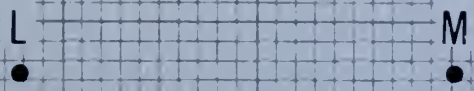
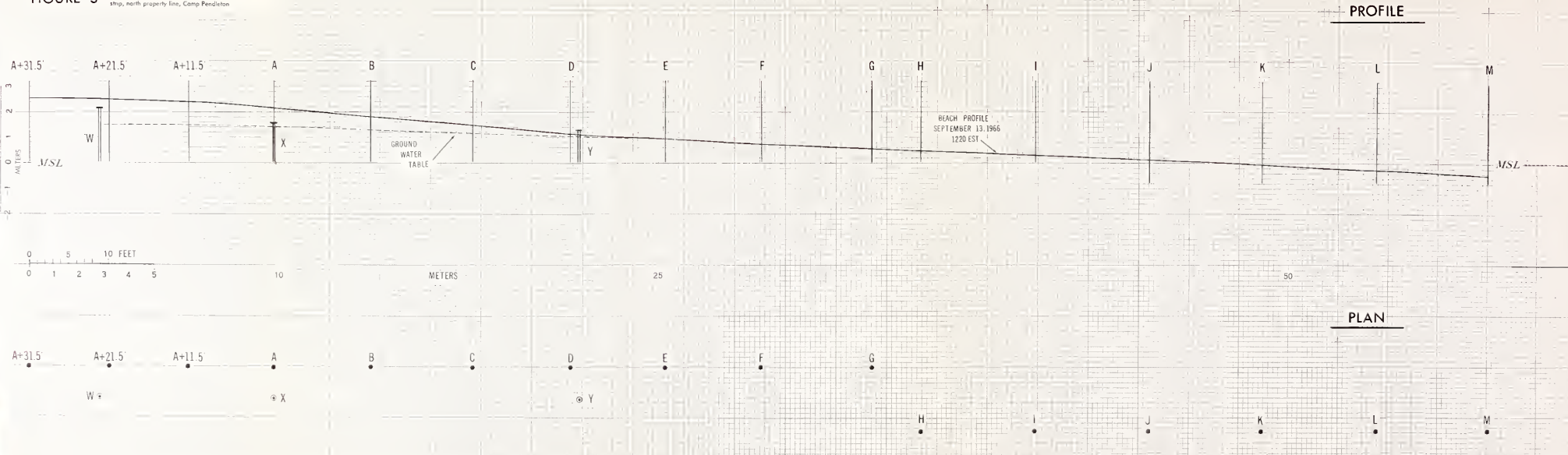


FIGURE 3 Layout of reference stations and well points at beach study strip, north property line, Camp Pendleton



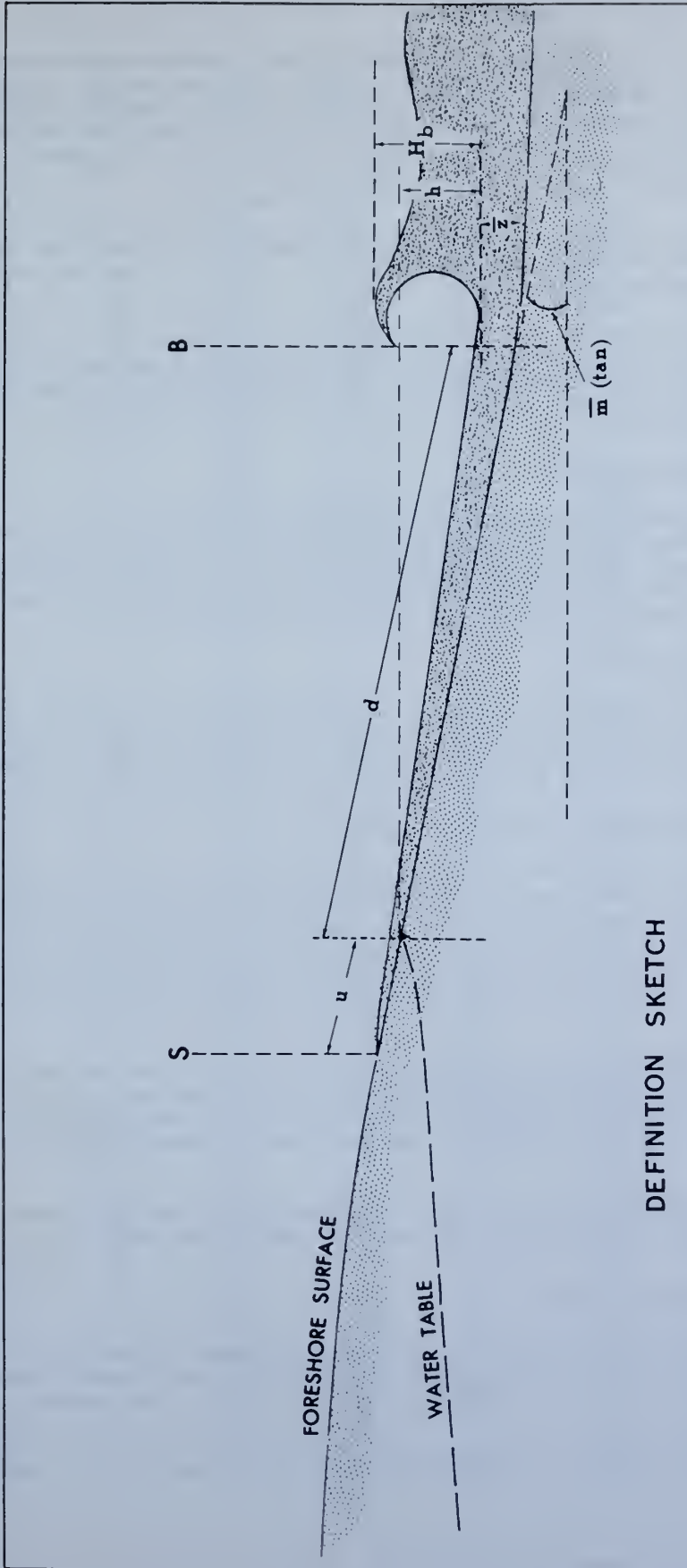


Fig. 4. Definition sketch for variables measured at beach study strip.

4.2.9 Mean longshore-current velocity (\bar{V})

The current velocity and direction were measured at the beach study strip (fig. 1C, plate 1) by timing the movement of the centers of patches of fluorescent dye as they moved parallel to shore. After three dye patches had been satisfactorily timed by stopwatch over a 15- or a 30-m course, a mean travel time was determined. This travel time was assumed to represent the mean velocity of the longshore current. Nearly all the dye charges were introduced at the inshore margin of the breaker line closest to shore. Thus, a small percentage of each dye patch was under the influence of swash motions.

Dye patches were illuminated by headlights and flashlights for nighttime observations and this proved adequate most of the time. Under certain conditions, foam obscured the dye patches and they could not be followed.

A field party from the U.S. Army Coastal Engineering Research Center studied fluctuations in the longshore-current system at the beach site using dye patches, balloons filled with water, and dye patches surrounding balloons. As a result of this study, the probable error in measurement of \bar{V} (app. A) appears to be on the order of ± 0.06 m/s (± 0.2 ft/s). Galvin's data are summarized in table 4.

4.2.10 Significant wave height (H_s)

Measures of wave height and period for waves beyond the breakers were desired so that wave steepness could be determined. The average height and period of the 1/3-highest waves were the measures selected. The value for H_s was determined from a significant-wave strip-chart analysis of wave records obtained from the Coastal Engineering Research Center's step-resistance wave gage located at the end of the fishing pier (fig. 2).

4.2.11 Significant wave period (T_s)

Consideration of the methods utilized in the significant-wave strip-chart analysis indicates that values for the periods of significant waves are good to ± 0.25 s for $T_s = 3$ to 6 s and ± 0.5 s for $T_s = 6$ to 20 s for most wave records. Note that T_s (app. A) is determined to the nearest 0.5 s for $T_s = 3$ to 6 s and to the nearest whole second for $T_s = 6$ to 20 s.

4.2.12 Elevation of beach surface at reference station (E_b)

Adequate profiles of the foreshore surface are required for precise determinations of foreshore volume changes. To this end, a series of reference stations (fig. 3) perpendicular to the beach was established using wooden piles (stations A+31.5 through G) or concrete reinforcing rods (stations H through M) jettied into the beach. Reference marks were painted on the rods and reference nails were driven into the piles. Precise elevations of the paint marks and nail heads (relative to a MSL bench mark datum) were then determined with an engineer's level.

To determine the altitude of the foreshore at a given station and instant of time a meter stick was used for measuring the distance between a reference mark or nail and the foreshore surface, to the nearest millimeter. Where the foreshore was above water, this value was probably good to ± 2 mm. Below water and under adverse breaker conditions, precision of measurements was only ± 10 mm.

A post study level check indicated that the reference marks and well points (see E_w and fig. 3) had retained their original pre-study altitudes. The values for E_b given in appendix B are relative to the MSL datum.

4.2.13 Elevation of groundwater table (E_w)

The water table beneath the foreshore was monitored because of the effects of excess pore water pressures in the lower foreshore face on erosion there, and because deposition on the upper foreshore is often greatly influenced by swash percolating into unsaturated sands above the water table.

Note: Figure 3 serves as a convenient plotting sheet for the B , E_b , E_w , and S data.

TABLE 4. - Longshore Current Data Collected by C. J. Galvin, September 9, 1966, 0930-1600 hr.

Run	Method	Time	V50-1	V50-2	V100-1	V100-2	V200	DELV1	DELV2
		MIN	FPS	FPS	FPS	FPS	FPS	FPS	FPS
1.0	B	0	1.00	-2.00	0.00	0.00	0.00	0.00	0.00
2.0	B	0	1.00	-2.00	0.00	0.00	0.00	0.00	0.00
3.0	B	0	0.67	-3.00	0.00	0.00	0.00	0.00	0.00
4.0	B	0	0.88	0.46	0.61	0.71	0.66	-0.41	0.11
5.0	B	0	-3.00	0.00	0.00	0.00	0.00	0.00	0.00
6.0	B	0	1.02	0.54	0.70	-2.00	0.00	-0.48	0.00
7.0	B	0	1.02	-2.00	0.00	0.00	0.00	0.00	0.00
8.0	B	0	1.00	-2.00	0.00	0.00	0.00	0.00	0.00
9.0	B	0	1.00	1.25	1.11	-2.00	0.00	0.25	0.00
10.1	B	40	1.11	1.25	1.18	1.25	1.21	0.14	0.07
10.2	B	0	1.43	1.43	1.43	1.33	1.38	0.00	-0.10
11.1	D	0	0.43	-1.00	0.00	0.00	0.00	0.00	0.00
11.2	B	0	1.00	-2.00	0.00	0.00	0.00	0.00	0.00
11.3	B	0	-2.00	0.00	0.00	0.00	0.00	0.00	0.00
12.1	DL	0	0.83	1.25	1.00	-1.00	0.00	0.42	0.00
12.2	B	0	0.56	0.67	0.61	0.91	0.73	0.11	0.30
12.3	B	0	0.91	0.91	0.91	0.71	0.80	0.00	-0.19
13.1	B	65	1.35	1.52	1.43	1.33	1.38	0.16	-0.10
13.2	B	0	1.85	1.79	1.82	1.43	1.60	-0.07	-0.39
14.1	B	0	0.94	0.96	0.95	-2.00	0.00	0.02	0.00
14.2	B	0	1.25	-2.00	0.00	0.00	0.00	0.00	0.00
15.1	B	78	1.67	2.50	2.00	1.05	1.38	0.83	-0.95
15.2	B	0	2.27	-2.00	0.00	0.00	0.00	0.00	0.00
16.0	BDP	120	1.43	-2.00	0.00	0.00	0.00	0.00	0.00
17.0	BDP	0	1.25	1.43	1.33	-2.00	0.00	0.18	0.00
18.0	BDP	0	1.67	1.11	1.33	-2.00	0.00	-0.56	0.00
19.0	BDP	0	1.14	1.92	1.43	-2.00	0.00	0.79	0.00
20.0	BDP	0	1.72	-2.00	0.00	0.00	0.00	0.00	0.00
21.0	BDP	0	1.47	1.92	1.67	1.49	1.57	0.45	-0.17
22.0	BDP	165	1.79	2.63	2.13	-3.00	0.00	0.85	0.00
23.0	BDP	0	0.94	-2.00	0.00	0.00	0.00	0.00	0.00
24.0	BDP	0	1.39	2.08	1.67	2.50	2.00	0.69	0.83
25.0	BDP	0	1.14	1.92	1.43	1.85	1.61	0.79	0.42
26.1	B	260	1.43	1.00	1.18	1.11	1.14	-0.43	-0.07
26.2	B	260	1.06	1.32	1.18	0.00	0.00	0.25	0.00
27.1	B	0	2.63	3.33	2.94	2.78	2.86	0.70	-0.16
27.2	B	0	2.63	3.13	2.86	2.38	2.60	0.49	-0.48
28.1	B	280	2.00	-2.00	0.00	0.00	0.00	0.00	0.00
28.2	B	280	-4.00	-2.00	1.43	1.32	1.37	0.00	-0.11
29.1	B	0	2.63	1.92	2.22	2.78	2.47	-0.71	0.56
29.2	B	0	2.50	3.33	2.86	3.23	3.03	0.83	0.37
30.1	B	289	3.13	1.72	2.22	1.64	1.89	-1.40	-0.58
30.2	B	289	3.33	3.33	3.33	3.03	3.17	0.00	-0.30
31.1	B	295	2.78	2.63	2.70	3.03	2.86	-0.15	0.33
31.2	B	295	2.78	2.78	2.78	2.33	2.53	0.00	-0.45
32.1	B	297	2.00	-4.00	0.00	1.06	2.22	0.00	1.06
32.2	B	297	2.00	2.50	2.22	2.22	2.22	0.50	0.00
33.1	BB	305	2.00	-4.00	0.00	0.81	1.67	0.00	0.81
33.2	BB	305	2.00	2.17	2.08	-2.00	0.00	0.17	0.00
34.1	BB	0	2.00	2.17	2.08	0.00	0.00	0.17	0.00
34.2	BB	0	2.00	1.56	1.75	1.92	1.83	-0.44	0.17
35.1	BB	315	2.78	2.94	2.86	2.56	2.70	0.16	-0.29
35.2	BB	315	2.94	3.13	3.03	2.56	2.78	0.18	-0.47
36.1	DDL	0	2.50	2.78	2.63	-1.00	0.00	0.28	0.00
36.2	DDL	0	2.38	2.08	2.22	-1.00	0.00	-0.30	0.00
37.1	DDL	324	2.27	1.79	2.00	-1.00	0.00	-0.49	0.00
37.2	DDL	324	2.38	1.56	1.89	-1.00	0.00	-0.82	0.00
38.1	DDL	0	3.33	-1.00	0.00	0.00	0.00	0.00	0.00
38.2	DDL	0	3.33	-1.00	0.00	0.00	0.00	0.00	0.00

TABLE 4. - (continued)

Run	Method	Time	V50-1	V50-2	V100-1	V100-2	V200	DELV1	DELV2
		MIN	FPS	FPS	FPS	FPS	FPS	FPS	FPS
39.1	DDL	0	1.67	-1.00	0.00	0.00	0.00	0.00	0.00
39.2	DDL	0	1.61	-1.00	0.00	0.00	0.00	0.00	0.00
40.1	DDL	330	1.67	-1.00	0.00	0.00	0.00	0.00	0.00
40.2	DDL	330	1.67	-1.00	0.00	0.00	0.00	0.00	0.00
41.1	BO	0	2.00	1.39	1.64	0.00	0.00	-0.61	0.00
41.2	BI	0	-4.00	1.39	1.92	2.44	2.15	0.00	0.52
42.1	BO	340	1.79	-4.00	0.00	-2.00	0.00	0.00	0.00
42.2	BI	340	2.08	2.08	2.08	-2.00	0.00	0.00	0.00
43.1	BO	0	1.72	3.13	2.22	1.69	1.92	1.40	-0.53
43.2	BI	0	3.13	-4.00	0.00	-2.00	0.00	0.00	0.00
44.1	BO	352	1.61	-3.00	0.00	-3.00	0.00	0.00	0.00
44.2	BI	352	2.38	3.33	2.78	-2.00	0.00	0.95	0.00
45.1	BO	362	2.38	3.13	2.70	2.63	2.67	0.74	-0.07
45.2	BI	362	2.50	2.94	2.70	1.92	2.25	0.44	-0.78
46.1	BO	0	1.25	2.38	1.64	2.17	1.87	1.13	0.53
46.2	BI	0	2.63	2.00	2.27	-2.00	0.00	-0.63	0.00
47.0	DP	372	2.27	2.17	2.22	2.50	2.35	-0.10	0.28
48.0	DP	380	2.17	1.56	1.82	2.00	1.90	-0.61	0.18

Explanation of column headings:

- Run - If the number after the decimal is 0, then only one balloon (or dye packet) was used in that run. If the number is not 0, that means two or three balloons were dropped; i.e., the 12th run included three separate measurements, 12.1, 12.2, 12.3.
- Time - Measured in minutes from time of first run. If time is not recorded, 0 is entered. All runs are listed in chronological order.
- V50-1 - Velocity over first 50 ft.
- V50-2 - Velocity over second 50 ft.
- V100-1 - Velocity averaged over first 100 ft.
- V100-2 - Velocity averaged over second 100 ft.
- V200 - Velocity averaged over entire 200 ft. Note: In the above velocity columns, 0 means not measured. Negative numbers: Minus 1.00, dye too dispersed to make measurement; -2.00, balloon touched bottom on beach face; -3.00, balloon lost permanently; -4.00, balloon lost temporarily.
- DELV1 - (V50-2) - (V50-1).
- DELV2 - (V100-2) - (V100-1). Note: For DELV1 and DELV2, a zero entry usually means that one or both of the items on the right side of the defining equation was not measured, but it may also mean that the two quantities on the right were equal.
- Method - B, balloon dropped singly or in simultaneous pairs; BB, balloon pairs, with second balloon dropped when the first reached 50-ft station; BI, balloon dropped in the middle of the surf zone; BO, balloon dropped at breaker point; BDP, balloon with LASIL dye packet attached; D, dye; DL, liquid dye; DP, LASIL dye packet; DDL, liquid dye pairs, with the second dropped when the first reached 50-ft station. Note: BI and BO were dropped simultaneously.

Three well points (W, X, and Y in fig. 3) were jetted into the beach along a line perpendicular to the coast and parallel to or concordant with the line of reference stations. The altitudes of the tops of the pipes were determined relative to an MSL bench mark datum by standard leveling procedures. Every 4 hr and at times of high and low water, caps were unscrewed from the well points and a measuring device inserted to determine the distance between the top of the well point and the free water surface in the well point. Three techniques were used for this purpose: 1) a meter stick was coated with powder so that the water-air interface could be clearly seen; 2) a flashlight beam was reflected off the top of the water column and a measuring stick inserted until it just touched the free water surface; and 3) an unpowdered piece of wooden quarter-round was inserted until a centimeter or two of its end was submerged. In all cases, the pertinent distance was measured immediately to the nearest mm, using a meter stick. The third method was used perhaps 60 percent of the time, the light-reflection method 37 percent of the time, and the powdered-stick method the remainder of the time. Values obtained (app. B) are probably precise to about ± 2.0 mm and are relative to the MSL datum.

4.2.14 Density of liquid (sea water) (ρ_l)

The dependency of sand movement on water density had been demonstrated in a previous study at Virginia Beach (Harrison and Krumbein, 1964), and for that reason variations in water density were carefully monitored in the present study. Samples of sea water for salinity determinations were taken at both the tide house (fig. 2) and at the beach strip (fig. 1C), as were measurements of water temperature (T_w). Only values for density of sea water (ρ_l) at the beach strip are reported (app. A). Each water sample was introduced into a citrate of magnesia bottle that had been well rinsed with the same local sea water from which the sample was taken. Salinities were determined using a Hytech Model 6210 laboratory salinometer. Salinity values are accurate to about ± 0.003 parts per thousand.

A nomograph was used for determining density from the temperature and salinity of sea water. In view of the precision of the T_w and salinity values, ρ_l values (app. A) are probably accurate to about ± 0.00005 g/cm³.

4.2.15 Temperature of the air (t_a)

The temperature of the surface water a short distance beyond the breaker zone is to some degree dependent upon the trend in air temperature during the preceding hours. Most of the time, in the course of this study, the temperature of the air at the tide house (fig. 2) was determined by simply holding a Taylor mercurial thermometer in the open air. Precision of measurement in this case was probably $\pm 0.3^\circ\text{C}$. During the last 14 days, the thermometer was mounted on the north side of the tide house and encased in a wooden, free-air-flow thermoscreen. Precision of these measurements (from September 2 until the end of the study; app. A) was probably $\pm 0.2^\circ\text{C}$.

4.2.16 Temperature of the water (t_w)

Water temperature was taken at both the tide house (fig. 2) and in the breaker zone at the beach site (fig. 1C). Only the water temperatures from the tide house are presented in this report. Precision-calibrated, Taylor mercurial thermometers, mounted in standard C&GS water samplers were used. Care was taken that the water samplers had time to come to equilibrium with the surrounding water and that the thermometers were shielded from wind while being read. Precision of the water temperature values, given in appendix A, is probably $\pm 0.2^\circ\text{C}$.

4.2.17 Mean wind direction (\bar{W}_d)

Moderate to strong winds blowing for several hours or more in a relatively constant direction may affect not only the temperature of the nearshore surface water----through turnover of the adjacent shelf waters----but also the movement of foreshore sand through the breaker zone, as a result of wind-induced bottom currents.

A Weather Bureau Model F420 wind system with a direct readout module was installed at the tide house (fig. 2). Wind direction was read every 2 or 4 hr, to the nearest 05° of azimuth. A given mean wind direction value (app. A) was estimated with a precision of about $\pm 3.0^\circ$.

4.2.18 Mean wind speed (\bar{W}_s)

The wind system was equipped with a direct readout module for wind speed. Mean wind speed was read every 2 or 4 hr, and the values, given in appendix A, are believed precise to about ± 1.0 m/s.

4.3 Measurements Made at Times of High and Low Water

Analyses of changes in elevation, quantity of material, grain size, etc., on the foreshore may be made most logically over intervals of tidal or half-tidal cycle length. For this reason, the measurements of beach elevation, of water table elevation, and of the positions of the swash reach and breaker zone (described in sec. 4.2) were also made at times of high and low water. Sand samples were taken for measurement of the variables associated with grains composing the foreshore surface. The three sand grain variables judged to be most critical in determining foreshore changes are listed below.

4.3.1 Mean nominal grain diameter of sand samples on the mid-foreshore (\bar{D})

Samples of the uppermost few millimeters of the foreshore were taken by hand at each station during times of high and low water. The samples were washed of salts, dried, and split to 7-8-g weights for analysis in a Woods Hole Rapid Sand Analyzer (Zeigler, *et al.*, 1960). This device was modified from the original Woods Hole design so that the fall tube was 10.2 cm ID instead of 5.1 cm. Also, the gate mechanism for introducing the samples was replaced with a screen (250-mesh) applicator. The general procedure for making such sand analyses has been outlined previously by Harrison and Morales-Alamo (1964). The mean nominal grain diameter, \bar{D} , was calculated by first using the formula for the mean time to settle 1 m:

$$M_v = \frac{P_{05} + 2P_{16} + 4P_{50} + 2P_{84} + P_{95}}{10},$$

where the P's are percentiles of a pressure versus time curve, each percentile being expressed in seconds. The M_v values were then converted to nominal grain diameter (mm) by using the tables of Zeigler and Gill (1959), for quartz particles with a Corey shape factor of 0.7 settling in pure water. Values for \bar{D} are probably precise to about ± 0.02 mm. The values presented in appendix A are for samples taken on the mid-foreshore at a given high or low water time (see also ρ_s values).

4.3.2 Density of solids (sand grains) on the mid-foreshore (ρ_s)

The relative densities of 25-g samples of surficial sand were determined using ASTM Test D 854-58 (Am. Soc. Test. Mater., 1964). The samples were taken from collections made at the reference stations shown in figure 3, at times of high or low water. Samples used for density determinations were selected from stations located as nearly half-way between the inshore margin of the breaker zone and the top of the swash as possible. Successive determinations of ρ_s were made on each sample until a meaningful average could be obtained. The measured values (app. A) are probably precise to ± 0.0003 g/cm³.

4.3.3 Standard fall velocity (\bar{v})

This is the average rate of fall of the particles of a sand sample settling in quiescent fresh water of infinite extent and at a temperature of 24°C. The mean settling time was determined using the modified Woods Hole Rapid Sand Analyzer described in subsection 4.3.1, and the statistic used for estimating \bar{v} was the same as that used for estimating \bar{D} .

All \bar{v} values (app. B) are corrected to a water temperature of 24°C using the graphs of Zeigler and Gill (1959). Precision of the \bar{v} values is probably of the order of ± 0.02 cm/s.

Note: The variables E_b , B, S, and E_w were also measured at the time of high and low water.

4.4 Measurements Derived From the Field Data

Certain measurements relating to beach geometry were made after plotting the field data for E_b , E_w , B, and S on cross-section paper. The average slope of the foreshore between B and S was measured for the analysis of changes in foreshore volume, as were distances giving the relationship between B, S, and the outcrop of the water table. Changes in foreshore volume also were determined from plotted profiles.

4.4.1 Mean foreshore slope (\bar{m})

Foreshore slopes were determined from cross sections drawn from the elevational (E_b) data, as plotted on a 1:1 scale. Values were measured to degrees and tenths with a protractor and then converted to the tangent of the slope angle (fig. 4). The probable error in a given slope measurement is of the order of $\pm 0.2^\circ$.

Two sets of foreshore slopes are given. Those for the basic time series (app. A) are for the mean slope between the inshore margin of the breakers and the top of the swash at a given instant. Slopes (table 5) used for investigating longshore current velocity are for the slope from the inshore margin of the breakers to a point about one-half to three-quarters of the way to the top of the swash. (When a longshore trough appeared on a profile, the toe of the foreshore slope was taken as the inshore margin of the trough.)

4.4.2 Distance between outcrop of water table on foreshore and inshore margin of breakers (d)

This variable is a measure of the length of the foreshore over which the hydraulic head, h, of the groundwater table may act and was thought to be important to consider when analyzing for erosion and/or deposition on the lower foreshore.

The value ("d", fig. 4) was obtained from profiles drawn on the beach surface using elevation data (E), from data on the elevation of the water table (E_w), and from the information for B (fig. 4). Results (app. A) are dependent upon: 1) validity of the projection of the water table, as measured in the well points (fig. 3) to its intersection with the foreshore surface; and 2) the error in measurement of B. Most values have a probable error of about ± 1.5 m.

4.4.3 Hydraulic head -- Vertical distance (fig. 4) between a horizontal plane passing through the outcrop of the water table on the foreshore and a horizontal plane through the bottom of the trough in front of the breaking wave (h)

This value (app. A) was obtained from 1:1 profiles of the surfaces of the groundwater table and foreshore, and the plane through the bottom of the wave trough. It is a measure of the groundwater head to be dissipated over the distance d at any instant of time. Errors in determining h are related to: 1) the projection of the groundwater table to its intersection with the foreshore surface; and 2) the errors related to the determination of B and z. For large values of h, the error is probably of the order of ± 0.04 m, becoming proportionately smaller for smaller values of h.

4.4.4 Length of unsaturated beach surface (fig. 4) between outcrop of water table on foreshore and top of swash (u)

This variable is important to analyses of deposition on the upper foreshore because swash that traverses the beach above the water table outcrop loses energy or disappears as it percolates into the unsaturated sand. Sand transported to the upper foreshore under such conditions tends to be deposited there.

The value for u (app. A) was obtained from profiles drawn of the beach surface using elevation data (E_b), from data on the elevation of the water table (E_w), and from the information on the position of the top of the swash (S). Values for u are dependent upon: 1) the validity of the projection of the water table to its intersection with the foreshore surface; and 2) the error in measurement of S. Most values have a probable error of ± 0.3 m for low values and ± 1.0 m for high values.

TABLE 5. - Observation Times and Corresponding Values for the Tangent of the Slope of the Lower Foreshore Used in a Study (Harrison, 1968) of Longshore Current Velocity

Date (da/mo)	Time (hr)	\bar{m} (tan)	Date (da/mo)	Time (hr)	\bar{m} (tan)		
8/23	1300	.0981	9/05	0010	.0507		
	1600	.0875		0430	.0454		
	1800	.0699		0830	.0594		
	2000	.0612		1215	.0542		
8/24	0000	.0384	9/06	1600	.0769		
				2005	.0542		
8/25	0800	.0437	9/07	1215	.0507		
	1200	.0454		1630	.0349		
	1600	.0699		9/08	0035	.0577	
	2000	.0367			0420	.0349	
8/26	0055	.0384	0800	.0384			
	0400	.0472	1205	.0489			
	0800	.0367	1600	.0332			
	1200	.0524	1945	.0314			
	1600	.0612	9/09	0000	.0384		
	2000	.0437		0530	.0437		
8/27	0000	.0507		0800	.0349		
	0400	.0910		1200	.0454		
	1600	.0559		1620	.0402		
	2000	.0262		2110	.0297		
	8/28	0000	.0524	9/10	0420	.0419	
		0400	.0454		0810	.0314	
0800		.0402	1203		.0297		
1155		.0349	2000		.0297		
1530		.0384	9/11		0800	.0332	
1745		.0384			1240	.0454	
1950	.0314	9/12		0430	.0577		
8/29	0000			.0647	0845	.0175	
	0410			.0297	1200	.0454	
	0805			.0963	9/13	0740	.0489
	1400		.0314	1600		.0349	
	1600		.0209	9/14		0000	.0437
	2000	.1016	0430			.0314	
8/30	0000	.0157	0800			.0524	
	0500	.0262	1205			.0349	
	0810	.0524	2000		.0402		
	1220	.0244	9/15		0800	.0437	
	1600	.0157		1540	.0349		
	2005	.0998		9/16	0015	.0262	
8/31	0000	.0419			0350	.0227	
	0410	.0262			0805	.0507	
	0800	.1016			1200	.0279	
	1200	.0787	1545		.0175		
	1600	.0454	2000		.0122		
	2000	.0875	9/17	0820	.0349		
9/01	0000	.0717		1030	.0402		
	0800	.0594		9/04	1320	.0262	
	9/04	1635			.0332	1635	.0332
		2030			.0402	2030	.0402

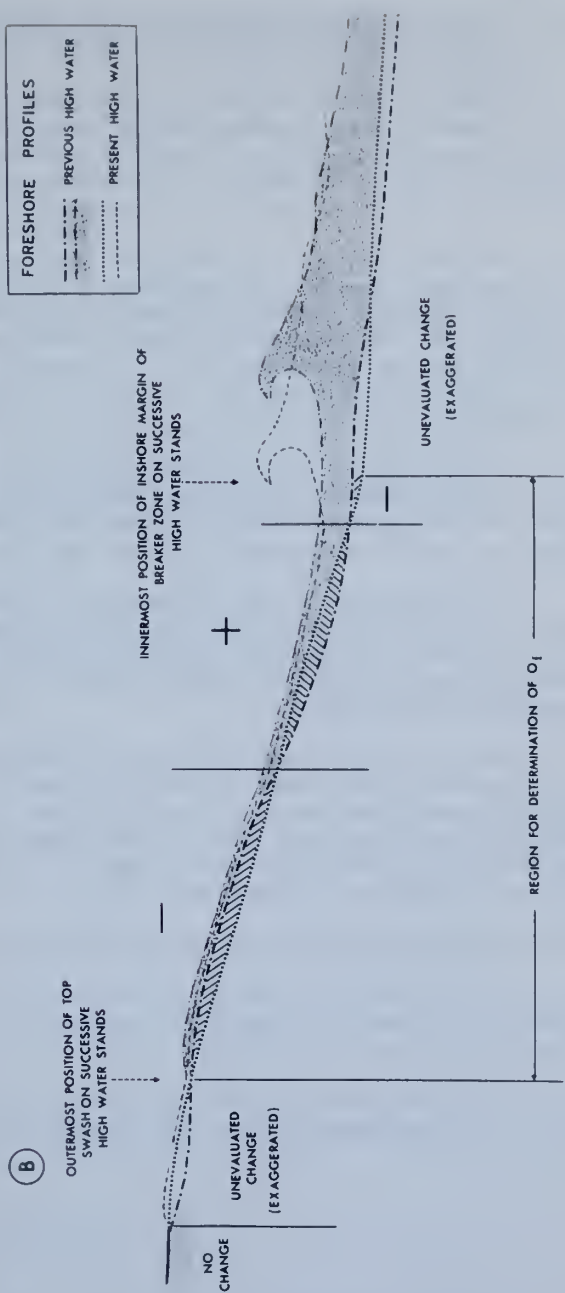
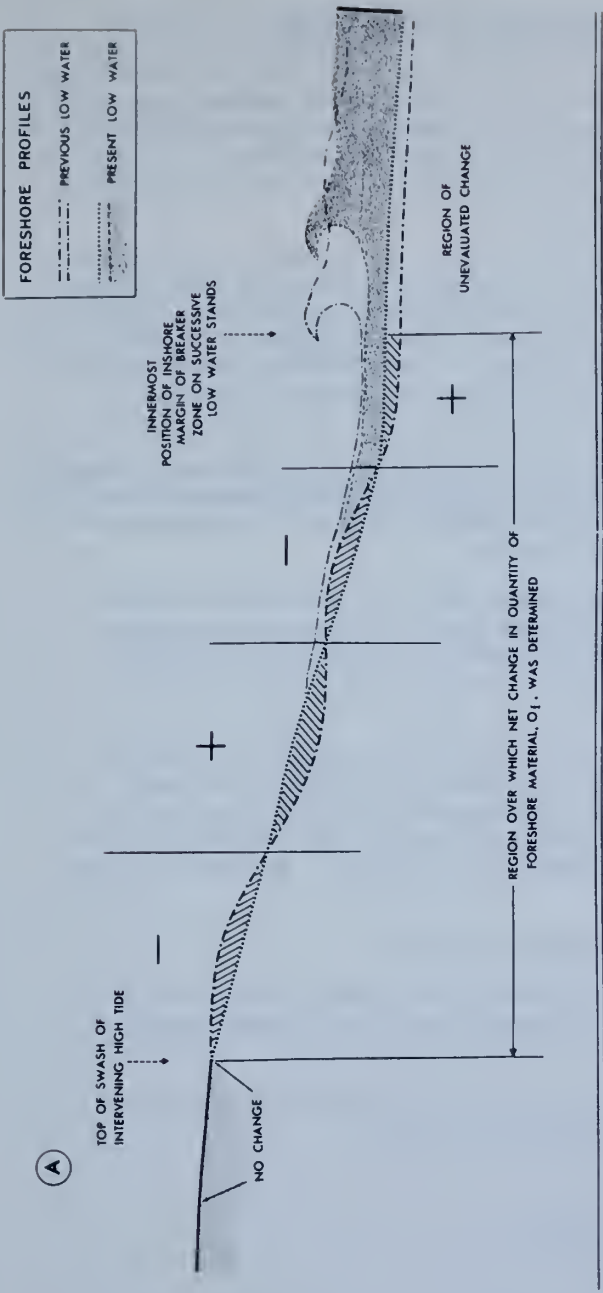


Fig. 5. Definition sketch for determination of Q_f (net change in quantity of foreshore material).

4.4.5 Quantity of sand eroded from (-) or deposited upon (+) the foreshore in one tidal cycle (Q_f)

Foreshore elevation data, E_b , were used to construct profiles of the beach surface (on a 1:1 ratio) using Albanene tracing paper. This type of paper has high stability and all profiles were stored flat in an air-conditioned room to prevent distortion. The profiles of successive high or successive low water stands were superimposed, and areas of accretion and erosion were determined with a planimeter.

Evaluation of the net change in quantity of material on the foreshore from one low tide to the next required planimetry of the areas of accretion and erosion lying between the inshoremost position of the breaker line on successive low water stands and the top of the swash at the intervening high water stand (see fig. 5A). The net change in area was then determined and converted to m^2 . To convert the change in area to change in volume (Q_f) the areal values were multiplied by 1.0 m, to represent the third dimension parallel to the shoreline.

The net change from one high tide to the next was obtained in the same way. In some cases, a small volume of change near the top of the swash had to remain unevaluated (see fig. 5B) as the foreshore there had been affected by the swash during only a small period of time, at only the beginning or end of the tidal interval.

The values for Q_f were determined by using profile data that were often obtained slightly before or slightly after the time of low or high water. Discrepancies between the true profiles at time of low or high water and the measured profiles are negligible, however, because of the very minor variation of the still-water level around the times of maximum tidal excursion.

Errors in the values of Q_f stem primarily from errors in measuring the elevation of the foreshore surface and errors in judgement in the connection of points for beach elevation during construction of the profiles. Errors incurred during planimetry are probably of least concern. None of the foregoing errors are cumulative. In most cases the total error in a given value for Q_f (app. A) is probably about $\pm 0.05 m^3$, assuming that the foreshore boundaries are adequately defined.

4.4.6 Rate of rise (+) or fall (-) of the still-water level ($\pm\eta$)

This variable is used in the analysis of foreshore volume changes and serves as a measure of the rate of change in the application of energy from waves or swash currents at a given point on the foreshore.

An hourly plot of $\pm\eta$ was made from the hourly E_t data obtained at the tide house (fig. 2). Values obtained (app. A) are valid to about $\pm 0.015 m/hr$.

5. DATA PROCESSING

With the exception of E_b , E_w , and \bar{v} (app. B), values for the variables described above were hand-plotted on a common time base, and smooth curves were drawn all by the same operator, connecting the plotted points for each variable. The continuous plots were then digitized at a 1-hr interval (0000, 0100, 0200 EDT, etc.).

The values for each variable are listed in appendix A. Underlined values denote actual measurements; all others were taken from the smooth curves. Gaps in the listings of certain variables in appendix A indicate that the time interval between successive observations was too great to permit meaningful interpolation from smooth curves.

Appendix C contains a special listing of variables used for investigating (Harrison, 1968) the dependent of foreshore volume changes in process elements acting over nine different lag times in a given tidal cycle. It is presented here for the convenience of the reader interested in utilizing such calculated ratios and dimensionless variables in his research. The data of appendix C are available on IBM cards from the senior author.

6. ACKNOWLEDGMENTS

Dr. C. J. Galvin, U.S. Army Corps of Engineers, Coastal Engineering Research Center (CERC), and Dr. R. B. McCammon, Gulf Research and Development Company, reviewed the manuscript and made helpful suggestions.

We also thank the firm of Langley, McDonald, and Overman, Consulting Engineers, for the use of their Sears Sea Sled; the U.S. Army, Fort Story, Virginia, for providing the services of two LARC V's and crews; the U.S. Naval Air Station, Oceana, Virginia, for providing aerial photographic coverage; and the City of Virginia Beach, Virginia, for numerous operational aids. Dr. Galvin, of CERC, kindly provided the data for table 4.

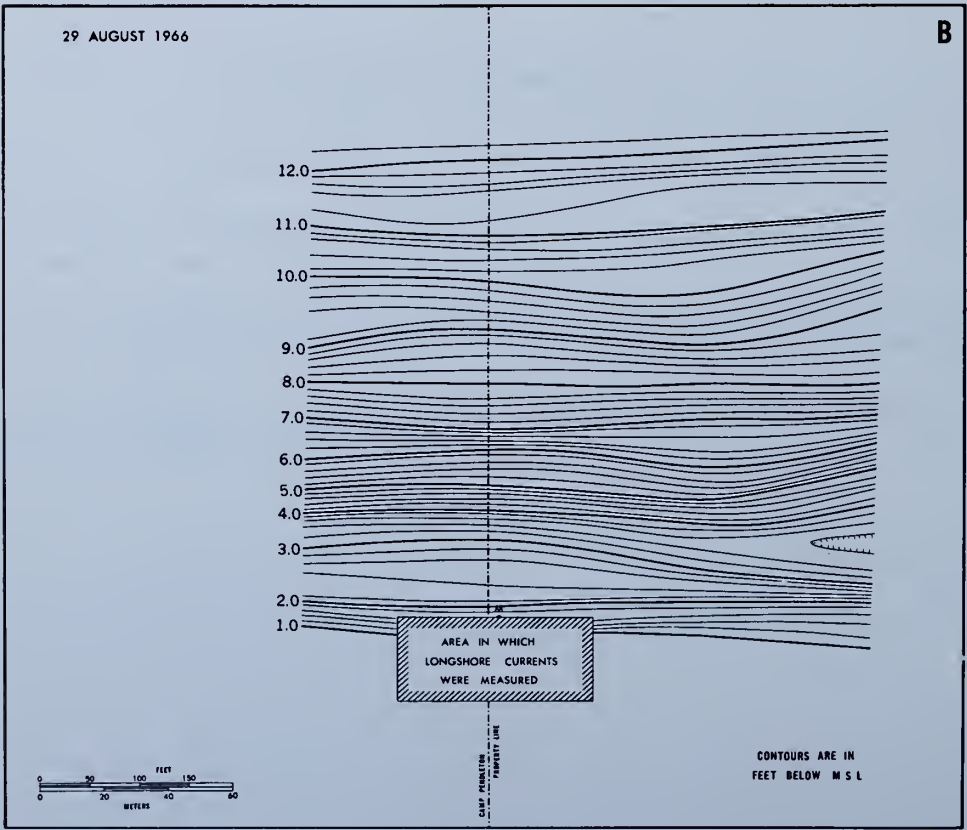
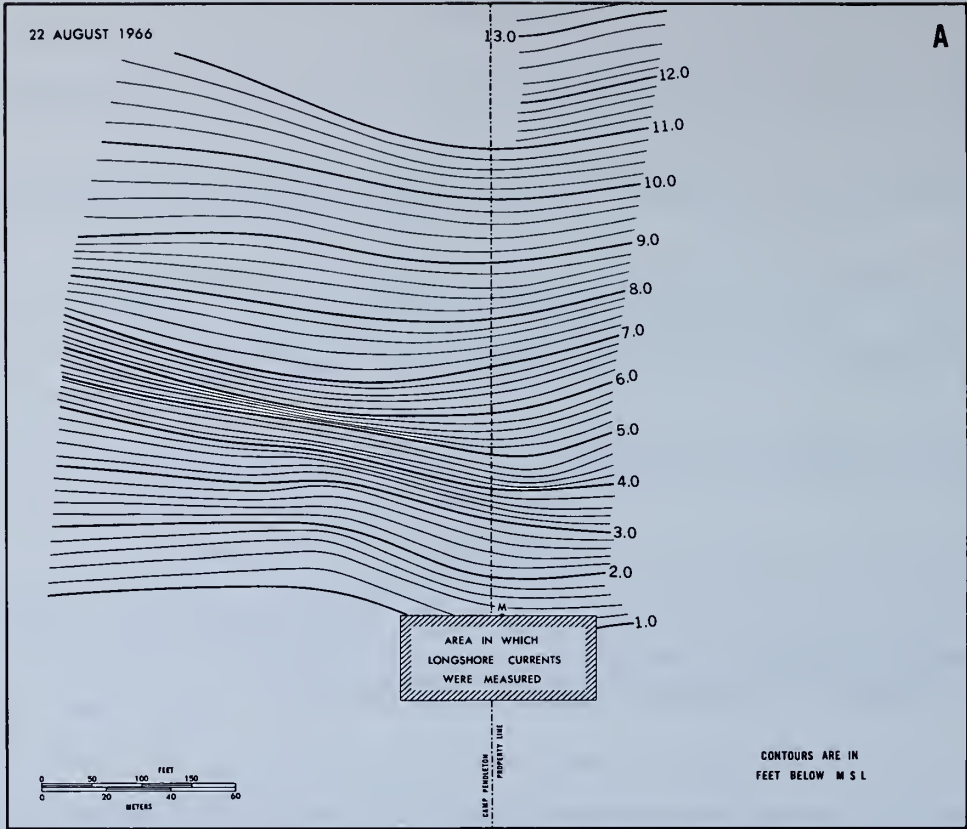
7. REFERENCES

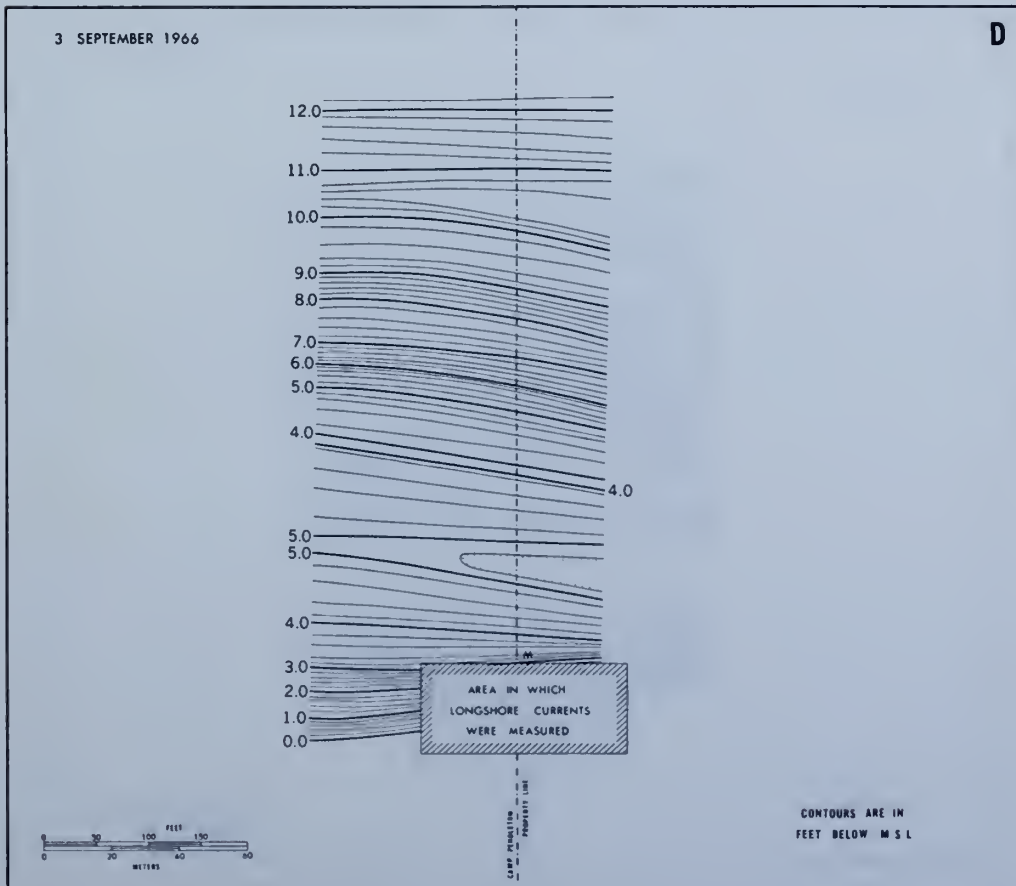
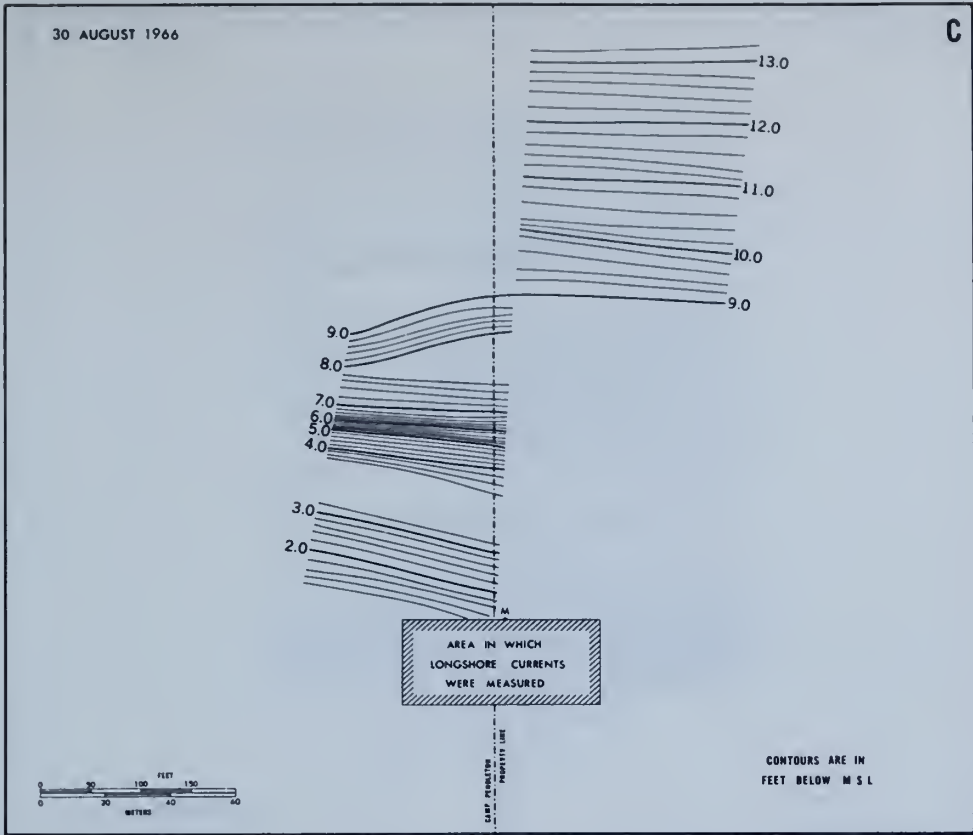
- American Society for Testing and Materials (1964), "Procedures for Testing Soils" (ASTM, Philadelphia).
- Harrison, W., M.L. Brehmer, and R.E. Stone (1964), "Nearshore tidal and non-tidal currents at Virginia Beach, Virginia," U.S. Army Corps of Engineers, Coastal Engineering Research Center, Tech. Memo. No. 5.
- Harrison, W., and K.A. Wagner (1964), "Beach changes at Virginia Beach, Virginia," U.S. Army Corps of Engineers, Coastal Engineering Research Center, Misc. Pap. No. 6-64.
- Harrison, W., and R. Morales-Alamo (1964), "Dynamic properties of immersed sand at Virginia Beach, Virginia," U.S. Army Corps of Engineers, Coastal Engineering Research Center, Tech. Memo. No. 9.
- Harrison, W., W.C. Krumbein, and W. Wilson (1964), "Sedimentation at an inlet entrance: Rudee Inlet, Virginia Beach, Virginia," U.S. Army Corps of Engineers, Coastal Engineering Research Center, Tech. Memo. No. 8.
- Harrison, W., and W.C. Krumbein (1964), "Interactions of the beach-ocean-atmosphere system at Virginia Beach, Virginia," U.S. Army Corps of Engineers, Coastal Engineering Research Center, Tech. Memo. No. 7.
- Harrison, W., and W.S. Wilson (1964), "Development of a method for numerical calculation of wave refraction," U.S. Army Corps of Engineers, Coastal Engineering Research Center, Tech. Memo. No. 6.
- Harrison, W. (1968), "Prediction in the Beach Environment," ESSA Prof. Pap. (In preparation).
- Inter-Agency Committee on Water Resources (1957), "Measurement and analysis of sediment loads in streams," Subcomm. on Sedimentation, Rept. 12 (U.S. Gov. Print. Off., Washington, D.C.).
- Helle, J.R. (1958), "Surf statistics for the coasts of the United States," U.S. Army Corps of Engineers, Beach Erosion Board, Tech. Memo. No. 79.
- Kolessar, M.A., and J.L. Reynolds (1966), "The Sears Sea Sled for surveying in the surf zone," U.S. Army Corps of Engineers, Coastal Engineering Research Center, Summary Rept. II.
- U.S. Congress (1953), "Virginia Beach, Virginia, beach erosion control study," 83rd Congress, 1st Session, House Doc. No. 186.
- Zeigler, J.M., and B. Gill (1959), "Tables and graphs for the settling velocity of quartz in water, above the range of Stokes' Law," Woods Hole Oceanographic Institution, Woods Hole, Mass., Ref. No. 59-36.
- Zeigler, J.M., G.G. Whitney, Jr., and C.R. Hayes (1960), "Woods Hole Rapid Sediment Analyzer," Sedimen. Petrol. 30, 490-495.

PLATES A - I

The following series of nine plates shows the bottom topography seaward along the beach study strip (fig. 1 C).

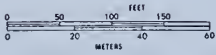
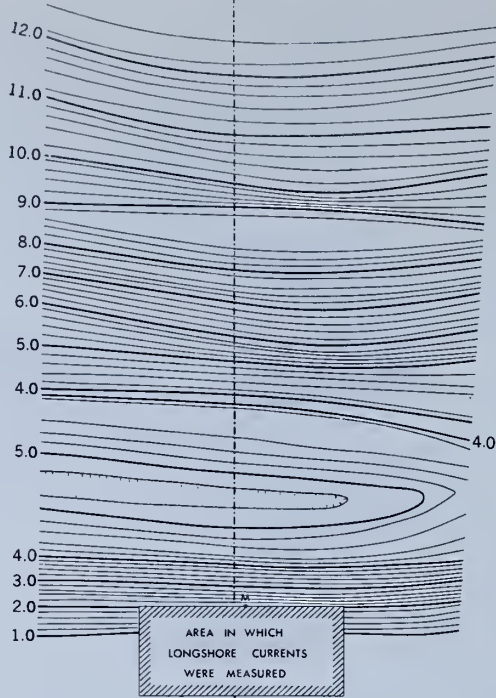
The symbol **M** on each plate denotes station "M" (fig. 3).





5 SEPTEMBER 1966

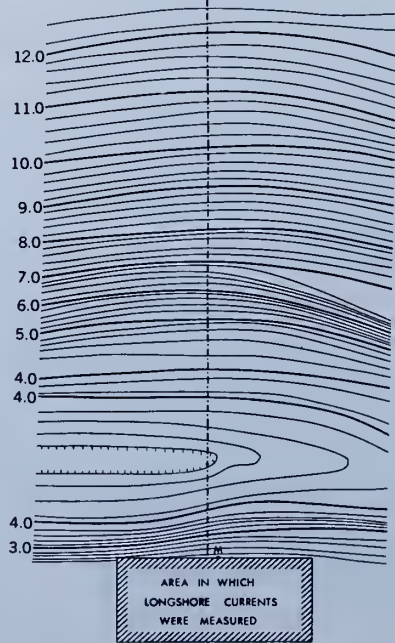
E



CONTOURS ARE IN
FEET BELOW M.S.L.

6 SEPTEMBER 1966

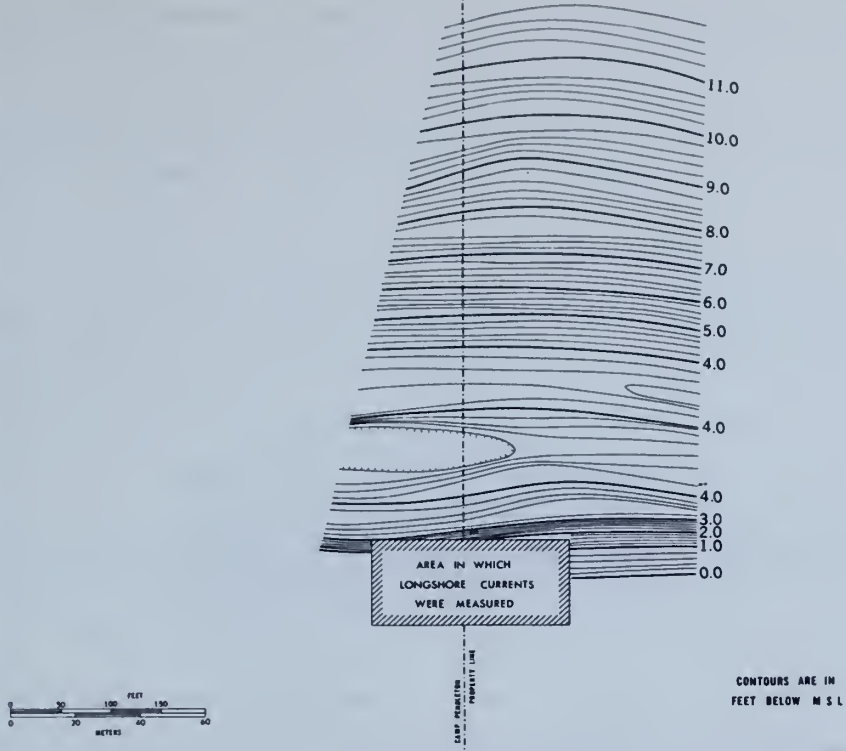
F



CONTOURS ARE IN
FEET BELOW M.S.L.

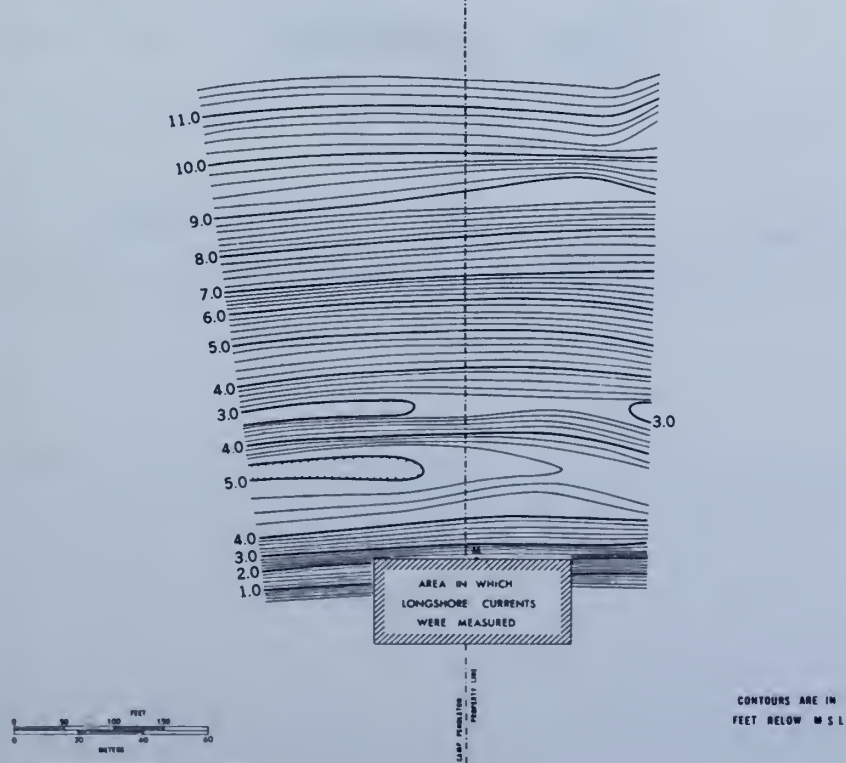
9 SEPTEMBER 1966

G

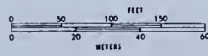
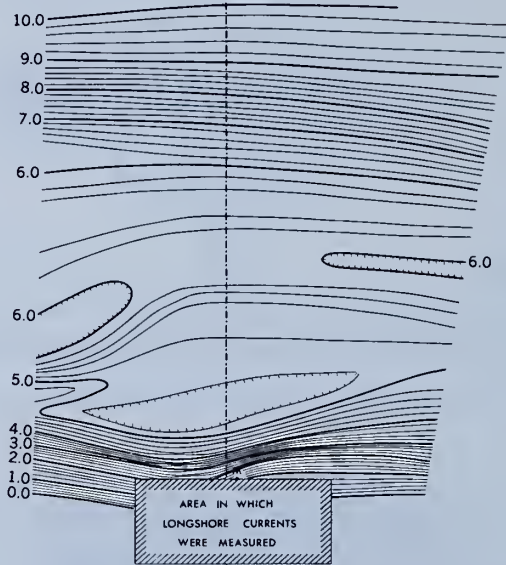


12 SEPTEMBER 1966

H



15 SEPTEMBER 1966



CONTOURS ARE IN FEET BELOW M S L

DATE: 08/21/66

Time hrs	B	d	\bar{D}	E_t	h	\bar{H}_b	H_{bs}	H_g	\bar{e}_b	\bar{m}	Q_f	R_a	S	t_a	t_w	\bar{T}_b	T_s	u	\bar{V}	W_d	W_g	\bar{z}	$\bar{\alpha}_b$	η	ρ_l	ρ_g	
	m	m	mm	m	m	m	m	m	m	(tan)	m ³	g cal/ cm ² /sec		(°C)	(°C)	sec	sec	m	m	()	m sec	m	(tan)	$\frac{m}{hr}$	g/cm ³	g/cm ³	
0000								.55									9.5							0.00			
0100				<u>2.073</u>				.56									9.5								-0.13		
0200				<u>1.890</u>				.55									9.4								-0.24		
0300				<u>1.615</u>				.55									9.4								-0.26		
0400				<u>1.341</u>				.55									9.2								-0.20		
0500				<u>1.158</u>				.55									9.2								-0.15		
0600				<u>1.067</u>				.55									9.2								0.00		
0700				<u>1.158</u>				.55									9.1								+0.13		
0800				<u>1.310</u>				.55									9.0								+0.20		
0900				<u>1.585</u>				.58									9.0								+0.34		
1000				<u>1.951</u>				.60									9.2								+0.34		
1100				<u>2.195</u>				.61									9.4								+0.16		
1200				<u>2.286</u>				.65									<u>9.6</u>								+0.05		
1300				<u>2.286</u>				.60									9.6								-0.07		
1400				<u>2.164</u>				.58									9.6								-0.19		
1500				<u>1.890</u>				.55									9.6								-0.25		
1600				<u>1.646</u>				.52									<u>9.6</u>								-0.28		
1700				<u>1.341</u>				.51									9.5								-0.28		
1800				<u>1.219</u>				.50									9.3								-0.07		
1900				<u>1.189</u>				.48									9.3								-0.02		
2000				<u>1.189</u>				.48									9.2								+0.12		
2100				<u>1.402</u>				.45									9.2								+0.21		
2200				<u>1.615</u>				.43									9.1								+0.26		
2300				<u>1.890</u>				.41									9.0								+0.23		

DATE: 08/22/66

Time hrs	B	d	\bar{D} mm	E_t m	h	\bar{H}_b m	H_{bs} m	H_s m	\bar{x}_b m	\bar{m} (tan)	Q_f m^3	R_n g cal/ cm^2/sec	S	t_a (°C)	t_w (°C)	\bar{T}_b sec	T_s sec	u	\bar{V} $\frac{m}{sec}$	W_d () $\frac{m}{sec}$	W_s $\frac{m}{sec}$	\bar{z} m	$\bar{\alpha}_b$ (tan)	η $\frac{m}{\bar{H}}$	ρ_l g/cm ³	ρ_s g/cm ³	
0000				2.042				.40									9.0								+0.06		
0100				2.042				.40									9.1									-0.03	
0200				1.981				.41									9.2									-0.12	
0300				1.768				.42									9.2									-0.20	
0400				1.585				.43									9.3									-0.23	
0500				1.341				.43									9.4									-0.23	
0600				1.158				.43									9.4									-0.13	
0700				1.097				.45									9.4									0.00	
0800				1.158				.45									9.4									+0.11	
0900				1.310				.45									9.4									+0.21	
1000				1.585				.44									9.2									+0.30	
1100				1.890				.43									9.1									+0.28	
1200				2.103			.87	.42									9.0									+0.16	
1300				2.195		.57	.85	.42									8.8									0.00	
1400			.261	2.164	.54	.85	.40	.40									8.7							.1033			
1500				2.073	.52	.85	.40	.40									8.6							.1052			
1600				1.951	.49	.85	.40	.40									8.4							.1104			
1700				1.737	.47	.82	.40	.40									8.3							.1122			
1800				1.585	.45	.80	.38	.38									8.2							.1139			
1900				1.219	.44	.80	.38	.38									8.0							.1157			
2000				1.158	.42	.79	.38	.38									8.0							.1175			
2100				1.219	.41	.79	.40	.40									8.2							.1192			
2200				1.372	.39	.78	.40	.40									8.4							.1210			
2300				1.585	.36	.78	.42	.42									8.6							.1228			

2.6648

DATE: 08/23/66

Time hrs	B	d	\bar{D}	E_t	h	\bar{H}_b	H_{bs}	H_g	\bar{H}_b	\bar{m}	Q_f	R_n	S	t_a	t_w	\bar{T}_b	T_s	u	\bar{V}	W_d	W_s	z	$\bar{\alpha}_b$	η	ρ_L	ρ_s
		m	mm	m	m	m	m	m	m	(tan)	m ³	g cal/ cm ² /sec		(°C)	(°C)	sec	sec	m	m SEC	(°)	m SEC	m	(tan)	m Hz	g/cm ³	g/cm ³
0000				<u>1.768</u>	.34	.78	.42									8.0	9.0	0.2					.1263	+0.16		
0100				<u>1.920</u>	.32	.76	.42									8.0	9.1	1.2					.1281	+0.10		
0200				<u>1.890</u>	.30	.75	.40									8.0	9.4	1.3					.1299	-0.07		
0300				<u>1.798</u>	.28	.75	.36									8.0	9.7	0.4					.1334	-0.13		
0400				<u>1.646</u>	.27	.73	.30									8.1	10.0	0.0					.1388	-0.15		
0500				<u>1.463</u>	.24	.73	.30									8.1	9.8	0.0					.1405	-0.15		
0600				<u>1.310</u>	.21	.72	.30									8.0	9.6	0.0					.1423	-0.18		
0700				<u>1.128</u>	.19	.70	.30									8.0	9.4	0.0					.1423	-0.14		
0800				<u>1.097</u>	.18	.68	.30									8.0	9.0	0.0					.1423	0.00		
0900	K	<u>14.5</u>	<u>.220</u>	<u>1.189</u>	0.52	.65	.31					I				<u>8.0</u>	<u>8.7</u>	<u>0.0</u>				0.12	.1441	+0.14		2.6458
1000	J	<u>13.0</u>		<u>1.372</u>	0.56	.63	.32					H				7.1	8.4	0.0				0.19	.1405	+0.22		
1100	J	<u>12.0</u>		<u>1.615</u>	0.60	.62	.34					G				6.5	8.2	0.0				0.24	.1370	+0.24		
1200	I	<u>11.5</u>		<u>1.859</u>	0.68	.45	.60	.37				F				6.2	8.0	0.0				0.31	.1299	+0.22		
1300	H	<u>10.5</u>		<u>2.073</u>	0.68	.49	.57	.40	.85			F				6.0	7.9	0.0	.72			0.38	.1139	+0.13	1.0199	
1400	H	<u>10.0</u>		<u>2.134</u>	0.68	.44	.54	.40	.85			E	<u>30.6</u>	23.7	5.8	5.8	7.9	0.0	.58			0.44	.0910	0.00	1.0198	
1500	H	<u>10.0</u>	<u>.352</u>	<u>2.103</u>	0.68	.38	.50	.41	.85	.1139		E	<u>26.0</u>	23.7	5.8	5.8	7.8	0.0	.52	209	5	0.44	.0875	-0.07	1.0198	2.6360
1600	I	<u>10.0</u>		<u>2.012</u>	0.60	.32	.47	.42	.85	.1051		E	<u>23.4</u>	23.7	6.0	6.0	8.0	0.0	.56	219	5	0.42	.1052	-0.15	1.0198	
1700	I	<u>10.0</u>		<u>1.798</u>	0.52	.28	.44	.41	.90	.0928		E	<u>22.6</u>	23.9	6.2	6.2	8.2	0.0	.62	232	4	0.37	.1104	-0.26	1.0197	
1800	J	<u>10.5</u>		<u>1.524</u>	0.42	.27	.41	.40	.90	.0805		F	<u>22.7</u>	24.3	6.4	6.4	8.5	0.0	.62	258	4	0.30	.1052	-0.26	1.0196	
1900	K	<u>10.5</u>		<u>1.310</u>	0.30	.27	.40	.41	.80	.0699		G	<u>24.5</u>	25.0	6.8	6.8	8.7	0.0	.46	288	4	0.22	.0857	-0.18	1.0195	
2000	K	<u>11.0</u>		<u>1.189</u>	0.20	.27	.39	.42	.80	.0647		H	<u>25.9</u>	25.6	7.2	7.2	9.0	0.0	.36	312	3	0.18	.0734	-0.09	1.0195	
2100	K	<u>11.5</u>	<u>.202</u>	<u>1.128</u>	0.16	.28	.40	.40	.70	.0630	+0.95	H	<u>25.9</u>	25.5	7.8	7.8	9.0	0.0	.40	320	3	0.16	.0770	0.00	1.0195	2.6444
2200	K	<u>12.0</u>		<u>1.219</u>	0.08	.30	.43	.38	.65	.0630		G	<u>25.5</u>	25.3	8.4	8.4	8.7	0.0	.48	321	3	0.22	.1033	+0.10	1.0193	
2300	J	<u>12.0</u>		<u>1.341</u>	0.08	.33	.45	.35	.55	.0647		G	<u>25.5</u>	25.1	9.0	9.0	8.4	0.9	.56	320	3	0.34	.1388	+0.18	1.0188	

DATE: 08/24/66

Time hrs	B	d	\bar{D}	E_t	h	\bar{H}_b	H_{bs}	H_s	\bar{h}_b	\bar{m}	Q_f	R_n	S	t_a	t_w	\bar{T}_b	T_s	u	\bar{V}	W_d	W_s	\bar{z}	$\bar{\alpha}_b$	η	ρ_l	ρ_s
		m	mm	m	m	m	m	m	m	(tan)	m^3	$\frac{g \text{ cal}}{cm^2 \text{ sec}}$		($^{\circ}C$)	($^{\circ}C$)	sec	sec	m	$\frac{m}{sec}$	($^{\circ}$)	$\frac{sec}{m}$	m	(tan)	$\frac{m}{hr}$	$\frac{g}{cm^3}$	$\frac{g}{cm^3}$
0000	J	12.0		1.615	0.16	.35	.47	.35	40	.0664			F	25.5	24.9	9.2	8.0	3.5	.60	321	3	0.43	.1656	+0.22	1.0183	
0100	J	12.0		1.737	0.24	.36	.47	.43	35	.0682			E	25.4	24.7	8.3	7.2	4.2	.54	341	6	0.45	.1763	+0.15	1.0182	
0200	J	13.0	.238	1.920	0.40	.36	.49	.58	25	.0717	+0.99		D	24.8	24.6	6.8	6.2	3.8	.46	017	9	0.46	.1763	+0.09	1.0182	2.6313
0300	J	14.0		1.920	0.52	.35	.49	.74	20	.0717			D	23.7	24.5	5.8	5.0	2.6	.36	020	10	0.46	.1673	0.00	1.0181	
0400	J	16.0		1.890	0.66	.34	.51	.90	20	.0647			E	22.7	24.5	5.4	4.0	1.4	.22	020	10	0.48	.1477	-0.08	1.0180	
0500	J	19.0		1.737	0.74	.31	.52	1.00	20	.0559			E	22.7	24.5	5.4	3.7	0.1	.10	021	9	0.48	.1192	-0.19	1.0180	
0600	K	22.0		1.524	0.76	.29	.54	.98	15	.0454			F	22.7	24.5	5.8	4.0	0.0	.02	022	8	0.49	.0875	-0.18	1.0179	
0700	K	24.5		1.402	0.72	.26	.59	.88	15	.0384			G	22.6	24.4	6.4	4.4	0.0	.08	024	7	0.50	.0489	-0.11	1.0178	
0800	L	25.5		1.310	0.68	.25	.55	.76	15	.0367			H	22.2	24.3	7.0	5.0	0.0	.16	029	6	0.50	.0052	0.00	1.0178	
0900	L	23.5	.328	1.341	0.62	.25	.56	.78	15	.0419	-1.44		H	19.7	24.2	7.3	4.8	0.0	.24	036	6	0.51	.0105	+0.04	1.0177	2.6193
1000	L	19.0		1.402	0.56	.26	.58	.82	20	.0540			G	17.2	24.1	7.3	4.6	0.0	.30	039	6	0.51	.0349	+0.09	1.0177	
1100	K	14.0		1.524	0.48	.31	.60	.95	35	.0682			F	17.2	23.9	6.9	4.2	0.0	.34	041	6	0.52	.0577	+0.16	1.0177	
1200	I	10.0		1.707	0.40	.38	.61	1.05	50	.0857			E	17.8	23.8	6.0	4.0	0.0	.36	050	5	0.52	.0752	+0.23	1.0177	
1300	H	7.5		1.951	0.32	.47	.68	1.04	60	.1033			E	18.8	23.7	5.8	4.2	0.0	.28	057	5	0.53	.0928	+0.21	1.0177	
1400	G	6.5		2.103	0.28	.56	.80	.95	55	.1175			D	19.8	23.6	6.0	4.6	0.2	.16	059	4	0.54	.1016	+0.12	1.0177	
1500	F	6.0		2.195	0.28	.64	.90	.72	55	.1281			D	20.0	23.5	6.5	5.3	1.4	.08	057	3	0.54	.1086	+0.01	1.0177	
1600	F	7.0	.372	2.164	0.32	.68	.95	.53	30	.1263	-0.85		D	20.0	23.5	7.0	6.0	1.2	.00	046	3	0.52	.1069	-0.08	1.0177	2.6318
1700	G	10.5		2.042	0.44	.66	.91	.45	25	.1104			D	20.7	23.6	7.3	6.5	0.2	.06	040	2	0.46	.1016	-0.16	1.0176	
1800	I	15.0		1.859	0.56	.57	.74	.38	25	.0840			E	21.5	23.7	7.2	7.0	0.0	.13	078	2	0.41	.0822	-0.20	1.0176	
1900	J	20.0		1.646	0.72	.44	.54	.32	25	.0594			E	22.0	23.9	6.8	7.6	0.0	.20	198	2	0.34	.0540	-0.23	1.0175	
2000	K	23.0		1.402	0.80	.30	.35	.30	30	.0402			F	22.2	24.0	6.0	8.0	0.0	.18	220	2	0.28	.0122	-0.22	1.0175	
2100	K	23.0		1.280	0.76	.24	.34	.31	30	.0402			H	21.8	24.1	5.5	8.0	0.0	.09	198	2	0.20	.0087	-0.11	1.0176	
2200	L	20.0	.291	1.189	0.64	.26	.37	.35	30	.0454	-0.15		I	21.6	24.0	5.4	7.8	0.0	.00	195	2	0.17	.0244	0.00	1.0177	2.6407
2300	K	21.0		1.250	0.52	.30	.44	.38	35	.0454			H	22.0	23.8	5.6	7.6	0.0	.16	204	2	0.22	.0314	+0.09	1.0177	

DATE: 08/25/66

TTime hrs	B	d m	\bar{D} mm	E_t m	h m	\bar{H}_b m	H_{bs} m	H_s m	$\bar{\lambda}_b$ m	\bar{m} (tan)	Q_f m^3	R_n g cal/ cm^2/sec	S	t_a (°C)	t_w (°C)	\bar{T}_b sec	T_s sec	u m	\bar{V} $\frac{m}{sec}$	W_{d_0} (°) sec	W_s $\frac{m}{sec}$	\bar{z} m	$\bar{\alpha}_b$ (tan)	η $\frac{m}{hr}$	ρ_l g/cm ³	ρ_s g/cm ³
0000	K	22.0		1.372	0.64	.36	.50	.42	35	.0454			G	22.2	23.7	5.8	7.0	0.0	.28	228	2	0.36	.0349	+0.14	1.0178	
0100	J	18.0		1.524	0.36	.42	.53	.40	40	.0524			G	21.8	23.5	6.3	6.6	0.0	.20	266	2	0.38	.0314	+0.18	1.0178	
0200	J	15.0		1.707	0.28	.44	.51	.39	40	.0577			F	21.6	23.3	6.8	6.2	0.0	.00	268	3	0.41	.0314	+0.16	1.0178	
0300	I	13.5		1.798	0.28	.42	.47	.37	45	.0577			E	21.6	23.1	7.1	6.0	1.0	.14	255	3	0.44	.0297	+0.06	1.0177	
0400	I	13.5	.222	1.829	0.32	.35	.41	.35	45	.0559	-0.65		E	21.6	22.9	7.2	6.0	1.7	.18	259	3	0.48	.0314	0.00	1.0177	2.6210
0500	I	13.5		1.798	0.34	.28	.42	.32	50	.0524			E	20.9	22.8	7.2	6.2	1.0	.12	260	2	0.47	.0349	-0.06	1.0178	
0600	J	14.0		1.707	0.36	.26	.44	.32	40	.0489			F	20.4	22.8	6.8	6.5	0.0	.00		C	0.44	.0349	-0.12	1.0179	
0700	J	14.0		1.554	0.40	.27	.50	.31	30	.0454			G	19.6	22.9	6.6	6.8	0.0	.12	180	1	0.39	.0314	-0.19	1.0181	
0800	K	15.0		1.341	0.44	.31	.55	.30	35	.0437			H	18.9	23.1	6.0	7.0	0.0	.24	121	1	0.32	.0349	-0.19	1.0182	
0900	K	16.5		1.189	0.48	.36	.57	.35	65	.0419			I	19.7	23.2	6.0	7.3	0.0	.34	087	2	0.27	.0472	-0.09	1.0183	
1000	K	17.0	.215	1.189	0.52	.41	.60	.38	100	.0437	-1.02		I	20.5	23.1	5.8	7.4	0.0	.40	092	2	0.25	.0699	0.00	1.0184	2.6370
1100	K	17.0		1.219	0.52	.45	.64	.41	135	.0454			I	18.7	23.0	5.5	7.7	0.0	.44	096	2	0.30	.1033	+0.08	1.0185	
1200	J	16.0		1.341	0.54	.48	.67	.49	155	.0489			H	17.0	22.9	5.0	8.0	0.0	.46	108	2	0.35	.1405	+0.17	1.0185	
1300	J	14.5		1.554	0.56	.50	.72	.48	135	.0540			G	17.5	22.8	5.4	8.2	0.0	.56	121	2	0.39	.1799	+0.24	1.0186	
1400	I	13.0		1.798	0.56	.54	.76	.44	105	.0577		.10	F	18.1	22.7	5.8	8.5	0.0	.68	138	3	0.38	.2162	+0.21	1.0185	
1500	I	11.5		1.951	0.56	.57	.80	.43	75	.0594		.12	E	18.8	22.7	6.1	8.8	0.0	.80	141	3	0.35	.2419	+0.13	1.0184	
1600	H	11.0		2.073	0.56	.60	.80	.43	50	.0630	-1.28	.18	E	19.5	22.7	6.3	9.0	0.5	.88	141	3	0.34	.2493	+0.09	1.0182	
1700	H	12.5	.327	2.073	0.60	.55	.72	.38	40	.0612		.25	E	21.2	22.7	6.4	8.6	0.6	.88	143	2	0.34	.2309	0.00	1.0183	2.6156
1800	I	15.5		2.012	0.60	.49	.60	.35	40	.0559		.11	E	22.2	22.7	6.2	8.0	0.0	.80	157	2	0.33	.1926	-0.10	1.0184	
1900	I	18.5		1.859	0.64	.41	.50	.31	45	.0489		-.01	F	21.4	22.6	5.9	7.3	0.0	.68	180	1	0.32	.1477	-0.23	1.0186	
2000	J	21.0		1.585	0.68	.35	.47	.30	60	.0454		-.03	F	20.5	22.6	5.2	7.0	0.0	.56	200	1	0.32	.1192	-0.26	1.0187	
2100	K	22.5		1.372	0.64	.34	.50	.30	60	.0419		-.03	G	20.1	22.5	5.0	7.2	0.0	.48	202	1	0.32	.0186	-0.19	1.0188	
2200	L	22.5		1.219	0.60	.34	.54	.30	60	.0437		-.03	H	20.0	22.4	4.7	7.4	0.0	.42	208	1	0.36	.1104	-0.10	1.0189	
2300	L	21.0	.205	1.219	0.56	.37	.57	.30	50	.0472		-.03	H	19.4	22.2	4.5	7.8	0.0	.40	213	1	0.40	.1228	0.00	1.0191	2.6248

DATE: 08/26/66

Time hrs	B	d	\bar{D}	E_t	h	\bar{H}_b	H_{bs}	H_s	\bar{x}_b	\bar{m}	Q_f	R_n	S	t_a	t_w	\bar{T}_b	T_s	u	\bar{V}	W_d	W_s	\bar{z}	$\bar{\alpha}_b$	η	ρ_l	ρ_s
		m	mm	m	m	m	m	m	m	(tan)	m^3	$\frac{g \text{ cal}}{cm^2 \text{ sec}}$		(°C)	(°C)	sec	sec	m	$\frac{m}{sec}$	$\frac{m}{sec}$	$\frac{m}{sec}$	m	(tan)	$\frac{m}{hr}$	$\frac{g}{cm^3}$	$\frac{g}{cm^3}$
0000	L	20.0		1.280	0.52	.39	.57	.30	50	.0524	-1.66	-.03	H	18.8	22.1	4.4	8.0	0.0	.36	219	1	0.43	.1370	+0.08	1.0191	
0100	K	19.0		1.372	0.48	.40	.54	.32	45	.0540		-.03	H	18.6	21.9	4.5	8.0	0.0	.36	223	2	0.47	.1495	+0.13	1.0192	
0200	J	17.5		1.524	0.44	.38	.50	.36	45	.0540		-.03	G	18.3	21.6	4.6	8.0	0.0	.35	238	2	0.51	.1495	+0.15	1.0195	
0300	I	16.0		1.676	0.40	.35	.45	.40	45	.0524		-.03	F	18.2	21.4	4.7	8.0	0.0	.32	257	2	0.54	.1423	+0.16	1.0197	
0400	I	15.0		1.829	0.36	.30	.44	.42	50	.0489		-.02	E	18.3	21.3	4.8	8.0	0.2	.32	270	3	0.58	.1281	+0.12	1.0199	
0500	I	15.0	.248	1.890	0.36	.28	.44	.38	55	.0472	-0.79	-.02	E	18.5	21.3	5.1	8.0	0.4	.36	271	3	0.58	.1210	0.00	1.0199	2.6339
0600	I	14.5		1.798	0.40	.30	.44	.35	55	.0437		-.02	D	18.8	21.2	5.5	8.0	0.2	.44	269	3	0.50	.1263	-0.12	1.0193	
0700	J	14.5		1.646	0.48	.30	.41	.32	55	.0437		.03	E	19.5	21.2	5.9	8.0	0.0	.56	269	2	0.36	.1405	-0.14	1.0192	
0800	J	16.0		1.524	0.52	.32	.41	.30	55	.0437		.15	F	20.0	21.1	6.2	8.0	0.0	.65	264	2	0.23	.1441	-0.16	1.0191	
0900	K	20.0		1.341	0.64	.29	.40	.30	55	.0489		.30	H	21.2	21.2	6.1	7.6	0.0	.61	264	2	0.27	.1459	-0.18	1.0193	
1000	L	23.0		1.189	0.68	.28	.40	.30	55	.0630		.40	J	22.7	21.3	5.9	7.4	0.0	.50	262	2	0.34	.1477	-0.13	1.0192	
1100	L	24.0	.296	1.097	0.70	.27	.43	.30	60	.0699	-0.82	.45	J	23.4	21.7	5.4	7.1	0.0	.38	222	2	0.36	.1423	0.00	1.0191	2.6303
1200	K	21.0		1.189	0.60	.30	.50	.30	60	.0507		.50	I	23.8	22.4	4.9	7.0	0.0	.33	137	2	0.26	.1405	+0.12	1.0190	
1300	J	17.5		1.341	0.60	.34	.59	.30	60	.0507		.50	G	24.1	23.3	4.8	7.2	0.0	.37	071	3	0.26	.1370	+0.17	1.0187	
1400	I	16.0		1.524	0.56	.39	.71	.30	50	.0559		.38	E	24.5	23.5	5.0	7.4	0.0	.47	072	3	0.27	.1317	+0.20	1.0184	
1500	I	14.0		1.737	0.56	.45	.82	.30	40	.0630		.34	D	23.8	23.7	5.2	7.8	0.0	.56	086	3	0.28	.1246	+0.22	1.0181	
1600	H	13.0		1.951	0.60	.51	.84	.30	35	.0682	+1.22	.31	C	23.3	23.9	5.4	8.0	3.4	.62	117	3	0.28	.1157	+0.16	1.0178	
1700	I	14.0		2.073	0.56	.53	.80	.30	30	.0682		.11	B	23.5	24.0	5.4	8.0	2.4	.64	141	3	0.30	.1086	+0.07	1.0176	
1800	I	15.5		2.103	0.52	.52	.75	.30	35	.0630		.08	C	23.8	24.0	5.6	8.0	0.0	.62	160	3	0.30	.1016	-0.01	1.0175	
1900	I	17.0		1.981	0.48	.47	.67	.30	35	.0540		.03	C	23.9	23.8	5.6	8.0	0.0	.60	170	3	0.32	.0981	-0.14	1.0174	
2000	J	18.0		1.829	0.48	.42	.60	.30	40	.0472		.00	E	23.9	23.7	5.6	7.9	0.0	.56	179	3	0.32	.1033	-0.21	1.0173	
2100	J	18.0		1.585	0.52	.34	.50	.30	40	.0454		.00	F	23.9	23.7	5.7	8.0	0.0	.48	182	3	0.32	.1157	-0.25	1.0172	
2200	J	18.5		1.341	0.62	.26	.42	.30	35	.0472		.00	G	23.8	23.7	5.6	8.0	0.0	.40	194	2	0.31	.1299	-0.21	1.0171	
2300	K	20.0		1.189	0.68	.20	.35	.30	30	.0507		.00	H	23.6	23.7	5.6	8.0	0.0	.32	200	2	0.29	.1423	-0.07	1.0170	

DATE: 08/27/66

Time hrs	B	d	\bar{D}	E_t	h	\bar{H}_b	H_{bs}	H_s	\bar{z}_b	\bar{m}	Q_f	R_n	S	t_a	t_w	\bar{T}_b	T_s	u	\bar{V}	W_d	W_s	\bar{z}	$\bar{\alpha}_b$	η	ρ_g	ρ_s
	m	m	mm	m	m	m	m	m	m	(tan)	m^3	$\frac{g \text{ cal}}{cm^2/sec}$		(°C)	(°C)	sec	sec	m	$\frac{m}{sec}$	($^\circ$)	$\frac{m}{sec}$	m	(tan)	$\frac{m}{hr}$	$\frac{g}{cm^3}$	$\frac{g}{cm^3}$
0000	K	21.0		1.189	0.68	.16	.27	.30	30	.0524		.00	H	23.3	23.7	5.6	8.0	0.0	.25	208	2	0.28	.1477	0.00	1.0169	
0100	K	20.5	.222	1.280	0.60	.15	.30	.30	30	.0559	+0.76	.00	H	23.2	23.7	5.8	8.0	0.0	.33	212	2	0.26	.1405	+0.07	1.0171	2.6356
0200	J	18.0		1.341	0.44	.19	.35	.30	40	.0647		.00	H	23.2	23.8	5.8	8.0	0.0	.48	222	2	0.28	.1228	+0.10	1.0172	
0300	I	12.0		1.494	0.30	.26	.41	.30	45	.0770		.00	G	23.1	23.8	5.8	8.0	0.0	.57	237	1	0.29	.1052	+0.25	1.0174	
0400	H	7.5		1.798	0.28	.32	.47	.30	50	.0875		.00	E	22.8	23.8	5.8	8.0	0.0	.60	249	1	0.30	.0875	+0.27	1.0176	
0500	H	8.0		1.859	0.40	.35	.50	.28	50	.0910		.00	E	22.0	23.6	5.7	8.3	3.6	.55	265	1	0.36	.0734	+0.03	1.0178	
0600	I	14.5	.244	1.859	0.56	.35	.53	.25	50	.0840	-0.85	-.04	D	21.0	23.5	5.8	8.9	4.7	.44	278	1	0.40	.0612	0.00	1.0179	2.6319
0700	I	19.0		1.829	0.64	.35	.54	.22	55	.0734		-.02	D	20.5	23.3	6.1	9.4	2.9	.28	285	2	0.38	.0524	-0.11	1.0181	
0800	J	19.0		1.676	0.60	.35	.54	.20	60	.0612		.11	E	20.4	23.0	6.4	10.0	0.0	.10	291	2	0.31	.0489	-0.17	1.0182	
0900	J	17.0		1.494	0.60	.35	.61	.20	60	.0540		.28	F	20.7	22.8	6.6	10.5	0.0	.00	296	3	0.28	.0559	-0.20	1.0183	
1000	L	21.0		1.280	0.60	.40	.70	.20	60	.0489		.40	G	21.2	22.8	6.8	11.2	0.0	.08	307	3	0.32	.0630	-0.19	1.0183	
1100	M+	38.0		1.128	0.68	.46	.80	.20	60	.0472		.52	H	21.9	23.1	7.2	11.6	0.0	.16	307	3	0.40	.0857	-0.09	1.0183	
1200	M+	57.0	.187	1.097	0.64	.54	.86	.21	60	.0454	+1.04	.58	H	22.8	23.4	7.6	12.1	0.0	.22	312	2	0.45	.0963	0.00	1.0182	2.6516
1300	M+	44.0		1.189	0.56	.56	.86	.22	60	.0437		.60	G	23.9	23.8	8.2	12.6	0.0	.30	316	2	0.46	.1033	+0.12	1.0182	
1400	M	29.0		1.341	0.48	.54	.78	.26	60	.0454		.57	G	25.0	24.4	8.6	13.2	0.0	.34	319	2	0.48	.1016	+0.19	1.0181	
1500	J	18.0		1.585	0.36	.46	.65	.28	60	.0489		.50	F	26.6	24.7	9.0	13.6	1.2	.38	317	2	0.50	.0963	+0.26	1.0178	
1600	I	12.0		1.676	0.30	.39	.56	.30	60	.0559		.38	E	27.6	24.8	9.1	13.8	2.8	.42	308	2	0.51	.0910	+0.23	1.0175	
1700	I	9.5		1.920	0.36	.38	.56	.31	70	.0840		.22	D	26.8	24.9	9.0	13.8	3.8	.45	292	2	0.52	.1210	+0.16	1.0175	
1800	I	10.5	.324	2.103	0.40	.43	.61	.35	90	.0963	+2.25	.10	C	26.0	24.9	9.2	13.8	4.2	.47	267	2	0.51	.1548	0.00	1.0174	2.6331
1900	I	14.5		2.164	0.60	.46	.66	.38	105	.0928		-.02	C	25.0	24.8	9.2	13.8	3.5	.48	245	2	0.48	.1908	-0.08	1.0174	
2000	J	21.0		2.073	0.76	.48	.70	.42	115	.0734		-.03	D	24.5	24.6	9.4	13.8	2.4	.51	229	2	0.45	.2259	-0.17	1.0173	
2100	K	23.0		1.920	0.80	.46	.64	.38	120	.0594		-.03	D	24.1	24.4	9.5	13.8	0.0	.50	223	2	0.40	.2254	-0.22	1.0174	
2200	L	21.0		1.707	0.68	.41	.48	.36	110	.0489		-.03	E	23.8	24.2	9.8	13.8	0.0	.49	233	3	0.34	.2016	-0.21	1.0175	
2300	M+	18.0		1.433	0.60	.31	.31	.32	95	.0415		-.05	F	23.6	24.0	10.2	13.8	0.0	.49	240	3	0.25	.1817	-0.19	1.0176	

DATE: 08/28/66

Time hrs	B	d	\bar{D}	E_t	h	\bar{H}_b	H_{bs}	H_s	\bar{x}_b	\bar{m}	Q_f	R_n	S	t_a	t_w	\bar{T}_b	T_s	u	\bar{V}	W_{d^0}	W_s	\bar{z}	$\bar{\alpha}_b$	η	ρ_k	ρ_s
		m	mm	m	m	m	m	m	(tan)	m^3	$g\ cal/cm^2/sec$			(°C)	(°C)	sec	sec	m	m	($^{\circ}$)	$\frac{m}{sec}$	m	(tan)	$\frac{m}{hr}$	g/cm^3	g/cm^3
0000	M ⁺ ₅₀	16.0		1.219	0.60	.17	.20	.30	90	.0367		-.04	G	23.2	24.0	10.6	13.8	0.0	.48	249	3	0.18	.1602	-0.08	1.0178	
0100	M ⁺ ₅	15.5	.196	1.219	0.56	.15	.25	.35	80	.0349	+1.43	-.04	H	22.8	24.0	10.8	13.7	0.0	.45	260	3	0.18	.1584	0.00	1.0179	2.6345
0200	M ⁺ ₃₀	16.0		1.280	0.48	.22	.36	.41	80	.0367		-.03	G	22.2	23.9	10.8	13.3	0.0	.46	261	3	0.26	.1620	+0.11	1.0179	
0300	M	17.0		1.433	0.40	.32	.50	.50	75	.0402		-.03	F	21.6	23.9	10.9	13.2	2.0	.47	262	3	0.38	.1890	+0.19	1.0179	
0400	J	17.0		1.646	0.40	.45	.59	.58	75	.0437		-.04	D	21.0	23.9	11.0	13.0	6.0	.48	264	3	0.44	.1944	+0.22	1.0180	
0500	J	16.5		1.859	0.52	.48	.58	.50	80	.0577		-.04	C	20.9	23.8	11.0	13.0	5.1	.51	264	3	0.44	.1926	+0.14	1.0180	
0600	I	16.5		1.951	0.64	.45	.55	.48	80	.0682		-.04	C	21.0	23.7	10.8	13.0	3.2	.56	268	3	0.46	.1871	+0.04	1.0180	
0700	I	17.5	.280	1.951	0.64	.39	.50	.45	90	.0717	+0.43	-.03	D	21.3	23.6	10.7	13.0	1.9	.62	282	3	0.47	.1835	-0.02	1.0180	2.6271
0800	J	20.0		1.859	0.60	.32	.45	.40	90	.0682		.07	E	21.8	23.5	10.5	13.0	0.0	.71	308	2	0.48	.1817	-0.13	1.0180	
0900	L	24.0		1.707	0.56	.25	.38	.38	90	.0612		.22	F	23.7	23.4	10.4	12.7	0.0	.72	310	2	0.49	.1799	-0.19	1.0179	
1000	M	30.0		1.494	0.52	.24	.35	.35	95	.0559		.36	G	25.5	23.4	10.4	12.5	0.0	.68	351	2	0.50	.1799	-0.20	1.0178	
1100	M ⁺ ₁₅	36.0		1.310	0.52	.25	.35	.33	95	.0507		.46	H	26.1	23.6	10.4	12.2	0.0	.56	359	2	0.51	.1799	-0.15	1.0177	
1200	M ⁺ ₃₅	43.0		1.189	0.50	.30	.34	.30	100	.0472		.58	H	26.6	24.5	10.6	12.0	0.0	.49	359	2	0.52	.1799	-0.09	1.0176	
1300	M ⁺ ₅₀	46.0	.229	1.128	0.52	.37	.37	.40	100	.0437	-0.13	.60	H	27.0	25.2	11.0	12.0	0.0	.54	360	2	0.54	.1817	0.00	1.0175	2.6413
1400	M ⁺ ₅₅	47.0		1.219	.44	.44	.44	.50	105	.0419		.52	H	27.3	25.3	11.6	12.0	0.0	.58	005	2	0.61	.1745	+0.16	1.0175	
1500	M ⁺ ₅₅	45.0		1.433	.50	.50	.52	.63	120	.0402		.49	G	26.7	25.3	12.2	12.0	0.4	.66	024	2	0.68	.1584	+0.23	1.0174	
1600	M ⁺ ₄₅	42.0		1.676	.54	.54	.57	.75	135	.0402		.38	F	26.0	25.3	12.4	12.0	2.1	.75	047	2	0.74	.1388	+0.25	1.0173	
1700	M ⁺ ₁₅	39.0		1.920	.54	.54	.57	.73	155	.0612		.24	E	26.0	25.3	12.1	12.0	2.0	.82	081	2	0.70	.1228	+0.22	1.0173	
1800	L	27.0		2.103	.50	.50	.55	.68	165	.0963		.10	E	26.0	25.2	11.6	12.0	1.5	.86	129	2	0.64	.1122	+0.14	1.0174	
1900	J	22.0		2.164	.44	.44	.52	.60	160	.1175		-.01	E	25.5	25.1	11.0	12.0	1.2	.88	166	2	0.60	.1122	0.00	1.0174	
2000	J	19.0		2.073	.37	.37	.50	.59	145	.1210	+1.08	-.04	E	24.5	25.0	10.8	12.0	0.7	.88	194	2	0.55	.1122	-0.13	1.0174	
2100	J	19.0		1.920	.33	.33	.45	.53	115	.1104		-.04	E	23.8	24.9	10.6	12.0	0.0	.84	204	2	0.50	.1139	-0.19	1.0175	
2200	K	21.0		1.707	.30	.30	.43	.50	85	.0875		-.04	F	23.4	24.8	10.2	12.0	0.0	.76	215	2	0.46	.1157	-0.25	1.0175	
2300	K	23.5		1.433	.30	.30	.42	.47	60	.0577		-.05	G	22.8	24.8	9.8	11.9	0.0	.68	220	2	0.41	.1192	-0.26	1.0175	

DATE: 08/29/66

Time hrs	B	d m	\bar{D} mm	E_t m	h m	\bar{H}_b m	H_{bs} m	H_s m	\bar{z}_b m	\bar{m} (tan)	Q_f m ³	R_n g cal/cm ² /sec	S	t_a (°C)	t_w (°C)	\bar{T}_b sec	T_s sec	u m	\bar{V} m/sec	W_{d^0} ()	W_s m/sec	\bar{z} m	$\bar{\alpha}_b$ (tan)	η m/hr	ρ_L g/cm ³	ρ_s g/cm ³
0000	L	25.0		1.219	0.92	.32	.42	.45	.45	.0402	+1.99		G	22.3	24.7	9.6	11.9	0.0	.58	228	2	0.36	.1228	-0.14	1.0175	
0100	L	25.5		1.158	0.76	.34	.44	.42	.45	.0314			H	21.9	24.7	9.4	11.6	0.0	.56	238	2	0.40	.1281	-0.02	1.0176	
0200	M	23.5	.183	1.158	0.60	.35	.45	.40	.55	.0297			H	21.6	24.6	9.3	11.4	0.0	.55	240	2	0.44	.1281	+0.01	1.0176	2.6194
0300	M+30	22.0		1.280	0.48	.36	.45	.40	.70	.0314			G	22.0	24.5	9.3	11.2	0.3	.60	242	2	0.48	.1317	+0.17	1.0177	
0400	M+45	20.0		1.524	0.44	.35	.46	.42	.90	.0367			F	22.7	24.4	9.4	11.0	1.4	.67	249	2	0.52	.1405	+0.22	1.0177	
0500	M+50	18.5		1.707	0.40	.35	.51	.47	1.00	.0507			F	22.9	24.3	9.7	11.2	1.6	.70	248	2	0.55	.1459	+0.22	1.0177	
0600	M+15	16.0		1.951	0.48	.36	.56	.53	1.10	.0822			F	22.9	24.4	10.0	11.4	1.0	.76	247	3	0.58	.1566	+0.16	1.0177	
0700	I	14.0		2.012	0.58	.38	.60	.60	1.15	.1016			E	22.9	24.5	10.5	11.7	0.3	.88	238	3	0.60	.1709	0.00	1.0177	
0800	H	13.5	.334	1.981	0.64	.45	.60	.68	1.20	.0998	+1.61		E	24.7	24.6	10.8	12.0	0.0	.96	226	3	0.59	.1799	-0.08	1.0176	2.6172
0900	J	14.0		1.859	0.70	.47	.55	.60	1.30	.0928			E	24.5	24.8	11.0	11.7	0.0	.98	216	3	0.55	.1817	-0.14	1.0176	
1000	L	17.0		1.707	0.76	.47	.54	.54	1.40	.0805			F	27.3	25.0	11.0	11.5	0.0	1.00	200	3	0.52	.1853	-0.23	1.0175	
1100	M+30	22.0		1.463	0.78	.45	.50	.50	1.45	.0664			F	26.9	25.2	10.8	11.2	0.0	1.01	186	4	0.48	.1890	-0.23	1.0174	
1200	M+60	28.5		1.250	0.80	.43	.49	.42	1.50	.0524			G	26.6	25.5	10.6	11.0	0.0	1.02	177	4	0.42	.1908	-0.19	1.0173	
1300	M+75	36.0		1.097	0.84	.40	.47	.50	1.50	.0402			H	26.9	25.8	10.4	10.5	0.0	1.02	163	4	0.40	.1944	0.00	1.0173	
1400	M+85	42.5	.195	1.158	0.92	.35	.47	.59	1.50	.0297	+2.22		H	27.2	26.2	10.1	10.0	0.0	1.00	158	4	0.40	.1944	+0.09	1.0172	2.6588
1500	M+15	47.0		1.280	0.96	.35	.48	.65	1.30	.0227			H	26.6	26.3	9.7	9.4	0.0	.96	147	4	0.46	.1871	+0.18	1.0172	
1600	M+30	48.0		1.524	0.76	.38	.49	.73	1.10	.0244			G	26.1	26.4	9.4	9.0	0.0	.94	144	4	0.54	.1781	+0.25	1.0172	
1700	L	41.0		1.768	0.60	.38	.49	.68	1.00	.0332			F	25.8	26.3	9.2	9.2	0.0	.90	150	4	0.62	.1745	+0.23	1.0173	
1800	J	30.0		1.981	0.48	.38	.51	.64	.95	.0524			E	25.5	26.2	9.0	9.5	0.0	.93	169	4	0.68	.1745	+0.17	1.0173	
1900	H	18.5		2.103	0.40	.37	.54	.61	.95	.0875			E	24.9	26.0	9.0	9.8	2.7	1.04	181	4	0.76	.1745	+0.07	1.0174	
2000	G	12.0	.437	2.134	0.38	.37	.54	.60	.95	.1033	-0.84		D	24.4	25.8	9.0	10.0	3.8	1.12	189	4	0.82	.1763	0.00	1.0175	2.6480
2100	H	10.0		2.062	0.44	.35	.50	.57	1.00	.0963			E	24.0	25.6	9.0	10.5	1.5	1.12	188	4	0.77	.1817	-0.14	1.0179	
2200	J	13.0		1.859	0.68	.34	.44	.52	1.05	.0805			E	23.4	25.2	9.2	11.0	0.0	1.04	188	4	0.59	.1890	-0.23	1.0182	
2300	K	20.5		1.615	0.84	.28	.36	.50	1.10	.0559			G	22.8	24.6	9.4	11.5	0.0	.95	192	4	0.39	.1944	-0.24	1.0185	

DATE: 08/30/66

Time hrs	B	d	\bar{D}	E_t m	h	\bar{H}_b m	H_{bs} m	H_s m	\bar{h}_b m	\bar{m} (tan)	Q_f m^3	R_n g cal/ cm^2/sec	S	t_a (°C)	t_w (°C)	\bar{T}_b sec	T_s sec	u	\bar{V} $\frac{m}{sec}$	W_d (°) sec	W_s $\frac{m}{sec}$	\bar{z} m	$\bar{\alpha}_b$ (tan)	η $\frac{m}{hr}$	ρ_λ g/cm ³	ρ_s g/cm ³
0000	L	25.0		1.341	0.94	.24	.31	.48	.120	.0332	+1.30		H	22.6	23.7	9.6	12.0	0.0	.86	191	4	0.30	.1944	-0.20	1.0189	
0100	L	25.5		1.158	0.84	.22	.36	.48	.120	.0367		I	22.4	22.3	9.8	11.7	0.0	.80	189	4	0.28	.1908	-0.13	1.0191		
0200	L	23.0	.201	1.097	0.76	.24	.40	.50	.105	.0419		I	22.2	22.2	9.8	11.5	0.0	.78	189	4	0.32	.1908	0.00	1.0193	2.6453	
0300	M	24.0		1.189	0.72	.27	.44	.51	.85	.0367		H	22.2	22.3	9.8	11.2	0.0	.76	192	3	0.36	.1890	+0.12	1.0195		
0400	M	26.5		1.341	0.72	.34	.51	.51	.75	.0314		G	22.3	22.5	9.6	11.0	0.0	.76	196	3	0.42	.1835	+0.19	1.0198		
0500	M	27.5		1.585	0.72	.40	.62	.53	.80	.0332		F	21.9	22.5	9.6	11.0	0.0	.78	200	2	0.48	.1835	+0.23	1.0198		
0600	M	26.5		1.768	0.74	.45	.72	.53	.115	.0384		E	21.6	22.5	9.2	11.0	0.0	.88	222	2	0.51	.1908	+0.18	1.0198		
0700	M	24.0		1.951	0.72	.51	.77	.53	.155	.0437		D	22.6	22.4	8.7	10.9	2.2	.96	178	2	0.57	.1926	+0.12	1.0199		
0800	L	20.5		2.012	0.72	.56	.77	.56	.200	.0472	+1.35		D	23.8	22.3	8.6	11.0	3.4	.96	091	2	0.59	.1871	0.00	1.0199	
0900	L	20.0	.273	1.951	0.72	.57	.68	.51	.220	.0454		D	25.0	22.2	9.0	11.0	2.4	.88	091	2	0.58	.1781	-0.09	1.0199	2.6387	
1000	M	22.5		1.829	0.76	.54	.58	.49	.230	.0402		F	26.0	22.1	9.8	11.0	0.0	.77	090	3	0.50	.1584	-0.19	1.0197		
1100	M	28.0		1.585	0.80	.44	.48	.47	.230	.0332		G	25.5	22.1	10.5	11.0	0.0	.64	090	3	0.42	.1370	-0.24	1.0195		
1200	M	35.5		1.372	0.88	.34	.40	.45	.220	.0262		H	24.9	22.2	11.0	11.0	0.0	.54	088	3	0.35	.1210	-0.21	1.0192		
1300	M	44.0		1.158	1.00	.30	.40	.50	.200	.0227		I	24.8	22.0	10.8	10.7	0.0	.52	088	4	0.33	.1157	-0.16	1.0191		
1400	M	49.5	.270	1.067	1.32	.30	.40	.52	.180	.0367	+1.85	I	24.9	22.0	10.2	10.5	0.0	.59	091	4	0.37	.1210	0.00	1.0189	2.6303	
1500	M	44.0		1.158	1.12	.33	.41	.56	.165	.0419		H	24.9	22.6	9.2	10.2	0.0	.71	093	5	0.44	.1299	+0.13	1.0188		
1600	M	34.0		1.310	0.68	.38	.43	.58	.150	.0367		G	24.9	23.8	8.4	10.0	0.0	.82	094	5	0.52	.1477	+0.20	1.0188		
1700	L	25.0		1.554	0.56	.42	.46	.61	.125	.0367		G	24.9	24.8	8.4	10.0	0.0	.96	124	5	0.54	.1656	+0.23	1.0188		
1800	J	17.5		1.768	0.44	.45	.51	.65	.95	.0559		F	24.9	24.9	8.9	10.0	0.0	1.08	125	5	0.56	.1853	+0.23	1.0188		
1900	I	12.0		2.012	0.40	.46	.56	.70	.75	.0840		E	25.2	24.9	9.6	10.0	0.7	1.12	123	5	0.58	.2035	+0.21	1.0188		
2000	H	11.0	.372	2.134	0.44	.45	.60	.74	.65	.1016	-0.82	D	25.5	24.9	9.9	10.0	1.1	1.08	122	4	0.59	.2126	+0.01	1.0189	2.6533	
2100	H	14.0		2.103	0.60	.42	.60	.69	.70	.0945		D	25.0	24.7	10.2	10.7	1.0	.90	119	4	0.55	.2053	-0.09	1.0189		
2200	I	19.0		1.951	0.84	.36	.55	.60	.100	.0805		E	24.5	24.6	10.3	11.5	0.2	.72	105	4	0.50	.1871	-0.17	1.0189		
2300	K	24.0		1.768	1.00	.33	.51	.54	.135	.0612		E	24.0	24.5	10.0	12.2	0.0	.52	097	3	0.46	.1691	-0.23	1.0189		

DATE: 08/31/66

Time hrs	B	d	\bar{D}	E_t	h	\bar{H}_b	H_{bs}	H_g	\bar{H}_b	\bar{m}	Q_f	R_n	S	t_a	t_w	\bar{T}_b	T_B	u	\bar{V}	W_d	W_s	\bar{z}	$\bar{\alpha}_b$	η	ρ_L	ρ_s	
		m	mm	m	m	m	m	m	m	(tan)	m^3	$\frac{g \text{ cal}}{cm^2 \text{ sec}}$		(°C)	(°C)	sec	sec	m	$\frac{m}{sec}$	(°)	$\frac{m}{sec}$	$\frac{m}{sec}$	m	(tan)	$\frac{m}{hr}$	$\frac{g}{cm^3}$	$\frac{g}{cm^3}$
0000	L	29.0		1.494	1.08	.30	.46	.50	155	.0437		-.05	F	23.7	24.4	9.7	13.0	0.0	.40	.091	3	0.41	.1584	-0.27	1.0190		
0100	L	31.0		1.250	1.04	.26	.44	.58	150	.0384		-.05	H	23.2	24.3	9.6	12.5	0.0	.42	.082	3	0.51	.1673	-0.21	1.0191		
0200	M	32.0		1.067	1.12	.25	.44	.61	135	.0402		-.05	I	22.7	24.3	9.4	12.0	0.0	.58	.068	3	0.66	.2035	-0.06	1.0192		
0300	M+ 35	32.0	.224	1.097	1.28	.25	.41	.68	110	.0437	+2.49	-.05	I	22.5	24.2	9.6	11.5	0.0	.78	.062	3	0.62	.2493	+0.08	1.0192	2.6543	
0400	M+ 100	53.5		1.219	1.60	.28	.41	.72	90	.0489		-.05	H	22.3	24.1	10.0	11.0	0.0	.99	.057	3	0.28	.2867	+0.18	1.0193		
0500	M+ 100	46.0		1.433	1.60	.38	.49	.75	120	.0540		-.05	G	22.5	24.1	10.4	10.7	0.0	1.16	.048	3	0.24	.3057	+0.23	1.0193		
0600	M+ 75	36.0		1.676	1.52	.48	.62	.80	160	.0594		-.04	F	22.7	24.1	10.6	10.4	0.0	1.28	.046	3	0.26	.3172	+0.19	1.0192		
0700	M+ 50	30.0		1.829	1.44	.52	.74	.84	205	.0647		-.01	E	22.8	24.1	10.8	10.2	0.0	1.36	.040	4	0.29	.3134	+0.15	1.0189		
0800	L	25.0		1.981	1.36	.60	.82	.89	235	.0682		.11	D	22.8	24.2	10.8	10.0	0.2	1.40	.041	4	0.32	.2962	+0.12	1.0188		
0900	J	22.5	.334	2.073	1.28	.61	.86	.89	235	.0734	+3.00	.21	D	23.5	24.3	11.0	11.0	0.9	1.39	.042	4	0.34	.2530	0.00	1.0186	2.6449	
1000	I	22.0		1.981	1.12	.62	.86	.90	220	.0787		.34	D	24.4	24.5	11.1	12.1	0.0	1.28	.053	4	0.38	.2035	-0.15	1.0185		
1100	I	22.5		1.798	0.96	.62	.82	.90	200	.0734		-.48	F	24.7	24.7	11.2	13.2	0.0	1.08	.051	4	0.40	.1673	-0.21	1.0184		
1200	I	23.0		1.585	0.86	.60	.75	.93	190	.0770		.52	F	24.9	24.8	11.4	13.0	0.0	.92	.048	4	0.42	.1584	-0.22	1.0183		
1300	J	23.5		1.372	0.84	.55	.63	.78	175	.0717		-.51	F	24.7	24.9	10.9	13.3	0.0	.86	.046	4	0.43	.1620	-0.20	1.0183		
1400	K	23.5		1.219	0.88	.46	.53	.63	155	.0664		.44	G	24.5	24.9	10.6	13.8	0.0	.84	.042	4	0.43	.1799	-0.13	1.0183		
1500	L	23.0	.246	1.128	0.92	.37	.45	.76	140	.0612	+0.44	.29	H	24.4	25.0	9.9	13.6	0.0	.88	.040	4	0.43	.2071	0.00	1.0183	2.6404	
1600	M	23.5		1.219	0.88	.30	.43	.97	120	.0594		.26	H	24.5	25.0	9.2	13.0	0.0	.94	.039	5	0.43	.2401	+0.14	1.0183		
1700	K	24.5		1.402	1.08	.26	.46	1.09	95	.0612		.23	F	24.0	25.0	8.8	13.3	0.0	.99	.039	5	0.44	.2586	+0.20	1.0182		
1800	J	24.0		1.615	.25	.52	.52	1.20	75	.0647		.15	C	23.7	25.0	8.8	13.7	0.0	1.02	.040	5	0.49	.2679	+0.28	1.0182		
1900	I	22.0		1.920	.28	.57	.57	1.25	60	.0717		-.03	A	23.9	24.8	9.0	12.8	0.0	1.04	.042	6	0.54	.2736	+0.29	1.0182		
2000	G	21.0	.286	2.103	.35	.60	.60	1.28	55	.0787	-2.37	-.07	A+	24.4	24.8	9.0	12.1	10.0	1.00	.043	7	0.60	.2679	+0.10	1.0182	2.6868	
2100	G	20.5		2.164	.39	.57	.57	1.37	45	.0857		-.07	A+	24.7	24.9	8.9	11.7	11.4	.92	.044	8	0.59	.2642	0.00	1.0181		
2200	H	21.0		2.103	.40	.56	.56	1.45	40	.0840		-.06	A+	24.8	24.8	8.5	11.7	8.4	.72	.046	8	0.56	.2456	-0.10	1.0181		
2300	I	20.5		1.951	.40	.55	.55	1.22	30	.0787		-.06	B	24.8	24.7	8.0	11.7	0.0	.54	.052	8	0.52	.2180	-0.19	1.0181		

DATE: 09/01/66

Time hrs	B	d m	\bar{D} mm	E_t m	h m	\bar{H}_b m	H_{bs} m	H_s m	\bar{x}_b m	\bar{m} (tan)	Q_f m^3	R_n g cal/ cm^2/sec	S	t_a (°C)	t_w (°C)	\bar{T}_b sec	T_s sec	u m	\bar{V} m sec	W_d (°) sec	W_s m sec	\bar{z} m	$\bar{\alpha}_b$ (tan)	η m hr	ρ_l g/cm ³	ρ_s g/cm ³
0000	J	21.5		1.737	.38	.54	1.02	30	.0699		-.05	E	24.9	24.5	7.6	11.7	0.0	.46	065	7	0.46	.1799	-0.23	1.0181		
0100	K	23.0		1.494	.35	.54	1.02	30	.0630		-.05	F	24.9	24.4	7.2	11.4	0.0	.47	057	7	0.40	.1370	-0.25	1.0181		
0200	L	24.0		1.250	.34	.54	1.05	40	.0559		-.05	G	24.9	24.4	6.7	11.0	0.0	.48	023	8	0.30	.1016	-0.17	1.0181		
0300	L	24.0	.387	1.219	.34	.51	1.10	60	.0524	-4.67	-.05	H	24.9	24.4	6.0	10.0	0.0	.51	022	8	0.31	.0805	0.00	1.0181	2.6500	
0400	L	22.5		1.280	.35	.54	1.20	85	.0540		-.04	G	24.9	24.4	5.6	9.2	0.0	.54	020	9	0.30	.0752	+0.18	1.0182		
0500	K	19.5		1.463	.40	.60	1.17	95	.0594		-.04	F	24.8	24.2	5.4	8.6	0.0	.56	018	8	0.34	.0875	+0.20	1.0181		
0600	J	16.0		1.676	.47	.67	1.17	100	.0682		-.03	D	23.8	24.1	5.9	8.3	0.0	.60	018	8	0.46	.1139	+0.24	1.0181		
0700	H	13.5		1.920	.55	.75	1.18	110	.0787		-.02	C	23.5	24.1	6.5	8.2	5.5	.62	012	8	0.60	.1477	+0.23	1.0180		
0800	G	12.0		2.134	.62	.85	1.20	120	.0857		.09	A	23.4	24.0	7.0	8.0	11.8	.64	011	8	0.68	.1781	+0.18	1.0180		
0900	F	18.5	.296	2.255	.64	.86	1.34	120	.0857	-5.07	.12	A+	23.0	24.1	7.2	8.4	8.5	.60	009	8	0.66	.1763	+0.06	1.0179	2.6647	
1000	F	24.0		2.255	.63	.85	1.50	115	.0770		.15	A+	22.8	24.1	6.8	8.5	7.0	.52	006	7	0.57	.1584	-0.08	1.0178		
1100	H	27.5		2.073	.58	.80	1.42	105	.0647		.32	A	23.8	24.2	6.0	8.4	1.8	.48	003	7	0.50	.1317	-0.17	1.0177		
1200	J	28.0		1.890	.54	.75	1.36	100	.0540		.47	C	24.3	24.1	5.2	8.2	0.0	.39	007	6	0.42	.1086	-0.19	1.0177		
1300	K	29.5		1.676	.49	.67	1.41	90	.0472		.52	D	25.1	24.2	5.0	7.8	0.0	.44	018	5	0.48	.0963	-0.24	1.0176		
1400	L	30.5		1.433	.45	.63	1.48	70	.0437		.52	E	25.5	24.3	5.6	7.4	0.0	.60	022	5	0.54	.0805	-0.21	1.0175		
1500	L	31.5		1.280	.43	.60	1.37	60	.0402	-5.73	.49	E	25.9	24.5	6.4	7.2	0.0	.80	022	5	0.61	.0630	-0.03	1.0175		
1600	L	31.0	.331	1.341	.41	.60	1.20	50	.0384		.40	D	26.0	24.7	7.3	7.0	0.0	.96	025	4	0.64	.0524	+0.10	1.0174	2.6521	
1700	L	29.0		1.463	.42	.62	1.08	50	.0384		.19	C	25.6	24.9	8.0	6.6	0.0	.96	009	4	0.66	.0349	+0.19	1.0175		
1800	K	26.0		1.707	.44	.65	.97	50	.0419		.09	A	24.8	24.9	8.4	6.3	0.0	.80	332	3	0.68	.0244	+0.23	1.0175		
1900	J	23.5		1.920	.47	.68	1.10	50	.0472		-.02	A+	24.9	24.8	8.4	6.0	0.0	.57	294	3	0.69	.0087	+0.23	1.0175		
2000	I	22.0		2.164	.52	.72	1.28	50	.0540	-1.88	-.02	A+	23.8	24.7	8.2	6.2	9.0	.28	273	3	0.70	.0000	+0.21	1.0176		
2100	H	23.0		2.286	.54	.75	1.16	50	.0612		-.03	A+	23.3	24.6	7.7	6.6	9.6	.14	258	2	0.64	.0000	+0.06	1.0176		
2200	H	25.5	.328	2.316	.54	.75	1.06	50	.0612		-.03	A+	22.8	24.4	6.9	7.0	6.6	.08	248	2	0.57	.0018	-0.06	1.0177	2.6724	
2300	I	29.0		2.164	.53	.75	1.11	50	.0524		-.04	A+	23.2	24.2	6.0	7.2	1.9	.05	250	1	0.50	.0035	-0.17	1.0177		

DATE: 09/02/66

Time hrs	B	d	\bar{D}	E_t	h	\bar{H}_b	H_{bs}	H_s	\bar{H}_b	\bar{m}	Q_f	R_n	S	t_a	t_w	\bar{T}_b	T_s	u	\bar{V}	W_{d0}	W_s	\bar{z}	$\bar{\alpha}_b$	η	ρ_l	ρ_s
		m	mm	m	m	m	m	m	m	(tan)	m^3	$\frac{g \text{ cal}}{cm^2 \text{ sec}}$		($^{\circ}C$)	($^{\circ}C$)	sec	sec	m	$\frac{m}{sec}$	($^{\circ}$)	$\frac{m}{sec}$	m	(tan)	$\frac{m}{hr}$	$\frac{g}{cm^3}$	$\frac{g}{cm^3}$
0000	J	33.0		1.981	1.40	.52	.74	1.18	52	.0419		-.04	A	24.5	23.8	5.4	7.0	0.0	.00	250	1	0.44	.0000	-0.22	1.0178	
0100	K	36.5		1.737	1.40	.52	.75	1.10	58	.0332		-.04	C	23.5	23.5	5.2	7.0	0.0	.00	244	2	0.39	.0018	-0.27	1.0178	
0200	L	38.5		1.463	1.40	.52	.76	.96	60	.0314		-.04	F	22.6	23.2	5.1	7.0	0.0	.00	249	3	0.36	.0018	-0.24	1.0178	
0300	L	38.5		1.310	1.36	.53	.79	.87	60	.0279		-.04	G	23.0	23.4	5.2	7.0	0.0	.00	257	3	0.34	.0000	-0.08	1.0179	
0400	L	37.5	.354	1.280	1.36	.54	.81	.78	55	.0297	-3.39	-.05	G	23.3	23.1	5.4	7.0	0.0	.00	264	3	0.32	.0000	+0.05	1.0179	2.6585
0500	L	37.0		1.402	1.36	.56	.86	.83	60	.0332		-.05	G	23.0	22.8	5.8	7.0	0.0	.00	280	3	0.41	.0000	+0.15	1.0180	
0600	K	36.0		1.585	1.32	.59	.92	.90	60	.0384		-.04	F	22.6	22.7	6.4	7.1	0.0	.02	286	3	0.50	.0070	+0.22	1.0181	
0700	K	35.5		1.829	1.28	.62	.96	.90	60	.0454		-.04	E	22.2	22.6	6.8	7.2	0.0	.03	298	3	0.58	.0140	+0.22	1.0181	
0800	J	34.5		2.012	1.24	.67	.99	.90	60	.0524		.10	C	22.0	22.7	7.2	7.3	0.0	.04	300	3	0.64	.0244	+0.20	1.0182	
0900	I	32.0		2.225	1.12	.70	.96	.85	60	.0682		.24	B	22.2	22.7	7.5	7.6	0.0	.05	307	3	0.64	.0262	+0.06	1.0183	
1000	G	24.0	.373	2.225	1.04	.70	.95	.80	55	.0770	+0.71	.30	B	22.5	22.9	7.4	8.0	0.0	.02	310	3	0.61	.0314	0.00	1.0183	2.6547
1100	H	24.0		2.164	1.00	.66	.90	.77	55	.0682		.39	B	22.7	23.0	7.2	8.2	0.0	.10	314	3	0.56	.0367	-0.13	1.0184	
1200	I	26.5		1.981	1.00	.60	.84	.76	55	.0489		.31	C	22.8	23.1	6.8	8.5	0.0	.19	315	4	0.52	.0367	-0.21	1.0184	
1300	J	30.0		1.737	1.08	.55	.76	.85	55	.0384		.41	D	23.0	23.3	6.4	8.6	0.0	.20	309	5	0.50	.0384	-0.26	1.0184	
1400	K	33.0		1.463	1.20	.49	.70	.90	55	.0332		.54	E	23.4	23.6	6.2	8.6	0.0	.20	304	5	0.48	.0402	-0.23	1.0183	
1500	K	34.5		1.310	1.24	.45	.65	.90	58	.0314		.45	F	23.6	23.9	6.2	8.8	0.0	.19	302	4	0.46	.0384	-0.13	1.0183	
1600	L	35.5	.378	1.219	1.24	.42	.62	.90	60	.0349	-0.20	.36	G	23.8	24.2	6.3	8.9	0.0	.19	297	3	0.44	.0332	0.00	1.0182	2.6553
1700	L	34.5		1.310	1.20	.41	.61	.82	62	.0437		.12	G	24.2	24.3	6.5	9.1	0.0	.18	286	2	0.48	.0262	+0.16	1.0182	
1800	L	33.0		1.524	1.12	.40	.60	.76	70	.0524		.09	F	24.9	24.3	6.8	9.3	0.0	.17	277	2	0.51	.0227	+0.21	1.0182	
1900	K	30.5		1.707	1.08	.41	.60	.68	80	.0577		-.01	E	26.5	24.2	7.0	9.4	0.0	.16	261	2	0.54	.0140	+0.18	1.0182	
2000	J	28.5		1.890	1.04	.44	.62	.60	88	.0577		-.04	D	28.3	24.1	7.2	9.6	0.0	.16	248	2	0.58	.0052	+0.18	1.0182	
2100	J	27.5		2.073	1.00	.46	.69	.66	100	.0524		-.04	B	26.8	24.1	7.4	9.8	0.9	.08	238	2	0.54	.0000	+0.13	1.0181	
2200	I	26.0	.370	2.134	0.96	.50	.75	.77	120	.0454	-0.62	-.04	A	23.8	24.1	7.7	9.9	4.2	.04	232	3	0.48	.0000	0.00	1.0179	2.6456
2300	I	25.0		2.103	0.94	.53	.82	.64	150	.0437		-.04	A	23.7	24.0	7.6	10.0	2.4	.20	246	3	0.46	.0000	-0.11	1.0175	

DATE: 09/03/66

Time hrs	B	d	\bar{D}	E_t	h	\bar{H}_b	H_{bs}	H_s	\bar{x}_b	\bar{m}	Q_f	R_n	S	t_a	t_w	\bar{T}_b	T_s	u	\bar{V}	W_d	W_s	\bar{z}	$\bar{\alpha}_b$	η	ρ_k	ρ_s
		m	mm	m	m	m	m	m	m	(tan)	m^3	$\frac{g \text{ cal}}{cm^2 \text{ sec}}$		($^{\circ}$)	($^{\circ}$)	sec	sec	m	m	($^{\circ}$)	$\frac{m}{sec}$	m	(tan)	$\frac{m}{hr}$	$\frac{g}{cm^3}$	$\frac{g}{cm^3}$
0000	I	24.5		1.920	0.92	.57	.90	.59	.170	.0419		-.05	C	23.7	23.8	7.6	10.0	0.0	.44	263	3	0.46	.0000	-0.22	1.0172	
0100	K	25.5		1.676	0.92	.60	.94	.54	.180	.0419		-.05	E	23.7	23.8	7.4	10.0	0.0	.48	260	4	0.46	.0000	-0.26	1.0173	
0200	L	27.5		1.402	0.88	.60	.94	.52	.165	.0402		-.05	F	23.9	23.9	7.4	10.0	0.0	.36	259	3	0.45	.0000	-0.24	1.0174	
0300	M	30.0		1.219	0.88	.60	.94	.43	.150	.0384		-.04	H	23.6	23.9	7.4	10.0	0.0	.20	260	3	0.44	.0000	-0.12	1.0174	
0400	M	31.5	.305	1.158	0.90	.59	.91	.38	.130	.0349	+1.32	-.04	H	23.5	23.9	7.6	10.0	0.0	.04	268	3	0.44	.0000	-0.01	1.0175	2.6450
0500	M	32.0		1.250	0.92	.59	.89	.41	.113	.0349		-.04	G	23.5	23.9	7.8	10.2	0.0	.00	284	3	0.47	.0070	+0.10	1.0175	
0600	L	31.0		1.372	0.88	.60	.86	.48	.110	.0367		-.04	F	23.5	23.9	8.0	10.4	0.0	.05	297	3	0.52	.0122	+0.17	1.0176	
0700	K	28.0		1.585	0.80	.60	.85	.50	.110	.0419		-.04	E	23.5	23.9	8.1	10.7	0.0	.12	314	4	0.58	.0175	+0.21	1.0176	
0800	J	23.5		1.798	0.68	.60	.85	.59	.110	.0489		.02	D	23.7	23.9	8.4	11.0	0.0	.16	339	3	0.62	.0227	+0.23	1.0176	
0900	I	17.0		2.042	0.52	.58	.85	.52	.110	.0577		.15	C	24.2	23.9	8.6	11.0	0.6	.12	360	3	0.60	.0262	+0.20	1.0178	
1000	H	13.5		2.134	0.40	.56	.85	.48	.112	.0664		.25	B	24.4	24.1	8.4	11.0	3.2	.08	360	4	0.55	.0279	+0.03	1.0179	
1100	G	12.0	.375	2.134	0.40	.55	.83	.41	.120	.0682	+2.05	.37	C	25.5	24.4	7.8	11.0	3.2	.04	002	4	0.50	.0279	0.00	1.0181	2.6740
1200	H	15.0		2.042	0.68	.54	.80	.37	.125	.0682		.41	D	26.5	24.6	6.9	11.0	0.0	.00	003	4	0.46	.0279	-0.18	1.0182	
1300	I	19.0		1.798	0.84	.48	.74	.30	.120	.0594		.49	E	27.5	24.7	6.1	10.5	0.0	.03	004	4	0.46	.0244	-0.24	1.0184	
1400	K	23.5		1.585	0.88	.43	.65	.22	.110	.0489		.48	F	28.1	24.7	5.4	10.1	0.0	.04	012	4	0.46	.0210	-0.20	1.0185	
1500	L	29.0		1.402	0.88	.38	.54	.20	.100	.0367		.41	G	27.7	24.7	5.0	9.5	0.0	.08	033	3	0.48	.0140	-0.16	1.0187	
1600	M	33.5		1.280	0.84	.36	.50	.19	.98	.0279		.31	G	27.2	24.9	4.9	9.0	0.0	.10	062	2	0.50	.0087	-0.07	1.0189	
1700	M+	35.5		1.280	0.80	.35	.51	.18	.90	.0244	+0.40	.18	H	26.6	25.6	5.2	9.0	0.0	.11	094	1	0.53	.0000	0.00	1.0189	
1800	M+	34.0		1.433	0.74	.36	.59	.18	.85	.0262		.08	G	26.2	25.9	5.6	9.0	0.0	.14	127	1	0.54	.0000	+0.17	1.0185	
1900	M	31.5		1.615	0.68	.38	.66	.19	.75	.0349		-.05	F	25.5	25.9	6.2	9.0	0.0	.08	156	2	0.58	.0000	+0.19	1.0180	
2000	L	26.5		1.798	0.60	.41	.70	.34	.72	.0454		-.07	E	25.0	25.7	6.8	9.0	0.0	.08	179	3	0.61	.0000	+0.16	1.0174	
2100	K	23.0		1.951	0.52	.45	.75	.34	.80	.0559		-.06	E	24.5	25.5	7.4	9.0	0.4	.08	196	3	0.64	.0000	+0.18	1.0170	
2200	J	20.5		2.134	0.48	.49	.79	.35	.100	.0647		-.07	C	24.2	25.4	7.8	9.0	2.1	.07	200	4	0.65	.0000	+0.16	1.0170	
2300	I	21.0	.396	2.134	0.48	.53	.79	.32	.120	.0664	-0.54	-.07	C	24.0	25.4	8.1	9.5	2.7	.06	207	4	0.67	.0000	-0.06	1.0170	2.6582

DATE: 09/04/66

Time hrs	B	d m	\bar{D} mm	E_t m	h m	\bar{H}_b m	H_{bs} m	H_s m	\bar{x}_b m	\bar{m} (tan)	Q_f m ³	R_n g cal/cm ² /sec	S	t_a (°C)	t_w (°C)	\bar{T}_b sec	T_s sec	u m	\bar{V} m/sec	W_d (°)	W_s m/sec	\bar{z} m	$\bar{\alpha}_b$ (tan)	η m/hr	ρ_l g/cm ³	ρ_s g/cm ³
0000	J	23.0		2.012	0.48	.54	.75	.35	135	.0524		-.07	D	23.8	25.3	8.2	10.0	2.4	.04	204	4	0.62	.0000	-0.14	1.0171	
0100	J	26.0		1.798	0.56	.52	.68	.30	150	.0437		-.07	D	23.8	25.3	7.8	9.7	0.0	.00	204	3	0.58	.0000	-0.18	1.0171	
0200	K	28.0		1.524	0.64	.46	.60	.25	140	.0367		-.07	E	23.6	25.0	7.0	9.5	0.0	.04	180	3	0.52	.0000	-0.21	1.0172	
0300	K	28.5		1.341	0.68	.39	.50	.21	125	.0349		-.06	F	23.2	24.8	5.6	9.2	0.0	.13	201	2	0.47	.0000	-0.19	1.0172	
0400	L	26.0	.316	1.250	0.68	.32	.42	.18	120	.0367	+1.42	-.07	G	23.0	24.6	4.7	9.0	0.0	.23	201	3	0.43	.0000	-0.06	1.0173	2.6588
0500	L	22.0		1.219	0.52	.25	.36	.18	120	.0437		-.07	G	23.3	24.3	4.6	9.0	0.0	.28	211	3	0.42	.0000	0.00	1.0173	
0600	K	17.5		1.280	0.36	.22	.35	.19	120	.0324		-.07	G	23.6	24.2	5.2	9.0	0.0	.26	218	3	0.42	.0000	+0.15	1.0174	
0700	I	13.0		1.402	0.24	.22	.35	.19	120	.0647		-.01	F	24.3	24.1	6.2	8.5	0.0	.24	220	3	0.41	.0052	+0.21	1.0174	
0800	H	10.0		1.554	0.20	.24	.35	.20	120	.0770		.07	D	25.2	23.9	7.4	8.0	4.9	.24	221	3	0.40	.0105	+0.20	1.0175	
0900	G	7.0		1.829	0.22	.28	.44	.19	120	.0857		.18	C	26.7	23.8	8.0	8.2	8.8	.26	220	3	0.42	.0140	+0.18	1.0174	
1000	F	6.5		2.041	0.24	.33	.55	.20	110	.0910		.32	B	27.6	23.9	8.2	8.4	10.0	.28	219	3	0.43	.0175	+0.15	1.0173	
1100	F	6.5		2.164	0.28	.39	.66	.20	98	.0893	+0.01	.42	B	28.8	23.8	8.0	8.6	9.6	.32	217	3	0.44	.0192	0.00	1.0172	
1200	G	10.5	.345	2.134	0.38	.45	.71	.20	80	.0734		.51	B	30.3	23.8	7.6	9.0	6.4	.34	217	4	0.46	.0192	-0.12	1.0171	2.6527
1300	I	19.5		2.073	0.56	.49	.66	.21	62	.0540		.55	C	31.5	23.6	6.9	8.4	1.9	.36	220	5	0.48	.0192	-0.20	1.0171	
1400	K	28.0		1.890	0.68	.49	.59	.26	50	.0367		.51	E	32.2	23.4	6.2	7.8	0.0	.38	222	6	0.49	.0175	-0.23	1.0174	
1500	L	31.5		1.676	0.72	.45	.52	.30	40	.0297		.46	E	32.6	23.3	5.8	7.4	0.0	.40	221	6	0.50	.0122	-0.22	1.0180	
1600	M	32.5		1.494	0.70	.35	.47	.33	35	.0314		.28	F	32.7	23.0	5.5	7.0	0.0	.40	220	7	0.50	.0087	-0.09	1.0185	
1700	M	30.5	.317	1.402	0.64	.25	.47	.32	30	.0349	-0.36	.11	G	32.3	23.1	5.3	7.2	0.0	.40	212	6	0.52	.0000	0.00	1.0189	2.6530
1800	M	27.5		1.402	0.60	.24	.50	.32	30	.0367		.11	G	31.3	23.1	5.1	7.5	0.0	.36	200	6	0.54	.0000	+0.06	1.0192	
1900	L	24.5		1.433	0.56	.30	.55	.32	30	.0384		-.02	F	29.6	23.1	5.1	7.8	0.0	.32	197	5	0.53	.0000	+0.12	1.0195	
2000	L	23.0		1.554	0.52	.39	.59	.35	30	.0419		-.06	F	27.8	23.1	5.2	8.0	0.6	.28	196	5	0.53	.0000	+0.16	1.0198	
2100	K	23.0		1.676	0.52	.46	.61	.31	30	.0472		-.06	E	27.1	23.0	5.6	7.3	2.0	.26	196	4	0.53	.0035	+0.16	1.0199	
2200	K	23.5		1.890	0.56	.51	.64	.29	32	.0507		-.06	D	26.6	22.9	6.0	6.5	1.7	.28	200	4	0.54	.0262	+0.13	1.0200	
2300	J	23.5		1.981	0.64	.50	.64	.25	32	.0524	+0.02	-.06	D	26.3	22.9	6.6	5.6	0.9	.34	218	4	0.54	.0437	0.00	1.0201	2.6491

DATE: 09/05/66

Time hrs	B	d	\bar{D}	E_t	h	\bar{H}_b	H_{bs}	H_s	\bar{h}_b	\bar{m}	Q_f	R_n	S	t_a	t_w	\bar{T}_b	T_s	u	\bar{V}	W_d	W_s	z	$\bar{\alpha}_b$	η	ρ_l	ρ_s
		m	mm	m	m	m	m	m	m	(tan)	m^3	$\frac{g \text{ cal}}{cm^2/sec}$		(°C)	(°C)	sec	sec	$\frac{m}{hr}$	$\frac{m}{sec}$	($\frac{m}{sec}$)	$\frac{m}{sec}$	m	(tan)	$\frac{m}{hr}$	$\frac{g}{cm^3}$	$\frac{g}{cm^3}$
0000	I	21.5		1.951	0.72	.48	.62	.22	30	.0507		-.05	D	25.6	22.8	7.0	5.2	0.3	.38	230	5	0.54	.0559	-0.07	1.0202	
0100	J	21.0		1.798	0.70	.44	.56	.20	25	.0454		-.05	D	25.0	22.7	7.2	5.8	0.0	.36	238	4	0.54	.0612	-0.21	1.0202	
0200	J	22.0		1.524	0.60	.36	.50	.20	20	.0402		-.05	E	24.6	22.6	7.1	6.6	0.0	.32	240	4	0.54	.0664	-0.25	1.0202	
0300	K	24.0		1.341	0.52	.30	.45	.20	18	.0367		-.04	E	24.0	22.4	6.3	7.6	0.0	.28	243	4	0.54	.0699	-0.15	1.0202	
0400	L	26.0	.275	1.250	0.48	.27	.40	.22	15	.0349		-.04	F	23.5	22.2	5.5	8.4	0.0	.24	251	3	0.54	.0734	-0.06	1.0202	2.6665
0500	M	26.5		1.219	0.48	.26	.43	.20	20	.0349	+0.67	-.04	H	23.1	21.9	5.1	8.8	0.0	.26	257	3	0.54	.0770	0.00	1.0202	
0600	M	25.5		1.280	0.52	.28	.47	.22	30	.0349		-.04	H	22.7	21.7	5.2	8.2	0.0	.27	259	4	0.50	.0770	+0.09	1.0202	
0700	L	23.5		1.402	0.52	.33	.54	.22	40	.0384		-.03	G	22.5	21.6	5.6	7.8	0.0	.28	258	5	0.46	.0805	+0.14	1.0202	
0800	K	21.5		1.554	0.52	.37	.60	.22	45	.0454		-.02	G	22.5	21.7	6.1	7.4	0.0	.32	260	5	0.42	.0840	+0.20	1.0202	
0900	J	19.5		1.829	0.52	.40	.61	.20	50	.0540		.11	F	23.3	21.7	6.8	7.6	0.0	.32	247	4	0.41	.0875	+0.25	1.0201	
1000	J	17.5		2.042	0.52	.42	.62	.20	60	.0647		.29	E	24.5	21.7	7.4	8.2	0.0	.32	227	3	0.42	.0910	+0.18	1.0199	
1100	I	16.0		2.164	0.50	.42	.62	.20	68	.0682		.40	D	25.7	21.9	7.6	8.6	0.5	.31	208	3	0.44	.0963	0.00	1.0197	
1200	I	15.5		2.134	0.48	.40	.60	.20	82	.0682	+1.15	.51	C	26.8	22.4	7.8	9.0	0.8	.24	200	2	0.45	.1033	-0.04	1.0195	
1300	J	15.0	.377	2.073	0.46	.40	.61	.20	103	.0647		.59	D	27.0	23.7	7.8	9.2	0.0	.20	200	1	0.46	.0981	-0.11	1.0192	2.6659
1400	K	14.5		1.890	0.46	.40	.63	.20	125	.0594		.28	D	27.2	24.4	7.5	9.4	0.0	.28	176	2	0.48	.0910	-0.21	1.0189	
1500	K	15.5		1.676	0.48	.41	.65	.20	140	.0540		.12	E	27.0	24.7	7.2	9.7	0.0	.35	168	3	0.50	.0805	-0.21	1.0185	
1600	L	17.5		1.494	0.50	.42	.68	.20	145	.0489		.22	F	26.8	24.7	6.8	10.0	0.0	.37	173	4	0.51	.0717	-0.14	1.0180	
1700	K	21.5		1.402	0.44	.42	.67	.20	138	.0454		.21	G	26.5	24.7	6.2	10.0	0.0	.32	180	4	0.53	.0630	-0.05	1.0178	
1800	L	25.5	.277	1.402	0.36	.42	.68	.20	120	.0454	+0.81	.03	H	26.0	24.6	5.6	10.0	0.0	.28	180	4	0.54	.0594	+0.02	1.0177	2.6537
1900	L	27.0		1.433	0.52	.42	.71	.20	105	.0454		-.02	G	25.4	24.6	5.4	10.0	0.0	.24	181	4	0.56	.0594	+0.06	1.0177	
2000	L	27.0		1.554	0.76	.43	.65	.20	100	.0489		-.08	F	25.0	24.6	5.6	10.0	0.0	.20	181	4	0.58	.0594	+0.12	1.0177	
2100	K	26.0		1.676	0.84	.46	.71	.23	95	.0540		-.09	E	24.8	24.6	6.8	10.2	0.0	.16	207	4	0.55	.0559	+0.18	1.0177	
2200	J	24.0		1.890	0.82	.51	.79	.25	110	.0577		-.09	D	24.8	24.6	8.5	10.4	0.0	.15	240	3	0.52	.0524	+0.19	1.0178	
2300	I	21.5		1.981	0.78	.57	.89	.30	150	.0577		-.09	D	24.8	24.5	10.3	10.7	4.0	.13	242	3	0.49	.0507	0.00	1.0178	

Time hrs	B	d	\bar{D}	F_t	h	\bar{H}_b	H_{bs}	H_s	\bar{x}_b	\bar{m}	Q_f	R_n	S	t_a	t_w	\bar{T}_b	T_s	u	\bar{V}	W_d	W_s	\bar{z}	$\bar{\alpha}_b$	η	ρ_k	ρ_s
	m	mm	m	m	m	m	m	m	(tan)	m^3	$\frac{g \text{ cal}}{cm^2 \text{ sec}}$		(°C)	(°C)	(°C)	sec	sec	m	$\frac{m}{sec}$	$\frac{m}{sec}$	$\frac{m}{sec}$	m	(tan)	$\frac{m}{hr}$	$\frac{g}{cm^3}$	$\frac{g}{cm^3}$
0000	I	17.5	.298	1.951	0.74	.60	.93	.31	.180	+1.15	-.09	C	24.5	24.5	24.5	10.7	11.0	4.9	.12	.247	3	0.46	.0524	-0.05	1.0179	2.6532
0100	I	18.0		1.890	0.72	.56	.85	.35	.190	.0507	-.09	D	23.5	24.4	24.4	11.9	10.6	1.4	.12	.252	3	0.43	.0559	-0.10	1.0180	
0200	J	20.0		1.737	0.76	.48	.72	.36	.175	.0472	-.09	E	23.3	24.1	24.1	11.0	10.4	0.0	.09	.261	3	0.40	.0612	-0.15	1.0182	
0300	K	22.5		1.585	0.80	.39	.59	.34	.130	.0454	-.09	F	23.4	23.8	23.8	8.7	10.2	0.0	.08	.287	3	0.38	.0734	-0.15	1.0184	
0400	L	24.0		1.433	0.80	.30	.48	.31	.70	.0472	+0.11	G	23.6	23.6	23.6	7.0	10.0	0.0	.06	.307	3	0.34	.0875	-0.14	1.0185	
0500	M	23.0		1.341	0.76	.27	.47	.32	.43	.0507	-.08	H	23.7	23.4	23.4	6.4	10.0	0.0	.13	.336	4	0.34	.0998	-0.08	1.0187	
0600	L	19.5	.329	1.280	0.64	.28	.51	.32	.38	.0559	-.08	H	23.8	23.3	23.3	6.4	10.0	1.0	.20	.358	4	0.34	.1016	0.00	1.0188	2.6544
0700	K	15.0		1.310	0.48	.30	.60	.32	.20	.0630	-.08	G	23.8	23.2	23.2	6.7	10.0	3.6	.28	.360	4	0.34	.0981	+0.15	1.0189	
0800	J	12.0		1.524	0.40	.33	.65	.22	.18	.0699	.01	E	23.7	23.1	23.1	7.0	10.0	5.4	.36	.350	3	0.34	.0981	+0.23	1.0190	
0900	I	11.0		1.768	0.30	.36	.68	.23	.20	.0752	.21	D	23.9	23.0	23.0	7.6	10.2	7.1	.40	.352	3	0.40	.1033	+0.21	1.0191	
1000	H	9.5		1.920	0.20	.38	.65	.25	.25	.0787	.33	B	24.2	23.0	23.0	8.0	10.4	8.4	.46	.348	3	0.53	.1052	+0.17	1.0188	
1100	H	9.0		2.103	0.10	.39	.62	.27	.30	.0822	.46	A	24.5	23.0	23.0	8.2	10.7	9.4	.52	.343	4	0.74	.1139	+0.06	1.0184	
1200	G	9.0	.310	2.134	0.04	.39	.60	.31	.35	.0840	.56	A	24.7	23.1	23.1	8.2	11.0	9.8	.56	.353	5	0.90	.1370	+0.01	1.0181	2.6719
1300	G	10.5		2.134	0.00	.39	.59	.27	.45	.0805	+0.33	B	25.2	23.7	23.7	8.1	10.2	9.6	.55	.044	6	0.96	.1370	-0.04	1.0180	
1400	G	11.5		1.981	0.12	.39	.58	.24	.75	.0805	.50	C	26.2	24.9	24.9	7.6	9.5	8.2	.48	.117	6	0.87	.1281	-0.15	1.0180	
1500	H	12.0		1.859	0.40	.38	.56	.20	1.00	.0805	.47	D	27.4	25.1	25.1	7.1	8.8	6.8	.42	.196	5	0.50	.0928	-0.21	1.0180	
1600	I	12.5		1.615	0.60	.37	.56	.20	1.20	.0770	.37	E	28.3	25.1	25.1	6.6	8.0	5.8	.38	.208	5	0.30	.0612	-0.23	1.0180	
1700	J	13.5		1.494	0.60	.35	.55	.18	1.15	.0699	.19	F	29.5	25.0	25.0	6.2	7.8	5.3	.42	.212	4	0.30	.0524	-0.12	1.0181	
1800	K	15.5	.240	1.402	0.60	.35	.55	.18	1.00	.0612	.08	G	28.6	24.7	24.7	6.2	7.5	4.8	.48	.206	3	0.34	.0612	-0.06	1.0182	2.6273
1900	L	17.5		1.372	0.60	.34	.54	.19	.80	.0559	-.04	G	26.5	24.4	24.4	6.0	7.2	3.9	.52	.203	3	0.36	.0787	0.00	1.0184	
2000	L	19.0		1.402	0.60	.35	.50	.20	.60	.0524	+1.04	F	24.7	24.2	24.2	5.8	7.0	2.6	.53	.206	3	0.38	.0981	+0.05	1.0185	
2100	K	21.0		1.494	0.64	.35	.50	.21	.60	.0507	-.08	E	23.5	24.1	24.1	5.8	6.1	1.2	.49	.242	3	0.41	.1192	+0.13	1.0185	
2200	J	22.0		1.646	0.72	.38	.51	.21	.60	.0472	-.08	D	22.8	24.0	24.0	5.5	5.2	0.3	.48	.289	3	0.43	.1388	+0.14	1.0185	
2300	J	24.0		1.768	0.76	.39	.55	.20	.60	.0454	-.07	C	22.8	24.0	24.0	5.1	4.3	1.4	.44	.281	2	0.45	.1512	+0.09	1.0185	

DATE: 09/07/66

Time hrs	B	d	\bar{D}	E_t	h	\bar{H}_b	H_{bs}	H_s	\bar{H}_b	\bar{m}	Q_f	R_n	S	t_a	t_w	\bar{T}_b	T_s	u	\bar{V}	W_d	W_s	z	$\bar{\alpha}_b$	η	ρ_l	ρ_s
		m	mm	m	m	m	m	m	m	(tan)	m^3	$\frac{g \text{ cal}}{cm^2 \text{ sec}}$		(°C)	(°C)	sec	sec	m	$\frac{m}{sec}$	$\frac{m}{sec}$	$\frac{m}{sec}$	m	(tan)	$\frac{m}{hr}$	$\frac{g}{cm^3}$	$\frac{g}{cm^3}$
0000	I	26.0		1.829	0.80	.39	.58	.20	60	.0437	+0.16	-.07	C	22.8	24.0	5.4	3.4	2.8	.40	272	2	0.48	.1584	0.00	1.0185	
0100	I	25.5	.316	1.798	0.72	.39	.57	.20	50	.0419		-.07	C	22.9	23.9	7.4	3.4	2.6	.32	241	3	0.50	.1530	-0.03	1.0184	2.6285
0200	J	24.0		1.768	0.64	.38	.54	.21	40	.0402		-.07	D	22.8	23.6	7.8	3.4	0.6	.23	286	5	0.49	.1405	-0.06	1.0185	
0300	J	23.0		1.646	0.52	.37	.50	.21	30	.0384		-.07	E	22.5	23.2	7.3	3.4	0.0	.14	301	7	0.48	.1139	-0.16	1.0185	
0400	L	21.5		1.768	0.46	.37	.47	.21	18	.0367		-.07	F	22.3	23.0	5.6	3.5	0.0	.06	360	8	0.48	.0770	-0.16	1.0185	
0500	L	21.5		1.341	0.44	.34	.46	.21	12	.0367		-.06	G	22.3	23.0	4.1	3.2	0.0	.00	001	9	0.48	.0437	-0.12	1.0186	
0600	M	25.5		1.219	0.70	.30	.45	.22	18	.0367		-.06	H	22.3	23.0	3.7	3.0	0.0	.00	002	9	0.47	.0175	-0.08	1.0187	
0700	M	28.0	.289	1.219	0.92	.27	.45	.27	20	.0402	-0.87	-.06	H	22.4	23.1	4.0	3.0	0.0	.00	010	9	0.46	.0035	+0.07	1.0189	2.6295
0800	L	26.0		1.310	0.76	.29	.46	.33	18	.0472		-.05	G	22.5	23.2	4.8	3.0	0.0	.00	020	9	0.46	.0332	+0.16	1.0189	
0900	K	25.0		1.524	0.76	.35	.55	.38	16	.0507		.01	F	22.6	23.4	5.4	3.2	0.0	.16	028	9	0.46	.0717	+0.25	1.0188	
1000	J	24.5		1.798	0.80	.42	.66	.44	15	.0540		.28	E	22.5	23.5	5.6	3.4	0.0	.34	039	8	0.44	.1139	+0.26	1.0185	
1100	I	24.5		2.012	0.88	.52	.78	.51	15	.0559		.31	D	22.4	23.6	5.6	3.7	0.0	.52	042	7	0.44	.1548	+0.16	1.0180	
1200	I	24.5		2.134	0.92	.60	.85	.60	25	.0559		.49	C	22.4	23.7	5.8	4.0	0.0	.68	048	6	0.44	.1871	+0.07	1.0178	
1300	I	24.0	.341	2.164	0.96	.64	.84	.52	43	.0540	-1.12	.54	C	22.6	23.7	5.7	4.2	0.0	.68	056	5	0.42	.2053	0.00	1.0177	2.6310
1400	I	24.0		2.103	0.98	.64	.79	.49	63	.0524		.53	C	23.0	23.8	5.6	4.4	0.0	.62	056	4	0.40	.2035	-0.09	1.0177	
1500	J	25.0		1.981	1.00	.60	.73	.48	80	.0489		.50	D	23.3	23.9	5.5	4.6	0.0	.54	049	4	0.37	.1799	-0.14	1.0178	
1600	K	25.5		1.829	0.96	.54	.67	.47	90	.0454		.29	E	23.5	24.1	5.2	5.0	0.0	.46	048	4	0.34	.1317	-0.15	1.0179	
1700	K	25.5		1.676	0.88	.47	.62	.52	90	.0402		.18	F	23.4	24.1	5.2	5.2	0.0	.39	049	3	0.32	.0540	-0.17	1.0179	
1800	K	24.0		1.494	0.82	.40	.56	.59	80	.0367		.03	F	23.4	24.0	6.0	5.4	0.0	.34	050	2	0.29	.0314	-0.16	1.0179	
1900	K	22.5		1.402	0.76	.35	.58	.68	70	.0332		-.09	F	23.3	24.0	6.9	5.7	0.0	.32	052	2	0.26	.0612	-0.06	1.0179	
2000	K	21.5	.320	1.372	0.70	.31	.50	.76	55	.0314	-0.05	-.10	F	23.3	23.9	7.4	6.0	0.0	.30	050	2	0.24	.0805	0.00	1.0178	2.6276
2100	K	20.5		1.433	0.64	.32	.50	.70	40	.0332		-.10	F	23.1	23.9	7.1	5.6	0.0	.29	041	3	0.29	.0910	+0.10	1.0178	
2200	K	20.5		1.554	0.60	.33	.50	.62	30	.0384		-.09	E	23.0	23.9	6.3	5.4	0.0	.29	034	4	0.36	.0805	+0.14	1.0178	
2300	K	19.5		1.707	0.58	.35	.55	.55	20	.0454		-.09	E	22.7	23.9	5.4	5.2	0.3	.30	038	5	0.39	.0524	+0.16	1.0179	

DATE: 09/08/66

Time hrs	B	d	\bar{D}	E_t	h	\bar{H}_b	H_{bs}	H_s	\bar{h}_b	\bar{m}	Q_f	R_n	S	t_a	t_w	T_b	T_s	u	\bar{V}	W_d	W_s	\bar{z}	$\bar{\alpha}_b$	η	ρ_l	ρ_s
		m	mm	m	m	m	m	m	m	(tan)	m^3	$\frac{g \text{ cal}}{cm^2 \text{ sec}}$		($^{\circ}C$)	($^{\circ}C$)	sec	sec	m	$\frac{m}{sec}$	($^{\circ}$)	$\frac{m}{sec}$	m	(tan)	$\frac{m}{hr}$	$\frac{g}{cm^3}$	$\frac{g}{cm^3}$
0000	J	19.0		1.859	0.56	.37	.60	.52	20	.0559		-.09	E	22.5	23.9	4.8	5.0	0.5	.32	.040	5	0.42	.0018	+0.09	1.0179	
0100	I	16.0		1.890	0.48	.37	.60	.64	20	.0612		-.09	E	22.2	23.8	4.6	4.4	0.2	.34	.039	6	0.43	.0018	+0.01	1.0179	
0200	I	19.0	.314	1.890	0.50	.39	.60	.79	20	.0559	+0.33	-.10	E	21.8	23.7	4.3	4.0	0.0	.37	.038	6	0.42	.0297	-0.05	1.0179	2.6308
0300	J	21.0		1.798	0.54	.39	.59	.87	20	.0507		-.10	E	21.5	23.7	4.2	3.7	0.0	.41	.032	7	0.42	.0612	-0.09	1.0179	
0400	J	22.5		1.707	0.60	.39	.56	1.01	20	.0454		-.10	F	21.1	23.6	4.0	3.0	0.0	.44	.025	7	0.41	.1086	-0.12	1.0179	
0500	K	23.0		1.554	0.56	.38	.55	.90	18	.0419		-.10	F	20.8	23.5	4.0	3.3	0.0	.51	.024	8	0.42	.1317	-0.17	1.0180	
0600	L	23.0		1.372	0.52	.37	.55	.77	18	.0402		-.11	G	20.6	23.4	4.2	3.6	0.0	.57	.024	8	0.43	.1530	-0.16	1.0181	
0700	L	23.0		1.310	0.48	.38	.55	.64	20	.0402		-.10	G	20.5	23.2	4.3	3.5	0.0	.66	.022	9	0.44	.1709	-0.02	1.0181	
0800	L	21.5		1.310	0.48	.40	.54	.61	20	.0402		.00	G	20.5	23.1	4.4	3.5	0.0	.72	.022	9	0.46	.1853	0.00	1.0182	
0900	L	19.5	.332	1.402	0.48	.40	.55	.61	22	.0419	+0.03	.14	C	20.5	23.1	4.6	3.4	0.0	.72	.020	9	0.47	.1835	+0.13	1.0183	2.6412
1000	K	18.0		1.554	0.54	.42	.56	.65	25	.0489		.29	F	20.8	23.2	4.8	3.6	0.0	.68	.017	9	0.48	.1620	+0.22	1.0181	
1100	K	17.5		1.829	0.64	.45	.59	.70	22	.0559		.41	D	21.0	23.3	5.0	3.8	1.6	.64	.008	9	0.50	.1352	+0.24	1.0180	
1200	K	20.0		1.981	0.66	.47	.62	.71	23	.0594		.52	C	21.5	23.4	5.2	3.5	7.4	.60	.005	9	0.50	.1228	+0.11	1.0179	
1300	J	23.0		2.073	0.60	.50	.68	.70	25	.0577		.46	B	21.7	23.3	5.2	3.4	7.8	.59	.360	9	0.57	.1228	+0.07	1.0178	
1400	J	26.0	.342	2.134	0.60	.50	.70	.67	28	.0507	-0.03	.51	C	22.0	23.2	5.2	3.4	2.5	.55	.001	9	0.64	.1299	0.00	1.0179	2.6420
1500	J	26.5		2.073	0.66	.51	.71	.60	30	.0507		.40	D	22.2	23.2	5.3	3.5	0.0	.52	.349	9	0.62	.1423	-0.08	1.0180	
1600	K	24.0		1.981	0.76	.52	.74	.60	30	.0507		.21	D	22.2	23.2	5.3	4.0	0.0	.54	.012	9	0.56	.1548	-0.11	1.0180	
1700	J	24.0		1.859	0.72	.51	.71	.60	30	.0489		.01	D	22.0	23.0	5.3	4.0	0.0	.60	.018	8	0.52	.1459	-0.14	1.0181	
1800	J	20.0		1.707	0.52	.48	.68	.60	30	.0454		-.03	D	21.9	22.9	5.4	4.0	0.0	.64	.020	8	0.46	.1210	-0.16	1.0181	
1900	J	19.5		1.554	0.32	.46	.65	.61	30	.0402		-.08	E	21.6	22.8	5.3	4.0	0.0	.68	.022	8	0.41	.0963	-0.14	1.0181	
2000	J	20.0	.269	1.463	0.28	.45	.63	.65	35	.0367	-1.38	-.08	F	21.5	22.7	5.0	4.0	0.0	.72	.023	8	0.36	.0910	-0.05	1.0182	2.6562
2100	K	20.5		1.463	0.30	.46	.68	.69	35	.0332		-.09	G	21.3	22.6	4.6	4.2	0.0	.72	.030	7	0.39	.1104	+0.06	1.0182	
2200	K	20.5		1.554	0.36	.49	.76	.76	35	.0332		-.10	G	21.1	22.7	4.2	4.4	0.0	.68	.028	7	0.41	.1405	+0.11	1.0183	
2300	K	20.5		1.676	0.46	.53	.85	.82	35	.0349		-.11	F	20.9	22.8	4.0	4.7	0.0	.64	.024	7	0.43	.1817	+0.14	1.0183	

DATE: 09/09/66

Time hrs	B	d	\bar{D} mm	E_t m	h m	\bar{H}_b m	H_{bs} m	H_s m	\bar{h}_b m	\bar{m} (tan)	Q_f m^3	R_n g cal/ cm^2/sec	S	t_a (°C)	t_w (°C)	\bar{T}_b sec	T_s sec	u m	\bar{V} m sec	W_d (°) m	W_s m sec	\bar{z} m	$\bar{\alpha}_b$ (tan)	η m hr	ρ_L g/cm ³	ρ_s g/cm ³
0000	J	20.0		1.829	0.56	.57	.86	.90	32	.0419		-.12	E	20.7	23.0	4.0	4.9	0.0	0.60	024	7	0.45	.2162	+0.14	1.0183	
0100	I	18.0		1.951	0.60	.60	.79	.91	30	.0524		-.12	E	20.4	23.0	4.0	5.0	0.0	.59	024	6	0.47	.2345	+0.10	1.0183	
0200	I	18.0		2.012	0.64	.57	.67	.95	30	.0577	-1.19	-.12	D	20.0	22.9	4.2	5.4	2.6	.56	018	5	0.49	.2309	0.00	1.0184	
0300	J	22.0	.344	1.981	0.72	.54	.58	.88	28	.0524		-.12	D	19.8	22.8	4.2	6.1	0.2	.52	006	4	0.50	.2217	-0.04	1.0184	2.6464
0400	K	27.5		1.920	0.84	.48	.55	.84	25	.0437		-.12	D	19.6	22.7	4.4	6.8	0.0	.48	002	3	0.48	.2035	-0.10	1.0184	
0500	L	30.5		1.768	0.68	.41	.53	.80	22	.0332		-.12	E	19.3	22.6	4.4	7.3	0.0	.48	338	3	0.48	.1853	-0.15	1.0184	
0600	L	29.5		1.615	0.36	.38	.53	.78	20	.0314		-.11	F	19.1	22.5	4.6	7.5	0.0	.47	303	3	0.46	.1673	-0.17	1.0184	
0700	L	26.5		1.433	0.10	.39	.55	.60	30	.0314		-.10	F	19.6	22.3	4.7	7.6	0.0	.46	305	3	0.46	.1495	-0.16	1.0185	
0800	L	23.0		1.341	0.04	.42	.58	.65	40	.0332	-0.12	.00	G	20.2	22.3	4.8	8.0	0.0	.45	308	2	0.45	.1405	-0.07	1.0186	
0900	L	20.0	.401	1.310	0.02	.46	.63	.58	50	.0367		.12	G	20.8	22.3	5.0	8.0	0.0	.44	310	3	0.44	.1263	+0.04	1.0188	2.6569
1000	K	19.0		1.433	0.16	.51	.70	.72	58	.0402		.30	G	21.3	22.3	5.2	8.0	0.0	.42	331	5	0.43	.1139	+0.16	1.0191	
1100	K	19.5		1.615	0.40	.55	.78	.85	62	.0419		.41	F	21.7	22.4	5.6	7.9	0.0	.41	001	7	0.42	.1052	+0.20	1.0193	
1200	J	20.5		1.829	0.60	.60	.85	1.02	62	.0419		.46	E	22.0	22.5	5.9	7.9	0.0	.40	009	8	0.41	.0981	+0.21	1.0196	
1300	J	22.0		2.042	0.72	.62	.85	.95	60	.0419		.50	D	22.3	22.6	6.2	7.9	0.0	.44	015	7	0.41	.0981	+0.19	1.0197	
1400	J	22.0		2.164	0.80	.62	.82	.90	50	.0437		.48	C	22.5	22.7	6.5	7.9	4.2	.52	019	6	0.40	.1016	+0.06	1.0198	
1500	I	22.0	.351	2.164	0.84	.61	.78	.90	40	.0472	-0.97	.47	B	22.7	22.9	6.8	7.4	7.0	.59	022	5	0.40	.1122	0.00	1.0198	2.6489
1600	J	22.0		2.134	0.84	.60	.77	.90	35	.0472		.39	B	22.9	23.1	7.1	7.0	6.8	.62	024	3	0.40	.1157	-0.06	1.0198	
1700	J	23.0		2.042	0.80	.59	.75	.80	30	.0454		.26	B	22.8	23.3	7.2	7.2	2.6	.64	032	2	0.40	.1192	-0.13	1.0198	
1800	J	24.0		1.859	0.80	.58	.74	.73	35	.0419		.08	C	22.5	23.3	7.0	7.4	0.0	.64	020	2	0.40	.1210	-0.21	1.0198	
1900	K	25.5		1.646	0.76	.56	.71	.66	40	.0402		-.08	E	21.9	23.1	6.6	7.7	0.0	.61	005	2	0.41	.1157	-0.21	1.0198	
2000	L	27.0		1.463	0.74	.55	.70	.60	50	.0367		-.11	F	21.5	23.1	6.2	8.0	0.0	.55	317	2	0.40	.1104	-0.15	1.0199	
2100	L	29.5		1.372	0.72	.52	.70	.59	60	.0367		-.12	G	21.6	22.8	5.8	7.6	0.0	.48	292	3	0.45	.0981	-0.06	1.0199	
2200	M	30.5	.340	1.341	0.68	.52	.70	.59	55	.0384	-0.32	-.12	G	21.8	22.7	5.3	7.2	0.0	.43	268	3	0.52	.0981	0.00	1.0199	2.6526
2300	M	30.0		1.433	0.64	.51	.71	.60	55	.0384		-.12	G	22.2	22.6	5.0	7.0	0.4	.40	248	3	0.59	.0963	+0.11	1.0199	

DATE: 09/10/66

Time hrs	B	d	\bar{D}	E_t	h	\bar{H}_b	H_{bs}	H_s	\bar{h}_b	\bar{m}	Q_f	R_n	S	t_a	t_w	\bar{T}_b	T_s	u	\bar{V}	W_d	W_y	\bar{z}	$\bar{\alpha}_b$	η	ρ_L	ρ_s	
	m	m	mm	m	m	m	m	m	m	(tan)	m^3	g cal/ cm^2/sec		(°C)	(°C)	sec	sec	sec	m	$\frac{m}{sec}$	(°)	$\frac{m}{sec}$	m	(tan)	$\frac{m}{hr}$	g/cm^3	g/cm^3
0000	L	29.0		1.554	0.60	.53	.74	.51	60	.0419		-.12	E	22.5	22.4	5.0	8.0	1.0	.40	240	3	0.66	.0963	+0.14	1.0199		
0100	L	27.5		1.707	0.56	.52	.73	.58	75	.0437		-.12	E	22.5	22.3	5.0	7.4	0.9	.40	239	3	0.65	.0981	+0.14	1.0199		
0200	K	25.0		1.829	0.50	.50	.73	.63	103	.0454		-.12	D	22.5	22.3	5.0	7.0	0.4	.40	242	3	0.62	.0981	+0.10	1.0199		
0300	J	23.5		1.890	0.48	.48	.72	.52	130	.0472		-.12	C	22.5	22.3	5.1	8.0	2.6	.39	252	3	0.59	.0981	+0.02	1.0200		
0400	J	22.0	.357	1.890	0.52	.46	.72	.43	150	.0472	+0.61	-.12	C	22.3	22.3	5.2	9.0	5.3	.39	267	4	0.56	.0963	0.00	1.0200	2.6405	
0500	J	23.0		1.829	0.58	.44	.66	.50	155	.0437		-.12	D	22.0	22.3	5.5	8.5	3.6	.40	285	4	0.52	.0963	-0.11	1.0200		
0600	J	26.0		1.676	0.64	.40	.60	.58	160	.0419		-.12	E	21.8	22.3	5.8	8.0	0.0	.34	304	4	0.49	.0963	-0.19	1.0200		
0700	L	28.5		1.463	0.68	.37	.55	.40	158	.0384		-.12	F	21.6	22.4	6.2	8.4	0.0	.26	322	4	0.46	.0945	-0.20	1.0200		
0800	M	30.5		1.310	0.70	.36	.50	.22	150	.0367		-.01	G	21.3	22.4	6.4	9.0	0.0	.20	333	4	0.44	.0928	-0.12	1.0200		
0900	M	30.5		1.219	0.64	.36	.50	.24	140	.0332		-.12	H	21.1	22.4	6.5	9.8	0.0	.20	339	4	0.45	.0805	0.00	1.0199		
1000	M	30.0	.302	1.250	0.56	.36	.54	.26	125	.0314	+0.96	.35	H	21.8	22.5	6.3	9.6	0.0	.20	337	4	0.46	.0524	+0.05	1.0198	2.6485	
1100	M	28.0		1.310	0.48	.38	.55	.29	110	.0402		.47	H	22.7	23.0	5.9	8.4	0.0	.20	325	3	0.48	.0332	+0.10	1.0197		
1200	L	25.0		1.494	0.44	.40	.57	.32	110	.0507		.49	C	23.8	24.2	5.4	7.0	0.0	.21	313	3	0.50	.0210	+0.20	1.0196		
1300	K	22.0		1.707	0.48	.43	.57	.30	110	.0524		.45	F	24.4	24.1	5.3	7.2	0.0	.24	001	3	0.48	.0244	+0.24	1.0196		
1400	J	21.0		1.951	0.56	.44	.58	.30	105	.0559		.49	E	24.7	24.0	6.0	7.2	0.0	.24	021	4	0.46	.0454	+0.22	1.0195		
1500	I	19.5		2.103	0.64	.45	.60	.29	103	.0559		.32	D	25.0	23.7	6.8	7.4	2.3	.25	001	4	0.43	.0752	+0.11	1.0195		
1600	I	19.0		2.164	0.72	.45	.60	.28	100	.0559	+2.05	.21	C	25.1	23.5	7.6	7.5	4.5	.28	001	3	0.40	.0963	+0.03	1.0195		
1700	I	18.5	.302	2.164	0.72	.45	.59	.27	110	.0540		.20	C	25.0	23.3	7.8	7.6	3.0	.28	001	3	0.37	.0945	-0.04	1.0194	2.6524	
1800	J	21.0		2.073	0.72	.45	.60	.25	117	.0489		.02	D	24.6	23.3	7.6	7.6	0.2	.28	015	2	0.34	.0875	-0.15	1.0189		
1900	K	25.5		1.859	0.76	.48	.63	.24	120	.0419		-.08	E	24.0	23.4	7.1	7.8	0.0	.25	044	2	0.31	.0699	-0.26	1.0184		
2000	L	28.0		1.585	0.84	.48	.65	.23	120	.0314		-.08	F	23.3	23.5	6.4	7.9	0.0	.24	110	2	0.28	.0524	-0.25	1.0181		
2100	L	26.0		1.372	0.92	.44	.62	.20	110	.0314		-.08	H	22.2	23.5	5.8	8.0	0.0	.17	200	2	0.28	.0384	-0.17	1.0180		
2200	M	23.0		1.250	0.96	.38	.55	.20	90	.0419		-.09	I	21.6	23.4	5.2	7.9	0.0	.12	224	2	0.28	.0244	-0.08	1.0181		
2300	M	22.0	.383	1.219	0.92	.33	.49	.20	72	.0507	+0.26	-.09	I	21.4	23.3	4.8	7.9	0.0	.04	246	2	0.36	.0105	0.00	1.0181	2.6459	

DATE: 09/11/66

Time hrs	B	d	\bar{D}	E_t	h	\bar{H}_b	H_{bs}	H_s	$\bar{\lambda}_b$	\bar{m}	Q_f	R_n	S	t_a	t_w	\bar{T}_b	T_s	u	\bar{V}	W_d	W_s	\bar{z}	$\bar{\alpha}_b$	η	ρ_d	ρ_s
	m	m	mm	m	m	m	m	m	m	(tan)	m^3	$\frac{g \text{ cal}}{cm^2 \text{ sec}}$		(°C)	(°C)	sec	sec	m	$\frac{m}{sec}$	()	$\frac{m}{sec}$	m	(tan)	$\frac{m}{hr}$	$\frac{g}{cm^3}$	$\frac{g}{cm^3}$
0000	M	23.0		1.280	0.76	.30	.45	.24	62	.0384		-.10	I	21.0	23.3	4.5	7.9	0.0	.00	.261	2	0.50	.0000	+0.10	1.0182	
0100	L	22.0		1.433	0.60	.33	.45	.28	60	.0437		-.10	H	20.8	23.3	4.6	7.9	0.0	.00	.267	2	0.50	.0000	+0.14	1.0182	
0200	K	19.5		1.554	0.50	.36	.48	.33	60	.0540		-.10	G	20.5	23.2	5.0	8.0	0.0	.00	.269	2	0.48	.0000	+0.11	1.0182	
0300	J	17.0		1.798	0.44	.41	.51	.32	60	.0630		-.10	F	20.2	23.2	5.6	8.0	0.0	.00	.268	2	0.46	.0000	+0.10	1.0182	
0400	I	15.0		1.890	0.44	.44	.55	.32	60	.0699		-.10	E	19.9	23.1	6.0	8.0	1.1	.00	.267	2	0.43	.0000	+0.08	1.0183	
0500	I	14.0	.360	1.951	0.48	.42	.50	.32	60	.0734	+1.17	-.10	E	19.7	22.9	6.2	8.0	1.8	.04	.272	2	0.40	.0000	0.00	1.0183	2.6433
0600	I	14.5		1.859	0.52	.38	.46	.31	60	.0664		-.10	E	19.5	22.8	5.7	8.0	0.6	.12	.275	2	0.38	.0052	-0.11	1.0184	
0700	J	16.5		1.737	0.56	.31	.43	.30	60	.0559		-.09	F	19.3	22.7	5.0	7.8	0.0	.20	.277	2	0.36	.0175	-0.15	1.0184	
0800	K	22.0		1.554	0.68	.25	.42	.30	60	.0419		-.01	G	19.2	22.7	4.4	7.6	0.0	.28	.279	2	0.33	.0262	-0.22	1.0185	
0900	L	27.0		1.310	0.76	.22	.42	.30	60	.0349		.13	H	20.0	22.9	4.0	7.2	0.0	.33	.284	3	0.32	.0105	-0.22	1.0185	
1000	M	29.0		1.158	0.84	.22	.44	.30	62	.0332		.29	H	21.0	23.2	4.1	6.9	0.0	.36	.299	3	0.31	.0314	-0.13	1.0185	
1100	M	28.0		1.067	0.88	.26	.45	.29	70	.0314	+0.75	.38	H	22.3	23.5	4.6	6.6	0.0	.38	.319	3	0.31	.1052	0.00	1.0184	
1200	L	22.5	.224	1.158	0.60	.32	.45	.29	82	.0349		.49	H	23.3	23.8	5.2	6.2	0.0	.40	.333	3	0.32	.1817	+0.13	1.0183	2.6501
1300	K	17.0		1.310	0.42	.38	.50	.28	89	.0419		.48	F	23.6	23.9	6.1	6.0	2.0	.41	.016	3	0.35	.2126	+0.22	1.0183	
1400	J	14.5		1.585	0.48	.42	.58	.28	82	.0540		.47	E	24.0	24.0	6.6	5.6	3.6	.40	.040	3	0.38	.2035	+0.30	1.0184	
1500	J	15.0		1.890	0.60	.44	.65	.27	72	.0612		.42	D	24.5	24.0	6.8	5.2	5.4	.40	.050	3	0.41	.1853	+0.27	1.0186	
1600	I	16.5		2.073	0.64	.42	.67	.25	60	.0612		.29	C	24.7	24.0	7.0	4.8	6.6	.40	.061	3	0.44	.1584	+0.15	1.0188	
1700	I	19.0		2.195	0.46	.40	.67	.25	58	.0489		.08	C	24.9	24.0	6.8	4.5	5.4	.37	.078	2	0.74	.1263	+0.09	1.0187	
1800	H	19.5	.339	2.225	0.32	.39	.64	.24	55	.0454	-1.20	.00	C	24.5	24.0	6.6	4.2	3.4	.34	.097	3	0.78	.0963	-0.03	1.0184	2.6388
1900	G	15.0		2.103	0.28	.37	.60	.23	55	.0540		-.10	C	23.8	24.0	6.4	3.8	2.8	.30	.118	3	0.54	.0647	-0.17	1.0180	
2000	H	12.0		1.890	0.36	.35	.55	.22	60	.0647		-.10	D	23.2	24.0	6.4	3.4	2.3	.26	.125	4	0.40	.0472	-0.24	1.0178	
2100	I	13.0		1.585	0.48	.33	.50	.20	50	.0682		-.10	E	22.8	24.0	6.3	3.0	0.0	.26	.127	4	0.38	.0384	-0.27	1.0177	
2200	J	17.5		1.310	0.68	.30	.45	.20	45	.0682		-.10	G	22.6	23.9	6.1	3.0	0.0	.25	.126	5	0.36	.0349	-0.25	1.0177	
2300	K	22.5		1.158	0.80	.30	.43	.20	40	.0647		-.11	H	22.7	23.9	5.8	3.0	0.0	.24	.125	5	0.35	.0332	-0.08	1.0177	

Time hrs	B	d	\bar{D}	E_t	h	\bar{H}_b	H_{bs}	H_s	\bar{h}_b	\bar{m}	Q_f	R_n	S	t_a	t_w	\bar{T}_b	T_s	u	\bar{V}	W_d	W_s	\bar{z}	$\bar{\alpha}_b$	η	ρ_l	ρ_s
	m	m	mm	m	m	m	m	m	m	(tan)	m^3	$\frac{g \text{ cal}}{cm^2 \text{ sec}}$		(°C)	(°C)	sec	sec	m	$\frac{m}{sec}$	(°)	$\frac{m}{sec}$	m	(tan)	$\frac{m}{hr}$	$\frac{g}{cm^3}$	$\frac{g}{cm^3}$
0000	L	25.5	.230	1.128	0.88	.28	.40	.20	35	.0630	-0.47	-.11	I	22.8	23.9	5.5	3.0	0.0	.24	123	4	0.34	.0332	0.00	1.0177	2.6421
0100	L	24.0		1.250	0.80	.28	.40	.20	30	.0594		-.11	H	22.9	23.9	5.1	3.0	0.0	.28	120	4	0.38	.0367	+0.12	1.0177	
0200	K	21.0		1.372	0.68	.28	.43	.20	20	.0577		-.10	G	22.8	23.9	4.9	3.0	0.0	.32	117	5	0.41	.0437	+0.19	1.0177	
0300	J	18.0		1.615	0.56	.29	.46	.24	10	.0577		-.10	F	22.8	23.9	4.7	3.0	0.5	.36	111	6	0.44	.0559	+0.27	1.0177	
0400	I	17.0		1.890	0.52	.30	.49	.30	10	.0594		-.10	D	22.7	23.7	4.5	3.0	2.0	.42	108	6	0.48	.0734	+0.25	1.0177	
0500	I	17.5		2.042	0.54	.35	.50	.36	10	.0630		-.10	D	22.8	23.7	4.5	3.0	3.6	.42	107	6	0.52	.0998	+0.11	1.0177	
0600	I	19.0	.336	2.103	0.56	.39	.53	.45	20	.0664	+0.50	-.10	C	22.9	23.5	4.7	3.0	4.5	.40	101	6	0.54	.1299	0.00	1.0177	2.6635
0700	J	21.0		2.012	0.56	.41	.56	.47	30	.0577		-.08	C	23.0	23.4	4.8	3.1	3.4	.40	098	6	0.51	.1620	-0.13	1.0177	
0800	J	23.0		1.859	0.60	.43	.60	.45	50	.0454		.00	D	23.2	23.4	4.8	3.5	2.0	.38	100	5	0.48	.1817	-0.18	1.0177	
0900	K	24.0		1.646	0.68	.43	.55	.46	80	.0384		.13	E	23.4	23.5	4.8	3.6	0.7	.36	100	5	0.44	.1853	-0.26	1.0177	
1000	L	25.5		1.372	0.76	.40	.54	.50	100	.0384		.12	F	23.5	23.5	4.8	3.7	0.2	.32	100	6	0.42	.1495	-0.26	1.0178	
1100	L	27.0		1.189	0.88	.35	.54	.50	110	.0419		.25	G	23.6	23.6	4.9	3.8	0.0	.28	100	6	0.38	.1139	-0.12	1.0178	
1200	M	30.0	.272	1.128	0.94	.34	.55	.50	120	.0472	+0.02	.32	H	23.7	23.7	4.8	4.0	0.0	.24	099	7	0.36	.0963	0.00	1.0178	2.6411
1300	M	32.5		1.189	0.96	.35	.56	.80	122	.0349		.47	F	23.7	23.7	4.7	4.4	0.0	.24	100	8	0.40	.0787	+0.11	1.0178	
1400	L	33.0		1.372	0.88	.40	.59	1.02	120	.0279		.45	E	23.5	23.7	4.8	5.0	0.0	.24	099	8	0.44	.0612	+0.24	1.0178	
1500	K	30.0		1.646	0.80	.45	.65	1.11	120	.0314			C	23.2	23.8	5.1	5.0	0.0	.24	098	7	0.52	.0437	+0.30	1.0178	
1600	J	24.5		1.951	0.76	.50	.70	1.20	120	.0384			C	23.0	23.7	5.3	5.0	0.0	.24	096	7	0.62	.0279	+0.29	1.0179	
1700	I	21.0		2.195	0.72	.55	.73	1.40	120	.0472			B	22.7	23.6	5.4	5.0	3.4	.08	096	7	0.76	.0244	+0.21	1.0179	
1800	H	20.0		2.347	0.76	.58	.75	1.49	110	.0540			B	22.5	23.6	5.6	5.3	10.0	.08	095	7	0.88	.0175	+0.10	1.0179	
1900	I	21.0	.359	2.347	0.86	.58	.75	1.45	90	.0524	-3.34		B	22.4	23.6	5.9	6.1	11.8	.28	091	7	0.86	.0105	-0.03	1.0180	2.6462
2000	I	32.0		2.195	1.00	.56	.75	1.42	75	.0454			B	22.2	23.6	6.2	6.6	0.2	.48	089	7	0.62	.0087	-0.20	1.0180	
2100	J	32.5		1.951	1.04	.49	.66	1.34	55	.0437			C	22.0	23.6	6.2	6.4	0.0	.36	087	7	0.55	.0035	-0.28	1.0181	
2200	K	30.5		1.646	0.96	.42	.55	1.26	38	.0454			E	22.1	23.5	6.0	6.0	0.0	.26	083	8	0.50	.0035	-0.31	1.0181	
2300	L	26.5		1.341	0.92	.34	.45	.96	25	.0472			H	22.2	23.4	5.8	5.9	0.0	.14	082	8	0.43	.0000	-0.25	1.0181	

DATE: 09/13/66

Time hrs	B	d	D	E _t	h	H _b	H _{bs}	H _s	z _b	m	Q _f	R _n	S	t _a	t _w	T _b	T _s	u	V	W _d	W _s	z	α _b	η	ρ _l	ρ _s
		m	mm	m	m	m	m	m	m	m	m ³	g cal/cm ² /sec		(°C)	(°C)	sec	sec	m	m	(°)	m	m	(tan)	$\frac{m}{hr}$	g/cm ³	g/cm ³
0000	M	23.5		1.158	0.88	.32	.41	.60	20	.0507			I	22.4	23.3	5.6	6.0	0.0	.00	83	8	0.36	.0035	-0.12	1.0182	
0100	M	22.5	.337	1.097	0.80	.37	.53	.82	20	.0507	+0.17		I	22.5	23.3	5.6	6.0	0.0	.03	83	8	0.35	.0035	0.00	1.0182	2.6490
0200	M	23.5		1.219	0.76	.47	.75	.98	20	.0454			H	22.6	23.2	5.6	5.6	0.0	.06	87	8	0.41	.0000	+0.19	1.0182	
0300	L	26.0		1.463	0.68	.60	.96	1.12	20	.0402			G	22.6	23.2	5.6	5.1	0.0	.08	87	8	0.47	.0000	+0.26	1.0182	
0400	K	28.5		1.737	0.60	.70	1.03	1.20	15	.0349			D	22.5	23.2	5.8	5.0	0.0	.10	90	8	0.52	.0000	+0.27	1.0182	
0500	I	29.5		2.012	0.56	.77	1.05	1.22	20	.0367			B	22.5	23.2	5.8	5.0	0.0	.10	99	8	0.56	.0035	+0.25	1.0182	
0600	G	28.5		2.195	0.52	.78	1.08	1.22	20	.0367			A	22.5	23.1	5.7	5.0	4.2	.00	107	8	0.60	.0262	+0.12	1.0183	
0700	F	26.0	.316	2.255	0.52	.75	1.05	1.18	20	.0384	-0.47		A	22.5	23.0	5.6	5.0	9.7	.16	109	8	0.64	.0647	0.00	1.0183	2.6550
0800	G	25.5		2.164	0.52	.65	.94	1.10	25	.0384			A	22.7	22.9	5.5	5.0	3.5	.28	106	8	0.58	.0945	-0.14	1.0183	
0900	H	26.0		1.981	0.56	.52	.76	1.03	30	.0367			B	23.0	22.9	5.6	5.0	0.0	.28	103	8	0.47	.1052	-0.23	1.0183	
1000	J	27.0		1.676	0.68	.39	.61	1.10	38	.0367			C	23.2	22.8	5.8	5.0	0.0	.28	100	8	0.37	.1052	-0.30	1.0183	
1100	K	31.0		1.402	0.80	.31	.49	1.15	40	.0367			E	23.2	22.8	5.9	5.1	0.0	.28	99	8	0.26	.1016	-0.27	1.0183	
1200	L	33.5		1.128	0.88	.29	.45	1.22	40	.0367	-0.52		F	23.0	22.8	6.0	5.2	0.0	.30	99	9	0.16	.0981	-0.21	1.0184	
1300	M	33.5	.314	1.006	0.88	.33	.52	1.33	40	.0384			G	22.8	22.9	5.8	5.2	0.0	.40	100	10	0.21	.0928	0.00	1.0184	2.6477
1400	M	32.0		1.036	0.80	.42	.66	1.36	40	.0384			F	22.6	23.0	5.8	5.4	0.0	.52	100	10	0.30	.0875	+0.16	1.0184	
1500	L	28.5		1.280	0.68	.52	.80	1.41	52	.0402			E	22.4	23.0	5.6	5.4	0.0	.60	100	10	0.38	.0840	+0.31	1.0184	
1600	K	25.0		1.310	0.56	.63	.86	1.50	65	.0437			D	22.4	23.0	5.4	5.5	0.0	.72	101	9	0.47	.0840	+0.36	1.0184	
1700	I	19.5		1.981	0.44	.65	.83	1.57	90	.0540			C	22.5	23.0	5.3	5.4	0.0	.58	101	9	0.56	.0787	+0.36	1.0184	
1800	G	15.5		2.316	0.44	.63	.76	1.67	120	.0630			B	22.6	23.0	5.2	5.4	0.0	.44	105	8	0.70	.0752	+0.27	1.0185	
1900	F	15.0	.330	2.408	0.56	.55	.70	1.69	145	.0717	-1.42		A	22.8	23.0	5.2	5.4	4.0	.25	106	8	0.74	.0717	+0.04	1.0185	2.6507
2000	F	17.5		2.408	0.66	.46	.68	1.70	140	.0734			A	22.9	22.9	5.2	5.4	3.3	.25	113	9	0.66	.0717	-0.05	1.0185	
2100	G	22.0		2.225	0.88	.39	.65	1.70	118	.0682			B	23.0	22.9	5.2	5.4	0.0	.25	118	9	0.56	.0717	-0.21	1.0186	
2200	I	27.5		1.981	1.02	.35	.62	1.66	75	.0594			C	23.0	22.9	5.2	5.0	0.0	.25	122	10	0.46	.0699	-0.32	1.0186	
2300	K	33.0		1.615	1.12	.35	.58	1.58	35	.0489			E	23.0	22.8	5.2	5.0	0.0	.25	124	10	0.36	.0699	-0.37	1.0186	

DATE: 09/14/66

Time hrs	B	d	D	E _t	h	H _b	H _{bs}	H _s	h _b	m	Q _f	R _n	S	t _a	t _w	T _b	T _s	u	V	W _d	W _s	z	α _b	η	ρ _l	ρ _s
	m	mm	m	m	m	m	m	m	m	m	m ³	g cal/cm ² /sec		(°C)	(°C)	sec	sec	m	m	(°)	sec	m	(tan)	m/HR	g/cm ³	g/cm ³
0000	M	37.0		1.310	1.14	.37	.57	1.50	22	.0384			C	23.0	22.8	5.2	5.0	0.0	.26	129	11	0.26	.0787	-0.25	1.0187	
0100	M ⁺ ₁₅	38.5		1.128	1.06	.39	.59	1.44	20	.0349			I	23.0	22.8	5.2	5.4	0.0	.32	130	11	0.30	.0963	-0.15	1.0187	
0200	M ⁺ ₁₅	37.0	.352	1.036	0.96	.41	.61	1.36	20	.0314	-0.18		I	23.0	22.8	5.0	5.8	0.0	.42	133	10	0.35	.1228	-0.01	1.0187	2.6416
0300	M ⁺ ₁₅	36.5		1.189	0.84	.45	.67	1.30	25	.0279			H	23.2	22.8	4.9	6.4	0.0	.52	137	9	0.40	.1459	+0.22	1.0188	
0400	M	35.5		1.463	0.76	.48	.72	1.20	30	.0297			E	23.3	22.8	4.8	7.0	0.0	.64	139	8	0.44	.1709	+0.32	1.0188	
0500	K	33.0		1.829	0.68	.50	.75	1.30	32	.0367			C	23.2	22.7	4.7	6.5	2.9	.76	142	8	0.49	.1980	+0.34	1.0188	
0600	G	28.0		2.134	0.56	.50	.76	1.41	30	.0559			B	23.1	22.7	4.8	6.2	3.0	.88	144	8	0.54	.2217	+0.25	1.0188	
0700	E	21.0		2.347	0.54	.52	.77	1.50	20	.0734			A	22.9	22.8	5.2	6.0	3.0	.92	144	9	0.58	.2438	+0.16	1.0189	
0800	E	13.0	.322	2.438	0.60	.52	.77	1.59	20	.0857	-2.00		A	22.8	22.8	5.8	6.0	2.3	.93	143	11	0.57	.2586	0.00	1.0189	2.6546
0900	G	14.5		2.347	0.72	.48	.73	1.58	60	.0840		.03	B	22.8	22.8	6.0	6.4	0.4	.91	139	11	0.46	.2530	-0.20	1.0189	
1000	I	23.0		2.073	0.88	.44	.66	1.58	110	.0717		.10	D	22.7	22.8	6.1	6.6	0.0	.88	130	11	0.36	.2345	-0.30	1.0189	
1100	L	34.5		1.737	1.00	.40	.60	1.56	150	.0559		.10	F	22.7	22.8	6.0	7.0	0.0	.83	128	11	0.26	.1962	-0.32	1.0190	
1200	M ⁺ ₃₀	40.0		1.463	1.04	.38	.57	1.56	180	.0384	-2.85	.12	I	22.8	22.8	5.4	7.4	0.0	.79	132	11	0.16	.1530	-0.32	1.0190	
1300	M ⁺ ₃₀	40.0		1.128	0.96	.39	.56	1.55	200	.0332		.18	J	22.9	22.9	5.4	7.8	0.0	.72	137	12	0.20	.1459	-0.25	1.0189	
1400	M ⁺ ₃₀	38.5	.356	1.036	0.86	.41	.59	1.51	210	.0297		.13	J	23.0	23.0	5.3	8.2	0.0	.59	140	11	0.25	.1495	0.00	1.0188	2.6494
1500	M ⁺ ₃₀	36.5		1.128	0.78	.43	.60	1.51	215	.0279		.19	H	23.4	23.1	5.5	8.6	0.0	.45	142	9	0.30	.1530	+0.19	1.0188	
1600	M	34.0		1.433	0.72	.44	.62	1.50	215	.0297		.21	D	23.7	23.3	6.0	9.0	0.0	.32	146	7	0.36	.1620	+0.33	1.0189	
1700	J	31.0		1.768	0.68	.50	.68	1.70	210	.0367		.20	B	23.7	23.4	6.7	9.0	0.0	.34	149	4	0.41	.1709	+0.34	1.0192	
1800	G	27.5		2.103	0.68	.57	.76	1.89	200	.0489		.14	A ⁺ ₁₂	23.5	23.3	7.4	9.0	0.0	.40	168	3	0.46	.1781	+0.31	1.0194	
1900	E	24.5		2.347	0.68	.64	.81	1.60	180	.0717		.03	A ⁺ ₂₂	23.0	23.2	7.7	8.6	0.0	.44	200	2	0.52	.1781	+0.20	1.0196	
2000	D	24.0	.352	2.499	0.76	.65	.82	1.08	150	.0910	-1.88		A ⁺ ₂₂	22.5	23.1	7.6	8.0	0.0	.49	244	2	0.56	.1673	+0.09	1.0197	2.6668
2100	E	25.0		2.499	0.88	.62	.76	1.00	125	.0910			A ⁺ ₁₂	21.8	23.0	7.1	8.5	0.0	.36	271	2	0.52	.1584	-0.02	1.0197	
2200	G	28.5		2.316	0.96	.54	.68	.95	100	.0734			B	21.5	22.8	6.4	9.0	0.0	.24	279	2	0.46	.1530	-0.24	1.0198	
2300	J	33.5		2.012	1.04	.39	.56	.90	75	.0577			D	21.0	22.7	5.6	8.8	0.0	.12	278	2	0.42	.1459	-0.34	1.0198	

DATE: 09/15/66

Time hrs	B	d	\bar{D}	E_t	h	\bar{H}_b	H_{bs}	H_s	\bar{h}_b	\bar{m}	Q_f	R_n	S	t_a	t_w	T_b	T_s	u	\bar{V}	W_d	W_s	z	$\bar{\alpha}_b$	η	ρ_l	ρ_s
		m	mm	m	m	m	m	m	m	(tan)	m^3	$\frac{g \text{ cal}}{cm^2 \text{ sec}}$		(°C)	(°C)	sec	sec	m	$\frac{m}{sec}$	($^{\circ}$)	$\frac{m}{sec}$	m	(tan)	$\frac{m}{hr}$	$\frac{g}{cm^3}$	$\frac{g}{cm^3}$
0000	L	37.5		1.646	1.14	.31	.52	.84	.62	.0454			F	20.7	22.7	5.1	8.6	0.0	.00	277	3	0.36	.1405	-0.36	1.0199	
0100	M	41.0		1.310	1.24	.31	.62	.80	.60	.0367			G	20.4	22.6	4.9	8.5	0.0	.06	277	3	0.29	.1405	-0.29	1.0200	
0200	M ¹ ₁₅	44.0	.341	1.097	1.28	.38	.76	.72	.55	.0332	-4.30		H	20.2	22.6	5.0	8.4	0.0	.12	277	3	0.28	.1459	-0.16	1.0200	2.6462
0300	M ¹ ₁₅	44.5		1.006	1.24	.48	.89	.67	.55	.0349			H	20.0	22.5	5.3	8.2	0.0	.20	275	3	0.32	.1477	0.00	1.0200	
0400	M	43.5		1.128	1.16	.60	.94	.60	.60	.0437			F	19.8	22.5	5.7	8.0	0.0	.28	274	3	0.38	.1495	+0.25	1.0201	
0500	L	40.0		1.463	0.92	.70	.99	.68	.75	.0454			E	19.8	22.5	6.3	7.6	0.0	.34	268	3	0.48	.1530	+0.38	1.0200	
0600	K	38.0		1.859	0.66	.81	1.08	.78	1.07	.0419			C	19.7	22.6	7.0	7.2	0.0	.42	262	3	0.58	.1530	+0.39	1.0199	
0700	J	36.0		2.225	0.40	.88	1.15	.78	1.35	.0367		.01	B	19.6	22.6	7.6	7.2	0.0	.50	264	4	0.66	.1477	+0.33	1.0199	
0800	I	35.0	.336	2.499	0.22	.89	1.20	.64	1.50	.0297	+0.67		A+	19.6	22.6	7.9	8.0	0.0	.60	271	4	0.76	.1370	+0.17	1.0198	2.6424
0900	I	35.0		2.560	0.24	.82	1.10	.52	1.35	.0227		.05	A+	19.5	22.6	8.0	8.0	0.0	.60	280	4	0.80	.1263	0.00	1.0197	
1000	J	37.5		2.438	0.40	.72	.96	.42	1.10	.0210		.12	A	20.2	22.7	7.8	8.0	0.0	.60	293	5	0.78	.1122	-0.20	1.0197	
1100	K	39.5		2.347	0.60	.60	.80	.33	.80	.0244		.23	B	21.0	22.7	7.0	8.0	0.0	.60	305	6	0.68	.0981	-0.30	1.0196	
1200	L	39.0		2.012	0.68	.52	.69	.25	.55	.0297		.32	E	22.0	22.7	6.0	8.0	0.0	.60	318	7	0.56	.0857	-0.36	1.0195	
1300	M	38.5		1.646	0.76	.45	.62	.29	.45	.0367		.53	H	22.8	22.9	5.8	8.0	0.0	.56	316	6	0.46	.0787	-0.36	1.0195	
1400	M ¹ ₁₅	44.0		1.310	0.96	.40	.58	.30	.55	.0419		.38	J	23.4	23.0	6.1	8.0	0.0	.48	319	5	0.40	.0857	-0.25	1.0195	
1500	M ¹ ₁₅	45.0	.411	1.158	1.00	.38	.57	.32	.75	.0472	-0.10	.40	J	23.4	23.0	6.7	8.0	0.0	.40	333	5	0.38	.0998	0.00	1.0195	2.6512
1600	M	39.0		1.219	0.96	.37	.57	.32	1.00	.0524		.22	H	23.0	23.0	7.1	8.0	0.0	.32	357	5	0.40	.1122	+0.18	1.0194	
1700	K	32.5		1.494	0.84	.39	.60	.40	1.15	.0577		.13	F	22.7	23.0	6.8	8.0	0.0	.26	360	4	0.44	.1139	+0.27	1.0194	
1800	I	26.5		1.768	0.72	.40	.64	.46	1.20	.0630		.02	D	22.2	23.0	6.4	8.0	0.0	.20	002	4	0.48	.1104	+0.37	1.0194	
1900	G	22.0		2.164	0.60	.42	.67	.39	1.25	.0682			B	21.7	23.0	5.9	7.4	0.0	.10	003	5	0.52	.0998	+0.35	1.0194	
2000	F	20.5		2.438	0.52	.41	.71	.32	1.23	.0752			A	21.2	22.9	5.4	6.6	0.0	.06	009	6	0.56	.0910	+0.22	1.0193	
2100	F	21.0	.386	2.620	0.52	.50	.74	.58	1.20	.0805	+0.39		A	20.7	22.9	5.0	6.0	0.0	.08	012	7	0.57	.0630	+0.09	1.0193	2.6389
2200	F	23.5		2.650	0.60	.53	.75	.88	1.05	.0822			A	20.2	22.9	4.8	5.4	0.0	.22	015	8	0.54	.0070	-0.01	1.0193	
2300	H	27.5		2.499	0.72	.54	.75	.97	.75	.0787			B	19.7	22.8	4.7	5.0	0.0	.38	018	9	0.50	.0875	-0.21	1.0193	

DATE: 09/16/66

Time hrs	B	d	\bar{D}	E_t	h	\bar{H}_b	H_{bs}	H_s	\bar{x}_b	\bar{m}	Q_f	R_n	S	t_a	t_w	\bar{T}_b	T_s	u	\bar{V}	W_d	W_s	\bar{z}	$\bar{\alpha}_b$	η	ρ_k	ρ_s
		m	mm	m	m	m	m	m	m	(tan)	m^3	$\frac{g\ cal}{cm^2/sec}$		(°C)	(°C)	sec	sec	m	$\frac{m}{sec}$	(°)	$\frac{m}{sec}$	m	(tan)	$\frac{m}{hr}$	$\frac{g}{cm^3}$	$\frac{g}{cm^3}$
0000	J	32.0		2.225	0.90	.53	.75	1.05	40	.0717			C	19.2		4.6	4.9	0.0	.52	019	10	0.46	.2035	-0.38	1.0194	
0100	K	36.5		1.798	1.04	.49	.73	1.02	30	.0594			E	18.5		4.6	4.9	0.0	.56	019	11	0.42	.2530	-0.42	1.0194	
0200	L	39.5		1.433	1.08	.45	.67	1.00	30	.0472			G	17.7		4.7	5.0	0.0	.54	015	11	0.38	.2493	-0.33	1.0193	
0300	M	40.0	.325	1.128	1.04	.44	.64	.98	30	.0332	-1.19		H	16.8		4.7	5.0	0.0	.58	010	11	0.34	.2364	-0.18	1.0193	2.6477
0400	M	39.5		1.067	0.88	.47	.65	.95	30	.0279			G	16.2		4.6	5.0	0.0	.68	007	11	0.34	.2254	0.00	1.0193	
0500	M	34.5		1.189	0.56	.52	.77	1.16	30	.0384			F	15.6		4.8	5.0	0.0	.88	008	11	0.39	.2180	+0.24	1.0193	
0600	L	29.5		1.524	0.36	.58	.98	1.37	30	.0577			D	15.2		4.9	5.0	0.0	1.08	011	11	0.43	.2162	+0.36	1.0190	
0700	K	22.5		1.890	0.12	.69	1.12	1.41	30	.0787			C	14.7		5.1	5.0	0.0	1.16	013	12	0.48	.2144	+0.34	1.0189	
0800	K	14.0		2.164	-0.12	.75	1.16	1.27	30	.1016			A	14.5		5.3	5.0	1.2	1.12	013	11	0.52	.2126	+0.26	1.0188	
0900	K	8.0	.363	2.408	-0.20	.77	1.07	1.13	30	.1229			A+	14.5		5.4	5.0	3.7	.96	014	10	0.56	.2035	+0.16	1.0188	2.6486
1000	K	7.0		2.438	-0.12	.74	.94	1.02	32	.1210	-3.60		A+	14.7		5.2	5.0	4.0	.77	012	10	0.61	.1944	-0.02	1.0188	
1100	L	10.0		2.316	0.04	.66	.81	.90	40	.0822			A	15.1		5.0	5.0	1.8	.63	012	9	0.66	.1799	-0.20	1.0188	
1200	L	15.5		2.073	0.28	.55	.75	.78	60	.0244			B	15.6		4.8	5.0	0.0	.48	013	8	0.66	.1620	-0.27	1.0188	
1300	M	22.5		1.768	0.48	.48	.65	.78	62	.0192			D	16.0		4.8	5.5	0.0	.46	018	7	0.48	.1495	-0.34	1.0187	
1400	M	30.0		1.402	0.64	.44	.55	.78	60	.0175			E	16.0		4.7	6.0	0.0	.46	020	6	0.23	.1405	-0.35	1.0187	
1500	M+	36.0		1.128	0.72	.44	.47	.78	60	.0175			G	16.5		4.8	6.5	0.0	.48	084	6	0.12	.1317	-0.21	1.0186	2.6470
1600	M+	39.0	.334	1.036	0.76	.44		.76	60	.0210	+0.00		G	16.8		4.9	7.0	0.0	.52	243	6	0.21	.1192	0.00	1.0185	
1700	M	35.5		1.097	0.68	.45	.78	.60	60	.0279			F	17.0		5.1	6.5	0.0	.56			0.37	.1139	+0.13	1.0185	
1800	K	29.0		1.310	0.52	.48	.76	.60	60	.0367			E	17.3		5.4	5.9	0.0	.61			0.58	.1086	+0.29	1.0184	
1900	I	24.5		1.646	0.40	.52	.75	.60	60	.0454			D	17.4		5.8	5.3	0.0	.66			0.66	.1016	+0.36	1.0183	
2000	H	23.0		2.012	0.40	.55	.74	.60	60	.0507			B	17.5		6.4	4.8	0.0	.72			0.76	.0945	+0.34	1.0183	
2100	H	24.5		2.316	0.48	.56	.57	.73	55	.0402			B	17.6		6.5	4.2	0.0				0.74	.0910	+0.22	1.0183	
2200	I	29.0	.372	2.438	0.60	.57	.58	.58	60	.0262	+1.54		B	17.6		6.5	4.0	0.0				0.62	.0875	0.00	1.0183	2.6389
2300	J	30.0		2.377	0.66	.59	.61	.40	60	.0262			B			6.5	4.0	1.4				0.56	.0840	-0.11	1.0184	

DATE: 09/17/66

Time hrs	B	d	\bar{D}	E_t	h	\bar{H}_b	H_{bs}	H_s	\bar{h}_b	\bar{m}	Q_f	R_n	S	t_a	t_w	\bar{T}_b	T_s	u	\bar{V}	W_d	W_s	z	$\bar{\alpha}_b$	η	ρ_l	ρ_s
		m	mm	m	m	m	m	m	m	(tan)	m^3	$\frac{g \text{ cal}}{cm^2 / sec}$		(°C)	(°C)	sec	sec	m	$\frac{m}{sec}$	($^{\circ}$)	$\frac{m}{sec}$	m	(tan)	$\frac{m}{hr}$	$\frac{g}{cm^3}$	$\frac{g}{cm^3}$
0000	K	31.5		2.225	0.66	.60	.63	.34		.0279			C			6.5	4.0	0.0				0.48	.0805	-0.26	1.0184	
0100	L	32.5		1.890	0.62	.60	.65	.37		.0314			D			6.6	4.1	0.0				0.48	.0787	-0.36	1.0185	
0200	L	33.5		1.524	0.56	.59	.67	.38		.0314			F			6.6	4.2	0.0				0.53	.0734	-0.37	1.0185	
0300	M	34.0		1.158	0.48	.59	.67	.40		.0314			C			6.6	4.3	0.0				0.58	.0630	-0.34	1.0185	
0400	M	34.5		0.975	0.40	.60	.66	.42		.0314	+1.70		C			6.6	4.4	0.0				0.63	.0559	-0.09	1.0186	
0500	M	35.0		0.945	0.32	.60	.69	.45		.0297			F			6.6	4.5	0.0				0.68	.0489	+0.04	1.0186	
0600	L	34.5		1.128	0.26	.60	.68	.49		.0297			E			6.7	4.6	0.0				0.73	.0419	+0.22	1.0187	
0700	L	33.5		1.372	0.20	.60	.68	.50		.0279			D			6.6	4.7	0.0				0.78	.0349	+0.30	1.0187	
0800	K	32.0		1.707	0.16	.59	.62	.50		.0279			C			6.5	5.0	1.0		272		0.83	.0262	+0.31	1.0187	
0900	K	30.0		1.981	0.12	.55	.58	.48		.0279			B			6.4	5.2	2.8	.20			0.88	.0244	+0.21	1.0187	
1000	J	27.0		2.134	0.02	.53	.55	.48		.0332			A			6.4	5.5	3.0	.23			0.93	.0402	+0.10		
1100	J	23.0	.238	2.195	-0.04			.44		.0384	+1.92		A			5.8	5.8	2.6		044	3	0.98	.0752	+0.01		2.6587
1200								.45														-0.07				
1300																						-0.17				

Date Time m/da hrs	E _B (m)												E _w (m)												v (cm/s)											
	A+3I	A+2I	A+12	A	B	C	D	E	F	G	H	I	J	K	L	M	W	X	Y	A	B	C	D	E	F	G	H	I	J	K	L	M				
9/14 0138				2.09	1.68	1.32	1.04	0.84	0.67	0.51	0.43	0.32	0.20	0.04	-0.27	-0.41	1.56	1.46	1.02	4.3	4.0	3.6	3.6	3.5	3.9	3.6	3.6	3.5	4.0	5.1	5.6	4.7				
9/14 0440				2.10	1.71	1.31	1.02	0.84	0.66	0.50	0.42	0.25	0.11	-0.04			1.50	1.39	1.04																	
9/14 0750				2.07	1.58	1.18	0.80										1.70	1.74																		
9/14 0755																																				
9/14 1200				2.02	1.56	1.22	0.91	0.72	0.50	0.29	0.30	0.28	0.22	0.06	-0.14	-0.29	1.67		0.93																	
9/14 1356																																				
9/14 1600				2.01	1.56	1.20	0.91	0.73	0.60	0.48	0.40	0.27	0.11	-0.04	-0.20	-0.37	1.58		0.92																	
9/14 2000	2.47	2.32	1.92	1.50	1.02	0.77	0.67																													
9/14 2014																																				
9/15 0220				1.90	1.51	1.12	0.82	0.58	0.43	0.30	0.26	0.20	0.22	0.11	-0.20	-0.44	1.79	1.57	0.80	5.2	4.3	4.4	4.1	3.9	5.1	5.6	5.5	5.4	5.3	4.9	6.2	4.5				
9/15 0415				1.83	1.44	1.05	0.77	0.60	0.45	0.32	0.24	0.39	0.40	0.06	-0.32	-0.48	1.72	1.50	0.74																	
9/15 0830	2.44	2.32	1.95	1.50	1.08	0.87	0.74	0.74	0.72								1.77	1.73		4.7	5.4	5.2	4.6	5.0	5.3	4.9	4.7									
9/15 1200	2.47	2.31	1.91	1.50	1.12	0.80	0.61	0.61	0.33	0.30	0.20	0.22	0.09	-0.04	-0.16	-0.29			0.84																	
9/15 1230				1.91	1.51	1.10	0.81	0.66	0.54	0.41	0.38	0.26	0.08	-0.11	-0.26	-0.34	1.48	1.50	0.83																	
9/15 1450				1.90	1.51	1.10	0.80	0.67	0.52	0.42	0.40	0.30	0.16	0.00	-0.38	-0.48	1.61	1.41	0.82	4.2	4.4	4.4	3.3	3.4	4.6	4.3	4.0	4.3	3.6	4.4	6.1	5.4				
9/15 1550																	1.60	1.40	0.80																	
9/15 2030	2.48	2.30	1.38	1.51	1.08	0.82	0.72	0.72	0.60	0.59							1.61			4.2	4.8	5.7	5.7	5.1	5.2	4.1	4.5									
9/15 2102																																				
9/16 0000	2.48	1.34	1.80	1.38	1.92	1.63											1.58	1.73		4.3	3.8	3.9	4.1	4.1	4.1	4.0	3.2	4.3	4.6	3.9	5.1	5.3				
9/16 0310																																				
9/16 0330	2.44	2.32	1.90	1.50	1.08	0.87	0.69	0.57	0.42	0.35	0.16	0.00	-0.14	-0.25	-0.38		1.55	1.38	0.87																	
9/16 0930	2.46	2.22	1.69	1.24	0.86	0.65											1.68	1.62		4.9	5.0	5.2	5.3													
9/16 1200				1.74	1.34	1.08	0.76	0.70	0.37	0.10	0.28	0.16	0.17	0.06	-0.09					4.6	4.1	4.7	4.8	3.9	4.7	5.2	5.0	4.4	4.6	4.8	5.0	5.7				
9/16 1544																																				

APPENDIX C

Data matrix used for investigating the dependence of the change in quantity of foreshore material ($\pm\Delta Q_f$) on eight dimensionless variables, distributed over nine lag periods. The dimensionally homogeneous form of the equation investigated is:

$$\pm\Delta Q_f = f \left[\left(\frac{H_b}{nT_b} \right)_{0-8}, \left(\frac{\rho_\ell}{\rho_s} \right)_{0-8}, \left(\frac{\bar{H}_b}{D} \right)_{0-8}, (\tan \bar{m})_{0-8}, (\tan \bar{\alpha}_b)_{0-8}, \left(\frac{\bar{H}_b}{z} \right)_{0-8}, (u/d)_{0-8}, (h/d)_{0-8} \right] (\bar{H}_b)^3_{0-8}$$

\bar{H}_b / nT_b	ρ_ℓ / ρ_s	\bar{H}_b / D	$\tan \bar{m}$	$\tan \bar{\alpha}_b$	\bar{H}_b / z	u/d	h/d	$\Delta Q_f / \bar{H}_b^3$	Tide cycle ends on water	End of cycle		Lag in hours from end of cycle	Lag #
										Date	Hours		
.000	.3855	1.386	.0630	.0770	1.45	0.00	.024	38.636	LOW	8/23	2100	00.0	0
-.095	.3858	1.217	.0664	.0770	1.80	0.00	.042	38.636	LOW	8/23	2100	1.5	1
-.050	.3863	0.982	.0805	.1086	1.45	0.00	.054	42.500	LOW	8/23	2100	3.0	2
-.068	.3866	0.938	.0963	.0945	0.90	0.00	.064	31.481	LOW	8/23	2100	4.5	3
-.286	.3868	1.086	.1139	.0875	0.75	0.00	.068	15.455	LOW	8/23	2100	6.0	4
.411	.3867	1.365	.0963	.0981	1.05	0.00	.062	8.763	LOW	8/23	2100	7.5	5
.101	.3863	1.567	.0805	.1334	1.45	0.00	.054	8.173	LOW	8/23	2100	9.0	6
.072	.3858	1.408	.0664	.1405	1.40	0.00	.046	14.407	LOW	8/23	2100	10.5	7
.061	.3854	0.898	.0630	.1441	1.25	0.00	.036	77.273	LOW	8/23	2100	12.0	8
.000	.3885	0.825	.0367	.0000	0.60	0.00	.016	- 77.778	LOW	8/24	0812	0.0	0
-.117	.3883	0.933	.0402	.0630	0.60	0.00	.010	- 63.636	LOW	8/24	0812	1.5	1
-.096	.3882	1.107	.0542	.1122	0.60	0.00	.010	- 46.667	LOW	8/24	0812	3.0	2
-.618	.3879	1.273	.0682	.1548	0.60	0.16	.022	- 35.897	LOW	8/24	0812	4.5	3
.176	.3874	1.469	.0717	.1763	0.65	0.36	.030	- 29.787	LOW	8/24	0812	6.0	4
.102	.0866	1.586	.0682	.1727	0.70	0.32	.030	- 29.787	LOW	8/24	0812	7.5	5
.059	.3860	1.561	.0647	.1441	1.05	0.20	.028	- 42.424	LOW	8/24	0812	9.0	6
.119	.3856	1.487	.0630	.0981	1.50	0.00	.026	- 58.333	LOW	8/24	0812	10.5	7
-.130	.3855	1.366	.0647	.0734	1.75	0.00	.026	- 63.636	LOW	8/24	0812	12.0	8
.000	.3853	0.896	.0454	.0210	1.10	0.00	.030	- 5.556	LOW	8/24	2202	0.0	0
-.110	.3852	0.806	.0367	.0000	0.95	0.00	.032	- 6.250	LOW	8/24	2202	1.5	1
-.086	.3857	1.325	.0594	.0542	1.00	0.00	.038	- 1.176	LOW	8/24	2202	3.0	2
-.139	.3860	1.771	.0963	.0945	1.20	0.00	.041	- 0.420	LOW	8/24	2202	4.5	3
-.360	.3865	1.853	.1263	.1086	1.35	0.22	.042	- 0.318	LOW	8/24	2202	6.0	4
.345	.3871	1.519	.1175	.1086	1.35	0.10	.042	- 0.463	LOW	8/24	2202	7.5	5
.118	.3875	1.333	.0998	.1016	1.20	0.00	.040	- 0.901	LOW	8/24	2202	9.0	6
.082	.3881	1.000	.0770	.0699	0.90	0.00	.032	- 2.564	LOW	8/24	2202	10.5	7
.127	.3884	0.826	.0540	.0349	0.70	0.00	.030	- 5.000	LOW	8/24	2202	12.0	8
.000	.3867	1.934	.0419	.0664	1.15	0.00	.028	- 15.217	LOW	8/25	0950	0.0	0
-.097	.3865	1.571	.0437	.0384	1.05	0.00	.028	- 29.167	LOW	8/25	0950	1.5	1
-.070	.3872	1.286	.0454	.0349	0.85	0.00	.028	- 52.500	LOW	8/25	0950	3.0	2
-.148	.3878	1.336	.0507	.0349	0.70	0.00	.027	- 43.750	LOW	8/25	0950	4.5	3
5.714	.3882	1.802	.0559	.0314	0.65	0.00	.023	- 16.406	LOW	8/25	0950	6.0	4
.187	.3877	1.872	.0577	.0314	0.85	0.14	.014	- 12.353	LOW	8/25	0950	7.5	5
.112	.3868	1.529	.0507	.0314	1.05	0.24	.022	- 17.797	LOW	8/25	0950	9.0	6
.148	.3860	1.047	.0454	.0349	1.15	0.04	.030	- 43.750	LOW	8/25	0950	10.5	7
.000	.3853	0.822	.0437	.0175	1.05	0.00	.030	- 75.000	LOW	8/25	0950	12.0	8
.000	.3883	1.805	.0489	.1263	0.85	0.00	.022	- 30.392	LOW	8/25	2308	0.0	0
-.142	.3887	1.478	.0437	.1086	0.85	0.00	.026	- 39.744	LOW	8/25	2308	1.5	1
-.078	.3888	1.296	.0437	.1157	0.95	0.00	.033	- 36.047	LOW	8/25	2308	3.0	2
-.133	.3887	1.443	.0507	.1656	1.25	0.00	.043	- 18.235	LOW	8/25	2308	4.5	3
-.900	.3887	1.662	.0594	.2272	1.65	0.28	.050	- 9.873	LOW	8/25	2308	6.0	4
.262	.3887	1.875	.0630	.2493	1.80	0.20	.050	- 7.176	LOW	8/25	2308	7.5	5
.139	.3882	1.849	.0577	.2199	1.65	0.00	.042	- 9.873	LOW	8/25	2308	9.0	6
.134	.3872	1.961	.0542	.1691	1.45	0.00	.034	- 12.400	LOW	8/25	2308	10.5	7
.279	.3863	2.091	.0454	.1086	1.25	0.00	.029	- 15.979	LOW	8/25	2308	12.0	8

$\bar{H}_b / n\bar{T}_b$	ρ_ℓ / ρ_s	\bar{H}_b / \bar{D}	$\tan \bar{m}$	$\tan \bar{\alpha}_b$	\bar{H}_b / \bar{z}	u/d	h/d	$\Delta Q_f / \bar{H}_b^3$	Tide cycle ends on	End of cycle		Lag in hours from end of cycle	Lag #
										water	Date		
.000	.3874	0.875	.0717	.1405	1.40	0.00	.030	- 36.363	LOW	8/26	1056	0.0	0
- .093	.3874	0.983	.0540	.1477	1.35	0.00	.032	- 33.333	LOW	8/26	1056	1.5	1
- .101	.3874	1.123	.0437	.1405	1.20	0.00	.031	- 24.242	LOW	8/26	1056	3.0	2
- .109	.3874	1.124	.0437	.1334	0.90	0.00	.029	- 29.630	LOW	8/26	1056	4.5	3
.000	.3872	1.160	.0489	.1228	0.65	0.18	.024	- 33.333	LOW	8/26	1056	6.0	4
.138	.3871	1.500	.0542	.1405	0.55	0.00	.024	- 22.222	LOW	8/26	1056	7.5	5
.165	.3872	1.900	.0540	.1477	0.75	0.00	.022	- 14.545	LOW	8/26	1056	9.0	6
.286	.3876	2.051	.0540	.1405	0.90	0.00	.022	- 12.500	LOW	8/26	1056	10.5	7
.000	.3881	1.805	.0472	.1228	0.85	0.00	.023	- 15.686	LOW	8/26	1056	12.0	8
.000	.3857	0.737	.0542	.1477	0.60	0.00	.028	162.500	LOW	8/26	2330	0.0	0
- .082	.3858	1.036	.0472	.1299	0.80	0.00	.026	54.167	LOW	8/26	2330	1.5	1
- .072	.3859	1.478	.0454	.1086	1.25	0.00	.027	16.667	LOW	8/26	2330	3.0	2
- .157	.3861	1.860	.0540	.0981	1.50	0.00	.038	7.143	LOW	8/26	2330	4.5	3
.000	.3863	2.063	.0664	.1052	1.55	0.00	.044	4.610	LOW	8/26	2330	6.0	4
.254	.3864	2.000	.0699	.1192	1.55	0.28	.048	4.610	LOW	8/26	2330	7.5	5
.118	.3867	1.552	.0594	.1334	1.50	0.00	.042	7.143	LOW	8/26	2330	9.0	6
.123	.3871	1.263	.0507	.1405	1.50	0.00	.032	13.830	LOW	8/26	2330	10.5	7
.157	.3873	1.034	.0577	.1405	1.45	0.00	.028	24.074	LOW	8/26	2330	12.0	8
.000	.3840	2.834	.0454	.0910	1.30	0.00	.012	7.047	LOW	8/27	1156	0.0	0
- .112	.3846	2.098	.0489	.0770	1.30	0.00	.020	13.125	LOW	8/27	1156	1.5	1
- .082	.3853	1.556	.0540	.0542	1.20	0.00	.032	24.419	LOW	8/27	1156	3.0	2
- .123	.3862	1.458	.0682	.0542	1.05	0.10	.032	24.419	LOW	8/27	1156	4.5	3
.000	.3867	1.428	.0857	.0594	1.00	0.38	.034	24.419	LOW	8/27	1156	6.0	4
.260	.3868	1.388	.0893	.0805	1.05	0.28	.046	26.923	LOW	8/27	1156	7.5	5
.056	.3864	1.087	.0770	.1052	1.05	0.00	.044	65.625	LOW	8/27	1156	9.0	6
.147	.3860	0.766	.0594	.1548	0.85	0.00	.036	210.000	LOW	8/27	1156	10.5	7
.000	.3855	0.691	.0542	.1477	0.55	0.00	.028	350.000	LOW	8/27	1156	12.0	8
.000	.3855	0.718	.0349	.1584	1.30	0.00	.037	483.333	LOW	8/28	0050	0.0	0
- .062	.3862	1.286	.0402	.1763	1.40	0.00	.038	72.500	LOW	8/28	0050	1.5	1
- .060	.3862	1.750	.0507	.2053	1.35	0.00	.038	19.595	LOW	8/28	0050	3.0	2
- .075	.3863	1.714	.0682	.2199	1.15	0.08	.037	13.063	LOW	8/28	0050	4.5	3
- .228	.3864	1.410	.0928	.1763	0.90	0.38	.038	17.059	LOW	8/28	0050	6.0	4
.104	.3862	1.149	.0928	.1334	0.80	0.36	.033	28.431	LOW	8/28	0050	7.5	5
.063	.3856	1.517	.0559	.0981	0.95	0.24	.022	17.059	LOW	8/28	0050	9.0	6
.081	.3848	2.250	.0472	.1016	0.85	0.00	.014	9.236	LOW	8/28	0050	10.5	7
.188	.3841	2.792	.0437	.1052	1.15	0.00	.010	8.735	LOW	8/28	0050	12.0	8
.000	.3852	2.050	.0437	.1799	0.55	0.00	.018	.000	LOW	8/28	1300	0.0	0
- .058	.3854	1.538	.0489	.1799	0.45	0.00	.012	.000	LOW	8/28	1300	1.5	1
- .033	.3861	0.923	.0559	.1799	0.55	0.00	.018	.000	LOW	8/28	1300	3.0	2
- .061	.3869	1.091	.0647	.1835	0.85	0.00	.028	.000	LOW	8/28	1300	4.5	3
.000	.3875	1.464	.0717	.1835	0.95	0.12	.042	.000	LOW	8/28	1300	6.0	4
.109	.3872	1.811	.0630	.1908	0.95	0.30	.038	.000	LOW	8/28	1300	7.5	5
.053	.3861	1.826	.0437	.1908	1.00	0.32	.025	.000	LOW	8/28	1300	9.0	6
.056	.3858	1.171	.0384	.1620	1.10	0.08	.036	.000	LOW	8/28	1300	10.5	7
.000	.3855	0.769	.0349	.1620	1.30	0.00	.038	.000	LOW	8/28	1300	12.0	8
.000	.3882	1.868	.0297	.1263	0.80	0.00	.033	51.282	LOW	8/29	0126	0.0	0
- .069	.3881	1.778	.0402	.1263	0.75	0.00	.036	60.606	LOW	8/29	0126	1.5	1
- .033	.3879	1.667	.0717	.1157	0.70	0.00	.034	74.074	LOW	8/29	0126	3.0	2
- .053	.3877	1.789	.1069	.1122	0.70	0.00	.030	51.282	LOW	8/29	0126	4.5	3
- .130	.3872	2.102	.1210	.1122	0.75	0.11	.025	28.986	LOW	8/29	0126	6.0	4
.092	.3863	2.500	.0963	.1122	0.70	0.12	.021	16.000	LOW	8/29	0126	7.5	5
.052	.3855	2.634	.0472	.1334	0.70	0.07	.019	12.739	LOW	8/29	0126	9.0	6
.054	.3851	2.439	.0402	.1584	0.65	0.00	.018	16.000	LOW	8/29	0126	10.5	7
.054	.3850	1.818	.0437	.1763	0.55	0.00	.018	30.250	LOW	8/29	0126	12.0	8

$\bar{H}_b / n\bar{T}_b$	ρ_L / ρ_s	\bar{H}_b / \bar{D}	$\tan \bar{m}$	$\tan \bar{\alpha}_b$	\bar{H}_b / \bar{z}	u/d	h/d	$\Delta Q_f / \bar{H}_b^3$	Tide cycle ends on	End of cycle		Lag in hours from end of cycle	Lag #
									water	Date	Hours		
.000	.3827	2.222	.0367	.1944	0.55	0.00	.028	35.156	LOW	8/29	1320	0.0	0
- .059	.3838	2.146	.0540	.1908	0.60	0.00	.036	26.471	LOW	8/29	1320	1.5	1
- .057	.3861	1.704	.0770	.1871	0.70	0.00	.044	23.196	LOW	8/29	1320	3.0	2
- .104	.3882	1.438	.0963	.1835	0.90	0.00	.038	23.196	LOW	8/29	1320	4.5	3
.000	.3886	1.152	.1033	.1763	1.00	0.00	.038	40.909	LOW	8/29	1320	6.0	4
.043	.3886	1.129	.0770	.1620	0.80	0.06	.030	52.326	LOW	8/29	1320	7.5	5
.050	.3886	1.358	.0384	.1405	0.70	0.08	.021	47.872	LOW	8/29	1320	9.0	6
.121	.3886	1.714	.0297	.1334	0.70	0.02	.030	47.872	LOW	8/29	1320	10.5	7
- .453	.3885	1.889	.0297	.1299	0.80	0.00	.033	57.692	LOW	8/29	1320	12.0	8
.000	.3852	1.171	.0419	.1944	0.85	0.00	.033	96.429	LOW	8/30	0202	0.0	0
- .038	.3850	0.891	.0349	.1944	0.85	0.00	.035	122.727	LOW	8/30	0202	1.5	1
- .038	.3847	0.856	.0384	.1835	0.80	0.00	.036	61.364	LOW	8/30	0202	3.0	2
- .061	.3844	0.875	.0910	.1871	0.60	0.00	.031	31.395	LOW	8/30	0202	4.5	3
- 1.028	.3842	0.860	.1016	.1763	0.45	0.30	.018	26.471	LOW	8/30	0202	6.0	4
.111	.3839	0.905	.0699	.1763	0.45	0.04	.018	24.545	LOW	8/30	0202	7.5	5
.055	.3835	1.070	.0332	.1763	0.60	0.00	.013	24.545	LOW	8/30	0202	9.0	6
.046	.3828	1.348	.0227	.1835	0.65	0.00	.017	28.723	LOW	8/30	0202	10.5	7
.119	.3825	1.846	.0297	.1871	0.60	0.00	.028	28.723	LOW	8/30	0202	12.0	8
.000	.3874	1.124	.0419	.1228	0.75	0.00	.027	68.519	LOW	8/30	1408	0.0	0
- .041	.3874	1.148	.0244	.1122	0.80	0.00	.022	61.667	LOW	8/30	1408	1.5	1
- .054	.3870	1.527	.0314	.1334	0.85	0.00	.026	25.000	LOW	8/30	1408	3.0	2
- .134	.3866	2.036	.0349	.1691	0.90	0.06	.032	10.511	LOW	8/30	1408	4.5	3
.000	.3864	2.036	.0472	.1871	0.95	0.18	.036	10.511	LOW	8/30	1408	6.0	4
.096	.3863	1.849	.0419	.1908	0.90	0.05	.034	15.678	LOW	8/30	1408	7.5	5
.058	.3859	1.739	.0349	.1835	0.85	0.00	.028	28.906	LOW	8/30	1408	9.0	6
.062	.3859	1.758	.0332	.1835	0.80	0.00	.028	56.061	LOW	8/30	1408	10.5	7
.136	.3852	1.333	.0419	.1908	0.85	0.00	.031	132.143	LOW	8/30	1408	12.0	8
.000	.3840	1.182	.0419	.2199	0.95	0.00	.038	136.111	LOW	8/31	0220	0.0	0
- .036	.3835	1.077	.0402	.1656	0.80	0.00	.038	111.364	LOW	8/31	0220	1.5	1
- .043	.3832	1.042	.0559	.1656	0.75	0.00	.038	74.242	LOW	8/31	0220	3.0	2
- .082	.3833	1.130	.0840	.1908	0.70	0.08	.042	41.525	LOW	8/31	0220	4.5	3
.000	.3837	1.216	.1016	.2089	0.70	0.56	.042	26.923	LOW	8/31	0220	6.0	4
.065	.3845	1.260	.0699	.1980	0.70	0.38	.036	25.258	LOW	8/31	0220	7.5	5
.066	.3856	1.292	.0402	.1727	0.70	0.00	.027	33.108	LOW	8/31	0220	9.0	6
.075	.3866	1.233	.0402	.1441	0.70	0.00	.020	52.128	LOW	8/31	0220	10.5	7
.000	.3873	1.111	.0419	.1228	0.75	0.00	.026	90.741	LOW	8/31	0220	12.0	8
.000	.3857	1.551	.0612	.2089	0.75	0.00	.037	8.182	LOW	8/31	1500	0.0	0
- .084	.3862	2.000	.0699	.1691	0.95	0.00	.042	3.191	LOW	8/31	1500	1.5	1
- .075	.3860	2.069	.0752	.1620	1.40	0.00	.053	2.083	LOW	8/31	1500	3.0	2
- .095	.3854	1.938	.0805	.1835	1.80	0.00	.058	1.891	LOW	8/31	1500	4.5	3
.403	.3851	2.638	.0734	.2530	1.90	0.06	.053	1.891	LOW	8/31	1500	6.0	4
.109	.3850	1.844	.0664	.3096	1.95	0.00	.041	2.195	LOW	8/31	1500	7.5	5
.064	.3848	1.714	.0594	.3172	1.85	0.00	.028	4.054	LOW	8/31	1500	9.0	6
.048	.3845	1.333	.0507	.2943	1.55	0.00	.026	13.636	LOW	8/31	1500	10.5	7
.120	.3840	1.111	.0437	.2493	1.05	0.00	.037	28.125	LOW	8/31	1500	12.0	8
.000	.3841	0.878	.0542	.1763	1.40	0.00	.042	-120.513	LOW	9/01	0300	0.0	0
- .062	.3831	0.883	.0594	.2309	1.00	0.00	.042	-120.513	LOW	9/01	0300	1.5	1
- .064	.3815	0.987	.0717	.2642	0.75	0.00	.042	-92.157	LOW	9/01	0300	3.0	2
- .098	.3804	1.143	.0805	.2717	0.60	0.18	.042	-73.438	LOW	9/01	0300	4.5	3
.000	.3797	1.270	.0857	.2680	0.60	0.53	.042	-73.438	LOW	9/01	0300	6.0	4
.063	.3793	1.143	.0770	.2680	0.65	0.30	.042	-142.424	LOW	9/01	0300	7.5	5
.033	.3809	1.000	.0647	.2605	0.70	0.00	.042	-261.111	LOW	9/01	0300	9.0	6
.052	.3832	1.120	.0594	.2493	0.65	0.00	.041	-213.636	LOW	9/01	0300	10.5	7
.000	.3854	1.510	.0577	.2089	0.70	0.00	.037	-92.157	LOW	9/01	0300	12.0	8

$\bar{H}_b / n \bar{T}_b$	ρ_l / ρ_s	\bar{H}_b / \bar{D}	$\tan \bar{m}$	$\tan \bar{\alpha}_b$	\bar{H}_b / \bar{z}	u/d	h/d	$\Delta Q_f / \bar{H}_b^3$	Tide cycle ends on	End of cycle		Lag in hours from end of cycle	Lag #	
										water	Date			Hours
.000	.3837	1.303	.0402	.0664	0.75	0.00	.030	- 71.250	LOW	9/01	1500	0.0	0	
-	.114	.3836	1.437	.0454	.0875	1.00	0.00	.038	- 54.808	LOW	9/01	1500	1.5	1
-	.166	.3830	1.688	.0540	.1122	1.20	0.00	.043	- 36.306	LOW	9/01	1500	3.0	2
-	.218	.3823	2.000	.0699	.1441	1.25	0.00	.031	- 25.110	LOW	9/01	1500	4.5	3
	.467	.3820	2.169	.0857	.1763	1.00	0.60	.021	- 21.756	LOW	9/01	1500	6.0	4
	.124	.3821	1.967	.0840	.1620	0.85	0.80	.018	- 27.805	LOW	9/01	1500	7.5	5
	.102	.3828	1.446	.0682	.1157	1.15	0.00	.024	- 54.808	LOW	9/01	1500	9.0	6
	.118	.3837	1.028	.0577	.0770	1.50	0.00	.033	-111.765	LOW	9/01	1500	10.5	7
	.000	.3841	0.883	.0542	.0840	1.40	0.00	.041	-146.154	LOW	9/01	1500	12.0	8
	.000	.3828	1.534	.0297	.0000	1.30	0.00	.035	- 21.338	LOW	9/02	0400	0.0	0
-	.142	.3822	1.507	.0297	.0000	1.30	0.00	.037	- 23.759	LOW	9/02	0400	1.5	1
-	.119	.3816	1.529	.0332	.0000	1.30	0.00	.039	- 23.759	LOW	9/02	0400	3.0	2
-	.155	.3810	1.606	.0472	.0000	1.20	0.10	.040	- 22.483	LOW	9/02	0400	4.5	3
1.862	.3808	1.662	.0612	.0000	1.05	0.50	.040	- 21.338	LOW	9/02	0400	6.0	4	
	.099	.3815	1.600	.0577	.0000	0.85	0.50	.037	- 23.759	LOW	9/02	0400	7.5	5
	.078	.3823	1.415	.0472	.0070	0.70	0.00	.033	- 34.536	LOW	9/02	0400	9.0	6
	.079	.3830	1.292	.0402	.0314	0.60	0.00	.030	- 45.270	LOW	9/02	0400	10.5	7
	.250	.3836	1.273	.0384	.0542	0.65	0.00	.030	- 45.270	LOW	9/02	0400	12.0	8
	.000	.3835	1.105	.0349	.0349	0.90	0.00	.034	- 2.703	LOW	9/02	1602	0.0	0
-	.152	.3835	1.237	.0314	.0384	1.00	0.00	.036	- 1.923	LOW	9/02	1602	1.5	1
-	.099	.3836	1.447	.0384	.0384	1.00	0.00	.037	- 1.205	LOW	9/02	1602	3.0	2
-	.157	.3837	1.733	.0594	.0349	1.05	0.30	.042	- 0.727	LOW	9/02	1602	4.5	3
	.000	.3836	1.866	.0770	.0314	1.15	0.00	.048	- 0.583	LOW	9/02	1602	6.0	4
	.131	.3834	1.838	.0612	.0244	1.25	0.00	.038	- 0.637	LOW	9/02	1602	7.5	5
	.125	.3833	1.676	.0454	.0140	1.30	0.00	.035	- 0.840	LOW	9/02	1602	9.0	6
	.158	.3832	1.611	.0349	.0000	1.30	0.00	.036	- 1.026	LOW	9/02	1602	10.5	7
	.491	.3829	1.521	.0297	.0000	1.30	0.00	.035	- 1.274	LOW	9/02	1602	12.0	8
	.000	.3846	1.934	.0349	.0000	1.05	0.00	.029	6.341	LOW	9/03	0408	0.0	0
-	.145	.3847	1.905	.0402	.0000	1.25	0.00	.034	6.019	LOW	9/03	0408	1.5	1
-	.092	.3847	1.818	.0419	.0000	1.63	0.00	.036	6.019	LOW	9/03	0408	3.0	2
-	.119	.3846	1.600	.0437	.0000	1.25	0.00	.033	7.386	LOW	9/03	0408	4.5	3
	.000	.3846	1.351	.0454	.0000	1.05	0.15	.031	10.400	LOW	9/03	0408	6.0	4
	.107	.3846	1.227	.0540	.0000	0.80	0.00	.032	13.402	LOW	9/03	0408	7.5	5
	.100	.3843	1.120	.0577	.0105	0.75	0.00	.032	17.568	LOW	9/03	0408	9.0	6
	.089	.3838	1.093	.0489	.0244	0.80	0.00	.033	18.841	LOW	9/03	0408	10.5	7
	.667	.3835	1.105	.0367	.0314	0.90	0.00	.035	17.568	LOW	9/03	0408	12.0	8
	.000	.3832	0.923	.0262	.0000	0.70	0.00	.022	8.511	LOW	9/03	1638	0.0	0
-	.158	.3821	0.982	.0367	.0140	0.90	0.00	.031	7.273	LOW	9/03	1638	1.5	1
-	.115	.3816	1.178	.0542	.0210	1.20	0.00	.042	4.396	LOW	9/03	1638	3.0	2
-	.108	.3807	1.406	.0664	.0279	1.35	0.00	.045	2.685	LOW	9/03	1638	4.5	3
	.000	.3807	1.459	.0682	.0279	1.30	0.33	.030	2.410	LOW	9/03	1638	6.0	4
	.112	.3812	1.499	.0594	.0244	1.10	0.00	.030	2.051	LOW	9/03	1638	7.5	5
	.102	.3824	1.739	.0489	.0210	0.90	0.00	.029	1.852	LOW	9/03	1638	9.0	6
	.127	.3837	1.846	.0384	.0140	0.90	0.00	.026	1.852	LOW	9/03	1638	10.5	7
	.250	.3846	1.873	.0332	.0035	0.95	0.00	.028	1.951	LOW	9/03	1638	12.0	8
	.000	.3826	0.857	.0384	.0000	0.65	0.00	.025	70.000	LOW	9/04	0438	0.0	0
-	.121	.3825	1.152	.0349	.0000	0.80	0.00	.023	25.455	LOW	9/04	0438	1.5	1
-	.095	.3825	1.315	.0384	.0000	0.95	0.00	.022	12.613	LOW	9/04	0438	3.0	2
-	.134	.3826	1.377	.0507	.0000	1.05	0.08	.022	9.396	LOW	9/04	0438	4.5	3
	.000	.3826	1.308	.0682	.0000	0.90	0.15	.022	10.526	LOW	9/04	0438	6.0	4
	.105	.3826	1.179	.0594	.0000	0.70	0.02	.022	14.433	LOW	9/04	0438	7.5	5
	.103	.3827	1.026	.0437	.0000	0.60	0.00	.022	21.875	LOW	9/04	0438	9.0	6
	.107	.3826	0.923	.0279	.0000	0.60	0.00	.022	29.787	LOW	9/04	0438	10.5	7
	.000	.3825	0.923	.0244	.0000	0.70	0.00	.022	29.787	LOW	9/04	0438	12.0	8

$\bar{H}_b / n\bar{T}_b$	ρ_z / ρ_s	\bar{H}_b / \bar{D}	$\tan \bar{m}$	$\tan \bar{\alpha}_b$	\bar{H}_b / \bar{z}	u/d	h/d	$\Delta Q_f / \bar{H}_b^3$	Tide cycle ends on	End of cycle		Lag in hours from end of cycle	Lag #
									water	Date	Hours		
.000	.3847	0.825	.0332	.0035	0.65	0.00	.022	- 16.667	LOW	9/04	1700	0.0	0
- .178	.3845	1.262	.0297	.0105	0.80	0.00	.022	- 4.348	LOW	9/04	1700	1.5	1
- .101	.3842	1.485	.0384	.0175	1.10	0.00	.025	- 2.542	LOW	9/04	1700	3.0	2
- .102	.3843	1.382	.0647	.0210	1.15	0.64	.035	- 2.885	LOW	9/04	1700	4.5	3
- 4.875	.3841	1.130	.0893	.0210	1.00	2.04	.044	- 5.085	LOW	9/04	1700	6.0	4
.065	.3840	0.912	.0893	.0175	0.80	1.02	.024	- 10.000	LOW	9/04	1700	7.5	5
.051	.3839	0.734	.0770	.0105	0.65	0.28	.024	- 21.429	LOW	9/04	1700	9.0	6
.059	.3830	0.698	.0594	.0035	0.55	0.00	.024	- 27.273	LOW	9/04	1700	10.5	7
.272	.3828	0.806	.0437	.0000	0.65	0.00	.024	- 18.750	LOW	9/04	1700	12.0	8
.000	.3825	0.939	.3437	.0770	0.55	0.00	.017	36.111	LOW	9/05	0500	0.0	0
- .182	.3828	1.036	.0454	.0699	0.45	0.00	.022	27.083	LOW	9/05	0500	1.5	1
- .072	.3837	1.298	.0402	.0664	0.50	0.00	.030	12.745	LOW	9/05	0500	3.0	2
- .114	.3845	1.586	.0489	.0559	0.65	0.00	.034	6.701	LOW	9/05	0500	4.5	3
- 1.087	.3850	1.724	.0542	.0454	0.80	0.08	.032	5.200	LOW	9/05	0500	6.0	4
.176	.3848	1.667	.0472	.0140	0.90	0.14	.026	5.200	LOW	9/05	0500	7.5	5
.144	.3846	1.279	.0402	.0000	0.95	0.00	.023	11.017	LOW	9/05	0500	9.0	6
.138	.3842	0.839	.0367	.0000	0.80	0.00	.023	36.111	LOW	9/05	0500	10.5	7
1.238	.3840	0.825	.0332	.0000	0.65	0.00	.022	36.111	LOW	9/05	0500	12.0	8
.000	.3835	1.302	.0454	.0594	0.75	0.00	.015	11.594	LOW	9/05	1800	0.0	0
- .176	.3835	1.273	.0472	.0612	0.80	0.00	.026	10.811	LOW	9/05	1800	1.5	1
- .078	.3835	1.143	.0540	.0805	0.90	0.00	.029	12.500	LOW	9/05	1800	3.0	2
- .095	.3836	1.081	.0630	.0981	0.95	0.00	.030	12.500	LOW	9/05	1800	4.5	3
- .410	.3837	1.108	.0682	.1086	0.90	0.05	.030	11.594	LOW	9/05	1800	6.0	4
.124	.3835	1.183	.0664	.0945	0.95	0.00	.028	10.811	LOW	9/05	1800	7.5	5
.070	.3832	1.219	.0540	.0875	0.95	0.00	.026	13.559	LOW	9/05	1800	9.0	6
.118	.3828	1.111	.0402	.0805	0.95	0.00	.020	22.222	LOW	9/05	1800	10.5	7
.182	.3825	0.964	.0349	.0734	0.75	0.00	.017	40.000	LOW	9/05	1800	12.0	8
.000	.3839	0.848	.0594	.1016	1.15	0.00	.031	11.369	LOW	9/06	0630	0.0	0
- .137	.3841	0.856	.0507	.1016	1.00	0.00	.035	11.364	LOW	9/06	0630	1.5	1
- .090	.3840	1.219	.0454	.0805	0.95	0.00	.041	4.237	LOW	9/06	0630	3.0	2
- .096	.3837	1.738	.0472	.0630	1.10	0.02	.042	1.678	LOW	9/06	0630	4.5	3
- .347	.3837	2.068	.0542	.0542	1.35	0.28	.041	1.101	LOW	9/06	0630	6.0	4
.191	.3835	1.830	.0594	.0559	1.25	0.02	.039	1.592	LOW	9/06	0630	7.5	5
.123	.3834	1.533	.0559	.0559	1.00	0.00	.032	2.577	LOW	9/06	0630	9.0	6
.194	.3834	1.355	.0489	.0559	0.75	0.00	.020	3.378	LOW	9/06	0630	10.5	7
1.265	.3834	1.365	.0454	.0594	0.70	0.00	.017	3.125	LOW	9/06	0630	12.0	8
.000	.3875	1.417	.0559	.0805	1.05	0.16	.042	26.923	LOW	9/06	1900	0.0	0
- .194	.3859	1.440	.0647	.0559	1.20	0.39	.050	22.340	LOW	9/06	1900	1.5	1
- .073	.3844	1.345	.0770	.0630	1.25	0.50	.044	20.588	LOW	9/06	1900	3.0	2
- .087	.3825	1.322	.0805	.1122	1.05	0.78	.012	17.797	LOW	9/06	1900	4.5	3
- .339	.3812	1.258	.0805	.1370	0.60	0.96	.000	17.797	LOW	9/06	1900	6.0	4
.476	.3810	1.238	.0840	.1228	0.55	0.90	.000	17.797	LOW	9/06	1900	7.5	5
.086	.3816	1.206	.0805	.1052	0.85	0.68	.015	19.091	LOW	9/06	1900	9.0	6
.060	.3825	1.062	.0734	.0981	1.20	0.44	.032	26.923	LOW	9/06	1900	10.5	7
.097	.3833	0.923	.0630	.0981	1.20	0.20	.031	38.889	LOW	9/06	1900	12.0	8
.000	.3875	0.966	.0419	.0000	0.65	0.00	.032	- 40.909	LOW	9/07	0712	0.0	0
- .207	.3875	1.152	.0349	.0244	0.70	0.00	.022	- 23.077	LOW	9/07	0712	1.5	1
- .094	.0875	1.213	.0384	.0734	0.80	0.00	.023	- 17.647	LOW	9/07	0712	3.0	2
- .174	.3875	1.206	.0402	.1228	0.85	0.00	.028	- 16.364	LOW	9/07	0712	4.5	3
- .574	.3875	1.238	.0419	.1548	0.85	0.14	.029	- 15.254	LOW	9/07	0712	6.0	4
.273	.3875	1.300	.0437	.1548	0.85	0.04	.030	- 15.254	LOW	9/07	0712	7.5	5
.129	.3876	1.286	.0472	.1405	0.80	0.00	.029	- 19.149	LOW	9/07	0712	9.0	6
.293	.3877	1.360	.0507	.1122	0.85	0.12	.032	- 23.077	LOW	9/07	0712	10.5	7
- 1.360	.3875	1.417	.0540	.0840	1.00	0.18	.044	- 23.077	LOW	9/07	0712	12.0	8

$\bar{H}_b / \eta \bar{T}_b$	ρ_L / ρ_s	\bar{H}_b / \bar{D}	$\tan \bar{m}$	$\tan \bar{a}_b$	\bar{H}_b / \bar{z}	u/d	h/d	$\Delta Q_f / \bar{H}_b^3$	Tide cycle ends on	End of cycle		Lag in hours from end of cycle	Lag #
									water	Date	Hours		
.000	.3874	1.000	.0314	.0805	1.30	0.00	.035	- 3.030	LOW	9/07	2000	0.0	0
- .204	.3871	1.169	.0332	.0454	1.50	0.00	.035	- 1.818	LOW	9/07	2000	1.5	1
- .168	.3871	1.508	.0402	.0542	1.50	0.00	.035	- 0.847	LOW	9/07	2000	3.0	2
- .215	.3870	1.785	.0472	.1584	1.40	0.00	.038	- 0.513	LOW	9/07	2000	4.5	3
- .381	.3869	2.000	.0542	.2016	1.40	0.00	.039	- 0.382	LOW	9/07	2000	6.0	4
1.326	.3869	1.936	.0559	.1980	1.40	0.00	.038	- 0.441	LOW	9/07	2000	7.5	5
.162	.3871	1.290	.0559	.1548	1.35	0.00	.036	- 0.800	LOW	9/07	2000	9.0	6
.074	.3873	1.220	.0542	.0910	0.95	0.00	.032	- 2.128	LOW	9/07	2000	10.5	7
.122	.3874	0.966	.0472	.0314	0.65	0.00	.032	- 4.545	LOW	9/07	2000	12.0	8
.000	.3856	1.212	.0419	.1799	0.80	0.00	.022	0.000	LOW	9/08	0732	0.0	0
- .170	.3860	1.169	.0419	.1548	0.80	0.00	.024	0.000	LOW	9/08	0732	1.5	1
- .203	.3862	1.219	.0437	.0875	0.85	0.00	.028	0.000	LOW	9/08	0732	3.0	2
- .300	.3867	1.238	.0507	.0630	0.80	0.00	.031	0.000	LOW	9/08	0732	4.5	3
.000	.3869	1.206	.0612	.0070	0.75	0.00	.032	0.000	LOW	9/08	0732	6.0	4
.262	.3871	1.175	.0540	.0052	0.70	0.08	.032	0.000	LOW	9/08	0732	7.5	5
.117	.3871	1.079	.0507	.0699	0.85	0.00	.034	0.000	LOW	9/08	0732	9.0	6
.150	.3873	1.016	.0332	.0875	1.35	0.00	.034	0.000	LOW	9/08	0732	10.5	7
- .444	.3874	1.000	.0314	.0699	1.35	0.00	.034	0.000	LOW	9/08	0732	12.0	8
.000	.3833	1.704	.0349	.1016	1.35	0.00	.012	- 13.402	LOW	9/08	2036	0.0	0
- .201	.3833	1.704	.0402	.0910	1.20	0.00	.012	- 13.402	LOW	9/08	2036	1.5	1
- .189	.3836	1.754	.0472	.1263	1.10	0.00	.021	- 10.400	LOW	9/08	2036	3.0	2
- .272	.3842	1.677	.0507	.1584	1.00	0.00	.030	- 9.220	LOW	9/08	2036	4.5	3
- .447	.3850	1.522	.0489	.1405	0.95	0.00	.025	- 9.774	LOW	9/08	2036	6.0	4
.408	.3854	1.433	.0577	.1228	0.95	0.36	.030	- 11.017	LOW	9/08	2036	7.5	5
.184	.3854	1.353	.0594	.1263	0.90	0.36	.033	- 13.402	LOW	9/08	2036	9.0	6
.120	.3854	1.254	.0489	.1620	0.85	0.00	.028	- 17.568	LOW	9/08	2036	10.5	7
.286	.3855	1.212	.0419	.1835	0.85	0.00	.022	- 20.313	LOW	9/08	2036	12.0	8
.000	.3833	1.100	.0349	.1263	1.15	0.00	.000	- 1.765	LOW	9/09	0905	0.0	0
- .173	.3837	1.000	.0314	.1441	0.95	0.00	.005	- 2.542	LOW	9/09	0905	1.5	1
- .162	.3842	1.027	.0314	.1691	0.85	0.00	.017	- 2.727	LOW	9/09	0905	3.0	2
- .279	.3846	1.371	.0384	.1944	0.95	0.00	.028	- 1.351	LOW	9/09	0905	4.5	3
- 1.217	.3847	1.623	.0542	.2199	1.15	0.22	.034	- 0.852	LOW	9/09	0905	6.0	4
.517	.3845	1.802	.0559	.2346	1.30	0.00	.030	- 0.694	LOW	9/09	0905	7.5	5
.275	.3841	1.774	.0419	.2016	1.45	0.00	.025	- 0.904	LOW	9/09	0905	9.0	6
.323	.3836	1.767	.0349	.1656	1.45	0.00	.018	- 1.200	LOW	9/09	0905	10.5	7
.000	.3833	1.704	.0332	.1122	1.40	0.00	.011	- 1.546	LOW	9/09	0905	12.0	8
.000	.3845	1.529	.0297	.0981	1.25	0.00	.023	- 2.837	LOW	9/09	2140	0.0	0
- .290	.3846	1.602	.0279	.1052	1.40	0.00	.026	- 2.548	LOW	9/09	2140	1.5	1
- .123	.3849	1.614	.0314	.1192	1.50	0.00	.030	- 2.273	LOW	9/09	2140	3.0	2
- .134	.3849	1.681	.0454	.1228	1.50	0.00	.032	- 2.051	LOW	9/09	2140	4.5	3
- .429	.3849	1.714	.0472	.1157	1.50	0.30	.035	- 1.852	LOW	9/09	2140	6.0	4
.000	.3848	1.756	.0454	.1052	1.55	0.26	.036	- 1.681	LOW	9/09	2140	7.5	5
.159	.3845	1.699	.0437	.0981	1.55	0.00	.034	- 1.681	LOW	9/09	2140	9.0	6
.143	.3840	1.506	.0419	.1052	1.50	0.00	.025	- 2.051	LOW	9/09	2140	10.5	7
.196	.3836	1.266	.0384	.1192	1.30	0.00	.011	- 3.200	LOW	9/09	2140	12.0	8
.000	.3845	1.200	.0314	.0630	0.90	0.00	.019	19.149	LOW	9/10	0936	0.0	0
- .119	.3857	1.175	.0367	.0981	0.85	0.00	.024	17.647	LOW	9/10	0936	1.5	1
- .112	.3860	1.224	.0419	.0981	0.85	0.00	.024	13.043	LOW	9/10	0936	3.0	2
- .425	.3861	1.286	.0454	.0981	0.85	0.16	.023	9.890	LOW	9/10	0936	4.5	3
1.171	.3861	1.352	.0472	.0981	0.85	C.24	.023	8.108	LOW	9/10	0936	6.0	4
.260	.3857	1.486	.0454	.0981	0.85	C.28	.023	6.383	LOW	9/10	0936	7.5	5
.226	.3851	1.529	.0419	.0981	0.80	0.34	.022	6.383	LOW	9/10	0936	9.0	6
.345	.3846	1.500	.0402	.0981	1.05	0.04	.021	6.767	LOW	9/10	0936	10.5	7
- .433	.3845	1.529	.0384	.0981	1.25	0.00	.023	6.383	LOW	9/10	0936	12.0	8

$\bar{H}_b / \eta \bar{T}_b$	ρ_l / ρ_s	\bar{H}_b / \bar{D}	$\tan \bar{m}$	$\tan \bar{\alpha}_b$	\bar{H}_b / \bar{z}	u/d	h/d	$\Delta Q_f / \bar{H}_b^3$	Tide cycle ends on	End of cycle		Lag in hours from end of cycle	Lag #
										water	Date		
.000	.3847	0.842	.0507	.0105	0.90	0.00	.048	9.091	LOW	9/10	2300	0.0	0
-.191	.3845	1.135	.0367	.0279	1.45	0.00	.040	4.054	LOW	9/10	2300	1.5	1
-.090	.3841	1.383	.0314	.0542	2.00	0.00	.030	2.703	LOW	9/10	2300	3.0	2
-.093	.3841	1.492	.0454	.0770	2.00	0.00	.033	2.885	LOW	9/10	2300	4.5	3
-.479	.3842	1.155	.0540	.0945	1.75	0.20	.039	3.297	LOW	9/10	2300	6.0	4
.257	.3842	1.500	.0559	.0840	1.35	0.19	.039	3.297	LOW	9/10	2300	7.5	5
.100	.3841	1.467	.0559	.0454	1.15	0.00	.027	3.529	LOW	9/10	2300	9.0	6
.113	.3844	1.367	.0507	.0210	1.00	0.00	.019	4.348	LOW	9/10	2300	10.5	7
.201	.3847	1.267	.0402	.0314	0.90	0.00	.017	5.455	LOW	9/10	2300	12.0	8
.000	.3843	1.156	.0332	.1052	0.80	0.00	.033	38.889	LOW	9/11	1100	00.0	0
-.110	.3846	0.917	.0349	.0000	0.80	0.00	.032	63.636	LOW	9/11	1100	1.5	1
-.079	.3852	0.893	.0419	.0210	0.80	0.00	.030	43.750	LOW	9/11	1100	3.0	2
-.167	.3853	1.091	.0612	.0105	0.95	0.00	.031	14.894	LOW	9/11	1100	4.5	3
.000	.3852	1.222	.0752	.0000	1.00	0.13	.034	8.235	LOW	9/11	1100	6.0	4
.241	.3849	1.135	.0664	.0000	1.00	0.00	.027	9.459	LOW	9/11	1100	7.5	5
.189	.3849	0.907	.0540	.0000	0.95	0.00	.022	17.949	LOW	9/11	1100	9.0	6
.135	.3848	0.805	.0419	.0000	0.60	0.00	.020	23.333	LOW	9/11	1100	10.5	7
.000	.3847	0.916	.0507	.0105	0.90	0.00	.048	16.279	LOW	9/11	1100	12.0	8
.000	.3852	1.217	.0630	.0349	0.80	0.00	.034	- 20.455	LOW	9/11	2356	0.0	0
-.100	.3857	1.200	.0664	.0349	0.85	0.00	.036	- 16.667	LOW	9/11	2356	1.5	1
-.058	.3859	1.158	.0682	.0419	0.85	0.00	.032	- 12.500	LOW	9/11	2356	3.0	2
-.080	.3860	1.125	.0577	.1052	0.80	0.19	.023	- 9.574	LOW	9/11	2356	4.5	3
-.494	.3858	1.157	.0454	.1122	0.85	0.20	.017	- 7.627	LOW	9/11	2356	6.0	4
.152	.3855	1.325	.0577	.1584	0.95	0.35	.032	- 6.081	LOW	9/11	2356	7.5	5
.074	.3849	1.517	.0612	.1980	1.15	0.35	.038	- 5.294	LOW	9/11	2356	9.0	6
.069	.3845	1.569	.0472	.2126	1.10	0.20	.029	- 7.031	LOW	9/11	2356	10.5	7
.154	.3843	1.391	.0349	.1405	0.95	0.00	.028	- 13.636	LOW	9/11	2356	12.0	8
.000	.3853	1.259	.0472	.0945	0.95	0.00	.030	1.282	LOW	9/12	1200	0.0	0
-.126	.3848	1.276	.0419	.1192	1.00	0.14	.029	0.980	LOW	9/12	1200	1.5	1
-.104	.3837	1.355	.0384	.1799	1.00	0.30	.027	0.676	LOW	9/12	1200	3.0	2
-.179	.3826	1.323	.0507	.1727	1.00	0.31	.026	0.625	LOW	9/12	1200	4.5	3
.000	.3821	1.164	.0664	.1299	0.80	0.26	.028	0.847	LOW	9/12	1200	6.0	4
.150	.3824	1.031	.0612	.0840	0.65	0.16	.032	1.389	LOW	9/12	1200	7.5	5
.070	.3825	1.036	.0594	.0559	0.60	0.00	.034	2.083	LOW	9/12	1200	9.0	6
.140	.3843	1.167	.0594	.0384	0.70	0.00	.034	2.273	LOW	9/12	1200	10.5	7
.000	.3852	1.217	.0630	.0349	0.80	0.00	.034	2.273	LOW	9/12	1200	12.0	8
.000	.3843	1.075	.0507	.0000	1.05	0.00	.022	4.255	LOW	9/13	0050	0.0	0
-.094	.3844	0.914	.0489	.0000	0.80	0.00	.025	6.061	LOW	9/13	0050	1.5	1
-.072	.3844	1.194	.0454	.0035	0.80	0.00	.030	2.500	LOW	9/13	0050	3.0	2
-.109	.3846	1.479	.0437	.0070	0.85	0.00	.031	1.274	LOW	9/13	0050	4.5	3
- 1.017	.3847	1.639	.0540	.0140	0.80	0.60	.030	0.976	LOW	9/13	0050	6.0	4
.199	.3848	1.652	.0507	.0175	0.80	0.40	.026	1.081	LOW	9/13	0050	7.5	5
.100	.3849	1.613	.0367	.0349	0.80	0.00	.024	1.600	LOW	9/13	0050	9.0	6
.097	.3851	1.500	.0279	.0542	0.85	0.00	.025	2.703	LOW	9/13	0050	10.5	7
.213	.3853	1.333	.0367	.0805	0.90	0.00	.030	4.255	LOW	9/13	0050	12.0	8
.000	.3853	1.048	.0384	.0981	2.05	0.00	.030	- 15.278	LOW	9/13	1310	0.0	0
-.055	.3851	0.921	.0367	.0981	2.05	0.00	.031	- 22.917	LOW	0/13	1310	1.5	1
-.068	.3847	1.206	.0367	.1052	1.75	0.00	.025	- 10.000	LOW	9/13	1310	3.0	2
-.176	.3836	1.841	.0367	.1052	1.40	0.00	.023	- 2.821	LOW	9/13	1310	4.5	3
.000	.3835	2.381	.0384	.0699	1.15	0.40	.022	- 1.303	LOW	9/13	1310	6.0	4
.227	.3837	2.469	.0367	.0175	1.20	0.00	.021	- 1.116	LOW	9/13	1310	7.5	5
.138	.3840	2.215	.0349	.0000	1.45	0.00	.021	- 1.475	LOW	9/13	1310	9.0	6
.121	.3840	1.612	.0437	.0000	1.45	0.00	.022	- 3.503	LOW	9/13	1310	10.5	7
.000	.3843	1.134	.0489	.0000	1.20	0.00	.022	- 10.000	LOW	9/13	1310	12.0	8

	$\bar{H}_b / n\bar{T}_b$	ρ_l / ρ_s	\bar{H}_b / \bar{D}	$\tan \bar{m}$	$\tan \bar{\alpha}_b$	\bar{H}_b / \bar{z}	u/d	h/d	$\Delta Q_f / \bar{H}_b^3$	Tide cycle ends on	End of cycle		Lag in hours from end of cycle	Lag #
											water	Date		
-	.000	.3855	1.200	.0314	.1228	1.75	0.00	.026	- 2.703	LOW	9/14	0200	0.0	0
-	.122	.3853	1.118	.0367	.0840	1.95	0.00	.040	- 3.636	LOW	9/14	0200	1.5	1
-	.057	.3849	1.038	.0489	.0699	1.75	0.00	.030	- 4.651	LOW	9/14	0200	3.0	2
-	.089	.3845	1.104	.0647	.0699	1.25	0.00	.025	- 3.922	LOW	9/14	0200	4.5	3
-	.590	.3842	1.394	.0752	.0699	0.85	0.32	.022	- 2.062	LOW	9/14	0200	6.0	4
-	.361	.3844	1.875	.0682	.0734	0.70	0.00	.022	- 0.926	LOW	9/14	0200	7.5	5
-	.106	.3844	2.062	.0540	.0770	0.95	0.00	.022	- 0.697	LOW	9/14	0200	9.0	6
-	.095	.3844	1.841	.0419	.0840	1.45	0.00	.024	- 1.026	LOW	9/14	0200	10.5	7
-	.157	.3845	1.333	.0402	.0875	1.85	0.00	.028	- 2.703	LOW	9/14	0200	12.0	8
-	.000	.3846	1.155	.0297	.1477	1.40	0.00	.023	- 47.101	LOW	9/14	1406	0.0	0
-	.064	.3843	1.086	.0349	.1477	2.40	0.00	.025	- 59.091	LOW	9/14	1406	1.5	1
-	.064	.3840	1.187	.0540	.2126	2.15	0.00	.037	- 50.781	LOW	9/14	1406	3.0	2
-	.088	.3838	1.446	.0770	.2530	1.25	0.00	.047	- 31.250	LOW	9/14	1406	4.5	3
-	.000	.3838	1.600	.0857	.2568	0.95	0.17	.046	- 23.050	LOW	9/14	1406	6.0	4
-	.149	.3840	1.545	.0664	.2346	0.90	0.17	.035	- 24.436	LOW	9/14	1406	7.5	5
-	.097	.3847	1.470	.0384	.1980	1.00	0.12	.023	- 26.000	LOW	9/14	1406	9.0	6
-	.111	.3853	1.362	.0279	.1620	1.25	0.00	.022	- 31.250	LOW	9/14	1406	10.5	7
-	.000	.3855	1.200	.0297	.1263	1.75	0.00	.025	- 43.919	LOW	9/14	1406	12.0	8
-	.000	.3847	1.412	.0367	.1477	1.55	0.00	.027	- 38.288	LOW	9/15	0300	0.0	0
-	.094	.3846	0.986	.0349	.1441	1.20	0.00	.027	-108.974	LOW	9/15	0300	1.5	1
-	.053	.3836	0.914	.0472	.1405	0.90	0.00	.027	-128.788	LOW	9/15	0300	3.0	2
-	.080	.3828	1.371	.0664	.1477	0.75	0.00	.026	- 38.288	LOW	9/15	0300	4.5	3
-	.873	.3823	1.771	.0910	.1585	1.00	0.00	.024	- 17.857	LOW	9/15	0300	6.0	4
-	.169	.3827	1.831	.0822	.1763	1.25	0.00	.023	- 15.455	LOW	9/15	0300	7.5	5
-	.078	.3832	1.634	.0489	.1763	1.30	0.00	.022	- 21.795	LOW	9/15	0300	9.0	6
-	.068	.3839	1.324	.0314	.1691	1.15	0.00	.020	- 40.865	LOW	9/15	0300	10.5	7
-	.135	.3844	1.211	.0279	.1548	1.25	0.00	.023	- 53.125	LOW	9/15	0300	12.0	8
-	.000	.3845	0.927	.0472	.1016	0.95	0.00	.022	- 2.727	LOW	9/15	1550	0.0	0
-	.065	.3847	1.037	.0402	.0840	0.90	0.00	.019	- 2.027	LOW	9/15	1550	1.5	1
-	.075	.3851	1.361	.0314	.0875	0.95	0.00	.018	- 1.064	LOW	9/15	1550	3.0	2
-	.108	.3856	1.877	.0227	.1052	1.00	0.00	.011	- 0.498	LOW	9/15	1550	4.5	3
-	.000	.3858	2.433	.0244	.1228	1.10	0.15	.006	- 0.272	LOW	9/15	1550	6.0	4
-	.124	.3859	2.657	.0314	.1441	1.20	0.00	.008	- 0.213	LOW	9/15	1550	7.5	5
-	.090	.3861	2.404	.0419	.1512	1.45	0.00	.018	- 0.282	LOW	9/15	1550	9.0	6
-	.102	.3861	1.929	.0454	.1512	1.65	0.00	.028	- 0.545	LOW	9/15	1550	10.5	7
-	.000	.3856	1.412	.0367	.1477	1.55	0.00	.027	- 1.351	LOW	9/15	1550	12.0	8
-	.000	.3849	1.446	.0279	.2162	1.40	0.00	.023	- 10.577	LOW	9/16	0400	0.0	0
-	.094	.3853	1.325	.0402	.2493	1.25	0.00	.024	- 12.941	LOW	9/16	0400	1.5	1
-	.076	.3858	1.400	.0594	.2456	1.30	0.00	.028	- 9.322	LOW	9/16	0400	3.0	2
-	.135	.3861	1.459	.0770	.1405	1.30	0.00	.028	- 7.006	LOW	9/16	0400	4.5	3
-	.000	.3862	1.377	.0822	.0000	1.05	0.00	.026	- 7.383	LOW	9/16	0400	6.0	4
-	.154	.3860	1.224	.0770	.0840	0.85	0.00	.024	- 9.910	LOW	9/16	0400	7.5	5
-	.064	.3854	1.083	.0682	.0981	0.80	0.00	.025	- 13.750	LOW	9/16	0400	9.0	6
-	.066	.3848	0.963	.0594	.1122	0.80	0.00	.025	- 18.644	LOW	9/16	0400	10.5	7
-	.099	.3845	0.927	.0542	.1122	0.70	0.00	.023	- 20.000	LOW	9/16	0400	12.0	8
-	.000	.3847	1.313	.0192	.1228	2.75	0.00	.019	1.176	LOW	9/16	1606	0.0	0
-	.104	.3847	1.294	.0175	.1370	2.70	0.00	.009	1.176	LOW	9/16	1606	1.5	1
-	.091	.3847	1.371	.0192	.1477	1.45	0.00	.004	0.901	LOW	9/16	1606	3.0	2
-	.155	.3847	1.722	.0577	.1691	0.75	0.12	.008	0.420	LOW	9/16	1606	4.5	3
-	2.387	.3846	2.038	.1175	.1944	0.85	0.53	.010	0.247	LOW	9/16	1606	6.0	4
-	.185	.3846	2.197	.1086	.2089	1.25	0.27	.008	0.211	LOW	9/16	1606	7.5	5
-	.123	.3846	2.000	.0787	.2126	1.60	0.00	.004	0.304	LOW	9/16	1606	9.0	6
-	.110	.3847	1.642	.0472	.2162	1.60	0.00	.010	0.602	LOW	9/16	1606	10.5	7
-	.000	.3848	1.446	.0279	.2235	1.45	0.00	.022	0.962	LOW	9/16	1606	12.0	8

$\bar{H}_b / n\bar{T}_b$	ρ_l / ρ_s	\bar{H}_b / \bar{D}	$\tan \bar{m}$	$\tan \bar{\alpha}_b$	\bar{H}_b / \bar{z}	u/d	h/d	$\Delta Q_f / \bar{H}_b^3$	Tide cycle ends on	End of cycle		Lag in hours from end of cycle	Lag #
									water	Date	Hours		
.000	.3855	1.690	.0314	.0489	0.65	0.00	.012	7.870	LOW	9/17	0448	0.0	0
- .099	.3859	1.635	.0332	.0630	0.70	0.00	.013	7.870	LOW	9/17	0448	1.5	1
- .073	.3862	1.594	.0332	.0734	0.70	0.00	.015	8.293	LOW	9/17	0448	3.0	2
- .092	.3860	1.622	.0297	.0805	0.70	0.00	.020	7.870	LOW	9/17	0448	4.5	3
- .292	.3859	1.594	.0262	.0875	0.75	0.00	.022	8.293	LOW	9/17	0448	6.0	4
.135	.3855	1.553	.0349	.0910	0.75	0.05	.016	9.189	LOW	9/17	0448	7.5	5
.074	.3852	1.556	.0507	.0981	0.80	0.00	.012	10.828	LOW	9/17	0448	9.0	6
.089	.3850	1.454	.0402	.1086	1.25	0.00	.013	14.407	LOW	9/17	0448	10.5	7
.259	.3847	1.313	.0262	.1192	2.25	0.00	.019	20.000	LOW	9/17	0448	12.0	8
.000	.3881	1.532	.0717	.1763	0.65	0.40	.030	21.277	HIGH	8/24	0224	0.0	0
.076	.3861	1.698	.0682	.1763	0.75	0.31	.015	21.277	HIGH	8/24	0224	1.5	1
.053	.3855	1.683	.0647	.1512	1.00	0.00	.008	25.641	HIGH	8/24	0224	3.0	2
.122	.3855	1.523	.0630	.0981	1.45	0.00	.018	37.037	HIGH	8/24	0224	4.5	3
.000	.3857	1.273	.0630	.0699	1.75	0.00	.036	45.455	HIGH	8/24	0224	6.0	4
- .049	.3862	1.031	.0717	.0875	1.70	0.00	.051	50.000	HIGH	8/24	0224	7.5	5
- .063	.3865	0.903	.0875	.1086	1.25	0.00	.061	45.455	HIGH	8/24	0224	9.0	6
- .167	.3868	0.957	.1052	.1052	0.80	0.00	.068	27.778	HIGH	8/24	0224	10.5	7
- 3.621	.3868	1.217	.1139	.0840	0.60	0.00	.065	13.514	HIGH	8/24	0224	12.0	8
.000	.3868	1.757	.1299	.1052	1.40	0.13	.044	3.091	HIGH	8/24	1520	0.0	0
.229	.3874	1.507	.1122	.1016	1.30	0.02	.043	5.121	HIGH	8/24	1520	1.5	1
.093	.3878	1.165	.0928	.0805	1.00	0.00	.038	12.319	HIGH	8/24	1520	3.0	2
.087	.3882	0.890	.0664	.0542	0.80	0.00	.032	31.481	HIGH	8/24	1520	4.5	3
.234	.3884	0.813	.0454	.0175	0.65	0.00	.028	47.222	HIGH	8/24	1520	6.0	4
.000	.3884	0.847	.0367	.0140	0.60	0.00	.026	47.222	HIGH	8/24	1520	7.5	5
- .117	.3882	0.966	.0437	.0770	0.60	0.00	.025	38.636	HIGH	8/24	1520	9.0	6
- .119	.3882	1.185	.0577	.1228	0.55	0.02	.028	25.758	HIGH	8/24	1520	10.5	7
.000	.3876	1.344	.0699	.1584	0.60	0.28	.030	21.795	HIGH	8/24	1520	12.0	8
.000	.3883	1.636	.0559	.0349	0.65	0.27	.023	13.830	HIGH	8/25	0356	0.0	0
.251	.3877	1.897	.0577	.0314	0.75	0.09	.015	7.647	HIGH	8/25	0356	1.5	1
.111	.3868	1.680	.0542	.0314	1.00	0.00	.019	8.784	HIGH	8/25	0356	3.0	2
.142	.3860	1.222	.0454	.0349	1.15	0.00	.029	18.056	HIGH	8/25	0356	4.5	3
.257	.3853	0.862	.0454	.0210	1.10	0.00	.030	40.625	HIGH	8/25	0356	6.0	4
- .127	.3852	0.833	.0454	.0000	0.95	0.00	.035	36.111	HIGH	8/25	0356	7.5	5
- .088	.3856	1.343	.0612	.0542	1.00	0.00	.039	7.143	HIGH	8/25	0356	9.0	6
- .135	.3861	1.775	.0963	.0945	1.25	0.00	.042	2.600	HIGH	8/25	0356	10.5	7
- .299	.3866	1.826	.1281	.1052	1.40	0.23	.044	2.159	HIGH	8/25	0356	12.0	8
.000	.3892	1.754	.0630	.2419	1.75	0.33	.052	7.027	HIGH	8/25	1632	0.0	0
.267	.3889	1.871	.0612	.2419	1.75	0.00	.047	6.667	HIGH	8/25	1632	1.5	1
.147	.3878	1.891	.0559	.1980	1.55	0.00	.038	9.220	HIGH	8/25	1632	3.0	2
.123	.3868	2.043	.0507	.1477	1.35	0.00	.032	11.712	HIGH	8/25	1632	4.5	3
.231	.3861	2.047	.0437	.0875	1.20	0.00	.028	15.294	HIGH	8/25	1632	6.0	4
.000	.3863	1.762	.0419	.0770	1.10	0.00	.028	25.490	HIGH	8/25	1632	7.5	5
- .080	.3869	1.381	.0454	.0349	0.95	0.00	.028	54.167	HIGH	8/25	1632	9.0	6
- .064	.3874	1.209	.0489	.0349	0.75	0.12	.027	72.222	HIGH	8/25	1632	10.5	7
- .158	.3881	1.591	.0540	.0349	0.60	0.26	.025	30.233	HIGH	8/25	1632	12.0	8
.000	.3872	1.134	.0472	.1228	0.65	0.19	.024	34.091	HIGH	8/26	0502	0.0	0
.151	.3871	1.455	.0542	.1370	0.50	0.00	.023	22.727	HIGH	8/26	0502	1.5	1
.165	.3872	2.051	.0540	.1405	0.75	0.00	.022	13.636	HIGH	8/26	0502	3.0	2
.228	.3876	1.805	.0542	.1441	0.90	0.00	.022	11.719	HIGH	8/26	0502	4.5	3
.000	.3882	1.404	.0472	.1228	0.90	0.00	.023	14.706	HIGH	8/26	0502	6.0	4
- .172	.3887	1.309	.0419	.1052	0.85	0.00	.027	20.833	HIGH	8/26	0502	7.5	5
- .078	.3889	1.452	.0454	.1192	0.95	0.00	.034	15.957	HIGH	8/26	0502	9.0	6
- .105	.3891	1.692	.0542	.1691	1.30	0.00	.044	8.242	HIGH	8/26	0502	10.5	7
.000	.3892	2.039	.0612	.2309	1.65	0.29	.050	4.518	HIGH	8/26	0502	12.0	8

$\bar{H}_b / \eta \bar{T}_b$	ρ_L / ρ_S	\bar{H}_b / \bar{D}	$\tan \bar{m}$	$\tan \bar{\alpha}_b$	\bar{H}_b / \bar{z}	u/d	h/d	$\Delta Q_f / \bar{H}_b^3$	Tide cycle ends on	End of cycle		Lag in hours from end of cycle	Lag #	
										Date	Hours			
.000	.3862	1.759	.0630	.1016	1.55	0.00	.046	7.092	HIGH	8/26	1800	0.0	0	
.236	.3865	1.636	.0699	.1122	1.55	0.25	.045	7.519	HIGH	8/26	1800	1.5	1	
.119	.3868	1.263	.0630	.1263	1.55	0.00	.039	10.989	HIGH	8/26	1800	3.0	2	
.121	.3871	1.263	.0542	.1370	1.50	0.00	.030	21.277	HIGH	8/26	1800	4.5	3	
.156	.3872	1.027	.0507	.1405	1.45	0.00	.028	37.037	HIGH	8/26	1800	6.0	4	
.000	.3874	0.933	.0699	.1441	1.40	0.00	.032	45.454	HIGH	8/26	1800	7.5	5	
-	.085	.3873	1.034	.0489	.1477	1.35	0.00	.033	37.037	HIGH	8/26	1800	9.0	6
-	.133	.3873	1.176	.0437	.1441	1.15	0.00	.030	30.303	HIGH	8/26	1800	10.5	7
-	.132	.3871	1.137	.0437	.1263	0.80	0.17	.025	41.667	HIGH	8/26	1800	12.0	8
.000	.3867	1.429	.0893	.0664	1.00	0.37	.034	- 19.767	HIGH	8/27	0530	0.0	0	
.552	.3867	1.306	.0875	.0910	1.05	0.11	.046	- 25.758	HIGH	8/27	0530	1.5	1	
.038	.3863	0.936	.0699	.1122	1.05	0.00	.044	- 77.273	HIGH	8/27	0530	3.0	2	
.115	.3860	0.721	.0559	.1405	0.75	0.00	.036	-212.500	HIGH	8/27	0530	4.5	3	
.107	.3857	0.829	.0542	.1477	0.55	0.00	.038	-141.667	HIGH	8/27	0530	6.0	4	
-	.137	.3858	1.166	.0472	.1299	0.80	0.00	.026	- 47.222	HIGH	8/27	0530	7.5	5
-	.083	.3858	1.652	.0454	.1086	1.25	0.00	.027	- 15.455	HIGH	8/27	0530	9.0	6
-	.136	.3861	1.983	.0540	.0981	1.50	0.00	.036	- 7.658	HIGH	8/27	0530	10.5	7
.000	.3862	2.080	.0734	.1052	1.50	0.00	.044	- 6.028	HIGH	8/27	0530	12.0	8	
.000	.3864	1.375	.0963	.1691	0.85	0.40	.037	25.882	HIGH	8/27	1820	0.0	0	
.061	.3862	1.143	.0805	.1157	0.75	0.32	.030	46.809	HIGH	8/27	1820	1.5	1	
.057	.3855	1.600	.0507	.0910	0.75	0.15	.019	25.882	HIGH	8/27	1820	3.0	2	
.100	.3846	2.422	.0454	.1052	0.95	0.00	.013	14.013	HIGH	8/27	1820	4.5	3	
.705	.3840	2.895	.0437	.0981	1.25	0.00	.010	13.253	HIGH	8/27	1820	6.0	4	
-	.200	.3842	2.300	.0472	.0840	1.35	0.00	.018	22.680	HIGH	8/27	1820	7.5	5
-	.079	.3851	1.636	.0542	.0559	1.25	0.00	.030	46.809	HIGH	8/27	1820	9.0	6
-	.101	.3860	1.458	.0647	.0559	1.10	0.00	.032	51.163	HIGH	8/27	1820	10.5	7
-	1.483	.3867	1.429	.0805	.0559	1.00	0.35	.032	51.163	HIGH	8/27	1820	12.0	8
.000	.3873	1.516	.0699	.1835	0.95	0.17	.043	6.081	HIGH	8/28	0630	0.0	0	
.145	.3872	1.846	.0577	.1908	1.00	0.34	.035	4.054	HIGH	8/28	0630	1.5	1	
.049	.3868	1.733	.0419	.1908	1.00	0.00	.027	7.627	HIGH	8/28	0630	3.0	2	
.045	.3865	1.100	.0367	.1620	1.15	0.00	.036	40.909	HIGH	8/28	0630	4.5	3	
.000	.3862	0.737	.0367	.1584	1.30	0.00	.038	150.000	HIGH	8/28	0630	6.0	4	
-	.097	.3863	1.455	.0419	.1835	1.45	0.00	.038	13.636	HIGH	8/28	0630	7.5	5
-	.065	.3862	1.746	.0540	.2089	1.30	0.00	.038	5.294	HIGH	8/28	0630	9.0	6
-	.071	.3863	1.655	.0787	.2126	1.10	0.17	.038	4.054	HIGH	8/28	0630	10.5	7
-	.137	.3864	1.344	.0963	.1727	0.85	0.40	.038	5.625	HIGH	8/28	0630	12.0	8
.000	.3872	2.316	.1122	.1122	0.70	0.12	.024	11.176	HIGH	8/28	1902	0.0	0	
.088	.3862	2.600	.0787	.1192	0.70	0.10	.020	6.738	HIGH	8/28	1902	1.5	1	
.052	.3856	2.348	.0402	.1405	0.70	0.05	.019	6.051	HIGH	8/28	1902	3.0	2	
.050	.3852	2.043	.0419	.1691	0.65	0.00	.018	8.559	HIGH	8/28	1902	4.5	3	
.167	.3852	1.644	.0437	.1835	0.55	0.00	.019	18.627	HIGH	8/28	1902	6.0	4	
-	.089	.3854	1.167	.0489	.1799	0.45	0.00	.015	43.182	HIGH	8/28	1902	7.5	5
-	.036	.3861	0.941	.0559	.1763	0.55	0.00	.018	67.857	HIGH	8/28	1902	9.0	6
-	.045	.3868	1.018	.0647	.1799	0.80	0.00	.025	43.182	HIGH	8/28	1902	10.5	7
-	.542	.3874	1.036	.0717	.1835	0.95	0.08	.040	39.583	HIGH	8/28	1902	12.0	8
.000	.3891	1.182	.1175	.1727	1.00	0.00	.046	27.119	HIGH	8/29	0708	0.0	0	
.044	.3889	1.129	.1175	.1548	0.85	0.06	.034	37.209	HIGH	8/29	0708	1.5	1	
.063	.3888	1.263	.0840	.1405	0.70	0.08	.021	34.043	HIGH	8/29	0708	3.0	2	
.084	.3887	1.714	.0454	.1299	0.70	0.02	.030	34.043	HIGH	8/29	0708	4.5	3	
.000	.3885	1.889	.0314	.1263	0.80	0.00	.033	41.026	HIGH	8/29	0708	6.0	4	
-	.076	.3883	1.676	.0297	.1228	0.80	0.00	.037	53.333	HIGH	8/29	0708	7.5	5
-	.029	.3881	1.514	.0384	.1192	0.75	0.00	.035	72.727	HIGH	8/29	0708	9.0	6
-	.057	.3879	1.789	.0699	.1122	0.75	0.00	.030	41.026	HIGH	8/29	0708	10.5	7
-	.391	.3874	2.205	.1016	.1122	0.75	0.11	.025	20.000	HIGH	8/29	0708	12.0	8

$\bar{H}_b / n\bar{T}_b$	ρ_l / ρ_s	\bar{H}_b / \bar{D}	$\tan \bar{m}$	$\tan \bar{\alpha}_b$	\bar{H}_b / \bar{z}	u/d	h/d	$\Delta Q_f / \bar{H}_b^3$	Tide cycle ends on	End of cycle		Lag in hours from end of cycle	Lag #
									water	Date	Hours		
.000	.3842	0.847	.1013	.1763	0.45	0.31	.026	- 20.588	HIGH	8/29	2000	0.0	0
.111	.3839	0.898	.0699	.1763	0.50	0.00	.017	- 19.091	HIGH	8/29	2000	1.5	1
.054	.3834	1.080	.0332	.1763	0.60	0.00	.013	- 19.091	HIGH	8/29	2000	3.0	2
.047	.3827	1.385	.0227	.1835	0.65	0.00	.019	- 22.340	HIGH	8/29	2000	4.5	3
.127	.3825	1.800	.0297	.1944	0.60	0.00	.029	- 22.340	HIGH	8/29	2000	6.0	4
- .400	.3833	2.154	.0472	.1944	0.60	0.00	.038	- 14.189	HIGH	8/29	2000	7.5	5
- .055	.3855	1.800	.0699	.1908	0.65	0.00	.044	- 11.538	HIGH	8/29	2000	9.0	6
- .085	.3877	1.516	.0875	.1835	0.80	0.00	.048	- 10.096	HIGH	8/29	2000	10.5	7
- .202	.3891	1.333	.0998	.1799	1.00	0.00	.045	- 12.353	HIGH	8/29	2000	12.0	8
.000	.3864	2.036	.0472	.1871	0.95	0.28	.036	7.670	HIGH	8/30	0808	0.0	0
.093	.3863	1.849	.0419	.1908	0.90	0.00	.034	11.441	HIGH	8/30	0808	1.5	1
.062	.3857	1.702	.0349	.1835	0.80	0.00	.026	21.094	HIGH	8/30	0808	3.0	2
.057	.3855	1.546	.0332	.1835	0.80	0.00	.028	40.909	HIGH	8/30	0808	4.5	3
.306	.3852	1.171	.0419	.1908	0.80	0.00	.031	96.429	HIGH	8/30	0808	6.0	4
- .038	.3850	0.898	.0349	.1908	0.85	0.00	.035	122.727	HIGH	8/30	0808	7.5	5
- .038	.3848	0.862	.0542	.1944	0.80	0.00	.036	61.364	HIGH	8/30	0808	9.0	6
- .062	.3844	0.840	.0875	.1944	0.65	0.00	.033	34.615	HIGH	8/30	0808	10.5	7
.411	.3842	0.871	.1033	.1763	0.45	0.30	.028	26.471	HIGH	8/30	0808	12.0	8
.000	.3838	1.200	.1033	.2126	0.70	0.58	.041	- 9.341	HIGH	8/30	2000	0.0	0
.065	.3847	1.278	.0699	.1944	0.70	0.23	.034	- 8.763	HIGH	8/30	2000	1.5	1
.071	.3859	1.333	.0367	.1656	0.70	0.00	.025	- 11.486	HIGH	8/30	2000	3.0	2
.059	.3868	1.228	.0419	.1405	0.70	0.00	.020	- 19.767	HIGH	8/30	2000	4.5	3
.130	.3874	1.111	.0367	.1228	0.75	0.00	.027	- 31.481	HIGH	8/30	2000	6.0	4
- .040	.3874	1.127	.0332	.1157	0.80	0.00	.024	- 28.333	HIGH	8/30	2000	7.5	5
- .062	.3870	1.600	.0349	.1370	0.85	0.00	.026	- 10.000	HIGH	8/30	2000	9.0	6
- .113	.3867	2.036	.0437	.1620	0.90	0.04	.031	- 4.830	HIGH	8/30	2000	10.5	7
- .651	.3864	2.036	.0472	.1871	0.95	0.16	.036	- 4.830	HIGH	8/30	2000	12.0	8
.000	.3851	1.851	.0717	.2530	1.90	0.04	.052	12.605	HIGH	8/31	0900	0.0	0
.109	.3850	1.873	.0664	.3057	1.90	0.00	.040	14.634	HIGH	8/31	0900	1.5	1
.091	.3848	1.733	.0594	.3172	1.85	0.00	.030	27.027	HIGH	8/31	0900	3.0	2
.045	.3845	1.333	.0542	.2943	1.55	0.00	.026	90.909	HIGH	8/31	0900	4.5	3
.105	.3840	1.111	.0437	.2493	1.30	0.00	.038	187.500	HIGH	8/31	0900	6.0	4
- .046	.3835	1.020	.0384	.1835	0.85	0.00	.039	166.667	HIGH	8/31	0900	7.5	5
- .036	.3832	0.984	.0437	.1584	0.75	0.00	.038	111.111	HIGH	8/31	0900	9.0	6
- .047	.3834	0.986	.0717	.1799	0.70	0.05	.042	76.923	HIGH	8/31	0900	10.5	7
- .166	.3837	1.129	.0928	.2053	0.70	0.56	.042	40.541	HIGH	8/31	0900	12.0	8
.000	.3895	1.279	.0857	.2642	0.60	0.54	.042	- 48.305	HIGH	8/31	2100	0.0	0
.086	.3896	1.127	.0770	.2717	0.65	0.23	.042	- 95.000	HIGH	8/31	2100	1.5	1
.030	.3812	1.000	.0647	.2680	0.65	0.00	.042	-158.333	HIGH	8/31	2100	3.0	2
.050	.3837	1.160	.0594	.2493	0.65	0.00	.040	-118.750	HIGH	8/31	2100	4.5	3
.192	.3855	1.551	.0577	.2089	0.70	0.00	.037	- 51.818	HIGH	8/31	2100	6.0	4
- .111	.3862	1.985	.0699	.1727	0.90	0.00	.042	- 20.213	HIGH	8/31	2100	7.5	5
- .075	.3860	2.105	.0770	.1584	1.20	0.00	.052	- 13.194	HIGH	8/31	2100	9.0	6
- .085	.3855	1.938	.0805	.1835	1.75	0.00	.058	- 11.975	HIGH	8/31	2100	10.5	7
- 1.409	.3851	1.851	.0717	.2530	1.90	0.05	.054	- 11.975	HIGH	8/31	2100	12.0	8
.000	.3820	2.169	.0822	.1656	1.10	0.34	.020	- 19.466	HIGH	9/01	0936	0.0	0
.175	.3822	2.033	.0857	.1799	0.85	0.92	.019	- 21.429	HIGH	9/01	0936	1.5	1
.106	.3829	1.600	.0752	.1370	1.00	0.06	.024	- 36.170	HIGH	9/01	0936	3.0	2
.104	.3838	1.111	.0612	.0875	1.40	0.00	.034	- 79.688	HIGH	9/01	0936	4.5	3
.213	.3841	0.883	.0542	.0770	1.50	0.00	.041	-130.769	HIGH	9/01	0936	6.0	4
- .493	.3833	0.853	.0559	.1016	1.15	0.00	.042	-141.667	HIGH	9/01	0936	7.5	5
- .061	.3816	0.960	.0664	.1548	0.80	0.00	.042	-108.511	HIGH	9/01	0936	9.0	6
- .071	.3803	1.127	.0770	.2126	0.65	0.08	.042	- 79.688	HIGH	9/01	0936	10.5	7
- .230	.3794	1.262	.0857	.2568	0.60	0.52	.042	- 79.688	HIGH	9/01	0936	12.0	8

$\bar{H}_b / n\bar{T}_b$	ρ_L / ρ_S	\bar{H}_b / \bar{D}	$\tan \bar{m}$	$\tan \bar{\alpha}_b$	\bar{H}_b / \bar{z}	u/d	h/d	$\Delta Q_f / \bar{H}_b^3$	Tide cycle ends on	End of cycle		Lag in hours from end of cycle	Lag #
									water	Date	Hours		
.000	.3808	1.662	.0612	.0000	1.05	0.56	.040	- 10.828	HIGH	9/01	2200	0.0	0
.105	.3815	1.662	.0559	.0000	0.80	0.46	.036	- 10.828	HIGH	9/01	2200	1.5	1
.085	.3823	1.538	.0454	.0070	0.70	0.00	.033	- 13.600	HIGH	9/01	2200	3.0	2
.066	.3830	1.354	.0402	.0279	0.60	0.00	.031	- 20.000	HIGH	9/01	2200	4.5	3
.227	.3836	1.273	.0384	.0542	0.65	0.00	.033	- 22.973	HIGH	9/01	2200	6.0	4
- .116	.3836	1.314	.0419	.0734	0.80	0.00	.038	- 21.250	HIGH	9/01	2200	7.5	5
- .121	.3831	1.469	.0472	.0981	1.05	0.00	.043	- 16.346	HIGH	9/01	2200	9.0	6
- .169	.3824	1.770	.0612	.1192	1.25	0.00	.032	- 10.828	HIGH	9/01	2200	10.5	7
- .897	.3820	2.068	.0787	.1584	1.20	0.25	.022	- 7.489	HIGH	9/01	2200	12.0	8
.000	.3836	1.903	.0752	.0314	1.20	0.00	.048	1.955	HIGH	9/02	0930	0.0	0
.133	.3833	1.784	.0542	.0244	1.25	0.00	.036	2.439	HIGH	9/02	0930	1.5	1
.116	.3832	1.662	.0507	.0140	1.30	0.00	.035	3.084	HIGH	9/02	0930	3.0	2
.197	.3828	1.583	.0332	.0000	1.30	0.00	.036	3.784	HIGH	9/02	0930	4.5	3
.000	.3823	1.521	.0279	.0000	1.30	0.00	.036	4.459	HIGH	9/02	0930	6.0	4
- .138	.3816	1.486	.0314	.0000	1.30	0.00	.036	4.965	HIGH	9/02	0930	7.5	5
- .125	.3816	1.529	.0367	.0000	1.25	0.00	.039	4.965	HIGH	9/02	0930	9.0	6
- .158	.3810	1.582	.0540	.0000	1.20	0.00	.040	4.698	HIGH	9/02	0930	10.5	7
- .740	.3808	1.636	.0612	.0000	1.05	0.53	.040	4.459	HIGH	9/02	0930	12.0	8
.000	.3846	1.351	.0367	.0000	1.00	0.13	.030	- 4.800	HIGH	9/02	2202	0.0	0
.105	.3846	1.227	.0559	.0000	0.80	0.00	.030	- 6.186	HIGH	9/02	2202	1.5	1
.100	.3842	1.120	.0577	.0140	0.75	0.00	.032	- 8.108	HIGH	9/02	2202	3.0	2
.089	.3836	1.093	.0472	.0244	0.85	0.00	.034	- 8.696	HIGH	9/02	2202	4.5	3
.000	.3834	1.120	.0349	.0349	0.90	0.00	.034	- 8.108	HIGH	9/02	2202	6.0	4
- .152	.3835	1.237	.0314	.0384	1.00	0.00	.036	- 5.769	HIGH	9/02	2202	7.5	5
- .100	.3837	1.447	.0384	.0384	1.00	0.00	.037	- 3.614	HIGH	9/02	2202	9.0	6
- .152	.3837	1.684	.0612	.0349	1.05	0.00	.042	- 2.290	HIGH	9/02	2202	10.5	7
- .946	.3837	1.867	.0770	.0349	1.15	0.00	.048	- 1.749	HIGH	9/02	2202	12.0	8
.000	.3806	1.418	.0664	.0279	1.25	0.34	.030	1.136	HIGH	9/03	1015	0.0	0
.171	.3814	1.568	.0559	.0244	1.00	0.00	.030	1.026	HIGH	9/03	1015	1.5	1
.098	.3827	1.739	.0437	.0175	0.90	0.00	.030	0.926	HIGH	9/03	1015	3.0	2
.110	.3840	1.858	.0367	.0105	0.90	0.00	.026	0.926	HIGH	9/03	1015	4.5	3
.231	.3846	1.934	.0349	.0000	1.05	0.00	.028	0.976	HIGH	9/03	1015	6.0	4
- .405	.3848	1.935	.0384	.0000	1.25	0.00	.033	0.926	HIGH	9/03	1015	7.5	5
- .107	.3849	1.846	.0419	.0000	1.35	0.00	.036	0.926	HIGH	9/03	1015	9.0	6
- .094	.3848	1.643	.0437	.0000	1.25	0.00	.034	1.081	HIGH	9/03	1015	10.5	7
- .559	.3847	1.397	.0454	.0000	1.05	0.13	.030	1.504	HIGH	9/03	1015	12.0	8
.000	.3826	1.214	.0682	.0000	0.90	0.12	.022	- 3.759	HIGH	9/03	2232	0.0	0
.104	.3826	1.095	.0559	.0000	0.70	0.00	.022	- 5.155	HIGH	9/03	2232	1.5	1
.103	.3825	0.959	.0402	.0000	0.60	0.00	.022	- 7.813	HIGH	9/03	2232	3.0	2
.109	.3826	0.867	.0367	.0000	0.60	0.00	.022	- 10.638	HIGH	9/03	2232	4.5	3
- .706	.3824	0.867	.0367	.0000	0.75	0.00	.023	- 10.638	HIGH	9/03	2232	6.0	4
- .190	.3820	0.922	.0454	.0140	0.95	0.00	.032	- 9.091	HIGH	9/03	2232	7.5	5
- .113	.3814	1.098	.0540	.0210	1.20	0.00	.043	- 5.495	HIGH	9/03	2232	9.0	6
- .097	.3809	1.309	.0682	.0279	1.40	0.00	.045	- 3.356	HIGH	9/03	2232	10.5	7
- .671	.3807	1.392	.0682	.0279	1.30	0.34	.030	- 3.012	HIGH	9/03	2232	12.0	8
.000	.3834	1.130	.0893	.0210	1.00	1.14	.044	0.000	HIGH	9/04	1102	0.0	0
.063	.3833	0.925	.0893	.0140	0.80	0.95	.032	0.000	HIGH	9/04	1102	1.5	1
.048	.3832	0.738	.0770	.0105	0.65	0.10	.024	0.000	HIGH	9/04	1102	3.0	2
.063	.3830	0.698	.0594	.0035	0.55	0.00	.025	0.000	HIGH	9/04	1102	4.5	3
- 1.359	.3828	0.801	.0437	.0000	0.65	0.00	.024	0.000	HIGH	9/04	1102	6.0	4
- .117	.3826	1.077	.0367	.0000	0.75	0.00	.023	0.000	HIGH	9/04	1102	7.5	5
- .094	.3825	1.296	.0367	.0000	0.95	0.00	.022	0.000	HIGH	9/04	1102	9.0	6
- .130	.3826	1.262	.0489	.0000	1.05	0.06	.022	0.000	HIGH	9/04	1102	10.5	7
- .642	.3826	1.238	.0664	.0000	0.95	0.12	.022	0.000	HIGH	9/04	1102	12.0	8

$\bar{H}_b / n\bar{T}_b$	ρ_l / ρ_s	\bar{H}_b / \bar{D}	$\tan \bar{m}$	$\tan \bar{\alpha}_b$	\bar{H}_b / \bar{z}	u/d	h/d	$\Delta Q_f / \bar{H}_b^3$	Tide cycle ends on	End of cycle		Lag in hours from end of cycle	Lag #
										water	Date		
.000	.3851	1.695	.0542	.0384	0.80	0.06	.032	0.000	HIGH	9/04	2308	0.0	0
.141	.3848	1.667	.0472	.0070	0.90	0.15	.026	0.000	HIGH	9/04	2308	1.5	1
.112	.3846	1.311	.0419	.0000	0.95	0.03	.023	0.000	HIGH	9/04	2308	3.0	2
.093	.3843	0.871	.0367	.0000	0.80	0.00	.023	0.000	HIGH	9/04	2308	4.5	3
- 1.202	.3840	0.794	.0332	.0035	0.65	0.00	.022	0.000	HIGH	9/04	2308	6.0	4
- .117	.3833	1.231	.0297	.0140	0.80	0.00	.022	0.000	HIGH	9/04	2308	7.5	5
- .111	.3833	1.433	.0437	.0175	1.10	0.00	.025	0.000	HIGH	9/04	2308	9.0	6
- .133	.3835	1.404	.0717	.0210	1.20	0.63	.037	0.000	HIGH	9/04	2308	10.5	7
- 2.500	.3834	1.159	.0893	.0210	1.05	1.14	.044	0.000	HIGH	9/04	2308	12.0	8
.000	.3837	1.108	.0682	.0981	0.95	0.06	.030	15.942	HIGH	9/05	1112	0.0	0
.082	.3836	1.210	.0594	.0910	1.00	0.00	.028	14.865	HIGH	9/05	1112	1.5	1
.067	.3830	1.199	.0454	.0840	1.05	0.00	.026	20.000	HIGH	9/05	1112	3.0	2
.145	.3826	1.085	.0367	.0770	0.85	0.00	.020	33.333	HIGH	9/05	1112	4.5	3
- 1.020	.3825	0.929	.0349	.0770	0.60	0.00	.017	61.111	HIGH	9/05	1112	6.0	4
- .164	.3826	1.011	.0349	.0699	0.45	0.00	.020	50.000	HIGH	9/05	1112	7.5	5
- .066	.3835	1.263	.0402	.0699	0.55	0.00	.028	23.404	HIGH	9/05	1112	9.0	6
- .125	.3843	1.568	.0577	.0594	0.65	0.00	.033	12.088	HIGH	9/05	1112	10.5	7
- 1.493	.3849	1.724	.0542	.0454	0.80	0.08	.034	8.800	HIGH	9/05	1112	12.0	8
.000	.3836	1.932	.0594	.0559	1.25	0.29	.042	5.946	HIGH	9/05	2300	0.0	0
.092	.3835	1.661	.0559	.0559	1.00	0.02	.039	9.322	HIGH	9/05	2300	1.5	1
.192	.3834	1.433	.0507	.0559	0.75	0.00	.032	13.750	HIGH	9/05	2300	3.0	2
.782	.3834	1.401	.0454	.0594	0.70	0.00	.020	13.750	HIGH	9/05	2300	4.5	3
- .689	.3835	1.333	.0472	.0630	0.75	0.00	.017	14.865	HIGH	9/05	2300	6.0	4
- .100	.3836	1.273	.0507	.0770	0.85	0.00	.028	14.865	HIGH	9/05	2300	7.5	5
- .076	.3837	1.127	.0594	.0910	0.90	0.00	.030	17.188	HIGH	9/05	2300	9.0	6
- .256	.3838	1.081	.0664	.1052	0.90	0.00	.030	17.188	HIGH	9/05	2300	10.5	7
- 1.105	.3838	1.135	.0682	.0981	0.95	0.06	.030	14.865	HIGH	9/05	2300	12.0	8
.000	.3810	1.258	.0840	.1299	0.50	0.98	.000	5.085	HIGH	9/06	1212	0.0	0
.232	.3811	1.206	.0805	.1122	0.65	0.85	.002	5.455	HIGH	9/06	1212	1.5	1
.097	.3818	1.175	.0770	.1052	1.05	0.62	.019	5.882	HIGH	9/06	1212	3.0	2
.059	.3827	1.000	.0664	.0981	1.25	0.44	.033	9.091	HIGH	9/06	1212	4.5	3
.446	.3836	0.892	.0540	.0981	1.10	0.16	.031	12.500	HIGH	9/06	1212	6.0	4
- .172	.3839	0.848	.0489	.0981	0.95	0.00	.032	13.636	HIGH	9/06	1212	7.5	5
- .088	.3840	1.138	.0454	.0770	0.95	0.00	.039	5.882	HIGH	9/06	1212	9.0	6
- .091	.3838	1.667	.0489	.0559	1.15	0.00	.042	2.128	HIGH	9/06	1212	10.5	7
- .313	.3836	2.000	.0540	.0542	1.35	0.23	.042	1.389	HIGH	9/06	1212	12.0	8
.000	.3875	1.238	.0437	.1584	0.85	0.25	.029	2.542	HIGH	9/07	0005	0.0	0
.170	.3876	1.267	.0472	.1477	0.80	0.04	.030	2.727	HIGH	9/07	0005	1.5	1
.148	.3876	1.286	.0507	.1228	0.80	0.00	.029	3.191	HIGH	9/07	0005	3.0	2
.576	.3876	1.360	.0540	.0910	1.00	0.12	.032	3.846	HIGH	9/07	0005	4.5	3
- .343	.3875	1.435	.0612	.0630	1.15	0.18	.044	3.846	HIGH	9/07	0005	6.0	4
- .126	.3862	1.412	.0752	.0559	1.25	0.31	.051	3.191	HIGH	9/07	0005	7.5	5
- .074	.3842	1.357	.0805	.0875	1.15	0.53	.041	2.727	HIGH	9/07	0005	9.0	6
- .123	.3821	1.300	.0787	.1299	0.75	0.82	.012	2.542	HIGH	9/07	0005	10.5	7
- .951	.3811	1.258	.0840	.1334	0.50	0.98	.000	2.542	HIGH	9/07	0005	12.0	8
.000	.3868	2.032	.0559	.1980	1.40	0.00	.039	- 4.198	HIGH	9/07	1242	0.0	0
.220	.3870	1.731	.0559	.1620	1.35	0.00	.038	- 7.006	HIGH	9/07	1242	1.5	1
.083	.3873	1.311	.0542	.1016	1.00	0.00	.035	- 17.188	HIGH	9/07	1242	3.0	2
.077	.3874	1.017	.0472	.0210	0.70	0.00	.031	- 40.741	HIGH	9/07	1242	4.5	3
- 1.474	.3874	0.967	.0367	.0035	0.65	0.00	.033	- 50.000	HIGH	9/07	1242	6.0	4
- .217	.3874	1.111	.0367	.0384	0.75	0.00	.027	- 30.556	HIGH	9/07	1242	7.5	5
- .120	.3875	1.233	.0384	.0875	0.80	0.00	.020	- 21.569	HIGH	9/07	1242	9.0	6
- .122	.3875	1.226	.0419	.1370	0.85	0.01	.026	- 20.000	HIGH	9/07	1242	10.5	7
- .557	.3875	1.238	.0437	.1548	0.85	0.08	.029	- 18.644	HIGH	9/07	1242	12.0	8

$\bar{H}_b / \eta \bar{T}_b$	ρ_l / ρ_s	\bar{H}_b / \bar{D}	$\tan \bar{m}$	$\tan \bar{\alpha}_b$	\bar{H}_b / \bar{z}	u/d	h/d	$\Delta Q_f / \bar{H}_b^3$	Tide cycle ends on	End of cycle		Lag in hours from end of cycle	Lag #
									water	Date	Hours		
.000	.3870	1.206	.0612	.0035	0.75	0.00	.032	4.545	HIGH	9/08	0112	0.0	0
.334	.3871	1.161	.0542	.0210	0.75	0.07	.034	5.319	HIGH	9/08	0112	1.5	1
.110	.3871	1.079	.0402	.0770	0.90	0.00	.034	6.410	HIGH	9/08	0112	3.0	2
.148	.3873	1.016	.0332	.0875	1.15	0.00	.034	7.576	HIGH	9/08	0112	4.5	3
- .486	.3872	1.063	.0332	.0630	1.40	0.00	.034	6.410	HIGH	9/08	0112	6.0	4
- .147	.3871	1.292	.0367	.0175	1.50	0.00	.034	3.378	HIGH	9/08	0112	7.5	5
- .200	.3871	1.600	.0454	.1228	1.45	0.00	.036	1.773	HIGH	9/08	0112	9.0	6
- .241	.3869	1.906	.0507	.1908	1.45	0.00	.038	1.101	HIGH	9/08	0112	10.5	7
- .561	.3868	2.019	.0540	.2053	1.40	0.00	.039	0.954	HIGH	9/08	0112	12.0	8
.000	.3853	1.471	.0489	.1299	0.95	0.00	.024	0.800	HIGH	9/08	1400	0.0	0
.355	.3854	1.412	.0594	.1192	0.95	0.44	.033	0.901	HIGH	9/08	1400	1.5	1
.150	.3854	1.324	.0559	.1370	0.90	0.24	.032	1.099	HIGH	9/08	1400	3.0	2
.183	.3854	1.265	.0454	.1763	0.85	0.00	.025	1.351	HIGH	9/08	1400	4.5	3
.000	.3856	1.212	.0419	.1835	0.80	0.00	.022	1.563	HIGH	9/08	1400	6.0	4
- .905	.3859	1.180	.0419	.1620	0.80	0.00	.024	1.818	HIGH	9/08	1400	7.5	5
- .158	.3861	1.188	.0419	.1299	0.85	0.00	.026	1.818	HIGH	9/08	1400	9.0	6
- .325	.3864	1.238	.0472	.0840	0.85	0.00	.028	1.695	HIGH	9/08	1400	10.5	7
- .442	.3867	1.206	.0577	.0210	0.80	0.00	.030	1.818	HIGH	9/08	1400	12.0	8
.000	.3848	1.706	.0577	.2309	1.30	0.12	.034	5.897	HIGH	9/09	0150	0.0	0
.382	.3845	1.731	.0559	.2199	1.40	0.00	.033	5.897	HIGH	9/09	0150	1.5	1
.271	.3842	1.667	.0349	.1763	1.45	0.00	.036	8.156	HIGH	9/09	0150	3.0	2
.341	.3837	1.684	.0332	.1192	1.40	0.00	.018	10.360	HIGH	9/09	0150	4.5	3
- .460	.3834	1.704	.0367	.0875	1.25	0.00	.012	11.856	HIGH	9/09	0150	6.0	4
- .181	.3833	1.778	.0437	.1122	1.15	0.00	.012	10.360	HIGH	9/09	0150	7.5	5
- .234	.3837	1.793	.0489	.1548	1.05	0.00	.025	8.156	HIGH	9/09	0150	9.0	6
- .327	.3844	1.640	.0507	.1477	1.00	0.00	.030	8.156	HIGH	9/09	0150	10.5	7
- 1.202	.3850	1.471	.0507	.1299	0.90	0.00	.024	9.200	HIGH	9/09	0150	12.0	8
.000	.3857	1.771	.0472	.1122	1.55	0.22	.038	4.202	HIGH	9/09	1420	0.0	0
.161	.3855	1.746	.0419	.0981	1.55	0.00	.036	4.202	HIGH	9/09	1420	1.5	1
.143	.3849	1.547	.0419	.1016	1.50	0.00	.032	5.128	HIGH	9/09	1420	3.0	2
.175	.3838	1.282	.0402	.1157	1.35	0.00	.022	8.000	HIGH	9/09	1420	4.5	3
- .896	.3835	1.084	.0349	.1334	1.05	0.00	.007	12.500	HIGH	9/09	1420	6.0	4
- .184	.3834	0.957	.0332	.1548	0.85	0.00	.001	18.182	HIGH	9/09	1420	7.5	5
- .164	.3838	1.013	.0332	.1763	0.80	0.00	.008	16.949	HIGH	9/09	1420	9.0	6
- .285	.3843	1.361	.0472	.2089	1.05	0.00	.022	8.475	HIGH	9/09	1420	10.5	7
- 13.902	.3847	1.643	.0559	.2309	1.25	0.26	.031	5.405	HIGH	9/09	1420	12.0	8
.000	.3861	1.352	.0472	.0981	0.85	0.25	.024	4.505	HIGH	9/10	0336	0.0	0
.357	.3857	1.429	.0454	.0981	0.85	0.28	.022	4.000	HIGH	9/10	0336	1.5	1
.208	.3852	1.507	.0419	.0981	0.80	0.33	.022	3.546	HIGH	9/10	0336	3.0	2
.272	.3846	1.500	.0402	.0981	1.05	0.03	.021	3.759	HIGH	9/10	0336	4.5	3
- .867	.3845	1.543	.0384	.1052	1.25	0.00	.023	3.546	HIGH	9/10	0336	6.0	4
- .211	.3846	1.588	.0367	.1192	1.45	0.00	.027	3.185	HIGH	9/10	0336	7.5	5
- .120	.3849	1.662	.0419	.1228	1.50	0.00	.030	2.703	HIGH	9/10	0336	9.0	6
- .204	.3850	1.681	.0454	.1228	1.50	0.08	.032	2.564	HIGH	9/10	0336	10.5	7
- .483	.3849	1.714	.0472	.1228	1.50	0.32	.036	2.315	HIGH	9/10	0336	12.0	8
.000	.3842	1.500	.0559	.0981	1.60	0.24	.040	22.527	HIGH	9/10	1626	0.0	0
.190	.3842	1.467	.0559	.0770	1.25	0.08	.035	24.118	HIGH	9/10	1626	1.5	1
.096	.3843	1.433	.0540	.0349	1.05	0.00	.024	25.625	HIGH	9/10	1626	3.0	2
.107	.3846	1.333	.0472	.0210	1.00	0.00	.017	32.031	HIGH	9/10	1626	4.5	3
.259	.3851	1.233	.0332	.0419	0.95	0.00	.018	40.196	HIGH	9/10	1626	6.0	4
- 1.108	.3854	1.161	.0349	.0805	0.85	0.00	.020	43.617	HIGH	9/10	1626	7.5	5
- .136	.3858	1.138	.0402	.0945	0.85	0.00	.024	40.196	HIGH	9/10	1626	9.0	6
- .104	.3861	1.206	.0437	.0981	0.85	0.04	.024	29.710	HIGH	9/10	1626	10.5	7
- .868	.3862	1.296	.0472	.0981	0.85	0.22	.023	21.134	HIGH	9/10	1626	12.0	8

$\bar{H}_b / \eta \bar{T}_b$	ρ_L / ρ_s	\bar{H}_b / \bar{D}	$\tan \bar{m}$	$\tan \bar{\alpha}_b$	\bar{H}_b / \bar{z}	u/d	h/d	$\Delta Q_f / \bar{H}_b^3$	Tide cycle ends on	End of cycle		Lag in hours from end of cycle	Lag #
									water	Date	Hours		
.000	.3851	1.167	.0734	.0000	1.00	0.13	.034	14.865	HIGH	9/11	0500	0.0	0
.247	.3850	1.162	.0664	.0000	0.95	0.00	.027	13.750	HIGH	9/11	0500	1.5	1
.200	.3849	0.960	.0540	.0000	0.75	0.00	.024	23.404	HIGH	9/11	0500	3.0	2
.145	.3848	0.831	.0419	.0000	0.65	0.00	.020	33.333	HIGH	9/11	0500	4.5	3
- .688	.3847	0.868	.0507	.0140	0.90	0.00	.048	30.556	HIGH	9/11	0500	6.0	4
- .213	.3846	1.117	.0367	.0314	1.45	0.00	.040	15.942	HIGH	9/11	0500	7.5	5
- .090	.3841	1.391	.0297	.0542	2.00	0.00	.030	9.910	HIGH	9/11	0500	9.0	6
- .079	.3841	1.492	.0454	.0770	2.00	0.00	.033	10.577	HIGH	9/11	0500	10.5	7
- .577	.3842	1.500	.0540	.0945	1.65	0.21	.039	12.088	HIGH	9/11	0500	12.0	8
.000	.3859	1.164	.0437	.1052	0.85	0.20	.020	- 20.339	HIGH	9/11	1740	0.0	0
.152	.3855	1.333	.0594	.1512	0.95	0.40	.038	- 16.216	HIGH	9/11	1740	1.5	1
.067	.3849	1.571	.0594	.1944	1.15	0.32	.037	- 14.118	HIGH	9/11	1740	3.0	2
.068	.3846	1.551	.0454	.2089	1.10	0.14	.027	- 21.818	HIGH	9/11	1740	4.5	3
.158	.3843	1.333	.0332	.1584	0.85	0.00	.032	- 44.444	HIGH	9/11	1740	6.0	4
- .183	.3845	0.979	.0332	.0419	0.80	0.00	.033	-100.000	HIGH	9/11	1740	7.5	5
- .073	.3850	0.824	.0367	.0140	0.80	0.00	.030	-109.091	HIGH	9/11	1740	9.0	6
- .103	.3853	0.984	.0540	.0175	0.90	0.00	.031	- 40.000	HIGH	9/11	1740	10.5	7
- .187	.3852	1.200	.0717	.0035	0.95	0.10	.030	- 16.216	HIGH	9/11	1740	12.0	8
.000	.3821	1.134	.0682	.1228	0.80	0.26	.028	10.000	HIGH	9/12	0550	0.0	0
.152	.3824	1.000	.0594	.0770	0.60	0.15	.032	16.667	HIGH	9/12	0550	1.5	1
.066	.3833	1.000	.0577	.0454	0.60	0.02	.034	25.000	HIGH	9/12	0550	3.0	2
.140	.3843	1.157	.0594	.0384	0.70	0.00	.034	25.000	HIGH	9/12	0550	4.5	3
.000	.3852	1.217	.0630	.0349	0.80	0.00	.034	25.000	HIGH	9/12	0550	6.0	4
- .167	.3857	1.200	.0682	.0349	0.85	0.00	.037	20.370	HIGH	9/12	0550	7.5	5
- .057	.3859	1.158	.0664	.0419	0.85	0.15	.033	15.278	HIGH	9/12	0550	9.0	6
- .084	.3860	1.125	.0577	.0594	0.80	0.20	.024	11.702	HIGH	9/12	0550	10.5	7
- .422	.3860	1.164	.0437	.1016	0.85	0.20	.017	9.322	HIGH	9/12	0550	12.0	8
.000	.3847	1.639	.0540	.0140	0.80	0.62	.030	- 16.585	HIGH	9/12	1832	0.0	0
.150	.3848	1.662	.0489	.0210	0.80	0.22	.026	- 19.318	HIGH	9/12	1832	1.5	1
.092	.3850	1.574	.0349	.0349	0.80	0.00	.024	- 30.631	HIGH	9/12	1832	3.0	2
.114	.3852	1.480	.0279	.0594	0.85	0.00	.027	- 49.275	HIGH	9/12	1832	4.5	3
.362	.3853	1.259	.0402	.0981	0.90	0.00	.030	- 87.179	HIGH	9/12	1832	6.0	4
.245	.3850	1.263	.0419	.1157	1.00	0.06	.030	- 72.340	HIGH	9/12	1832	7.5	5
- .098	.3840	1.400	.0384	.1727	1.05	0.28	.027	- 45.946	HIGH	9/12	1832	9.0	6
- .144	.3830	1.323	.0437	.1835	1.00	0.32	.026	- 42.500	HIGH	9/12	1832	10.5	7
- .833	.3821	1.194	.0612	.1477	0.90	0.28	.028	- 53.125	HIGH	9/12	1832	12.0	8
.000	.3835	2.413	.0384	.0630	1.15	0.40	.022	- 1.025	HIGH	9/13	0656	0.0	0
.195	.3837	2.469	.0367	.0105	1.25	0.00	.020	- 0.913	HIGH	9/13	0656	1.5	1
.139	.3840	2.154	.0349	.0000	1.45	0.00	.022	- 1.312	HIGH	9/13	0656	3.0	2
.114	.3841	1.606	.0454	.0000	1.45	0.00	.022	- 3.020	HIGH	9/13	0656	4.5	3
.000	.3843	1.104	.0507	.0000	1.10	0.00	.022	- 8.824	HIGH	9/13	0656	6.0	4
- .090	.3844	0.914	.0489	.0000	0.85	0.00	.024	- 13.636	HIGH	9/13	0656	7.5	5
- .068	.3846	1.167	.0454	.0000	0.75	0.00	.028	- 6.081	HIGH	9/13	0656	9.0	6
- .110	.3846	1.452	.0437	.0070	0.80	0.00	.031	- 3.020	HIGH	9/13	0656	10.5	7
- 1.054	.3847	1.639	.0540	.0105	0.80	0.54	.030	- 2.195	HIGH	9/13	0656	12.0	8
.000	.3841	1.569	.0734	.0699	0.75	0.32	.022	- 10.902	HIGH	9/13	1930	0.0	0
.110	.3843	1.969	.0630	.0770	0.75	0.00	.022	- 5.800	HIGH	9/13	1930	1.5	1
.102	.3844	2.063	.0489	.0805	1.10	0.00	.022	- 5.052	HIGH	9/13	1930	3.0	2
.093	.3845	1.625	.0402	.0875	1.60	0.00	.026	- 10.284	HIGH	9/13	1930	4.5	3
.638	.3845	1.156	.0384	.0910	1.95	0.00	.029	- 28.431	HIGH	9/13	1930	6.0	4
- .071	.3844	0.921	.0367	.0981	2.05	0.00	.032	- 60.417	HIGH	9/13	1930	7.5	5
- .065	.3841	1.079	.0367	.1052	1.85	0.00	.027	- 37.179	HIGH	9/13	1930	9.0	6
- .126	.3836	1.619	.0384	.1052	1.45	0.00	.023	- 10.902	HIGH	9/13	1930	10.5	7
- 1.309	.3835	2.286	.0384	.0840	1.15	0.32	.022	- 3.887	HIGH	9/13	1930	12.0	8

$\bar{H}_b / n\bar{T}_b$	ρ_s / ρ_s	\bar{H}_b / \bar{D}	$\tan \bar{m}$	$\tan \bar{a}_b$	\bar{H}_b / \bar{z}	u/d	h/d	$\Delta Q_f / \bar{H}_b^3$	Tide cycle ends on	End of cycle		Lag in hours from end of cycle	Lag #
										water	Date		
.000	.3839	1.610	.0857	.2568	0.95	0.17	.046	- 14.184	HIGH	9/14	0754	0.0	0
.146	.3841	1.545	.0630	.2309	0.90	0.16	.034	- 15.038	HIGH	9/14	0754	1.5	1
.097	.3847	1.471	.0349	.1944	1.00	0.12	.022	- 16.000	HIGH	9/14	0754	3.0	2
.106	.3852	1.326	.0279	.1584	1.35	0.00	.022	- 20.619	HIGH	9/14	0754	4.5	3
- .823	.3855	1.200	.0314	.1192	1.80	0.00	.026	- 27.027	HIGH	9/14	0754	6.0	4
- .122	.3854	1.102	.0367	.0840	1.95	0.00	.030	- 36.364	HIGH	9/14	0754	7.5	5
- .057	.3849	1.029	.0507	.0699	1.70	0.00	.029	- 46.512	HIGH	9/14	0754	9.0	6
- .089	.3846	1.104	.0664	.0699	1.25	0.00	.024	- 39.216	HIGH	9/14	0754	10.5	7
- .462	.3841	1.455	.0752	.0699	0.85	0.30	.022	- 18.018	HIGH	9/14	0754	12.0	8
.000	.3823	1.829	.0963	.1620	1.10	0.14	.024	- 4.084	HIGH	9/14	2038	0.0	0
.128	.3827	1.803	.0752	.1763	1.30	0.00	.023	- 4.084	HIGH	9/14	2038	1.5	1
.071	.3834	1.549	.0454	.1691	1.25	0.00	.022	- 10.241	HIGH	9/14	2038	3.0	2
.067	.3840	1.268	.0297	.1620	1.15	0.00	.021	- 18.681	HIGH	9/14	2038	4.5	3
.259	.3845	1.183	.0279	.1512	1.35	0.00	.023	- 22.973	HIGH	9/14	2038	6.0	4
- .099	.3843	1.114	.0332	.1477	2.10	0.00	.024	- 28.814	HIGH	9/14	2038	7.5	5
- .074	.3840	1.118	.0454	.1691	2.50	0.00	.034	- 30.909	HIGH	9/14	2038	9.0	6
- .072	.3839	1.354	.0717	.2272	1.65	0.00	.046	- 18.681	HIGH	9/14	2038	10.5	7
- .278	.3838	1.548	.0857	.2568	1.00	0.00	.048	- 13.600	HIGH	9/14	2038	12.0	8
.000	.3859	2.507	.0244	.1263	1.10	0.16	.006	1.096	HIGH	9/15	0850	0.0	0
.119	.3860	2.627	.0349	.1441	1.25	0.00	.009	0.954	HIGH	9/15	0850	1.5	1
.091	.3862	2.344	.0437	.1477	1.50	0.00	.019	1.318	HIGH	9/15	0850	3.0	2
.110	.3861	1.899	.0454	.1477	1.65	0.00	.028	2.481	HIGH	9/15	0850	4.5	3
- .885	.3855	1.353	.0349	.1477	1.50	0.00	.027	6.701	HIGH	9/15	0850	6.0	4
- .077	.3849	0.991	.0349	.1441	1.20	0.00	.027	16.667	HIGH	9/15	0850	7.5	5
- .053	.3839	0.922	.0472	.1405	0.85	0.00	.027	19.697	HIGH	9/15	0850	9.0	6
- .079	.3829	1.429	.0682	.1512	0.85	0.00	.027	5.200	HIGH	9/15	0850	10.5	7
- .875	.3824	1.800	.0928	.1584	1.00	0.00	.025	2.600	HIGH	9/15	0850	12.0	8
.000	.3862	1.351	.0822	.0349	1.00	0.00	.024	2.128	HIGH	9/15	2136	0.0	0
.121	.3859	1.205	.0752	.0910	0.85	0.00	.024	2.885	HIGH	9/15	2136	1.5	1
.062	.3855	1.050	.0664	.1052	0.85	0.00	.023	4.054	HIGH	9/15	2136	3.0	2
.050	.3848	0.938	.0594	.1122	0.90	0.00	.023	5.455	HIGH	9/15	2136	4.5	3
.134	.3845	0.934	.0507	.1122	0.95	0.00	.023	5.455	HIGH	9/15	2136	6.0	4
- .129	.3847	0.988	.0419	.0875	0.95	0.00	.019	4.688	HIGH	9/15	2136	7.5	5
- .070	.3851	1.221	.0349	.0840	0.95	0.00	.018	2.885	HIGH	9/15	2136	9.0	6
- .079	.3856	1.667	.0244	.0981	1.00	0.00	.012	1.389	HIGH	9/15	2136	10.5	7
- .162	.3859	2.265	.0210	.1157	1.00	0.14	.016	0.656	HIGH	9/15	2136	12.0	8
.000	.3845	2.111	.1263	.1980	0.95	0.54	-.999	- 8.314	HIGH	9/16	0940	0.0	0
.173	.3845	2.141	.0998	.2126	1.40	0.18	-.008	- 8.314	HIGH	9/16	0940	1.5	1
.110	.3847	1.930	.0717	.2126	1.65	0.00	-.002	- 12.718	HIGH	9/16	0940	3.0	2
.140	.3847	1.592	.0419	.2199	1.60	0.00	.012	- 24.497	HIGH	9/16	0940	4.5	3
- 1.000	.3850	1.415	.0279	.2272	1.25	0.00	.023	- 37.629	HIGH	9/16	0940	6.0	4
- .068	.3852	1.364	.0454	.2493	1.30	0.00	.024	- 40.110	HIGH	9/16	0940	7.5	5
- .078	.3856	1.429	.0647	.2382	1.25	0.00	.028	- 29.200	HIGH	9/16	0940	9.0	6
- .164	.3860	1.459	.0787	.1052	1.25	0.00	.028	- 23.248	HIGH	9/16	0940	10.5	7
2.653	.3862	1.368	.0822	.0279	1.00	0.00	.026	- 25.887	HIGH	9/16	0940	12.0	8
.000	.3859	1.559	.0262	.0875	0.75	0.00	.020	8.205	HIGH	9/16	2212	0.0	0
.086	.3855	1.556	.0489	.0910	0.75	0.06	.016	9.091	HIGH	9/16	2212	1.5	1
.075	.3851	1.499	.0454	.0981	0.90	0.00	.012	11.348	HIGH	9/16	2212	3.0	2
.136	.3849	1.353	.0332	.1086	1.55	0.00	.013	16.495	HIGH	9/16	2212	4.5	3
.000	.3847	1.313	.0210	.1192	2.75	0.00	.018	18.824	HIGH	9/16	2212	6.0	4
- .104	.3847	1.294	.0175	.1334	2.75	0.00	.010	18.824	HIGH	9/16	2212	7.5	5
- .083	.3847	1.343	.0192	.1477	1.60	0.00	-.002	15.385	HIGH	9/16	2212	9.0	6
- .163	.3847	1.639	.0542	.1691	0.75	0.05	-.005	7.805	HIGH	9/16	2212	10.5	7
- 1.404	.3846	2.028	.1192	.1835	0.85	0.52	-.999	4.113	HIGH	9/16	2212	12.0	8

$\bar{H}_b / n\bar{T}_b$	ρ_l / ρ_s	\bar{H}_b / \bar{D}	$\tan \bar{m}$	$\tan \bar{\alpha}_b$	\bar{H}_b / \bar{z}	u/d	h/d	$\Delta Q_f / \bar{H}_b^3$	Tide cycle ends on water	End of cycle		Lag in hours from end of cycle	Lag #
										Date	Hours		
.000	.3843	1.821	.0367	.0664	0.00	0.22	.002	14.286	HIGH	9/17	1048	0.0	0
.201	.3840	1.833	.0297	.0279	0.00	0.13	.005	11.446	HIGH	9/17	1048	1.5	1
.091	.3843	1.844	.0279	.0279	0.65	0.00	.008	9.268	HIGH	9/17	1048	3.0	2
.114	.3848	1.791	.0279	.0349	0.65	0.00	.010	8.796	HIGH	9/17	1048	4.5	3
.909	.3853	1.714	.0297	.0542	0.65	0.00	.012	8.796	HIGH	9/17	1048	6.0	4
- .227	.3857	1.667	.0314	.0630	0.65	0.00	.013	8.796	HIGH	9/17	1048	7.5	5
- .077	.3861	1.622	.0314	.0734	0.75	0.00	.015	8.796	HIGH	9/17	1048	9.0	6
- .090	.3861	1.622	.0297	.0805	0.75	0.00	.017	8.796	HIGH	9/17	1048	10.5	7
- .279	.3859	1.568	.0262	.0840	0.75	0.00	.020	9.744	HIGH	9/17	1048	12.0	8

Empirical Equation for Longshore Current Velocity¹

W. HARRISON

ESSA Research Laboratories, Norfolk, Virginia 23510

Ninety-eight observations of longshore current velocity, beach slope, and the breaker height, period, angle, crest length, and trough depth were made on an Atlantic ocean beach. Precision inshore surveys during the observation period revealed an essentially plane beach with an offshore bar parallel to the shoreline during two-thirds of the study period. Analysis of replicate measurements of current velocity revealed no topographically-induced non-"uniformity" in the current and suggested that an individual determination of velocity was within about ± 10 percent of the true velocity value.

A linear multi-regression analysis performed on the data resulted in the following empirical correlation, for the four strongest independent variables:

$$\bar{V} = -0.170455 + 0.037376 (\bar{\alpha}_b) + 0.031801 (\bar{T}_b) + 0.241176 (H_{b_s}) + 0.030923 (\bar{m})$$

where \bar{V} is in meters per second, $\bar{\alpha}_b$ is the mean acute angle between the breaker front and the shoreline in degrees, \bar{T}_b is in seconds, H_{b_s} is the significant breaker height in meters, and \bar{m} is the mean beach slope in degrees. The total reduction of variance R^2 for $\bar{\alpha}_b$ is 0.46 and for $\bar{\alpha}_b$ plus \bar{T}_b it is 0.53; H_{b_s} and \bar{m} each add 0.02 to successive values of R^2 . The similarity between this equation and that obtained by Sonu et al. (1967), who used similar variables and analytical techniques, suggests that a general equation of this type may be valid for many Atlantic beaches. The present equation may be applied to values of H_{b_s} , \bar{T}_b , and \bar{m} falling within certain specified ranges, when $\bar{\alpha}_b$ falls between about 2.0° and 15.0°.

INTRODUCTION

As pointed out by Galvin [1967, p. 287], 'reliable data on longshore currents are lacking over a significant range of possible flows.' An attempt to remedy this situation was made [Harrison et al., 1968] at Virginia Beach, Virginia, in August and September of 1966. Ninety-eight observations of longshore current velocity and related variables were made before, during, and after the passage of wave trains from hurricane Faith and a moderate 'northeaster.'

The data for the 1966 field study were subjected to linear multiregression analysis in order to assess the relative importance of the following independent variables in determining longshore current velocity: breaker angle, period, height, crest length and trough depth, and the beach slope. Results of the correlation analyses are quite unlike those of the author's earlier studies [Harrison and Krumbein, 1964; Harrison et al., 1965] that used offshore wave data, but they are quite similar to the results of Sonu

et al. [1967] in which shallow-water and breaking-wave data at Nags Head, North Carolina, were used. Inasmuch as a major goal of previous longshore current studies has been to develop a method for prediction of the velocity of the longshore current, a prediction equation for the data is presented here for testing in future studies.

DATA

The variables (Figure 1) used in this study are listed in Table 1, together with their observed ranges and probable errors. A complete listing of all the measurements and details of the measurement techniques can be found in Harrison et al. [1968], together with nine charts of the inshore bottom topography. The charts, based on three precision (± 0.03 meter of water depth) transects in a square 250 meters on a side, indicate a roughly plane beach for about one-third of the longshore current observations and a bar-trough topography generally parallel to the shoreline for the remainder of the observations. No radical changes in the alignment of the bar-trough topography parallel to the shoreline were observed during the 26-day-long study

¹ Contribution 15 of the Land and Sea Interaction Laboratory (LASIL) Atlantic Oceanographic Laboratories, ESSA, Norfolk, Virginia 23510.

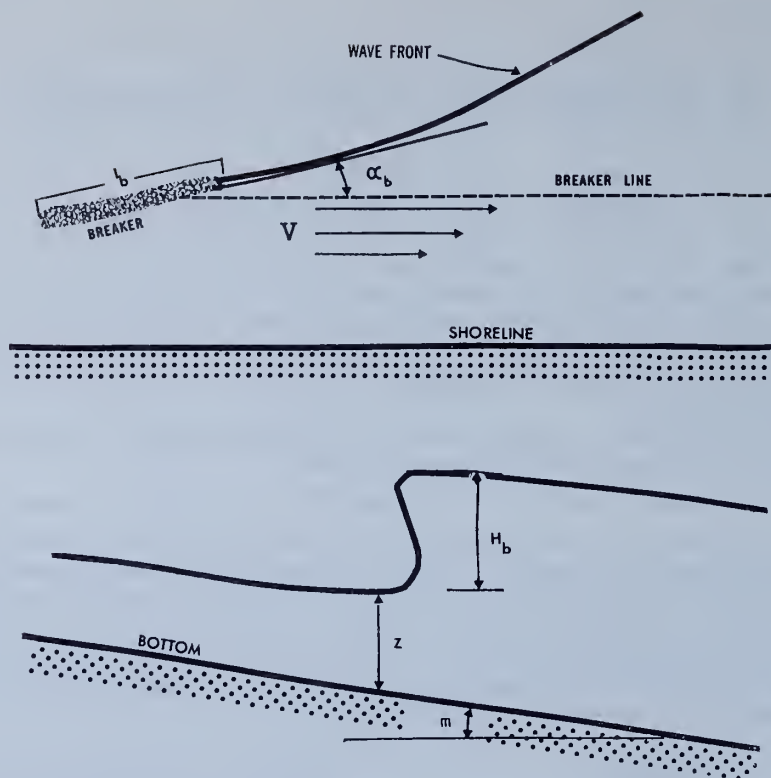


Fig. 1. Definition of variables.

period, nor was even one rip current observed anywhere in the study area.

The current velocity was measured by timing the movement of the centers of patches of fluorescent dye as they moved parallel to shore in or close to the zone of maximum flow. Three dye patches were timed by stopwatch over a

15- or 30-meter course, depending on the prevailing velocity of flow. A mean travel time was determined for the three satisfactory trials. Nearly all the dye charges were introduced at the inshore margin of the breaker line closest to shore. The center of each dye patch had to remain coherent for a given trial to be judged

TABLE 1. Variables Screened in Development of Empirical Predictor Equations

Symbol	Description	Range in Values	Probable Error
\bar{H}_b	Mean height of breaking waves	0.15-0.89 m	± 0.06 m, low waves; ± 0.12 m, high waves
H_{b_s}	Height of significant breaking waves	0.21-1.22 m	± 0.06 m, low waves; ± 0.12 m, high waves
\bar{l}_b	Mean crest length of breaking waves	10.0-235.0 m	Within 10%, at best
\bar{m}	Mean slope of foreshore	0.70° - 5.80°	$\pm 0.2^\circ$
\bar{T}_b	Mean period of breaking waves	4.0-12.8 sec	± 0.2 sec
\bar{V}	Mean longshore current velocity	0.17-1.14 m/sec	± 0.06 m/sec
\bar{z}	Mean trough to bottom distance in front of a breaking wave	0.07-0.98 m	± 0.005 m
$\bar{\alpha}_b$	Mean acute angle between shoreline and crest of breaking wave	1.00° - 16.6°	± 1.0 - 2.0° , for a given breaker

satisfactory. Where more than one breaker line was present, the flow in the current zone most inshore may have been influenced by the flow of the longshore current in the next closest offshore zone.

Breaker heights and periods were measured in nearly all cases by an observer standing in the breakers and a recorder near the breakers. The heights of fifty successive breaking waves were measured against a wave staff, and the mean breaker period was calculated using the elapsed time required to measure the fifty waves.

The slope of the lower foreshore was determined from profiles drawn at a 1:1 scale. Profile data were based on measurements of the elevation of the beach surface made every 4 hours. The measurements were referenced to a MSL datum plane painted on permanent, 1/2-inch steel reference rods.

The trough-to-bottom distance, z , in front of a breaking wave was measured because it is a reasonable estimate of the amount of water in the longshore current zone. Also, some investigators have noted a direct correlation between V and the volume of water in the surf zone.

Three to eight determinations of the acute angle α_b between the shoreline and the crest of a breaking wave were made just before or just after determination of \bar{V} using a tripod-mounted azimuthal circle equipped with sights. The tripod was set up as close to the inshore margin of the breaker zone as possible, and values of α_b were measured to the nearest degree. For the first half of the study period, a base line parallel to the shoreline was estimated by eye. For the other half of the study period, the center of the tripod was lined up with two steel rods previously positioned on a base line determined to be 'parallel to the shoreline.' Such positioning of the tripod reduced observer variability, as far as determination of the bearing of one side of angle α_b was concerned. The bearing of the other side of α_b was determined by sighting down the crests of breaking waves at some distance (50–500 meters) from the tripod. Because of the straightness of the shoreline in the study area and the lack of significant beach rhythms during the study period, the value obtained for an individual α_b is thought to be valid to ± 1 or 2 degrees. The range for several mean values of α_b was variable, depending on the nature of the deep-water wave trains causing the breakers.

The minimum and maximum crest length, l , of breaking waves was estimated visually by comparison with a measured base line on shore. Crest length was estimated because $l \times H_b$ is a measure of the amount of water that enters the longshore current zone per unit time. For a given α_b and constant H_b and T_b , the greater is the crest length the more water that enters the longshore current zone and is available for driving the current. At times, considerable variability was noted in crest length, and the 'mean crest length' values were but crude estimates. The significance of \bar{l} under such circumstances is open to question. For a number of longshore current measurements, during a period of high \bar{V} , high \bar{H}_b , and high l (≈ 400 meters), the mean crest length values were probably valid to within 10%.

Wind velocity in the along-shore direction was one of the variables used in previous studies by *Harrison and Krumbein* [1964] and by *Sonu et al.* [1967], but it exhibited only weak correlations with \bar{V} . Also, local wind was not employed in the present data set because, throughout the 26-day sampling period, winds were generally light and variable (*Harrison et al.* [1968], maximum speed: 11m/sec for 2 hours in direction of current).

CURRENT 'UNIFORMITY' AND ESTIMATING V

An evaluation of the 'uniformity' of the long shore current was obtained from data [*Harrison et al.*, 1968, Table 4] collected at the study site by C. J. Galvin (as part of an investigation by the U.S. Army Coastal Engineering Research Center) on the nineteenth day of the 26-day study. For 7 hours Galvin timed the movement of balloons filled with fresh water or dye patches over a 61.0-meter course. The upcurrent end of Galvin's measuring course overlapped, by a few meters, the course used by the author for measurements of \bar{V} . The 61.0-meter course was divided into two 30.5-meter lengths, and the upcurrent length was further divided into two 15.3-meter lengths. The differences in measured velocities between the first and second 15.3-meter distances (DEL V1, Table 2) and between the first and second 30.5-meter distances (DEL V2) were subjected to a null-hypothesis test, using the Student's t distribution [*Snedecor*, 1965, pp. 45,56]. The results of this test (Table 2), which used time-successive velocity pairs, indicated that there was no statistical reason to reject the hypothesis that the velocities in the first and second

TABLE 2. Results of Null Test

DEL V1	N=47	t = 1.458	P=0.16	Null hypothesis not rejected
DEL V2	N=32	t = -0.661	P>0.50	Null hypothesis not rejected

15.3-meter distances or in the first and second 30.5-meter distances were the same at the 95% level of confidence. According to normal statistical usage, the null hypothesis cannot be rejected unless the 95% level is exceeded ($P \leq 0.05$ [Snedecor, 1965, Table 2.7.1]). Thus, there is no statistical basis for assuming that the currents in different segments of the 61.0-meter course had significantly different velocities. Assuming that this statistical inference is valid, one could postulate 'uniformity,' of a sort, for the flow over the 61.0-meter distance. This is significant in view of the slightly undulatory nature of the inshore bottom contours [Harrison *et al.*, 1968, Figure G] during this 7-hour measurement period.

Differences in measured velocities between adjacent 15.3-meter or 30.5-meter segments, then, may be largely due to the varying position of the flow indicator (dye patch, balloon, etc.) relative to the mean streamlines of flow as the indicator moves across the two measurement courses. Cross-stream velocity variation is significant in a longshore current, and visual selection of the center of a dye patch can be rather subjective. Turbulence in the flow may cause movement of a flow indicator back and forth across the mean streamlines as the indicator moves from the beginning of one segment to the end of the next. This motion of the velocity indicators along path lines that cut the mean streamlines leads to an *estimate* of V , rather than a measurement of V in the strict sense. It is largely for this reason that a mean of several samples of V , along a fixed course, is more meaningful than a single sample (or 'measurement').

An evaluation of the magnitude of the estimate of V , afforded by timing the speed of an indicator, was obtained by comparing the mean value for the velocity over the 61.0-meter distance with the mean of the deviations in velocity between the two 30.5-meter distances. The mean of the deviations in velocity between the two 30.5-meter lengths was equal to 20% of the mean velocity over the entire 61.0-meter length.

Because the deviations between the two 30.5-meter lengths were both positive and negative, one may assume that an individual determination of V is generally within $\pm 10\%$ of the true V , under similar conditions. It is probably valid to apply such a value over the entire 26-day period because the bottom topography was no more complex on days other than the day of Galvin's measurements, and his velocities were close to the average of the velocities measured in this study.

METHODS OF ANALYSIS

The procedure adopted for selecting predictors involves expressing \bar{V} as a linear function of a number of variables (predictors) X_n ($n = 1, \dots, N$).

Thus

$$\bar{V} = A_0 + A_1X_1 + A_2X_2 + \dots + A_nX_n + \dots + A_NX_N$$

where the coefficients A_n ($n = 0, \dots, N$) are determined by the method of least squares.

One limitation of the linear analysis is that some variables that have only a small linear effect may become quite strong in a model that explicitly includes nonlinear effects. It is also true, however, that the linear model is generally the best one for initial work with many variables.

The 'screening procedure' [cf. Miller, 1958] was used for the multiregression analysis of this study. Basically, the technique is shown below.

$$\bar{V} = A_1 + B_1X_1 \quad (1)$$

$$\bar{V} = A_2 + B_2X_1 + C_1X_2 \quad (2)$$

$$\bar{V} = A_n + B_nX_1 + C_{n-1}X_2, \dots, NX_n \quad (3)$$

where A is constant and B_1, B_2, C_1, C_2 , etc., are regression coefficients.

The procedure is first to select the best single predictor (X_1) for regression equation 1. The second regression equation (2) contains X_1 and X_2 , which contributes most to reducing the residual after X_1 is considered. This is usually, but not always, the best subset of X_i from the original set. In the somewhat analogous field of meteorology, however, studies have shown that by this screening procedure a highly reliable set of predictors can be selected. Sonu *et al.* [1967, p. 533] attempted both linear and nonlinear re-

gression techniques on a very similar set of data and concluded that 'the nonlinear regression of a product form does not necessarily improve the level of the correlation.'

RELATIONSHIP SCREENED

The following formulation was screened: $\bar{V} = f(\bar{H}_b, H_{bs}, \bar{T}_b, \bar{m}, l/\bar{H}_b, \bar{H}_b/\bar{z}, \bar{H}_{bs}/\bar{z}, \bar{\alpha}_b)$ (4)

It is recognized that certain of the correlations, such as those involving \bar{H}_b , l/\bar{H}_b , and \bar{H}_b/\bar{z} could be spurious cf. *Benson*, 1965], owing to the commonality of the variable \bar{H}_b . It is hoped that the X_i with variables in common will not be selected, in the first screening run, before one each of the following X_i are chosen: (1) a breaker height, (2) a breaker period, (3) a beach slope, and (4) a wave direction. The prime dependence of \bar{V} on these four variables is mentioned by *Galvin* [1967, p. 288]. If predictors with variables in common are chosen in the first run, a decision will have to be made as to which of them must be excluded from the next screening run.

Results of the first screening run (Table 3) indicate the prime dependence of \bar{V} on breaker angle. A much lesser dependency of \bar{V} on the breaker period is noted, and relatively minor contributions of the significant breaker height and the beach slope are seen.

These results compare well with the results reported by *Sonu et al.* [1967], who made a linear multiregression analysis of similarly defined variables from an area of slightly complicated near-shore topography at Nags Head, North Carolina. *Sonu et al.* found the wave angle to be the strongest predictor by far, followed by wind velocity in the along-shore direction, wave height, bottom slope, and wave period. The results of Table 3 are

TABLE 3. Predictors Selected by Screening Process ($N = 98$)

Equation	Variables	R^{2*}
1	$\bar{\alpha}_b$	0.46
2	$\bar{\alpha}_b, \bar{T}_b$	0.53
3	$\bar{\alpha}_b, \bar{T}_b, H_{bs}$	0.55
4	$\bar{\alpha}_b, \bar{T}_b, H_{bs}, \bar{m}$	0.57

* R^2 is the percentage of total variance of the predict and \bar{V} explained by the X_i , or predictors. See *Harrison and Pore* [1967, p. 44] for additional explanation.

quite different from those obtained by *Harrison et al.* [1965], who screened offshore wave data, and it is now doubtful [cf. *Galvin*, 1967, p. 299] that empirical equations involving offshore wave data can have predictive value.

The prediction equation (5) for the variables in Table 3 indicates that all the X_i are positively correlated with \bar{V} . The equation is

$$\begin{aligned} \bar{V} = & -0.170455 \\ & + 0.037376(\bar{\alpha}_b) + 0.031801(\bar{T}_b) \\ & + 0.241176(H_{bs}) + 0.030923(\bar{m}) \end{aligned} \quad (5)$$

Figure 2 shows a plot of observed versus predicted values for equation 5, using the data from which the equation was derived.

Equation 6, [*Sonu et al.*, 1967, Table 2] is presented for comparison with equation 5.

$$\begin{aligned} \bar{V} = & -1.39 + 0.06(\bar{\alpha}_b) - 0.01(\bar{T}_b) \\ & + 0.20(\bar{H}_b) + 0.14(\bar{m}) + 0.05(W) \end{aligned} \quad (6)$$

where \bar{V} is in feet per second, $\bar{\alpha}_b$ in degrees, \bar{T}_b in seconds, \bar{H}_b in feet, \bar{m} in per cent slope, and W is in miles per hour. The ordering of the first four variables and the magnitudes of the constant and coefficients (when converted to the metric system) are similar to those of equation 5. Only the role of wave period, which is negative in equation 6, is significantly different in the two equations. Students of longshore currents are about equally divided [cf. *Sonu, et al.*, 1967, Table 1] on the sign of the wave period in their equations for \bar{V} .

EQUATION TESTING

It is impossible to test equation 5 as adequately as might be desired with the published data [cf. *Galvin and Nelson*, 1967] of other field studies. Published data do not cover the entire range covered by the data of this study, and differences in the definition of some of the variables and (or) imprecision in the techniques used for measurement complicate unnecessarily the interpretation of 'test' results. A few data from *Galvin and Nelson's* [1967] compilation will be subjected to equation 5, however.

The data of *Putnam et al.* [1949] are plotted in Figure 2. Analysis of the cluster of data points above the perfect prediction line suggests that, when wave angles are moderate (5° - 15°) but values for \bar{T}_b , \bar{m} , and H_{bs} are large, the predicted longshore current velocity tends to be greater

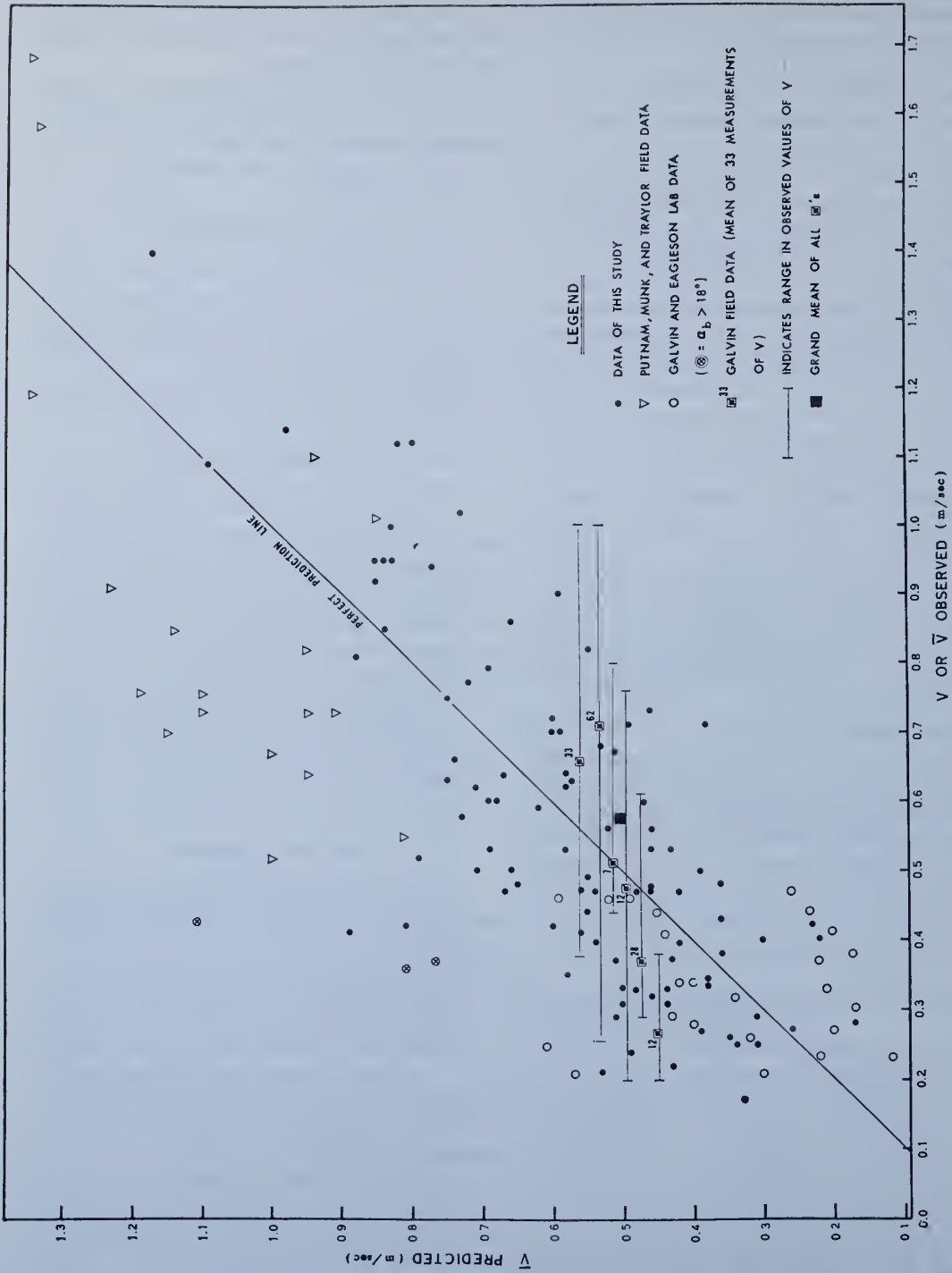


Fig. 2. Predicted versus observed values for mean longshore current velocity, using equation 5, and results of the application of equation 5 to the field data of Putnam et al. [1949] and the laboratory data of Galvin and Eagleson [1965].

than the observed. Such an interpretation assumes that the breaker heights and periods from Putman et al. were exactly what they measured from the beach, and that the beach slopes they determined from 'soundings . . . taken along the pier' were valid at the locations where current velocities were measured. Further, some of their observations of V were made using a weighted plywood cross equipped with a flotation can. The inertia of such a device might lead to smaller 'observed' velocities than equation 5 would predict.

If equation 5 is to be tested adequately, it should be applied initially to data gathered in a similar environment and to data for variables defined and measured in a manner similar to that of this study. The unpublished data of *Sonu et al.* [1967], for example, would probably be suitable for testing with equation 5, although measurements of \bar{V} were gathered in the vicinity of a fishing pier and H_b was 'visually observed over the inner bar.'

Figure 2 shows the application of equation 5 to Galvin's set of independent observations of V at Virginia Beach. These observations permit 'testing' of equation 5 over a limited range of synchronous data. All Galvin's 15.3-meter values [*Harrison et al.*, 1968, Table 4], plus all his second 30.5-meter values, were used in computing the V values of Figure 2. In all cases but one, the perfect prediction line falls within the ranges in the observed V values during the several measurement intervals. The values of V vary from the perfect prediction by 0.00 to 0.18 m/sec, with a mean variance of 0.10 m/sec. Many more observations of \bar{V} , covering a much wider range of conditions, will have to be tested in the fashion shown by Galvin's field data (Figure 2) before a reliable assessment of the predictive value of equation 5 can be obtained. If after such testing the equation is judged reliable, it may serve as a useful empirical guide for velocity predictions in similar beach environments, in the absence of a proven theory.

The laboratory data of *Galvin and Eagleson's* [1965] study, as listed in *Galvin and Nelson* [1967, Table 4], were subjected to equation 5 and are plotted in Figure 2. The three plots (Figure 2) at widest variance from the perfect prediction line are for values of α_b greater than 18° . Analysis of the cluster of laboratory plots below the perfect prediction line reveals that, in general, observed

values of V are higher than predicted values when α_b is less than 5° . To what extent these discrepancies result from the inability of laboratory experiments to simulate nature is not known, but, if the experiments simulated nature perfectly, equation 5 would apply only when α_b ranged between about 5° and 15° .

CONCLUDING DISCUSSION

The most significant result of this study is probably the relative importance of the four independent variables. As in the study of *Sonu et al.* [1967], angle of breaker incidence is by far the most important variable influencing current velocity. The linear multiregression analysis by *Sonu et al.* of the field and laboratory data of *Putnam et al.* [1949] also showed the same result. (The R^2 values of *Sonu et al.* [1967, p. 529, and Table 3] are misleadingly high for the field data because of the few observations in comparison to the number of X_i [cf. *Harrison and Pore*, 1967, p. 49, Figure 19].)

A secondary, but nevertheless important result of this investigation, is the appearance of a linear multiregression equation similar in kind to that derived from the field investigation reported by *Sonu et al.* It is possible, therefore, that this type of regression equation will find wider application than might originally have been thought. This is of importance in view of *Galvin's* [1967, p. 303] conclusion that 'at present the best approach to a meaningful prediction of longshore current velocity is through empirical correlation of reliable data.' Assuming then, that a multiregression equation such as (5) is worthy of additional testing or refinement, what restraints should be placed on its initial application to natural data?

Sonu et al. felt that α_b was of such overriding importance that the other variables in their empirical correlation could be ignored. Unfortunately, their one-predictor equation [*Sonu et al.*, 1967, p. 529] does not yield a positive V until α_b is greater than about 3° . Equation 5, on the other hand, yields a positive V when α_b is zero. The magnitude of \bar{V} (when $\alpha_b = 0$) varies from a minimal one $\bar{V} = 0.02$ m/sec for small values of \bar{T}_b (3.0 sec), \bar{m} (1°), and H_{b_0} (0.3 meter), to an improbably large one ($\bar{V} = 0.78$ m/sec) for high values of \bar{T}_b (10.0 sec), \bar{m} (5°), and H_{b_0} (2.0 meters). Thus, although α_b may be expected to be the most important variable in determining V ,

the use of a given empirical equation like (5) or (6) must be governed by an understanding of the range in α_b over which the equation logically will apply.

Pending analysis [cf. *Harrison and Krumbein*, 1964, p. 27] of nonlinear relationships between \bar{V} and the X_i , and pending testing of equation 5 with data covering a side range in values of the variables, it would seem desirable to apply equation 5 only when H_{bs} , \bar{T}_b , and \bar{m} fall within the ranges given in Table 1, and only when α_b is between about 2.0° and 15.0° .

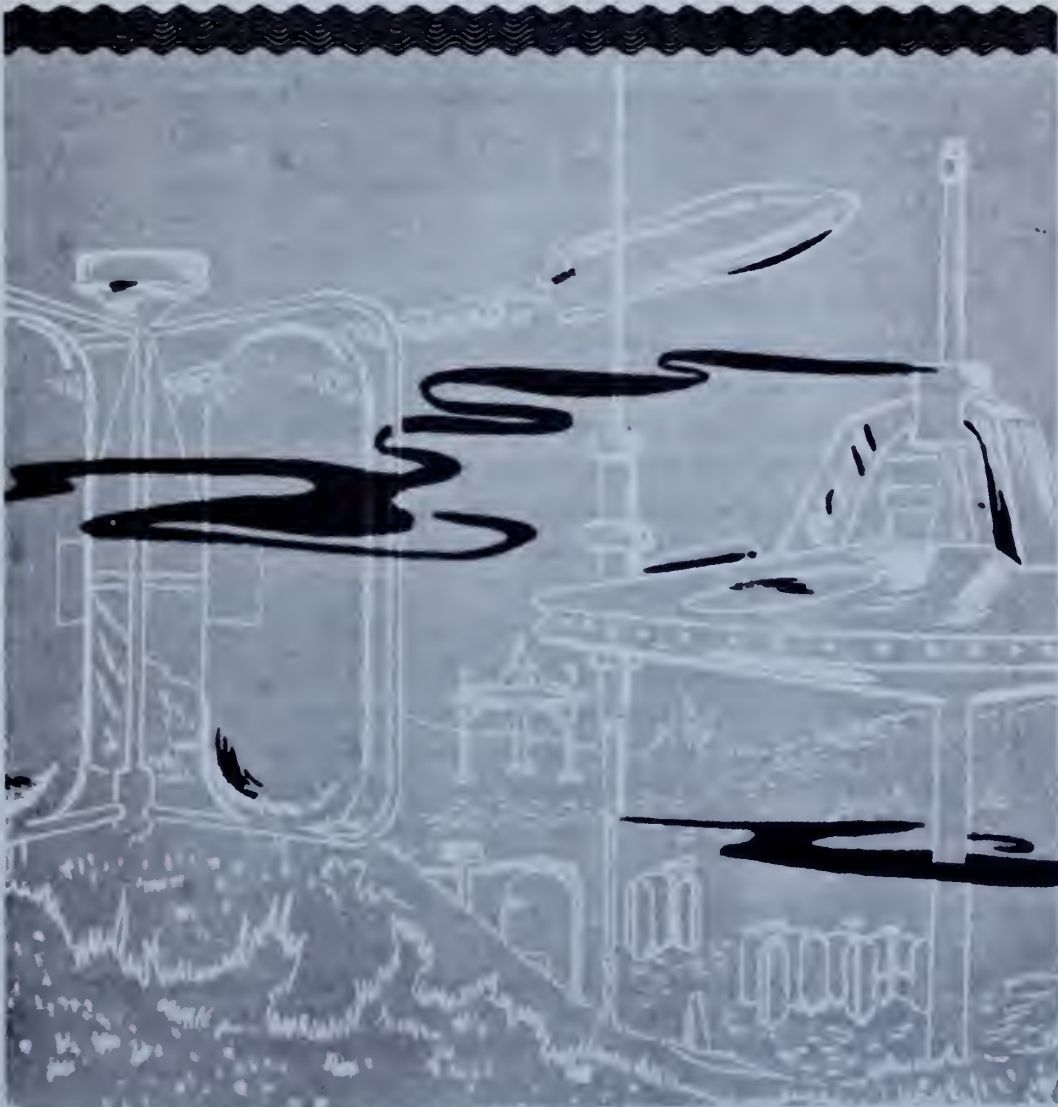
Acknowledgments. N. A. Pore, Weather Bureau ESSA, programmed the screening run. The U. S. Army Coastal Engineering Research Center supported C. J. Galvin and his assistants in the collection of data at Virginia Beach. I thank C. J. Galvin, R. J. Byrne, and C. J. Sonu for review of the manuscript.

REFERENCES

- Benson, M. A., Spurious correlation in hydraulics and hydrology, *J. Hydraulics Div., Am. Soc. Civ. Engrs.*, 91, 35-41, 1965.
- Galvin, C. J., Jr., Longshore current velocity: A review of theory and data, *Rev. Geophys.* 5(3), 287-304, 1967.
- Galvin, C. J., Jr., and P. S. Eagleson, Experimental study of longshore currents on a plane beach, *U. S. Army Corps Engrs., Coastal Eng. Res. Center Tech. Mem.*, 10, 1-80, 1965.
- Galvin, C. J., Jr., and R. A. Nelson, Compilation of longshore current data, *U. S. Army Corps Engrs., Coastal Eng. Res. Center Misc. Paper*, 2-67, 1-19, 1967.
- Harrison, W., and W. C. Krumbein, Interactions of the beach-ocean-atmosphere system at Virginia Beach, Virginia: *U. S. Army Corps Engrs., Coastal Eng. Res. Center Tech. Mem.*, 7, 1-102, 1964.
- Harrison, W., and N. A. Pore, An approach to correlation and prediction in the drift-runoff-wind system, in *Circulation of Continental Shelf Waters off the Chesapeake Bight, ESSA Admin. Prof. Paper*, 3, 1-82, 1967.
- Harrison, W., N. A. Pore, and D. R. Tuck, Jr., Predictor equations for beach processes and responses, *J. Geophys. Res.*, 70, 6103-6109, 1965.
- Harrison, W., E. W. Rayfield, J. D. Boon, III, G. Reynolds, J. B. Grant, and D. Tyler, A time series from the beach environment, *ESSA Res. Lab. Tech. Mem.*, AOL-1, 1-85, 1968.
- Miller, R. G., The screening procedure. Studies in statistical weather prediction, *Final Rept. Contract AF19(604)-1590*, 86-95, Travelers Weather Research Center, Hartford, Conn., 1958.
- Putnam, J. A., W. H. Munk, and M. A. Traylor, The prediction of longshore currents, *Trans. Am. Geophys. Union*, 30, 337-345, 1949.
- Snedecor, G. W., *Statistical Method*, Iowa State University Press, Ames, Iowa, 1965.
- Sonu, C. J., J. M. McCloy, and D. S. McArthur, Longshore currents and near-shore topographies, *Proceedings Tenth Conference on Coastal Engineering*, pp. 524-549, American Society of Civil Engineers, New York, 1967.

(Received March 11, 1968;
revised July 11, 1968.)

Reprinted from
PROCEEDINGS OF THE CONFERENCE ON
CIVIL ENGINEERING IN THE OCEANS
ASCE Conference
San Francisco, California
September 6-8, 1967



SHEAR STRENGTH AND OTHER PHYSICAL PROPERTIES
OF SEDIMENTS FROM SOME OCEAN BASINS

GEORGE H. KELLER

ABSTRACT

Measurement of mass physical properties such as wet density, shear strength, water content, and grain size have been made on a large number of sediment cores collected from the North Atlantic and North Pacific Ocean basins. These samples represent several types of deep-sea sediment as well as different depositional environments within the basins. Some degree of correlation is found between these properties and sediment type, currents, and local topography. Areas of the deep-sea floor consisting of "red clay" commonly display lower shear strengths and bulk densities than those areas blanketed by calcareous oozes. In the vicinity of the continental margins, the mass physical properties vary considerably as the sediment supply and depositional environment change. Sediments from carbonate environments or areas of relatively high relief normally have higher shear strengths. This investigation has led to a delineation of various portions of the sea floor on a basis of the mass physical properties and gives an indication of the range of these parameters for submarine sediments.

INSTITUTE FOR OCEANOGRAPHY - ESSA
MIAMI, FLORIDA

INTRODUCTION

Only in recent years has much attention been given to the mass physical or engineering properties of submarine sediments other than to those found in harbors and in relatively shallow coastal waters. Prior to 1950, when offshore petroleum exploration began to be important, very few data were obtained from beyond the breaker zone. Only in the past ten years have serious attempts been made to investigate the mass physical properties of deep-sea sediments. These studies have mainly been undertaken by marine geologists who, using the doctrine of Hutton, "the present is the key to the past", are trying to understand the depositional history of ancient marine deposits by studying the mass properties of recent deep-sea sediments.

Early studies by such investigators as Hamilton, 1959; Richards, 1961, 1962; and Moore, 1962 have provided the impetus for the increased interest more recently shown in this field of study by many marine geologists and civil engineers.

The marine geologist has gained a clearer understanding of several problems by adapting soil mechanics practices to submarine sediments. Studies of the consolidation characteristics of deep sea sediments (Hamilton, 1964) have been significant in contributing to a better understanding of the depositional history in the ocean basins since their formation. The requirements of various military programs for an increased knowledge of the sea-floor environment also has lead to a greater interest in the mass properties of submarine sediments (Hamilton, et.al., 1956; Smith, 1962; and Keller, 1964).

Many of the published studies on the mass physical properties of submarine sediments pertain to specific relationships such as sound velocity and porosity, density and depth, consolidation and depositional history (Hamilton, 1956; Igelman and Hamilton, 1963) or have discussed the mass properties of a local area (Moore and Shumway, 1959; Fisk and McClelland, 1959; Harrison, et al., 1964). Although only relatively few deep-sea sediment cores have been collected in the past ten years from the North Atlantic and North Pacific basins for the purpose of studying the mass physical properties (roughly 600 to 700 cores), it is possible to now gain some insight into the range of values we can expect to find in various parts of these basins.

This paper is an attempt to bring together all the available data, published and unpublished, pertaining to the variation of sediment type, shear strength, water content, and wet unit weight in the North Atlantic and North Pacific Ocean basins. This study is based on the data obtained from approximately 500 sediment cores (Atlantic 300, Pacific 200) the majority of which were collected and analyzed by the U. S. Naval Oceanographic Office, data published by Moore (1962) for the North Pacific and Fisk and McClelland (1959) for the Gulf of Mexico have been incorporated in this study.

Core samplers used to collect the sediments are those normally used by marine geologists and leave much to be desired in the way of providing "undisturbed samples". The coring techniques commonly used are similar to those described by the U. S. Hydrographic Office (1955, pp. 52-65). Deficiencies of these samplers have been pointed out and attempts made to improve the quality of samples (Richards

and Kellar, 1961). Cores used in this study vary in length from 12 inches to 20 feet with an average of about seven feet. After considering the size of the ocean basins and the relatively short lengths of the cores, it was decided to average the respective parameter values over the entire length of each core. This was done after critically evaluating the data and removing any values that were obviously in error as a result of the sampling or testing procedures. The data presented here should be considered as representing an average value for the upper few feet of the sea floor. Studies involving the variation of these properties with depth have been presented elsewhere (Richards, 1962; Harrison et.al, 1964; Moore, 1964) and will not be discussed.

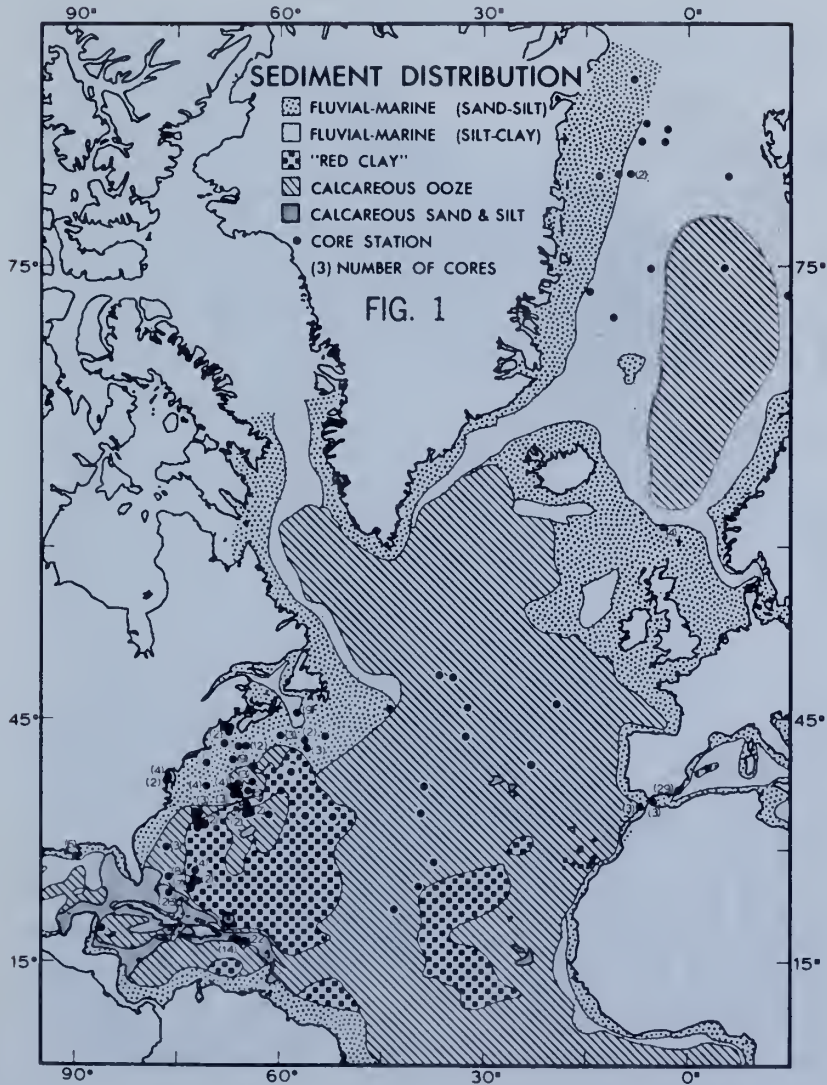
NORTH ATLANTIC AND NORTH PACIFIC BASINS

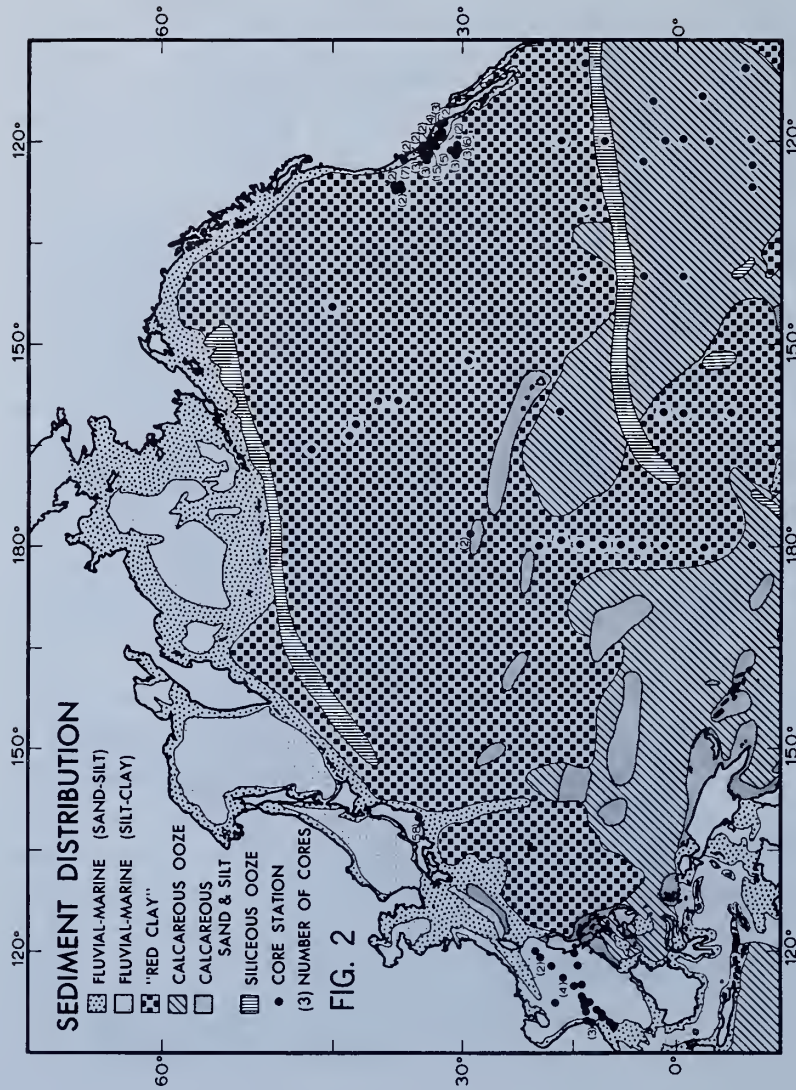
Although the North Atlantic and North Pacific Ocean basins are major ocean basins, the sea floor underlying these areas differ considerably from each other. The Atlantic is a much smaller basin (approximately half the area of the Pacific) and as such is influenced more by runoff from the surrounding land masses than is the Pacific. Bottom topography is notably different in the two basins. The Atlantic basin is more or less separated into east and west halves by the Mid-Atlantic Ridge with somewhat similar topography on either side of the ridge. On the other hand, the Pacific basin has numerous ridges, trenches, scarps, island chains and seamounts all of which play an important role in the deposition of the sediments. The mean depth of the Pacific is greater than that of the Atlantic which is also a factor influencing the sediment distribution. The significance of these differences as related to the mass physical properties is discussed below.

SEDIMENT TYPES

The sediment distribution shown in Figures 1 and 2 is based mainly on data obtained from the files of the U. S. Naval Oceanographic Office and supplemented by the work of Arrhenius (1963). For the purpose of this study the sediment types have been divided into six classes: (1) fluvial-marine (sand-silt) representing the coarser fraction (larger than 0.016 mm); (2) fluvial-marine (silt-clay) the finer fraction (smaller than 0.016 mm) of material derived from terrestrial drainage; (3) "red clay" is a term applied to inorganic pelagic clays which vary considerably in color, but are usually chocolate brown; (4) calcereous ooze is used here to define sediment composed of at least 30 percent calcium carbonate which is in the form of skeletal material from various planktonic animals and plants; (5) calcereous sand and silt consist of shell fragments and coralline debris of sand and silt-size particles; (6) siliceous oozes are deposits containing 30 percent or more of siliceous skeletal material derived from either diatoms or radiolarians.

Pelagic sediments of the North Pacific show several conspicuous differences from those of the North Atlantic basin (Figs. 1 and 2). The percentage of sea floor covered by "red clay" is at least four times that found in the North Atlantic. These deposits are indicative of very slow rates of deposition and frequently reflect the remoteness of land areas to the Pacific Ocean. Approximately 10 to 15 percent of the Pacific is at least 930 miles from the nearest land; such areas are almost absent from the Atlantic.





Lack of calcium carbonate deposits over a major part of the North Pacific sea floor may be attributed to various circumstances. The great depths in some areas result in the dissolution of the calcareous skeletons before they can reach the sea floor. Calcium carbonate is seldom found at depths greater than 12,000 ft. In other areas where the carbonate particles do reach the ocean floor, the rate of sedimentation is often so slow that the carbonates are exposed much longer to the corrosive action of the deep waters and are then dissolved before they can be buried.

In contrast to the Pacific, the greater influx of terrigenous sediment and the shallower depths in the Atlantic result in the deposition and burial of the carbonate particles before they can be dissolved. Siliceous ooze are almost absent from the North Atlantic, but are found over extensive areas of the Pacific. These deposits frequently occur in areas where the dissolution of calcium carbonate exceeds its production as well as in regions where the accumulation of siliceous skeletons is greater than that of "red clay".

River inflow from the bordering land areas is much more significant in the Atlantic than the Pacific as seen by the distribution of fluvial-marine sediments. These deposits comprise a large portion of the sea floor in the Atlantic, but are only of importance in the most northern and far western portions of the Pacific. The differences between the North Pacific and North Atlantic basins are also evident from a study of the engineering properties of the sediments which is discussed in the following sections.

SHEAR STRENGTH

Sediment cores used in this study were composed essentially of fine grained cohesive material with a few stringers of fine sand occurring in a small number of the samples. Shear strength of a cohesive sediment is a function of the cohesion and internal friction of the material and the effective stress normal to the shear plane, more simply expressed as:

$$s = c + \bar{\sigma} \tan \phi$$

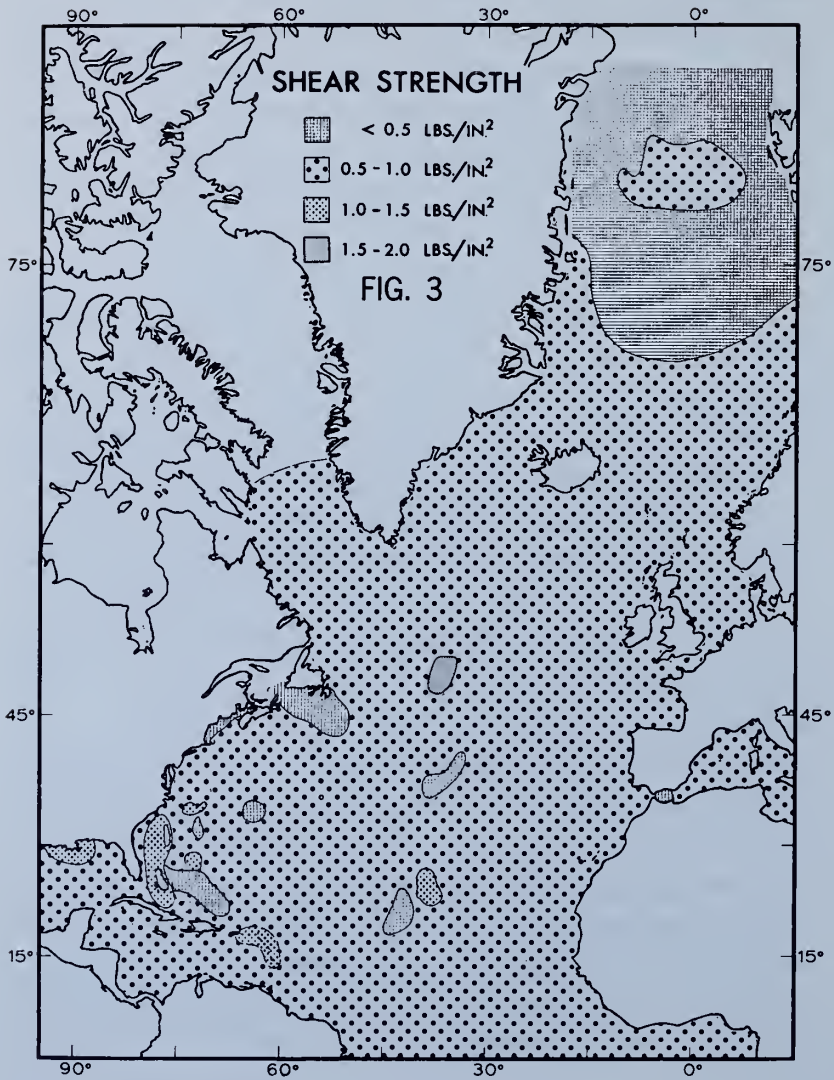
where c is the cohesion, $\bar{\sigma}$ is the effective stress and ϕ is the angle of internal friction. Fine grained, saturated sediments stressed without loss of pore water behave with respect to the applied load as if they were cohesive materials without any internal friction ($\phi = 0$). In this instance, shear strength then is equal to cohesion ($s = c$). For a more detailed discussion of shear strength the reader is referred to such soil mechanics texts as those by Terzaghi and Peck (1948, p. 87) and Taylor (1948, p. 362).

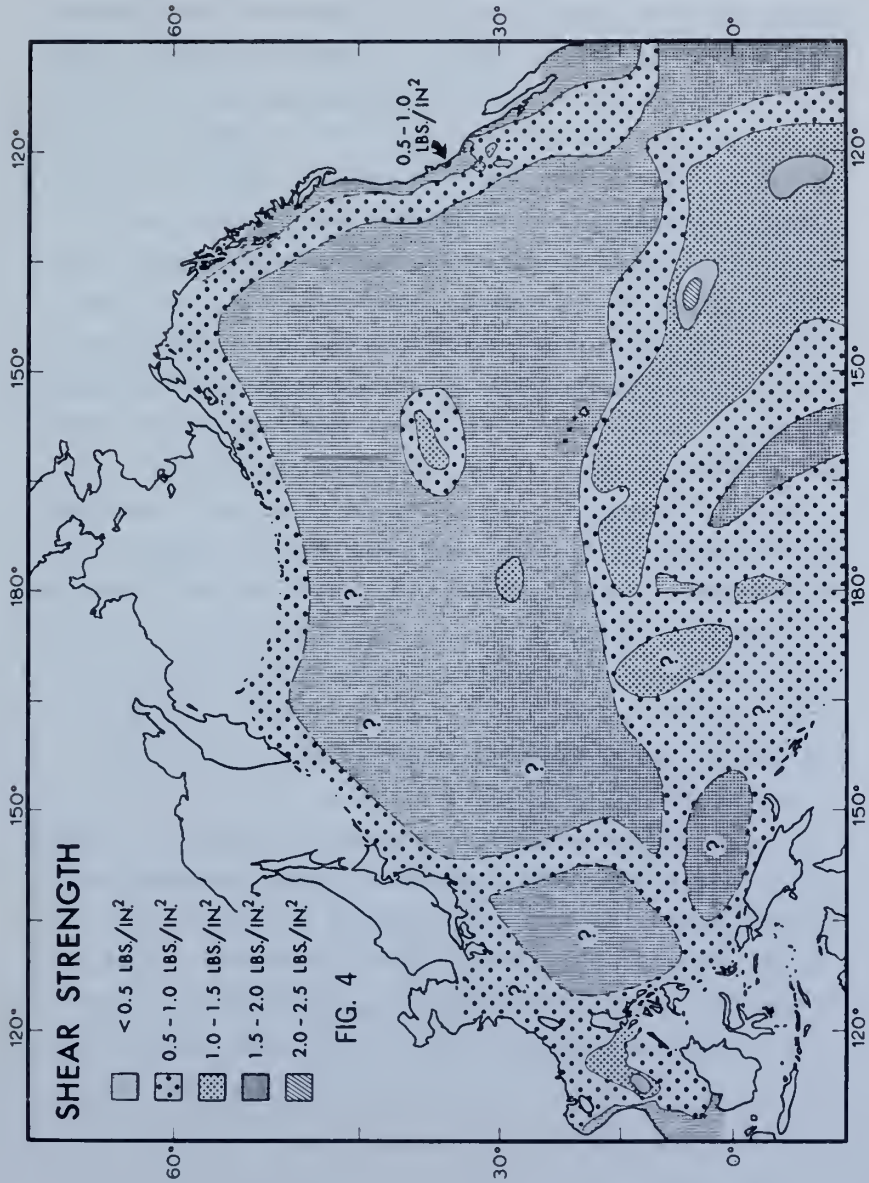
Measurement of shear strength was made mainly by either of two methods: the laboratory vane shear or the unconfined compression test. The vane shear technique provides a rather simple yet suitable test for the relatively soft submarine sediments. In some instances, it was the only test that could be used because of the very low shear strengths encountered. This test is made by inserting a small four-bladed vane into the sample and applying an increasing torque until a shear occurs (Evans and Sherratt, 1948; Richards, 1961).

Unconfined compression tests were made on many of the more cohesive samples. The test procedure is similar in principle to the standard test described in various soil mechanics texts.

However, both the equipment and procedure were modified slightly to accommodate the relatively weak submarine sediments (Richards, 1961). For the purpose of this study, the sediments were considered to be clays or materials behaving like clays and the shear strength was taken as one-half of the unconfined compressive strength.

Average shear strength values in the ocean basins range from less than 0.5 to 2.5 psi for the upper few feet of sea-floor sediments (Figs. 3 and 4). Sediments with a shear strength of 0.5 to 1.0 psi appear to predominate in the North Atlantic basin. Shear strengths of 1.0 to 1.5 psi are the highest observed in the North Atlantic and are associated with calcareous deposits. Values of less than 0.5 psi are often found in coastal areas where local drainage or current conditions strongly influence the depositional environment. In these areas, minor changes in the environment can result in significant variations in the mass properties of the sediments. Other areas of low shear strength are found in association with "red clay" deposits and in pockets of sediment along the Mid-Atlantic Ridge. The most prominent portion of the Atlantic basin displaying shear strengths of less than 0.5 psi is that east of Greenland. As shown by these values, (Fig. 3) and other observations to be discussed later, this section of the sea floor differs considerably from other portions of the North Atlantic. This particular depositional environment is probably influenced considerably by a large current gyral composed primarily of the north-flowing Norwegian Current on the east and the south-flowing East Greenland Current to the west. Sediment influx from Greenland and the Arctic undoubtedly are also an important influence on the sedimentary characteristics of this area.





In contrast to the North Atlantic, large portions of the North Pacific sea floor are covered with sediments whose average shear strength is less than 0.5 psi. These areas coincide closely with the distribution of "red clay" and comprise a major portion of the sea floor. Localities of higher shear strength occur within the area of low shear strength as a result of changes in bottom topography influencing the depositional environment. Local currents in and around topographic features can account for changes in the distribution of certain sediment properties. It has been found that on topographic "highs" shear strengths are slightly higher than in the surrounding areas (R. J. Smith, personal communication). This may be attributed to the winnowing effect of currents which tend to keep the "highs" free of softer sediments.

Shear strength values are generally higher along the margins of the basin and in the lower latitudes. Coarser sediments and shallower water depths, normally found closer to land, account for the general pattern shown in Figure 4. In areas of increased calcium carbonate, such as the low latitudes, shear strength is also found to increase. The highest range of values 2.0 to 2.5 psi observed thus far occur in the calcareous oozes of the Pacific basin (Fig. 4).

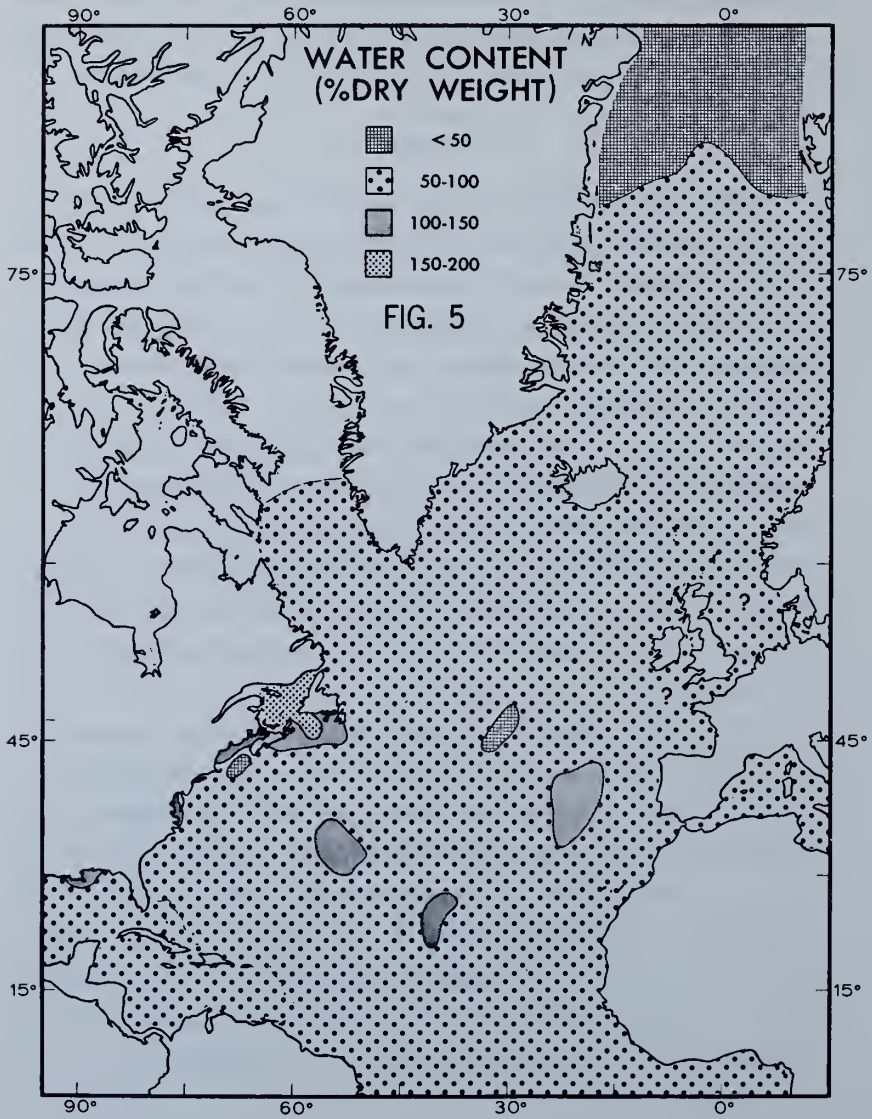
A comparison of the overall data presented in Figures 3 and 4 indicates that North Atlantic sediments possess relatively higher shear strengths than do those of the North Pacific. It is also evident from these data, that the North Pacific basin can be divided into two sedimentary provinces, each distinctly different from the other. The northern portion consists of sediment

possessing strengths ranging from 0.25 to 0.5 psi; in the lower latitudes, values of 1.0 to 1.5 psi predominate. The North Atlantic does not display these sedimentary provinces except for the area east of Greenland discussed earlier.

WATER CONTENT

Water content used here is the ratio, expressed as a percent, of the weight of water to the weight of oven dried (110°C) solids in a given sediment mass. The procedure for this determination is described in most texts dealing with soil mechanics and is not discussed. In a few instances, when sediment cores were not analyzed immediately after they were taken, or the core liners were not coated with an impervious wax, the measured water content values may be lower than one would actually find in place. As shown by Keller, et.al. (1961), the clear plastic liners used in deep-sea coring devices are not impervious to water and moisture loss does take place through the walls of these liners. The averaging approach used in this study has reduced any such errors to a minimum.

Water content values in the North Atlantic range from 30 to 175 percent, but more commonly are between 50 and 100 percent (Fig. 5). The relatively high water contents found in the vicinity of Newfoundland and Nova Scotia undoubtedly result from the influence local drainage and current conditions have on the depositional environment. The patches of low and high water content material observed in the basin are probably related to areas where topographic irregularities in the sea floor strongly influence the currents. Sufficient data are, however, not available to

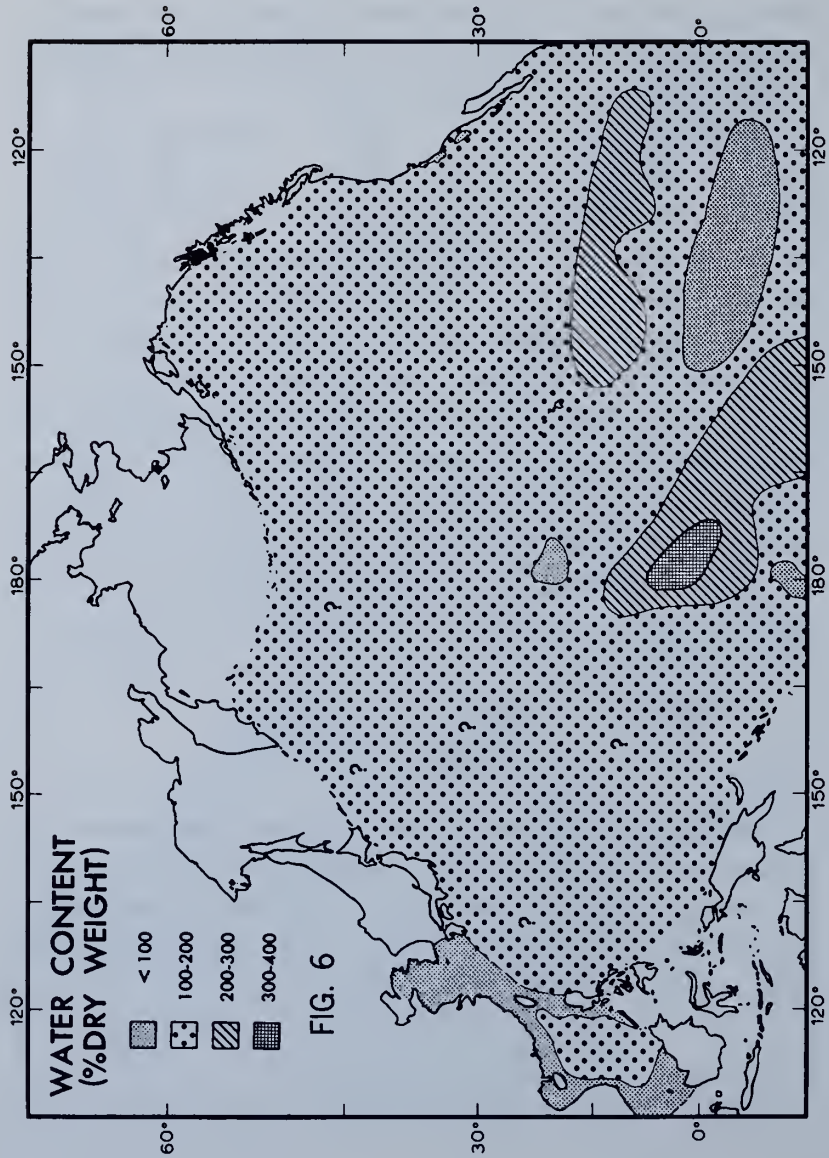


adequately discuss the reason for the presence of these isolated deposits. The area east of Greenland is unique, in that some of the lowest observed water contents in the North Atlantic are found there.

In the North Pacific, water contents are generally higher than those reported for the North Atlantic. Water content varies from 50 to 375 percent, but more frequently ranges from 100 to 200 percent (Fig. 6). The higher values are often found in association with "red clay" deposits, whereas, calcareous sediments and those deposited in local coastal areas appear to possess relatively low water contents. This is probably a result of grain size variation; the fine-grained sediments possess high water content, whereas, the coarser carbonate material and coastal sediments have relatively low water contents. This relationship in submarine sediments was discussed by Richards and Keller (1962). This line of reasoning can also be used when comparing the North Atlantic to the North Pacific. North Pacific sediments on the whole are finer grained than those of the North Atlantic and also display higher water contents.

WET UNIT WEIGHT

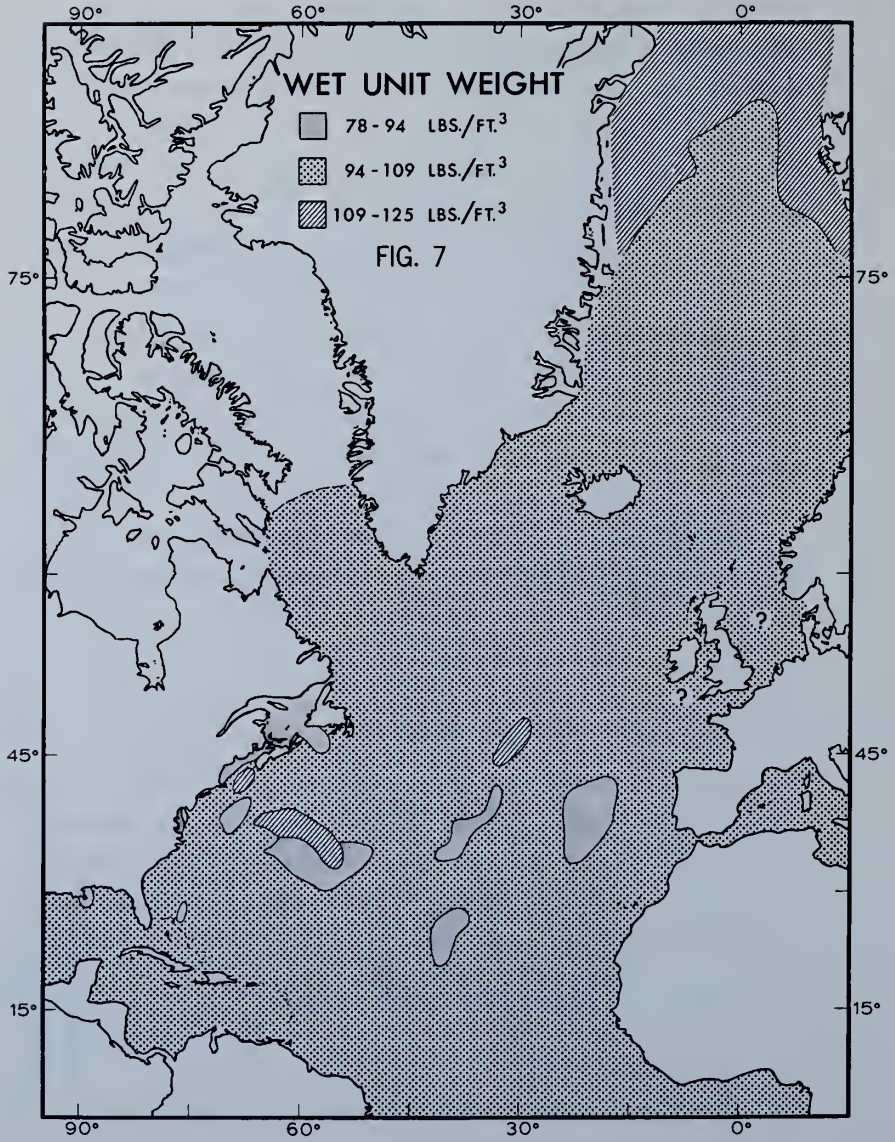
Wet unit weight or wet bulk density is the weight per unit of total volume of a sediment mass. Samples taken from the sea floor are sufficiently close to 100 percent saturation to allow use of the term saturated unit weight, which is the in-place bulk density. It is that value which is reported here.

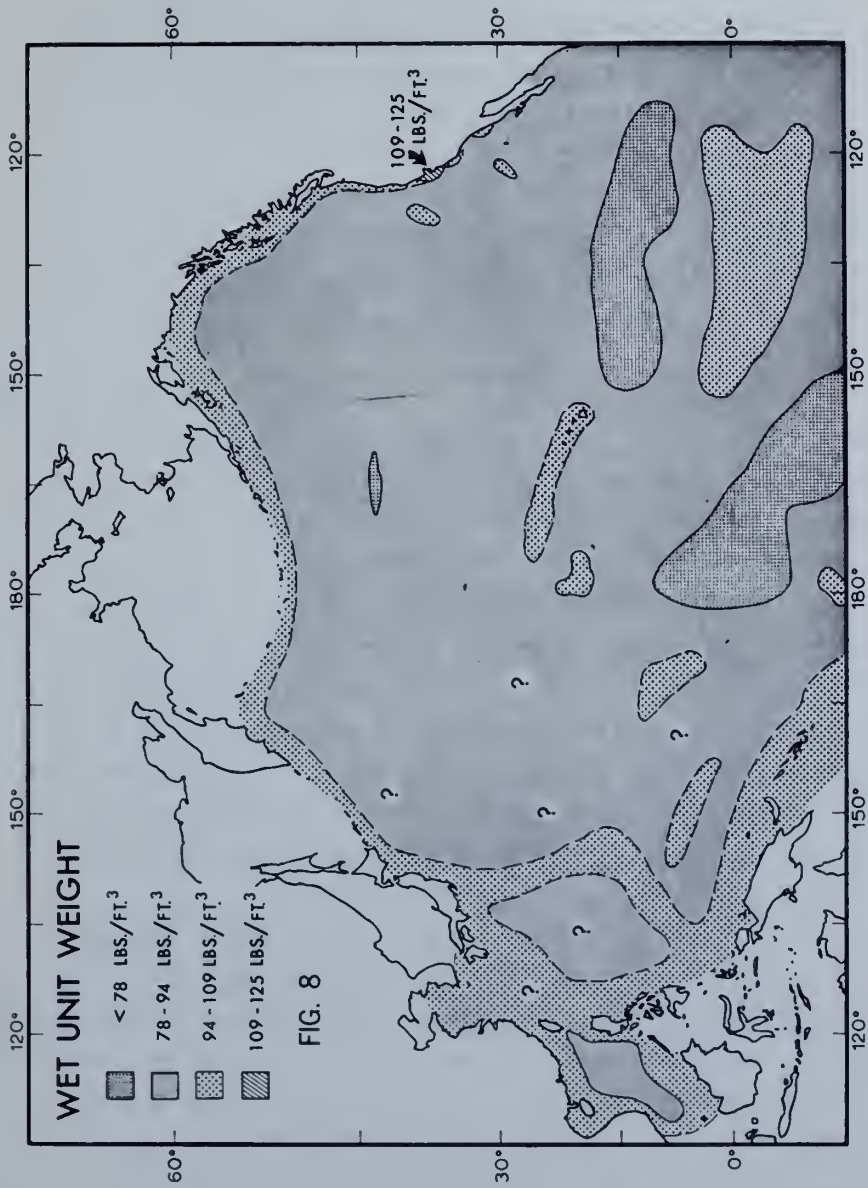


Bulk densities are slightly higher in the North Atlantic relative to the North Pacific. Sediment densities of 94 to 109 pcf. constitute a major portion of the Atlantic sea floor, whereas, extensive regions of the Pacific are covered with sediments ranging in density from 79 to 94 pcf. (Figs. 7 and 8). Areas of relatively low density material — less than 78 pcf. — have been found in the North Pacific, but as yet have not been observed in the North Atlantic. These low densities are common to areas of "red clay". The low values occurring in the vicinity of 3°S and 170°W may possibly be attributed to the particular depositional environment caused by the numerous islands found in that area. Other areas of low density material are associated with the relatively flat abyssal floor which rules out the possibility of bottom topography influencing the depositional environment in these particular areas. No explanation is readily available for the occurrence of these low density sediments. The areal extent of these lower density sediments will undoubtedly increase as additional data become available.

The distribution of 94 to 109 pcf. values around the margin of the Pacific is based on the extrapolation of density and sediment type observations from the South China Sea and from off California.

The highest densities observed are those east of Greenland where values as high as 125 pcf. are reported. This unique area of relatively high densities can most likely be correlated with an influx of heavy minerals from Greenland and Vestspitsbergen. This has not been verified by heavy mineral analyses of the sediments.





DISCUSSION

Observations made thus far show clearly a direct relationship between sediment type and the mass physical properties as might be expected. A direct relationship between mass properties and such factors as water depth or ocean currents is also observed in some areas. The isolated patches of various parameters seen in Figures 3 through 8 can, with a degree of certainty, be attributed to the influence of local bottom topography and currents although there may not be any change in the sediment type in the area of these variations.

In addition to the basic relationships between such parameters, as cohesion, water content, and bulk density, which have been discussed by various authors, (Tarzaghi and Pack, 1948; Hamilton and Menard, 1956; and Richards, 1962), some generalizations can be made based on the present study. The extensive "red clay" deposits commonly possess high water content, but low shear strength and bulk density. Exceptions to this are usually in areas effected by variation in the sea-floor topography. Calcareous deposits are more or less the opposite with relatively low water content, but with high shear strength and bulk density. The presence of various types of skeletal debris along with the cementation characteristics of certain calcareous deposits accounts strongly for a wide variation of mass properties from one deposit to another.

Mass properties in coastal areas vary considerably from area to area because of the influence that local drainage and currents have on the depositional environment. In the vicinity of major rivers shear strength and bulk density are relatively low, whereas, water content values are higher than those found on the deep-sea floor.

The area east of Greenland deserves special mention because of its noticeable difference from the other areas studied. This area is a small basin in itself and is strongly influenced by both currents and inflow of sediment from the adjacent land masses. The low water content and high bulk density values can be attributed to the generally coarse, heavy-mineral-rich deposits found in this basin. The presence of relatively low shear strength values in this same area cannot readily be explained. The low strength values are generally found in conjunction with clayey sediments which possess high water content and low densities. The possibility that these samples were overly disturbed cannot be ruled out.

The data presented here now gives some indication of the range of mass physical property values we can expect to find in the surface sediments — one to ten feet — of the North Pacific and North Atlantic basins.

In areas where data are not available, the values shown are extrapolated from known values occurring in similar sediments and water depths. It must be noted that relatively crude sampling techniques were used in obtaining most of the sediment samples. Shear strength values are reduced considerably as the amount of sample disturbance increases. Although many of the samples were collected with improved coring devices such as the Hydro-plastic corer (Richards and Keller, 1961), the samples are far from being undisturbed. With the advent of in-place measurements on the sea floor by means of instruments such as the nuclear sediment density probe (Keller, 1965), it can be expected that significant

discrepancas will be found when comparing these new data with those available today.

It is anticipated that as more data are collected, the distribution patterns of these various parameters will increase in complexity. The Atlantic Ocean, with its mid-ocean ridge and great influx of terrigenous sediment, will display a much greater variation and complexity than presently seen. On the other hand, relatively little change in the distribution pattern is expected over much of the North Pacific as a result of the more uniform depositional environment. Greater lateral variation than is presently observed can also be expected in the low latitudes of the southwest North Pacific where numerous islands and trenches interrupt the sea floor.

SUMMARY

Although the 500 sediment cores used in this study represent only a small portion of the North Atlantic and North Pacific sea floor, it is possible to gain some insight into the values and distribution of various mass physical properties and the range of values that can be expected in these basins.

1. Sediment types vary considerably between the North Atlantic and North Pacific basins. The vastness and remoteness of the North Pacific as well as its great depth is clearly reflected in the extensive deposits of "red clay", which are considered to be an indication of a very slow rate of deposition. Sediments of the smaller North Atlantic basin tend to be coarser and possess higher percentages of calcium carbonate as

shown by the vast deposits of fluvial-marine and calcareous ooze deposits. This is attributed, in part, to the extensive drainage into the Atlantic and to the relatively shallow water depths found there as compared to the Pacific Ocean. Siliceous oozes are noticeably absent from the North Atlantic, but do occur in some portions of the Pacific.

2. Shear strength varies from 0.25 to 2.5 psi, but more commonly is within a range of 0.5 to 1.5 psi. In comparison, sediments of the North Atlantic appear to be slightly stronger than those of the North Pacific.
3. Water content varies from 50 to 375 percent, and ranges between 50 and 100 percent in the North Atlantic and between 100 to 200 percent in the North Pacific. The finer Pacific sediments possess a considerably higher water content than the relatively coarser sediments of the North Atlantic.
4. Sediment bulk densities are found to range from 74 to 125 pcf., but more frequently vary from 78 to 109 pcf. Bulk densities are generally lower in the North Pacific, (78 to 94 pcf.) than in the North Atlantic, (94 to 109 pcf.).

The data presented here clearly reflect the contrasting depositional environments of the North Atlantic and North Pacific basins. The remoteness of the Pacific basin to land areas is indicated by the extensive deposits of "red clay". These sediments possess relatively high water contents, but low shear strengths and bulk densities. Carbonate deposits in the low latitudes of the Pacific

generally display higher shear strengths and densities, but lower water contents than the "red clay" to the north.

In contrast to the Pacific, the North Atlantic sediments possess lower water contents, but higher shear strengths and bulk densities. Although this study shows a rather simple distribution pattern for the various parameters in the North Atlantic, it is expected that this will increase in complexity as more data become available.

REFERENCES

- Arrhenius, G., (1963): Pelagic Sediments, in The Sea: Ideas and Observations on Progress in the Seas: Hill, M. N. ed., V. 3, pp. 655-727.
- Evans, I., and G. G. Sherratt, (1948): A simple and convenient instrument for measuring the shear resistance of clay soils: Jour. Sci. Instruments and Physics in Industry, V. 25, pp. 411-414.
- Fisk, H. N., and B. McClalland, (1959): Geology of continental shelf off Louisiana: Its influence on offshore foundation design. Geol. Soc. America Bull., V. 70, pp. 1369-1394.
- Hamilton, E. L., (1956): Low sound velocities in high porosity sediments: Jour. Acoustical Soc. America, V. 28, pp. 16-19.
- Hamilton, E. L., (1959): Thickness and consolidation of deep-sea sediments: Geol. Soc. America Bull., V. 70, pp. 1399-1424.
- Hamilton, E. L., (1964): Consolidation characteristics and related properties of sediments for experimental Mohole (Guadalupe site): Jour. Geoph. Research, V. 69, pp. 4257-4269.

- Hamilton, E. L., and H. W. Menard, (1956): Density and porosity of sea-floor surface sediments off San Diego, California: Amer. Assoc. Petroleum Geologists, V. 40, pp. 754-761.
- Hamilton, E. L., G. Shumway, H. W. Menard, and C. J. Shippek, (1956): Acoustic and other physical properties of shallow water sediments off San Diego: Jour. Acoustical Soc. America, V. 28, pp. 1-15.
- Harrison, W., M. P. Lynch, and A. G. Altschaeffl, (1964), Sediments of lower Chesapeake Bay, with emphasis on mass properties: Jour. Sed. Petrology, V. 34, pp. 727-755.
- Igelman, K. R., and E. L. Hemilton, (1963): Bulk densities of mineral grains from Mohole samples (Guadalupe site). Jour. Sed. Petrology, V. 33, pp. 474-478.
- Keller, G. H., (1964): Investigation of the application of standard soil mechanics techniques and principles to bay sediments: in proc. 1st U. S. Navy Symposium on Military Oceanography, pp. 329-360.
- Keller, G. H., (1965): Deep-sea nuclear sediment density probe: Deep-Sea Res., V. 12, pp. 373-376.
- Keller, G. H., A. F. Richards, and J. H. Recknagel, (1961): Prevention of water loss through CAB plastic sediment core liners: Deep-Sea Res., V. 8, pp. 148-151.
- Moore, D. G., (1962): Bearing strength and other physical properties of some shallow and deep-sea sediments from the North Pacific: Geol. Soc. America Bull. V. 73, pp. 1163-1166.
- Moora, D. G., (1964): Shear strength and related properties of sediments from experimental Mohole (Guadalupe site). Jour. Geoph. Research, V. 69, pp. 4271-4291.

- Moore, D. G., and G. Shumway, (1959): Sediment thickness and physical properties: Pigeon Point Shelf, California: Jour. Geoph. Research, V. 64, pp. 367-374.
- Richards, A. F., (1961): Investigations of deep-sea sediment cores, I. Shear strength bearing capacity, and consolidation: U. S. Hydrographic Office Tech. Rept. 63, 70 pages.
- Richards, A. F., (1962): Investigations of deep-sea sediment cores, II. Mass physical properties: U. S. Hydrographic Office Tech. Rept. 106, 146 pages.
- Richards, A. F., and G. H. Keller, (1961): A plastic-barrel sediment corer: Deep-Sea Res., V. 8, pp. 306-312.
- Richards, A. F., and G. H. Keller, (1962): Water content variability in a silty clay core from off Nova Scotia: Limnology and Oceanography, V. 7, pp. 426-427.
- Smith, R. J., (1962): Engineering properties of ocean floor soils, Amer. Soc. for Testing and Materials, Spec. Tech. Publication No. 322, pp. 280-302.
- Taylor, D. W., (1948): Fundamentals of soil mechanics: New York, John Wiley, & Sons, Inc., 700 pages.
- Terzaghi, K., and R. B. Peck, (1948): Soil mechanics in engineering practice: New York, John Wiley & Sons, Inc. 566 pages.
- U. S. Navy Hydrographic Office, (1955): Instructions manual for oceanographic observations: Hydrographic Office Publication No. 607, Washington, 210 pages.

Mass Physical Properties of Submarine Sediments in the Atlantic and Pacific Basins

G. H. KELLER and R. H. BENNETT

U.S.A.

Abstract: Measurements of mass properties (bulk density, porosity, cohesion, water content, and grain size) have been made on a large number of sediment cores collected from various portions of the Atlantic and Pacific oceans. These samples represent several types of deep-sea sediment as well as different depositional environments within the basins. Some degree of correlation is found between these properties and sediment type, currents, and local topography. Portions of the Pacific sea floor consisting of "red clay" commonly display lower cohesion and bulk density, but higher water contents than those areas blanketed by calcareous oozes. This relationship is not as clearly defined in the Atlantic basin. Atlantic sediments are found to be denser and stronger (greater cohesion) than those of the Pacific. In contrast, such properties as water content and porosity are usually higher in the Pacific than in the Atlantic. In the vicinity of the continental margins, the mass physical properties vary considerably as the sediment supply and depositional environment change. Sediments from carbonate environments or areas of relatively high relief normally possess greater cohesion. This investigation has led to a delineation of various portions of the sea floor on a basis of the mass physical properties and gives an indication of the range of these parameters for deep-sea sediments.

Introduction

Only in recent years has much attention been given to the mass physical or engineering properties of submarine sediments other than to those found in harbors and in the relatively shallow coastal waters. Prior to 1950, when offshore petroleum exploration began to be important, very few data were obtained from beyond the breaker zone. Only in the past ten years have serious attempts been made to investigate the mass physical properties of deep-sea sediments. These studies have mainly been undertaken by marine geologists, who, using the doctrine of Hutton, "*the present is the key to the past*", are trying to understand the depositional history of ancient marine deposits by studying the mass properties of recent deep-sea sediments.

Early studies by such investigators as Hamilton, 1959; Richards, 1961, 1962; and Moore, 1962 have provided the impetus for the increased interest more recently shown in this field of study by many marine geologists and civil engineers.

The marine geologist has gained a clearer understanding of several problems

by adapting soil mechanics practices to submarine sediments. Studies of the consolidation characteristics of deep-sea sediments (Hamilton, 1964) have been significant in contributing to a better understanding of the depositional history in the ocean basins since their formation. The requirements of various military programs for an increased knowledge of the sea-floor environment also has lead to a greater interest in the mass properties of submarine sediments (Hamilton *et al.*, 1956; Smith, 1962; and Keller, 1964).

Many of the published studies on the mass physical properties of submarine sediments pertain to specific relationships such as sound velocity and porosity, density and depth, consolidation and depositional history (Hamilton, 1956; Igelman and Hamilton, 1963) or have discussed the mass properties of a local area (Moore and Shumway, 1959; Fisk and McClelland, 1959; Harrison *et al.*, 1964). Although only relatively few deep-sea sediment cores have been collected in the past ten years from the North Atlantic and North Pacific Basins for the purpose of studying the mass physical properties (roughly 600 to 750 cores), it is possible now to gain some insight into the range of values we can expect to find in various parts of these basins.

This paper is an attempt to bring together all the available data, published and unpublished, pertaining to the variation of sediment type, shear strength, water content, wet unit weight and porosity in the North Atlantic and North Pacific Ocean basins. This study is based on the data obtained from approximately 500 sediment cores (Atlantic 300, Pacific 200) the majority of which were collected and analyzed by the U.S. Naval Oceanographic Office. Data published by Moore (1962) for the North Pacific and Fisk and McClelland (1959) for the Gulf of Mexico have been incorporated in this study.

Coring devices used to collect the samples are those normally used by marine geologists and leave much to be desired in the way of providing "undisturbed samples". The coring techniques commonly used are similar to those described by the U. S. Navy Hydrographic Office (1955, pp. 52-65). Deficiencies of these samplers have been pointed out and attempts made to improve the quality of samples (Richards and Keller, 1961). Cores used in this study vary in length from 30 cm to 3.7 m with an average of about 2 m. After considering the size of the ocean basins and the relatively short lengths of the cores, it was decided to average the respective parameter values over the entire length of each core. This was done after critically evaluating the data and removing any values that were obviously in error as a result of the sampling or testing procedures. The data presented here should be considered as representing an average value for the upper 2.0 to 2.5 m of the sea floor. Studies pertaining to the variation of the mass properties with depth have been presented elsewhere (Richards, 1962; Harrison *et al.*, 1964; Moore, 1964) and will not be discussed here.

North Atlantic and North Pacific basins

Although the North Atlantic and North Pacific Ocean basins are major ocean basins, the sea floor underlying these areas differ considerably from each other. The Atlantic is a much smaller basin (approximately half the area of the Pacific) and as such is influenced more by runoff from the surrounding land masses than is the Pacific. Bottom topography is notably different in the two basins. The Atlantic basin is more or less separated into east and west halves by the Mid-Atlantic Ridge with somewhat similar topography on either side of the ridge. On the other hand, the Pacific basin has numerous ridges, trenches, scarps, island chains and seamounts all of which play an important role in the deposition of the sediments. The mean depth of the Pacific is greater than that of the Atlantic which is also a factor influencing the sediment distribution. The significance of these differences as related to the mass physical properties is discussed below.

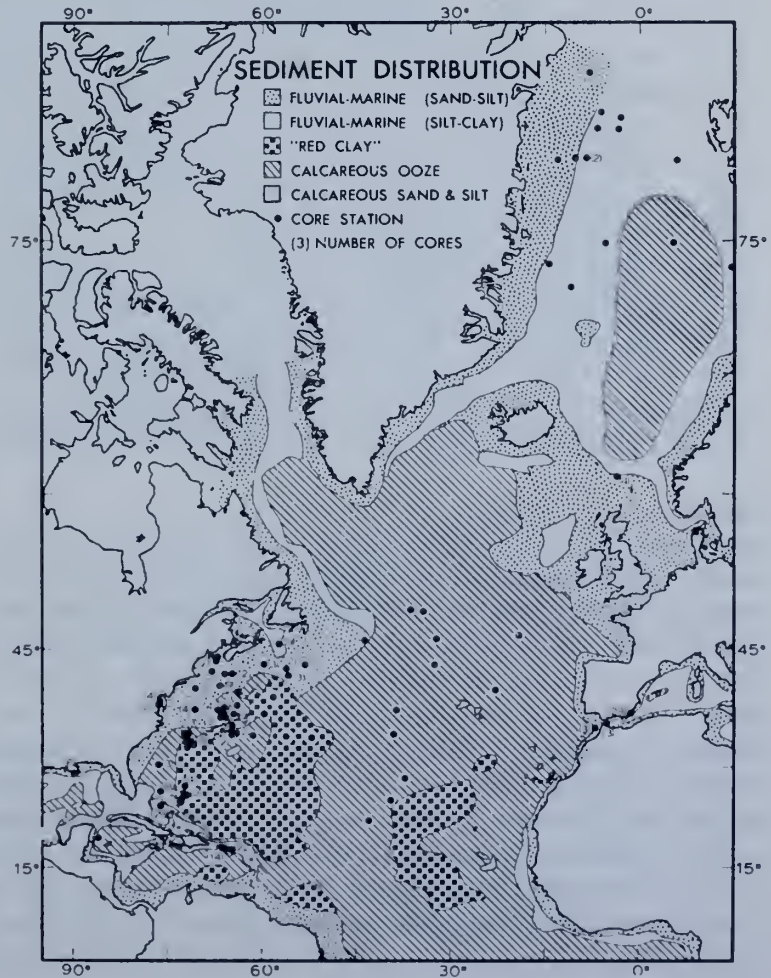


Fig. 1

Sediment types

The sediment distribution shown in Figures 1 and 2 is based mainly on data obtained from the files of the U. S. Naval Oceanographic Office and supplemented by the work of Arrhenius (1963). For the purpose of this study the sediment types have been divided into six classes: (1) fluvial-marine (sand-silt) representing the

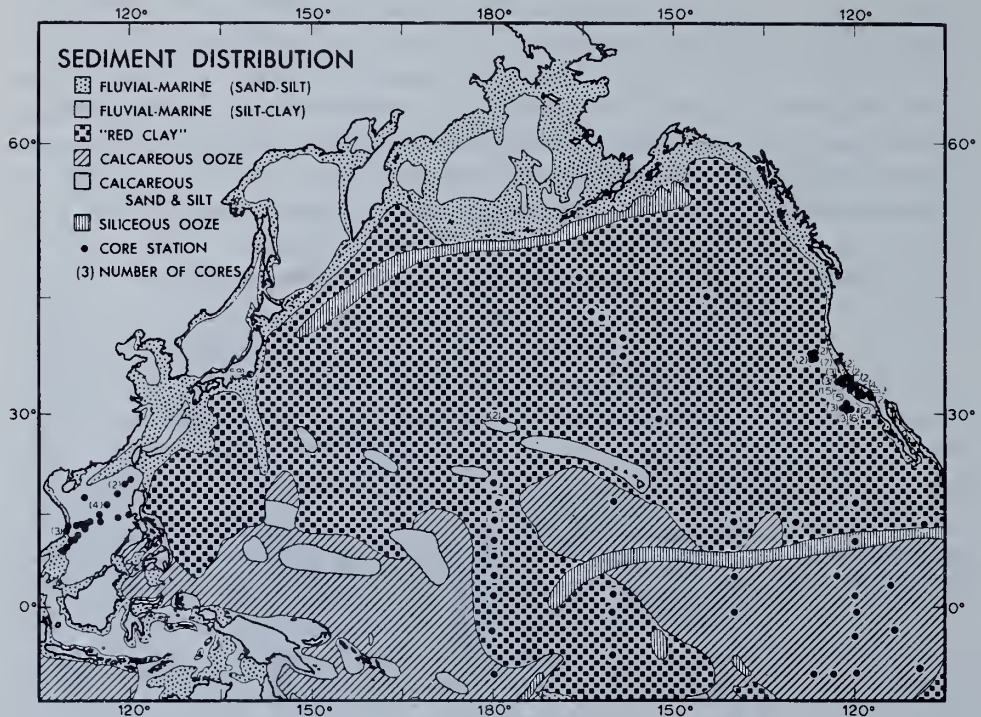


Fig. 2

coarser fraction (larger than 0.016 mm); (2) fluvial-marine (silt-clay), the finer fraction (smaller than 0.016 mm) of material derived from terrestrial drainage; (3) "red clay" is a term applied to inorganic pelagic clays which vary considerably in color, but are usually chocolate brown; (4) calcareous ooze is used here to define sediment composed of at least 30 per cent calcium carbonate which is in the form of skeletal material from various planktonic animals and plants; (5) calcareous sand and silt consist of shell fragments and coralline debris of sand and silt-size particles; (6) siliceous oozes are deposits containing 30 per cent or more of siliceous skeletal material derived from either diatoms or radiolarians.

Pelagic sediments of the North Pacific show several conspicuous differences from those of the North Atlantic basin (Figs. 1 and 2). The percentage of sea floor covered by "red clay" is at least four times that found in the North Atlan-

tic. These deposits are indicative of very slow rates of deposition and frequently reflect the remoteness of land areas to the Pacific Ocean. Approximately 10–15 per cent of the Pacific is at least 1500 km from the nearest land; such areas are almost absent from the Atlantic. Lack of calcium carbonate deposits over a major part of the North Pacific sea floor may be attributed to various circumstances. The great depths in some areas result in the dissolution of the calcareous skeletons before they can reach the sea floor. Calcium carbonate is seldom found at depths greater than 3.7 km. In other areas where the carbonate particles do reach the ocean floor the rate of sedimentation is often so slow that the carbonates are exposed much longer to the corrosive action of the deep waters and are then dissolved before they can be buried.

In contrast to the Pacific, the greater influx of terrigenous sediment and the shallower depths in the Atlantic result in the deposition and burial of the carbonate particles before they can be dissolved. Siliceous oozes are almost absent from the North Atlantic, but are found over extensive areas of the Pacific. These deposits frequently occur in areas where the dissolution of calcium carbonate exceeds its production as well as in regions where the accumulation of siliceous skeletons is greater than that of “red clay”.

River inflow from the bordering land areas is much more significant in the Atlantic than the Pacific as seen by the distribution of fluvial-marine sediments. These deposits comprise a large portion of the sea floor in the Atlantic, but are only of importance in the most northern and far western portions of the Pacific. The differences between sediments in the North Pacific and North Atlantic basins are also evident from a study of the engineering properties which is discussed in the following sections.

Shear strength

Sediment cores used in this study were composed essentially of fine grained cohesive material with a few stringers of fine sand occurring in a small number of the samples. Shear strength of a cohesive sediment is a function of the cohesion and internal friction of the material and the effective stress normal to the shear plane, more simply expressed as:

$$s = c + \bar{\sigma} \tan \Phi$$

where c is the cohesion, $\bar{\sigma}$ is the effective stress and Φ is the angle of internal friction. Fine grained, saturated sediments stressed without loss of pore water behave with respect to the applied load as if they were cohesive materials without any internal friction ($\Phi = 0$). In this instance, shear strength then is equal to cohesion ($s = c$). For a more detailed discussion of shear strength the reader is referred to such soil mechanics texts as those by Terzaghi and Peck (1948, p. 87) and Taylor (1948, p. 362).

Measurement of shear strength was made by either of two methods: the laboratory vane shear or the unconfined compression test. The vane shear technique provides a rather simple yet suitable test for the relatively soft submarine sediments. In some instances, it was the only test that could be used because of the very low shear strengths encountered. This test is made by inserting a small four-bladed vane into the sample and applying an increasing torque until a shear occurs (Evans and Sherratt, 1948; Richards, 1961).

Unconfined compression tests were made on many of the more cohesive samples. The test procedure is similar in principle to the standard test described in various soil mechanics texts, however, both the equipment and procedure were modified slightly to accommodate the relatively weak submarine sediments (Richards, 1961). For the purpose of this study, the sediments were considered to

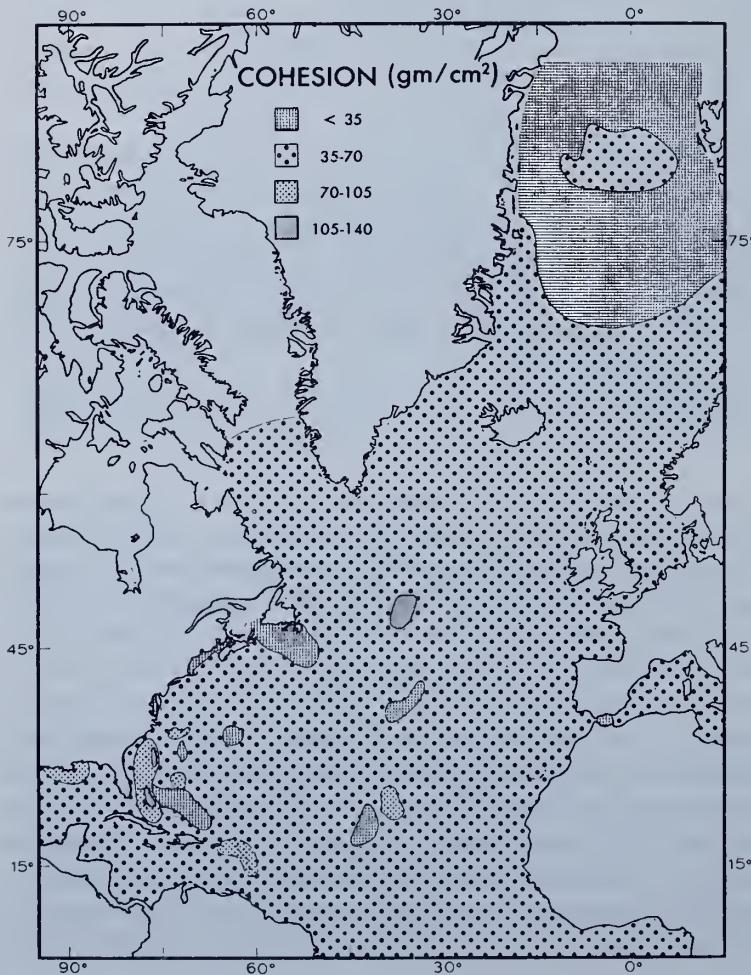


Fig. 3

be clays or materials behaving like clays and the shear strength was taken as one-half of the unconfined compressive strength.

Average shear strength values in the ocean basins range from less than 35 g/cm² to 175 g/cm² for the upper 1 to 7 meters of the sea floor (Figs. 3 and 4). Sediments with a shear strength of 35 to 70 g/cm² appear to predominate in the North

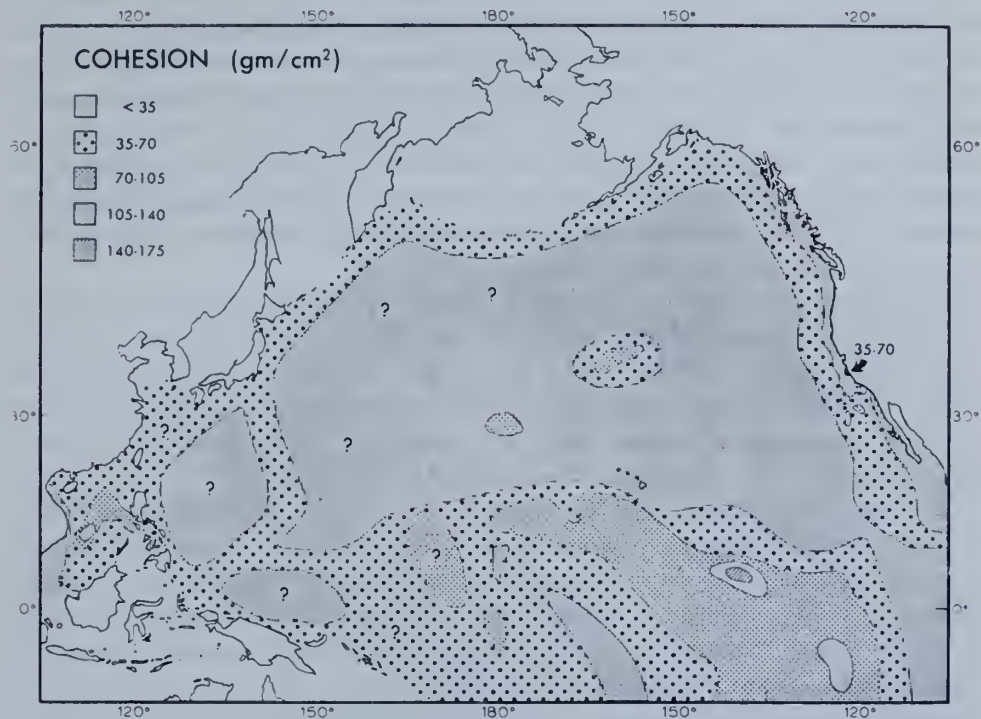


Fig. 4

Atlantic basin. Shear strengths of 70 to 105 g/cm² are the highest observed in North Atlantic and are associated with calcareous deposits or those high in calcium carbonate. Values of less than 35 g/cm² are often found in coastal areas where local drainage or current conditions strongly influence the depositional environment. In these areas, minor changes in the environment result in significant variations in the characteristics of the sea floor. Other areas of low shear strength are found in association with “red clay” deposits and in pockets of sediment along the Mid-Atlantic Ridge. The most prominent portion of the Atlantic basin displaying shear strengths of less than 35 g/cm² is that east of Greenland. As shown by these values (Fig. 3) and other observations to be discussed later, this section of the sea floor differs considerably from other portions of the North Atlantic. This particular depositional environment is probably influenced considerably by a large current gyral composed primarily of the north-flowing Nor-

wegian Current on the east and the south-flowing East Greenland Current to the west. Sediment influx from Greenland and the Arctic undoubtedly is also an important influence on the sedimentary characteristics of this area.

In contrast to the North Atlantic, large portions of the North Pacific sea floor are covered with sediments whose average shear strength is less than 35 g/cm^2 . These areas coincide closely with the distribution of "red clay" and comprise a major portion of the sea floor. Localities of higher shear strength occur within the area of low shear strength as a result of changes in bottom topography influencing the depositional environment. Local currents in and around topographic features can account for changes in the distribution of certain sediment properties. It has been found that on topographic "highs" shear strengths are slightly higher than in the surrounding areas (R. J. Smith, personal communication). This may be attributed to the winnowing effect of currents which tend to keep the "highs" free of softer sediments.

Shear strength values are generally higher along the margins of the basin and in the lower latitudes. Coarser sediments and shallower water depths, normally found closer to land, account for the general pattern shown in Figure 4. In areas of increased calcium carbonate, such as the low latitudes, shear strength is also found to increase. The highest range of values — 140 to 175 g/cm^2 — observed thus far occur in the calcareous oozes of the Pacific basin (Fig. 4).

A comparison of the overall data presented in Figures 3 and 4 indicates that North Atlantic sediments possess relatively higher shear strengths than do those of the North Pacific. It is also clear from these data that the North Pacific basin can be divided into two sedimentary provinces, each distinctly different from the other. The northern portion consists of sediment possessing strengths ranging from 17 to 35 g/cm^2 ; in the lower latitudes values of 70 to 105 g/cm^2 predominate. The North Atlantic does not display these sedimentary provinces except for the area east of Greenland discussed earlier.

Water content

Water content used here is the ratio, expressed as a per cent, of the weight of water to the weight of oven dried (110°C) solids in a given sediment mass. The procedure for this determination is described in most texts dealing with soil mechanics and is not discussed. In a few instances, when sediment cores were not analyzed immediately after they were taken, or the core liners were not coated with an impervious wax, the measured water content values may be lower than one would actually find in place. As shown by Keller *et al.* (1961), the clear plastic liners used in deep-sea coring devices are not impervious to water and moisture loss does take place through the walls of these liners. The averaging approach used in this study has reduced any such errors to a minimum.

Water content values in the North Atlantic range from 30 to 175 per cent, but

more commonly are between 50 and 100 per cent (Fig. 5). The relatively high water contents found in the vicinity of Newfoundland and Nova Scotia undoubtedly result from the influence local drainage and current conditions have on the depositional environment. The patches of low and high water content material observed in the basin are probably related to areas where topographic irregularities in the sea floor strongly influence the currents. Sufficient data are, however, not available to adequately discuss the reason for the presence of these isolated deposits. The area east of Greenland is unique, in that some of the lowest observed water contents of the North Atlantic are found there.

In the North Pacific, water contents are generally higher than those reported for the North Atlantic. Water content varies from 50 to 375 per cent, but most frequently ranges from 100 to 200 per cent (Fig. 6). The higher values are often found in association with "red clay" deposits, whereas calcareous sediments and

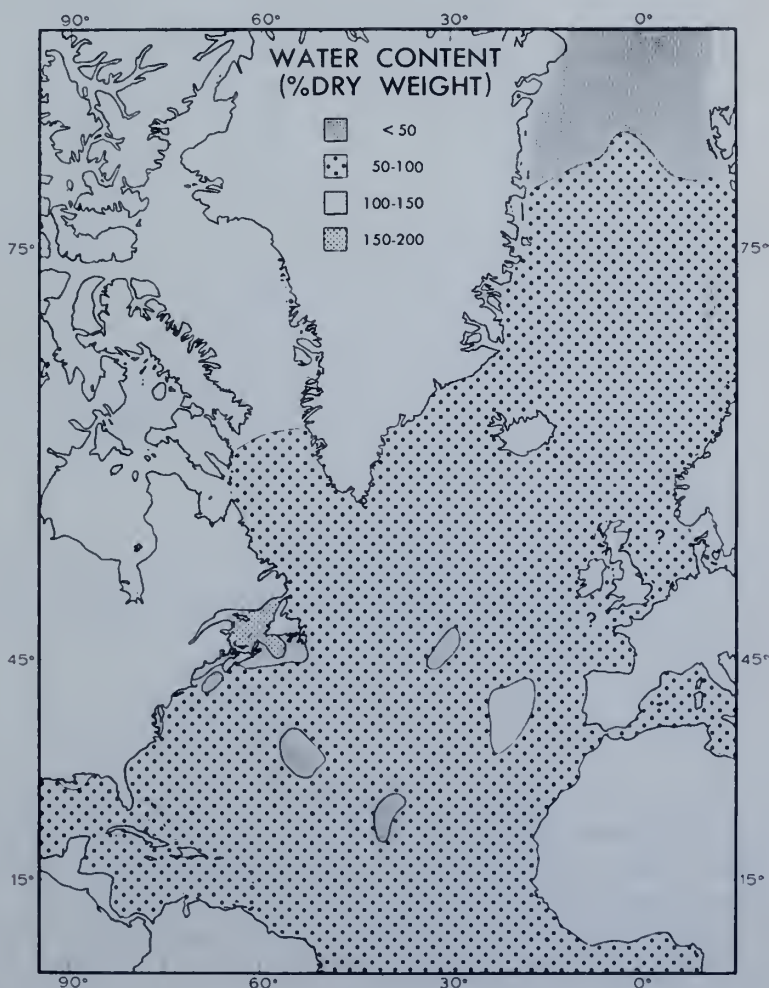


Fig. 5

those deposited in local coastal areas appear to possess relatively low water contents. This is probably a result of grain size variation; the fine-grained sediments possess high water content, whereas the coarser carbonate material and coastal sediments have relatively low water contents. This relationship in submarine sediments was discussed by Richards and Keller (1962). This line of reasoning

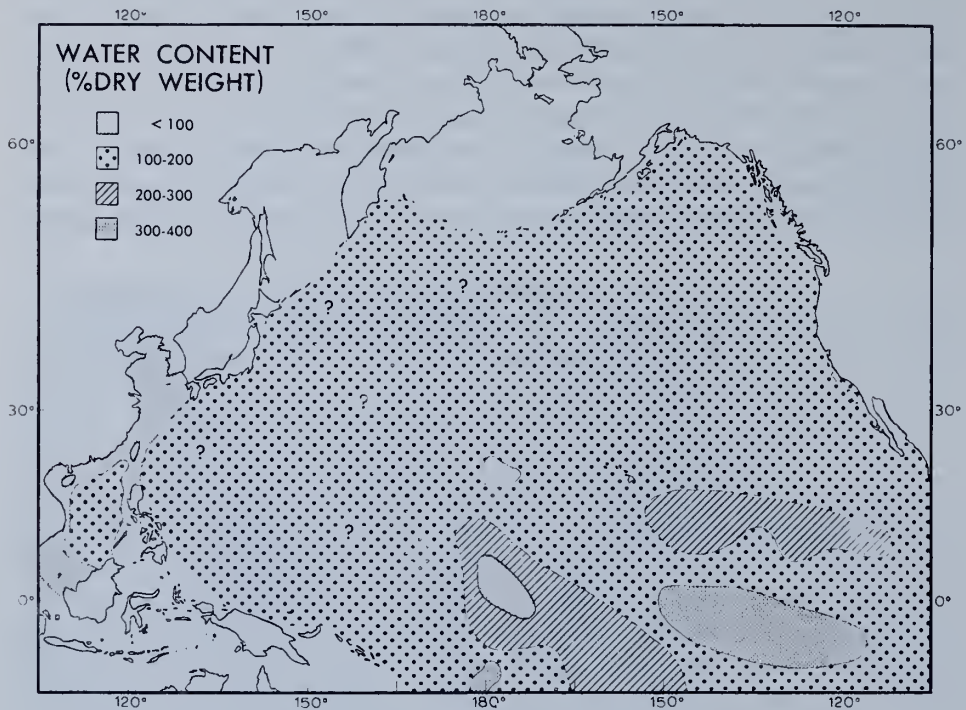


Fig. 6

can also be used when comparing the North Atlantic to the North Pacific. North Pacific sediments on the whole are finer grained than those of the North Atlantic and also display higher water contents.

Wet unit weight

Wet unit weight or wet bulk density is the weight per unit of total volume of a sediment mass. Samples taken from the sea floor are sufficiently close to 100 per cent saturation to allow use of the term saturated unit weight, which is the in-place bulk density. It is that value which is reported here.

Bulk densities are slightly higher in the North Atlantic relative to the North Pacific. Sediment densities of 1.50 to 1.75 g/cm³ constitute a major portion of the

Atlantic sea floor, whereas extensive regions of the Pacific are covered with sediments ranging in density from 1.25 to 1.50 g/cm³ (Figs. 7 and 8). Areas of relatively low density material — less than 1.25 g/cm³ — have been found in the Pacific, but as yet have not been observed in the North Atlantic. These low densities are common to areas of “red clay”. The low values occurring in the vicinity of 30°S and 170°W possibly may be attributed to the particular depositional environment caused by the numerous islands found in that area. The other areas of low density material are associated with the relatively flat abyssal floor which rules out the possibility of bottom topography influencing the depositional environment. No explanation is readily available for the occurrence of these low density sediments. The areal extent of these lower density sediments will undoubtedly increase as additional data become available.

The distribution of 1.50 to 1.75 g/cm³ values around the margin of the Pacific

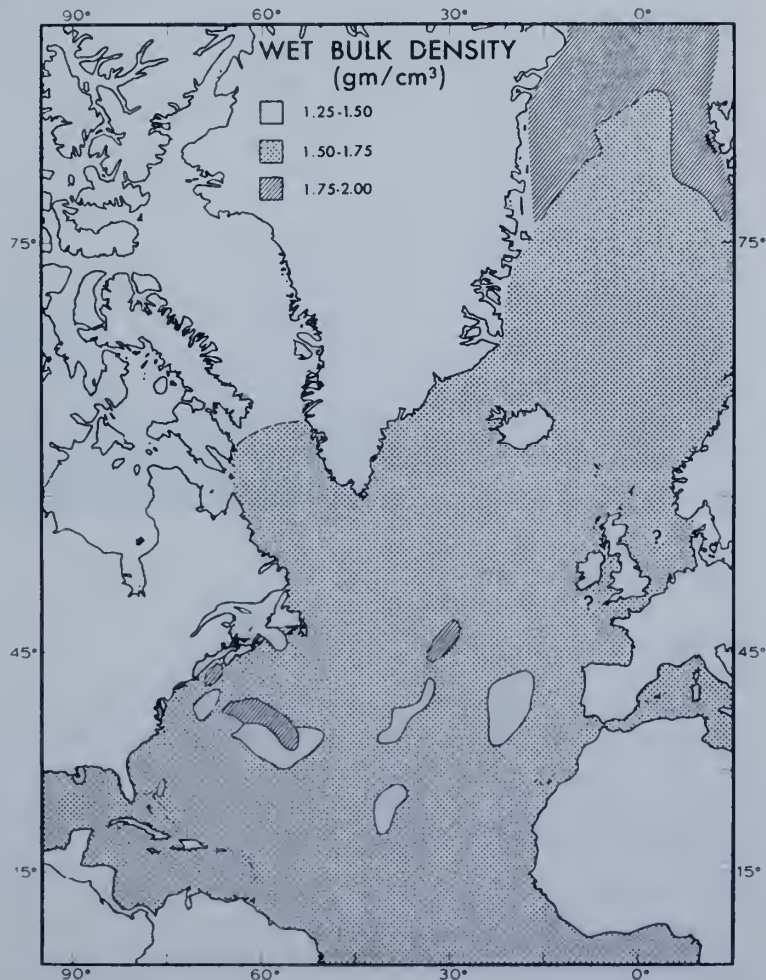


Fig. 7

is based on the extrapolation of density and sediment type observations from the South China Sea and from off California.

The highest densities observed are those east of Greenland where values as high as 2.0 g/cm³ are reported. This unique area of relatively high densities can be most likely correlated with an influx of heavy minerals from Greenland and Vestspitsbergen. This has not been verified by heavy mineral analyses of the sediments.

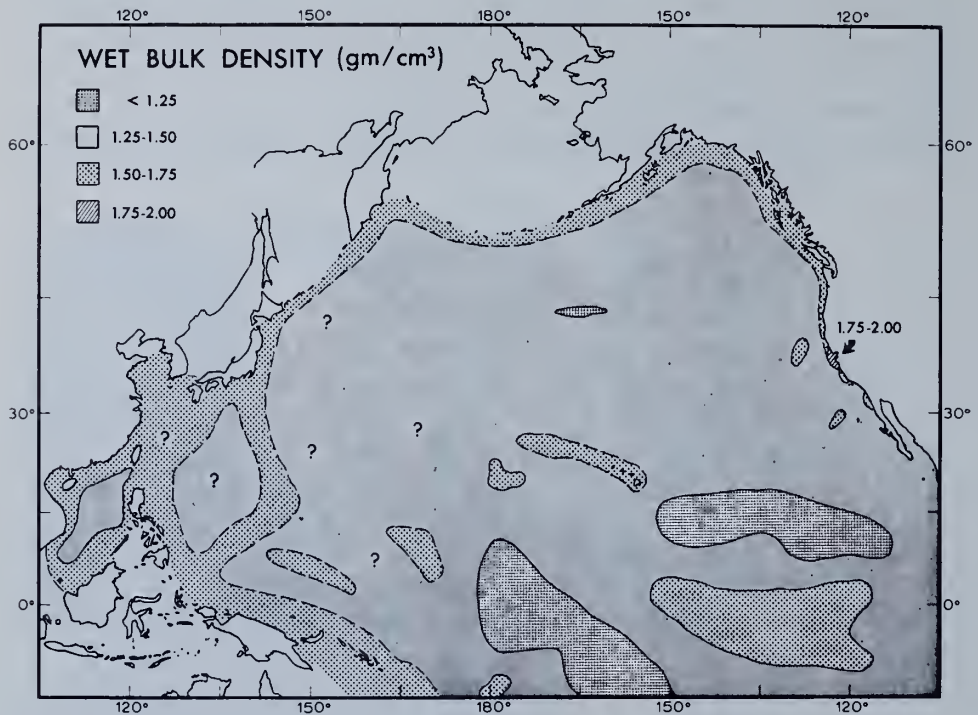


Fig. 8

Porosity

Porosity is the ratio of the volume of voids (pores) in a given mass to the total volume of the sediment mass. Based on the measured water content, bulk density and grain specific gravity values, the void ratio, e , (the ratio of the volume of the voids to the volume of the solids) can be calculated. Porosity, n , is then simply determined using the relationship

$$n = \frac{100 e}{1 + e}$$

Porosity of submarine sediments is found to range from 40 to 90 per cent, but

commonly ranges from 60 to 80 per cent. Extreme values can be found, but are relatively rare. Maximum porosity of a mass of similarly packed spheres of uniform size is 74 per cent regardless of size. Actual sediments are not spheres nor do they generally consist of one grain size. Small grains between large ones tend to reduce porosity and the presence of flat grains tend to increase porosity. Clayey sediments comprise a major portion of the sea floor and because these sediments have large surface areas and are predominantly flat grained, porosity is usually high.

Sediment porosity values seldom exceed 70 per cent in the North Atlantic and more frequently are lower than 65 per cent (Fig. 9). The relatively high values are found mainly associated with fine sediments, whereas the lower values frequently occur in conjunction with coarser deposits. This is a crude relationship at best and caution must be used when applying this generalization.

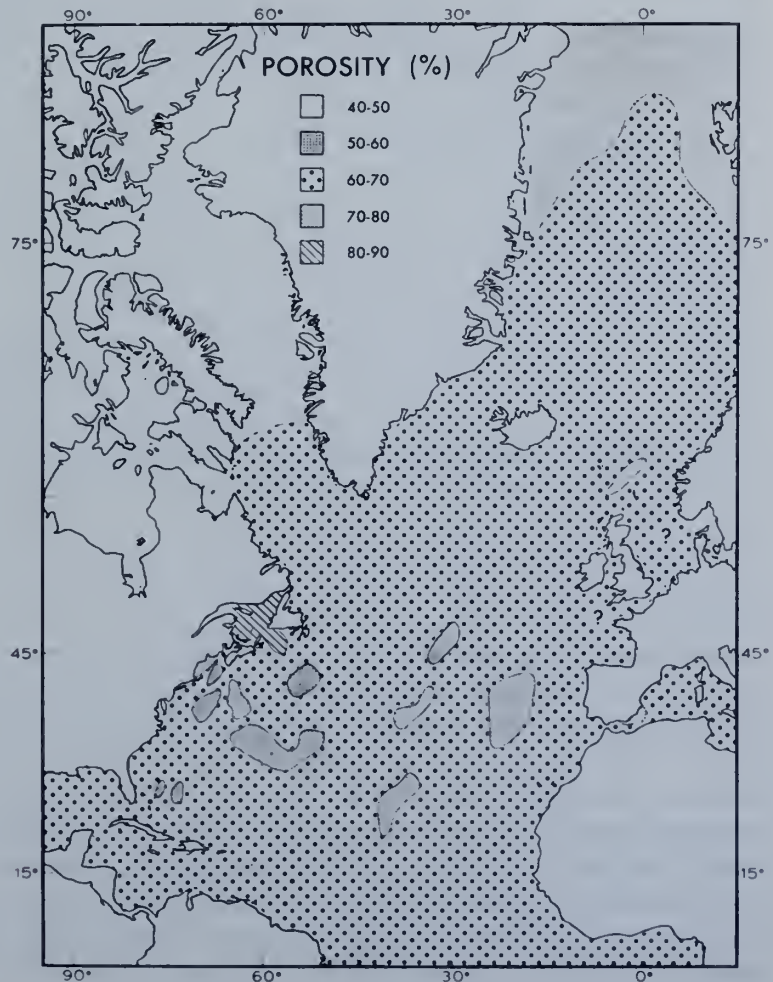


Fig. 9

In the North Pacific, porosity values are commonly higher than those observed in the Atlantic. Porosities of 70 per cent or greater are observed over much of the North Pacific basin. Lower values appear mainly along the coastal margin or in areas where water depths are relatively shallow (Fig. 10). No correlation can be made between porosity and sediment type from the available data, other than to say calcareous oozes appear to have a lower porosity than do "red clays".

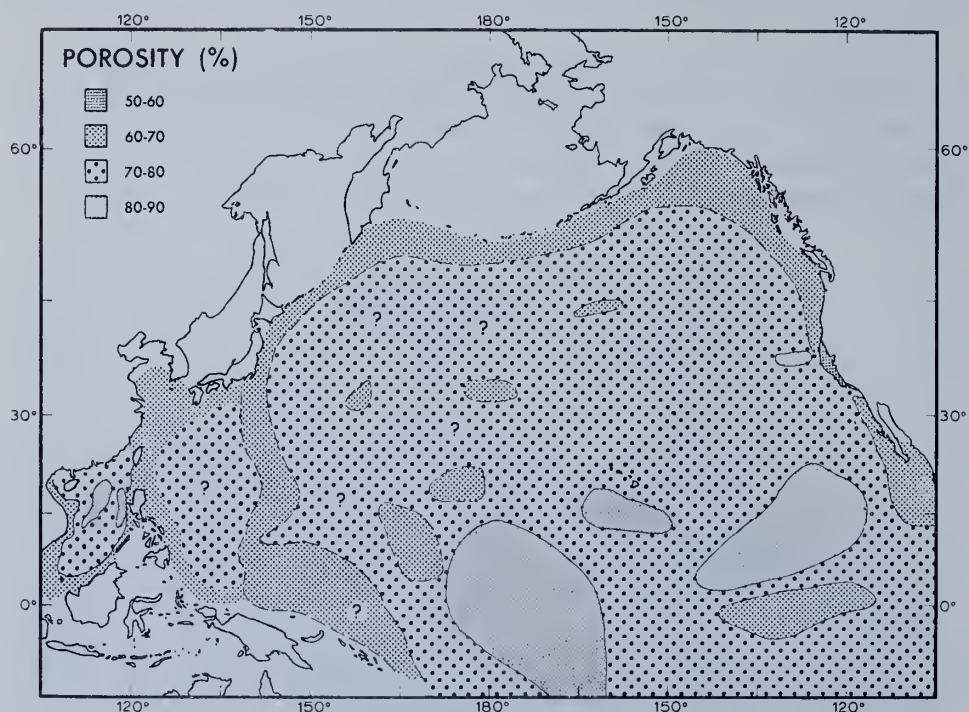


Fig. 10

Discussion

Observations made thus far show clearly a direct relationship between sediment type and the mass physical properties as might be expected. A direct relationship between mass properties and such factors as water depth or ocean currents is also observed in some areas. The isolated patches of various parameters seen in Figures 3 through 10 can with some degree of certainty be attributed to the influence of local bottom topography and currents although there may not be any change in the sediment type in the area of these variations.

In addition to the basic relationships between such parameters as cohesion, water content, bulk density and porosity which have been discussed by various authors, (Terzaghi and Peck, 1948; Hamilton and Menard, 1956; and Richards,

1962), some generalizations can be made based on the present study. The extensive "red clay" deposits commonly possess high water content and porosity, but low shear strength and bulk density. Exceptions to this are usually in areas affected by variation in the sea-floor topography. Calcareous deposits are more or less the opposite with relatively low water content and porosity, but with high shear strength and bulk density. The presence of various types of skeletal debris along with the cementation characteristics of certain calcareous deposits accounts strongly for a wide variation of mass properties from one deposit to another.

Mass properties in coastal areas vary considerably from area to area because of the influence that local drainage and currents have on the depositional environment. In the vicinity of major rivers shear strength and bulk density are relatively low, whereas porosity and water content values are higher than those found on the deep-sea floor.

The area east of Greenland deserves special mention because of its noticeable difference from the other areas studied. This area is a small basin in itself and is strongly influenced by both currents and inflow of sediment from the adjacent land masses. The low water content and high bulk density values can be attributed to the generally coarse and probable heavy-mineral-rich deposits in this basin. The presence of relatively low shear strength values in this same area cannot readily be explained. The low strength values are generally found in conjunction with clayey sediments which possess high water content and low densities. The possibility that these samples were overly disturbed cannot be ruled out.

The data presented here now give us some indication of the range of mass physical property values we can expect to find in the surface sediments — .3 to 3.3 m — of the North Pacific and North Atlantic basins.

In areas where data are not available, the values shown are extrapolated from known values occurring in similar sediments and water depths. It must be kept in mind that relatively crude sampling techniques were used in obtaining most of the sediment samples. Shear strength values are reduced considerably as the amount of sample disturbance increases. Although many of the samples were collected with improved coring devices such as the Hydro-plastic corer (Richards and Keller, 1961), the samples are far from being undisturbed. With the advent of in-place measurements on the sea floor by means of instrumentation such as the nuclear sediment density probe (Keller, 1965), it can be expected that significant discrepancies will be found when comparing these new data with those available today.

It is anticipated that as more data are collected, the distribution patterns of these various parameters will increase in complexity. The Atlantic Ocean, with its mid-ocean ridge and great influx of terrigenous sediment, will display a greater variation and complexity than presently seen. On the other hand, relatively little change in the distribution pattern is expected over much of the North Pacific as a result of the more uniform depositional environment found there. Greater lateral

variation than is presently observed can be also expected in the low latitudes of the southwest North Pacific where numerous islands and trenches interrupt the sea floor.

Summary

Although the 500 sediment cores used in this study represent only a small portion of the North Atlantic and North Pacific sea-floor, it is possible to gain some insight into the distribution of various mass physical properties and the range of values that can be expected in these basins.

- (1) Sediment types vary considerably between the North Atlantic and North Pacific basins. The vastness and remoteness of the North Pacific as well as its great depth is clearly reflected in the extensive deposits of "red clay". Sediments of the smaller North Atlantic basin tend to be coarser and possess higher percentages of calcium carbonate as shown by the vast deposits of fluvial-marine and calcareous ooze deposits. This is attributed, in part, to the extensive drainage into the Atlantic and to the relatively shallow water depths found there. Siliceous oozes are noticeably absent from the North Atlantic, but do occur in some portions of the Pacific.
- (2) Shear strength varies from 17 to 175 g/cm² and commonly is within a range of 35 to 105 g/cm². In comparison, sediments of the North Atlantic appear to be slightly stronger than those of the North Pacific.
- (3) Water content varies from 50 to 375 per cent, and ranges between 50 and 100 per cent in the North Atlantic and between 100 and 200 per cent in the North Pacific. The finer Pacific sediments possess a considerably higher water content than the relatively coarser sediments of the North Atlantic.
- (4) Sediment bulk densities are found to range from 1.18 to 2.00 g/cm³, but more frequently vary from 1.25 to 1.75 g/cm³. Bulk densities are generally lower in the North Pacific — 1.25 to 1.52 g/cm³ — than in the North Atlantic — 1.52 to 1.75 g/cm³.
- (5) Observed porosity values range from 40 to 50 per cent, but usually vary from 60 to 80 per cent. Sediment porosities are considerably higher in the North Pacific than in the North Atlantic.

The data presented here clearly reflect the contrasting depositional environments of the North Atlantic and North Pacific. The remoteness of the Pacific basin to land areas is indicated by the extensive deposits of "red clay". These sediments possess relatively high water contents and porosities, but low shear strengths and bulk densities. Carbonate deposits in the low latitudes of the Pacific generally display higher shear strengths and densities, but lower water contents and porosities than the "red" clay to the north.

In contrast to the Pacific, the North Atlantic sediments possess lower water contents and porosities, but higher shear strengths and bulk densities. Although

this study shows a rather simple distribution pattern for the various parameters in the North Atlantic, it is expected that this will increase in complexity as more data become available.

References

- Arrhenius, G. (1963): Pelagic sediments, in *The Sea: Ideas and observations on progress in the seas*. M. N. Hill (ed.), Vol. 3, pp. 655—727.
- Evans, I. and Sherratt, G. G. (1948): A simple and convenient instrument for measuring the shear resistance of clay soils. *Jour. Sci. Instruments and Physics in Industry*, Vol. 25, pp. 411—414.
- Fisk, H. N. and McClelland, B. (1959): Geology of continental shelf off Louisiana: its influence on offshore foundation design. *Geol. Soc. Amer. Bull.*, Vol. 70, pp. 1369—1394.
- Hamilton, E. L. (1956): Low sound velocities in high porosity sediments. *Jour. Acoust. Soc. America*, Vol. 28, pp. 16—19.
- (1959): Thickness and consolidation of deep-sea sediments. *Geol. Soc. Amer. Bull.*, Vol. 70, pp. 1399—1424.
- (1964): Consolidation characteristics and related properties of sediments from experimental Mohole (Guadalupe site). *Jour. Geoph. Res.*, Vol. 69, pp. 4257—4269.
- Hamilton, E. L. and Menard, H. W. (1956): Density and porosity of sea-floor surface sediments off San Diego, California. *Amer. Assoc. Petrol. Geol.*, Vol. 40, pp. 754—761.
- Hamilton, E. L., Shumway, G., Menard, H. W. and Shipek, C. J. (1956): Acoustic and other physical properties of shallow-water sediments off San Diego. *Jour. Acoust. Soc. Amer.*, Vol. 28, pp. 1—15.
- Harrison, W., Lynch, M. P. and Altschaeffl, A. G. (1964): Sediments of lower Chesapeake Bay, with emphasis on mass properties. *Jour. Sed. Petr.*, Vol. 34, pp. 727—755.
- Igelman, K. R. and Hamilton, E. L. (1963): Bulk densities of mineral grains from Mohole samples (Guadalupe site). *Jour. Sed. Petr.*, Vol. 33, pp. 474—478.
- Keller, G. H. (1964): Investigation of the application of standard soil mechanics techniques and principles to bay sediments, in *Proc. 1st U. S. Navy Symposium of Military Oceanography*, pp. 329—360.
- (1965): Deep-sea nuclear sediment density probe. *Deep-Sea Res.*, Vol. 12, pp. 373—376.
- Keller, G. H., Richards, A. F. and Recknagel, J. H. (1961): Prevention of water loss through CAB plastic sediment core liners. *Deep-Sea Res.*, Vol. 8, pp. 148—151.
- Moore, D. G. (1962): Bearing strength and other physical properties of some shallow and deep-sea sediments from the North Pacific. *Geol. Soc. Amer. Bull.*, Vol. 73, pp. 1163—1166.
- (1964): Shear strength and related properties of sediments from experimental Mohole (Guadalupe site). *Jour. Geoph. Res.*, Vol. 69, pp. 4271—4291.
- Moore, D. G. and Shumway, G. (1959): Sediment thickness and physical properties: Pigeon Point Shelf, California. *Jour. Geoph. Res.*, Vol. 64, pp. 367—374.
- Richards, A. F. (1961): Investigations of deep-sea sediment cores, I. Shear strength bearing capacity, and consolidation. *U. S. Hydrographic Office Tech. Rept.* 63, 70 p.
- (1962): Investigations of deep-sea sediment cores, II. Mass physical properties. *U. S. Hydrographic Office Tech. Rept.* 106, 146 p.
- Richards, A. F. and Keller, G. H. (1961): A plastic-barrel sediment corer. *Deep-Sea Res.*, Vol. 8, pp. 306—312.
- (1962): Water content variability in a silty clay core from off Nova Scotia. *Limnology and Oceanography*, Vol. 7, pp. 426—427.

- Smith, R. J. (1962): Engineering properties of ocean floor soils. Amer. Soc. for Testing and Materials, Spec. Tech. publ. No. 322, pp. 280—302.
- Taylor, D. W. (1948): Fundamentals of soil mechanics. John Wiley & Sons, Inc., New York, 700 p.
- Terzaghi, K. and Peck, R. B. (1948): Soil mechanics in engineering practice. John Wiley & Sons, Inc., New York, 566 p.
- U. S. Navy Hydrographic Office (1955): Instructions manual for oceanographic observations. Hydrographic Office Publ. No. 607, Washington, 210 p.

[Manuscript received August 8, 1967]

East-West Profile from Kermadec Trench to Valparaiso, Chile

G. H. KELLER AND G. PETER

Atlantic Oceanographic Laboratories, ESSA, Miami, Florida 33130

Introduction. Although several studies have been made of parts of the East Pacific rise and the Peru-Chile trench, comparatively little is actually known about the tectonic framework of the South Pacific basin. Most tracklines are either short or pursue some form of a sawtooth pattern over a prominent feature. Very few continuous geophysical traverses have been made across the South Pacific. A straight shelf-to-shelf traverse usually offers unique data for studying the bathymetric and tectonic relationships of an ocean basin. In this sense, it is felt that the data presented here will be of value to the scientists investigating this remote area.

During a recent (October 1967) cruise by the ESSA ship *Oceanographer*, the South Pacific was crossed approximately at the 35°S parallel from the Kermadec trench to Valparaiso, Chile. In conjunction with magnetic observations, bathymetric data were obtained with a narrow-beam (3°) echo sounder. Position control was maintained with a satellite navigation system.

Although it is realized that a single traverse frequently raises more questions than it answers, it is felt that in light of the scarcity of data from the South Pacific, attention should be drawn to several features revealed by the data obtained during this cruise. The ship traversed a complex portion of the South Pacific, where three major tectonic features, the Austral seamount chain, the East Pacific rise, and the Chile rise, were the dominant structural elements. Bathymetric and magnetic data are discussed in light of their reflection of the major tectonic elements along the *Oceanographer* traverse.

Austral seamount chain. An area characterized by elevated rough topography and bordered by seamounts ranging in height from 3000 to 3250 meters was located approximately 1610 km west of the crest of the East Pacific rise, between 125°40'W and 132°30'W. These features distinctly set off this segment of the sea floor

from that of the neighboring area (Figure 1). Present charts show that the Austral chain trends in a southeast direction from Samoa to approximately 142°W. By projecting this trend to the southeast, it coincides with the area of rough topography and bordering seamounts just described. The width of the elevated block (352 km) agrees with the approximate width of the Austral chain (282 km) farther to the northwest. In view of the prominence of this feature, it is unlikely that it is an isolated structure. The general NW-SE structural trend of the area (observed on most bathymetric maps) supports the proposed conjecture that it trends NW-SE and possibly represents the extension of the Austral chain. The possibility that this feature is trending mainly north-south was ruled out when it was not observed along an east-west traverse by the *Eltanin* 29 cruise at 28°S.

A further projection of this trend, supported by correlation with a similar feature recorded during the *Eltanin* 20 cruise at 45°S [Pitman and Heirtzler, 1966], intersects the East Pacific rise in the vicinity of 47°S. It is here that the rise undergoes a noticeable change in trend from nearly north-south to northeast-southwest. It may only be a coincidence that the Austral chain intersects the rise in this area, or it may in some way be related to the bend in the rise.

Rift zones. A rift-like depression (1000 meters deep and 20 km wide) was found at the crest of the East Pacific rise at 111°20'W. A similar depression was also observed by the *Eltanin* 21 cruise, which crossed the rise at 40°S [Pitman and Heirtzler, 1966]. Such a feature has not been reported from elsewhere along this rise, and it appears to be only of local extent rather than an extensive median rift.

A pronounced depression was found 250 km east of the crest of the East Pacific rise (designated as G in Figure 1). The feature is 2200 meters deep and varies in width from 16 km at its lip to 1 km at its base. This feature cannot

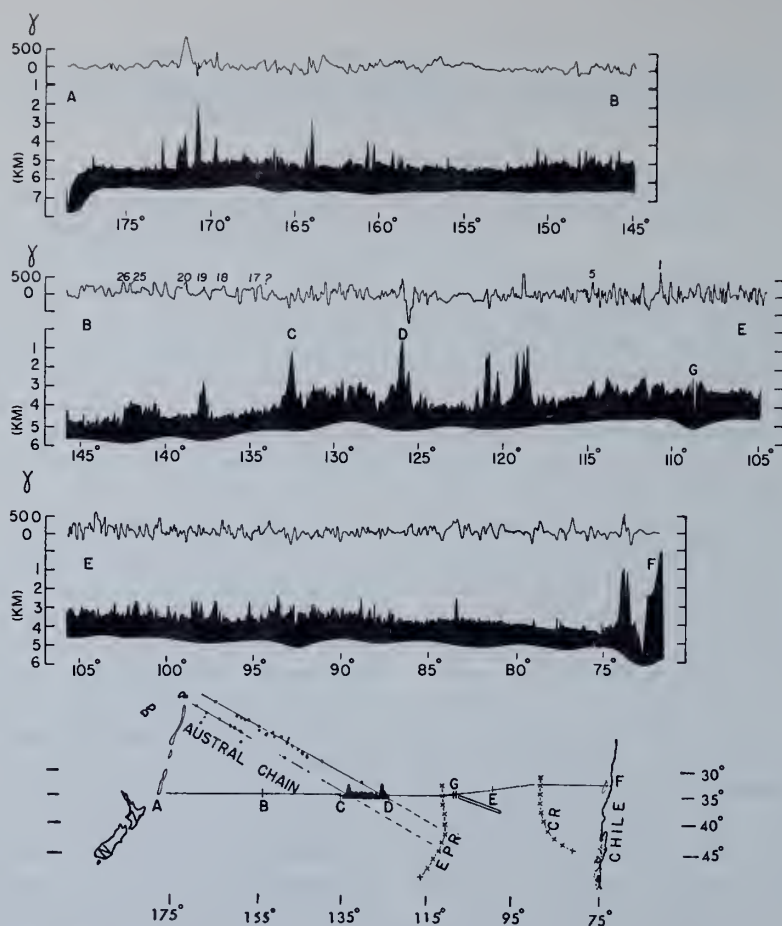


Fig. 1. Bathymetric and magnetic profile from the Kermadec trench to Valparaiso, Chile.

be detected in either the *Eltanin* 21 (40°S) profile to the south or the *Conrad* 8 crossing shown by *Burckle et al.* [1967] farther to the north (30°S). The absence of this rift-like depression to the north and south indicates the unlikelihood that this is a major feature paralleling the East Pacific rise.

The possibility of a transverse fracture trending northwest-southeast and intersecting the east flank of the East Pacific rise in the vicinity of 35°S has been discussed on the basis of seismicity [*Sykes*, 1963] and topography [*Menard et al.*, 1964]. Based on the available data, it is possible that the feature (G) is a portion of this transverse fracture (Figure 1).

Chile rise. Earlier studies of the South Pacific have shown the Chile rise intersecting the East Pacific rise in the vicinity of 35°S [*Menard*, 1961]. As more bathymetric data

become available from this part of the basin, the evidence for an intersection of the two rises appears to become weaker. *Menard et al.*, [1964] proposed that the Chile rise may be a southward extension of the Galapagos rise and that it does not intersect the East Pacific rise at all. Examination of the *Oceanographer* bathymetric profile suggests that the crest of the Chile rise is approximately 1800 km east of the crest of the East Pacific rise, at about 32°S, 91°W. Although this is slightly east of the crest line proposed by *Menard et al.* [1964], it lends support to their deduction that the Chile rise does not intersect the East Pacific rise.

Fault blocks. Several step-like breaks in the sea floor were observed along the *Oceanographer* traverse. They are shown in an idealized sketch of the bathymetric profile (Figure 2) in order to depict the general relationship of the major

topographic features on a single profile. The breaks may be 'north-south' faults, following the tectonic grain of such features as the Kermadec trench, the East Pacific rise, and the Peru-Chile trench, but such a determination cannot be made from a single profile. In each instance, the uplifted portion of the block was to the east and throws varied from 220 to 550 meters. Little or no indication of these faults was observed from the magnetic data. Without additional observations, the extent of these faults and their significance with respect to the structure of the South Pacific basin are not clear.

It is apparent from the bathymetric profile (Figure 2) that in this area there is a distinct difference between the crustal elevation in the eastern and in the western portions of the South Pacific. In the eastern half of the basin (east of 135°W) the mean depth is about 3300 meters; to the west it is commonly in excess of 4000 meters.

Magnetic anomaly pattern. The recognized characteristic worldwide magnetic pattern starts at approximately 148°W. Several prominent anomalies occur west of 148°W, but their character or extent are not known and therefore cannot be correlated with other anomalies reported for the western South Pacific. The western end of the recognized magnetic pattern appears to be compressed, but anomalies 26, 25, 22, 21, 20, 19, and 18 can be identified [Pitman *et al.*, 1968]. Anomaly 17 does not have its typical shape; and from this point eastward to

115°W the pattern cannot be recognized. The Austral chain intersects the pattern between 133° and 125°W, and it is likely the cause for the disruption of the pattern. The anomalies over this volcanic chain are sharper and their higher frequency indicates a shallower source.

The typical crestal type anomalies start at 120°W. A broad anomaly, which does not appear to be part of the worldwide pattern, separates the crestal anomalies and the anomalies related to the Austral chain between 121° and 123°W.

A closer study of the magnetic anomalies suggest that the Austral seamount chain, not only superimposed its magnetic effect on this part of the worldwide magnetic pattern, but also caused (or formed as a result of) a crustal extension. This extension can be measured on the magnetic pattern by comparing the distance between two known anomalies, one on the flank and one on the crest. Because a single distance measurement could be interpreted to be the function of the rate of crustal spreading in a given segment of the sea floor [Vine and Matthews, 1963; Vine, 1966], distance ratios were computed and compared with values for other areas in the Pacific. Comparisons indicate that the distance ratio between anomalies 26 and 18 and anomalies 18 and 5 along this profile is 1 to 4; the ratio between these same anomalies in the North Pacific and elsewhere in the South Pacific is 1 to 2 (measured on the North Pacific standard profile and on EL-19S southeast of New Zealand [from Pitman *et al.*, 1968]). Similar disruption

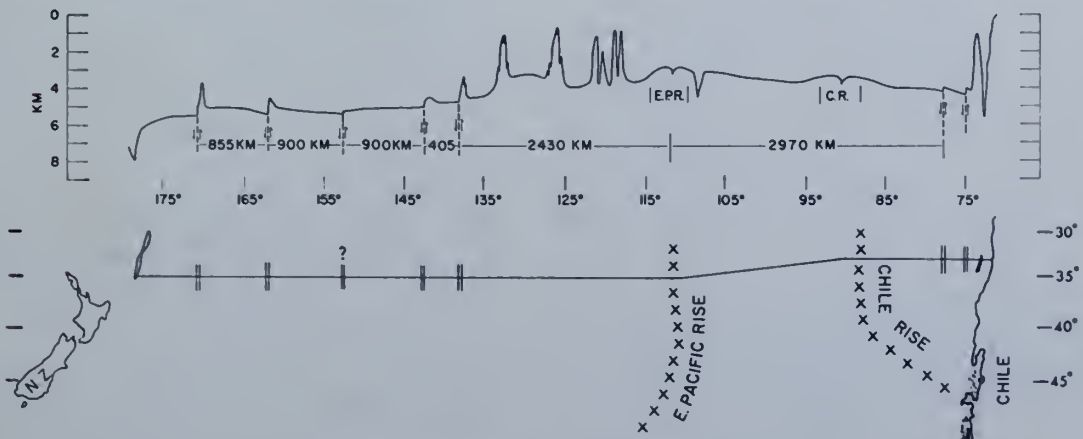


Fig. 2. Generalized bathymetric profile from the Kermadec trench to Valparaiso, Chile, showing the prominent fault blocks.

of the magnetic pattern and new crust formation were suggested by Raff [1962] for the area south of the Murray fracture zone.

The central anomaly (a broad anomaly with three small peaks, indicated as anomaly 1 on Figure 1) is somewhat distorted at this crossing. Axial symmetry, although not obvious, may be carried to anomaly 5 on the eastern side of the East Pacific rise. From this point eastward the magnetic pattern cannot be recognized, possibly because of the tectonic interference from the Chile rise. A recognizable pattern or symmetry does not seem to be associated with the Chile rise. East of 84°W the amplitude and wavelength of the anomalies resemble the typical 'flank anomaly' pattern. The section is too short to identify the pattern, if it is part of the worldwide system, without additional data.

Acknowledgments. We wish to express our appreciation to Robert Fleisher, who assisted in the shipboard portion of this study, and to Dr. Dale C. Krause, who critically reviewed this manuscript.

REFERENCES

- Burekle, L. H., J. Ewing, T. Saito, and R. Leyden, Tertiary sediment from the East Pacific rise, *Science*, *157*, 537, 1967.
- Menard, H. W., The East Pacific rise, *Sci. Am.*, *205*, 52, 1961.
- Menard, H. W., T. E. Chase, and S. M. Smith, Galapagos rise in the southeast Pacific, *Deep-Sea Res.*, *11*, 233, 1964.
- Pitman, W. C., III, and J. R. Heirtzler, Magnetic anomalies over the Pacific-Antarctic ridge, *Science*, *154*, 1164, 1966.
- Pitman, W. C., III, E. M. Herron, J. R. Heirtzler, Magnetic anomalies in the Pacific and sea floor spreading, *J. Geophys. Res.*, *73*, 2069, 1968.
- Raff, A. D., Further magnetic measurements along the Murray fault, *J. Geophys. Res.*, *67*, 417, 1962.
- Sykes, L. R., Seismicity of the South Pacific Ocean, *J. Geophys. Res.*, *68*, 5999, 1963.
- Vine, F. J., Spreading of the ocean floor: New evidence, *Science*, *154*, 1405, 1966.
- Vine, F. J., and D. H. Matthews, Magnetic anomalies over oceanic ridges, *Nature*, *199*, 947, 1963.

(Received June 10, 1968.)

DEPOSITIONAL ANTICLINES versus TECTONIC "REVERSE DRAG"

RICHARD J. MALLOY

Environmental Science Services Administration
Atlantic Oceanographic Laboratories
Miami, Florida

A B S T R A C T

Recent high resolution seismic reflection profiles have revealed the presence of base-of-slope depositional anticlines in the Florida Straits. Depth profiles across Santaren and Nicholas channels are deepest along the sides of the channels at the slope base. Channel axes are somewhat shoaler due to anticlinal deposits of sediment.

A large anticline of deposition covering approximately 3100 square kilometers (900 square nautical miles) has formed adjacent to the Miami Terrace escarpment. Presumably the high energies of the Florida Current have produced this feature on a grand scale by a mechanism believed to be widespread, but little recognized. It is suggested that these asymmetrical base-of-slope anticlines of deposition find their counterpart in ocean basin seamount-moat-swell sequences, along deep sea channels which are flanked by levees of asymmetrical depositional anticlines, and in most other depositional areas of the sea floor where deep currents flow along scarps of locally steep slopes.

The base-of-slope depositional anticline concept, when applied to "reverse drag" anticlines associated with scarps in the Gulf of Mexico and in the ancient sediments of the Gulf Coast, appears to satisfy the data better than previously proposed models. It is concluded, therefore, that depositional anticlines are widespread in space and time.

INTRODUCTION

"When the combined action of waves and currents extends a barrier into deep water, an embankment is formed which, in many cases, becomes of very grand proportions. In the formation of embankments the debris of which they are composed is swept along the surface of the barrier or terrace leading to them and deposited when deep water is reached. This process continues until the embankment has been built up to the water surface . . . Both bars and embankments, where seen in cross-section, having a more or less well-defined anticlinal structure. An arch of this character is termed an anticline of deposition." (Russell, 1888).

Originally "anticline" was a non-generic term, descriptive only of a feature whose strata dipped away in opposite directions from a common ridge or axis. The term, however, has grown to mean strata arched by folding. Anticlines which are known remotely, as by reflection seismology, or fragmentally, as through the bore hole, or casually, are automatically ascribed to folding. This convention that an anticline is necessarily a fold may have caused other mechanisms to be overlooked. Deposition has been relegated to an insignificant role in the formation of anticlines. The presence of large anticlines of deposition in the Florida Straits and elsewhere suggests that their importance as contributors to continental geology should be reassessed.

To what extent the mechanism of deposition is actually involved in the formation of anticlines is problematic. If the mechanism is extensive, the problem is one of recognition, and a review of depositional anticlines presently forming on the sea floor may serve as a key to their being recognized in the geologic records of the past.

DEPOSITIONAL ANTICLINES IN THE
FLORIDA STRAITS

Figure 1 is a bathymetric map of a portion of the sea floor east of Miami, Florida (from Kotoed and Malloy,

1965). Proceeding from west to east the map shows a north-south scarp formed at the seaward terminus of prograded sediments (Uchupi, 1966). The surface of the Miami Terrace slopes less than one degree to the southeast. Where sediment-free, the terrace is deeply etched by karstlike topography. Unconsolidated sediments are ponded synclinally, trapped behind the coral reefs which lip the outer edge of the terrace. The Miami Terrace extends eastward to what appears to be a sediment-free limestone slope which forms the western side of a long, closed trough. East of this trough is a broad rise which slopes eastward down to the flat, central portion of the strait.

Figures 2, 3, 4, and 5 are seismic reflection profile records with the tracklines shown in Figure 1. A 3000-joule arcser with a 12', 10-phone array was used to obtain the high resolution records. Echo events were recorded unfiltered. The scarp of progradation, terrace, slope, trough, and rise are shown in Figure 4. It is clear from the seismic profiles that the sediment rise is anticlinal, strongly asymmetrical, with an internal structure which shows that the axial plane has migrated westward with building of the anticline. The strata thicken westward, toward the limestone slope. If the flat floor of the strait (east of the anticline) is projected beneath the anticline, the sediment thickness above this projected floor measures 457 m (1500') based on the minimal sound transmission velocity of 1463 m/s. On Cross-section B-B' the western dip-slope of the anticline measures a maximum of $4\frac{1}{2}^\circ$ and the gentle eastern dip-slope measures less than 1° . The anticline extends from $25^\circ 10'N$ to $26^\circ 10'N$, a distance of 111 km (60 nm) and ranges in width from 22 km to 37 km (12 nm to 20 nm). This anticline has an area of about 3100 square km (900 square nm) with a maximum structural closure in cross-section of about 293 m (960'). In addition to the western flank of the major anticline, Figure 5 shows a smaller, buried anticline formed against the sub-surface extension of the scarp of the Miami Terrace escarpment. Both flanks dip approximately 7° .

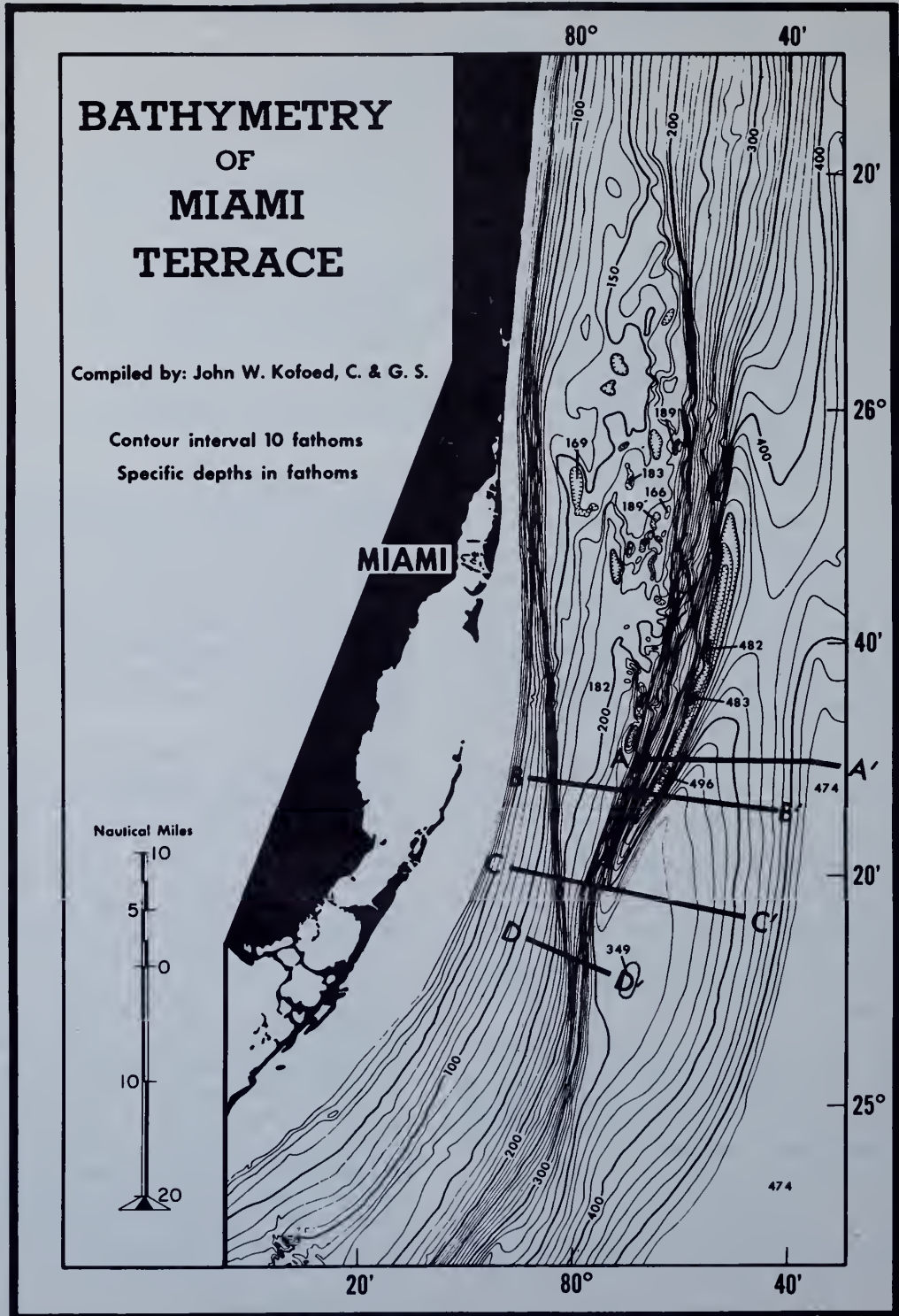


Figure 1. Bathymetric map of the Miami Terrace, escarpment, trough, and rise. Location of seismic profiles is shown. Figure from Kofoid & Malloy (1965).

Base-of-slope trough and rise deposits are common in the Florida Straits. Off Miami Beach at the base of the Miami Terrace escarpment (Fig. 1) there is a well-developed trough-rise sequence. In Santaren and Nicholas channels on either side of Cay Sal Bank, which lies 185 km (100 nm) south of Miami, Florida, the sea floor is deeper on either side of the narrow straits than in the middle of the channels (unpublished map). These troughs are separated in each instance by a sediment accumulation with anticlinal structure.

Cross-section A-A' (Fig. 2) shows the entire width of the anticline off Miami Beach. The crest of the anticline is at 677 m (370 fathoms) and the trough depth is 851 m (465 fathoms). Cross-section B-B' (Fig. 3) shows the crest depth to be 650 m (355 fathoms) and the trough depth at 851 m (465 fathoms). On Cross-section C-C' (Fig. 4) the crest rises to 631 m (345 fathoms). These data show the anticline to have a north plunge.

Megascopic examination of several short cores taken on the rise shows the sediment to be predominantly fine calcareous sand. R. Dietz and J. Kofoed dived in the Aluminant to the bottom of the long, closed trough at the base of the terrace escarpment (Fig. 1) and reported (personal communication) the bottom sediment as coarse to pebble-sized shell fragments.

Shown on Cross-section D-D' (Fig. 5) is a smaller buried anticline. The seaward margin of prograding sediments has coincidentally formed a gentle scarp directly above the buried anticline. The escarpment of the buried Miami Terrace forms the slope against which this base-of-slope anticline has formed. Each flank has an apparent dip of about 7°.

SIMILAR FEATURES

Much of the sea-floor topography in the Florida Straits is formed by base-of-slope depocenters. An examination of these and similar features may suggest a common cause.

Base-of-slope Trough and Rise Deposits:

Circumvolcanic moats and associated rises are probably the best known examples of base-of-slope features. Originally they were believed to be caused by isostatic sinking of the volcanic mass (Menard and Dietz, 1951), and their genesis was later made an issue in the subsidence-versus-erosion (or differential deposition) controversy by Dietrich and Ulrich (1961). Based on seismic reflection profiling evidence, such features recently have been considered to be caused by differential deposition (Hamilton, 1967). These seismic profiler data show the seamount-associated rises to be gently anticlinal. Hamilton (1967) pointed out that the nondepositional moat is not to be confused with the huge moats and arches described by Menard (1964) which encircle the Hawaiian Islands where the crest of the arch lies out 150 km to 180 km (81 nm to 97 nm) from the volcanoes, or with the Line Islands' crest which lies 240 km (130 nm) from the land mass. These moats range from 0.5 km to 1.5 km (1640' to 4920') in relief, which is also the elevation of the arch above the surrounding sea floor. However, Menard and Dietz (1951) described several volcanic moats whose magnitude could be ascribed to differential deposition. Menard and Dietz (1951) showed profiles of seamounts in the Gulf of Alaska seamount province with the moats ranging in relief from 9 m

to 183 m (30' to 600') and with the crests of the arches ranging from 3.7 km to 13 km (2 nm to 7 nm) from the base of the volcanic slope. The slopes of the volcanoes range upward to 16°, but most are more gentle. The slopes of the arches are very gentle, usually in the 1° to 3° range. Moated seamounts are not peculiar to the Pacific. Figure 6 shows a seamount in the North Atlantic encircled completely by a moat and partially by an arch.

Bottom profiles and sparker lines from widely scattered areas reveal that the scarp-associated trough and rise sequence is widespread. Detailed sparker work in the Gulf of Maine (Malloy and Harbison, 1965) showed that most of the bedrock basins were only partially filled with sediments and that many of the basins had well-developed troughs at the bedrock-sediment contact. Depressions at the base of fault scarps southwest of Montague Island, Alaska, occur at the bedrock-sediment contact (Malloy and Merrill, in press). Dowling (1968), using seismic reflection profiling data, reported a base-of-slope trough and anticlinal rise (suggestive of deposition) at the base of the Sigsbee Scarp in the Gulf of Mexico, which he ascribed to tectonism. Weeks et al. (1967) show several examples of subsurface "reverse drag" in the seismic reflection profile records made in the Andaman Sea. Their Figure 5 shows a base-of-slope trough and anticlinal rise in the southern part of the Andaman Sea. Lowrie and Heezen (1967) described a base-of-slope deposit formed against a knoll near Hudson Canyon. A 12-kHz echo sounder showed the accumulation to be anticlinal. Lowrie and Heezen (1967) list other areas of moated knolls: in the Mediterranean off Gibraltar, in the Canary Passage, and on the Crozet Plateau in the Indian Ocean.

Leveed Seachannels:

Leveed seachannels were shown by Buffington (1952) to have a wide distribution. They were suggested by Kuenen (1950) to be depositional, and this interpretation was later corroborated by Hamilton (1967) using seismic reflection profiling data.

Figure 7 shows a portion of a fathogram made by crossing normal to a leveed seachannel in the Gulf of Alaska Abyssal Plain. Including both levees, this seachannel measures 70 km (38 nm) across. The higher levee is elevated 137 m (450') above the surrounding sea floor. The channel relief (measured to the higher levee) is 91 m (300') and the channel width (levee crest to levee crest) is 7.4 km (4 nm) (P. J. Grim and F. P. Naugler, in preparation).

PROBABILITY OF ONE CAUSATIVE MECHANISM

The universal asymmetry of these anticlinal deposits, with their steeper limbs flanking axes of bottom-current concentration, suggests that they are caused by a common mechanism.

It is suggested that the base-of-slope trough and anticlinal rise sequence is caused by the periodic deposition of sediment by bottom contour currents which are naturally channeled against a scarp to form a high-energy zone along it. The sea floor beneath the high-energy concentration becomes an elongated zone of less deposition than the bottom adjacent to it. The scarp-concentrated high current energy disallows sedimentation to occur, and any sediment which may have been delivered to the site of the scarp either by pelagic sedi-

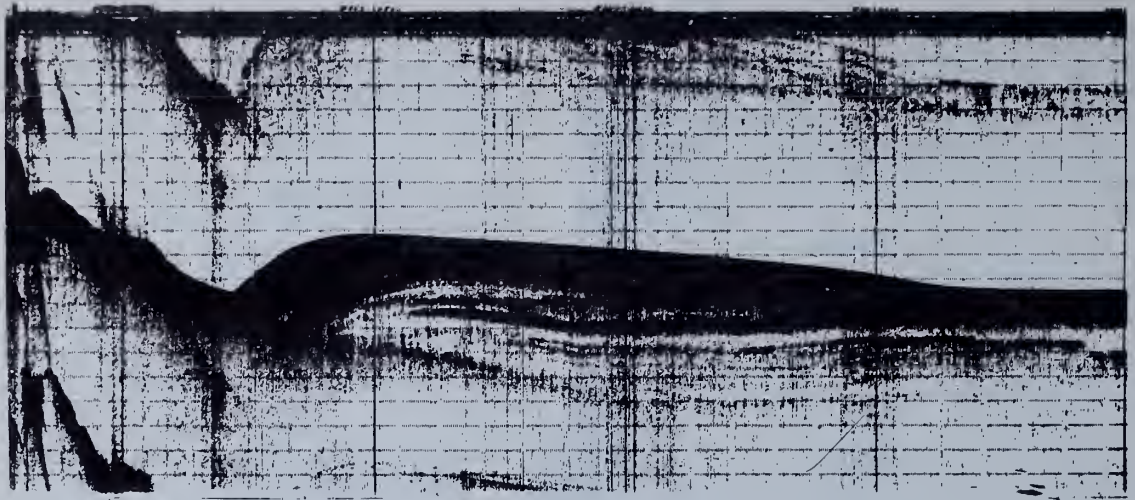


Figure 2. Seismic reflection profile A-A' (location on Fig. 1). Vertical lines mark fixes every 30 minutes, or 4 nm. Record was made using a 2-second sweep marked off in .1 second increments (40 fathoms in sea water).

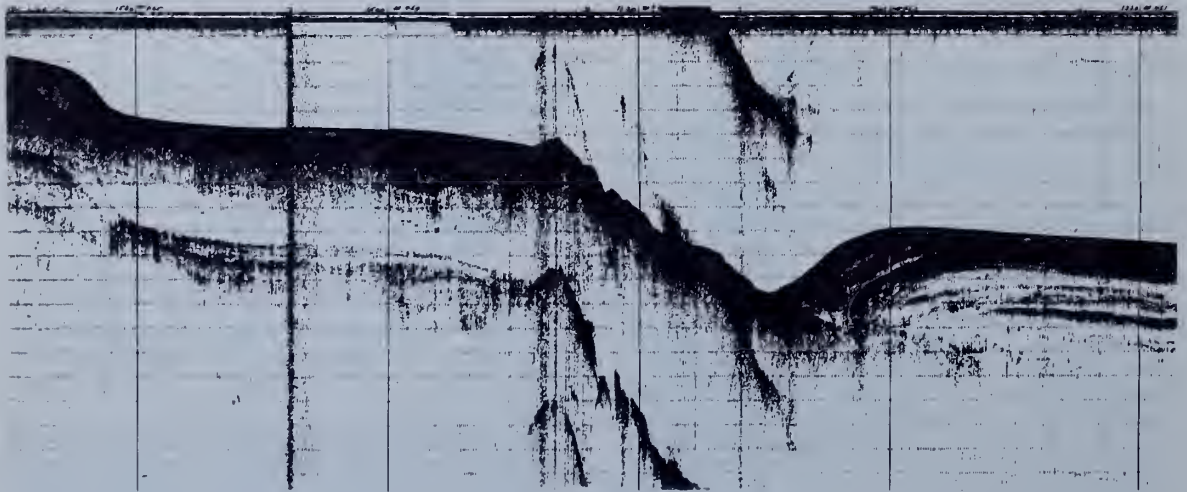


Figure 3. Seismic reflection profile B-B' (location on Fig. 1). Vertical lines mark fixes every 30 minutes, or 4 nm. Record was made using a 2-second sweep marked off in .1 second increments (40 fathoms in sea water).

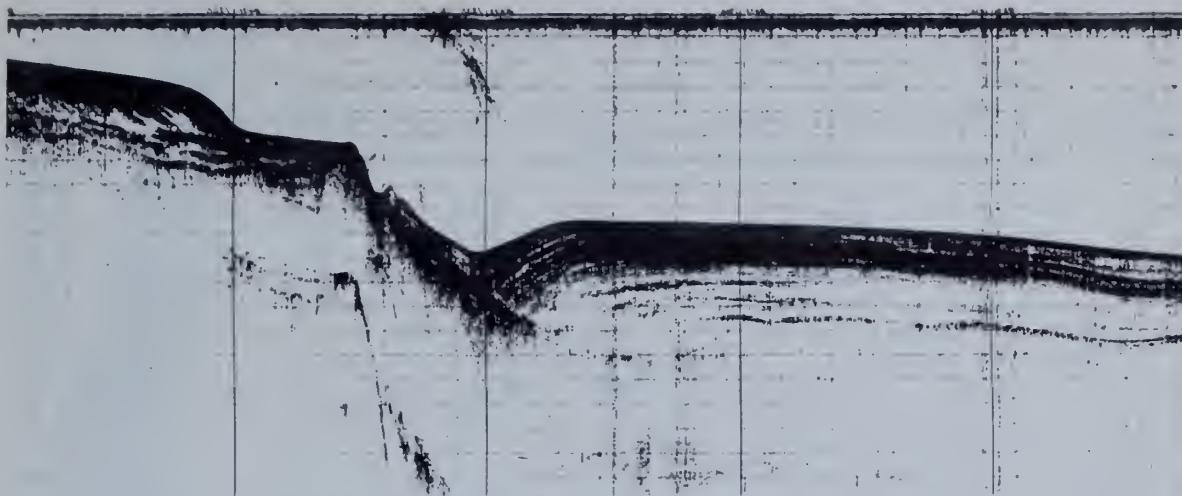


Figure 4. Seismic reflection profile C-C' (location on Fig. 1). Vertical lines mark fixes every 30 minutes, or 4 nm. Record was made using a 2-second sweep marked off in .1 second increments (40 fathoms in sea water).

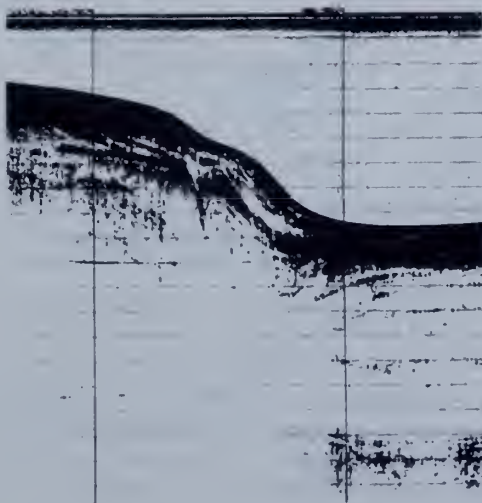


Figure 5. Seismic reflection profile D-D' (location on Fig. 1). Vertical lines mark fixes every 30 minutes, or 4 nm. Record was made using a 2-second sweep marked off in .1 second increments (40 fathoms in sea water).

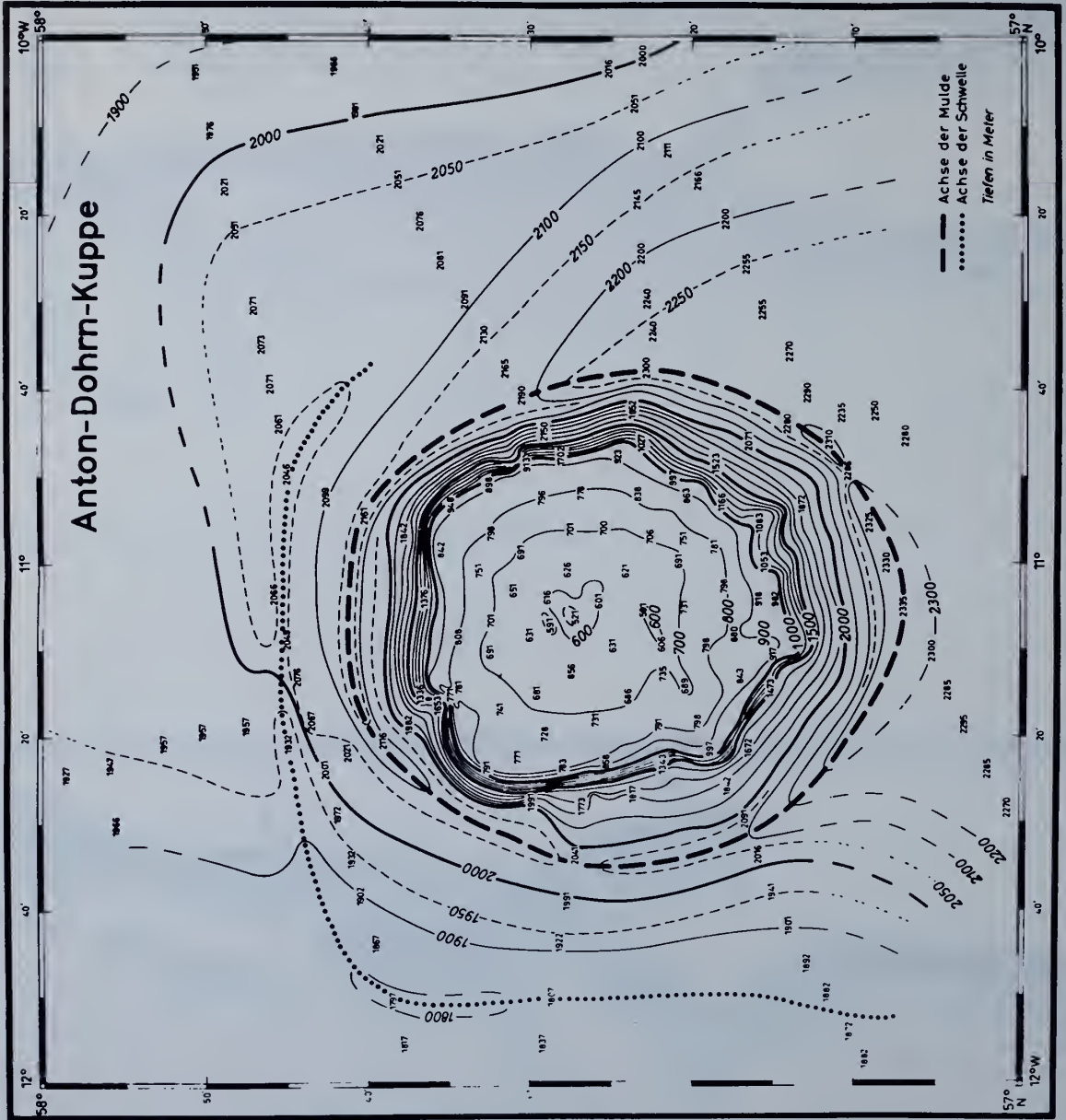


Figure 6. Bathymetry of an Atlantic seamount published by Dietrich and Ulrich (1961).

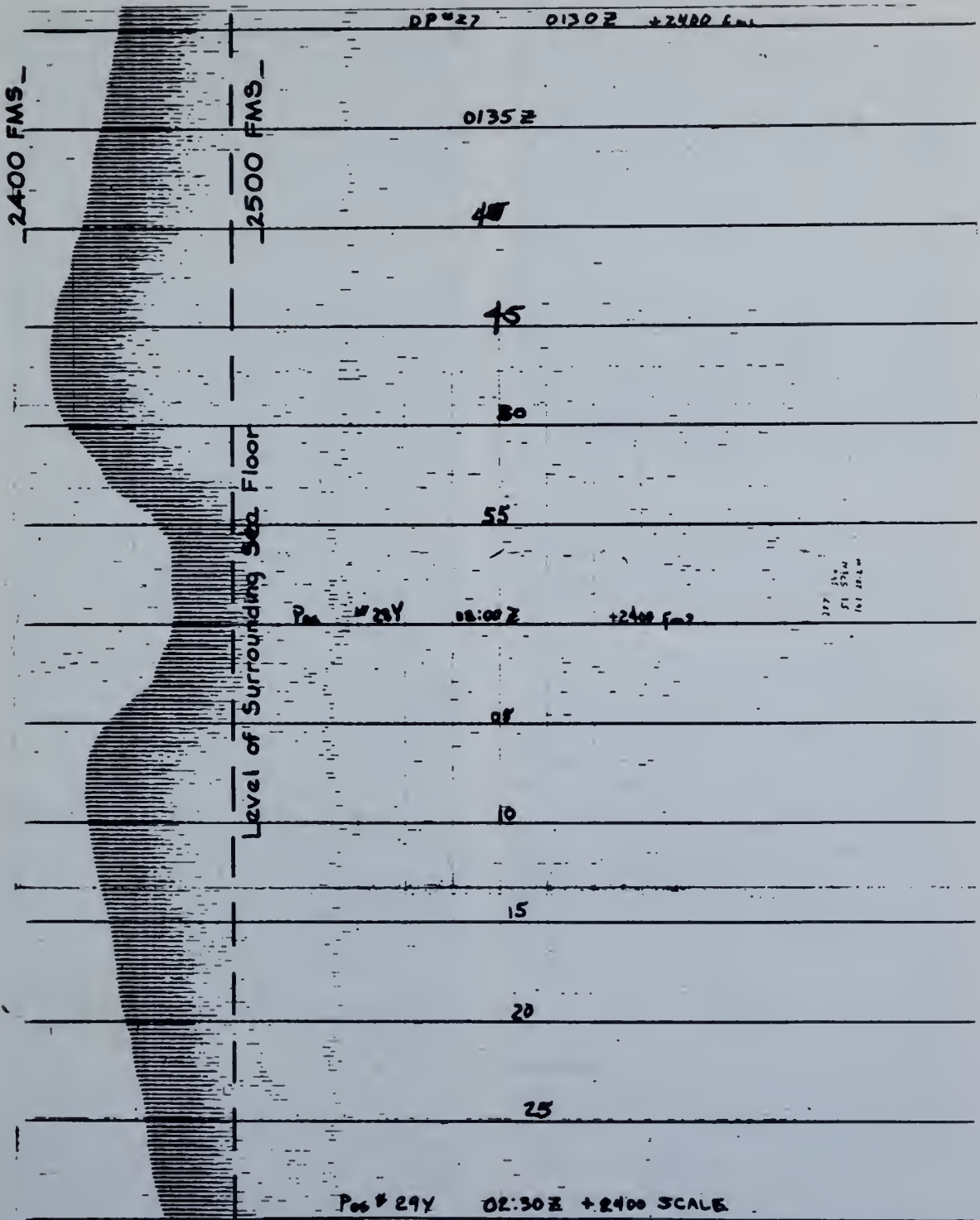


Figure 7. Fathogram record of a seachannel crossing in the Gulf of Alaska Abyssal Plain, courtesy of P. Grim and F. Naugler (in preparation). Axis is at 51°57.5'N, 161°28.2'W. View is down channel, looking west. Horizontal lines are 36.6 m (20 fathoms) based on a sound transmission velocity of 4800 f/s (1463 m/s). Vertical lines are 5 minute fix marks, approximately 1.25 nm apart. Complete dimensions are in text.

mentation or by current transport will be deposited as close to the scarp as the energy balance will allow. As with a leveed seachannel and the Miami Terrace anticline, initial deposition will be at some distance from the axis of high-energy concentration. But subsequent deposition will be affected by this new sea-floor topography in that a migration of the sediment accumulation will take place pressing closer to the high-energy zone as the levee is constructed. By repetition, this phenomenon eventually builds a levee which is self-perpetuating and becomes more effective as a depositional barrier with each spillover. Eventually equilibrium will be attained for the forces acting on that particular area of the sea floor. Current velocity, sediment load, grain size, and scarp height and slope probably represent the principal parameters which will affect the topographic and structural architecture of the equilibrium state. Apparently, however, turbidites and other deposited marine sediment will sculpture roughly the same final scene under widely varying conditions of the four parameters of current velocity, sediment load, grain size, and dip of the scarp slope. This is suggested strongly by the fact that depositional anticlines are presently being formed in such diverse environments as the abyssal depths of the Pacific and Atlantic oceans, around volcanic slopes, on either side of seachannels reported in all oceans, in the Florida Straits, at the base of the Sigsbee Scarp in the Gulf of Mexico, etc.

The crest of the elongated scarp-parallel deposit is believed to migrate toward the fault plane or scarp until the scarp-facing dip-slope reaches its maximum angle dictated by the energies involved and the type of sediment. At any rate, as with its analog, the seachannel levee, the feature will be built upward in time, flanked with its up-slope scarp until the scarp is covered.

PROBABILITY OF PRESERVATION

Which depositional anticlines, if any, will be preserved in the geologic record: (1) The seamount-associated, (2) the seachannel-associated, or (3) the sea-scarp-associated features? If sea floor spreading, as amplified by Dietz (1966) is valid, then features formed in the true oceanic province are destroyed as they became accreted to the continental mass. Thus, the seamount girdling anticlines and the twin anticlines of the seachannels of the abyssal sea floor would not survive their being welded to the continent. Anticlines which form in intra-cratonic basins of deposition would, however, be expected to survive. As the basin subsides under the weight of sediment deposition, base-of-slope depositional anticlines should be preserved and remain recognizable in the section, although their flanks may have been steepened by gravity folding. Their asymmetry and juxtaposition to scarps would be expected to survive post-depositional folding and uplift.

The principle of uniformitarianism suggests that these base-of-slope anticlines have formed in the geologic past. That the features are depositional suggests that they have been preserved in the record. That anticlines have been the object of extensive, world-wide surface and subsurface search since the announcement of the anticline theory of oil accumulation in 1860 suggests that these depositional anticlines have also been found, but not recognized.

UBIQUITY OF CONTEMPORANEOUS NORMAL FAULTING

The intra-cratonic basin of deposition provides the necessary conditions (sedimentation and basinward-facing scarps)

for forming base-of-slope, anticlinal deposits. Hardin and Hardin (1961) have demonstrated the wide occurrence of normal faults which strike parallel to the bottom contours in the Gulf of Mexico. They point out that most of these faults are contemporaneous — that is, movement occurred during deposition. All contemporaneous faults observed by Hardin and Hardin (1961) were normal and displayed thicker sections on the down-thrown side of the fault. Contemporaneous faults are also known as growth faults, depositional faults, progressive faults, and sometimes hinge-line faults.

Most faults in the Gulf of Mexico are "contour" faults — that is, they strike parallel to the bottom contours. They are also termed "strike faults," since the slopes of the Gulf of Mexico are essentially dip-slopes. On the Gulf Coast these faults occur in broad, curved zones which parallel the coast from eastern Louisiana into northeastern Mexico, becoming progressively younger toward the Gulf. Faults similar in character, and possibly identical in origin to Gulf Coast regional contemporaneous faults, occur in the Ganges-Brahmaputra Delta (Sengupta, 1966), the Niger Delta (Short and Stauble, 1967), and the McAlaster Basin of Oklahoma (Koinm and Dickey, 1967).

DEPOSITIONAL ANTICLINES VERSUS TECTONIC "REVERSE DRAG"

Conditions appear to be favorable for the formation and preservation of depositional anticlines in intra-cratonic basins, but they have not been reported. The well-known and commonly-occurring "reverse drag" anticline is strikingly similar to the scarp-associated depositional anticline in shape, size, and habitat.

There have been many explanations set forth as to the forces which form "reverse drag" anticlines. The recently-proposed mechanism of Hamblin (1965) and Cloos (1968) is widely employed. Dowling (1968) uses this mechanism in explaining a large "reverse drag" anticline at the base of the Sigsbee Scarp in the north-central Gulf of Mexico.

Hamblin (1965) reviewed the published explanations of the mechanism for forming "reverse drag" anticlines on the down-thrown side of normal faults. Hamblin (1965) concluded that normal fault "reverse drag" is attributable to the transected beds of the hanging wall sagging into the gap opened by horizontal extension. His explanation continues by suggesting that these forces are the same which form antithetic faults, but that failure occurs by folding, not by fracturing. Cloos (1968), working with clay models, reported success in creating hanging-wall reverse drag by subjecting modeling clay to simple tension, although in order for the model to effect "reverse drag" it appeared necessary to thin the clay strata by erosion, a phenomenon rarely, if ever, observed in nature.

The conditions necessary to form anticlines by tectonic sag also satisfy the conditions necessary to form anticlines by deposition. In a basin subsiding by the weight of clastic deposits and compaction, normal faults are commonly formed. These faults dip basinward and strike parallel to the bottom contours and also to the structural strike of the subsurface. The fault planes have been shown to dip less at depth, which is the crux of the tectonic sag explanation. As set forth by Hamblin (1965), the near-surface vertical forces of gravity

are translated along the fault plane into horizontal forces at depth. This horizontal tension affects the steeper, shallower reaches of the fault to cause the two fault blocks to pull apart. Into this "incipient gap" the strata of the down-thrown block sag, producing the asymmetrical anticline.

Since most of these normal faults are contemporaneous, causing a thicker sequence of strata on the down-faulted block, the fault must have reached the surface to form a scarp. The formation of the commonly-observed roll-over at the base of normal faults can be explained by deposition against this sea scarp by the mechanism suggested herein for the formation of the depositional anticlines forming on the sea floor today.

Both models appear to satisfy the observed data, with exceptions. The shortcomings of the tectonic sag model include:

(1) Observations by Dickey et al. (1968) in southwestern Louisiana include: "The stratigraphic units which are over-thickened on the down-thrown side may thin for a few miles, although regional thickening is to the south. This situation results in a northward dip in the deeper horizons, contrary to the regional southward dip. This dip reversal often provides structural closure for the oil and gas fields." Thinning of sediments is best explained by differential deposition or erosion, and erosion would not be expected to occur on the down-thrown block of a contemporaneous fault.

(2) Another objection to the tectonic sag model is found in figures published by Hamblin (1965). His Figure 11 (pictured here as Figure 8) is depicted as "showing typical reverse drag in the Gulf Coast area." But the beds forming the crestal axis of the anticline are *higher* than the beds of the upthrown side of the fault. This is particularly clear when the beds of the footwall are projected through the fault *below* their correlatives. For these beds to have sagged into the reverse drag posture calls for post-depositional normal faulting. But the apparent movement contradicts this. This "reverse drag," however, comports with depositional "reverse drag," where normal faulting preceded deposition. The mechanics of deposition against this slope could have produced the typical trough-rise relationship. The same difficulty is experienced in explaining Hamblin's (1965) Figure 10 (down-thrown strata are shown higher than upthrown correlatives) with the same solution offered: post-fault deposition of the trough-rise sequence. The same difficulty in the tectonic sag model is brought out by a figure published by Short and Stauble (1967). Their Figure 8 shows beds forming the crestal axis of the "reverse drag" anticline as being structurally higher than the regionally dipping beds of the upthrown block.

(3) Another characteristic of "reverse drag" anticlines is the close-spaced facies changes which occur along the strike of the roll-over. The depositional model explains these observed data better than the tectonic sag model.

(4) An objection to the tectonic model is its lack of uniformitarianism as compared to the deposition model. The depositional anticlines presently forming on the sea floor are outlined in the dip-slope topography of the sea floor. The trough-rise sequences at the slope bases are too common to suppose that they have all been simultaneously sagged into that posture. The anticline of deposition is, on the other hand, a topographic rise throughout the major part of its

cycle of development, thus the ubiquitous moats and rises, and troughs and rises along sea scarps suggest this more uniformitarianistic model for the formation of normal fault "reverse drag" anticlines.

(5) A final argument against the formation of the base-of-slope trough-rise sequences by de-collation can be found in considering the leveed seachannel. No slope is involved. Asymmetrical anticlinal deposits are seen to form on either side of an axis by periodic turbiditic spillover.

CONCLUSIONS

Depositional anticlines have been shown to be widely reflected in the topography of the sea floor. A mechanism other than tectonic sag has been shown to be capable of producing "reverse drag" similarly at the base of normal faults and other sea scarps. Base-of-slope anticlines have probably formed in intra-cratonic basins, and have been preserved, but have remained unrecognized. The ultimate resolution of which folds are tectonic and which are depositional will follow only after additional research specifically addressed to this issue. Depositional anticlines steepened by post-burial tectonism may prove to be a common occurrence, synthesizing in nature two mechanisms made diametric by this discussion.

REFERENCES

- Buffington, E. C., 1952, Submarine "Natural Levees": *J. Geol.*, v. 60, p. 473-479
- Cloos, Ernst, 1968, Experimental Analysis of Gulf Coast Fracture Patterns: *Amer. Assoc. Petrol. Geol. Bull.*, v. 52, no. 3, p. 420-464
- Dickey, P. A., Shriram, C. R., and Paine, W. R., 1968, Abnormal Pressures in Deep Wells of Southwestern Louisiana: *Science*, v. 160, no. 3828, p. 609-615
- Dietrich, Gunter von, and Ulrich, Johannes, 1961, Zur Topographie de Anton-Dohrn-Kuppe: *Meeresforschungen*, Band XVII, Heft 1, p. 3-7
- Dietz, R. S., 1966, Passive continents, spreading sea floors and collapsing continental rises: *Am. Jour. Sci.*, v. 264, p. 177-193
- Dowling, J. J., 1968, Measurements in the Gulf of Mexico: The Mississippi Delta—DeSoto Canyon Area: Annual Report of the Geosciences Division 1966-67, Southwest Center for Advanced Studies, Dallas, Texas p. 7-8
- Hamblin, W. K., 1965, Origin of "Reverse Drag" on the Downthrown Side of Normal Faults: *Bull. Geol. Soc. America*, v. 76, p. 1145-1164
- Hamilton, E. L., 1967, Marine Geology of Abyssal Plains in the Gulf of Alaska: *Jour. Geophys. Res.*, v. 72, no. 16, p. 4189-4213
- Hardin, F. R., and Hardin, G. C., 1961, Contemporaneous Normal Faults of Gulf Coast and their relation to Flexures: *Amer. Assoc. Petrol. Geol. Bull.*, v. 45, p. 238-248
- Kofoed, J. W., and Malloy, R. J., 1965, Bathymetry of the Miami Terrace: *Southeastern Geology*, v. 6, no. 3, p. 159-164
- Koehn, D. N., and Dickey, P. A., 1967, Growth Faulting In McAlaster Basin of Oklahoma: *Amer. Assoc. Petrol. Geol. Bull.*, v. 52, no. 5, p. 710-718

- Kuenen, Ph. H., 1950, *Marine Geology*: New York, John Wiley & Sons, Inc.
- Lowrie, A., Jr., and Heezen, B. C., 1967, Knoll and Sediment Drift near Hudson Canyon: *Science*, v. 157, no. 3796, p. 1552-1553
- Malloy, R. J., and Merrill, G. F. (In Press) Vertical Crustal Movement on the Sea Floor Associated with the 1964 Alaska Earthquake: The Prince William Sound, Alaska, Earthquake of 1964—Vol. II, Part C, U. S. Gov't Printing Office
- Malloy, R. J., and Harbison, R. N., 1965, *Marine Geology of the Northeastern Gulf of Maine*: Tech. Bull. No. 28, U. S. Coast & Geodetic Survey, 15 p., 4 maps
- Menard, H. W., 1964, *Marine Geology of the Pacific*; McGraw-Hill, New York, 271 p.
- Menard, H. W., and Dietz, R. S., 1951, Submarine Geology of the Gulf of Alaska: *Bull. Geol. Soc. America*, v. 62, p. 1263-1285
- Russell, I. C., 1888, *Geol. Mag.*, n.s., v: 5, p: 342
- Sengupta, S., 1966, Geological and Geophysical Studies in Western Part of Bengal Basin, India: *Amer. Assoc. Petrol. Geol. Bull.*, v. 50, no. 5, p. 1001-1017
- Short, K. C., and Stauble, A. J., 1967, Outline of Geology of Niger Delta: *Amer. Assoc. Petrol. Geol. Bull.*, v. 51, no. 5, p. 761-770
- Thorsen, C. E., 1963, Age of Growth Faulting in Southeast Louisiana: *Gulf Coast Assoc. Geol. Soc., Trans.*, v. 13, p. 103-110
- Uchupi, E., 1966, Shallow Structure of the Straits of Florida: *Science*, v. 153, p. 529-531
- Weeks, L. A., Harbison, R. N., and Peter, G., 1967, Island Arc System in Andaman Sea: *Amer. Assoc. Petrol. Geol. Bull.*, v. 51, no. 9, p. 1803-1815



Figure 8. Figure from Hamblin (1965) showing downthrown block structurally *higher* than upthrown block.

Reprinted from SCIENCE Vol. 161, No.3846

Murray Fracture Zone: Westward Extension

Abstract. The Murray Fracture Zone is one of the principal east-west rifts in the crust of the northeast Pacific basin. As judged by bathymetric and magnetic surveys, the Murray approaches the Hawaiian Archipelago as a well-defined zone of ridges and troughs accompanied by strong, linear magnetic anomalies. It loses its topographic expression on encountering the Hawaiian Arch but can be traced magnetically to its intersection with the Hawaiian Ridge in the vicinity of Laysan Island (near 172°W). All evidence tends to discount a previously suggested genetic relation between the Murray Fracture Zone and the Necker Ridge.

The long, linear fracture zones (1), which trend in an east-west direction across the northeast Pacific basin and offset well-defined patterns of north-south trending magnetic anomalies, are of primary significance and must be considered in any geological model of the earth. One of these, the Murray Fracture Zone, lies between and parallels two others, the Mendocino and the Molokai fracture zones. The Murray

Fracture Zone has been traced from a point off the coast of southern California westward for more than 4000 km. It has been suggested (2, 3) that before reaching the Hawaiian Archipelago, the Murray bends abruptly southwestward and continues into the Necker Ridge which trends southwestward from Necker Island (Fig. 1). Detailed bathymetric and magnetic data (4), however, indicate that the Murray

passes well north of Necker Island and intersects the Hawaiian Ridge near Laysan Island (Fig. 2).

The Murray Fracture Zone approaches the Hawaiian structure (west of 157°W) as a well-defined bathymetric feature (Figs. 1 and 2a). It occurs as a band of parallel asymmetrical ridges and troughs trending generally west-southwest. Between 157°W and 161°W it has a ridge-to-trough relief on the order of 1000 m, with a maximum depth of 6520 m occurring at about 158°W in one of the troughs. Bathymetric profiles of the Murray Fracture Zone in this region are almost identical to one at 152°30'W which Menard (1, fig. 3.3) presents as a typical example of the double-asymmetrical-ridge type of fracture zone. The topography is accompanied throughout by a wide band of linear magnetic anomalies characterized

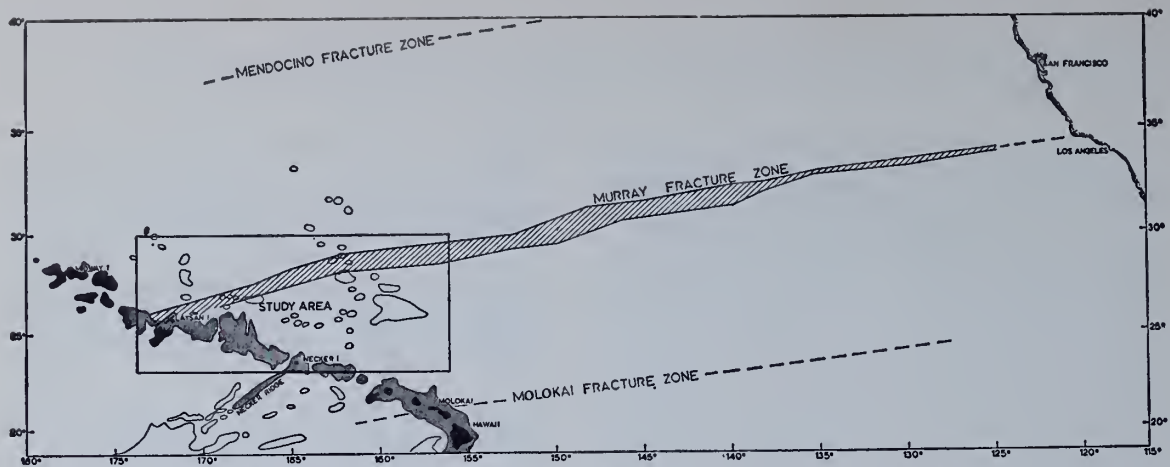


Fig. 1. Murray Fracture Zone and the Hawaiian Ridge. The ridge (stippled areas) and other topographic features (limited to the Hawaiian area) are defined by 3700 m contours (from U.S. Coast and Geodetic Survey chart 9000). Bathymetric and magnetic trends within the outlined area are shown in Fig. 2.

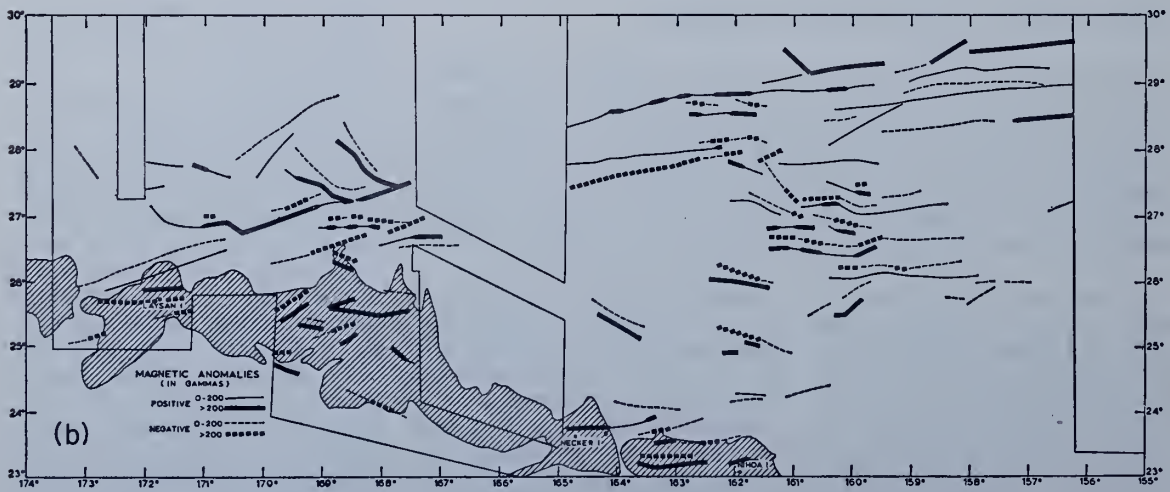
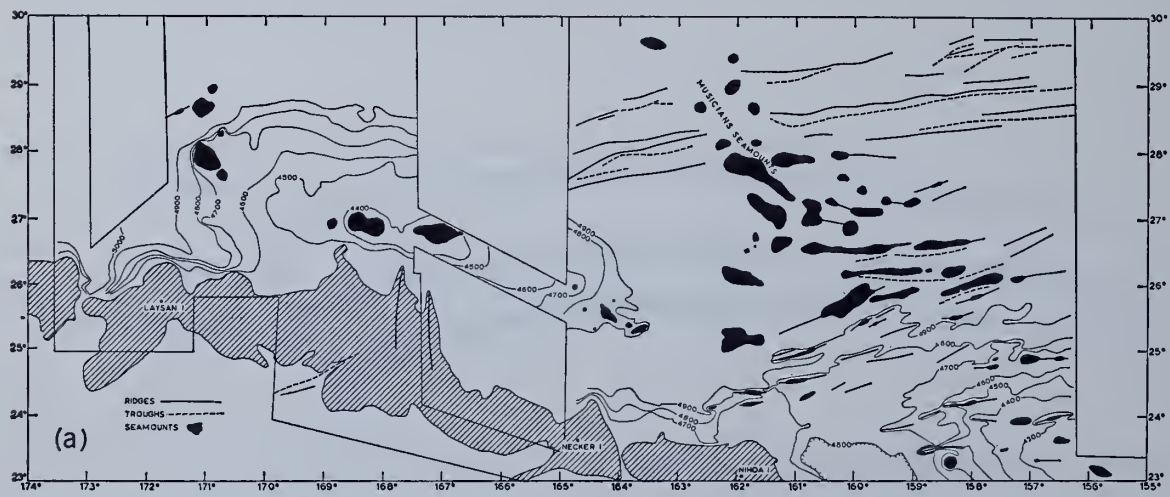


Fig. 2. Bathymetric trends (a) and magnetic trends (b) along the Murray Fracture Zone north of the Hawaiian Islands. Areas shoaler than 400 m are shown in black for seamounts (a) and are hatched over the Hawaiian Ridge (a and b). Selected contours are used to show the location of the Hawaiian Arch and Deep (a). Outlined areas indicate regions for which there is no detailed data.

by strong positive magnetic lineations along the northern margin (Fig. 2b). At about 161°30'W the Murray Fracture Zone encounters and is masked for about 130 km by the northwest trending Musicians Seamount Province. The northern limit of the Hawaiian Arch also lies within this region (5). Thus three structural features intersect at approximately the same location (28°30'N and 162°W). Several changes take place in the Murray Fracture Zone as it passes westward across this intersection: (i) it loses about half of its vertical relief, (ii) its trend changes about 5° toward the south, and (iii) it acquires a strong negative magnetic lineation along its southern margin. Its general morphological character is retained, and it continues as a well-defined zone to 165°W before entering a region for which detailed data are lacking.

Data coverage resumes west of 167°30'W, but here the Murray has lost its bathymetric expression completely. The characteristic magnetic lineations show that the Murray Fracture Zone continues across the relatively smooth Hawaiian Arch and that it intersects the Hawaiian Ridge in the vicinity of Laysan Island. Between 167°30'W and 170°30'W the trend is represented by a pair of large magnetic lineations which are offset or rotated at the crest of the arch where several large seamounts are located. At this same location two large anomalies branch off the main trend of the Murray, extend northwesterly for about 130 km, and die out before reaching an elongate dipole anomaly perpendicular to them. These anomalies have no bathymetric expression—a suggestion that they result from deep-seated intrusives whose surface expression has been covered and smoothed by materials forming the Hawaiian archipelagic apron (6). The various features may reflect the intersection of the Murray Fracture Zone with a zone of tension along the crest of the arch. A decrease in the intensity of the anomalies, and discontinuities in the individual lineations, occur where they encounter the Hawaiian Deep which is unusually well developed along the general trend of the lineations.

The observed bathymetric and magnetic relations along the Murray Fracture Zone are similar to those associated with the Molokai Fracture Zone as it intersects the Hawaiian Ridge farther south near the island of Molokai. Malahoff *et al.* (3) show that the Molokai Fracture Zone loses its bathymetric ex-

pression as it encounters the Hawaiian Deep but can be traced magnetically across the Ridge and westward for several hundred miles.

According to Malahoff *et al.* (7), most magnetic anomalies in the Hawaiian area can be divided into two groups: (i) local dipole anomalies related to centers of volcanism and (ii) elongate dipole anomalies related to dike complexes and crustal rift zones. Both types of magnetic expression are apparent in Fig. 2b. Local dipole anomalies are shown by relatively short, parallel pairs of positive and negative lineations, randomly oriented around a general east-west trend. As Malahoff *et al.* found to the east (7), most dipoles in this area exhibit normal polarization (positive anomaly to the south) with respect to the present magnetic field of the earth and in almost all cases are associated with pronounced topographic features. Several large east-west ridges located near 160°W have elongate anomalies associated with them, but only locally do their single-peak values exceed 200 gammas (shown by heavy lines) ($1 \text{ gamma} = 10^{-5}$ oersted). Hence, the anomalies appear due to topographic effects (near-surface volcanism) rather than deep-seated intrusives along a major rift zone. The second group of magnetic anomalies are long and linear, do not necessarily have topographic expression, generally trend in one of two major directions, and in places maintain high amplitudes over great distances. These may be caused by deep-seated intrusives along primary rift zones. One trend is associated with the Murray Fracture Zone and closely parallels the ridge and trough topography of the Murray east of 165°W, while west of 167°30'W, where there is no bathymetric expression, the "rift zone" magnetic anomalies clearly continue the trend across the crest of the arch. The other principal trend suggestive of primary fracturing is shown by a series of east-west lineations along portions of the ridge. These elongate anomalies have little correlation with local topography and closely parallel regional trends of the ridge.

An east-west interruption of the general northwest trend of the Hawaiian Ridge occurs near 169°W (Fig. 1). This configuration could be explained by left-lateral displacement of the ridge along the Murray Fracture Zone; however, large right-lateral displacements are indicated along the eastern portion of the Murray (8), and evidence suggests that these displacements increase

westward. A more plausible explanation of this east-west deviation in trend is that the Murray Fracture Zone is older and, as a zone of weakness, influenced formation of this portion of the ridge.

The topographic lineations which continue the trend of the Necker Ridge northeast of Necker Island do not appear to be related to primary fracturing. This conclusion is based on the lack of high-amplitude elongate magnetic anomalies within this zone and also on the fact that the bathymetric trends, although somewhat subtle, are more pronounced than those of the magnetics, a relation opposite to that generally observed along zones of primary rifting.

Several cross-cutting bathymetric and magnetic structures trending northeast occur within the Murray Fracture Zone between 156°W and 160°W, and also the Murray appears to be slightly offset, left laterally along a similar trend, between 148°W and 152°W (Fig. 1). These subtle relations may be connected to the similar trending bathymetric lineations associated with the Necker Ridge. If so, this would indicate that these structures postdate the Murray Fracture Zone.

Bathymetric charts of the region west of the ridge (9) show several lineations in the form of strings of abyssal hills (ridges?) and regional offsets in bathymetry, which conform in trend and general position to an extension of the Murray Fracture Zone.

FREDERIC P. NAUGLER
BARRETT H. ERICKSON

*Pacific Oceanographic Research
Laboratory, Environmental
Science Services Administration,
Seattle, Washington 98102*

References and Notes

1. H. W. Menard, *Marine Geology of the Pacific* (McGraw-Hill, New York, 1964), p. 260.
2. G. P. Woollard, in *Continental Margins and Island Arcs*, W. H. Poole, Ed. (Geological Survey of Canada Paper 66-15, 1965), p. 296.
3. A. Malahoff, W. E. Strange, G. P. Woollard, *Science* 153, 521 (1966).
4. These data were collected by the U.S. Coast and Geodetic Survey ships *Pioneer* and *Surveyor* during project SEAMAP. For brief résumé of the USC&GS SEAMAP survey, see T. V. Ryan and P. J. Grim, "A new technique for correcting echo soundings," *Intern. Hydrograph. Rev.*, in press.
5. F. Naugler and T. V. Ryan, ESSA Research Laboratories technical report, Boulder, Colo., in preparation.
6. H. W. Menard, *Bull. Geol. Soc. Amer.* 40, 2195 (1956).
7. A. Malahoff, W. E. Strange, G. P. Woollard, *Poc. Sci.* 20, 265 (1966).
8. A. D. Raff, *J. Geophys. Res.* 67, 417 (1962).
9. G. V. Udintsev, Ed., *General Bathymetric Map of the Ocean: Pacific Ocean* (Department of Geodetic Cartography, Geology Commission, Moscow, 1964).

Reprinted from *ENCYCLOPEDIA OF GEOMORPHOLOGY*, Reinhold, 1968

Alpine, Turkish, Persian, Himalayan, and Burmese Mountains, and the island chains of Indonesia, New Guinea, the Solomons, New Hebrides, and New Zealand. The other, the "East Asian-Cordilleran Belt" or "circum-Pacific Belt", surrounds the Pacific Ocean; its members extend from Indonesia to the Aleutian Islands, and from there to West Antarctica.

Some of the island arc systems are relatively simple and form a *single island arc* which consists of a single chain of volcanic islands. Prominent examples (see Fig. 2) are the Aleutian, the Kurile and the Mariana Island groups. With further tectonic development, *double island arcs* may be formed. These consist of an outer arc of sedimentary islands and a parallel inner arc of volcanic islands. Most of the single island arcs contain submerged or scattered traces of a second line (Brouwer,

Reprinted with permission from THE ENCYCLOPEDIA OF GEOMORPHOLOGY, R. W. Fairbridge, Reinhold, 1968.

ISLAND ARCS, GENERAL

There are several thousand islands in the oceans of the world, many of them are part of groups or chains of islands. If these island chains describe segments of an arc which are generally convex outward from the continental areas and are part of the major globe-encircling active orogenic belt systems, they are called *island arcs*.

General Distribution and Description

Island arc systems are morphologic indications of tectonic activity found roughly along two mutually perpendicular great circles (Fig. 1). According to Wilson (1954), they are parts of two vast and complex zones of fracture about the earth. These zones include the major mountain chains of the continental areas and the major island arc systems of the oceanic areas. One of the major orogenic systems, the "Eurasian-Melanesian Belt", or "Mediterranean—Tethyan Belt", includes the Atlas,

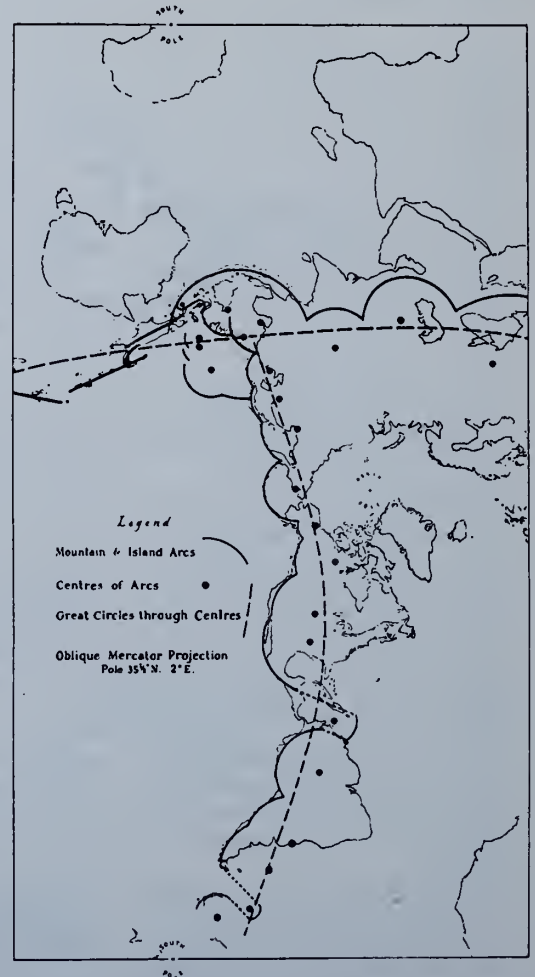


FIG. 1. Distribution of the active orogenic belts (from J. T. Wilson, 1954). (By permission of The University of Chicago Press.)

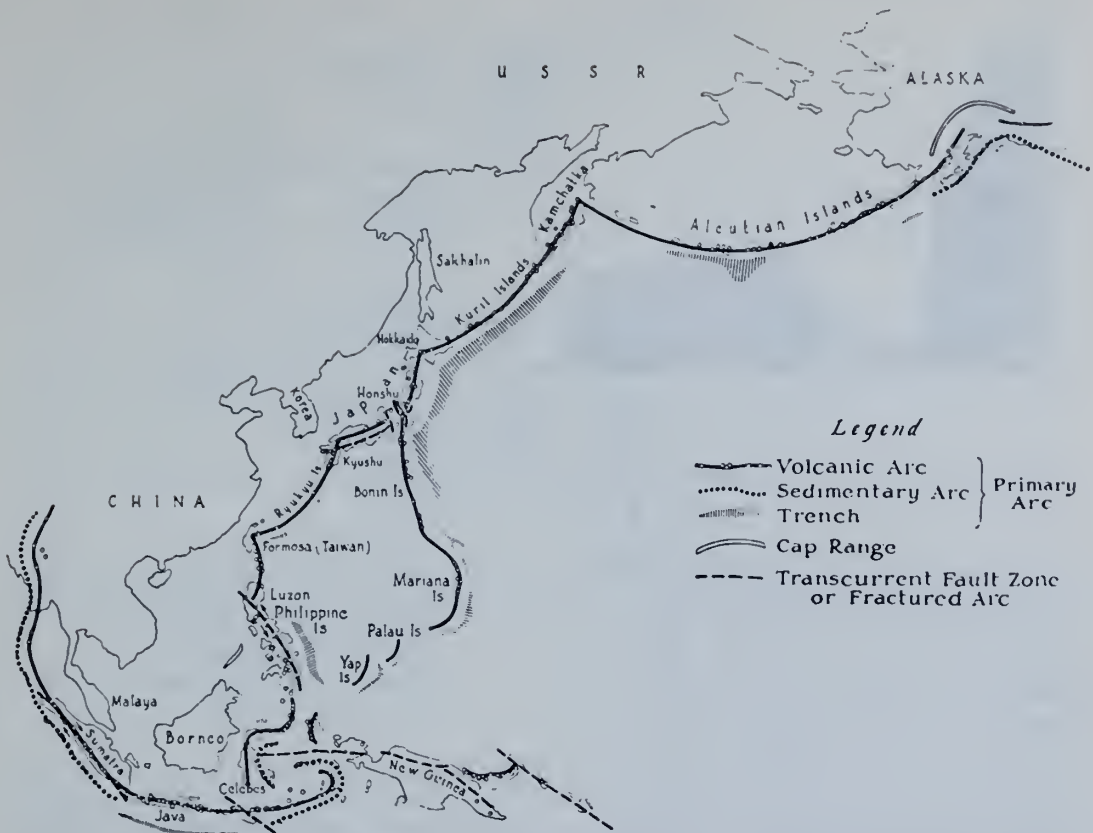


FIG. 2. Distribution of island arcs in the northwest Pacific Ocean (from J. T. Wilson, 1954). (By permission of The University of Chicago Press.)

1951; Hobbs, 1925). Double island arcs are not as numerous as the single island arc systems, but an excellent example is found in the northeast Indian Ocean. Here the Andaman and Nicobar Islands form an outer arc of sedimentary islands and there is an inner volcanic trend which manifests itself in two isolated volcanic islands and a chain of submarine volcanoes (see *Andaman Sea*, Vol. 1). Less obvious examples are Kodiak Island, part of a sedimentary arc, and the volcanic trend on the Alaska Peninsula. In this latter case, the clear arcuate trends of the single arc systems are less well defined, since a portion of this double arc system is part of the continent itself.

Certain single and double island arcs exhibit large transcurrent (or strike-slip) fault zones which suppress the ideal arcuate pattern. These island arcs are called *fractured island arcs*. Typical examples of these are the Melanesian arcs from the Philippines to New Zealand.

Morphologic Associations

There are several fundamental morphologic relationships between the island arcs themselves and the sea floor from which they rise.

In case of the relatively simple single island arcs, the chain of volcanic islands is characteristically associated with a deep-sea trench on its convex side. Whereas the island arc-deep sea trench system may be several thousand kilometers in length, the width of the system is generally only a few hundred kilometers. Many of the volcanoes on the islands have elevations of 1–2 km above sea level, and the adjacent deep-sea trench may reach depths exceeding 10 km. The greatest depth surveyed in the Mariana Trench is approximately 11 km. Thus, together with the cordilleran-trench combinations (e.g. Andes-Peru Trench) with relief in excess of 15 km, the island arc-deep sea trench systems represent the maximum relief features found on the earth's surface.

Moving toward a single island arc from the open ocean, the deeper ocean basin, which may have an average depth of 4–5 km, becomes shallower at first (by approximately 1 km), then dips with increasing steepness into the deepest portions of the trench (Fig. 3). The ocean floor rises somewhat more sharply on the inner wall of the trench, up to the island platform itself. The shallower part of the deep-sea floor seaward of the trench is called the

ISLAND ARCS, GENERAL

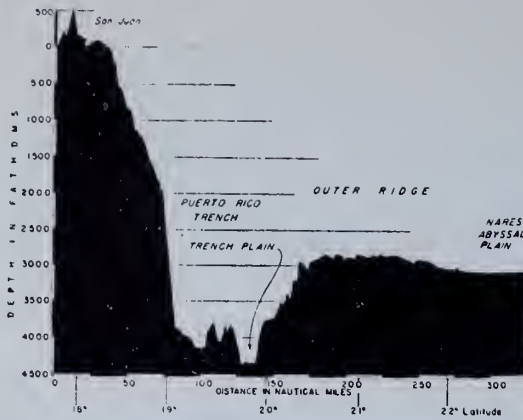


FIG. 3. Cross section of the Puerto Rico Trench (after Ewing and Heezen, 1955). Vertical exaggeration: 50 to 1.

outer ridge, and it is generally an area of rugged (but relatively small-scale) bottom relief features and a complex crustal structure. The insular slope of the island arc is also riddled with canyons and sharp, usually small-scale, topographic depressions and elevations. However, as contrasted to the outer ridge, the insular slope frequently shows benches and ridges which can be followed parallel to the island arc sometimes for several hundred kilometers. Menard (1964) says: "Almost everyone who sees an echogram of the side benches and bottom troughs of trenches believes that they are produced by normal faulting. That is, the benches are the upper surfaces of fault blocks which have moved down into the trenches and been rotated away from the trenches so they are excellent traps for sediment. Likewise, the troughs in the center can hardly be anything but grabens." Studies of the Aleutian Arc (Gibson and Nichols, 1953; Gates and Gibson, 1956) showed that several canyons, sharp depressions, and ridges are connected to known fault zones mapped on the islands. Location of volcanic necks, plugs and dikes were found to be connected to tensional faulting on several islands of the Aleutian Arc (Knappen, 1929; Coats, 1950).

Well-developed double island arcs are less common than the single arcs and consist of two generally parallel arcuate trends (Fig. 4). As recognized half a century ago by Brouwer, the inner arc consists of volcanic islands or when the islands themselves are not present, a drowned ridge or a zone of submarine volcanoes. The volcanoes are characteristically steep cones of the explosive, andesitic type. On the outer, convex side of this andesitic volcanic arc there is another island chain composed chiefly of sedimentary rocks (limestones, tuffs, greywackes, shales, cherts). These are cut in places by ultrabasic and serpentine intrusions. The greywacke chert serpentine facies is the so-called Steinmann Trinity characteristic of axial orogenic belts. These forma-

TABLE I. ISLAND ARCS

	Name		Ocean
Single Island Arcs	Antillean Arc	Puerto Rico Trench	Atlantic
	Sandwich (Scotia) Arc	South Sandwich Trench	Atlantic
	Aleutian Arc	Aleutian Trench	Pacific
	Kurile Arc	Kurile-Kamchatka Trench	Pacific
	Japan Arc (including Bonin)	Japan Trench	Pacific
	Palau Arc	Palau Trench	Pacific
Yap Arc	Yap Trench	Pacific	
Double Island Arcs	Ryukyu Arc (Nansei Shoto)	Ryukyu Trench	Pacific
	Mariana Arc	Mariana Trench	Pacific
	Kodiak-Alaska Peninsula	Aleutian Trench	Pacific
	Indonesian Arc	Java Trench	Indian
Fractured Island Arcs	Philippine Arc	Philippine Trench	Pacific
	Solomon-New Hebrides Arc	New Britain and New Hebrides Trench	Pacific
	Tonga-Kermadec Arc	Tonga-Kermadec Trench	Pacific

tions are involved in complex overthrust or nappelippe tectonics, directed outward (ideally exposed, for example, on Timor). The length of the double island arcs, similarly to the single arcs, may reach several thousand kilometers, the overall width of the double arc-trench system is approximately 500 km.

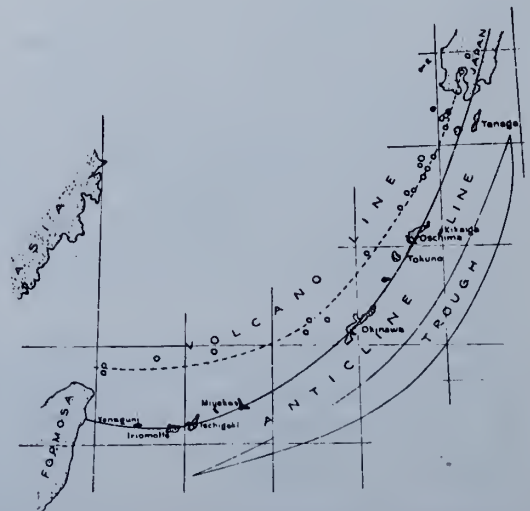


FIG. 4. The Ryukyu (Riukiu or Nansei Shoto) island arcs, including both a volcanic line (poorly developed), anticlinal belt (Cenozoic limestones, etc.), and a contemporary trough or trench (from Hobbs, 1944).

ISLAND ARCS, GENERAL

of the earth's active orogenic belts, are closely related to seismic activity which occurs along these belts. Although there is some scatter in distribution, shallow earthquakes (25 km) are associated with the area of the trench and outer arc, medium depth earthquakes (100-300 km) are located under the volcanic island ridge, and deep earthquakes (400-700 km) are located farther toward the continent. The rugged topography of the island arcs is related to present-day volcanism, young fractures and the earthquake activity. Vertical movements of extreme youth are shown by coastal terraces that in places (e.g., Timor, New Guinea) may be traced to over 4000 feet above sea level. Gravity anomalies and other geophysical attributes of the island arc-trench systems, and the basic crustal structures associated with them are discussed in Vol. V.

Development and Origin

The origins of island arcs and of the orogenic belts are still subjects of geological and geophysical debates. The earthquakes are generally attributed to an inclined fracture zone, but compressional, tensional and strike-slip movements all have been suggested for the nature of this fracture system (Fig. 5). It is generally agreed, however, that during the course of a hundred million years or so the single island arcs develop into double island arcs and then into marginal mountain ranges. Rock suites, similar to those of island arcs, can also be found deep inside several continents. These show the location of mobile belts in the earlier geological history of the earth and suggest that the development of continents occurred through the marginal addition of island arcs.

GEORGE PETER
R. E. BURNS

References

- Brouwer, H. A., 1951, "The movement of island arcs," *Quart. J. Geol. Soc. London*, **106**, 231-239.
- Coats, R. R., 1950, "Volcanic activity in the Aleutian Arc," *Bull. U.S. Geol. Surv.*, **974-B**, 35-49.
- Ewing, M., and Heezen, B. C., 1955, "Puerto Rico Trench Topography and Geophysical Data," in (Poldervaart, A., ed.), "Crust of the Earth," 255-267, *Geol. Soc. Am. Spec. Paper* **62**.
- Fisher, R. L., and Hess, H. H., 1963, "Trenches," in "The Sea," Vol. 3, pp. 411-436, New York and London, Interscience Publishers.
- Gates, O., and Gibson, W. M., 1956, "Interpretation of the configuration of the Aleutian Ridge," *Bull. Geol. Soc. Am.*, **67**, 127-146.
- Gibson, W. M., and Nichols, 1953, "Configuration of the Aleutian Ridge, Rat Islands-Semisopchnoi I. to west of Boulder I.," *Bull. Geol. Soc. Am.*, 1173-1181.
- Hawkes, D. D., 1962, "The structure of the Scotia Arc," *Geol. Mag.*, **99**, 85-91.
- Hess, H. H., 1939, "Island arcs, gravity anomalies and serpentine intrusions: A contribution to the ophiolite problem," *Rept. Int. Geol. Congr. (U.S.S.R.) 1937*, **17**, 263-283.
- Hobbs, W. H., 1925, "The unstable middle section of the island arcs," *Gedenboek Verbeek, Verh. Geol.-Mijn. Gen. Ned. en Kol., Geol. Ser.*, **8**, 219-262.
- Hobbs, W. H., 1944, "Mountain growth, a study of the southwestern Pacific region," *Proc. Am. Phil. Soc.*, **88**, 221-268.
- Knappen, R. S., 1929, "Geology and mineral resources of the Aniakchak District," in "Mineral Resources of Alaska," *Bull. U.S. Geol. Surv.*, **797**, 161-223.
- Lake, P., 1931, "Island arcs and mountain building," *Geogr. J.*, **78**, 149-160.
- Menard, H. W., 1964, "Marine Geology of the Pacific," New York, McGraw-Hill Book Co., 271pp.
- Sykes, L. R., 1966, "Seismicity and deep structure of island arcs," *J. Geophys. Res.*, **71**, 2981-3006.
- Wilson, J. T., 1954, "The Development and Structure of the Crust," in (Kuiper, G. P., editor) "The Earth as a Planet," Chicago, University of Chicago Press, 749pp.

Cross-references: *Islands; Mountain Systems; Submarine Geomorphology*. Vol. I: *Andaman Sea; Bathymetry; Ocean Bottom Features; Trenches*. Vol. V: *Island Arcs—Geophysics and Tectonics*.

Reprinted from INTERNATIONAL HYDROGRAPHIC REVIEW, Vol. 45, No. 2

A NEW TECHNIQUE FOR ECHO SOUNDING CORRECTIONS

by T.V. RYAN and P.J. GRIM

Environmental Science Services Administration,
Pacific Oceanographic Research Laboratory,
Seattle, Washington.

The argument that reasonably complete maps of the oceans are the first requisite for studies leading to an understanding of oceanic structures and processes was advanced by the U. S. National Academy of Sciences Committee on Oceanography in 1959 (NASCO 1959). The U. S. Coast and Geodetic Survey (USC&GS) accepted this thesis and as a pilot project in 1961 launched a survey of unparalleled scope in the North Central Pacific. As of January 1967, 33 ship months had produced the areal coverage illustrated in figure (1).

The basic plan, now known as SEAMAP (Scientific Exploration And Mapping Program) provides for continuous echo sounding and magnetic and gravity observations on a line spacing of 10 nautical miles (18.52 km) under Loran-C control. Oceanographic station observations (temperature, salinity, oxygen) and geological samples (dredge hauls and cores) are also being obtained. In addition to the basic plan, many additional observations and special investigations have been carried out concurrently by Environmental Science Service Administration (ESSA) scientists and by other research laboratories. These supplementary programs include studies of deep currents, light transmissivity, biological populations and primary productivity, time changes in properties, bottom photography, natural and man-induced radio-activity, etc.

In view of the immense quantity of echo soundings which were to be obtained from the survey, it was apparent that a computerized technique was essential for processing position data and correcting the soundings for sound velocity. With a computer (IBM Model 1620) committed to the task, and the relatively large volume of oceanographic station data obtained during the survey, it was felt that an improved method for correcting echo soundings could be devised.

Three prominent factors enter into the problem : (1) The basic relationship among the independent variables, i.e., temperature, salinity and pressure, and the dependent speed of sound; (2) The approximations used to describe the speed of sound in the specific water volume in which the echo soundings are made (it should be noted that the speed of sound usually

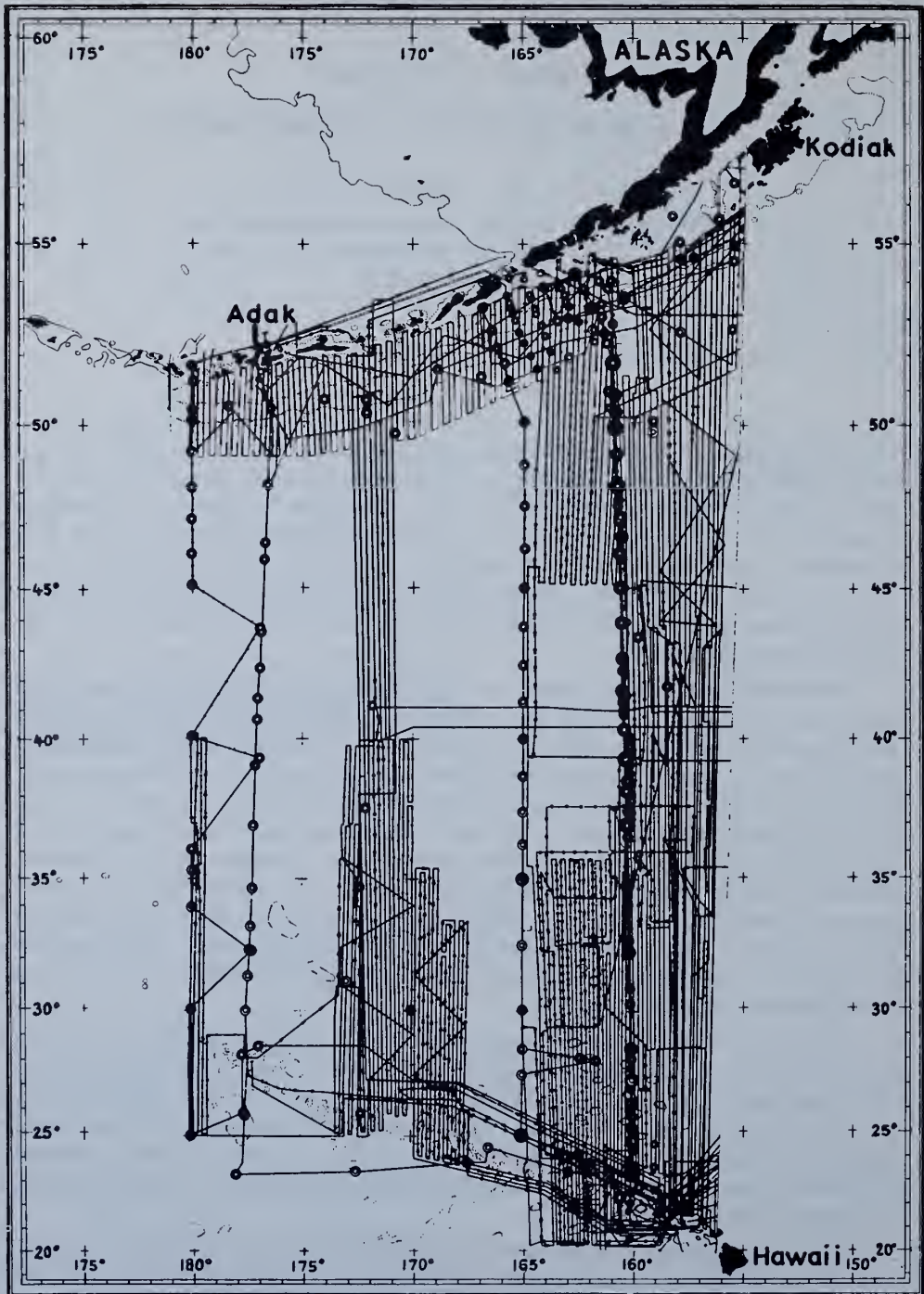


FIG. 1. — North Pacific SEAMAP Surveys.

varies in a non-linear fashion with latitude, longitude, depth and time); and (3) The computational technique one uses to compute the correction and apply it.

1. THE BASIC RELATIONSHIP

Modern studies and field tests (DEL GROSSO, 1952; BYERS, 1954; MCKENZIE, 1960; WILSON, 1960) argue that the well known tables and equations which were developed by MATTHEWS (1939) and KUWAHARA (1939) from theoretical considerations relating temperature, salinity, and pressure to sound velocity (*), although remarkably accurate, are systematically different from the results of empirical studies. BYERS (1954) attributes the discrepancy to an error in the published values for the isothermal compressibility of water, a factor which both MATTHEWS and KUWAHARA recognized as a weak point in their calculations. The values used by MATTHEWS and KUWAHARA for compressibility are based on measurements made in 1893

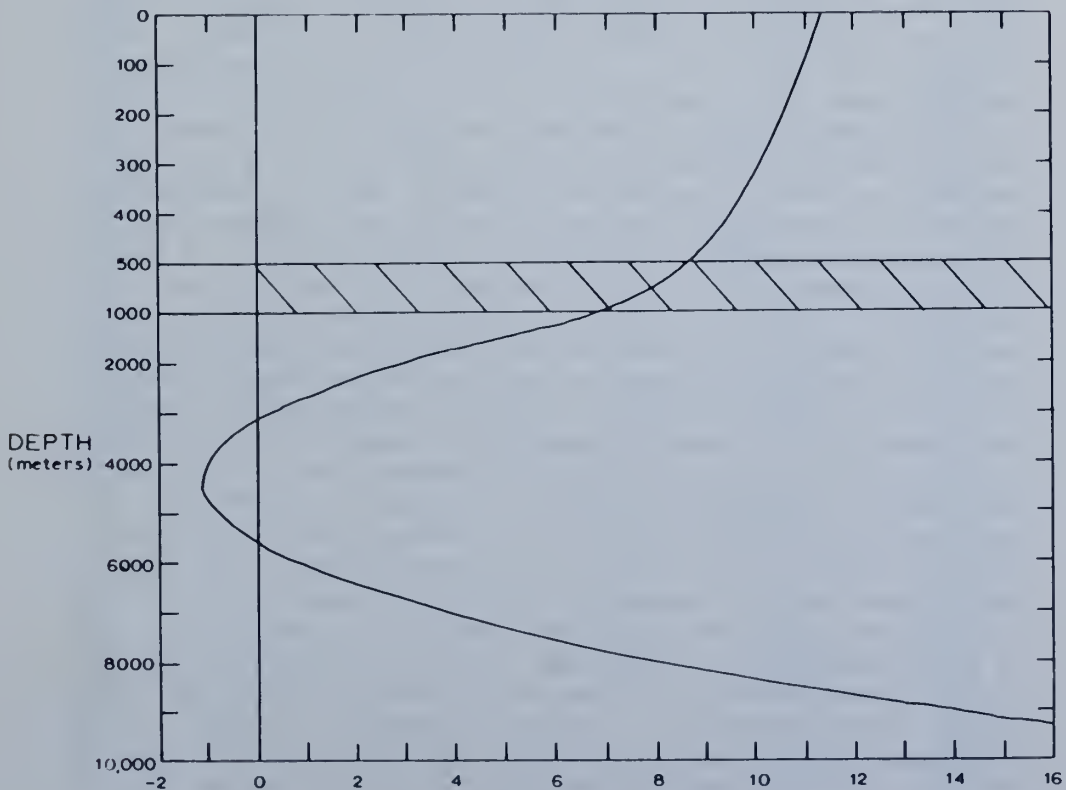


Fig. 2. Velocity difference (ft/sec), Wilson minus Kuwahara. Comparison of sound velocity values, Surface to 9 000 metres, given by Wilson's equation and Kuwahara's tables (from SOWEN, 1961).

(*) Popular usage favors the term 'velocity' for 'speed' of sound although the value is a scalar not vector quantity. In accordance with the custom the term 'velocity' will be used hereafter instead of 'speed'.

and 1908. Figure 2 from SOWER (1961), presents a comparison of KUWAHARA's velocities (which are essentially identical with those of Matthews) with values computed from the WILSON (1960) equation for a typical oceanographic condition. Acceptance of Wilson's equation by marine scientists was confirmed when in 1963 the U.S. National Oceanographic Data Center replaced Kuwahara's equation with Wilson's equation for computing the velocity of sound from oceanographic station data. Thus with regard to the basic relationship among the independent variables, we decided that the system must be based on Wilson's equation (1960).

2. — CLASSIFICATION OF THE ENVIRONMENT

MATTHEWS' tables (1939) divide the world's oceans into 52 areas on the basis of echo sounding conditions. It is not evident what criteria MATTHEWS used for drawing the area boundaries, but it is certain that in 1939 he had only a small fraction of the oceanographic station data which are available today for evaluating the acoustic characteristics of the ocean. In the SEAMAP area the C&GS has occupied 151 stations well distributed with regard to space and the period of the survey. With this relatively dense and appropriate body of data available, we chose to use it exclusively to study the sound velocity structure of the region. The spacial and temporal variability in Mean Vertical Sound Velocity (*) (MVSV), (computed by a method to be described later) throughout the SEAMAP region was examined by plotting geographically the Mean Vertical Sound Velocity, at each of the 151 oceanographic stations, to 200, 1 000 and 5 000 metres. These depths were chosen to provide a basis for (a) evaluating the maximum effect of seasonal variability (200 metre level), (b) representing a depth of a large portion of the soundings (5 000 metres) and (c) providing a look at an intermediate depth (1 000 metres). The plotted values were then contoured. As expected from the known physical characteristics of the North Pacific, the contours were found to have a decided east-west trend. The region was then divided into a sufficient number of latitudinal zones with boundaries such that the variability in each zone, resulting from geophysical and seasonal changes, did not exceed an acceptable tolerance. The tolerance (due to both areal and seasonal effects) deemed acceptable was 4 metres at 200 metres (fathometer resolution is about 3.6 m), and 0.5 % of depth at depths greater than 1 000 metres. The zone boundaries and the Mean Vertical Sound Velocity, in terms of "R", which is the Mean Vertical Sound Velocity divided by the fathometer velocity (**), at 200, 1 000 and 5 000 metres are illustrated in figures 3, 4 and 5. To reduce clutter, 1.0000 has been subtracted from "R" and the decimal point omitted. The "R"

(*) Mean Vertical Sound Velocity (MVSV) is the mean velocity of the sound wave from the ocean surface to the depth of interest, assuming the wave travels vertically downward, and the velocity changes in a linear fashion within each layer.

(**) Fathometer Velocity is the assumed velocity of sound in sea water used by the instrument manufacturer when building the readout device. The USC&GS fathometers use 1 463.43 m/sec (800 fms/sec) as a fathometer velocity. See 'Fathometer Depth' below.

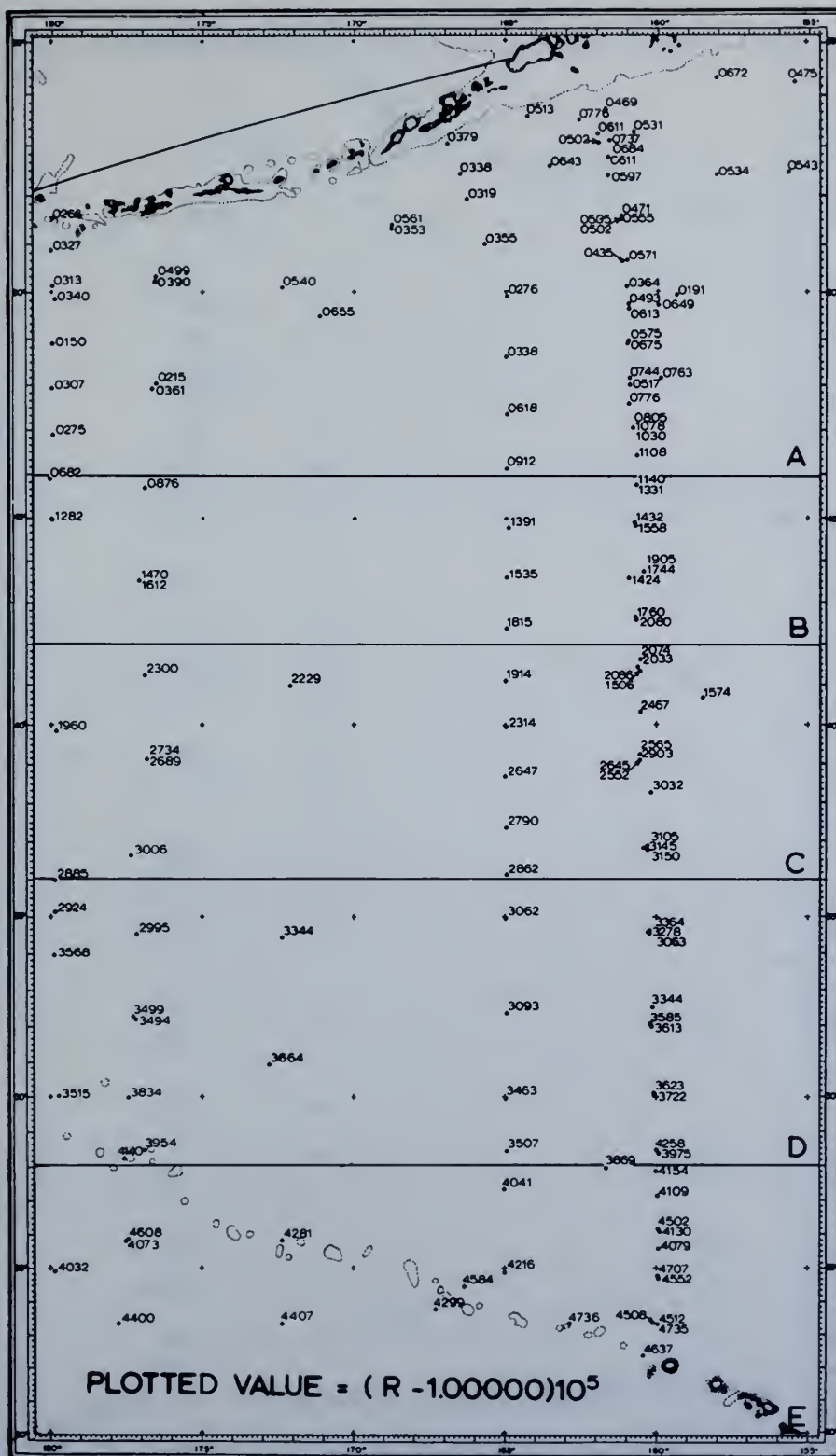


FIG. 3. — Ratio R for 0 to 200 metres.

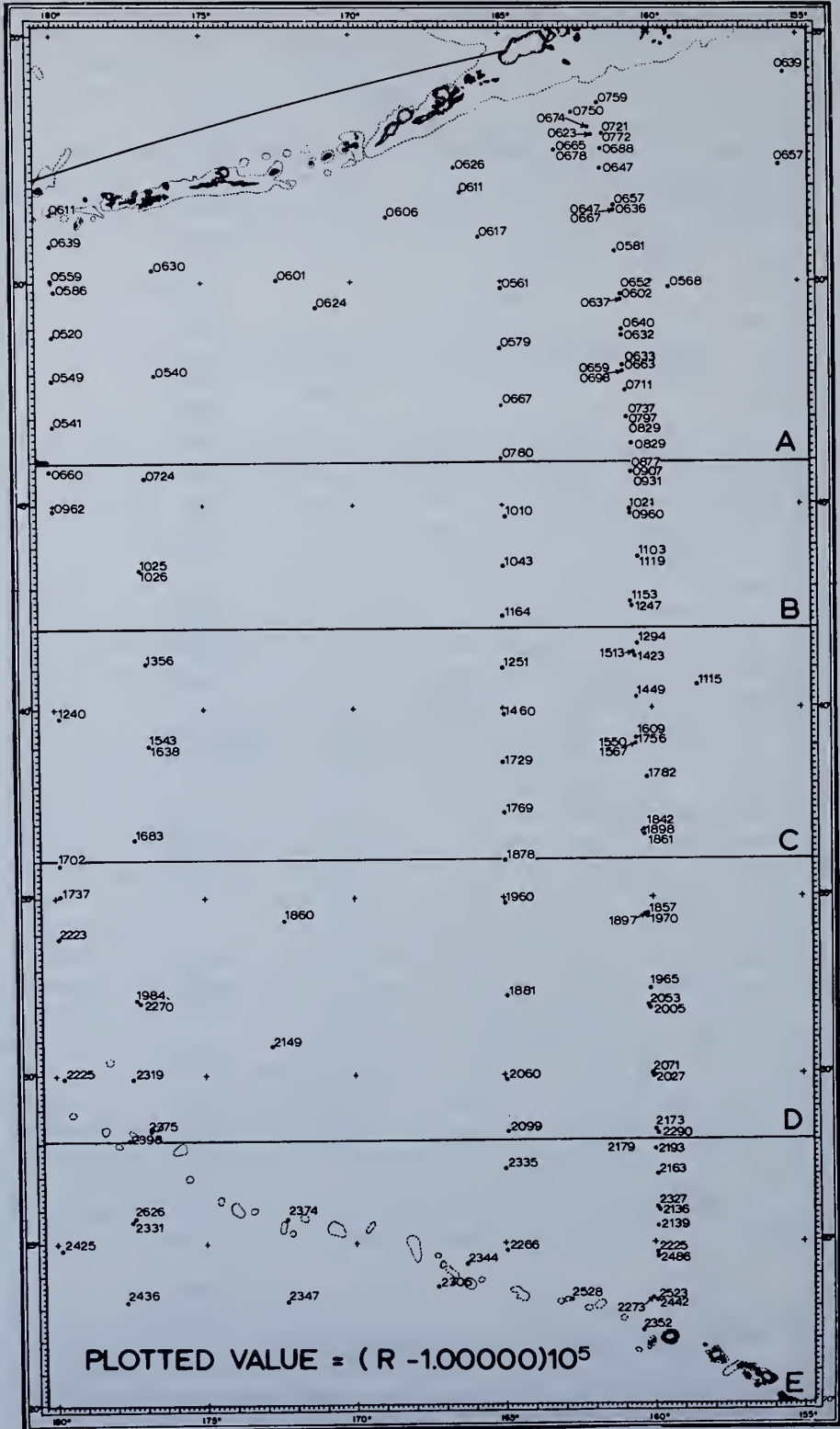


FIG. 4. — Ratio R for 0 to 1000 metres.

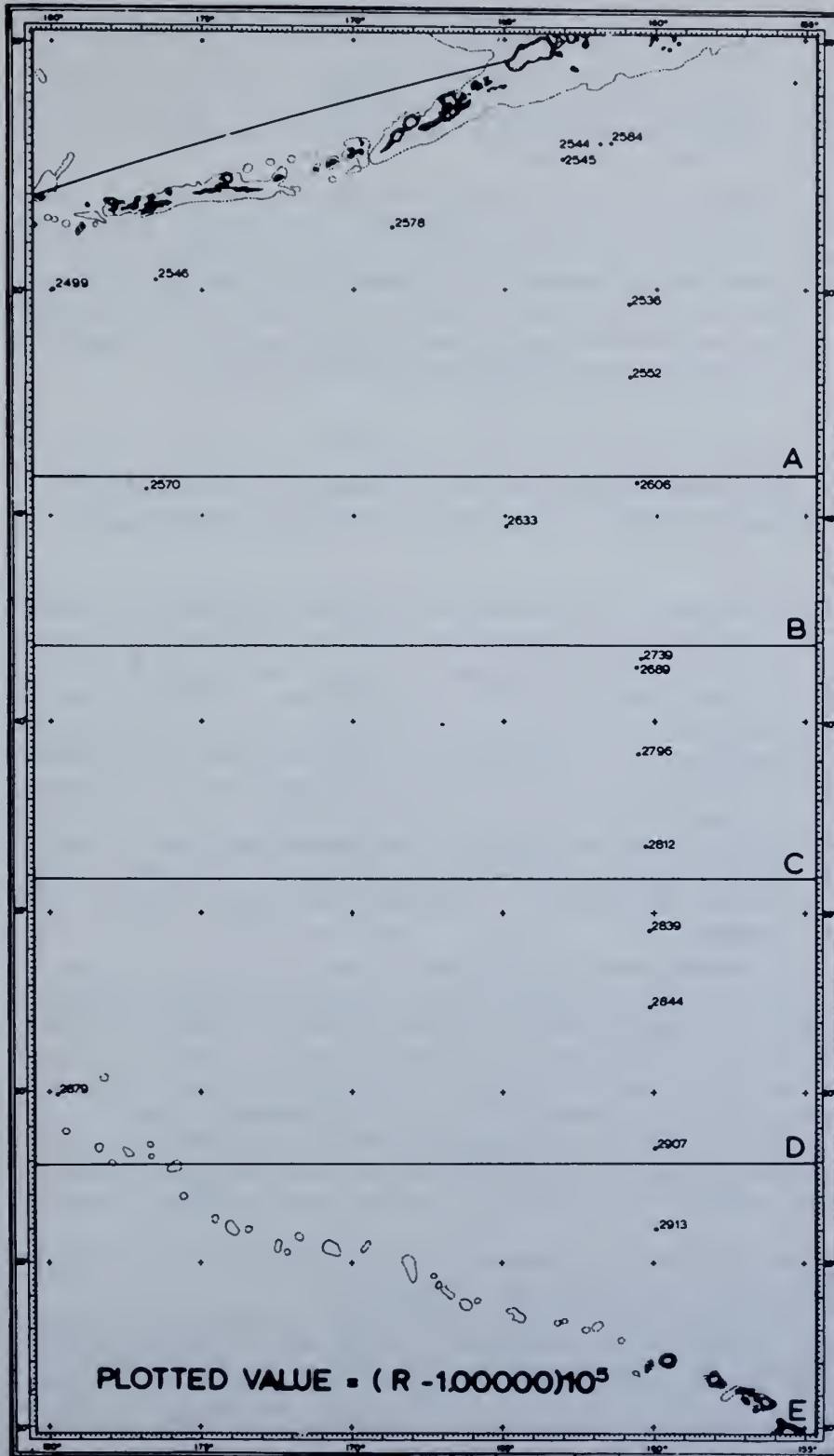


FIG. 5. — Ratio R for 0 to 5 000 metres.

value, therefore, shows the proportional error in the "raw" fathometer depth (*). For example, in the upper right corner of figure 3, the value 0.475 means that a fathometer reading of 200 m would be 0.475 % too shallow; at the same location at 1 000 m we learn from figure 4 that the reading is 0.639 % too shallow; and from figure 5 we see it would be 2.534 % too shallow at 5 000 m.

Our original intent was to multiply the raw soundings by the appropriate "R" values, to yield the corrected sounding. Difficulties in fitting an equation to the plot of "R" versus depth, forced us to develop an alternate approach which will be discussed later. Having found that the variability was such that the SEAMAP region could be divided into 5 zones, each with an acceptably low variability in "R", the problem remained to characterize each zone by a single Mean Vertical Sound Velocity curve.

3. — THE COMPUTATION OF MEAN VERTICAL SOUND VELOCITY AND APPLICATION OF THE SOUND VELOCITY CORRECTION

The oceanographic station data "detail" punch cards, prepared routinely by the U. S. National Oceanographic Data Center (NODC), list sound velocity computed from Wilson's equation for each oceanographic standard depth (**). A program (identified as VEL I) was written to compute certain statistical properties of the sound velocity for each oceanographic standard depth based on all stations lying within each zone : The statistical values computed are the lowest velocity, the average velocity, the highest velocity, the standard deviation of the velocities from the average value and the number of observations used in the calculations. The number of stations available in each zone is fixed; however, as the stations sample to various depths, the number of available observations decreases with increasing depth.

A reproduction of the output of this program is shown in the appendix. The average velocities computed by this program for the oceanographic standard depths comprise the data which are used to compute the Mean Vertical Sound Velocity for the zone in which the echo soundings are made. The maximum and minimum values found within each zone at each depth are used to compute the maximum error in the sounding correction which would result from natural variability in the zone. To provide sound velocity data for depths which exceed the depths of the oceanographic stations (in all zones stations to at least 5 000 metres were available) values of

(*) Fathometer Depth is the depth scaled from the fathometer. It is a product of 1/2 the travel time for the sound wave from the surface to bottom to surface, times the velocity assumed by the instrument manufacturer.

(**) Oceanographic Standard Depth. These are depths at which the oceanographic parameters, measured and derived, are routinely listed by most oceanographic laboratories. When necessary, the independent variable is determined at the standard depth by an interpolation formula. The oceanographic standard depths used by the National Oceanographic Data Center are 0, 10, 20, 30, 50, 75, 100, 125, 150, 200, 250, 300, 400, 500, 600, 700, 800, 900, 1 000, 1 100, 1 200, 1 300, 1 400, 1 500, 1 750, 2 000, 2 500, 3 000, and at 1 000 m intervals to bottom.

RESULTS (PARTIAL) FROM VEL I PROGRAM FOR ZONE B

DEPTH IN M.	LOW VELOCITY	AVERAGE VELOCITY	HIGH VELOCITY	STANDARD DEVIATION	NUMBER OF OBS.
10.	1486.2	1502.08	1523.2	14.074	10
20.	1486.3	1501.28	1521.5	13.159	10
30.	1486.3	1497.60	1513.9	10.115	10
50.	1484.1	1488.05	1495.2	3.530	10
75.	1477.2	1483.77	1489.5	3.713	10
100.	1476.5	1484.02	1489.5	4.171	10
125.	1476.4	1484.07	1489.1	3.495	10
150.	1477.7	1483.75	1488.6	3.125	10
200.	1480.0	1482.90	1486.6	2.116	10
250.	1477.5	1480.21	1483.1	1.980	10
300.	1475.6	1478.14	1481.5	1.908	10
400.	1473.9	1475.29	1477.6	1.219	10
500.	1473.9	1474.64	1475.8	.619	10
600.	1474.9	1475.23	1475.9	.337	10
700.	1475.5	1476.05	1476.7	.398	10
800.	1476.4	1476.88	1477.3	.286	10

temperature, salinity, and pressure were extrapolated to 9 000 metres. We now have a means of characterizing the environment by a "mean station" and can express quantitatively the maximum error that our approximation can cause.

Given the data from the "mean station", which we assume expresses within allowable tolerances for areal and temporal variability the velocity of sound for each oceanographic standard depth, it is still necessary to compute the effective velocity for the sound wave travelling vertically from the surface to the reflecting bottom. We have called this the Mean Vertical Sound Velocity. Various techniques (*) have been used; however, in essence all divide the water column into a number of layers in each of which a constant, average velocity is assumed to apply. In the real ocean the speed changes continuously with depth and thus with a finite number of layers sound is travelling through layers in which the speed is continuously changing. A simple calculation will show that the true Mean Vertical Sound Velocity through a layer in which the velocity changes is something less than the arithmetic average of the velocity in the bounding surfaces of the layer. Use of the simple averaging technique thus yields a velocity which is too fast.

With a digital electronic computer it is practical to compute an average speed utilizing the equation $dt = \frac{dz}{v}$ which recognizes the fact that the speed changes in each layer. Integration of the equation over each layer yields the time required to transit the layer. By summing the times and dividing by the total depth, a more accurate Mean Vertical Sound Velocity is obtained. The mathematics of this procedure are given in the appendix.

Given an acceptable method for computing the Mean Vertical Sound Velocity to each oceanographic standard depth, one can compute the fathometer depth which when corrected equals the oceanographic standard depth, by the equation :

$$\begin{aligned} \text{fathometer depth} &= \\ &= \frac{(\text{fathometer velocity})}{\text{MVSV}} (\text{oceanographic standard depth}) \end{aligned} \quad (1)$$

The correction to be applied to the fathometer depth is :

$$\text{correction} = \text{oceanographic standard depth} - \text{fathometer depth} \quad (2)$$

This important point is illustrated as follows :

The fathometer in reality simply records a figure based on one half of the time for the sound wave to reach the sea bottom and return. It expresses this time as its product with the constant fathometer velocity and reads out in fathometer depth. Therefore, the time, t_z , required for the

(*) MATTHEWS averaged the temperature and salinities from the upper and lower surface of each layer and computed a speed from the 'average' temperatures, salinities, and pressures. Since the speed of sound is not a linear function of temperature and salinity, strictly speaking the simple average of the bounding temperatures and salinities does not yield precise values for determining the average velocity within the layer. If the range in temperatures and salinities across the layer is small, the error due to this simplification is trivial.

sound wave to reach the bottom at depth z , can be computed from the equation :

$$t_z = \frac{\text{fathometer depth}}{\text{fathometer velocity}} \quad (3)$$

and since

$$\text{true depth} = t_z (\text{MVSV}) \quad (4)$$

by combining equations (3) and (4), we derive

$$\text{true depth} = \frac{\text{fathometer depth}}{\text{fathometer velocity}} (\text{MVSV})$$

or rearranging terms,

$$\text{fathometer depth} = \frac{\text{fathometer velocity}}{\text{MVSV}} (\text{true depth}) \quad (5)$$

As oceanographic standard depths are "true" depths, we can solve for the fathometer depth which corresponds to each oceanographic standard depth, and then, by computing the correction at each fathometer depth according to equation (2), produce a table of corrections to be applied to those fathometer depths. Note that this procedure departs from MATTHEWS (and others) who computed the correction from oceanographic data listed at "true" depths and then prepared correction tables which in effect apply the correction to "true" depths. In practice one enters a table (or other correction technique) with a fathometer depth to "look up" the correction. Since fathometer depths are usually too shallow, the correction obtained is for a column of water shallower than the real column. The refinement incorporated by the present method eliminates another very small but systematic error, which varies in different regions but generally results in too large a correction above 1 000 metres and too small a correction below. At 5 000 metres it can amount to 3 metres. A computer program (VEL II) was written to compute the corrections at each fathometer depth corresponding to an oceanographic standard depth, utilizing the accepted Mean Vertical Sound Velocity of each zone. The output from this program is illustrated in the appendix. It includes (1) the correction as computed from the *accepted* Mean Vertical Sound Velocity, and (2), the corrections computed from the maximum and (3), minimum Mean Vertical Sound Velocities found in that zone. Also computed are the ratios of the Mean Vertical Sound Velocity to the fathometer velocity for all three types of Mean Vertical Sound Velocities.

The corrections computed from the sets of maximum and minimum Mean Vertical Sound Velocity for each zone are used to establish the maximum error in the correction that could result within a zone, as a result of the variability in the environment. Figure 6a indicates the standard deviation from the mean sound velocity for all depths for all five zones, and figure 6b illustrates the maximum probable error in the echo sounding correction which one might expect as a result of the variability indicated in figure 6a.

As a result of Program VEL II we have a listing, for each zone, of the corrections to be applied to the fathometer depths which when corrected are the oceanographic standard depths from 10 metres to 9 000 metres.

RESULTS (PARTIAL) FROM VEL II PROGRAM FOR ZONE B

ACCEPTED MVSV			MINIMUM MVSV			MAXIMUM MVSV			TRUE DEPTH
1	2'	3	1	2	3	1	2	3	4
9.740	2.599	1.02668	10	0	1.01583	10	0	1.04112	10
19.481	5.187	1.02662	20	0	1.01650	19	1	1.04084	20
29.238	7.617	1.02605	30	0	1.01630	29	1	1.03968	30
48.839	11.609	1.02377	49	1	1.01586	48	2	1.03512	50
73.454	15.461	1.02105	74	1	1.01458	73	2	1.03005	75
98.089	19.105	1.01948	99	1	1.01334	97	3	1.02703	100
122.668	23.322	1.01901	123	2	1.01260	122	3	1.02522	125
147.308	26.918	1.01827	148	2	1.01210	146	4	1.02399	150
196.624	33.756	1.01717	198	2	1.01179	196	4	1.02219	200
245.999	40.007	1.01626	247	3	1.01158	245	5	1.02073	250
295.454	45.464	1.01539	297	3	1.01119	294	6	1.01947	300
394.526	54.737	1.01387	396	4	1.01039	393	7	1.01741	400
493.699	63.014	1.01276	495	5	1.00980	492	8	1.01580	500
592.858	71.321	1.01203	594	6	1.00948	591	9	1.01477	600

COLUMN IDENTIFICATION:

1. Fathometer depth
 2. Correction for sound velocity to fathometer depth
 3. Ratio = $\frac{\text{MVSV}}{\text{Fathometer velocity}}$
 4. True depth
- Columns 1, 2, 4 in metres.
Column 2' in decimetres.

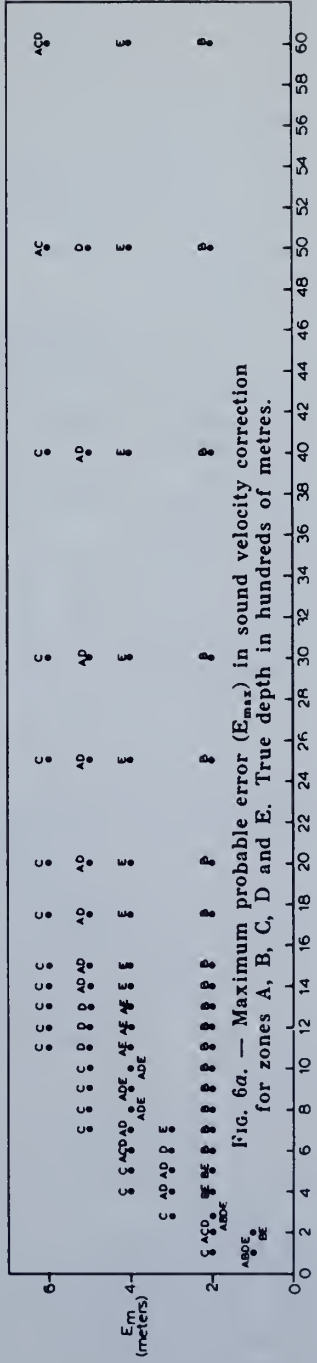
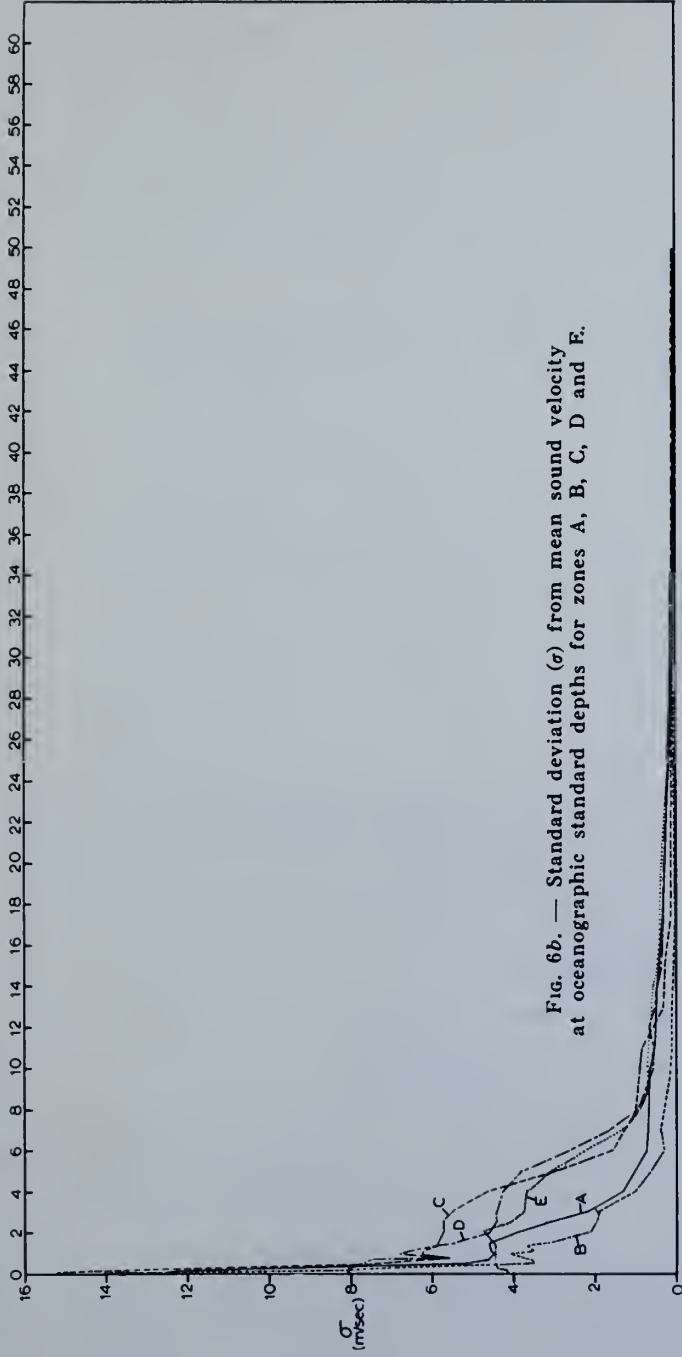


TABLE I

*Fathometer corrections for North Central Pacific SEAMAP Survey
Surface to 1 500 metres*

(fathometer velocity = 1 463 m/sec)

Equation : $\text{Corr} = bM + cM^2 + dM^3 + eM^4$

Where M = Fathometer depth in metres

Corr = Correction in metres to be added
to fathometer depth

ZONES	CONSTANTS			
	<i>b</i>	<i>c</i>	<i>d</i>	<i>e</i>
Zone A (46° to 56° N)	+ 6.0424 × 10 ⁻³	- 3.3660 × 10 ⁻⁶	+ 5.2830 × 10 ⁻⁹	- 1.2858 × 10 ⁻¹²
Zone B (42° to 46° N)	+ 2.04564 × 10 ⁻²	- 2.2860 × 10 ⁻⁵	+ 1.7232 × 10 ⁻⁸	- 3.9494 × 10 ⁻¹²
Zone C (36° to 42° N)	+ 2.52993 × 10 ⁻²	- 2.2670 × 10 ⁻⁵	+ 1.4598 × 10 ⁻⁸	- 3.0225 × 10 ⁻¹²
Zone D (28° to 36° N)	+ 4.3265 × 10 ⁻²	- 4.0874 × 10 ⁻⁵	+ 2.2439 × 10 ⁻⁸	- 4.1810 × 10 ⁻¹²
Zone E (20° to 28° N)	+ 5.3085 × 10 ⁻²	- 5.4265 × 10 ⁻⁵	+ 3.0317 × 10 ⁻⁸	- 5.7826 × 10 ⁻¹²

TABLE II

*Fathometer corrections for North Central Pacific SEAMAP Survey
1 500 metres to 10 000 metres*

(fathometer velocity = 1 463 m/sec)

Equations : $\text{Corr} = a + bM + cM^2 + dM^3 + eM^4$

Where M = Fathometer depth in metres

Corr = Correction in metres to be added
to fathometer depth

ZONES	CONSTANTS				
	<i>a</i>	<i>b</i>	<i>c</i>	<i>d</i>	<i>e</i>
Zone A (46° to 56° N)	- 0.36	+ 2.800 × 10 ⁻³	+ 3.244 × 10 ⁻⁶	+ 3.530 × 10 ⁻¹⁰	- 1.203 × 10 ⁻¹⁴
Zone B (42° to 46° N)	+ 4.64	"	"	"	"
Zone C (36° to 42° N)	+ 7.64	"	"	"	"
Zone D (28° to 36° N)	+ 14.64	"	"	"	"
Zone E (20° to 28° N)	+ 17.64	"	"	"	"

These are the data by which the echo soundings are corrected. The corrections for each zone are plotted against the fathometer depths to which they apply and smooth curves drawn through the data points. By means of a least square curve-fitting procedure, a polynomial expression is derived to match the empirical curves. This expression, therefore, yields a correction as a continuous function of depth for each zone. We have found that a fourth order equation will fit the curves with departures less than 0.3 metre above 1 500 metres. Below 1 500 metres a single polynomial expression will fit the curves for all zones merely by changing the a_0 term, with departures not exceeding 1 metre. The coefficients of the polynomials for the SEAMAP zones are listed in tables I and II. The correction versus depth curve and polynomial expressions for zone B are shown in figure 7.

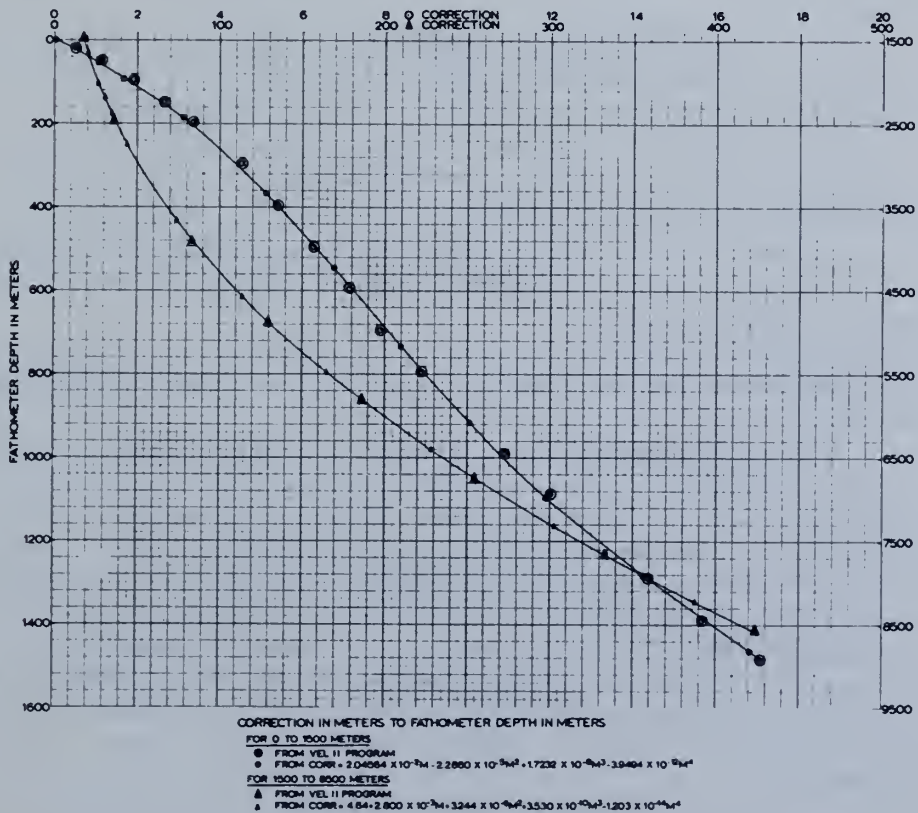


FIG. 7. — Corrections to fathometer depths for sound velocity for Zone B.

A simple computer program provides a look-up routine whereby the coefficients appropriate to the zone in which a sounding is made are used with the fathometer depth to 'solve' the polynomial for the correction. This correction is then added to the fathometer depth to yield the corrected depth.

As a supplement to the computer method, conventional tables have been prepared from the polynomial coefficients which provide for 'manual'

correction of fathometer readings when the situation does not warrant computer assistance. The tables have been prepared in two parts to yield corrected depths in metres and fathoms.

4. — SUMMARY

The method described here embodies the following features.

1. Echo sounding corrections for sound velocity are available as a continuous function of depth, and are calculated and applied without manual effort.

2. The procedure is based on Wilson's formula which is generally accepted as superior to the MATTHEWS-KUWAHARA values. The differences, though small, are systematic, resulting in a slightly deeper ocean.

3. The procedure is designed to utilize all data on the environment available from the U.S. NODC, and yields quantitative information as to the probable error in the corrections.

4. A minor refinement in calculating the Mean Vertical Sound Velocity is achieved by means of an equation which recognizes that the velocity changes within each layer.

5. A minor refinement in applying the correction is achieved by developing the corrections as a function of fathometer depths rather than true depths.

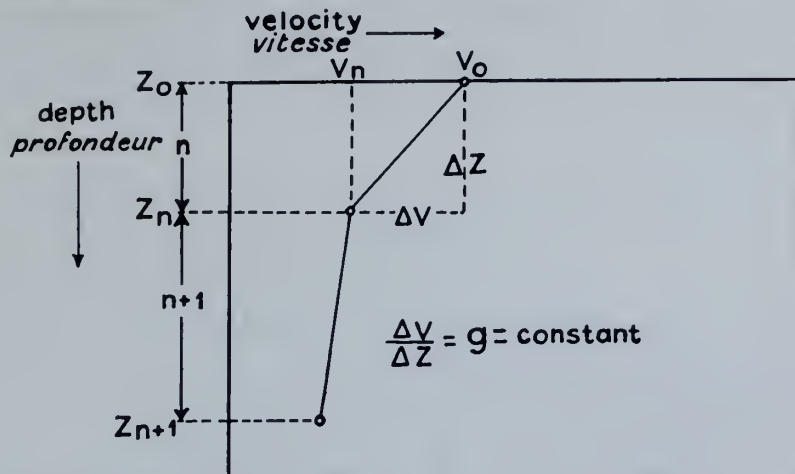
6. Although corrections are made as a continuous function of depth, "scarp" as large as 7 metres in water depths of 5 660 metres can occur when track lines cross zone boundaries. These artificial scarps could be eliminated by using an interpolation technique between zones. As the boundary location is known, the cartographer can compensate for artificial scarps if they should occur.

We are indebted to Mr. R. K. REED for reviewing the manuscript and Mr. James L. STEPHENS for drafting the figures. The developmental work was accomplished on the IBM 1620 computer which was made available by Admiral H. J. SEABORG, Director, Pacific Marine Center, Seattle, Washington.

METHOD FOR COMPUTING THE MEAN VERTICAL SOUND VELOCITY (MVSV) FROM VELOCITIES GIVEN AT THE OCEANOGRAPHIC STANDARD DEPTHS

The MVSV is the mean velocity of a sound wave travelling from the ocean surface to any depth, Z_n where Z_n is one of the oceanographic standard depths. As the actual sound velocity usually changes continuously with depth, the derivation of a MVSV is complex; as a simplification the

water column is considered to consist of a number of layers bounded by the oceanographic standard depths, within each of which the sound velocity gradient is constant.



In each layer, the time required for the sound wave to pass vertically through the layer is

$$t_n = \frac{z_{n+1} - z}{v} = \frac{\Delta z}{v} \quad (1)$$

where Z_n is an oceanographic standard depth, Z_{n+1} is the next deeper oceanographic standard depth, and V is the sound velocity. Within each layer the sound velocity is assumed to vary as a linear function of depth. It is clear that the velocity at any depth Z within the layer is

$$v_z = v_0 + \left(\frac{\Delta v}{\Delta z}\right) z = v_0 + gz \quad (2)$$

(note g has a negative sign)

where g is the gradient of velocity within the layer.

Substituting the expression V from equation (2), into equation (1), and taking the derivative of equation (1)

$$dt = \frac{dz}{v_0 + gz}$$

and integrating over the depth interval n from layer Z_0 to Z_n ,

$$\int dt = \int_{z_0}^{z_n} \frac{dz}{v_0 + gz} = t_n = \frac{1}{g} \ln(v_0 + gz) \Bigg|_{z_0}^{z_n}$$

$$t_n = \frac{1}{g} \ln(v_0 + gz_n) - \frac{1}{g} \ln v_0$$

but $v_0 + gz_n = v_n$, so

$$t_n = \frac{1}{g} \ln(v_n - v_0) = \frac{1}{g} \ln \frac{v_n}{v_0}$$

which yields the time for the sound wave to pass through the first layer.

Similarly for all other layers to a depth Z_N :

$$T_N = \sum t_n + t_{n+1} + t_{n+2} \dots t_N$$

the mean velocity for the sound wave to get to depth Z_N is therefore

$$VMVS_N = \frac{Z_N}{T_N}$$

REFERENCES

- BYERS, R.T. : Formulas for Sound Velocity in Sea Water, *Jn of Marine Research*, 13, 1, pp. 113-121, 1954.
- Del GROSSO, V.A. : The Velocity of Sound in Sea Water at Zero Depth, *Naval Research Laboratory Rpt. 4002*, June 1952.
- KUWAHARA, S. : Velocity of Sound in Sea and Calculations of the Velocity for use in Sonic Sounding, *Hydrographic Review*, Vol. 16, pp. 123-140, 1939.
- MacKENZIE, K.V. : Formulas for Computation of Sound Speeds in Sea Water, *Jn of the Acoustic Society of America*, 32, 1, pp. 100-104, Jan. 1960.
- MATTHEWS, D.J. : Tables of the Velocity of Sound in Pure Water and Sea Water for use in Echo Sounding and Sound Ranging, *British Admiralty Hydrographic Department No. 282*, 1939 (second edition).
- NASCO. See Chapter 9 of "OCEANOGRAPHY 1960 to 1970" a report of the Committee on Oceanography of the (U.S.) National Academy of Sciences 1959.
- SOWER, L.A. : Sound Velocity Formulas *Informal Oceanographic Manuscripts No. 30-61* (Unpublished Manuscript) U.S. Navy Oceanographic Office Dec. 1961.

Reprinted from SCIENCE Vol. 161, No. 3843

Iron-Manganese Nodules from Nares Abyssal Plain: Geochemistry and Mineralogy

Abstract. Three nodules from a core taken north of Puerto Rico are composed chiefly of an x-ray amorphous, hydrated, iron-manganese oxide, with secondary goethite, and minor detrital silicates incorporated during growth of the nodules. No primary manganese mineral is apparent. The nodules are enriched in iron and depleted in manganese relative to Atlantic Ocean averages. The formation of these nodules appears to have been contemporary with sedimentation and related to volcanic activity.

Three iron-manganese nodules were recovered from a 95-cm core taken on Nares Abyssal Plain (25°N, 65°W), a deep southeastern extension of Hatteras Abyssal Plain (1), from a depth of 5729 m. Two of the nodules came from the top 5 cm of the core; the third, from a depth of 73 cm. They provided a rare opportunity for study of geochemical variations of nodules with depth in a sediment column; they were spherical, 3 cm in diameter, and friable, showing uniform distribution of black submetallic grains in an ocherous matrix; a unique feature was their identical size, shape, texture, mineralogy, and concentration of minor elements although the 73-cm nodule predates the other two by at least 30,000 years on the

basis of estimates of the rate of accumulation of clay in the North Atlantic (2). The core sediment was typically abyssal (3), had uniform texture, contained sparse micronodules, and was oxidized throughout; there was no physical evidence of disturbance of sediment within the core, and the extremely friable nature of the nodules precludes any post-formational transport.

The nodules were crushed, and washed repeatedly by centrifugation and decantation for removal of soluble salts and adherent clay. Subsamples were taken for x-ray diffraction, differential-thermal, thermogravimetric, and atomic-absorption analyses. The fractions for x-ray diffraction analysis were examined under a microscope, and ap-

parent mineral phases were segregated. Bulk samples were used for all other analyses.

The fractions for x-ray diffraction analysis were ground in ethanol and dried at 70°C. Other bulk samples, for determination of phase relations at elevated temperatures, were heated in a muffle furnace in air for 72 hours at 200°, 500°, 650°, 870°, or 1000°C (each sample at one temperature) before cooling in air. All samples were mounted in silica capillaries and x-rayed in a powder camera with Mn-filtered Fe radiation.

Differential-thermal and thermogravimetric analyses were used to determine thermal stability, recrystallization, and dehydration, and to supplement and confirm x-ray diffraction results in the determination of composition and phase relations in the nodules. Thermograms and dehydration curves were obtained between 25° and 1200°C.

A sample, ranging from 0.5 to 1.0 g, was collected from each nodule and ignited at 1000°C; the ignition loss was measured, and the sample was leached with concentrated hydrochloric acid. The resultant solution was filtered, and the filtrate was diluted to a known volume. The concentrations of the elements investigated were determined by atomic-absorption spectroscopy (Table 1); analytical error is 5 percent of the amount present. The insoluble material was collected on filter paper, ignited, and measured (Table 1). The elemental values are expressed as weight percentages on a detrital-mineral-free basis. Ignition loss and insoluble residue, determined gravimetrically, are expressed as weight percentages of the bulk nodule.

No primary manganese mineral was detected in the nodules, although spectroscopic analysis demonstrated the presence of 13 to 19 percent (by weight) manganese (Table 1). Other studies of iron-manganese nodules have reported the presence of some form of manganese mineral on the basis of x-ray diffraction analyses which, alone, are inadequate for accurate characterization of the mineralogy of nodules. X-ray diffraction analyses of the black submetallic grains indicated that the material is amorphous, but the ocherous matrix consists of cryptocrystalline goethite.

Our studies indicate that the manganese is diadochic in an x-ray-amorphous, hydrous, iron oxide phase; this conclusion is based partly on x-ray dif-

Table 1. Chemical compositions (percentages by weight) and characteristics of iron-manganese nodules compared with some Atlantic averages. Results: 1 and 2, for the two surface nodules; 3, for the 73-cm nodule; 4, average of 16 other analyses (8).

Result	Element						Ignition loss	Insoluble residue*	Mn:Fe ratio
	Fe	Mn	Co	Cr	Cu	Zn			
1	28.42	19.35	0.41	0.01	0.14	0.07	41.22	27.10	0.681
2	31.61	17.52	.39	.02	.16	.05	34.39	19.59	.554
3	34.96	13.21	.37	.02	.14	.05	37.72	25.40	.378
4	25.85	21.20	.58	.003	.22	.10			.820

* After ignition loss.

Table 2. X-ray powder data for nodule phases in the range 500° to 1000°C, hematite, and jacobsite; for the last two, lines of intensity less than 20 are not included. For the nodule phases, line intensities were determined visually; Fe radiation, $\lambda = 1.9373 \text{ \AA}$; camera diameter, 114.6 mm. Lines for detrital-silicate phases are not included. Abbreviations: I, intensity; v, very (V refers to breadth only); w, weak; B, broad; m, medium; s, strong.

Hematite, ASTM 13-534 (d Å, I)	Nodule phases (d Å, I)				Jacobsite, ASTM 10-319 (d Å, I)
	500°C	650°C	870°C	1000°C	
3.66,25	3.66,vwB	3.66,mwB 2.97,wB	3.68,mw 2.98,m	3.679,vw 2.981,m	3.005,35
2.69,100	2.70,mwB	2.69,s	2.70,m 2.54,vs	2.699,w 2.544,vvs	2.563,100
2.51,50	2.51,mwB	2.52,vsVB	2.52,m	2.21,w 2.107,mw	2.206,vvw 2.107,m
2.201,30	2.20,wB	2.20,mw 2.101,wB	2.21,w 2.107,mw	2.206,vvw 2.107,m	2.124,25
1.838,40	1.837,vwB	1.833,mwB	1.839,w	1.8430,vw	
1.690,60	1.692,wB	1.687,ms 1.617,wB	1.692,mw 1.621,m 1.488,s	1.6923,vw 1.6227,m 1.4904,ms	1.6355,35 1.5031,40
1.484,35	1.483,vwB	1.483,ms			
1.452,35	1.450,vwB	1.449,m	1.452,mw	1.4543,vw	

fraction analyses of bulk samples heated to between 200° and 1000°C. At no stage was a discrete manganese oxide phase observed although, from studies of amorphous manganese oxide gels (4), crystallization of some form of an oxide below 500°C is expected. Below 200°C, dehydration occurs and the nodules lose as much as 20 percent water by weight. Between 200° and 400°C the predominant iron-manganese oxide phase crystallizes as Mn-hematite with an empirical formula $\alpha\text{-Fe}_{2-x}\text{Mn}_x\text{O}_3$; simultaneously goethite from the ocherous matrix undergoes dehydroxylation to $\alpha\text{-Fe}_2\text{O}_3$ (hematite). Above 650°C the Mn-hematite and hematite spinel (jacobite); the transition is nearly complete at 870°C (Table 2).

Other workers (5) have shown that the lower limit for the formation of Fe-Mn spinel from stoichiometric mixtures of the oxides is approximately 1000°C. If manganese is diadochic in an iron mineral such as the Fe-Mn oxide phase observed in these nodules, jacobite could be formed appreciably below 1000°C.

Differential-thermal analyses provide further evidence of the existence of a hydrous iron-manganese oxide phase. Thermograms of the nodules compare favorably with those reported by other workers (6, 7) for hydrated iron oxide gels. No observed reaction could be attributed to the crystallization of manganese oxide from a gel, although differential-thermal studies of prepared mixtures (7) clearly show a resolved exothermal doublet in the range 200° to 400°C, corresponding to the crystallization of iron and manganese oxides from their respective gels.

The ocherous matrix of the nodules consisted chiefly of cryptocrystalline goethite; their sediments and insoluble residues contained abundant illite, mi-

nor chlorite and kaolinite, and traces of montmorillonite, quartz, amphibole, plagioclase, and potassium feldspar. The nodules appeared to have no nuclei, although rare shards, and porcelainous grains apparently pseudomorphic aftershards, were observed under the microscope. The porcelainous grains were chiefly montmorillonite with minor phillipsite. No carbonate mineral was observed in nodules or sediment.

We suggest that formation of these nodules was contemporary with sedimentation and apparently related to volcanic activity; the basis for our argument is the occurrence within the nodules of large percentages of detrital silicates (from sedimentation) (see Table 1), and of rare shards and shard pseudomorphs from volcanic activity.

The nodules were enriched in iron and depleted in manganese relative to average values for the Atlantic Ocean (Table 1); nevertheless our values fall within the reported ranges for these elements (8). The Mn:Fe ratios of the nodules, differing appreciably, are considerably lower than most reported values for Atlantic nodules (8, 9).

Although the manganese content of the surface nodules is significantly greater than that of the 73-cm nodule (Table 1), no evidence suggests that manganese has migrated. Migration of manganese requires an environment that reduces manganese IV to manganese II (10), and there is no evidence in this core of such a reducing environment. The most probable oxidation state is manganese IV which has t_{2g}^3 electron distribution. The ligand-field stabilization energy associated with this electron distribution is $6/5 \Delta_0$ (11), which is maximum. Manganese II has a $t_{2g}^3e_g^2$ electron configuration and no ligand-field stabilization energy; therefore the energy difference between the

two states may be sufficient to deter the migration of manganese IV.

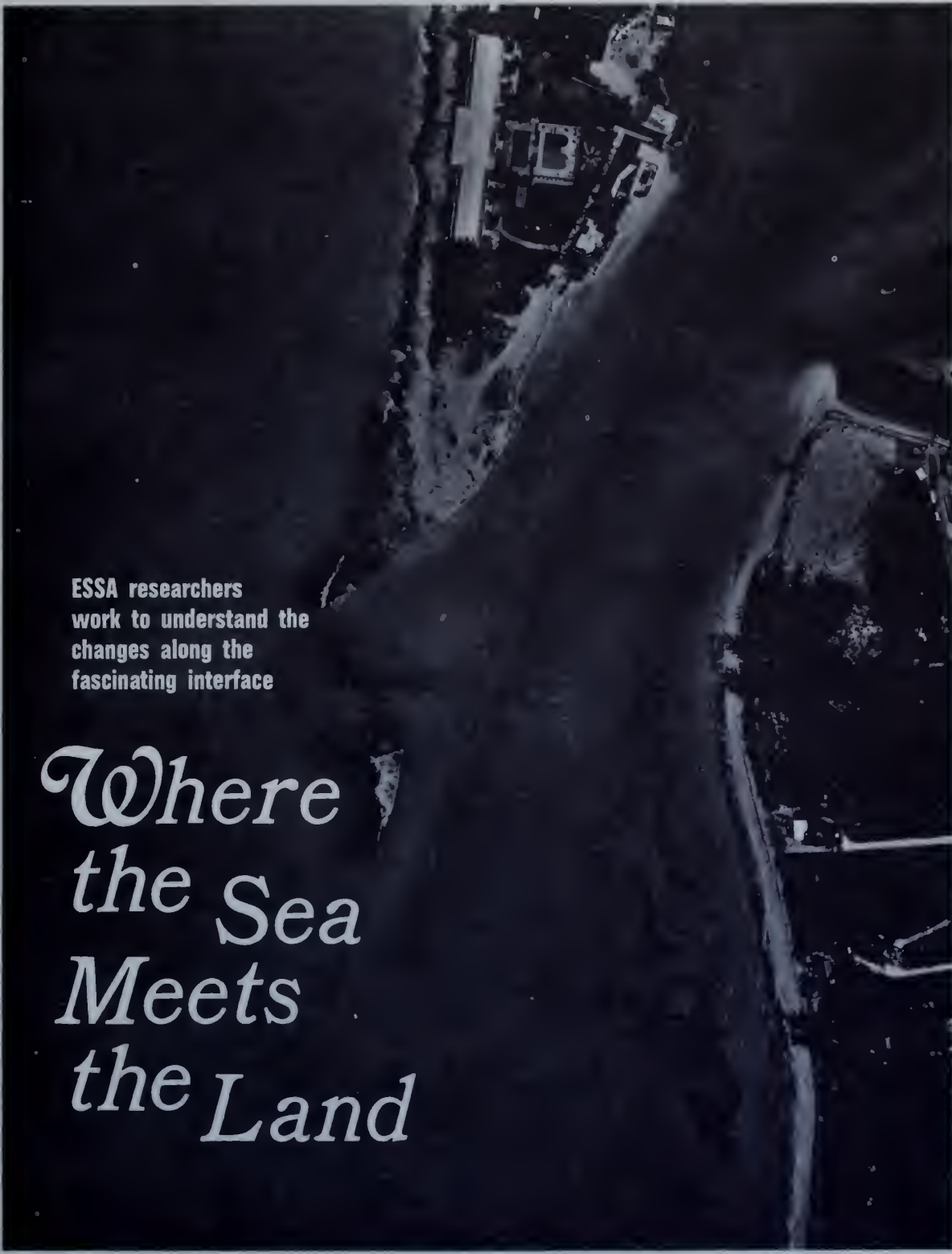
The contents of minor elements (Cr, Co, Cu, and Zn) were similar for the three nodules (Table 1), but our values for them are considerably less than average values for the Atlantic Ocean, with the exception of Cr which is greater by an order of magnitude than reported values (8). Our overall analyses suggest a similar history of formation of all three nodules.

R. E. SMITH, J. D. GASSAWAY
H. N. GILES

Research and Development Department,
Naval Oceanographic Office,
Washington, D.C. 20390, and Atlantic
Oceanographic Laboratories, 901 South
Miami Avenue, Miami, Florida 33130

References and Notes

1. B. C. Heezen, M. Tharp, M. Ewing, *Geol. Soc. Amer. Spec. Paper* 65 (1959).
2. K. K. Turkian, in *Chemical Oceanography*, J. P. Riley and G. Skirrow, Eds. (Academic Press, New York, 1965), vol. 2, p. 102.
3. D. B. Ericson, M. Ewing, G. Wollin, B. C. Heezen, *Geol. Soc. Amer. Bull.* 72, 244 (1961).
4. C. Klingsberg and R. Roy, *Amer. Mineralogist* 44, 819 (1959).
5. B. Mason, *Geol. Fören. Stockholm Förh.* 65, 95 (1943); A. Maun and S. Sömiya, *Amer. J. Sci.* 260, 230 (1962).
6. M. A. Gheith, *Amer. J. Sci.* 250, 677 (1952); R. C. Mackenzie, in *The Differential Thermal Investigation of Clays*, R. C. Mackenzie, Ed. (Mineralogical Society, London, 1957), p. 299.
7. H. N. Giles and R. E. Smith, in preparation.
8. J. L. Mero, *The Mineral Resources of the Sea* (Elsevier, New York, 1965).
9. J. P. Willis and L. H. Ahrens, *Geochim. Cosmochim. Acta* 26, 751 (1962).
10. K. Boström, in *Researches in Geochemistry*, P. H. Abelson, Ed. (Wiley, New York, 1967), p. 421; F. T. Manheim, in *Symposium on Marine Geochemistry* (Graduate School of Oceanography, Rhode Island Univ., 1965), p. 217.
11. F. A. Cotton and G. Wilkinson, *Advanced Inorganic Chemistry* (Interscience, New York, 1966), p. 1136.
12. We thank D. J. Termini, National Bureau of Standards, for lending a thermogravimetric analyzer; and C. Milton, George Washington University, for reviewing the manuscript. Publication approved by the commander, U.S. Naval Oceanographic Office.

An aerial, black and white photograph of a coastal area. A large, multi-story building with a flat roof is visible in the upper center, surrounded by some vegetation and a road. The terrain appears to be a mix of built-up areas and natural land. The overall tone is dark and grainy.

ESSA researchers
work to understand the
changes along the
fascinating interface

*Where
the Sea
Meets
the Land*

IN LATE August 1966, Hurricane Faith lathered the Atlantic, north of Haiti, sending powerful waves far beyond her circumscribed violence. To some — such as the swimmers who were to drown in rip currents coursing through the surf at Wrightsville Beach, North Carolina — these waves held an ominous promise. To others — like the scientists and technicians of the Land and Sea Interaction Laboratory, of ESSA's Atlantic Oceanographic Laboratories — they provided a rare opportunity for the study of exceptional breakers and their forceful effects on beaches.

On August 29, when the first waves of Hurricane Faith began to crash in on the beach at Virginia Beach, Virginia, swimsuit clad LASILites, led by laboratory director Dr. Wyman Harrison, were poised for action, ready to struggle into the churning surf on an around-the-clock schedule of observations that would numb them for 20 straight days. Their objective would be to amass data on winds, waves, tides, currents, and sea-water properties — enough data to permit them to explain the dramatic shift from significant beach deposition to radical beach erosion as a hurricane approaches shore.

On September 1, far to the north of Cape Cod, LASIL oceanographer Dr. Robert Byrne,* was waiting with time-lapse cameras and a series of wave gages to make photographs and electrical traces of the giant breakers that would come hulking over the outer bar near Truro, Massachusetts.

Once the mighty waves had subsided, the cast of swimsuit players would return to its offices for the drudgery of preparing thousands of bits of data for computer analysis. It would be nearly a year after Faith had blown through the North Atlantic that an ESSA computer would grind out an equation which would — in just one line of cryptic symbols — give a precise formulation of how hurricane waves can

modify a beach. And Dr. Byrne, poring over his photographs a few weeks after the waves had subsided, would find to his amazement that the huge waves that had passed over Cape Cod's outer bar had been disturbed in such a way that somehow, without even breaking, they had each reformed into several smaller waves. His precise traces obtained from the wave gages would eventually add an important new wrinkle to oceanographers' understanding of the ways that large waves "deform" in shallow water.

The foregoing illustrates the major part of LASIL's mission of putting land-sea interactions on a quantitative basis. Although formerly it was known, for example, that long, low waves tended to move sand onto a beach and that short, high waves eroded beaches, LASIL has gone the extra mile by developing equations that tell *how* long and *how* high the waves will be before beach erosion or deposition begins. Such quantitative information is vital to engineers and others whose design of coastal structures must be based upon a precise understanding of the relationships involved.

A variety of tools — some primitive, some elegant — are used to accomplish LASIL's objectives.

Lt. John Boon, assigned to LASIL from the C&GS, is working on his master's thesis in a cooperative program between LASIL and the Virginia Institute of Marine Science. He is studying the movement of beach sand using fluorescent sand grains and a "cookie cutter" on a pipe. He dumps a vial of dyed sand in the surf and then, at timed intervals, he and several Girl Scout volunteers dash back and forth into the brine to pick up plugs of sand with the cookie cutter. The plugs, marked for identification, are taken back to the laboratory where ultraviolet (black) light is shined upon them, and the fluorescent grains in each sample are counted. From these data, and information on wave activity and currents, Boon can develop equations for the speed and direction of beach sand movement under different conditions. *continued*

* *Then of Woods Hole Oceanographic Institution.*



LASIL technician E. W. Rayfield samples hurricane surf at Virginia Beach. (Left) The inlet between North and South Bimini, B.W.I. (Right) Lt. John Boon with Girl Scout volunteers who aided research project on movement of beach sand.



Vastly more elegant than Lt. Boon's cookie cutter is the C&GS's "ODESSA" system used by LASIL in a study of the interaction between tidal currents, underwater sand waves, and the transport of fluorescent sand grains. The study was conducted in a tidal inlet between the islands of North and South Bimini in the Bahamas. "ODESSA" is a complete system of telemetering oceanographic sensors and with it LASIL monitored the inlet currents at 16 points.

In deploying the "ODESSA" system, it was first necessary to mount the sensor packages rigidly on tripods at the Lerner Marine Laboratory on North Bimini. These tripods were taken one by one on a workboat to the proper points in the inlet, where they were emplaced during slack water. Electrical cables from the sensors were then connected to recording units on shore. Once running, the "ODESSA" faithfully kept track of the speed and direction of the currents as water rushed in and out of the inlet.

The most exciting part of the inlet study involved keeping track of the movement of sand waves on the floor of the inlet. For this, it would be necessary for the LASIL workers to become "menfish." Donning SCUBA or HOOKAH gear, the oceanographers first placed a rigid, 200-foot "ruler" on the bottom, oriented perpendicular to the crests of the sand waves and made perfectly level. Then, as the current waxed and waned, flooded and ebbed, LASIL menfish made repeated runs back and forth along the ruler with underwater movie cameras. There, 20 feet down in the crystal clear

Bahamian water, they trapped the motion of foot-high dunes and pearly-white sand as the sea floor undulated rhythmically along in the direction of the currents.

LASIL staged something of an underwater ballet in order to freeze the movement of individual sand grains which — by their skipping over the backs, crests, and steep fronts of the dunes — cause the downcurrent motion of the dune forms.

Choreography for the sampling runs involved a lead player who cut open tubes of fluorescent sand laid out on the bottom parallel to one of the dune crests. At precisely timed intervals, this leader would signal three other SCUBA-dancers holding paint rollers. These diver-dancers would press the roller on the bottom and glide off over a prescribed downcurrent course, unrolling a plastic film covered with silicone grease. At the end of the 60-foot-long "stage," the film was expended and the divers would kick to the surface. Another diver would then flutter to the stage and coax the plastic film up off the bottom. In a skiff on the surface, a "stagehand" would reel the film out of view of the audience of lobsters, grouper, and an occasional barracuda.

Study of the brilliantly fluorescent grains on the LASIL tapes is permitting testing of a backlog of theoretical and laboratory work on sediment transport by currents. Thus, LASIL's research program carries forward a vital environmental approach to understanding the various interactions along the boundary where the sea meets the land. □

(Right) Hurricane Faith waves attacking the shore of Cape Cod. Photo was taken on Sept. 2, 1966 at Truro, Mass., from seaside cliffs 130 ft. in elevation. The waves shown have deformed to multiple crests in passing over the off-shore bar. The waves in the foreground, about to break, are about seven feet in height. (Below) LASIL staff members set an ODESSA sensor in place at Bimini, B.W.I.



RESEARCH LABORATORIES
Pacific Oceanography Laboratory
Honolulu, Hawaii
January 1968

Deep Sea Release Mechanism



Technical Memorandum RLTM-POL 1

U.S. DEPARTMENT OF COMMERCE
ENVIRONMENTAL SCIENCE SERVICES ADMINISTRATION
RESEARCH LABORATORIES

Research Laboratories Technical Memorandum-POL 1

DEEP SEA RELEASE MECHANISM

T. J. Sokolowski
G. R. Miller

Joint Tsunami Research Effort

PACIFIC OCEANOGRAPHY LABORATORY
ESSA TECHNICAL MEMORANDUM NO. 1

HONOLULU, HAWAII
JANUARY 1968



TABLE OF CONTENTS

	<u>Page</u>
Abstract	1
1. INTRODUCTION	1
2. DESCRIPTION	1
3. TESTING	6
4. SUMMARY	6
5. ACKNOWLEDGEMENTS	6
6. REFERENCES	7

DEEP SEA RELEASE MECHANISM

T. J. Sokolowski and G. R. Miller

Many oceanographic measurements are most easily obtained by dropping a weighted instrument package to the ocean floor. After the measurements are made the weight is released and the buoyant instrument package floats to the surface for recovery. This report describes a release device actuated by the closing of an electrical switch.

Key Words: oceanographic measurements, release device, actuated, solenoid plunger, and valve.

1. INTRODUCTION

One commonly used release device (Van Dorn, 1953) depends on a magnesium link but the uncertainties in corrosion rates cause large errors in release times. The release device described in this report is actuated by the closing of an electrical switch. A solenoid plunger breaks a glass "valve" that equalizes the pressure in a fluid-filled cylinder and permits a piston to be extracted (fig. 1).

2. DESCRIPTION

The release device consists of three main parts (fig. 2). The first part contains the solenoid and a sleeve. The next section consists of a glass tube valve or differential pressure release, an auxiliary pressure release and the piston housing. The third component is the expendable piston.

The solenoid has approximately 1000 turns of No. 30 HNC NYCIAD wire that is completely filled and encased in plastic. The chrome-plated plunger has a brass screw with a nut at one end, which serves as the striking device to break a small glass tube. The power source to activate the solenoid is a compact 45-V battery contained in the instrument package. The striking device of the plunger is held at a

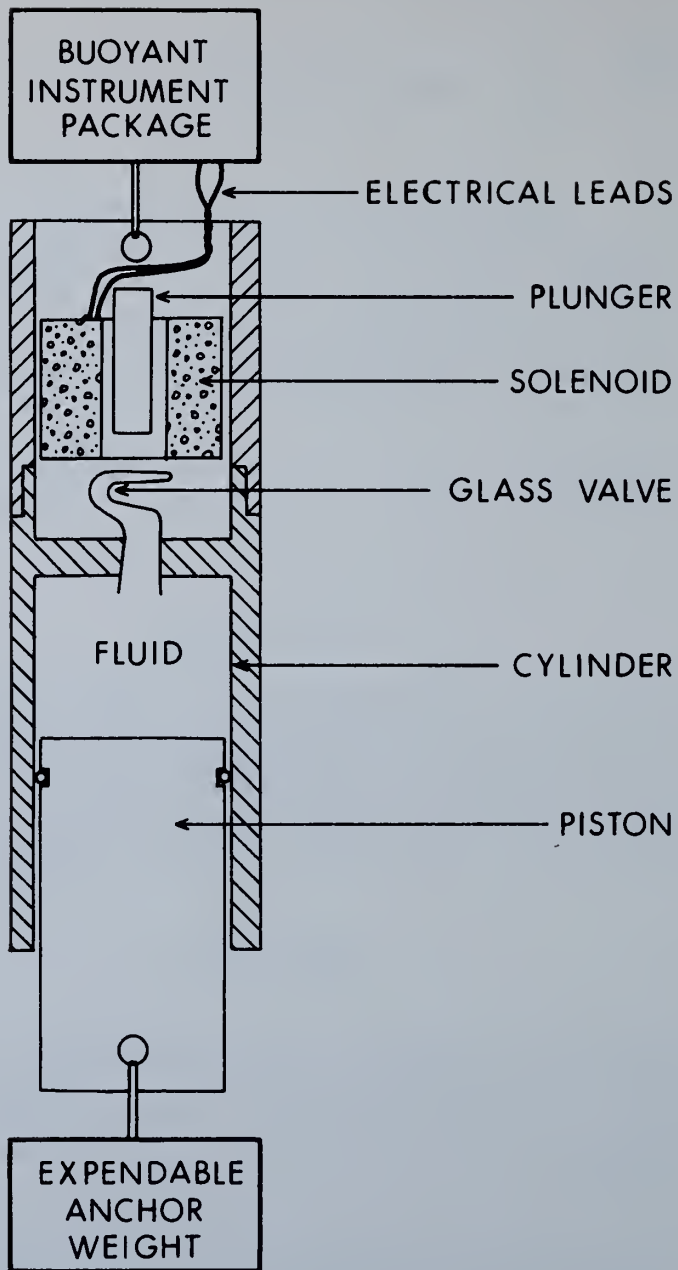


Figure 1. Schematic showing basic principles of operation of release device.

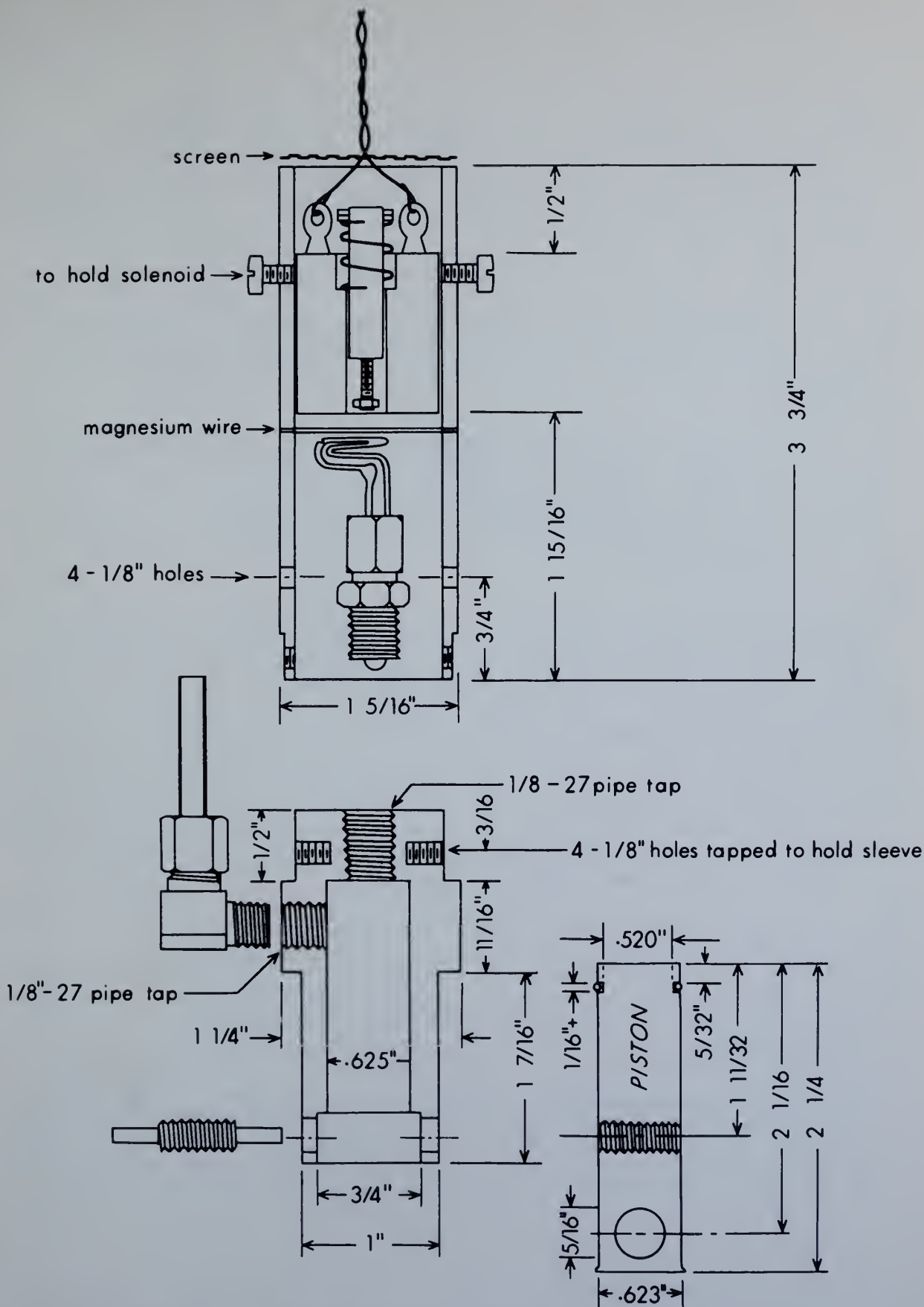


Figure 2. Engineering drawing of the individual parts and their size.

approximately .05 in. from the glass tube by a very flexible stainless steel spring. A thin magnesium wire (taut) attached to the sleeve is placed between the plunger and the glass tube to insure against prebreakage of the glass by the plunger during surface handling. The sleeve houses the solenoid and also serves as a connection between the piston housing and the instrument package. The solenoid is held in place near the top of this housing. A band across the top diameter of this sleeve stops the plunger from coming out of the solenoid.

The glass tube, having a shape of a question mark, is held firmly in place on top of the piston housing. This glass tube is broken by the solenoid striking device. It is etched near the sharp bend to insure breakage.

When the glass is broken the pressure differential in the piston housing no longer exists and the piston may then slide out of the rest of the mechanism. The expendable brass piston is the only part of the mechanism that is eventually left behind with the anchor. A tension of about 5 lb is sufficient to separate the piston from the rest of the release device.

As a back-up in case the glass fails to be broken, a magnesium rod will deteriorate and release the pressure differential. The circumference of the protruding magnesium rod has been coated with FLECTO VARATHAN liquid plastic, and only the diameter face of the rod is exposed to sea water. This delays the chemical deterioration of the magnesium rod considerably and allows the mechanism to be submerged for long periods of time. Figure 3 shows two graphs of deterioration rates as a function of time. The solid line is the deterioration rate at the surface pressure in sea water. The dashed line is the deterioration rate at 7500 psi measured in a limited amount of sea water and at 25°C. These two curves are not to be considered as absolutely accurate but only as a guideline for the deterioration rate.

When the piston is inserted all the remaining voids in the housing are filled with silicone oil. A magnesium pin near the bottom holds the piston firmly in place so that the device will not separate during surface handling. Once the instrument package is released from the surface, this magnesium pin begins to deteriorate. After the pin has completely deteriorated, the increased pressure at depth produces a pressure differential that will support a heavy load. The maximum load that can be supported at any depth is given by the product of the area of the piston head times the hydrostatic pressure. When the glass is broken the pressure differential no longer exists and the piston slips out of the piston housing. The instrument package is then free to float to the surface leaving the expendable brass piston and anchor behind.

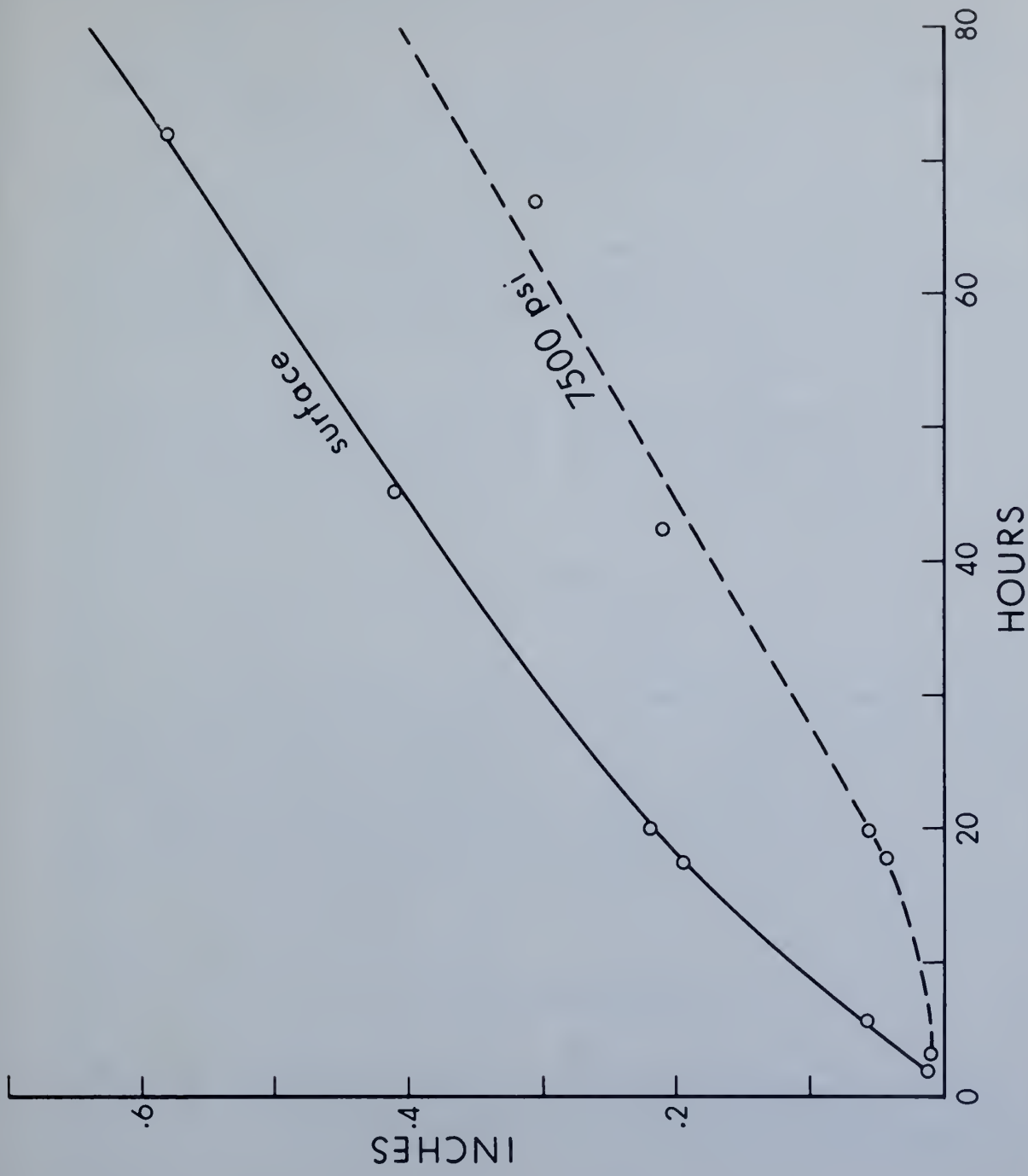


Figure 3. Chemical deterioration rate of the magnesium auxiliary release. Solid line represents the deterioration at surface pressure. Dashed line represents the deterioration at 7500 psi.

3. TESTING

This instrument was tested at atmospheric and higher pressures. The higher pressure range was between 7500 psi and 9000 psi. The pressure chamber used was ESSA's housed at the University of Hawaii Look Laboratory.

The surface testing was done in approximately 3 ft of sea water using a 5-lb weight as the anchor. In this test the mechanism performed as expected, releasing the anchor at each specified time.

The higher pressure testing was performed at 25°C; at present no refrigerated test chamber is available. Various parts of the mechanism were tested separately at 9000 psi. The solenoid was tested at 9000-psi cycling the pressure. Tests of the complete mechanism were made at pressures up to 7500 psi.

The back-up magnesium release rod was tested at surface pressures and at 7500 psi for various lengths of time. The chemical deterioration test at 7500 psi was performed using a small volume of sea water in a container and may not be accurate.

4. SUMMARY

This release mechanism has an advantage over dissolving link releases of immediately freeing the instrument package after a pre-determined length of time. The timing mechanism and power supply are contained in the instrument package. The release is made of brass for ease in machining but could be made of other suitable materials. The instrument was tested at surface and higher pressures and performed satisfactorily in all tests. The deterioration curves are not to be considered as accurate but only to provide an approximation in establishing the length of the magnesium rod to be used for various lengths of submergence time.

5. ACKNOWLEDGEMENTS

The author thanks Dr. Jan M. Jordaan, Director of Look Laboratory, and his staff for the use of the laboratory facilities and their cooperation in performing the required tests.

6. REFERENCES

Van Dorn, William G. (1953), "The marine release-delay timer," Oceanographic Equipment Report No. 2, University of California, Scripps Institution of Oceanography No. 53-23, February 18.

OCEAN-WIDE SURVEYS, BOTH METEOROLOGICAL AND OCEANOGRAPHIC

HARRIS B. STEWART, JR.

ESSA Institute for Oceanography, U.S. Department of Commerce
 Washington, D.C.

Any ocean-scale survey activity would be less than efficient if it were purely oceanographic or purely meteorological. Oceanic and meteorological phenomena are too closely interrelated to attempt to understand one through ocean-wide surveys without considering the other at the same time.

To digress for a moment, this same philosophy has been extended to the administrative end of the scientific spectrum with the recent merger of the Weather Bureau, the Coast and Geodetic Survey, and the Central Radio Propagation Laboratory of the National Bureau of Standards to form a new group within the Department of Commerce which labors under the burdensome—but descriptive—title of the Environmental Science Services Administration. ESSA is a new concept—"lumping" versus the usual governmental operation of "splitting." So far it is working well, and we who are involved in it have great hopes for the future.

ESSA, to carry out the research required to provide adequate services in relation to the marine environment, is establishing the ESSA Institute for Oceanography. Its establishment will be formally announced on the 26th of December. Just a word about this might be in order, since institutes of and for oceanography are fairly close to a lot of our hearts out here. What we're doing is this: We hope to be providing to ESSA the research needed in order to carry out their missions in the field of marine products and services. It is not to be a purely basic research institute as such in competition even scientifically or financially with Scripps or Woods Hole and Lamont, rather we envision this as a research group that will be trying to bridge what some of us consider a considerable gap between basic research conducted elsewhere and the people who are banging on our doors for information on the ocean. This involves everyone from the Jerry Namiases in the long-range forecasting business screaming for sea-surface information, through the people concerned with putting up oil rigs who want to know the currents that they are going to be involved in as they work in the ocean, to the minerals people, the fisheries people, everyone concerned with the ocean as an environment. This will be the thing then that we will be working on in our Institute for Oceanography. It will be located, at least temporarily, in Washington, D.C. Eventually, of course, we hope for a coastal site somewhere, but that will be long in coming, I'm afraid.

Joe Reid had my talk this morning all scheduled and a name tied to it, and my first reaction was to change the name, but my second reaction was to become sufficiently informed myself so that I could

speak to the same title Joe had planned. Therefore, what I would like to do is tell you something of ocean-wide surveys both from the meteorological point of view and the oceanographic point of view.

Jerry Namias alluded briefly to something called the World Weather Watch, and I think it's worth cluing you in briefly on the World Weather Watch as a concept. As I discuss this, please keep it within your oceanographic frame of reference. Think of this as perhaps an oceanographic possibility although being developed primarily for meteorological purposes. To commemorate the United Nations' 20th birthday, 1965 was designated as International Cooperation Year, and in speaking of this President Johnson said: "We will move ahead with plans to devise a world-wide weather system, using the satellite facilities of all industrialized countries. The space age has given us an unparalleled capacity to predict the course of the weather. By working together on a global basis we can take new strides toward coping with the historic enemies: storms, droughts and floods."

The World Weather Watch is an interesting idea. The rapidly evolving capabilities of modern weather instrumentation together with the very large advances which have been made in the understanding of the atmosphere have led people to plan a truly global observation network for meteorology. The motivating idea was that better weather service for all nations really offers the best hope for understanding the atmospheric environment in which we all live. Again keep the oceanographic framework in mind as I go through this meteorological approach.

The World Weather Watch is a system of observing, collecting, processing, and distributing weather information, using the latest developments in communications, data processing, instrumentation, and space technology. Its objective is to remedy age-old deficiencies in weather operations which have prevented meteorologists from providing weather predictions of longer range, greater accuracy, and more usefulness. The plan is being worked out through WMO (World Meteorological Organization). There are some 125 nations now involved in WMO. Already there is an international weather network, but it reflects the widely differing capabilities of the internal weather services of the various countries involved. In many instances several nations cooperate in joint efforts to collect vital weather information. The United States and some western European countries, for example, share the task of maintaining the ocean weather stations.

But the present weather observing and communication networks fall far short of providing the weather

services that are required today. The network of upper air observations, for example, is way below the minimum requirements for about 80% of the earth, for half the globe these observations are totally inadequate, so the meteorologists have considerable problems. But one thing they have done is to establish this World Weather Watch. No one nation could be expected to provide it all—it had to be done on an international basis. As Jerry Namias said, the perfection of mathematical models is coming along, but they need the information that is to be put into them, and I agree with him in that I think it quite probable that when we have good mathematical models and adequate input of global weather data to these models, we will be able to increase our ability for long-range forecasting. But again, this depends on global-scale data—it's nothing that can be done with one man and one lab somewhere—it requires a large network for obtaining meteorological data.

In 1961 after the first Tiros satellite, President Kennedy expressed the desire of the United States to cooperate with other nations in space technology for peaceful purposes, and, speaking to the United Nations, he said the United States "would propose cooperative efforts between all nations in weather predictions and eventually in weather control" (they keep talking about weather control, but this is a long, long way away). And United Nations Resolution 1721, which concerned international cooperation in the peaceful uses of outer space and embodied the idea of cooperative meteorological work, was approved unanimously by the General Assembly of the UN on December 20, 1961, just four years ago today. In the field of meteorology the resolution proposed that the World Meteorological Organizations study means of developing a global weather network to receive, process, and transmit information received from weather satellites.

Specifically, the resolution requested WMO in collaboration with UNESCO and ICSU (the International Council of Scientific Unions) to draw up a proposal for appropriate organizational and financial arrangements and get going with it. In the first report to the United Nations submitted in 1962 WMO recommended the creation of a World Weather Watch combining satellite information with an expanded network of continental information to bring better weather services to all nations of the world. And it is coming along. Plans are developing, and—as these things do—it requires committees and panels, and meteorologists, at least in the United States, are working closely with the National Academy of Sciences Committee on Atmospheric Sciences, and it is coming along—the plan is taking shape, funds for it are being planned—are being budgeted (no one knows how these will come out, it's always sort of a problem), but the point to be made is that the meteorologists are moving right along in this field of developing a global observational network for improving weather prediction and especially long-range weather forecasting throughout the world.

It would be very interesting to me to see the word "meteorological" replaced with "oceanographic"

throughout the foregoing discussion. And there are trends in this direction. One of the aspects of the World Weather Watch is that over much of the ocean there are no means of obtaining meteorological data. The early plans for the World Weather Watch include a series of ocean buoys transmitting meteorological data. It is our intention that the buoys will also be able to obtain oceanographic information.

Again this creates something of a problem because I personally am convinced that right now we do not have a buoy that can sit out there and operate six-eight months with high reliability. It just isn't here yet. There are a lot of plans, ideas, lots of developmental work, particularly the work that ONR is doing, but to get the buoy that will sit in one place for as much as six months with the sensors operating effectively with no deterioration of the data right now is not possible. There are people working on it, but it seems to me that we have to stop talking about great global buoy networks without having the backup to go along with it, and we just don't have it yet. Good buoys are one thing that a lot of people are working on, some of you here are involved in it. It is primarily a technological problem rather than a scientific problem, and I'm a firm believer that if enough bucks are poured into it, it can be solved. Never underestimate the profit motive as a means for getting something done. I think this is also true for oceanography as a whole. People say, for example, that there are not enough oceanographers to justify adding funds to the program on a large scale. My answer is "horsefeathers." With enough money poured into it, oceanographers "will come out of the woodwork." There will be people from other disciplines who are currently working on problems unrelated to the ocean who can just as well translate their effort to similar problems in the ocean.

The same thing happened when we were first talking about a large effort in space. If you look back at some of the Congressional hearings, the standard question was "How can we possibly mount a large-scale space program, we have no space scientists in the United States." Yet when the dollars were placed on the line, "space scientists" came from everywhere. The same thing could happen in oceanography. But I get sidetracked. That then is a brief summary of the World Weather Watch as it now stands.

Now what about the ocean business? Certainly the problem of systematic surveys in the ocean is nothing new to the CalCOFI people. Your organization's program has been one of continuing systematic surveys for some 17 years. Within the Federal Government, where we have been trying to do this on an oceanic scale, we had some of the same problems that CalCOFI has had. Processing, working up, and publishing the data has been a real bugaboo for us. First, a few words as to how this effort got started.

The National Academy of Sciences Committee on Oceanography (NASCO) in their monumental 12-chapter report had a Chapter 9 called Ocean-wide Surveys. This was no brand-new concept. This had been proposed over and over again. It was proposed by the International Council for the Exploration of the

Seas at the end of the last century. It was either ICES or what later developed into ICES. It was proposed by the Navy in the early 1920's—something called the Matthew Fontaine Maury Oceanographic Research Expedition. I've seen a volume this thick of justification as to why the Navy should get into the oceanographic survey business and I have framed in my office a copy of the letter from the Bureau of the Budget saying that the President had looked at this program and found that submission of this program at this particular time was not consistent with the President's present budgetary ideas. This circumlocution means no bucks, so it died again. We still have the same trouble; but within the Federal Government in Washington, we've tried to see what could be done about implementing this latest recommendation to get going on taking a systematic look at the world's ocean.

The Interagency Committee on Oceanography, in trying to put things into categories so that you can label them and add them up to find out how much money is going into what, made an unfortunate split between surveys and research. I think it was a mistake—we have had to live with it ever since, and it has been darn difficult at times. In the Coast and Geodetic Survey, for example, we knew we couldn't get any money for research, we never got any money for research. Thus if we called our effort a research effort, we never would have gotten started. So we had to call it a survey effort. We are a survey organization, and by calling it a survey effort we were able to get it started. Other organizations doing exactly the same thing called it research. But when you start totalling this up to see how much money is going into one aspect of oceanography and how much money into another, you run into definitional problems. The way I like to sort it out is to say that the systematic survey effort is looking at the "what," the "where," and the "when," whereas research-motivated work is looking primarily at the "why" and the "how." I think it is a legitimate way to split them up. In other words, the survey effort is primarily a descriptive effort, looking at the "what's," the "where's," and the "when's," whereas the research effort is trying to understand why and how these things are as they are.

Now in order to find out about the "why's" and the "how's," you have to go back and do the descriptive work first, so these two approaches are inextricably related, and it is criminal that we had to try and make a split between them for budgetary purposes. The hydrographers, the nautical charting people, for years have been doing systematic surveys along the coasts of the world producing nautical charts. These guys are good at it—they have what I like to call a tolerance for tedium that most of us just don't share. If something exciting isn't happening or if we can't see some scientific problems that we want to attack, oceanographers feel it's pretty dull. But fortunately the hydrographers have this tolerance for tedium—this ability to do the same thing day in and day out over and over and over, and they're good at it. What we have done is try and utilize this capability of doing good, systematic, technical, accurate work and utilize this capability for oceanography. What we have

tried to do is translate the recommendations of Chapter 9 of the NASCO report, Ocean-wide Surveys, into an operational reality. To say it is coming along well would be stretching the point a bit. It's limping, just barely limping, but we're beginning to get some interesting results out of it.

As to what the program is, we have, in the classic Washington tradition, given it a code name (you seem to do better getting funds for things when they have a code name) and we struggled to find one for this for a long time. There had been considerable confusion between the continuing historical missions of the agencies—that is, the nautical charting of the Geodetic Survey and of the Naval Oceanographic Office—and the attempt to get started on the ocean survey program. Both ended up as survey items in the budget presentation, so there was confusion as to what bucks were for what. So it became imperative to point out that the specific ocean survey program was different, that it was separate from the continuing historical mission of the agencies. So to point out this difference very strongly during the hearings before the Panel on Oceanography of the President's Science Advisory Committee (PSAC), we called it the "Federal Oceanic Exploration and Mapping Program" which came out "FOEMP" as an acronym, and actually FOEMP! wasn't a bad description of what we had been able to accomplish to date. It has been coming along really very slowly. A lot of work, a lot of good work, has been done but the support has not been there. So we have come up with a better name: it's called Project SEAMAP for Scientific Exploration and Mapping program, and we're going to stick with that title now, Project SEAMAP.

What SEAMAP involves is the systematic mapping of the bottom topography, gravity, and magnetics on underway surveys plus such meteorological observations and sea-surface observations that can be made underway. In this respect I'll be particularly interested this afternoon to listen to Lee Alverson, Ahlie Ahlstrom and Tim Parsons and the rest of the papers on your agenda.

For a long time we have been trying to instill in biologists a feel for the systematic approach to biological surveys, the point being that if we can get this survey rolling, there will be ships doing systematic survey work in the world oceans, ships that can be biologically useful. What is it that the biologists want that can be obtained on a systematic global basis? We are sure that there are such data. I was interested to hear from Maurice Blackburn just recently of developments on measuring pigment material well underway. In the early stages we talked with the Bureau of Commercial Fisheries people in Honolulu. They said, in effect, "Yes, we're very sympathetic; there are a lot of things we would like to learn on this basis, but we don't have the people to do the work. Our shelves now are just stocked with plankton samples that we can't work up—what good would it do to get another 500,000 plankton samples?" So there are some real problems on taking a biological look on a global basis. But the point I want to make is that we're still fighting to get this project SEAMAP going, and to me it would be

criminal to have the project going without a solidly based biological program. The meteorological part is coming along very well—why can't we get the biologists to cooperate?

The work done to date on this program has been in the North Pacific between the Hawaiian Islands and the Aleutian Islands starting at 153°W and working all the way over to 180°. We have done a series of north-south lines; generally they have been 10 nautical miles apart. This, of course, is meaningless unless you have accurate navigational control. I won't beat the navigational drum any more. It has been one of my pet ones for a number of years; but the point is that we had Loran-C control. We now on the *Pioneer* have TRANSIT—the Navy Navigational Satellite System, and hopefully we can hang on to it. We got ours through a little different route from that of the private institutions, and so far we have been able to hang on to it. It hasn't been pulled back by the Navy; we hope to hang on to this thing. The system works—it's a good system. The accuracy is classified, other aspects of the system are also classified, but the point is that it works and we can tell where we are on the surface of the ocean. This really is the fulcrum on which this whole ocean survey business depends—having good navigational control.

Question: What observations are planned for the SEAMAP program? The plan as proposed by the ICO covers the whole spectrum—it reads like a Montgomery-Ward catalog of oceanography, and it is meaningless as far as I'm concerned. It is ridiculous to try to do everything at once; we're under political pressure at this point of the game. But what is actually being observed now? There is one ship working on this—the *Pioneer* of the Coast and Geodetic Survey. The observations being made underway are continuous echo sounding, gravity, magnetics, BT's every two hours (hopefully next year some expendable BT's will be added to this), meteorological observations, regular radiosonde balloon releases, and surface weather observations. We are also using the logs of the Bureau of Commercial Fisheries for fish and bird sightings. We monitor sea-surface temperature, and sea-surface salinity is determined on all BT bucket samples. These make up the underway observations.

In addition each year we have hove-to or station operations which include a research input. For four years we had a series of stations—hydrographic stations—running from the Hawaiian Islands to the Aleutians. These data have been worked up, and they are now in the process of publication by the Seattle laboratory. Cores have been taken when there was a requirement for them. Our own feeling has been that the best place in the world to store cores, if nobody is going to look at them, is at the bottom of the ocean where they were in the first place. So when there are specific requirements, we will do coring.

We've cooperated with the University of Washington and the Geological Survey in doing some dredging on the rift zones seaward of the Hawaiian volcanoes. Dredge samples from these studies enabled the people from Hawaii, the geologists, to come up with some very interesting correlations between the size of

vesicles in pillow lavas, lavas extruded under water, and other characteristics of the lavas as a function of the depth at which the lavas were originally emplaced. This is turning out to be a very interesting new tool for geologists to use to determine the depth at which pillow lavas were extruded on the ocean floor. In the early days of the SEAMAP program we also did some cesium 137 collections for Ted Folsom. We have done other specific projects like this. We collected water samples at depth in the North Pacific for NIO in England, and we have done some biological work for the Bureau of Commercial Fisheries, particularly for the Hawaiian group that wanted samples in specific places. We did work on magnetics with Vic Vacquier who was interested in the possibility of extending some of his crustal displacements. He wanted to see how far these things ran, so we ran some specific magnetic crosslines for him.

We have been concentrating, so far, primarily on the time-independent variables: gravity, magnetics, topography, and so on. The whole problem of the time-dependent variables, as Warren Wooster has pointed out over and over again, is a different problem. Joe Reid alluded to it this morning. We also include within the philosophy of project SEAMAP the systematic collection of information on the time-dependent variables. This problem is a real stinker as you all know. We are proceeding very slowly. Perhaps we are overly conservative, but I don't think so. I personally am tired of the grandiose schemes of loading our ocean with buoys (a) before we have the buoy that will do the job or (b) before we know what we really want to measure, or where. What we hope to do, following the suggestion of the new NASCO report now in the draft stages, is to carry out their suggestions that a small test buoy network be established, and so far the item has been able to remain in our 1967 budget (how long it will stay there is hard to say). We are requesting funds to plant on the east coast shelf an array of five buoys of which the prototype is being delivered to us this week. The system was developed within the Coast Survey and will measure current direction and speed, pressure, temperature, and salinity. These will be in sensors that can go on the cable. We plan to plant five, if we have funds for them, in a fairly tight network on the east coast shelf somewhere out of the Gulf Stream system. With these we will take a look at the whole spectrum of variations, the range of frequencies, and the scales of these variations. And when we have accumulated a volume of data, what we then hope to do is to make copies of these and farm them out to physical oceanographers in the United States and elsewhere. Hopefully we will then have a meeting to sit down, take a look at these data and see what people feel are the things to measure on the larger, more systematic scale.

Question: What sort of an array of buoys do you plan? It's not set yet, we don't know and are open to suggestions; probably they would be arranged in a square with one in the middle. How far apart, we are not yet sure. We would plan it to be close enough to shore so that we can intersperse the buoy measurements with ship observations so that we can fill in some of

the space holes. Question: What is the cost per copy? By the time you get your anchoring gear and the buoy itself we think it's going to run about \$30,000 per buoy. It isn't terribly expensive as buoys go. Question: How do you get the data back? These are both telemetered and/or stored in the buoy on incremental magnetic tape. The man handling the whole project is Mark Goodhart of the Coast Survey. They have done considerable modification to the Geodyne current meter and the tests so far show it has worked very well not only in slow currents but also in currents of two to three knots. So we will continue to be working on buoys, for within this SEAMAP project is a requirement for the measurement of the time-dependent variables. But, this phase is going very slowly and conservatively, which I think is as it should be.

One thing that Jerry Namias mentioned this morning struck a very responsive chord. This was the requirement for long series of data so that you can take a look at time variations systematically. What this always brings to my mind is tidal data, for here in fact is one of the best—if not the best—long series of oceanographic data. They go back into the last century. Generally these are available, with some gaps in the record, on an hourly basis. This is an incredible time series of data. Some people have been well aware of this. Gunnar Roden, for example, has dug many times into our tidal data bank and has utilized these data to come up with new ideas. Walter Munk has done a lot with these long series of tidal data, things that couldn't be done before electronic computers were here. Bernie Zetler from the Institute of Oceanography has been working with Walter Munk on this and has come back from his work with Walter this summer with something which to me was very interesting. I'll pass it on as far as I understand it and suggest that you talk with Walter to get the details on it. To me it was very intriguing. They were using a very long series of hourly tidal height data at San Francisco. They were applying to it new analytical techniques using the BOMM program developed here at Scripps. They were taking a look at the whole range of spectrum of frequencies that occurred in this tremendously long series of hourly tidal heights running back 80 years or so.

Instead of looking for what they thought would be there, they looked at the whole thing to see what actually was there. They found some interesting things. For example, there was a 5-day cycle that appeared as a line on their frequency chart that no one ever suspected. You'd never think of a 5-day frequency in tide; but they also came up with another thing as they looked at these. They found what they are calling a "radiation term." What they feel is that this is a variation in sea level that is a function of the incoming solar radiation. Actually the sun warmed up the water column sufficiently during the day to put a measurable steric variation in sea level, and they are convinced that is what it is. To me what this meant is that all of a sudden we have a tool for going back historically and taking a look at the variations in what I would call the "effective incoming radiation." So here is a whole storage bin of air-sea inter-

action data that suddenly people tripped on, and it's all there in the records just waiting for someone to go ahead and take a look at long-term variations in this effective incoming radiation. This may tie in with some of the solar activity we were speaking of a minute ago. In other words, this is the sort of thing that can happen when you get long series of dependable data.

One other thing, while we're on this ocean-scale survey subject and talking on tides, is a program that is now in the thinking and planning stages, and funds have been budgeted here and there for. Hopefully it will come off. This is the IAPO-Walter Munk plan for an ocean-wide look at deep-sea tides. There has been a lot of interest generated in taking a look at deep-sea tides on a global basis. One nice thing, of course, is that this does not have to be done synoptically, so you are not going to have to have instruments all over the ocean at the same time. Rather the plan is to run a profile dropping the instruments, say, across the Pacific, then coming back and picking them up later on—hopefully. We now have, as you know, cotidal charts that are theoretical. They are based on coastal and island data. We don't really have much of a feel for what happens to a tidal wave as it comes up on to the Continental Shelf—what sort of modification takes place. The idea of going out with bottom-mounted tide gauges on a global scale and taking a look at the whole movement of tide in the ocean is a fascinating idea, and it can very probably be done. People have been working on deep-sea gauges. Aeries in France, Jim Snodgrass and Walter Munk here, Steacy Hicks of the Coast Survey, and many others have been working on deep-sea gauges, and they are beginning to get pretty good results. These things will work. So here is another look on a global scale—this one at the phenomenon on tides.

One other aspect of this large-scale business is one other look at the time-dependent variations which is going on even now. This is called Gulf Stream Studies—'65. I realize it isn't your ocean, and I apologize: but it's a lot like your Kuroshio, so what we Atlantic oceanographers can say is that we are looking at the Gulf Stream and maybe this will help with understanding your Kuroshio. This was a project dreamed up three years ago when air-sea interaction was an especially good budgetary word, and we thought that maybe by using that word which people were latching onto, we would get some additional funds to do something we had been wanting to do all along. This is the way you have to play it in Washington, as you know. So what we proposed was to take a long look at the Gulf Stream. We knew perfectly well that if we in the Weather Bureau and the Coast and Geodetic Survey said that we were going to go into a Gulf Stream program, that it probably would be shot down in flames before we ever got started. So what we did was this: we called in the Gulf Stream people, brought them to Washington for three full days of sessions. This was Henry Stommel, John Knauss, Fritz Fuglister, Tak Ichiye, Bill Richardson, and Ray Montgomery. All came in for three days, and all sat down in a conference room on

the top floor of the Department of Commerce. We said, "Let's be perfectly frank about it. We have the facilities—both meteorological and oceanographic. What we would like to do is take a look at the Gulf Stream, but we want your guidance. We want to know what are the major scientific problems that have to be solved; don't worry about the justifications, we'll tie it in with fish and weather and national defense in the national budget; all we want to know is the scientific problems involved." They were fairly good sessions. On the basis of those sessions we planned a Gulf Stream survey—Gulf Stream Studies 1965. It is going along pretty well. It started actually in August and it's going for one full year. Let me just briefly show you the way it's working, and then I'll get back to these survey studies.

This program is in three phases. For the first at Miami and at Bimini in the Bahamas we had continuously recording tide gauges. Originally we hoped to have the one at Bimini telemetered into Miami so that we could have these on a two-pen recorder. This way we could see immediately the variations and the difference in sea level across the straits. We ran into some telemetering problems with the Canaveral people who were a little touchy about what radio frequencies were used; and rather than get all the new equipment that would be required, we decided that it wasn't really that important to have these data in real time. Thus we waited until we could see the records that would now come in, and we could get hourly heights. Bill Richardson of Miami was working with these data, and we hoped to get some feel for variations in the volume flow through the straits as indicated by variations in sea level across the straits of Florida. Also as part of this program, Bill Richardson has been working with the pop-up current integrator, a very clever gadget. With accurate positioning, you drop it to the bottom and then wait until it comes up to the surface, and the difference between the point where it was dropped and the point where it is recovered is a measure of the net transport that was going on at the time.

The second phase of Gulf Stream Studies—'65 is a standard section running about 150 miles out from Charleston, S.C., done by the Coast Survey Ship *Pierce* with meteorologists aboard making regular upper air observations. The *Pierce* occupies 28 deep stations of which every other one goes to the bottom. This profile is run once every two weeks. This projection is not very accurate. There is no great directional change in the Gulf Stream at Cape Hatteras. If you look at it on the globe, it is one straight run all the way out.

The third aspect, and the one most interesting to me, is continuing the work that Fritz Fuglister was doing, that is, taking a look at the Gulf Stream meanders in the area northeast of Cape Hatteras. Using the Braincon vee-fin towed at 200 meters we pick up the 15° isotherm. Actually the ship is navigated as a function of the temperature at 200 meters. If the temperature gets warmer, we come to the left; if colder, we come to the right, and this way we are able to follow the left-hand (downstream) edge of

the Gulf Stream. These meander trips are made once each month, with the first one made in August.

What we have found is that these large-scale meanders are the norm rather than an exception. When we first started, Henry Stommel became particularly interested in looking at an eddy if we found one. He was sure that these large circular eddies formed and broke away, but he was hoping we would find one so he could go out and look at it. It turned out that we found several of these. The first one we found south of the main stream in September. On the October trip we found that it was still about in the same place, but it had moved to the west, and we found another one over to the east. These large eddies do break away and maintain their integrity at least during periods on the order of three months. We also found very large changes in the position of these meanders. Where at one time we followed a meander like this (drawing on the blackboard), the next time a month later when the ship went out, the meander had moved some 50 miles to the east.

This, then, is another way of taking a look at some of these time-dependent variables. I think this program is going to work out pretty well—I think we will learn a good deal about the Gulf Stream. We held a meeting in November at which the Fuglisters and the Knausses, the Richardsons, and the Ichiyes were all there, and we had a delightful time hashing out what we found to date and what modifications should be made in the program as we go along.

But I want to get back to your ocean and what has been found in some of these systematic surveys in the North Pacific—the area covered through last June, primarily north-south lines with occasional cross lines. The cross lines have not been adequate to date, and this is being improved. We'll talk right now about the work underway. The 1961 data have been almost completely processed and are already being used in papers by George Peter on the geophysics of this area.

The results of the magnetic observations from the area across the Aleutian trench show the same general thing that the only previous systematic survey of this type had also shown. As you recall, the work of Mason, Raff, Vacquier, et al., showed the magnificent magnetic topography off the west coast of the United States. That was magnetic topography found as the result again of systematic surveys off the west coast done by the *Pioneer*, but done on a classified survey for the Navy. We still don't have the bathymetry from that survey in our own shop, but the magnetics were not classified, and Vacquier and company found very intriguing ridge and trough magnetic topography off the west coast. If we examine the Aleutian Trench area with the magnetic anomalies superimposed on top of the topography we find these long magnetic trends, the same sort of thing that Vacquier, Raff, and Mason found farther down off the west coast of the United States. In other words, what these are are magnetic trends that do not follow the pattern of the topography. Now if you took a single trackline of a research ship going through this area and plotted the magnetics, it would look the same

way it does in any other ocean—just a single track-line. If you tried putting two or three of these track-lines together, it would help some, but what I'm contending is that it is the systematic, back-and-forth, tedious survey job that turns up information like this.

I checked with George Peter before I left on Friday. He was quite excited. He has continued to work up this information farther to the South and has found that these lineations do not, as he at first suspected, continue down to join up with the magnetic trends found off the west coast, but these magnetic lineations peter out and become quite irregular in the general area of the Mendocino fracture zone. They then pick up below that, so that the Mendocino is having some reflection in the magnetic data. But this again is the sort of thing that can be discovered only by a systematic survey. We're looking from 45°N to 55°N and from 150°W to 159°W.

One other thing about how this ocean survey program is progressing. I'd like to be much more optimistic than I can—we just had budget sessions this past week and I'm anything but optimistic. A ship that we had in our '67 budget for doing this type of work was disallowed—we're not even sure where we are going to get the funds to repair the *Pioneer* which is badly in need of major overhaul before she can go back to sea. However, we do have two bright spots in the horizon with the delivery sometime this winter of the *Oceanographer* and the *Discoverer*, two large oceanographic survey ships. Each is 3,800 tons, 303 feet length over-all, with 4,200 square feet of lab space. Lots of versatility was designed into them. For example, the lab is of modular construction so you can switch it around to do what you wish. These ships have really good possibilities. One will be operating in the Pacific, one will be in the Atlantic, and both doing project SEAMAP, laeud, we hope, with a good deal of research work going on at the same time. We've done a lot of homework for this program. A recent operations research study carried out at considerable expense has come up with mathematical planning models which we are already using. I can go into details later, perhaps, for those of you who are interested. It was very interesting, though, that after a very detailed research analysis

of the whole thing, they came up with almost the identical number that the NASCO people had come up with for the number of ship-years operation required to survey the whole ocean. NASCO did it over a few drinks at the Cosmos Club one night, and these people to whom we paid X number of bucks came out with the same number, so it was legitimate. It was about 285 ship-years. Granted this would have to be done like the World Weather Watch, on an international basis. The oceans are just too big to try to do it by ourselves. However, we approach the international basis cautiously, for if you have to strike the median level of competence of all the countries involved, this would perhaps fall short of the achievement level that we have in mind. Probably what will be done internationally at first—again a recommendation of Warren Wooster and the NASCO group—is to have some of the larger maritime countries, perhaps the United States, Canada, and the United Kingdom, undertake a portion, say, of the North Atlantic. Then the others come along as they can meet our standards.

The other point that I really want to make is that be it meteorology and the World Weather Watch, or be it oceanography and project SEAMAP, over and above research activity, the systematic collection of meaningful data in both the atmosphere and the ocean can contribute tremendously to our knowledge of both of these environments. Both areas must be pursued with considerably more vigor than in the past if we are ever to realize any real benefits of new and needed knowledge.

DISCUSSION

Schaefer: Are the buoys being planned by ESSA as part of World Weather Watch designed to obtain sub-surface temperatures through the mixed layer? It would be important to do this both for oceanography and also for the weather-forecasting problem.

Stewart: They are being planned to have this capability. No bid proposals have been requested—the buoys are still being considered by ESSA. Not only NASCO and MASCAS, but also the oceanographic element within ESSA has insisted that oceanographic capabilities be included in any buoys for the World Weather Watch.

By Dr. WARREN B. STEWART JR.
Director, Atlantic Oceanographic Laboratory,
ESSA Research Laboratories, Miami, Fla.



An expert's view of
ocean scuba diving:

"You'll love it ...

**don't let
it kill you.**

THIS summer some 300,000 persons in the United States will don ducklike flippers, a cyclopan faceplate, heavy weight belt and one or more air tanks, and wade into the ocean through the surf or roll in over the gunwale of a boat somewhere off the coast.

More people than ever will learn the sheer joy of unfettered swimming, suspended above the bottom and glorying in the magnificence of the seascapes beneath. Once you have tried it, you return again and again to that quiet realm of gentle motion, graceful creatures, swaying seaweed and oceanic peace. You travel in a three-dimensional world. You are free. You are an explorer, enjoying new sights, new sounds, new sensations, new motions, new peace.

It is a good feeling and you will love it. Don't let it kill you.

Most of the Americans who go scuba diving this summer will come back, but a tragically large number will die in the ocean. Since 1960 in Florida alone, some 40 scuba divers have perished in the Atlantic — and most of these deaths could have been avoided.

The really dangerous aspect of scuba diving (and scuba is an acronym for self-contained underwater breathing apparatus) is that anyone can do it. You can don the gear with no instruction, wade into the ocean and swim underwater on a man-to-man basis with the fish who have lived there all their lives. There are no special valves to master, no dials to read, no special techniques to learn; you don't even have to be a strong swimmer. This is the great danger of scuba diving. Anyone can do it — as long as all goes well.

Many problems can arise, however, and the reactions to these problems are what sort out the living from the dead. What happens if your faceplate gets kicked off at 50 feet? If you run out of air at 100 feet? If your intake hose fills with water? What happens if you lose your weight belt and pop to the surface holding your breath? If you get stuck in a wreck and another diver comes down to help you out and offers you his mouthpiece?

These are the mechanical, the technical problems that require that you have a complete scuba indoctrination and checkout in a pool before you ever approach the ocean. This pre-ocean training is vitally important. Like learning to drive a car, you must first learn how to operate the equipment and how to react when the unexpected happens. Any person who scuba dives in the ocean — or anywhere else, for that matter — without first having a complete checkout with a qualified instructor is asking for deadly trouble. It is this group that makes up a portion of the member of divers who do not come back.

Even after you have had the full course in a pool, there is still the transition between that shallow, clean, uninhabited, tideless,

currentless inclosure and the ocean. It is the many differences between the pool and the real ocean that claim another portion of the divers who do not come back. It is to this group, this summer, that this article is directed.

What, in fact, are the peculiarly oceanic things that can threaten the pool-trained scuba diver? What should he know about the ocean if he is to increase his chances of coming back from his first dive or from his fiftieth?

The ocean is a magnificently complex environment. Those who spend their lives studying it are the first to admit that we know very little about it.

Currents are a universal oceanic phenomenon. If you have trained in a pool, the concept of currents has not yet been faced. Learn them and respect them. If you are entering the ocean from a beach through the surf, you will encounter currents as soon as you leave the dry land and enter the water. With your big fins made for swimming rather than for walking, moving out through the shallows can be difficult. Some move into the water backwards so their fins do not impede their progress. Others will carry their fins until they reach swimming depth and put them on there. Longshore currents are usually present between the shoreline and the surf zone, and you should be prepared to be carried parallel to the shore as soon as you stop walking and start swimming.

Rip currents — those narrow swift-moving currents that move seaward the water that piles up at the beach from wave action — are common along most of our long sand beaches. An experienced scuba diver might use a rip to carry him out into deeper water with less expenditure of his own energy, but an inexperienced diver might panic when he finds himself carried seaward at a fast clip. Learn about rip currents and how to spot them.

Once in your diving area, whether you have come out through the surf or rolled in off a boat, your first task on the bottom is to check the local current. Wear a compass on your wrist. They are cheap, and good ones are available. Lie motionless for a moment and see which way you move. If the water is shallow, the swell large, and the current small, you will find yourself moving back and forth as each wave crest and trough moves overhead.

Learn to use this action, and swim harder with the surge than you do with the back-surge. If the surge is really big, you will find that the sediment on the bottom moves with the surge in what marine geologists call "sheet flow," and you will move too. You and the sand will be moving in the same direction and at the same speed, and there appears to be no relative motion. As the forward surge stops and the sand settles to the bottom, you suddenly discover that you have been moving, and the "Einstein effect"

continued

There is fun and fascination in scuba diving, but also great danger. . . .



sharks may be nearby . . .



sea urchins can puncture . . .



a wreck can be a trap . . .



Author Dr. Harris B. Stewart, Jr. in wet suit preparing for dive. (Right) Swimmer Sled capable of speeds up to 2½ knots and depths of 150 feet, carrying two divers.



Photo by North American Rockwell Corp.

can leave you confused. In some instances this totally unworldly effect has led to sheer panic. Learn of it and enjoy it. It is one of the many new sensations you will discover in ocean diving.

In most of our offshore areas within diving depth there is a current over and above the surge related to waves moving overhead. In places like the Santa Barbara Channel off California, these currents can be so strong that a diver hanging onto a rock outcrop at fifty feet finds himself waving like a flag. If you have a tending boat overhead — and it is a lot safer to have someone up there whose sole purpose in life is monitoring your and your fellow diver's bubbles — pop up and tell the man in the boat that you are encountering strong currents to the east so that he will know which way to move to follow you. It is quite probable that he is in a different regime of currents and has the additional problem of wind and that the boat is not drifting the same way that you are, some fifty feet below him. If currents in a dive are strong to the east, this is no indication that they will be the same when you go back to the same diving area the next week. Off most of our coasts, we have fairly strong tidal currents that change direction with time, so you will have to check the current direction each time you dive.

Even though the surface water may be warm as you enter it, the temperature at depth will probably be considerably colder. Most offshore areas have what oceanographers call a thermocline. This is an area where there is a relatively rapid decrease in water temperature with increasing depth. Know what the local temperature regime is, and dress accordingly. You may be perfectly comfortable with only swim trunks at the surface, but at fifty feet you may find that without a full wet suit your teeth are chattering so badly that you have trouble keeping your mouthpiece in place.

There are numerous organisms in the sea that are potentially dangerous to scuba divers. Many of these, such as sharks and the sharp-spined sea urchins, fortunately look dangerous, and obviously should be avoided. If you are heavily weighted and tend to sink, look beneath you as you settle to the bottom. The spines of the sea urchin are

sharp. They can puncture the toughest of wet suits and inflict an annoying wound.

Although there are many stories about scuba divers who have driven off sharks by hitting their noses with an underwater camera or an abalone iron, there are also stories about sharks having been caught and found to have swim fins or face plates or even a leg in their stomachs. If there are sharks of any sort in the water, the really clever thing is to get back to back with your fellow diver and head for the surface as fast as you can. The best course of action — if there are sharks in your area — is to have a cup of coffee aboard and wait until they move off.

One of the best ways to attract sharks if there are none in the dive area is to spear a few fish and have them dangling on a line at your belt. What you are doing is setting yourself up as bait. If you are spearfishing, get the fish in the boat as soon as possible unless you are interested in attracting sharks. They are mean, regardless of species. Have infinite respect for them. If you must have photographs of sharks to impress your friends with your bravery, invest in a simple shark cage. This is merely a small cage to contain not the sharks but you. Take your pictures through the bars, and your friends will never know. You will be just as heroic, and the chances of your getting back with all your arms and legs are considerably enhanced.

Be aware of restricted underwater visibility. In murky waters, things can come upon you undetected faster than they can in clear water. If you are being towed on a line behind a boat or are using one of the several underwater sleds now on the market, don't move so fast that you are unable to stop within the distance you can see. It is the old problem of overdriving your headlights on the road at night. Restricted underwater visibility can come from a heavy overcast sky, from sediment thrown into suspension by storm waves, or by a heavy plankton bloom that causes a "snowfall" of organic material. Unless you know the area and the potential hazards in it, avoid diving if the visibility is less than six or eight feet. The fun of diving is drastically curtailed if the visibility is low, so unless you are in the business commercially, come to the surface

and wait until next weekend. It is safer.

Night diving for the experienced diver can be a totally different and exciting experience, but the hazards are multiplied many-fold. Any night dive must be very carefully planned in advance with particular care taken to insure good communication between the divers and the tending boat. Although the visibility underwater at night is nil, there is in most waters and particularly in the tropical waters a phenomenon that is totally undetected during daylight hours. The oceanographers give it the complex name of "bioluminescence." Actually, it is the living light given off by various marine organisms when they are agitated. If there are in the water suspended small organisms that luminesce, any motion of a diver at night will agitate them into giving off light, and the experience is indescribable. Diving, for example, on a bottom mounted oil rig, you may find that the entire structure is outlined in the subdued neon lighting of bioluminescence. This is due to the turbulence which the rig causes as the current rushes past it. This turbulence is enough to agitate the organisms in the water to the extent that they give off their bioluminescence, and your first exposure to his can be quite startling. In the same environment, you can flick your swim fin and find that great galaxies of swirling light are cast off into the dark reaches of space. A night dive in tropical waters can be very exciting, but it must be planned with sufficient care that when you come up from your experience you have a boat waiting for you.

Finally, be it scuba diving, navigating, fishing, swimming on the surface, boating in your power boat, sailing in your dinghy or your cruising sloop, or just body surfing or swimming, the real secret of getting back safely is based to a large degree on understanding the ocean as a dynamic entity. Probably this is most important while scuba diving. Here you as an individual are completely immersed in the alien world. If you are going into the ocean, learn about it, and your chances of coming back alive will be increased. It is an utterly fascinating environment, but like any alien environment, it can kill you if you don't know about it and respect it. □

Reprinted from GULF UNIVERSITIES RESEARCH CORPORATION
Gulf of Mexico Investigations, Publication No. 107

issues and programs . . .

Environmental Science Services Administration

DEPARTMENT OF COMMERCE

Harris B. Stewart, Jr.
Director
Atlantic Oceanographic Laboratories

"The Environmental Science Services Administration" may be a lengthy and cumbersome name, but it does in fact describe nicely our major mission—the providing of scientific services relating to the environment. For the Gulf of Mexico, ESSA's major involvement is related to the many scientific services available to the operator and researcher. You are, I am sure, familiar with many of these—such as our weather forecasts and our nautical charts. But there are quite a few with which you may not be familiar. Did you, for example, know that ESSA publishes monthly mean surface water temperature and salinity values together with the maximum and minimum for some 20 stations in the Gulf of Mexico from Key West around the coast to Progreso on the Yucatan Peninsula? Or that there are 19 Automatic Picture Transmission stations in the Gulf region which receive satellite cloud pictures on a daily basis?

Perhaps the best way to give you a run-down on ESSA's activities in the Gulf of Mexico is to start with our scientific satellite program, work down through our meteorological program, and end with our marine activities including our oceanographic research work.

THE NATIONAL ENVIRONMENTAL SATELLITE CENTER

ESSA's National Environmental Satellite Center does not have plans for a specific Gulf of Mexico research project but some of its world-wide programs are well suited to exploration in the Gulf. These programs include studying sea state and sea surface temperatures using satellite pictures and infrared radiation from Nimbus I and II. The chief drawback of these studies has been a lack of supporting information from aircraft concerning the sea surface. In addition, plans are underway to let a contract for a comparison of satellite readings and surface temperatures in two areas, one of strong and one of very weak horizontal sea surface temperature gradients. Also of interest is the distribution of cloud cover over the Gulf region and the computation of the heat budget.

Data Acquisition and Dissemination

The Satellite Center does have plans for data acquisition and dissemination for the Gulf area, and these include:

1. *The Advanced Vidicon Camera System (AVCS) and High Resolution Infrared Radiometer (HRIR)* scanning radiometer coverage for hurricane data and sea surface temperature measurements over the Gulf.

2. *WEFAX dissemination* of analyses, satellites and conventional, including digital mosaics, neph-analyses, and maps.

3. *Geostationary spacecraft.* Within the next few years we expect data from geostationary spacecraft for continuous coverage of storms in the Gulf. The spacecraft could also be used as part of a data collection and relay system.

Automatic Picture Transmission

Presently, there are 19 Automatic Picture Transmission (APT) stations in the Gulf region which receive satellite data on a daily basis.

Data Exchange

If some arrangements could be made with the Gulf Universities Research Corporation and ESSA / NESR for a data exchange, it would be most useful and appreciated. In order to have reliable data of the surface conditions on the ocean to go along with any future attempts at a Nimbus shot, members of NESR have been contacting individuals and organizations which could provide good observations of surface weather and cloud cover, sea state, vertical temperature profile, and sea surface temperature. This information is of particular interest at local noon and local midnight which will be close to the time of satellite passage.

It is hoped that the sea surface temperature measurements will be made in several ways: buoy readings such as NOMAD, ship bucket and recording probe readings, and ship and aircraft radiometer readings. For shipboard measurements, care should be taken to prevent the contamination of the sea surface temperature by the presence or movement of the ship. Such data will be used to provide the actual sea surface conditions and the parameters of

the atmosphere which can be used to correct the satellite readings for atmospheric attenuation.

METEOROLOGICAL PROGRAMS

Moving now from space down into the atmosphere, you are all familiar with the ESSA Weather Bureau's routine weather forecasts, but their Marine Weather Service for the Gulf of Mexico is perhaps less well known.

Marine Weather Service

The ESSA-Weather Bureau issues warnings of tropical and extratropical storms when required, and routinely issues forecasts of wind and weather, generally at 6-hour intervals, for segments of the Gulf of Mexico and the adjoining coastal waters.

Hurricane Warning System

One primary responsibility of the Weather Bureau is the provision of the hurricane warning service. The National Hurricane Center at Miami prepares forecasts of hurricanes for the Gulf of Mexico and shares hurricane warning responsibility for the Gulf with the New Orleans Office, dividing at 85° West Longitude. Coastal and area marine forecasts and warnings for the Gulf are issued by our offices in Miami, New Orleans, and San Antonio. Details of the Hurricane Warning Service are given in a 40-page brochure called "Hurricane, The Greatest Storm on Earth" prepared by ESSA and published by the Government Printing Office.

Communications Network

Synoptic data to support the basic analyses and forecasts issued by the National Meteorological Center in Suitland, Maryland, as guidance for the Weather Bureau service programs, are supplied by a network of surface and upper air reports covering the northern hemisphere, including surface reports from cooperating merchant ships. A radar net and the meteorological satellites supplement these data. Reports are also obtained from offshore platforms in cooperation with the oil industry. An extensive international communication net collects and moves this mass of synoptic data to processing centers.

The warnings and forecasts are disseminated over AM and FM commercial radio and TV broadcast stations and over commercial and Coast Guard marine radio stations. In addition, ESSA-Weather Bureau has continuous VHF-FM radio weather broadcasts in operation at Corpus Christi, Galveston, New Orleans, Tampa, and Lake Charles. Another is planned for Brownsville, and at a later date others are planned to cover the remaining principal areas of boating activity.

Expanding the Data Net

ESSA expects soon to have guidance on sea and swell available from the National Meteorological Center that will make it possible for our field offices to include more of this information in their marine forecasts.

Long range plans call for additional dissemination capability, including radiofacsimile as well as the additional VHF-FM stations. Additional marine oriented forecast products, such as sea surface temperature and mixed layer depth, are also planned.

A forecast service is dependent on an adequate data net. The Weather Bureau's long range plans call for buoys in sparse data areas of the Gulf, automatic stations at shore points where observers are not available, more cooperative observation stations and off-shore platforms, and the additional communication facilities to handle the increased data flow.

OCEANOGRAPHIC RESEARCH WORK

Moving from the atmosphere down to the waters of the Gulf of Mexico, ESSA's scientific services include the nautical charts produced by the Coast and Geodetic Survey as one of our more important services to the marine community.

The shared use of our coastal waters by transportation, scientific, and industrial interests poses technical, navigational, and legal problems that must be solved in order to manage efficiently the resources of the Gulf of Mexico shelf areas. Already the petroleum industries are extending operations offshore into water depths greater than 200 meters.

Shipping Safety Fairways

Over the past ten years there has been a steady increase in the number of offshore oil wells and each step seaward increases the hazards to marine navigation. The greatest concentration of these structures is located around the Louisiana Delta area; however, they are now spreading across the entire Gulf Shelf. The area is becoming so hazardous that the Federal Government has established, and chartered "traffic lanes" to help guide vessels safely through this maze toward their destination. The lanes are known officially as "Shipping Safety Fairways."

Ships are not required to use these lanes, but they are expected to stay within them as a matter of safety. The fairways are shown on approximately 45 Coast and Geodetic Survey nautical charts covering the Gulf coast from Port St. Joe, Florida to Galveston, Texas. A recent review of the Fairways by Government and industrial interests may result in changes which will subsequently be reflected on the nautical charts.

Offshore Oil Areas

Mineral leasing areas and blocks have been overprinted on C&GS Chart 1116 for the benefit of commercial and recreational fishing interests, tug boat operators, U. S. Coast Guard air-sea rescue operations, and mariners in general for fixing their position while navigating through the oil lease areas. Due to numerous requests from marine interests, and in view of the value of this information to U. S. Coast Guard air-sea rescue operations, plans are

now underway to overprint these areas also on Charts 1115 and 1117.

Nautical Charts for Small Craft

The explosive growth of recreational small craft from 3.5 million in 1950 to over 8 million in 1966, has had a marked effect on the economy. More than 40 million persons spend \$3 billion annually to participate in this activity. Nearly 550,000 small craft were registered in 1967 by the States along the Gulf coast. To provide these small boat operators with a compact navigational instrument especially designed for their needs, the C&GS is now converting the conventional Intracoastal Waterway series of nautical charts to the folded small-craft format. Nine of these charts have been completed and placed on issue. Complete small-craft coverage of the Intracoastal Waterway and major connecting waterways is planned for the end of 1971. New large scale conventional charts are planned for Mobile Bay and for the new ship channel through Matagorda Bay to Point Comfort.

Large Scale Charting

Our long-range nautical chart maintenance plans provide for the offshore extension of the 122 series of conventional charts when the larger scale coverage has been completed for the inland harbors and waterways. Chart 1282, covering the approaches to Galveston Bay, is the first of this series scheduled for reconstruction. This improvement in existing coverage will furnish more detailed coverage of the oil lease areas and better approaches to the major harbors of the Gulf.

Gulf Bathymetric Maps

As part of the C&GS program to produce detailed 1:250,000 scale bathymetric maps of the U. S. Continental Shelf, compilation will begin on four maps in the Gulf area in FY 1969. Two of these maps will be seaward of the Mississippi delta and two will be off the coast of Texas. Negotiations are now underway with a representative of the Texas Offshore Group to obtain additional depth data needed to supplement C&GS basic hydrographic survey information in the compilation of the Texas maps.

Boundary Delimitation

The increasing interest in the marine environment is producing an increasing interest in boundary delimitation.

All coastal boundaries are delimited from the legal coastline or baseline. Determination of the location of the baseline involves, among other things, two fundamental surveying procedures: (1) establishment of the appropriate tidal datum plane (mean low water on the Gulf Coast) by tide gages in place for at least one year of continuous observations and (2) serial photomapping of the horizontal delineation of the line formed by the intersection of the shore and the appropriate tidal datum plane. These surveying procedures have been carried out as reg-

ular functions of ESSA's Coast and Geodetic Survey but primarily for producing navigational charts.

Unique Texas Coast

The Gulf coast boundary of Texas is unique in that the Supreme Court has interpreted the intent of Congress as fixing its boundary as the mean low water line as of the time it became a State. (This ruling will also apply to Florida, by analogy, as of the time its boundary was approved by Congress in 1868.)

During the past few weeks the C&GS has been asked for technical aid in locating the baselines of California, Louisiana, Texas and Massachusetts. A series of special maps has been prepared for joint use by the Federal Government and Texas in determining as nearly as possible the low water line as it was when Texas became a State. At the request of the Justice Department and the Bureau of Land Management, the C&GS recently resurveyed islets in Atchafalaya Bay, Louisiana, to see if they still exist and, if so, their position and mean low water line.

Coastal Use Studies

As multiple use of the coastal zone increases, it seems clear there will be an increasing demand for C&GS services for boundary determination purposes.

Tide Services

Other ESSA scientific services for the Gulf of Mexico include the Tide Tables and the Tidal Current Tables. Daily tide predictions are published for seven reference stations in the Gulf: Key West, St. Petersburg, St. Marks River Entrance, Pensacola, Mobile, Galveston, and Tampico Harbor plus tidal difference tables for over 350 additional stations between Key West and Progreso, Mexico, on the Yucatan Peninsula. Daily tidal current predictions are published for four reference stations in the Gulf: Key West, and the harbor entrance at Tampa Bay, Mobile Bay, and Galveston Bay, with tables of difference for some 120 additional places between Key West and Brownsville. The Coast Survey vessel MARMER is even now based out of New Orleans to carry out detailed surveys to update this publication for the mouths of the Mississippi.

Tide Station Reports

Once each weekday surface seawater temperature and density measurements are made at most of the Coast and Geodetic Survey's tide stations. C&GS Publication 31-1 summarizes these data through 1964 and lists monthly means, annual means and extremes of surface water temperatures and salinities at stations from Greenland to southern Brazil along the Atlantic coasts of North and South America. This listing includes some 20 stations from Key West to Progreso and these are listed as Annex IV. You might be interested to know that here at Galveston at the Galveston Channel the long term mean surface water temperature is 72.3°F with maximum and minimum temperatures of 102° and

35°. The long term mean surface water salinity is 24.0 o/oo with a maximum of 40.1 o/oo and a minimum of 0.4 o/oo. These temperature and salinity data constitute a valuable time-series of Gulf data. Fifty-five cents buys you the whole of the Atlantic Coast of North and South America, and for an additional fifty cents you can buy the whole Pacific—not a bad bargain. The *United States Coast Pilot*, Volume 5, covers the entire Gulf of Mexico with information of value to navigators but inconvenient to show on nautical charts. This volume covers navigation regulations, outstanding landmarks, channel and anchorage details, dangers, general weather information, routes, pilotage information, and port facilities. This volume is updated every five years or so, and annual supplements are published early each year and distributed free of charge.

GSY Research

In the research area, the Gulf of Mexico is specifically involved in the work of ESSA's Atlantic Oceanographic Laboratories and of the National Hurricane Research Laboratory all at Miami. Zetler of AOL's Physical Oceanography Laboratory as part of his planning for the Gulf Science Year has just recently reviewed Marmer's 1954 paper on tides and sea level in the Gulf and believes the original interpretation of the tidal regime in the Gulf to be completely in error. Where Marmer interpreted the data as indicating a closed basin with a resonance period corresponding to that of the diurnal tides, Zetler has found that the data do not support this, and he is now in the process of proposing a new explanation based on the movement of water into and out of the basin in tidal periods. The data for his analysis are at best sketchy, and Zetler proposes as part of the Gulf Science Year that the required tidal current data in the Yucatan Channel and Florida Straits be obtained along with bottom tide measurements within the Gulf of Mexico and data from more coastal tide stations along the east coast of Florida. These data are needed to test his hypothesis and to solve the problem of the reasons for the observed tidal patterns in the Gulf of Mexico.

Sea-air Relationship Studies

AOL's Sea-Air Interaction Laboratory (SAIL) also hopes to take part in future Gulf studies. Their main interest is in the sea-air relationship to the

frequent cyclogenesis in the central and northeastern Gulf. These storms develop rapidly and bring moderate to heavy precipitation to the south and east coast areas. Use of the instrumentation developed for the BOMEX project planned for 1969 would provide new insights into the air-sea relationship. These instruments include the boundary layer instrument package for use from tethered balloons, airborne dropsondes, and air-dropped XBT's with the data coordinated with those from buoys and coastal radars. Most of this work will be in close cooperation with the research meteorologists at the National Hurricane Research Laboratory and will utilize the instrumented aircraft of ESSA's Research Flight Facility also based in Miami.

Marine Geology

AOL's Marine Geology and Geophysics Laboratory plans a cooperative effort with Texas A&M to core and dredge two outcrops in the DeSoto Canyon area in the northeast Gulf of Mexico. In this same area in 1969 our marine geologists plan a 20-day geophysical/geological exploration including the west Florida escarpment. Participants from Texas A&M's Department of Oceanography will also be along on this one.

National Hurricane Research

ESSA's National Hurricane Research Laboratory has as its two major missions the improvement in predictions of formation, motion, and changes in intensity of hurricanes and other tropical cyclones and the developing of increased understanding of the physical processes that govern the life cycle of hurricanes with the ultimate development of a theoretical model which will simulate the hurricane in all of its phases. Insofar as hurricanes cross the Gulf of Mexico, the hurricane research work of NHRL will also be carried out in the Gulf of Mexico.

As the American Mediterranean, the Gulf of Mexico should be one of the most studied and best understood bodies of water anywhere in the world. It reflects little credit on us that this is not the case. ESSA will be glad to participate in the Gulf Science Year to the extent possible, for the Gulf holds secrets we need to know if we are to provide the best possible services for the environmental sciences.

Reprinted from the Orlando SENTINEL, FLORIDA INDUSTRIES EXPOSITION

FLORIDA'S FUTURE

OCEANOGRAPHICALLY SPEAKING

By Harris B. Stewart, Jr.

IF YOU SUBSCRIBE to Lincoln's statement that government should do for the people only those things that they can not do for themselves, then certainly the immense and expensive task of exploring, mapping, and understanding the ocean is a job for the government.

The federal government has, in fact, undertaken this task in a fairly large way, and a recent publication, "Marine Science Affairs - a Year of Plans and Progress," is the President's report to the Congress in which he outlines the federal program in oceanography for the coming fiscal year (available from the Superintendent of Documents, U. S. Government Printing Office, Washington, D. C. 20402 at a cost of \$1).

Part of the federal task in oceanography should be accomplished through federal agencies such as ESSA, the Bureau of Commercial Fisheries, Coast Guard, Navy, and others. Part should be accomplished through non-governmental agencies but with the financial support of the federal government. In this latter category fall the various colleges and universities which receive support for their teaching and research work in the marine sciences. For the Fiscal Year 1969 which begins this coming July, the total amount of the federal involvement in oceanography comes to some \$516 million as reflected in the President's budget now before the Congress. Over half of this (\$297 million) is requested for the Department of Defense with the rest going to some 10 other departments or independent agencies. The total represents an increase in the support of marine science of about 15 per cent over the present fiscal year.

Marine science is thus a growing federal program, and the hopes for greater expansion in the years ahead are promising. Florida, because of its good climate for year-round oceanographic operations, its numerous and good colleges and universities, and its vigorous activities in trying to attract oceanographic operations to the State, has become a leading - if not the leading - state in oceanographic activities.

Part of these activities are federal, and the present list is impressive: the Environmental Science Services Administration (ESSA) of the U. S. Department of Commerce has at Miami the Atlantic Oceanographic Laboratories made up of the Sea-Air Interaction Laboratory, the Marine Geology and Geophysics Laboratory, and the Physical Oceanography Laboratory.

ALSO IN MIAMI is ESSA's National Hurricane Research Laboratory, its Research Flight Facility, the USC&GS Ship Discoverer, and an Engineering Development Laboratory. The Department of the Interior's Bureau of Commercial Fisheries has their Tropical Atlantic Biological

Laboratory and their ship the UNDAUNTED at Miami, and Biological Laboratories at St. Petersburg Beach and at Gulf Breeze; and the Bureau of Sport Fisheries and Wildlife has a Marine Gamefish Laboratory at Panama City and plans for an additional laboratory on the Florida East Coast.

The Navy has perhaps the largest involvement of the federal oceanic activities in Florida, and this includes their Atlantic Undersea Test and Evaluation Center (AUTEC) Headquarters at West Palm Beach, the Mine Defense Laboratory at Panama City, the Naval Training Device Center and the Naval Research Laboratory's Underwater Sound Reference Division both at Orlando, the Naval Ordnance Laboratory Test Facility at Fort Lauderdale, and both the Underwater Swimmers School and the Fleet Sonar School at Key West.

Other federal agencies include the Corps of Engineers of the Department of the Army, the U. S. Coast Guard of the Department of Transportation, and the Geological Survey of the Department of the Interior, all with varying degrees of involvement in the ocean off Florida.

ALL OF THE COLLEGES and universities in Florida that have programs in marine research and education have federal support to some degree. Probably the University of Miami's Institute of Marine Sciences and the Department of Oceanography at Florida State University are presently the largest recipients of federal support, but Nova University at Fort Lauderdale and Florida Atlantic University at Boca Raton also have federal support for their oceanographic activities as do at least five others in the state.

Ocean industry in Florida benefits some from federal contracts, and the recent publication of the Florida Council of 100, "Oceanography in Florida - 1968," lists some 38 major industries actively working on oceanographic projects, and

these run alphabetically from Airpax Electronics in Fort Lauderdale to Westinghouse's Sea Technology Division in Sarasota.

Because of the heavy governmental commitments in Florida's oceanographic endeavors - commitments to federal agencies, education institutions, and private industry - what happens in Washington will to a very large measure and to a very real degree determine what will happen to Florida's future in the sea. State sponsored activities and private oceanographic efforts unrelated to the federal government are steadily increasing in Florida, but the major oceanographic effort in the State is presently funded primarily by federal funds.

There really is no such thing as "federal funds." They are your funds and mine merely funnelled through the federal government via the tax route to accomplish something that we want done and that we can not afford to or are unable to do for ourselves. Therefore, to a large measure, the future course of oceanography in Florida depends on what the taxpaying public is able to convince the Congress and the Executive Department of the federal government that it most needs.

THE SOOTHISAYERS along the Potomac predict that in a few years we will see a sharp increase in the federal funds for oceanography. If this becomes a reality, then Florida with its heavy involvement in ocean science and technology can expect a comparable expansion in the federally supported programs and projects within the State.

With such expansion will come those ancillary industries that support marine programs, will come more marine science students in Florida's colleges and universities, more people, more marine activity, more research and survey ships, more economic growth, and more knowledge of the global sea produced with the Florida label on it. But this will not just happen.

It takes people to make it happen, people who will let their voices be heard where it will do some good, people willing to work with city, county, and State oceanography committees and panels trying to lure ocean oriented businesses to Florida. Although the impact of the federal government on oceanography in Florida is now substantial, the real future of Florida in oceanography depends heavily on the future impact of Florida's people on the federal government.



U. S. Coast Guard Ship "Discoverer."

About The Author
Of
Florida's Future

Oceanographically
Speaking

BORN September 19, 1922, in Auburn, N. Y. He is the son of a Presbyterian minister and a grandson of the late Rev. George Black Stewart, President of Auburn Theological Seminary. He was graduated from the Phillips Exeter Academy in 1941, and entered Princeton University that fall. He left college in 1942 to spend four years in the Army Air Force, where he served as flying instructor and as a pilot in the southwest Pacific. He returned to Princeton in the fall of 1946 and was graduated with an AB degree in Geology in 1948.

He made one expedition to the Persian Gulf as a hydrographic surveyor with the U. S. Navy Hydrographic Office, establishing shoreline control for offshore surveys in the waters of Kuwait and the Neutral Territories at the head of the Persian Gulf. Upon the return of the expedition in 1949, he accepted a position as instructor at the Hotchkiss School in Lakeville, Conn., leaving there in 1951 to undertake graduate studies at the Scripps Institution of Oceanography in La Jolla, Calif. He received his MS in oceanography in 1952 and his Ph.D. in 1956. While at Scripps, Dr. Stewart participated in a two-month marine geological expedition to the Gulf of Alaska, and was a member of the 1952-53 Capricorn Expedition to the South Pacific. While still in graduate school, he was a member of Geological Diving Consultants, Inc., a group of diving geologists mapping the California offshore area for the oil companies. In 1956 and 1957, Dr. Stewart was project director of the extensive current surveys carried out off San Diego, and in the fall of 1957 went to the U. S. Coast and Geodetic Survey as Chief Oceanographer.

From 1957 through 1965 he was engaged in enlarging the oceanographic activities of the Coast and Geodetic Survey and acted as Chief Scientist — both aboard the USC&GS Ship EXPLORER during its 1960 Oceanographic Expedition, and aboard the Manila to Colombo portion of the USC&GS Ship PIONEER's participation in the International Indian Ocean Expedition in 1964. He was Deputy Assistant Director of the Coast and Geodetic Survey for Oceanography until December of 1965

when he was appointed to head the newly created Institute for Oceanography of the Environmental Science Services Administration. When the Washington components of this group were moved to Miami, Fla., in 1967, Dr. Stewart continued as director of the same group under the new name of ESSA's Atlantic Oceanographic Laboratories. He served as Chairman of the International Programs Panel of the Interagency Committee on Oceanography while in Washington, and has been a member of the U. S. delegation to the five sessions of the Intergovernmental Oceanographic Commission.

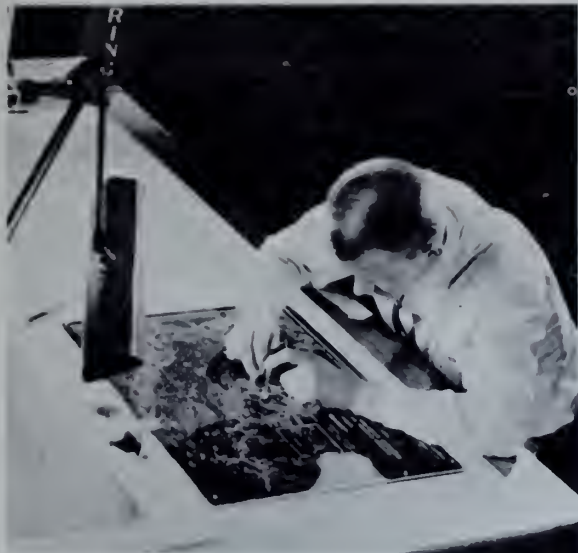
Dr. Stewart is the author of numerous scientific papers on sedimentation, submarine geology, and physical oceanography, and author of the books, "The Global Sea" and "Deep Challenge." He holds memberships in the American Geophysical Union, American Geographic Society, Marine Historical Association, American Asso-



ciation of Petroleum Geologists, Marine Technology Society, and the New York Academy of Sciences. He is a fellow of the American Association for the Advancement of Science, the Geological Society of America, and the Washington Academy of Sciences. He was Chairman of the U. S. Delegation to the 1966 meeting on International Oceanographic Data Exchange, Copenhagen; and Chairman, U. S. Delegation, meeting of the Intergovernmental Oceanographic Commission Bureau and Consultative Council, Paris, 1966.

He is a member of the Florida Commission on Science and Technology, and the Miami Committee of 21.

In 1959 he married Elise Bennett Cunningham of Dover, Mass. They have one daughter, Dorothy Cunningham Stewart, born in 1961, and they reside in Coral Gables, Fla.



Scientists Aid Weekend Sailors

By **HARRIS B. STEWART, Jr.**,
Director ESSA's Atlantic
Oceanographic Laboratories

When John Cabot sailed along the Florida coast in 1497, in all probability he was the first white man to see this lush, green shore, and he certainly had no chart. In the sixteenth century, "La Florida" began to show up on the maps of the great European cartographers. For the following two centuries there was a gradual improvement in the nautical charts of the Florida coast, but the groundwork for the modern nautical chart was really laid when in 1807 the U.S. government established the Coast Survey (now the Coast and Geodetic Survey of ESSA, U.S. Department of Commerce) to undertake a survey of the coasts of the new nation. The first precise nautical charting surveys of the East Coast were not started until 1832, and it was another 30 years before the first good charts of the Florida Coast were made. The original copper plate from which the Coast Survey's 1863 chart of the east coast of southern Florida and the Bahama banks was printed has recently come to Miami and hangs in my office along with other old charts of the Florida coast.

The nautical chart is published to enable both commercial shipping and pleasure boat operators to navigate safely. A lot of precise work and

accurate surveying goes into these charts. Today's nautical chart involves tidal measurements so the soundings can be reduced to a common reference level, aerial photography for shoreline delineation and additional geodetic control, establishment of shore points for navigational control of offshore survey launches or larger survey vessels, and of course, the actual sounding launch or ship operations to determine the depth of the water.

Then there are hours and hours of plotting fix positions on the large "boat sheet" on which the original field survey is worked up. The sounding records—from continuously recording echo sounders—are checked and the depths logged and plotted on the "boat sheet" after they have been reduced for tidal corrections and for other corrections including speed of sound in the seawater at that time. This last one is needed because the echo sounders actually measure not the water depth but rather the time it takes a sound pulse to travel from the ship to the ocean bottom and back. The speed of sound in the sea varies with the density of the water, water temperature and salinity. Then the recorded "depth" must be corrected for density variations. It is a complex, fascinating operation, and a practised crew of hydrographic engineers carrying out their survey at sea

is as fine an example of a smooth man-machine operation as you could ever hope to see.

The charts they turn out are good—at least they are good for the time the survey was made. But storms change the shoreline, currents shift the position of shoals, man dredges new channels in one place and heaps up his spoil dumps in another and creates new land such as Dodge Island. New piers, jetties, marinas, buoys and lights, a submerged wreck, an offshore structure, all of these things make the task of the nautical chartmaker a never ending one.

But what of the charts themselves? For the Miami and Florida Keys area, there is a whole set at various scales ranging from the small-scale chart of all of Florida, Cuba, and the Gulf of Mexico (C&GS Chart No. 1007 at the scale of 1:2,160,000 or about 29 nautical miles per inch) down to the large-scale chart of Miami Harbor (C&GS Chart No. 547 at a scale of 1:10,000 or about 850 feet per inch). A recent innovation for the small boat operator is the special Small Craft Series. The one most used here is C&GS No. 141 covering the area from Miami down to Marathon in the Keys with a series of large-scale charts and larger-scale insets all accordian folded for ease of handling in the confined quarters of most small boats. This special series includes



listings of docking facilities, availability of fuel and supplies, as well as tide tables, tidal current tables, and marine weather information. But no chart is any more useful than the ability of the boat operator to use it.

A few tips might be helpful. Learn how to read and use charts properly. Important chart corrections are issued immediately through the local and weekly Notices to Mariners. As new additions of the charts you use become available, get them and use the obsolete ones for wall decorations, not for navigation. Finally, if you find a place where you feel the chart is in error, don't just complain, do something about it. Write to the Director, ESSA Coast and Geodetic Survey, Rockville, Maryland 20852, and tell him what it is and where it is, and the next time a survey party is in the area, they will check it out and see that the next edition of the chart is accurate.

A nautical chart is a thing of beauty. The history of nautical charting of Florida's waters is fascinating. The modern nautical charts of south Florida area may save your boat and your life if you have them and know how to use them. For further information, write directly to the Coast and Geodetic Survey. They work to compile and publish the charts—they want to be sure that you get the most you can from them. ☀

Reprinted from TRANSACTIONS, NATIONAL SYMPOSIUM ON OCEAN SCIENCE AND ENGINEERING OF THE ATLANTIC SHELF, The Marine Technology Society, Philadelphia, Pa. March 19-20, 1968

KEYNOTE ADDRESS

SCIENCE, SURVEYS, AND THE CONTINENTAL SHELF

Harris B. Stewart, Jr.
ESSA Atlantic Oceanographic Laboratories
Miami, Florida

The United States Continental Shelf out to the 200-meter depth curve amounts to some 850,000 square miles. If this number is hard to visualize, it might help if you think of it as over twice the area covered by the states of Maine, New Hampshire, Vermont, Massachusetts, Connecticut, Rhode Island, New York, New Jersey, Pennsylvania, Delaware, Maryland, Virginia, North Carolina, South Carolina, Georgia, and Florida. Certainly if the Continental Shelf also had twice as many Senators and Representatives as these states do, we would be much farther along in our knowledge and utilization of this vast amount of U.S. territory.

Since the Continental Shelf does not have direct congressional representation, it is up to us, the scientists, engineers, technicians, and administrators to develop and present sufficiently cogent justifications that those who control the purse-strings and determine program priorities will allocate to the research on and development of our Continental Shelf the support required. We need this support if these 850,000 square miles are to be understood and utilized for the betterment of our lot on the remaining 3,669,209 square miles of the United States on which our population of 200,000,000 now lives.

What are the reasons that the United States should concern itself at all with its Continental Shelf, and how can those of us already concerned get our message across so that the United States can move ahead with the task of meaningful exploration and utilization?

As our churches are filled with those who already "have religion" and those who need it most do not attend, so too is this hall today filled with people who already know of the importance of our Shelves while those we really need to reach are elsewhere. At the risk of saying some things that many of you already know, I will proceed in hopes that through you as missionaries and through the published Transactions of these sessions, our message will get out and those who can do something to further Shelf research and development will hear it and will act.

Over half of the population of the United States is concentrated in its 24 coastal states. It is these coastal areas where the demand for waste disposal facilities is greatest and the spectre of pollution looms the largest. It is these same areas to which the populace is turning for more facilities for recreation, more swimming beaches, more boat-launching ramps and marinas, more seashore parks, more good fishing spots, and more places where a man can just sit and watch the sea; yet these same areas are in many states being taken over by an unplanned and uncontrolled expansion of activities with absolutely no concern for present or future recreational uses. Our estuaries and coastal marshlands

constitute an ecological niche where many of our sport and commercial fish species spend at least a part of their life cycle, yet these same estuaries and marshlands are constantly being forced to give way to the encroachments of civilization while the United States between 1955 and 1965 dropped from second to fifth place in commercial fish production. These same waterways are the marine route to our great coastal metropolitan areas; yet few of our seaports are modernized, turn-around times are overly long, port facilities in many places are antiquated and inefficient, and far from being the exciting and colorful waterfronts of a century ago are now in many cities the areas most in need of urban renewal, areas carefully avoided by all except those with business there.

These, then, are our estuaries. These are our coastal areas with the great conflicts among those who would use for their own particular purposes these great resources held in common. Waste disposal, recreation, sport and commercial fishing, commerce and navigation - these are the main competitors for our estuaries. It is up to us, the scientists and engineers, to provide to the decision-makers the facts they need in order to make intelligent and rational decisions on the present and future uses of our estuaries. Without the basic environmental knowledge, the use of our estuaries will go to the richest contender, the loudest complainer, or the faction with the greatest political influence. It is only through adequate knowledge of our entire estuarine ecosystem, its processes, dynamics, interactions, and the ranges through which its many characteristics vary, that we will be able to have adequate knowledge on which can be based the important decisions of the future.

Providing this knowledge is a major task of the people here today. Providing these people with the wherewithal to obtain this knowledge is the job primarily of government - federal, state, and local. So the appeal today is primarily to the governmental administrators: if you ever hope to stop the present trend of complete destruction of our great estuarine resources, plan now for their optimum use. But that planning must be based on a complete knowledge of all the interactions, all of the magnificently complex processes which operate in our estuaries. It is the coastal laboratories and the marine scientists and engineers that must provide this knowledge. These are the groups that must be supported now if our estuaries are ever to be anything but the mismanaged, polluted, azoic, unattractive waterways they are fast becoming.

It may seem that I have dwelt overly long on the estuarine areas which comprise a relatively small percentage of our Continental Shelves, but it is in these areas that we are already facing major problems. These are our areas of coastal crisis. The rest of the Continental Shelf, however, still presents a picture that is a bit more optimistic. Granted, we know even less about our Continental Shelf than we do about our estuaries, but we still are a fairly long way from its complete ruin. There is more time for adequate planning for the exploration and use of our Shelf, but the time to start has long since passed. Our work on the U.S. Continental Shelf has been piecemeal and ill supported. We do not yet have our Shelf adequately mapped. Only the Atlantic Shelf data have been compiled into a bathymetric map of the Shelf and Slope topography, and that at a scale of 1:1,000,000 is useful primarily for gross planning and as a nice wall decoration. Great portions of complex shelf off Alaska have yet to be

adequately charted for navigation. Off the Atlantic coast, we really know little more of the general circulation than we did at the time Haight published his summary over 25 years ago (Haight, F. J., 1942, Coastal Currents Along the Atlantic Coast of the United States, USC&GS Spec. Pub. No. 230, G. P. O., Washington, D. C.). We have no system to predict wave and breaker heights routinely along our coasts. We have far from adequate knowledge of the distribution and variations in the abundance of Shelf organisms, let alone those species that can be caught commercially. The sardine problem on the West Coast and the menhaden problem on this coast are the classic examples. We do not have geological maps of our Shelf. Sediment distribution maps are spotty and have to be at such small scales because of the sparseness of the data that they too are of use primarily as wall decorations. We know practically nothing of the distribution of mass physical properties of Shelf sediments. We have a good deal of tidal data along the coast, but the motion of the tide wave across our Continental Shelf will remain in the realm of speculation until bottom-mounted gauges finally become operational and provide us with the information. Our knowledge of the Gulf Stream and its variations is still terribly limited. It is only within the past few years with the development of deep-towed thermister units that we have made any significant advances over the classic work of Pillsbury aboard the steamer Blake in the latter part of the last century. The sub-bottom structure of the Continental Shelf is known publicly along only a few isolated profiles. I say "publicly" because the oil companies and their geophysical contractors probably have most of the Shelf pretty well covered; but until such knowledge ceases to have any economic advantage for the company that holds it, the data are more secure than Top Secret military data. We have no surveys of the mineral resources on our Shelf. The Heavy Metals Program of the Geological Survey and the fledgling and underfunded program of the Bureau of Mines are making a start on this mineral resource evaluation, but it is just that - a start. State boundaries have not been delineated on the Shelf let alone our boundaries with Canada and Mexico. Even were these boundary lines shown on charts, there is no operational coast-wide system by which the offshore ship or boat operator could adequately position himself in relation to such boundaries.

I do not mean to deprecate in any way the many excellent surveys and research projects that have been carried out on the Atlantic Continental Shelf. What I do mean to say is that the area of the ocean closest to our own shores is still so inadequately mapped, so poorly understood in all its facets, that we are kidding ourselves if we think we are anywhere near ready to make even the most primitive use of such resources as might be on our Shelves. The petroleum companies are, of course, the big exception here. They had the economic squeeze that drove them to the Shelf. I contend that there are other "squeezes" to which we should also be responsive - the need for food, the need for safe disposal of our unwanted wastes, the need for improved weather forecasts, the need for better charts for the shipping which crosses our Shelf, the need for preserving our beaches, the need for predicting waves and surf and tides and coastal currents for the engineers who would build or operate on our Shelf, the need for finding new sources for the minerals that are being used up on land, and of course the need for the military protection of this very same Shelf and the country itself. Far from the least important, but certainly one of the most difficult to justify in this era of blind adherence to the cost/benefit ratio as the ultimate

justification, is the satisfaction of scientific curiosity. This is the real stimulus for the many individual scientists on whom the developing of our fund of basic knowledge must ultimately depend. This, perhaps above all others, is the most compelling reason for learning about our Continental Shelf. What a pity that our present preoccupation with potential benefits and economic returns for our scientific efforts precludes our even suggesting to the budgeteers that the satisfaction of intellectual curiosity is as adequate a motive for the actions of nations as it is for those of individuals!

Operating then on the contentions that (a) we need to have knowledge of our Continental Shelf if we are to utilize it and its resources in some sort of optimum fashion, and (b) that we presently do not have enough knowledge to do this or even an adequate program to insure that such knowledge will be available in the future, the question boils down to one of how we can obtain this knowledge.

President Johnson in his January 1968 State of The Union Message said:

"This year I propose that we launch, with other nations, an exploration of the ocean depths to tap their wealth, energy, and abundance."

Knowing the Federal Government as I do, you can be sure that the "Potomac oceanographers", as Athelstan Spilhaus used to refer to them, will be hard at it developing a program of exploration to back up this excellent proposal of the President. I am sure that this is the first time that marine exploration has received such coverage in the State of the Union message. This, to me, represents a real challenge to the marine scientists and engineers of the United States. This is a loud clear call for the best marine minds in the country to work together to develop a truly meaningful program of marine exploration. Hopefully the Continental Shelf because of its accessibility and potential will be adequately covered in any such developing plan for "exploration of the ocean depths". But can we rest on "hopefully"? I would think not, certainly not if we are as concerned about the Atlantic Continental Shelf as the presence of this many people here today would seem to indicate.

I respectfully submit that if we sit here today and tomorrow listening to the excellent papers the program lists, clap respectfully - even enthusiastically, and then return to our offices, companies, and laboratories leaving this Presidential challenge unmet, we have no one but ourselves to blame if the United States mounts an ocean exploration program without its including adequate coverage of the Continental Shelf. Each of us must be willing to contribute something of his talents, something of his time, and something of himself to furthering our exploration and understanding of the Continental Shelf. The SEAS Committee (Scientific Exploration of the Atlantic Shelf), the group in the south planning the Gulf Science Year For 1970, and the group assembled here today comprise a group of real experts on the Continental Shelf. Make this talent available to your government. Help in the planning. Make the United States program for the exploration and utilization of our Continental Shelf a very meaningful reality. The United States needs to know about our Shelf. The planning for any Shelf exploration program needs the experience and knowledge

of the best minds available. This is the challenge.

With the demise of the old Interagency Committee on Oceanography, the role of coordinator of Federal programs in oceanography has become the task of the National Council on Marine Resources and Engineering Development headed by the Vice President. If a program of ocean exploration is to develop, it will certainly be the Marine Council, its staff, and various panels that will put the program together. It is this group to which you should offer your assistance. This is the group where your ideas and experience can best be utilized. If you really want the United States to mount a program aimed at providing the needed knowledge of the Continental Shelf, you must be prepared to help in the preparation of such a program. Let's be perfectly frank. The increased support for Continental Shelf research and surveys which we all would like to see depends upon program endorsement by the Federal Government. The Marine Council will not endorse a mediocre program. It must be good. You are the scientists and engineers that can make it good. I hope that in the meetings scheduled for today and tomorrow, in the corridors, and in the inevitable informal sessions that will develop among scientists with similar interests that you seriously consider how you as scientists and engineers, either singly or collectively, can rise to the challenge of preparing a coordinated national effort aimed at the mapping and understanding of the Continental Shelf of the United States.



The "Researcher," ESSA's prize exploration ship, will be making Miami its home this year.

The Southside Fleet

A growing fleet of oceanographic ships will berth on the south side of the new Port of Miami on Dodge Island this year. Dr. Harris B. Stewart, director of the Atlantic Oceanographic Laboratories of ESSA, tells the story of Miami's new ocean frontier.

By Harris B. Stewart

DRIVING ACROSS the bridge into the new Port of Miami on Dodge Island, it is hard to realize that a few short years ago the bustling port complex was a group of four small uninhabited islands covered with scrub casuarina.

Today, the island has a railroad with delivery spurs, two large cargo buildings each covering 200,000 square feet, a rising passenger terminal, which will be the best and most modern on the entire eastern seaboard, large ships coming and going tended by a fleet of fork lifts and trucks, and always men; men with lists constantly checking, men directing the movement of cranes and lifts, men shoving and sweating and shouting, men busy pumping the lifeblood of a busy port. If you haven't been out to Dodge Island, you should go. Its bustling business typifies the new Miami approach to the ocean as a major resource of southeast Florida.

Although Miamians are familiar with the "Ariadne," "Sunward," "Jamaica Queen," and the "Cabo Izarra," and will soon become familiar with

the new Miami-based cruise ships, new "Bahama Star," "Flavia," "Boheme," "Starward," and "Freeport," there is still another fleet of ships that is, or soon will be, based at Dodge Island. These are the oceanographic research ships: "Discoverer" of the Environmental Science Services Administration (ESSA), "Pillsbury" of the Institute of Marine Sciences of the University of Miami, and "Undaunted" of the Bureau of Commercial Fisheries. To these will be added the 2,800-ton ESSA research ship, "Researcher," this coming year.

By next April Dodge Island will see the greatest concentration of oceanographic research ships ever assembled in Florida. The "Oceanographer," "Discoverer," "Surveyor," and "Mount Mitchell," all operated by the ESSA Coast and Geodetic Survey, will be berthed at Dodge Island at the same time, preparing for the Barbados Oceanographic and Meteorological Experiment, called BOMEX for short. BOMEX will also include ships of the Coast Guard,

Continued on Page 20

The Southside Fleet

Continued from Page 18

Bureau of Commercial Fisheries and the Navy, and any or all of these could well be at Dodge Island at one time.

Even while the new passenger terminal and the increase of Miami-based cruise ships have caught the headlines and the fancy of Miami's press, there have been developing, at the same time, plans for a unique cooperative research ship facility along the south side of Dodge Island. Preliminary plans are already on the drawing boards, and negotiations have reached the stage where the Federal Government and the Dade County Government are working out the lease arrangement. This new Dodge Island facility will be a complex of attractive low buildings housing offices and machine shops, covered storage space, and open storage area to provide the

shoreside support for the growing fleet of oceanographic research ships operated by ESSA, the University of Miami and the Bureau of Commercial Fisheries. Hopefully, this facility will be completed next summer along with the bulk-heading of the entire south side of Dodge Island.

The research ship facility on Dodge Island is one more manifestation of the growing oceanographic activity in the Miami area. Funds are now available for construction of the new Marine Science Center at UM's Institute of Marine Sciences on Virginia Key, and construction should commence soon.

The new oceanographic research building of ESSA's Atlantic Oceanographic Laboratories is well along in the design stage, and construction funds are being requested in the fed-

eral budget to be submitted to the Congress the first of the year. This new building will house ESSA oceanographers, meteorologists, and ocean engineers and will include laboratories, seminar and conference rooms, a museum, a two-story library, an electronics shop and the various support activities required of present-day scientists concerned with understanding the magnificent intricacies of the ocean and the atmosphere and their complex interactions. Ground breaking should be late next year with completion in 1970.

Other reflections of Miami's dynamic ocean-oriented growth are to be found at the Miami Shipyard on the Miami River at Southwest Second Avenue. Here, under the ownership of Jim Brown, the former shipyard

Continued on Page 22

Southside

Continued from Page 20

office building has become a center for ocean engineering activities. In addition to the shipyard programs themselves, this building now houses the Reynolds Submarine Service Corp., operators of the research submarine, "Aluminaut," and their main office has just moved to Miami from Washington, D.C.

In the same building is the recently-dedicated Engineering Development Branch of the Systems Development Office of the ESSA Coast and Geodetic Survey. This group is involved with the design and development of oceanic buoy systems and sensors for measuring the physical characteristics of the ocean.

The Coast and Geodetic Survey also has the office of the Miami Ship Base there, pending the completion of the new ship facility on Dodge Island.

Oceans General, a newly formed ocean engineering group, is housed there along with HydroTech Service Corp. This latter group has moved to Miami within the past year. It services various types of exotic underwater equipment and is constructing a large hydrophone calibration facility at Miami Ship Yard.

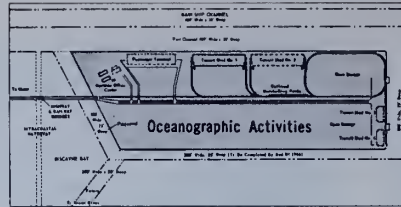
The roof of the building has sprouted some six large antennas for test and communication, and listening in on one of the daily coffee sessions in this Miami Shipyard building is all that would be needed to convince you that Miami is indeed well launched into her ocean era.

Other things are happening, too, that reflect Miami's growing involvement in things oceanic. Marine Acoustical Services has recently been purchased by Tracor, reflecting the respect of out-of-state capital for Miami's oceanic capabilities. MAS operates a fleet of commercial survey and research ships and has recently launched a new oceanographic ship whose time was already booked solid when she was launched.

In response to the increasing demand for technicians specifically trained for marine work, Miami-Dade Junior College instituted a Marine Science Technology program which, in its first semester, has over forty enrollees.

Seacamp, the unique Miami-based

Continued on Page 24



Master plan for the Port of Miami includes room for the oceanographic facilities.

Continued from Page 18

summer camp for teenagers interested in oceanography, had its largest and most successful summer yet on Big Pine Key, and scientists from the various Miami oceanographic activities were guest lecturers.

The Miami Museum of Science also reflects this ocean interest and has just opened a coral reef exhibit that is exciting and unique.

In other areas, the Dade Development Department has published quality brochures covering the county's marine activities, and these have been widely disseminated. The newly-formed Florida State Commission on Marine Sciences and Technology has established its offices in Coral Gables and is deeply involved in projects ranging from studying the delineation of Florida's offshore boundaries to looking into the possibilities of strengthening the state's posture in marine science. National associations of bankers, architects, and industrial developers are planning Miami meetings this winter with oceanography as a major theme and with local oceanographers taking part. The 1969 annual meeting of the Marine Technology Society is slated for Miami Beach in June.

The word is spreading. The years ahead can expect to see more marine research groups, more oceanographic ships, more new oceanography buildings, more meetings and conferences of national significance, more marine scientists and engineers, and with all of these, more of the ancillary and supporting activities that help the local economy.

In oceanographic activities, Miami has reached what the nuclear physicists call "critical mass." Those here for years have attracted new ones, and they in turn have attracted more, and the system is a self-perpetuating and expanding one that spells nothing but good for Miami in the years ahead. ☀

PENN STATE UNIVERSITY LIBRARIES



A000072022320